Mechanosensitivity in Cells and Tissues 6

Andre Kamkin
Ilya Lozinsky *Editors*

Mechanically Gated Channels and their Regulation

Springer

Mechanically Gated Channels and their Regulation

Mechanosensitivity in Cells and Tissues

Volume 6

Series Editors

A. Kamkin
Department of Fundamental and Applied Physiology, Russian State Medical University, Ostrovitjanova Str. 1, 117997 Moscow, Russia

I. Lozinsky
Department of Fundamental and Applied Physiology, Russian State Medical University, Ostrovitjanova Str.1, 117997 Moscow, Russia

First Editors of the Series

I. Kiseleva: 2008–2012

For further volumes:
http://www.springer.com/series/7878

Andre Kamkin • Ilya Lozinsky
Editors

Mechanically Gated Channels and their Regulation

Foreword by Maik Gollasch

Springer

Editors
Andre Kamkin
Department of Fundamental
and Applied Physiology
Russian State Medical University
Moscow
Russia

Ilya Lozinsky
Department of Fundamental
and Applied Physiology
Russian State Medical University
Moscow
Russia

Editorial Assistant
Natalia E. Lapina
Division of Neurosurgical Research
Medical Faculty Mannheim
Ruprecht Karls-University Heidelberg
Mannheim
Germany

ISBN 978-94-007-5072-2 ISBN 978-94-007-5073-9 (eBook)
DOI 10.1007/978-94-007-5073-9
Springer Dordrecht Heidelberg London New York

Library of Congress Control Number: 2012953484

Foreword

Research on mechanosensation and mechanotransduction is a challenge for all clinician-scientists, in part because of the complexities of the relevant basic science, and because it is crucial for maintaining life and is observed on many levels of the organism. In recent years, few fields have changed so dramatically as those in biology of mechanosensationa and mechanotransduction. The main areas of progress involve molecular identification of candidates within large and different families of ion channels, identification of their interacting molecules, validation by methods of molecular biology, cell biology and electrophysiology, and identification of biological and cellular systems *in vivo*. The application of these methods has made all steps of discoveries not only faster, but also more precise. It is common for medical students, staff at all levels of training, researchers in the field to feel some apprehension about tackling these challenges, and clear overviews in this field are highly valued.

Hence, it is mandatory for those of us involved in research and teaching of mechanobiology to keep pace with the continuous progress in this field, by receiving the experts' overview, as presented in this book.

In this context, the current book will fill a real need. Andre Kamkin and Ilya Lozinsky have drawn together an international expert team of expert scientist in mechanobiology and ion channels and tasked them to bring an overview in 15 chapters about recent discoveries in this emerging field of research.

I congratulate the editors and all contributors for their in-deep view into this in this rapidly growing field, for their consistent and disciplined use of an easy understanding format, and strongly recommend the book to all those who wish to deepen their understanding of the role of mechanobiology and ion channels in health and diseases, in the interest of better care for our patients.

Berlin, Germany

Maik Gollasch, MD PhD
Professor of Medicine
Charité University Medicine

Editorial

Mechanically Gated Channels

Andre Kamkin and Ilia Lozinsky

Cell reaction to mechanical stress is the oldest type of reaction from the point of view of evolution. Therefore response to mechanical stress is typical for all organisms, from bacteria to mammals. R. Kaufmann and U. Theophile (a.k.a. Ravens) in 1967 and M. J. Lab in 1968 were the first to suggest that mechanical changes in heart during contraction or other mechanical stress modulate its electric activity. In 1986 A. Kamkin and I. Kiseleva for the first time reported existence of mechanically induced potentials in cardiac fibroblasts (Kamkin et al. 1986, 1988; Kiseleva et al. 1987). Now it is known that mechanical stress of the cell triggers electrophysiological and biochemical responses in cells. Mechanical stress can influence physiological processes at the molecular, cellular, and systemic level. During last 30 years of investigation of cellular membrane responses to mechanical stress there was a major progress in both phenomenological description of the ongoing processes and investigation of the cellular response mechanisms to mechanical stress. It was shown than one of the mechanisms via which the cell responds to mechanical stress is mediated by ion channels reacting to membrane tension. Such channels were originally called mechanosensitive channels (MSCs: Guharay and Sachs 1984), and were redefined as mechanically gated channels (MGCs: Kirber et al. 1990) in the same manner as it was done with voltage and ligand gated channels. MGCs, reacting to the membrane tension, were shown to play the key role in one of the mechanisms, through which the cell responds to mechanical stimulus. Sachs and Morris (1998) noted that MGCs are channels that recognize mechanical deformation as a proper physiological signal and react to mechanical stimulation with changes in kinetics. MSCs, as a term, is now days usually used to describe channels that only modulate their permeability in response to mechanical stress (Morris et al. 2006; Moris and Juranka 2007; Morris and Laitko 2007). For example mechanosensitivity of Na_V channels (Moris and Juranka 2007), Ca_V channels (Calabrese et al. 2002), and K_V channels (Piao et al. 2006) has been convincingly shown. Definition of this term in such way allows further division of MSCs into two groups—mechanosensitive voltage-gated channels and mechanosensitive ligand-gated channels (Kamkin and Kiseleva 2008). MGCs convert the mechanical force, which is exerted on the cell membrane, into electrical signals. Cellular signaling in response to mechanical stress starts rapid induction of immediate-early genes, which acts as transcription factors, and triggers long-term changes in gene expression. However, the plasma membrane of the cell remains the primary target for mechanical stimulation. It responds to variable physical stress with changes of the open probability of MGCs. MGCs can

produce considerable currents in cells and therefore play an important role in forming their electric response. Both mechanosensitivity and mechanotransduction are fundamental physiological processes which are responsible for sensing of mechanical forces and their transformation into electrical or (and) biochemical signals.

Today many channels have been recognized as being MGCs, and include the prokaryotic MGSs of large, small, mini conductance and potassium dependent (MscL, MscS, MscM and MscK, respectively), the eukaryotic transient receptor potential (TRP) type cation channels (TRPC6, TRPV4, TRPY1), 2P-type potassium channels (TREK-1, TREK-2, TRAAK) and sodium channels from DEG/MEC/ENaC family (ENaC, MEC4/MEC10).

The structure and function of prokaryotic MGCs MscL and MscS have provided us with much of what we know today. Thus the first part of the volume is opened with an article devoted transmission of force from lipids. The manuscript employs a multidisciplinary approach to study of bacterial mechanosensitive ion channels (Cranfield et al. 2013). Authors stress that much of what we know about structure and function of these channels derives mostly from prokaryotic sources and from patch clamp electrophysiology techniques and X-ray crystallography. Then authors describe new investigation techniques such as electron paramagnetic resonance (EPR) spectroscopy, förster resonance energy transfer (FRET) imaging and nuclear magnetic resonance (NMR) spectroscopy. Authors discuss those methods along with possible data, which can be acquired by them, for better understanding of the molecular principles underlying mechanosensory transduction in living cells.

Now it seems important to discuss a number of topics, linked to the role of K_{2P} channels, which determine the basal level of leak K^+ ions and therefore influences resting potential, since a number of such channels is sensitive to mechanical stress. About 10 years ago, the identification of K_{2P} channels experimentally proved the existence of "leak channels", which were predicted to underlie the basal leakage of K^+ by Hodgkin and Huxley in 1952. Recently a new member of this family is identified. It consists of two 2TM/1P region-containing subunits, linked in tandem, and its functional channel is a dimer of the 4TM/2P subunits.

Several K_{2P} channels have been recently cloned. Three of them: $K_{2P}2.1$ (TREK-1), $K_{2P}10.1$ (TREK-2), $K_{2P}4.1$ (TRAAK) can be activated by mechanical stress. Previously it has been shown in the inside–out patch configuration that positive pressure is significantly less effective, compared with negative pressure, in opening of channels, suggesting that a specific membrane deformation (convex curving) preferentially opens these channels (Maingret et al. 1999; Patel et al. 1998). However it is quite likely that this line of argument has the same limitations, which we already discussed earlier. This was shown for the K_{2P} MGCs (Honoré et al. 2006).

At the whole-cell level, $K_{2P}2.1$ and $K_{2P}4.1$ are modulated by cellular volume. For example, hyperosmolarity closes the channels (Maingret et al. 2000a, b; Patel and Honoré 2001; Patel et al. 1998). Both the number of active channels and the sensitivity to mechanical stretch are strongly enhanced after treating the cell-attached patches with the cytoskeleton disrupting agents, colchicines and cytochalasin D (Maingret et al. 1999). This suggest that mechanical force might be transmitted directly to the channel via the lipid bilayer and does not require the integrity of the cytoskeleton

(Maingret et al. 1999; Patel et al. 1998, 2001). Both $K_{2P}2.1$ and $K_{2P}4.1$ are blocked by amiloride and Gd^{3+} (Maingret et al. 1999, 2000a, b).

In general the observation that channels, which are responsible for generation of K^+-leak current, can be activated by mechanical stress, suggests their direct contribution to regulation of cellular functions, one of which would be the maintenance of the resting membrane potential. Thus the second part of the volume is opened with an article devoted to mechanosensitive K2P channels, TREKking through the autonomic nervous system (Lamas 2013). TREK channels are leak potassium channels that are extensively expressed in the central, somatic peripheral and as recently demonstrated in the autonomic nervous system, where they are thought to play an important role in the modulation of neuronal excitability.

Two chapters are devoted to transient receptor potential vanilloid (TRPV1 and TRPV4) channels role in cell signaling. First of those two chapters demonstrates that the TRPV1 channel is a polymodal receptor that has been implicated in several physiological and pathological processes. TRPV1 channel can be directly activated by acidic pH, bioactive lipids, cysteine-modifying molecules, extracellular cations, voltage, elevated temperatures and several exogenous molecules such as capsaicin and toxins from animals. Its function can be modulated by the action of protein kinases, lipids, the cytoskeleton, second messengers and many proteins involved in signaling processes (Jara-Oseguera and Rosenbaum 2013).

The second review deals with the molecular mechanism of multifunctional MGC TRPV4. TRPV4 is functionally active in many tissues, including nerve, bone, lung, kidney and blood vessels. TRPV4 is a direct MGC, and cytoskeleton proteins such as actin, tubulin and integrin bind to the channel, helping it to respond to mechanical stimuli (Suzuki and Mizuno 2013).

Following Fifth Chapter discusses mechanical stretch and intermediate-conductance Ca^{2+}-activated K^+ channels (Hayabuchi et al. 2013). Authors describe the role and regulation of intermediate-conductance Ca^{2+} -activated K^+ (IKca) channels in cardiovascular pathophysiologies such as hypertension and restenosis. Cell membrane stretch activates IKca channels. The activation is associated with extracellular Ca^{2+} influx through stretch-activated nonselective cation channels, and is also modulated by the F-actin cytoskeleton and the activation of PKC. In this review authors discuss the physiological and pathophysiological role of IKca channel in cells.

Chapter 6 is devoted to sensing mechanism of stretch activated ion channels (Niisato and Marunaka 2013) and summarizes our current knowledge of MGCs. It demonstrates that physical force including osmotic pressure, hydrostatic pressure, gravity, shear stress and membrane tension is a crucial signal to control cellular functions such as proliferation, differentiation, development and cell death. Chapter includes the discussion of prokaryotic MGSs—MscL and MscS, the eukaryotic TRP channels (TRPV, TRPM, TRPC, TRPP), Degenerin/epithelial Na^+ channel (DEG/ENaC) superfamily—ASIC (acid-sensing ion channel), ENaC (epithelial Na^+ channel), MGCs in renal tubules.

Chapter 7 is devoted to ion channels in cardiac fibroblasts.Authors separately discuss MGCs and their regulation. Authors highlight that discussion of mechanisms of generation of mechanically induced potentials (MIPs) in cardiac fibroblasts is impossible without consideration of other membrane ion channels, which are present in those cells (Abramochkin et al. 2013). Cardiac fibroblasts generate delayed rectifier current (I_K), transient potassium current (I_{to}), inward rectifier potassium current (I_{Kir}), Ca^{2+}-activated K^+ current ($I_{K(Ca)}$), TTX-sensitive sodium voltage-gated current ($I_{Na.TTX}$), TTX-sensitive sodium voltage-gated current ($I_{Na.TTXR}$), volume-sensitive chloride current ($I_{Cl.vol}$), voltage gated proton current (I_{Hv}), non-selective cation currents, besides mechanosensitive MG currents. Manuscript describes single mechanically gated channels (MGCs), recorded simultaneously with whole cell MG currents. All of those currents, which are mentioned above, together with MG currents contribute to alterations of fibroblast membrane potential (resting potentials and MIPs).

Following Chap. 8 discusses the role of nitric oxide in the regulation of ion channels in the cardiomyocytes. It describes regulation of MGCs conduction via NO. This manuscript shows that in description of the cardiac function under normal or pathological conditions separate consideration of nitric oxide effects on mechanically gated channels aside from consideration of its simultaneous effect on voltage gated channels of cardiac cell would be misleading (Makarenko et al. 2013). Chapter focuses on discussion of the modulatory effect of nitric oxide on voltage gated Na^+-, Ca^{2+}-, K^+-channels, which are the major contributors to generation of cardiac action potential and alterations of its shape under normal or pathological conditions. It also describes the effect of nitric oxide on leak channels (two-pore potassium channels), some of which are known to be mechabosensitive. It is concluded with discussion of nitric oxide effects on mechanically gated ion channels and mechanically gated currents.

Chapter 9 describes the role of ion channels in cellular mechanotransduction of hydrostatic pressure. Studies reviewed herein suggest that multiple mammalian cell types are sensitive to pure hydrostatic pressure within normal physiological ranges, and the signals may be mediated by activities of membrane-bound ion channels and transporters (Champaigne and Nagatomi 2013). The lack of success thus far in identifying a single hydrostatic pressure-sensitive protein structure or complex, such as an ion channel, implies that the mechanosensation process of hydrostatic pressure is likely to be a multifaceted process that exploits an unconventional sensing mechanism.

Chapter 10 discusses lipid-mediated mechanisms involved in the mechanical activation of TRPC6 and TRPV4 channels in the vascular tone regulation (Inoue et al. 2013). In this review, authors focus on the lipid-mediated regulation of two TRP channels abundantly expressed in the cardiovascular system, i.e. TRPC6 and TRPV4, with particular interest in the synergistic interaction between receptor-mediated and mechanical stimulations, and discuss their complex functional antagonism in vascular tone and blood pressure regulation.

Following chapter is devoted to stretch effects on atrial conduction (Masè and Ravelli 2013). In this chapter authors discuss the experimental and clinical evidence

which supports the role of stretch-induced conduction disturbances in the creation of an arrhythmic substrate. After an introduction concerning the methodological challenges and technical advancements involved in the investigation, the effects of acute stretch on macroscopic conduction properties are described along with the potential microscopic determinants of the observed changes. The mechanisms through which stretch-induced conduction changes may contribute to the generation, maintenance and stabilization of arrhythmic conditions are pointed out, complementing the effects on conduction produced by acute stretch with the even more deleterious changes induced by chronic dilatation.

Then the reader will find the discussion of early activation of intracellular signals after myocardial stretch (Cingolani et al. 2013). Authors present the updated experimental evidence that led them to propose the autocrine/paracrine mechanism underlying the Anrep effect, as well as its resemblance to signals that have been described for cardiac hypertrophy development and heart failure. Interesting novel data supporting a crucial role for stretch-induced mineralocorticoid receptor activation, EGFR transactivation and increased mitochondrial production of reactive oxygen species leading to NHE-1 stimulation is thoroughly described. A clear understanding of the early triggering mechanisms that stretch imposes to the myocardium allows to design novel weapons to win the battle against cardiac hypertrophy and failure, a major disease spread worldwide.

The following chapter describes recent findings regarding effects of angiotensin II action in the heart (De Mello 2013). The influence of angiotensin II (Ang II) on cardiac structural and electrophysiological remodeling is reviewed including the novel concept that the renin angiotensin aldosterone and the mineralocorticoid receptors are involved in the regulation heart cell volume. The role of Ang II AT1 receptors as mechanosensors which are activated by mechanic stretch independently of Ang II, is discussed. The effect of Ang II and renin on cell volume and the consequent activation of ionic channels is reviewed as well as its implications to cardiac arrhythmias (De Mello 2013).

After that the Volume includes the description of mechanosensitivity of pancreatic β-cells, adipocytes, and skeletal muscle cells (Nakayama et al. 2013). Pancreatic β-cells, adipocytes, and skeletal muscle cells, all of which are related to the core concerns in metabolic syndrome causing cardiovascular diseases, are also responsive to mechanical stimuli, such as osmotic change and stretching, and show a variety of functions, including insulin release from β-cells, depression of adipocyte differentiation, and translocation of glucose transporter 4 (GLUT4) in skeletal muscle cells. Furthermore, the fish-oil-derived ω-3 polyunsaturated fatty acid such as eicosapentaenoic acid (EPA) combined with cyclic stretching significantly reduces the adipocyte differentiation. The present article provides with a unitary discussion of three peripheral organs from the viewpoint of mechanosensitivity, which aids in recognizing the importance of biomechanical factors in physiological and pathological conditions, and may potentially have therapeutic consequences.

The final chapte of the Volume is devoted to the role of the primary cilium in chondrocyte response to mechanical loading (Wann et al. 2013). Articular cartilage, like many other living tissues, experiences a complex physiological mechanical loading

environment which regulates cell function and tissue homeostasis through a process of mechanotransduction. This chapter explores the rapidly evolving area of primary cilia and their response to mechanical forces with a particular focus on articular cartilage for which mechanical loading is critical for homeostasis and functionality. Understanding the role of the primary cilium in mechanobiology will aid the development of novel therapeutic strategies for pathologies, such as osteoarthritis, that involve disruption of primary cilia function.

Thus, the volume dwells on the major issues of mechanical stress influencing the ion channels and intracellular signaling pathways. This book is a unique collection of reviews outlining current knowledge and future developments in this rapidly growing field. In our opinion the book presents not only the latest achievements in the field but also brings the problem closer to the experts in related medical and biological sciences as well as practicing doctors. Knowledge of the mechanisms which underlie these processes is necessary for understanding of the normal functioning of different living organs and tissues and allows to predict changes, which arise due to alterations of their environment, and possibly will allow to develop new methods of artificial intervention. We also hope that presenting the problem will attract more attention to it both from researchers and practitioners and will assist to efficiently introduce it into the practical medicine.

References

Abramochkin DV, Lozinsky I, Kamkin A (2013) Ion channels in cardiac fibroblasts: Link to mechanically gated channels and their regulation. In: Kamkin A, Lozinsky I (eds) Mechanosensitivity in cells and tissues 6. Mechanically gated channels and their regulation. Springer, Berlin

Calabrese B, Tabarean IV, Juranka P, Morris CE (2002) Mechanosensitivity of N-type calcium channel currents. Biophys J 83(5):2560–2574

Champaigne KD, Nagatomi J (2013) The role of ion channels in cellular mechanotransduction of hydrostatic pressure. In: Kamkin A, Lozinsky I (eds) Mechanosensitivity in cells and tissues 6. Mechanically gated channels and their regulation. Springer, Berlin

Cingolani HE, Villa-Abrille MC, Caldiz CI, Ennis IL, Cingolani OH, Morgan PE, Aiello EA, Pérez NG (2013) Early activation of intracellular signals after myocardial stretch: Anrep effect, myocardial hypertrophy and heart failure. In: Kamkin A, Lozinsky I (eds) Mechanosensitivity in cells and tissues 6. Mechanically gated channels and their regulation. Springer, Berlin

Cranfield CG, Kloda A, Nomura T, Petrov E, Battle A, Constantine M, Martinac B (2013) Force from lipids: a multidisciplinary approach to study bacterial mechanosensitive ion channels. In: Kamkin A, Lozinsky I (eds) Mechanosensitivity in cells and tissues 6. Mechanically gated channels and their regulation. Springer, Berlin, pp 1–33

De Mello WC (2013) Recent aspects of angiotensin II action in the heart. Implications for myocardial ischemia and heart failure. In: Kamkin A, Lozinsky I (eds) Mechanosensitivity in cells and tissues 6. Mechanically gated channels and their regulation. Springer, Berlin, pp 367–378

Guharay F, Sachs F (1984) Stretch-activated single ion channel currents in tissue cultured embryonic chick skeletal muscle. J Physiol (Lond) 352:685–701

Hayabuchi Y, Sakata M, Ohnishi T, Kagami S (2013) Mechanical stretch and intermediate-conductance Ca^{2+}-activated K^+ channels in arterial smooth muscle cells. In: Kamkin A, Lozinsky I (eds) Mechanosensitivity in cells and tissues 6. Mechanically gated channels and their regulation. Springer, Berlin, pp 159–187

Honoré E, Patel AJ, Chemin J, Suchyna T, Sachs F (2006) Desensitization of mechano-gated K2P channels. Proc Natl Acad Sci USA 103(18):6859–6864

Inoue R, Hu Y, Duan Y, Itsuki K (2013) Lipid-mediated mechanisms involved in the mechanical activation of TRPC6 and TRPV4 channels in the vascular tone regulation. In: Kamkin A, Lozinsky I (eds) Mechanosensitivity in cells and tissues 6. Mechanically gated channels and their regulation. Springer, Berlin, pp 281–301

Jara-Oseguera A, Rosenbaum T (2013) TRPV1 in cell signaling: molecular mechanisms of function and modulation. In: Kamkin A, Lozinsky I (eds) Mechanosensitivity in cells and tissues 6. Mechanically gated channels and their regulation. Springer, Berlin, pp 69–102

Kamkin A, Kircheis R, Kiseleva I (1986) New type of cell in the frog atria? In: Challenges in prevention, diagnostics and treatment of cardio-vascular diseases. Springer, Moscow. p. 11

Kamkin A, Kiseleva I (2008) Mechanically gated channels and mechanosensitive channels. In: Kamkin A, Kiseleva I (eds) Mechanosensitivity in cells and tissues. mechanosensitive ion channels. Springer, Berlin, pp xiii–xviii

Kamkin A, Kiseleva I, Kircheis R, Kositzky G (1988) Bioelectric activity of frog atrium cells with non-typical impulse acvity. Abhandlungen der Akademie der Wissenschaften der DDR (Abteilung Mathematik – Naturwissenschaft – Technik) 1:103–106

Kaufmann R, Theophile U (1967) Autonomously promoted extension effect in Purkinje fibers, papillary muscles and trabeculae carneae of rhesus monkeys. Pflugers Arch Gesamte Physiol Menschen Tiere 297(3):174–189

Kirber MT, Ordway RW, Clapp LH, Sims SM, Walsh JV Jr, Singer JJ (1990) Voltage, ligand, and mechanically gated channels in freshly dissociated single smooth muscle cells. Prog Clin Biol Res 334:123–143

Kiseleva IS, Kamkin AG, Kircheis R, Kositski GI (1987) Intercellular electrotonical interaction in the cardiac sinus node in the frog. Reports of Academy of Science of USSR 292(6):1502–1505

Lab MJ (1968) Is there mechano-electric transduction in cardiac muscle? The monophasic action potential of the frog ventricle during isometric and isotonic contraction with calcium deficient perfusions. S Afr J Med Sci 33:60

Lamas JA (2013) Mechanosensitive K_2P channels, TREKking through the autonomic nervous system. In: Kamkin A, Lozinsky I (eds) Mechanosensitivity in Cells and Tissues 6. Mechanically gated channels and their regulation. Springer, Berlin, pp 35–68

Maingret F, Fosset M, Lesage F, Lazdunski M, Honore E (1999) TRAAK is a mammalian neuronal mechano-gated K^+ channel. J Biol Chem 274:1381–1387

Maingret F, Lauritzen I, Patel AJ, Heurteaux C, Reyes R, Lesage F, Lazdunski M, Honore E (2000a) TREK-1–1 is a heat-activated background K^+ channel. EMBO J 19:2483–2491

Maingret F, Patel AJ, Lesage F, Lazdunski M, Honoré E (2000b) Lysophospholipids open the two P domain mechano-gated K^+ channels TREK-1 and TRAAK. J Biol Chem 275:10128–10133

Makarenko EYu, Lozinsky I, Kamkin A (2013) The role of nitric oxide in the regulation of ion channels in the cardiomyocytes: Link to mechanically gated channels. In: Kamkin A, Lozinsky I (eds) Mechanosensitivity in cells and tissues 6. Mechanically gated channels and their regulation. Springer, pp 245–262

Masè M, Ravelli F (2013) Stretch effects on atrial conduction: a potential contributor to arrhythmogenesis. In: Kamkin A, Lozinsky I (eds) Mechanosensitivity in cells and tissues 6. Mechanically gated channels and their regulation. Springer, Berlin, pp 303–325

Moris CE, Juranka PF (2007) Na_V channel mechanosensitivity: activation and inactivation accelerate reversibly with stretch. Biophys J 93(3):822–833

Morris CE, Laitko U (2007) The mechanosensitivity of voltage-gated channels may contribute to cardiac mechano-electric feedback. In: Kohl P, Franz MR, Sachs F (eds) Cardiac mechano-electrical feedback and arrhythmias: from pipette to patient. Saunders, Philadelphia, pp 33–41

Morris CE, Juranka PF, Lin W, Morris TJ, Laitko U (2006) Studying the mechanosensitivity of voltage-gated channels using oocyte patches. Methods Mol Biol 322:315–329

Nakayama K, Tanabe Y, Obara K, Ishikawa T (2013) Mechanosensitivity of pancreatic β-cells, adipocytes, and skeletal muscle cells: the therapeutic targets of metabolic syndrome. In: Kamkin A, Lozinsky I (eds) Mechanosensitivity in cells and tissues 6. Mechanically gated channels and their regulation. Springer, Berlin, pp 379–403

Niisato N, Marunaka Y (2013) Sensing mechanism of stretch activated ion channels. In: Kamkin A,Lozinsky I (eds) Mechanosensitivity in cells and tissues 6. Mechanically gated channels and their regulation. Springer, Berlin, pp 189–213

Patel AJ, Honoré E (2001) Properties and modulation of mammalian 2P domain K^+ channels. TRENDS Neurosci 24(6):339–345

Patel AJ, Honoré E, Maingret F, Lesage F, Fink M, Duprat F, Lazdunski M (1998) A mammalian two pore domain mechano-gated s-like K^+ channel. EMBO J 17:4283–4290

Piao L, Li HY, Park CK, Cho IH, Piao ZG, Jung SJ, Choi SY, Lee SJ, Park K, Kim JS, Oh SB (2006) Mechanosensitivity of voltage-gated K^+ currents in rat trigeminal ganglion neurons. J Neurosci Res 83(7):1373–1380

Sachs F, Morris CE (1998) Mechanosensitive ion channels in nonspecialized cells. Rev Physiol Biochem Pharmacol 132:1–77

Suzuki M, Mizuno A (2013) The Molecular Mechanism of Multifunctional Mechano-Gated Channel TRPV4. In: Kamkin A, Lozinsky I (eds) Mechanosensitivity in cells and tissues 6. Mechanically gated channels and their regulation. Springer, Berlin, pp 103–157

Wann AKT, Thompson CL, Knight MM (2013) The role of the primary cilium in chondrocyte response to mechanical loading. In: Kamkin A, Lozinsky I (eds) Mechanosensitivity in cells and tissues 6. Mechanically gated channels and their regulation. Springer, Berlin, pp 405–426

Contents

Contributors

Denis V. Abramochkin Department of Fundamental and Applied Physiology, Laboratory of Electrophysiology, Russian State Medical University, Ostrovitjanova 1, Moscow 117997, Russia

Ernesto A. Aiello Centro de Investigaciones Cardiovasculares, Facultad de Ciencias Médicas, Universidad Nacional de La Plata, Calle 60 y 120, 1900 La Plata, Argentina

Andrew Battle School of Pharmacy, Griffith University, Gold Coast Campus, QLD 4022, Australia

Claudia I. Caldiz Centro de Investigaciones Cardiovasculares, Facultad de Ciencias Médicas, Universidad Nacional de La Plata, Calle 60 y 120, 1900 La Plata, Argentina

Kevin D. Champaigne Department of Bioengineering, Clemson University, 315 Rhodes Hall, Clemson, SC 29634-0905, USA

Horacio E. Cingolani Centro de Investigaciones Cardiovasculares, Facultad de Ciencias Médicas, Universidad Nacional de La Plata, Calle 60 y 120, 1900 La Plata, Argentina
e-mail: cicmes@infovia.com.ar

Oscar H. Cingolani Division of Cardiology, Johns Hopkins University Hospital, 720 Rutland Avenue, Ross 835, Baltimore, MD 21205, USA

Maryrose Constantine Mechanosensory Biophysics Laboratory, Molecular Cardiology and Biophysics Division, Victor Chang Cardiac Research Institute, 405 Liverpool St, Darlinghurst, NSW 2010, Australia

Charles G. Cranfield Mechanosensory Biophysics Laboratory, Molecular Cardiology and Biophysics Division, Victor Chang Cardiac Research Institute, 405 Liverpool St, Darlinghurst, NSW 2010, Australia
e-mail: c.cranfield@victorchang.edu.au

Walmor C. De Mello Department of Pharmacology, School of Medicine, Medical Sciences Campus, UPR, San Juan, PR 00936-5067, USA
e-mail: walmor.de-mello@upr.edu

Yubin Duan Department of Physiology, Graduate School of Medical Sciences, Fukuoka University, Fukuoka 814-0180, Japan

Irene L. Ennis Centro de Investigaciones Cardiovasculares, Facultad de Ciencias Médicas, Universidad Nacional de La Plata, Calle 60 y 120, 1900 La Plata, Argentina

Yasunobu Hayabuchi Department of Pediatrics, University of Tokushima, Kuramoto-cho-3-18-15, Tokushima 770-8503, Japan
e-mail: hayabuchi@clin.med.tokushima-u.ac.jp

Yaopeng Hu Department of Physiology, Graduate School of Medical Sciences, Fukuoka University, Fukuoka 814-0180, Japan

Ryuji Inoue Department of Physiology, Graduate School of Medical Sciences, Fukuoka University, Fukuoka 814-0180, Japan
e-mail: inouery@fukuoka-u.ac.jp

Tomohisa Ishikawa Department of Pharmacology, School of Pharmaceutical Sciences, University of Shizuoka, 52-1 Yada, Suruga-ku, Shizuoka City, Shizuoka 422-8526, Japan

Kyohei Itsuki Department of Physiology, Graduate School of Medical Sciences, Fukuoka University, Fukuoka 814-0180, Japan

Andrés Jara-Oseguera Departamento de Fisiología, Facultad de Medicina, Universidad Nacional Autónoma de México, D.F., México

Shoji Kagami Department of Pediatrics, University of Tokushima, Kuramoto-cho-3-18-15, Tokushima 770-8503, Japan

Andre Kamkin Department of Fundamental and Applied Physiology, Laboratory of Electrophysiology, Russian State Medical University, Ostrovitjanova 1, Moscow 117997, Russia
e-mail: Kamkin.A@g23.relcom.ru

Anna Kloda School of Biomedical Sciences, The University of Queensland, St Lucia, QLD 4072, Australia

Martin M. Knight Institute of Bioengineering, School of Engineering and Materials Science, Queen Mary University of London, Mile End Rd, E1 4NS, London, UK

J. Antonio Lamas Laboratory of Neuroscience, CINBIO, Department of Functional Biology, University of Vigo, 36310 Vigo, Spain
e-mail: antoniolamas@uvigo.es

Ilya Lozinsky Department of Fundamental and Applied Physiology, Laboratory of Electrophysiology, Russian State Medical University, Ostrovitjanova 1, Moscow 117997, Russia

Ekaterina Yu. Makarenko Department of Fundamental and Applied Physiology, Laboratory of Electrophysiology, Russian State Medical University, Ostrovitjanova 1, Moscow 117997, Russia

Boris Martinac Mechanosensory Biophysics Laboratory, Molecular Cardiology and Biophysics Division, Victor Chang Cardiac Research Institute, 405 Liverpool St, Darlinghurst, NSW 2010, Australia

Yoshinori Marunaka Department of Molecular Cell Physiology, Graduate School of Medical Sciences, Kyoto Prefectural University of Medicine, Kyoto 602-8566, Japan

Michela Masè Laboratory of Biophysics and Biosignals and BIOTech, Department of Physics, Faculty of Science, University of Trento, Via Sommarive 14, 38123, Povo-Trento, Italy
e-mail: mase@science.unitn.it

Astuko Mizuno Department of Molecular Pharmacology, Jichi Medical university, Yakushiji 3311-1, Tochigi, Japan

Patricio E. Morgan Centro de Investigaciones Cardiovasculares, Facultad de Ciencias Médicas, Universidad Nacional de La Plata, Calle 60 y 120, 1900 La Plata, Argentina

Jiro Nagatomi Department of Bioengineering, Clemson University, 315 Rhodes Hall, Clemson, SC 29634-0905, USA
e-mail: jnagato@clemson.edu

Koichi Nakayama Department of Molecular and Cellular Pharmacology, Faculty of Pharmaceutical Sciences, Iwate Medical University, Yahaba, Iwate 028-3694, Japan
e-mail: nakyamk@iwate-med.ac.jp

Naomi Niisato Department of Molecular Cell Physiology, Graduate School of Medical Sciences, Kyoto Prefectural University of Medicine, Kyoto 602-8566, Japan
e-mail: naomi@koto.kpu-m.ac.jp

Takeshi Nomura Mechanosensory Biophysics Laboratory, Molecular Cardiology and Biophysics Division, Victor Chang Cardiac Research Institute, 405 Liverpool St, Darlinghurst, NSW 2010, Australia

Kazuo Obara Department of Pharmacology, School of Pharmaceutical Sciences, University of Shizuoka, 52-1 Yada, Suruga-ku, Shizuoka City, Shizuoka 422-8526, Japan

Tatsuya Ohnishi Department of Pediatrics, University of Tokushima, Kuramoto-cho-3-18-15, Tokushima 770-8503, Japan

Néstor Gustavo Pérez Centro de Investigaciones Cardiovasculares, Facultad de Ciencias Médicas, Universidad Nacional de La Plata, Calle 60 y 120, 1900 La Plata, Argentina

Evgeny Petrov Mechanosensory Biophysics Laboratory, Molecular Cardiology and Biophysics Division, Victor Chang Cardiac Research Institute, 405 Liverpool St, Darlinghurst, NSW 2010, Australia

Flavia Ravelli Laboratory of Biophysics and Biosignals and BIOTech, Department of Physics, Faculty of Science, University of Trento, Via Sommarive 14, 38123, Povo-Trento, Italy
e-mail: ravelli@science.unitn.it

Tamara Rosenbaum Departamento de Neurodesarrollo y Fisiología, División Neurociencias, Instituto de Fisiología Celular, Universidad Nacional Autónoma de México, México, D. F., México
e-mail: trosenba@ifc.unam.mx

Miho Sakata Department of Pediatrics, University of Tokushima, Kuramoto-cho-3-18-15, Tokushima 770-8503, Japan

Makoto Suzuki Edogawabashi clinic, 348 Yamabuki, Shinjyuku, Tokyo, Japan
e-mail: msuzuki@edogawabashi-clinic.com

Yoshiyuki Tanabe Department of Molecular and Cellular Pharmacology, Faculty of Pharmaceutical Sciences, Iwate Medical University, Yahaba, Iwate 028-3694, Japan

Clare Thompson Institute of Bioengineering, School of Engineering and Materials Science, Queen Mary University of London, Mile End Rd, E1 4NS, London, UK

María C. Villa-Abrille Centro de Investigaciones Cardiovasculares, Facultad de Ciencias Médicas, Universidad Nacional de La Plata, Calle 60 y 120, 1900 La Plata, Argentina

Angus K. T. Wann Institute of Bioengineering, School of Engineering and Materials Science, Queen Mary University of London, Mile End Rd, E1 4NS, London, UK
e-mail: m.m.knight@qmul.ac.uk

Chapter 1
Force from Lipids: A Multidisciplinary Approach to Study Bacterial Mechanosensitive Ion Channels

Charles G. Cranfield, Anna Kloda, Takeshi Nomura, Evgeny Petrov, Andrew Battle, Maryrose Constantine and Boris Martinac

1.1 Introduction

The first mechanosensitive (MS) channels were reported in embryonic chick skeletal muscle (Guharay and Sachs 1984) and frog muscle (Brehm et al. 1984). Over the last twenty five years this type of ion channels have been identified in a variety of living cells from all evolutionary provenances including bacteria, achaea, yeasts, green algae, plants, animals and humans. Today many channels have been recognized as being *MS* or *stretch activated (SA)*, and include the prokaryotic MS channels of large, small, mini and potassium dependent conductance (MscL, MscS, MscM and MscK respectively), the eukaryotic transient receptor potential (TRP) type cation channels (TRPC6, TRPV4, TRPY1), 2P-type potassium channels (TREK-1, TREK-2, TRAAK) and sodium channels from the DEG/MEC/ENaC family (ENaC, MEC4/MEC10) to name but a few (Hamill and Martinac 2001; Martinac 2004; Chalfie 2009). The structure and function of prokaryotic MS channels MscL and MscS have provided us with much of what we know today as to how MS channels function and are regulated (Fig. 1.1) (Martinac 2007).

In bacteria, these channels serve to protect the cells from hypo-osmotic shock. In conditions of hypotonicity a bacterial cell will typically expand or swell. This swelling is a result of *turgor* pressure, which causes the cell membrane to stretch, and it is known that this stretching of the cell membrane is the main factor responsible for the opening of these MS channels. Opening of MS channels releases ions and other small osmolytes from within the cytoplasm of the bacteria so that turgor pressure will be reduced, and the bacteria can continue to function in their new hypotonic

C. G. Cranfield (✉) · T. Nomura · E. Petrov · M. Constantine · B. Martinac
Mechanosensory Biophysics Laboratory, Molecular Cardiology and Biophysics Division, Victor Chang Cardiac Research Institute, 405 Liverpool St, Darlinghurst, NSW 2010, Australia
e-mail: c.cranfield@victorchang.edu.au

A. Kloda
School of Biomedical Sciences, The University of Queensland, St Lucia, QLD 4072, Australia

A. Battle
School of Pharmacy, Griffith University, Gold Coast Campus, QLD 4022, Australia

A. Kamkin, I. Lozinsky (eds.), *Mechanically Gated Channels and their Regulation,* Mechanosensitivity in Cells and Tissues 6,
DOI 10.1007/978-94-007-5073-9_1,

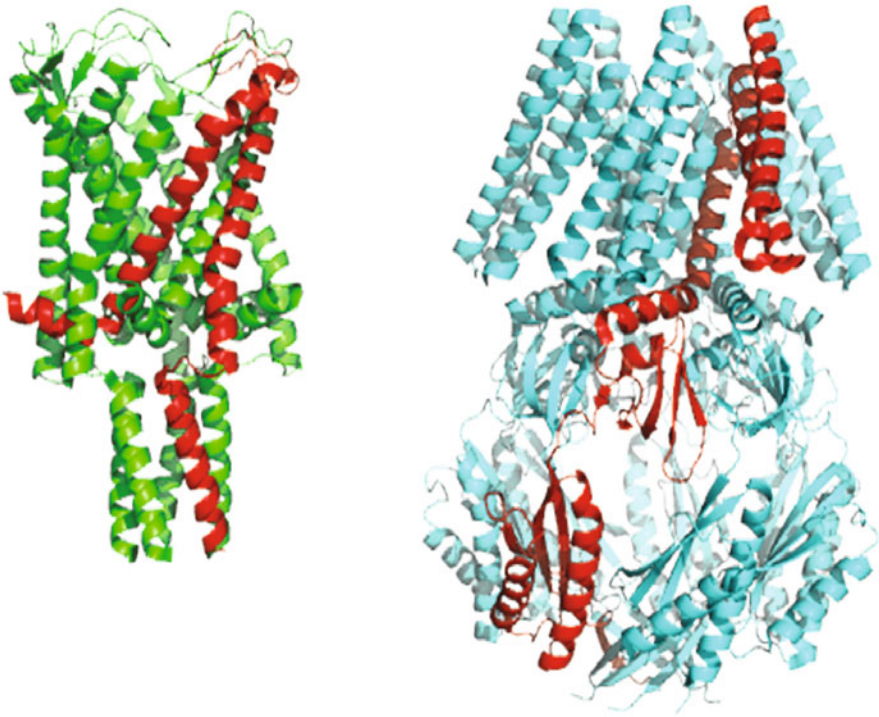

Fig. 1.1 Crystal structures of the homo-pentamer MscL (*left*) and the homo-heptamer MscS (*right*). An individual subunit of each protein is contrasted

environment. There is much evidence, however, that turgor pressure and stretch activation alone are not the only factors that determine whether bacterial MS channels open. Recently it has become clear that acyl chain length, the presence of amphipaths, and even the curvature of the membrane itself, can all play a part in determining whether these MS channel open or close (Martinac 2007; Yoshimura and Sokabe 2010). Here we outline the various methods that have been employed to identify the structure, function and lipid interaction of these unique types of channels.

1.1.1 Some Background on the Mechanics of MS Channel Activation by Membrane Tension

MscL and MscS channels are often misleadingly referred to as pressure sensitive channels. This is somewhat misleading as it is not pressure but membrane tension or strain that is the key stimulus in activating (or inactivating) MS channels (Gustin et al. 1988; Sachs 2010). If we assume the membrane has an elasticity associated with it, we can look to use Hook's law to calculate this tension:

$$T = K\Delta x/x_0 \tag{1.1}$$

Here K is the spring constant (S.I. units N/m), Δx is the difference in diameter between the open and closed states of the channel, and x_0 is diameter of the closed channel (Morris 1990). However this is a simplistic model that assumes the channel is being pulled from just 2 sides. In reality the multi-oligomeric forms of the MscS and MscL channels reside in an elastic membrane plane, and so instead of x we need to use an area term, A, which for a perfectly cylindrical channel would simply be πr^2, to give:

$$T = K\frac{\Delta A}{A_0} \tag{1.2}$$

where ΔA is the increase in the channel surface area under strain, A_0 is the membrane area occupied by the closed channel under zero strain and K is the membrane elasticity constant (Guharay and Sachs 1984). In a patch pipette however, when pressure is applied, the membrane tension is a function of both the applied pressure and the radius of curvature of the membrane patch according to the simple formula that follows Laplace's law:

$$T = P\frac{r}{2} \tag{1.3}$$

where T is membrane tension, P is pressure, and r is the radius of the membrane curvature (Sokabe et al. 1991; Sachs 2010). Armed with this equation it then becomes a relatively simple task to measure the tension required to open MS channels such as MscL and MscS so long as the patch membrane radius can be accurately determined in the patch pipette in situ (Sokabe and Sachs 1990; Sokabe et al. 1991; Sukharev et al. 1999).

Various lipid compositions and the presence of various amphipaths, are factors that will all have an impact on the elasticity (K) of the lipid bilayer, which will in turn have an effect on the pressure/tension thresholds of opening bacterial MS channels (Perozo et al. 2002b; Moe and Blount 2005; Nomura et al. 2011). What is also becoming clear is that there may be other factors that also influence channel opening that are not directly coupled to the membrane tension, such as membrane localized curvature (Cui et al. 1995; Meyer et al. 2006; Yoo and Cui 2009).

1.2 What Patch-Clamp Recordings of Bacterial Mechanosensitive Channels Tell us of Lipid-Channel Interactions

1.2.1 Why are Spheroplasts Suitable for Researching MS Channels from Bacteria?

The cell of *E. coli*, a rod-shaped Gram-negative bacterium, is only about 1 μm wide and 2 μm long which is almost the same as a diameter of the tip of the patch pipette. Hence a larger bacterial body (with cell wall excluded) is essential for patching the

cytoplasmic (inner) membrane. This can be achieved by preparing giant spheroplasts from bacterial cells (Ruthe and Adler 1985; Martinac et al. 1987; Blount et al. 1996). The preparation of giant spheroplasts presented a major technical advancement allowing for the electrophysiological investigation of *E. coli* cell membranes, and thus ultimately leading to discovery of bacterial MS channels. The term *spheroplast* is used to signify the double membrane of Gram-negative *E. coli* rather than *protoplasts* formed from eukaryotic cells or Gram-positive bacteria. To make giant spheroplasts, *E. coli* cells are treated with antibiotic *cephalexin* to form long filaments (‘*snakes*’). The cell wall of the snakes is then disrupted by *lysozyme* and *EDTA* to enable the formation of giant spheroplasts. The following is a brief description of the method used for electrical recording from giant spheroplasts (for details of the giant spheroplast preparation method see (Martinac et al. 1987; Blount et al. 1999).

1.2.2 Patch-Clamp Recording from Giant E. Coli Spheroplasts

Most recordings of giant spheroplasts are performed using the inside-out patch configuration, although recording from whole-protoplasts has also been reported (Cui et al. 1995). The pipette solution typically consists of 200 mM KCl, 40 mM $MgCl_2$ and 5 mM HEPES (adjusted to pH 7.2 with KOH), whereas the bath solution contains 250 mM KCl, 90 mM $MgCl_2$ and 5 mM HEPES (adjusted to pH 7.2 with KOH). Negative pressure can be applied through the patch pipette to the membrane patch via a syringe or high-speed pressure clamp apparatus (such as an HSPC-1 (ALA Scientific Instruments Inc., Farmingdale, NY)) and concurrently measured using a pressure gauge.

1.2.3 What Results have been Obtained from Mutagenesis Study using Spheroplasts?

The patch-clamp technique made it possible to record the currents and activity of single MS channels in situ from native bacterial membranes (Martinac et al. 1987). MscL and MscS, the MS channels from *E. coli,* are the best studied and characterized MS channels to date (Fig. 1.1). MscL (*MS c*hannel of *l*arge conductance) consists of five 15 kDa subunits, 136 amino acids per subunit (Sukharev 1994a, b). It has a conductance of ~3 nS and does not have any selectivity for ions (Sukharev et al. 1993). On the other hand, *E. coli* MscS (*MS c*hannel of *s*mall conductance) consists of seven ~30 kDa subunits, 286 amino acids per subunit (Levina et al. 1999). The conductance of MscS is ~1 nS (Martinac et al. 1987; Sukharev 2002) and has a weak preference for anions (Martinac et al. 1987; Sukharev 2002; Sotomayor et al. 2006). A crystal structure of MscL homologue from *Mycobacterium tuberculosis* (Tb-MscL) (Chang et al. 1998) and *E. coli* MscS (Bass et al. 2002) has been resolved by X-ray crystallography at a resolution of 3.5 and 3.9 Å, respectively. MscL monomer consists of two helical transmembrane (TM) domains, TM1 and TM2, cytoplasmic N- and C-terminal domains and a periplasmic loop domain that is connecting TM1

and TM2 domains (Chang et al. 1998), whereas MscS monomer consists of three TM domains, (TM1, TM2 and TM3) and has a large cytoplacmic domain (Bass et al. 2002). Here, we address the recent findings on the structure and gating mechanism of MscL and MscS channels obtained from patch-clamp recordings from giant *E. coli* spheroplasts expressing mutant channels of both channel proteins.

MscL and MscS are activated directly by lateral tension in the membrane lipid (Sukharev et al. 1993; Häse et al. 1995; Sukharev 2002). To understand the entire gating mechanism, we need to clarify the relationship between tension sensor and gate, which are functional units of gating mechanism. Random (Ou et al. 1998) and a comprehensive site-directed mutagenesis (Yoshimura et al. 1999) studies indicate that the hydrophobic residues that are located at the cytoplasmic half of TM1 form constriction in the channel pore dubbed the "*hydrophobic lock*". Substitution of G22 for hydrophilic residues caused poor cell growth in the presence of IPTG and exhibited spontaneous channel activity in patch-clamp experiments (Yoshimura et al. 1999). In addition, cysteine (Levin and Blount 2004) and histidine (Iscla et al. 2004) scanning mutagenesis experiments suggested that G26 also was a part of the hydrophobic gate.

A number of loss-of-function (LOF) mutants of MscL were found in the TM1 and TM2 domains as well as in the periplasmic loop by random mutagenesis (Maurer and Dougherty 2003; Yoshimura et al. 2004). Furthermore, asparagine-scanning mutagenesis identified seven LOF mutants that are located at the periplamic end of TM1 and TM2 domains and lining the periplasmic rim (Yoshimura et al. 2004). These results suggest that lipid-protein interactions are critical for MscL gating. A similar MscS study also indicated that interaction between the membrane lipids and both ends of the TM α-helices were important for the MscS sensitivity to membrane tension (Nomura et al. 2006).

One of the main structural differences between MscS and MscL is that MscS has a large (∼17 kDa) cytoplasmic domain (Bass et al. 2002). It has been proposed that the cytoplasmic domain would cause a dynamic conformational change during the gating transition from the closed to the open state (Koprowski and Kubalski 2003; Miller et al. 2003a, b; Grajkowski et al. 2005; Nomura et al. 2008; Machiyama et al. 2009; Gamini et al. 2011). In the closed state, two hydrophobic rings, L105 and L109 of TM3a form the constriction pore (Anishkin and Sukharev 2004) and G121 and G113 of TM3b which are related to desensitization and inactivation, respectively (Akitake et al. 2007; Edwards et al. 2008). During the gating transition, TM3a helices become tilted and rotated and D62 which is located in the loop that connects TM1 and TM2 makes a salt bridge with R128 or R131 to stabilize the open state (Sotomayor and Schulten 2004; Nomura et al. 2008).

1.3 Reconstitution of MS Channels into Liposomes

Liposome reconstitution was essential for molecular identification of the MscL protein, which enabled cloning of the corresponding *mscL* gene as the first MS channel gene that became available for structure and function studies of MS channels (Sukharev et al. 1994a, b). The reconstitution method used for this unortodox

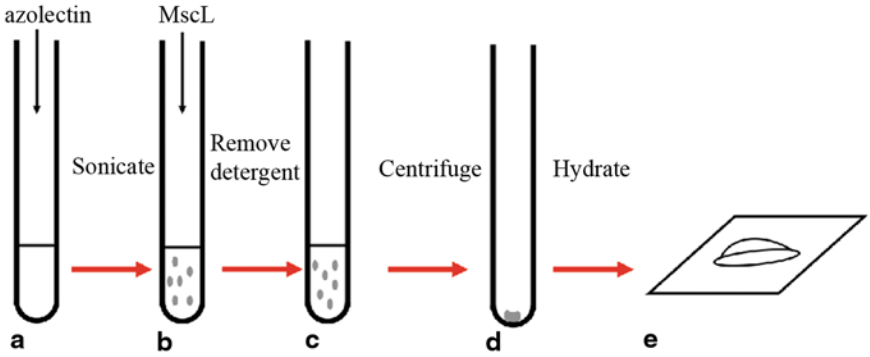

Fig. 1.2 The Dehydration/Rehydration (*D/R*) method of reconstitution of MS channels into liposomes. **a** The lipid is dissolved in a suitable solvent (e.g. chloroform or ethanol) and added to a dry test tube. The solvent is removed under a stream of N_2. **b** Buffer solution and protein (e.g. MscL) are added and the mixture sonicated. The detergent is removed by use of Biobeads **c** and the solution centrifuged under high g (typically 240,000) for 30 min. The pellet is collected **d**, placed on a microscope slide **e**, and dried under vacuum overnight at 4 °C. The dried pellet is then rehydrated with buffer at 4 °C for a further 24 hr.

approach in cloning of an ion channel was a refinement of the method reported by Criado and Keller (Criado and Keller 1987), where the bacterial membrane vesicles were introduced into azolectin liposomes and $MgCl_2$ was subsequently used in the recording solution to induce *blisters* (unilamellar or paucilamellar liposomes) in the multilamellar liposomes, which resulted in better gigaohm seal formation for MS channel recording (Delcour et al. 1989). Later, Häse and co-workers (Häse et al. 1995) demonstrated the functional activity of a purified extraction of a recombinant MscL in azolectin liposomes. This method is used today as the standard for MscL reconstitution into liposomes and is termed the *Dehydration/Rehydration* (D/R) method (Fig. 1.2). It requires two days preparation time but gives very good reconstitution efficiencies with MscL in particular at protein/lipid ratios of 1/4000 and even 1/50000 (wt/wt) being possible. Both wild-type and mutant channels show functional activity using this method (Martinac et al. 2010; Petrov et al. 2011). Additionally the D/R method proves effective for MscL reconstitution into pure, or mixtures of pure lipids (Perozo et al. 2002b; Moe and Blount 2005; Powl and Lee 2007).

In contrast to MscL, *E. coli* MscS has been difficult to reconstitute into liposomes with the majority of reports using MscS expressed in giant spheroplasts. The first reported successful reconstitution by Sukharev (Sukharev 2002) using the D/R method required reconstitution efficiencies of 1/200 (w/w) in azolectin liposomes. In a more recent report by Vásquez and co-workers (Vásquez et al. 2007), MscS was successfully reconstituted into polar lipid membranes derived from *E. coli*, also at a 1/200 ratio. Using Electron Paramagnetic Resonance (EPR) they were also able show the presence of MscS in DOPC (1,2-dioleoyl-sn-glycero-3-phosphocholine), DOPC:DOPE (1,2-dioleoyl-sn-glycero-3-phosphoethanolamine) and DOPC:DOPG

(1,2-dioleoyl-sn-glycero-3-phospho-(1′-rac-glycerol) liposome mixtures. Interestingly, to date there has been no evidence for functional MscS activity in pure PC (phosphatidylcholine) lipids alone from patch-clamp studies. In addition to MS channels from *E. coli,* other prokaryotic MS channels have successfully been incorporated into liposomes using this method. Some examples of these include the Archaeon *Haloferax volcanii* (Le Dain et al. 1998) through liposome reconstitution of the native protein. MscMJ and MscMJLR, two MS channels from *M. jannashii*, were also identified as having *E. coli* MscS- and MscL-like activity, respectively, when reconstituted into liposomes (Kloda and Martinac 2001a, b).

A second technique termed the *sucrose method* was developed to improve both MscL and MscS reconstitution into liposomes (Fig. 1.3) (Battle et al. 2009). This method has the advantage of giving very good reconstitution efficiencies for both MscL and MscS, with MscS showing functional activity from patch-clamp recordings at a 1:1000 wt/wt ratio. It also offers significant time-savings over the D/R method with functional channel activity of both MscS and MscL being reported in 3 h. Continued shaking overnight further improves the reconstitution. This method has been successful for reconstitution of both WT and mutant channels.

An electroformation technique is also successful for incorporation of MscL into liposomes that has been developed commercially by Nanion technologies GmbH (München, Germany; http://www.nanion.de/products/port-a-patch/port-a-patch-data.html). The Vesicle Prep Pro® uses a solvent free approach to prepare giant unilamellar liposomes through an electro-swelling procedure (Fig. 1.4).

1.4 The Lipid Bilayer Model of MS Channels Activation

Tension developed in the lipid bilayer of cellular membranes leads to conformational rearrangements of MS ion channels followed by opening of their large non-selective pores. The bilayer tension is transduced into open and closed conformational changes of the MS channel proteins followed by exchange of solutes on a millisecond time scale. Such rapid ion fluxes provide a defence mechanism against sudden changes in osmolarity that protect microbial cells from lysis (Booth et al. 2005; Martinac 2007). Tension induced stretching of the bilayer is accompanied by a proportional change in the bilayer thickness, and this bilayer thinning is believed to contribute to the stability of the open conformation of the channel (Hamill and Martinac 2001). The role of the lipid bilayer in bacterial MS channel gating has been investigated using a combination of mechanical membrane stretch, site directed spin labelling, EPR spectroscopy and molecular dynamic studies (see also Sect. 1.5). This led to the discovery that hydrophobic mismatch and membrane curvature are potential triggers for MS channel gating via the bilayer mechanism (Hamill and Martinac 2001; Perozo et al. 2002b; Meyer et al. 2006).

The lipid-protein hydrophobic mismatch can be induced experimentally by reconstitution of MS ion channels in lipid bilayers of different thickness as demonstrated for gramicidin, an antibiotic compound isolated from the soil bacterial species *Bacillus brevis*. Gramicidin A is a simple hydrophobic peptide that is not long enough to span the membrane as a monomer but it can form a functional cation channel upon

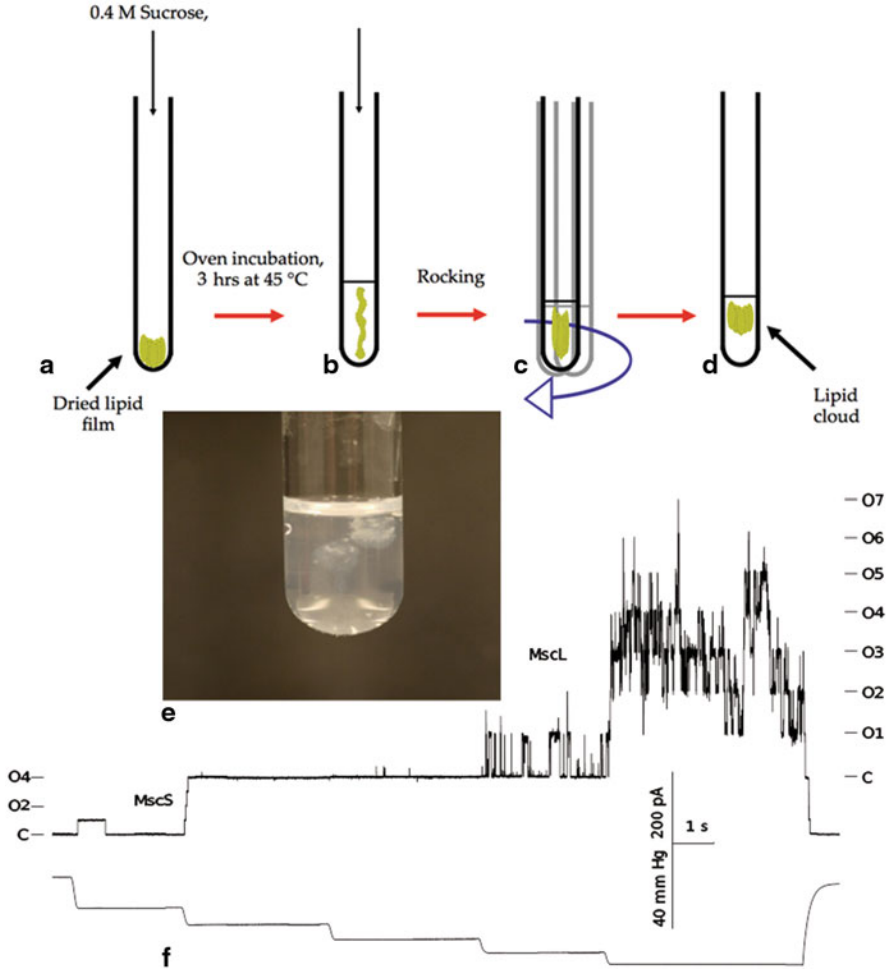

Fig. 1.3 Sucrose method of reconstitution of MS channels. **a** The lipid is dissolved in a suitable solvent, added to a test tube, then dried under an N_2 stream. **b** 0.4 M sucrose is then added to test tube, the solution placed in an oven at 45–55 °C for 3 h after which time a thin lipid film is formed. **c** Rocking is continued at room temperature on a flatbed shaker for a further 3 h resulting in a lipid cloud floating in solution **d**. **e** Photograph of the lipid cloud in a test tube. **f** Patch-clamp recording of MscS and MscL co-reconstituted into azolectin liposomes using the sucrose method. The pipette voltage was +30 mV. (Adapted from Battle et al. 2009 with permission of Elsevier Limited and FEBS Letters via copyright clearance centre)

dimerization (Urry et al. 1971; Koeppe and Anderson 1996). However, small changes in phospholipid acyl chain length (i.e., PC20–PC18) can switch gramicidin A from a stretch-activated to a stretch-inactivated channel, demonstrating that mechanosensitivity of an ion channel protein depends on the composition of the lipid bilayer (Martinac and Hamill, 2002). The effect of bilayer thickness on the gating properties

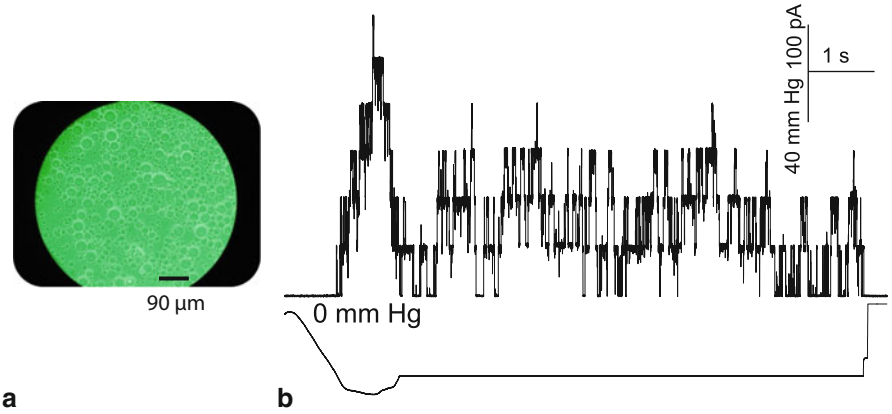

Fig. 1.4 **a** Giant unilamellar liposomes containing MscL prepared using the electro-formation method. **b** Patch-clamp recording of MscL reconstituted into azolectin liposomes prepared using the electroformation method, pipette voltage +30 mV. (Adapted from Cranfield et al. 2011 with permission of Springer Verlag via copyright clearance centre)

of the MscL channel has been investigated by reconstitution of the recombinant protein into bilayers made from lipids of different acyl chain length. The MscL channel required a free energy of activation of approximately 16–17 kT in azolectin liposomes (Hamill and Martinac 2001; Kloda et al. 2006). However, in bilayers made of phospatidylcholine lipids with acyl chains of 16, 18 and 20 hydrocarbons, the free energy G_0 of activation of MscL was significantly different being ∼4 kT for PC16, ∼9 kT for PC18 and ∼24 kT for PC20 (Perozo et al. 2002b). Similarly, EPR spectroscopic measurements of MscL reconstituted into thicker bilayers reduced the mobility of the spin probe and increased spin to spin coupling of residues lining the MscL permeation pathway. In contrast, reduction in bilayer thickness promoted a decrease in spin-spin coupling (Perozo et al. 2002b). Furthermore, decreasing the bilayer thickness lowered the threshold of MscL activation and stabilized channel intermediates during transition from closed to open states (Perozo et al. 2002b). These data indicate that the thinner bilayer better matches the open channel than the closed channel. This is further supported by the molecular dynamics stimulation study of MscL, which confirmed that the thinner bilayer matches better the open conformation compared to closed conformation of the channel (Gullingsrud et al. 2001).

Studies focusing on dissecting the molecular mechanism that underlies the function of MS channels are often based on the use of amphipaths. Amphipaths are molecules that possess both hydrophobic and hydrophilic elements, such as found in detergents, in active lipid substances such as fatty acids and phospholipids of biological membranes. Amphipatic molecules are capable of altering the curvature of the plasma membrane of cells due to their biochemical properties such as charge, shape and size of the polar head, and degree of hydration. For example, anionic amphipaths such as trinitrophenol (TNP) are crenators of erythrocytes, whereas cationic

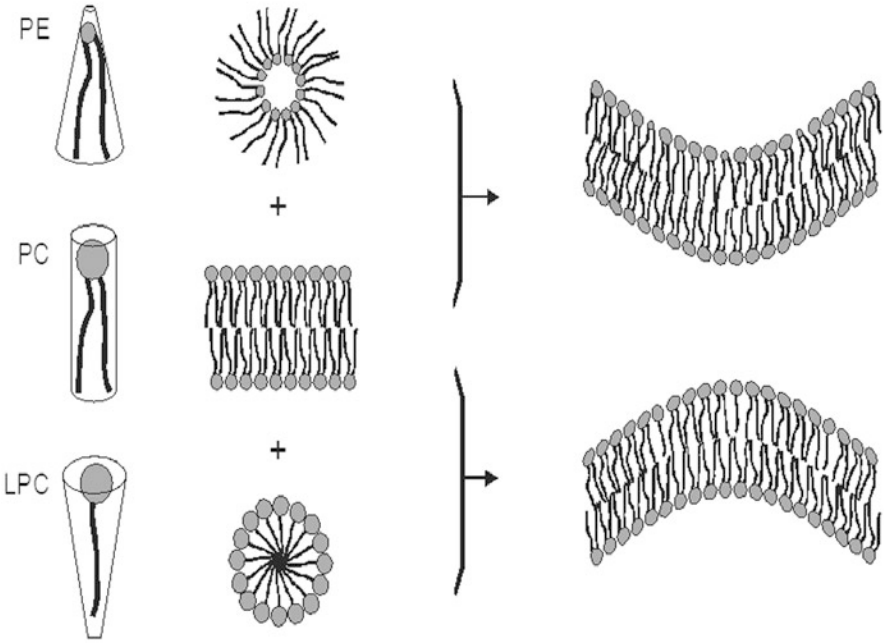

Fig. 1.5 The effect of amphipathic molecules on topology of biological membranes. Insertion of amphipaths into a natural lipid bilayer alters its curvature. Cylindrical natural lipids such as phosphatidylcholine (*PC*) (*middle*) have a neutral effect on biological membranes. Inverted cones e.g. lysophosphatidylcholine (*LPC*) tend to stabilize convex curvature of biological membranes, whereas cone shaped molecules such as phosphatidylethanolamine (*PE*) tend to curve the membrane in the opposite way (courtesy of E. Perozo).

amphipaths such as chlorpromazine (CPZ) cause the erythrocyte membrane to form cups (Sheetz and Singer 1974). The hydrophobic (lipid-like) group typically consist of a hydrocarbon moiety whereas the hydrophilic region has typically either polar (uncharged) or ionic (anionic or cationic) groups. The hydrophilic elements have a bilayer-coupling effect such that differential incorporation of an amphipathic molecule into the respective leaflets of the lipid bilayer can change the bilayer intrinsic curvature, imitating membrane stretch (Fig. 1.5).

Both types of MS ion channels of *E. coli* (MscS and MscL) are activated by amphipaths. The *E. coli* MscS and its archaeal homologue, MscMJ (the MS channel of *M. jannaschii*) can be activated by oppositely charged amphipathic molecules, the cationic *CPZ* and the anionic *TNP*; whereas MscL is sensitive to *lysophosphatidylcholine* (LPC) (Martinac et al. 1990; Kloda and Martinac 2001b; Perozo et al. 2002a, b). Amphipathic drugs strongly support the bilayer model of MS channel activation in which the mechanical gating force comes from the bilayer-protein hydrophobic surface matching and bilayer curvature. In the lipid bilayer model asymmetrical effects of amphipaths may be explained in terms of compensatory

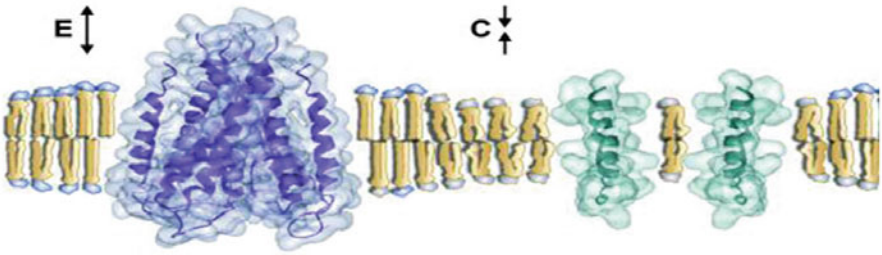

Fig. 1.6 The effect of lipid bilayer on conformational changes of inserted ion channel proteins. The bilayer deformations e.g. lipid acyl chain extension (E) or lipid acyl chain compression (C) can cause rearrangement of transmembrane domains that are transduced into a channel's open/closed conformations, thus affecting channel gating. (Modified from Mitra et al. 2004 with permission PNAS copyright clearance centre, Copyright 2004 National Academy of Sciences, USA)

conformational changes due to differential lipid acyl chain extension and/or compression that create the inner or outer monolayer distortion (Fig. 1.6) (Martinac et al. 1990; Hamill and Martinac 2001).

An MS channel that displays asymmetrical hydrophobic mismatch with respect to each monolayer might therefore be expected to respond differentially, depending upon the direction of membrane curvature (Hamill and Martinac 2001).

Studies based on the use of amphipaths indicate that the MscL channel could gate in response to intrinsic curvature created by asymmetries in the lipid bilayer pressure profile at the lipid-protein junction. Addition of lysophosphatidylcholine (LPC) to the external leaflet of the lipid bilayer trapped the channel in the fully open state (Perozo et al. 2002a, b) and increased channel diameter by 16 Å as determined by FRET spectroscopy (Fig. 1.7) (Corry et al. 2005, 2010). In contrast phosphatityletanolamine, the principal phospholipid in bacterial cell membranes increased the tension threshold for MscL channel activation, most likely through changing the biophysical properties of the lipid bilayer of the lipid membrane (Moe and Blount 2005). Molecular simulation studies of the MscL channel embedded in curved lipid bilayers provided some insight into the possible mechanism of MS channel activation through the geometry of the surrounding lipid bilayer. In a dome shaped lipid bilayer, MscL showed large conformational changes that could trigger channel gating on a very short simulation time scale of 9.5 ns (Meyer et al. 2006).

As shown experimentally the functioning of MS channels is closely dependent on the properties of the lipid bilayer. *In vivo* experiments in native bacterial membranes showed that upregulation of MS channels is related to synthesis of stress sigma factor (RpoS) that protects cells from osmotic stress during stationary growth phase (Stokes et al. 2003). The RpoS factor controls synthesis of cyclopropane fatty acids that can influence the biophysical properties of the cellular membranes by increasing membrane fluidity and thus could affect gating properties of MS ion channels which are sensitive to such changes. Recent studies demonstrated that MscS channel protein concentrates at the poles of *E. coli* cells and co-localizes with the *cardiolipin*, the concentration of which increases with the osmolarity of the growth medium

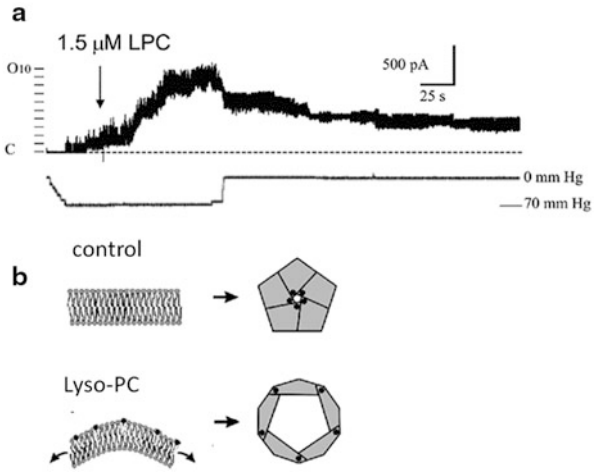

Fig. 1.7 Amphipaths induce asymmetries within the lipid bilayer and stabilize the open MscL channel pore. **a** Single channel current trace of MscL reconstituted into phosphatidylcholine liposomes and recorded in the presence of LPC. **b** A schematic showing that LPC induced asymmetries in the intra-bilayer pressure profile trapped the channel in a fully open state. The curved arrows indicate the change in transbilayer pressure profile corresponding to membrane tension that opens the channel. (Modified from Perozo et al. 2002b with permission from author Martinac)

(Romantsov et al. 2010; Renner and Weibel 2011). Cardiolipin (also referred to as diphosphatidylglycerol) is a doubly negatively charged phospholipid that is most likely asymmetrically distributed between the two leaflets of the bacterial membrane bilayer given that it is asymmetrically distributed in the inner mitochondrial membrane of yeast (Gallet et al. 1997) and that mitochondria contain bacterial lipids (van Meer et al. 2008). Therefore, it could locally affect its shape and thus MS channel gating. Indeed, cardiolipin has been shown to modify rectification and gating behaviour of the MscS channel upon reconstitution into lipid bilayers (Battle et al. 2011). This provides further evidence that bacterial MS channels can sense curved surfaces of cellular membranes and thus may play an important role in bacterial physiology by providing protection during challenging periods of cell growth and division.

1.5 What Electron Paramagnetic Resonance Spectroscopy and Molecular Dynamic Simulations Studies Tell us of Bacterial Mechanosensitive Ion Channel-Lipid Interaction

1.5.1 Electron Paramagnetic Resonance (EPR) Spectroscopy

Site-directed spin labelling (SDSL) and electron paramagnetic resonance (EPR) spectroscopy have successfully been used for the study of the structural dynamics of bacterial MS channels. Closed-to-open transitions and corresponding structural

changes in both MscL and MscS have been characterized using this technique offering the advantage of studying the channels in their natural lipid environment by reconstituting them into artificial liposomes of different lipid composition. Combined with patch-clamp recordings this approach helped to shed light on how basic physical properties of the lipid bilayer such as thickness, curvature and/or pressure profile affect MS channel gating (Perozo 2006; Corry and Martinac 2008; Martinac et al. 2008).

For SDSL EPR spectroscopy a single cysteine residue is introduced into a protein in which, prior to SDSL labelling with a nitroxide spin label, all non-disulfide bonded cysteines are removed by site-directed mutagenesis. A nitroxide spin label is characterised by a N-O group containing the unpaired paramagnetic electron required to produce an EPR signal. In oligomeric ion channels, including MS channels, SDSL EPR measurement of the distances between the spin labels is used to determine the spatial orientation of the secondary structural elements of the channel protein which enables computational modelling of the channel structure with a spatial resolution at the level of the backbone fold. Solvent accessibility (aqueous vs. hydrophobic membrane lipid environment) and the polarity of the spin label micro-environment are examined by employing paramagnetic collisional probes such as molecular oxygen O_2 and NiEdda as relaxing agents which enables the determination of the location of the transmembrane relative to the extracellular channel domains, as well as their movements between the two environments, on the millisecond time scale. The combination of continuous wave (CW) and pulsed EPR methods is used to measure the distances between the structural channel domains in the range ∼0.5–8 nm (Mchaourab and Perozo 2000).

Whereas patch-clamp sieving experiments examining permeation of large organic cations through the MscL channel pore indicated that the MscL pore could expand to ∼30 Å in diameter (Cruickshank et al. 1997), SDSL EPR spectroscopy helped to determine the nature of the conformational transitions leading to the opening of the MscL channel pore. Prior to characterizing the open channel structure using this approach, a closed structure of MscL in the lipid bilayer was determined by SDSL EPR (Perozo et al. 2001). Aside from significant differences between the EPR data and the MscL crystal structure that were found in the C-terminal domain of MscL (Chang et al. 1998), the EPR study confirmed that the crystal structure of the transmembrane TM1 and TM2 domains was an accurate representation of the channel structure in a membrane bilayer (Fig. 1.8). The experimental trick that enabled determination of the MscL structural rearrangements during the channel opening by SDSL EPR was based on measuring the changes in membrane intrinsic curvature induced by the asymmetric addition of the amphipath LPC. This created large EPR spectroscopic changes (Perozo et al. 2002b) (Fig. 1.7). There is an overall very good agreement between the results of the EPR spectroscopic studies and the electrophysiological sieving experiments. The EPR experiments showed that the open channel pore of MscL was at least 25 Å in diameter, which was the minimum pore diameter that could be determined by the CW EPR used in these studies (Perozo et al. 2002a). The residues forming the channel gate are in the open state and so further apart resulting in a sharper EPR spectrum exhibiting an overall change in

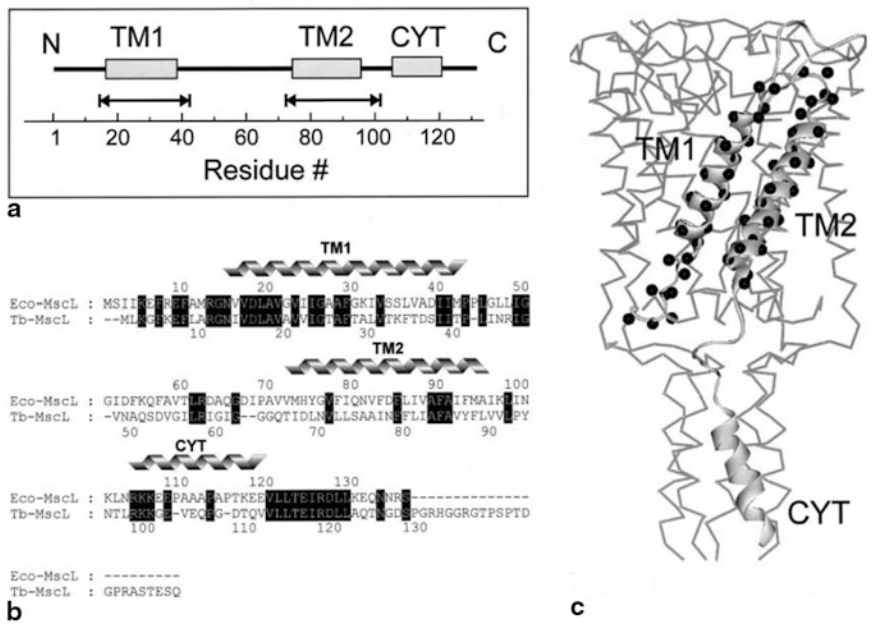

Fig. 1.8 **a** Linear representation of the membrane topology of Eco-MscL. The helical portions of the Eco-MscL monomer (the transmembrane domains TM1 and TM2 and the cytoplasmic helix CYT) are represented by rectangles. The scale corresponds to the amino acid residue numbering. The double-headed arrows designate the amino acid residues replaced by reactive cysteines used for spin labeling. **b** Sequence alignment of Eco-MscL and Tb-MscL. Identical residues are highlighted (*black*). The residues corresponding to two transmembrane helical domains (TM1 and TM2) and the cytoplasmic helix (CYT) are marked. **c** Single MscL subunit showing amino acid residues subjected to cysteine scanning mutagenesis (*black spheres*). The single MscL monomer is represented as a part of the channel pentamer according to the 3-D crystal structure of the channel. (Reproduced from Perozo et al. 2001 with permission from author Martinac)

line shape relative to the EPR spectrum characteristic of the closed state. To generate such a large pore, both TM1 and TM2 domains are significantly tilted with respect to the membrane normal ($\sim$45°). Consequently, the channel flattens and expands in the membrane plane from $\sim$55 Å in diameter in the closed state to $\geq$ 70 Å in the open state (Perozo et al. 2002a). The water-filled open channel pore is almost exclusively lined by the TM1 helices, largely in agreement with other studies of the MscL gating mechanism (Gullingsrud et al. 2001; Sukharev et al. 2001b; Iscla et al. 2007; Corry et al. 2010). As discussed in detail in Sect. 1.4 the open channel structure in the EPR experiments showed that a hydrophobic surface match between the bilayer and the hydrophobic transmembrane portion of the channel could stabilize intermediate conformations of MscL meaning less tension was required to open the channel in thin bilayers ($<$18 hydrocarbons per acyl chain) compared to thick bilayers ($>$18 hydrocarbons per acyl chain) (Perozo et al. 2002b). This finding corresponds

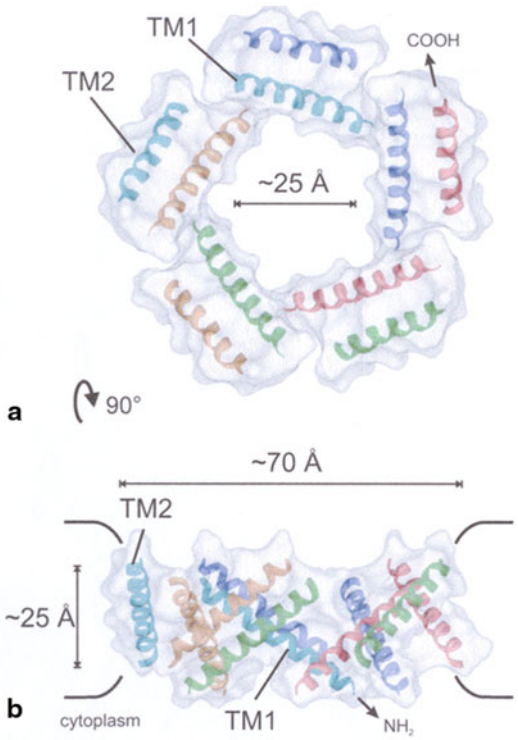

Fig. 1.9 Extracellular **a** and side **b** views of TM1 and TM2 in the open state. Structures are shown within a translucent molecular surface representation of the whole molecule (without extracellular loop or the c-terminal end). The side view is shown in relation to a hypothetically distorted bilayer. (Adapted from Perozo et al. 2002a with permission from author Martinac)

well with the notion that any fractional change in membrane area caused by stretching the membrane is accompanied by a proportional change in the thickness of the lipid bilayer (h), so that

$$\Delta A/A_0 \cong -\Delta h/h_0 \tag{1.4}$$

where h_0 and A_0 are the unstressed membrane thickness and area, respectively.

The overall change in diameter between closed and open conformations of the MscL channel was also determined by other methods including molecular modeling (Sukharev et al. 2001a, b), engineering inter-subunit disulfide bonding (Betanzos et al. 2002; Iscla et al. 2007), and site-directed fluorophore-labeling Förster resonance energy transfer spectroscopy (SDFL FRET) (Corry et al. 2005, 2010). In accordance with the SDSL EPR studies (Perozo et al. 2002a) all these alternative approaches yielded an overall change in MscL diameter of 15–16 Å upon opening (Fig. 1.9). Such a large conformational change is in excellent agreement with the opening of the large 30 Å diameter pore associated with a 20-nm^2 in-plane MscL protein expansion (Chiang et al. 2004). These MscL channel properties account not only for its very large unitary conductance of ~3 nS and its lack of ion specificity (passing any particles with a molecular weight $\leq$ 1,000), but also with its physiological role as

an efficient emergency valve to release solutes from bacteria challenged by hypo-osmotic shock (Levina et al. 1999; Booth et al. 2005).

Structural dynamics of MscS of *E. coli* has also been investigated using CW-EPR spectroscopy (Vásquez et al. 2008a, b). In contrast to MscL, whose gating remains largely unaffected by membrane voltage, MscS is activated by both tension in the lipid bilayer and voltage (Martinac et al. 1987; Sukharev 2002). However, voltage itself is insufficient to open the channel. Instead, it modulates the channel activity cooperatively with membrane tension once the channel has been activated by stretching the membrane.

The MscS crystal structure obtained at 3.9 Å resolution revealed that the functional channel is composed as a homoheptamer of three-transmembrane (TM) domain subunits (Bass et al. 2002). Although originally interpreted as an open MscS structure, the functional state depicted by the crystal structure could initially not be associated with a specific functional state of the channel. A combination of SDSL EPR spectroscopy and molecular dynamics simulations, however, enables a better determination of the native molecular structure of closed MscS in a lipid bilayer (Vásquez et al. 2008b). Here, the closed conformation of MscS is characterized by a more compact packing of the TM domains than in the crystal structure so that the TM domains are realigned towards the normal of the membrane. In addition, the N-terminal domain, previously unresolved by X-ray crystallography, forms a short helical hairpin of 26 amino acid residues preceding the extracellular ends of the TM1 and TM2 helices and is seemingly in close contact with the lipid bilayer.

The 3D-model of membrane-embedded MscS in the closed state obtained by SDSL EPR made it possible to investigate further the closed-to-open structural rearrangements of the channel using the same approach (Vásquez et al. 2008a). To open MscS, the amphipath LPC was also used here as was previously done with MscL. The study showed that during channel opening the TM1 helices tilted and rotated enabling the TM2 helices to become exposed to the membrane lipids and thus allowing the TM3 helices to expand, tilt and rotate, resulting in an opening of the channel pore of at least 11 Å in diameter. By taking into account the MscS unitary conductance of ~1 nS, and non-saturability in high salt and weak ionic selectivity, this result indicates that a water-filled pore of a fully open channel is ~16 Å in diameter (Sukharev 2002; Kung et al. 2010). In the open state the TM1 and TM2 domains remain in continuous contact with the lipid bilayer and are therefore thought to form the MscS mechanosensor for bilayer tension (Nomura et al. 2006; Vásquez et al. 2008a; Booth et al. 2011; Malcolm et al. 2011). Furthermore, the role of the voltage sensor has also been attributed to the TM1 and TM2 transmembrane domains because of the three arginine residues present in those domains (Bass et al. 2002; Bezanilla and Perozo 2002). This view is in agreement with the results of the initial patch-clamp characterization of MscS showing that higher open probabilities were observed with more positive membrane voltage being applied to a membrane patch (Martinac et al. 1987). Importantly, the voltage was only effective so long as membrane tension over the activation threshold was applied to the patch pipette.

1.5.2 Molecular Dynamic Simulations

Molecular dynamic (MD) simulations indicate large conformational changes occurring during opening of both MscL and MscS comparable to those obtained by the experimental methods described in the previous section.

The *sine-qua-non* to perform MD simulations of a protein is the availability of its 3D structure at an atomic resolution. In most cases the structure is obtained by X-ray crystallography as in the case of MscL and MscS, which are at present the only MS channels fulfilling this condition (Kubalski 2005). MD simulations of both channels have over the last decade aimed primarily at unravelling the gating pathway between the closed and open configuration in these channels (Gullingsrud et al. 2001; Bilston and Mylvaganam 2002; Kong et al. 2002; Colombo et al. 2003; Sotomayor and Schulten 2004; Vora et al. 2006; Vásquez et al. 2008a). MD simulations have also investigated the mechanism of molecular protein-lipid interactions between these MS channel proteins and their surrounding lipids whereby membrane tension is translated into channel opening (Elmore and Dougherty 2003; Gullingsrud and Schulten 2004; Meyer et al. 2006; Malcolm et al. 2011). As well, MD simulations have also been used to investigate how changes of the lipid headgroups or the length of the acyl chains would alter the membrane tension required to gate the channels (Elmore and Dougherty 2003; Corry and Martinac 2008). Furthermore, MD simulation studies have been employed to understand the hydration properties of the channels and the role the hydrophobic lock of MscL and MscS plays in regulating their function (Anishkin and Sukharev 2004; Sotomayor and Schulten 2004; Spronk et al. 2006; Anishkin et al. 2010).

Given the short nanosecond time scales of MD simulations, large conformational changes in both MscL and MscS could only be observed when an external mechanical force was applied to these proteins. Thus, most of the MscL simulations have investigated the channel structural changes under the influence of an external force whose application to the channel protein varied between studies including surface tension applied to the MscL protein without a lipid bilayer (Gullingsrud et al. 2001); direct force application to the outer TM2 helix or anisotropic pressure coupling to a bare MscL protein (Bilston and Mylvaganam 2002); pressure applied to the bilayer around MscL (Colombo et al. 2003); and targeted force inducing conformational change of MscL from its crystal structure to a pre-determined end structure (Kong et al. 2002). In comparison, most of the MD simulations done with MscS have aimed to resolve the contention about the channel functional state represented by its crystal structure (Bass et al. 2002). All MD simulation studies suggest thus far that the crystal structure does not represent the fully open state of the pore, but rather indicate that the structure is representative of an inactive state of the channel. As neither the open state nor the closed state crystal structures of MscS have been completely resolved, the only MscS gating pathway from its closed to open conformation has to date been obtained using EPR spectroscopy, and computational analyses (Vásquez et al. 2008a).

1.6 Application of MTS Reagents in Studies of Bacterial MS Channels

Another approach in studying the structure and function of MscL and MscS is to use the negatively (2-sulfonatoethyl methanethiosulfonate sodium salt ($MTSES^-$)) and positively (2-(trimethylammonium)ethyl methanethiosulfonate bromide ($MTSET^+$)) charged methanethiosulfonate (MTS) compounds combined with cysteine site-directed mutagenesis. In particular, this approach has been employed to investigate pore permeation and gating properties of these MS proteins. Attaching MTS reagents to various cysteine loci in the gating region of these MS channels induces spontaneous opening of the channels. Both $MTSES^-$ and $MTSET^+$ have successfully been used to study pore permeation in MscL channels. For example, application of 4–10 mM of $MTSES^-$ to the patch pipette was shown to lead to full opening of single MscL channels (Yang and Blount 2011).

One of the first studies employing MTS reagents probed water accessibility of the G22 residue (mutated to G22C for the MTS study) of MscL, which together with several other residues including A21, V23, I24, I25, G26 and A27 forms the hydrophobic gate of the *E. coli* MscL (Yoshimura et al. 2001). The study confirmed previous findings by the same authors showing that a hydrophobic moiety at the G22 position makes the channel harder to open, whereas a hydrophilic addition at the same position makes it easier to open the channel (Yoshimura et al. 1999). The G22C was found to be accessible to MTS reagents from the periplasmic side in the closed state, whereas the channel had to be open to access this site from the cytoplasmic end. Together, these results indicate that exposure of the hydrophobic constriction of the channel gate to a hydrophilic environment is the main energy barrier to gating the channel by membrane tension (Hamill and Martinac 2001). Several other studies employing MTS compounds investigated structural transition from the closed to the open states of MscL *in vivo* (Bartlett et al. 2004) and/or by the patch-clamp recording from giant *E. coli* spheroplasts (Batiza et al. 2002; Li et al. 2009; Yang and Blount 2011). Collectively, these studies helped to identify residues lining the lumen of the MscL pore in different conformational states of the channel and suggested a clockwise rotation and tilting of the TM1 helix during the MscL gating, consistent with the data obtained from SDSL EPR spectroscopy (Perozo et al. 2002a), but inconsistent with another model for MscL gating which proposed a slight TM1 rotation in the counter-clockwise direction (Sukharev et al. 2001b; Betanzos et al. 2002). Moreover, these studies showed that the MscL crystal structure (Chang et al. 1998) did not depict a fully closed structure but rather a nearly closed state of the channel; a result that was further confirmed by a study introducing single-site histidine substitutions into the MscL structure and assessing the ability of divalent metal ions of Ni^{2+}, Cd^{2+} and Zn^{2+} to affect channel activity (Iscla et al. 2004).

$MTSET^+$ was also used to show that the crystal structure of MscS did not depict an open channel structure as originally proposed (Bass et al. 2002), but rather the structure of a non-conducting channel in its inactivated state (Belyy et al. 2010). TM3 helices are normally attached toTM1 and TM2 transmembrane domains in the

closed and open MscS conformations, and to the cytoplasmic β domain in closed and inactivated states. A current model of MscS gating proposes that MscS enters an inactivated state when the pore-forming TM3 helices decouple from the lipid-facing TM1 and TM2 helices and join together in a narrow conformation similar to the conformation represented by the crystal structure (Anishkin et al. 2008a, b; Koprowski et al. 2011). This model was further supported by the finding that $MTSET^+$ at position L111C completely abolished the return of the MscS channel from inactivated to the resting MS state (Belyy et al. 2010). After treatment with 1 mM $MTSET^+$ the MscS response to saturating membrane tension remained unchanged, which, however, changed upon the channel inactivation. The inactivated state was stabilized upon modification by $MTSET^+$, indicative of state-dependent modification by the positively charged MTS reagent.

1.7 Studying the Effects of High Hydrostatic Pressure on Bacterial Mechanosensitive Ion Channels

Deep sea organisms, through millions of years of evolution, learnt to survive under extreme conditions such as *high hydrostatic pressure* (HHP) (Ashcroft 2000). Under pressures of tens of megaPascals (MPa) biomembranes, the tertiary and quaternary structure of proteins, and nucleic acids are all functionally altered (Macdonald 1984). As well, HHP has direct influence on biophysical characteristics of biomembranes (viscosity, thickness, compactness of hydrocarbon chains etc.) (Braganza and Worcester 1986). Nevertheless, life does exist under HHP as animals of varying complexity have even been discovered near bottom of the Mariana Trench (> 80 MPa). How they have adapted to such harsh conditions is still largely unknown. MS channels can be a tool to study the effects of HHP on membrane bound proteins in order to answer some of the mysteries surrounding life under high pressure (Macdonald and Martinac 2005; Petrov et al. 2011).

In order to investigate how HHP can modify structure and function of macromolecules and biomembranes innovative approaches need to be employed. Patch-clamp electrophysiology recording under high pressure utilizes a device called a "flying-patch" (Braganza and Worcester 1986; Heinemann et al. 1987). The key element of this device is a cylindrical plastic protecting chamber placed on electrode (Fig. 1.10). Once the membrane patch is attached to the electrode tip, the chamber is slid down towards the tip of the electrode. A few microliters of bath solution from recording chamber are captured inside and held in place by capillary forces. Thus the most fragile part—the electrode tip with membrane patch—is isolated and surrounded by bath solution. This can then be positioned inside a high pressure chamber. HHP steps can then be applied to membrane patch and ion channel currents recorded simultaneously.

Due to the technical design of high pressure chamber, it is impossible to apply suction to the inside of the electrode and stretch the patch membrane—a necessary requirement to open MS channels. Thus it is necessary to already have the MS

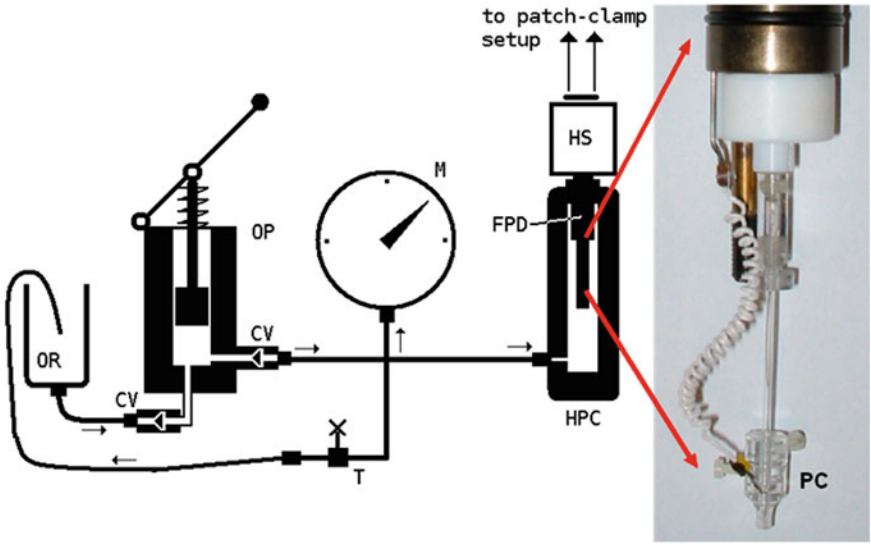

Fig. 1.10 High pressure setup and "flying-patch" device (photo). *OP*, oil pump; *CV*, check valve; *OR*, oil reservoir; *M*, manometer; *HPC*, high pressure chamber; *FPD*, "flying-patch" device; *HS*, patch-clamp headstage; *T*, tap; *PC*, protecting chamber. (Figure reproduced from Cranfield et al. 2011 with permission of Springer Verlag via copyright clearance centre)

channel in the open state, partially at least. Using bacterial mechanosensistive ion channels this has been achieved in two ways: (i) by using MscS/MscK, which are more MS than MscL and applying the negative pipette voltage across membrane (–40 to –60 mV); or (ii) by using a mutated variants of the channels which have been found to gate spontaneously without tension. The substitution of a hydrophilic glutamate residue at position 22 in MscL (Yoshimura et al. 1999) is one such mutation that has been used for this purpose (Yoshimura et al. 1999; Petrov et al. 2011).

It was previously shown that MscS decreases its activity under HHP (Macdonald and Martinac 2005). This was evident by its reduced opening probability. These observations were reproducible and the HHP did not denature the channel because fully open states were observed at all applied pressures (0–90 MPa) and channels recovered their activity when returned to lower pressures (Petrov et al. 2007). G22E mutants of MscL on the other hand demonstrated longer openings at subconducting levels when exposed to HHP (Petrov et al. 2011). This increase of activity was observed regardless of whether the channels were from spheroplasts or azolectin membranes.

The difference in these effects between the two MS channels could lie in the fact that MscS was the WT channel. In order to open MscS channels energy has to be spent to expose the hydrophobic amino acids of the channel pore to water molecules. Under HHP (< 100 MPa) it is likely that the channel is becoming more compact and so occupying less volume (Wann and Macdonald 1980; Macdonald

and Martinac 2005). If so, then a decrease in the free volume of the channel under HHP would make a closed state more favourable. As well, given that membranes under HHP are stiffer and the hydrocarbon tails of phospholipid molecules are more compact (Braganza and Worcester 1986), it is conceivable that HHP could hamper the movement of the TM1-TM2 *hairpin* which is vital to the gating process (Bass et al. 2002). In the case of the G22E-MscL mutant there is a substitution (glycine to glutamate) at the narrowest part of the MscL channel which impairs the hydrophobic lock and causes excess hydration. Under the influence of HHP there may be increased water permeation, which in turn interferes with the "hydrophobic lock" mechanism of the pore-forming helices of the G22E-MscL pentamer, hindering channel closure (Petrov et al. 2011).

1.8 Liposome Efflux Assays

Membrane bound MS ion channels that have been cloned, recombinantly expressed and purified can normally be readily reconstituted into artificial liposomes (see Sect. 1.3. above). By filling these liposomes with a high concentration of a self-quenching fluorophore such as calcein or carboxy-fluorescein, channel activity can be quantified according to the leakage of these fluorophores from their liposomal compartments into the surrounding media. Once free of the confines of the liposomes, overall fluorescence is increased as the dye becomes dispersed and is no longer self-quenched (Fig. 1.11). The method of liposome creation for this assay typically involves extruding lipids containing reconstituted protein in a solution of very highly concentrated fluorophore (typically of the order of 50 mM) through a membrane. This typically produces unilamellar vesicles of a size corresponding to the pore size of the membrane used. Extruders for this application are commercially available (AVESTIN). Following extrusion, the liposomes can typically be separated from their fluorophore containing media by using a Sephadex G50 gravity fed column.

After the separation of free dye the liposomes are ready to be used for whatever experimental assay is required. Results can be easily measured using a fluorescence plate reader. As a positive control, the detergent *Triton-X* is typically added to break open all the liposomes and releases all the fluorophore to the surrounding media, causing a considerable increase in overall fluorescence (Foo et al. 2011).

Liposome efflux assays have been used to assess the functioning of MscL channels in response to various mechanical and chemical stimulations. The effectiveness of liposome assays using MscL can be improved further by creating a gain of function (GOF) mutant. This can readily be achieved by replacing the glycine at the pore constriction site (G22) with cysteine, and then labelling the cysteines with [2-(triethylammonium)ethyl] methanethiosulfonate bromide (MTSET). This creates positive charges within the constriction site forcing the channel to open (Yoshimura et al. 2001; Bartlett et al. 2004, 2006) (Sect. 1.6). Powl et al. used this GOF mutant to demonstrate that the addition of anionic lipids such as phosphatidylglycerol,

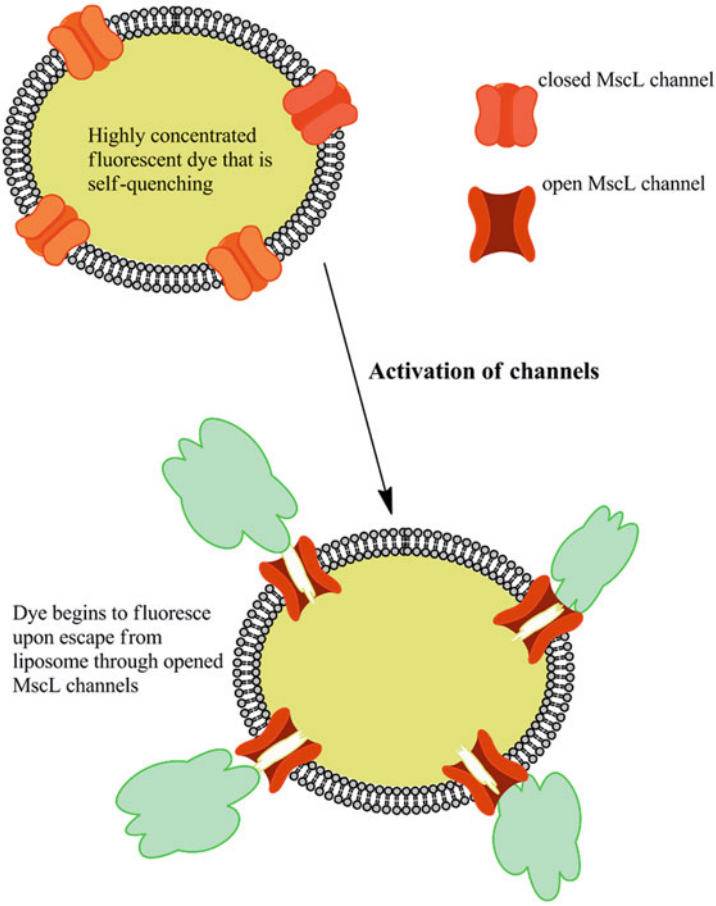

Fig. 1.11 Liposome efflux assay. A highly concentrated self-quenching fluorescent dye is incorporated into liposomes reconstituted with mechanosensitive (*MS*) ion channels (typically MscL). In response to some stimulus or drug, the channels open and the dye is released into the surrounding media where it is no longer quenched and overall fluorescence increases.

phosphatidic acid, and cardiolipin to phosphatidylcholine liposomes increases the flow of the fluorophore through these MscL channels (Powl et al. 2008).

Li et al used a liposome efflux assay to verify that 2 separately distinct residue pairs, G26/I92 and V23/I96, in MscL do interact upon channel opening (Li et al. 2009). They did this by mutating the select residues such that they would electrostatically repulse each other when brought into close contact. This electrostatic repulsion led to a loss of function which was readily detectable using a liposome efflux assay. Koçer et al. have used MscL mutants that were chemically modulated to function as nanovalves incorporated into liposomes which can then open in response to various stimuli such as light or pH changes (Koçer et al. 2005, 2006). Van de Bogaart

et al used a variation of fluorescence correlation spectroscopy with their liposomes in order to demonstrate that small protein molecules can pass through the pore of MscL channels incorporated into liposomes (van den Bogaart et al. 2007a). They labelled their liposome membranes with the fluorophore DiO (excitation max 484 nm, emission max 501 nm), and then incorporated various AlexaFluor 633 (excitation max 632 nm, emission max 647 nm) labelled proteins into them. They were then able to monitor fluorescence signals in a confocal volume over time in 2 distinct wavelength bands. By correlating the intensities of the 2 signals they were able to distinguish between liposomes with both fluorophores, and those liposomes where the AlexaFluor labelled proteins had leaked out through MscL pores. The same group used a similar technique to demonstrate the pore size of the antimicrobial agent in honey bee venom, *melittin*, in liposomes of various lipid compositions (van den Bogaart et al. 2007b).

1.9 Advanced Fluorescence Techniques to Characterise Bacterial Mechanosensitive Ion Channels

Modern fluorescence microscopy techniques have created many new and innovative ways to study the interactions and structures of ion channels (Martinac and Cranfield 2012). Techniques such as total internal reflection fluorescence (TIRF) microscopy, Förster Resonance Energy Transfer (FRET), Bioluminescence Resonance Energy Transfer (BRET), Fluorescence Lifetime Imaging (FLIM), Stimulated Emission Depletion (STED) microscopy, Stochastic Optical Reconstruction Microscopy (STORM), Photoactivated Localisation Microscopy (PALM), and Fluorescence Correlation Spectroscopy (FCS) are highly useful tools for detecting what occurs at the nanometer level. In this section we will primarily focus on the applications of FRET as it is the most frequently used and established method for the characterisation of bacterial MS ion channels within their lipid environment.

FRET involves the transfer of the energy from an excited donor fluorophore to a nearby quencher or acceptor molecule, so long as the acceptor molecule is within a distance ∼1–100 Å (Förster 1959). This is advantageous as many inter- and intra-protein interactions occur within this distance range. This transfer of energy occurs through dipole-dipole interactions and is radiationless, thus no photons are emitted during the energy transfer process. If the acceptor molecule is itself a fluorophore the transfer of energy to it may cause emission of a photon at a longer wavelength and with lower energy than the fluorescence that would normally be emitted by the donor. The amount of energy transferred to the acceptor is dependent upon the distance and the relative dipole orientations of the donor with respect to the acceptor molecules. The FRET efficiency (E) is the fraction of energy that is transferred between donor and acceptor molecules. It can be measured by dividing the donor fluorescence intensity (or lifetime—see FLIM below) in the presence of the acceptor with the value in the absence of the acceptor and subtracting this from 1. This value can then be used to determine the distance between donor and acceptor molecules according to the

equation:

$$r = R_0 \left[\left(\frac{1}{E} \right) - 1 \right]^{1/6} \tag{1.5}$$

where r is the distance between fluorescence dipoles and R_0 is the *Förster distance,* which is the distance at which energy transfer is 50 %. R_0 is dependent on the freedom of movement of the donor and acceptor molecules with respect to each other, and the relative overlap between the donor's emission spectrum and the acceptors' absorption spectrum. We recommend Lakowicz (2006) for those interested in better understanding of calculating the value of R_0 (Lakowicz 2006). For many applications, however, the calculation of the exact distance between donor and acceptor FRET pairs is not necessary as it is often sufficient just to know that FRET is occurring. From the FRET efficiency measurements alone it is often possible to conclude that relevant fluorescently labelled protein regions are either closer or further apart with respect to each other, which can provide valuable structural information. If the accuracy of intra- and inter-molecular distances is of particular importance to the experiment the use of Fluorescence Lifetime Imaging (FLIM) to measure FRET is recommended. The fluorescence lifetime is the average time the stimulated electron of a fluorophore spends in the excited state prior to its decline to the ground state. FLIM is an advantageous technique as lifetimes are independent of a fluorophore's localised concentration. Although quantification of FRET efficiency using FLIM is preferred, it does however require more sophisticated equipment and analysis. If FRET occurs between a donor fluorophore and the acceptor there will be a reduction in the fluorescence lifetime of the donor fluorophore, and it is this difference in the lifetime of the donor, in the presence and absence of the acceptor, that can be used to calculate the FRET efficiency.

The open channel structure of MscL was elucidated using FRET (Corry et al. 2005, 2010). These structural changes were detected from the fluorescence intensity emitted from cysteine mutants tagged with a FRET pair consisting of Alexa-Fluor 488 as the donor and Alexa-Fluor 568 as the acceptor. MscL channels incorporated into liposomes were stimulated to open via the application of the amphipath LPC to the lipid bilayer. The researchers were able to determine that the diameter of the MscL protein expanded by 16 Å upon channel opening (Corry et al. 2005, 2010) in a very good agreement with the EPR spectroscopic studies (Perozo et al. 2002a).

In addition FRET was used to investigate the conformational dynamics of the cytoplasmic domain in the MS channel of small conductance (MscS) during the channel opening (Machiyama et al. 2009). MscS possesses a large cytoplasmic domain which is required for its activity and stability (Martinac et al. 2008). By labelling point mutations in the cytoplasmic domain of MscS with a FRET pair, and using LPC to stimulate channel opening, Machiyama et al were able to demonstrate that the cytoplasmic domain of the channel swells when the channel opens and that this expansion is a result of an electrostatic interaction between the transmembrane and cytoplasmic domains (Machiyama et al. 2009).

FRET was performed on fluorescently labelled derivatives of single Gramicidin A (gA) channels incorporated into planar membranes. Gramicidin A is an antibiotic isolated from *Bacillus brevis* that is able to form channels that are sensitive to mechanical stretch and changes in membrane thickness (Martinac and Hamill 2002; Markin et al. 2006). gA monomers are not large enough to span typical lipid bilayers, so in order to form channels gramicidin needs to form homodimers that will span the lipid membrane (see Sect. 1.4. above). Borisenko et al were able to visually identify gA homodimers using FRET by separately labelling 2 populations of monomers, one with a donor, and one with the acceptor. They did this whilst simultaneously recording channel electrical activity using a specially designed imaging chamber (Borisenko et al. 2003).

Single molecule FRET for the study of bacterial channels has the ability to detect structural fluctuations at the single channel level without confounding FRET signals that can occur between channels in a group or cluster (Weiss 2000; Roy et al. 2008). In another gramicidin study single molecule FRET was measured from within a patch pipette enabling simultaneous current traces of channels opening with subsequent single molecule FRET images (Harms et al. 2003).

Tryptophan residues have also been used as the fluorescence donor to study lipid-protein interactions. Powl et al. (2003) incorporated a tryptophan residue into the transmembrane regions of MscL. They then incorporated 2 lipids of differing acyl chain lengths into their lipid bilayer, one containing bromine atoms to act as a fluorescence acceptor molecule. By measuring the amount of tryptophan quenching at various brominated lipid concentrations they were able to calculate the lipid binding constants for their lipid pairs. By varying lipid chain lengths and/or the site of the tryptophan residue in the protein they were then able to demonstrate that MscL distorts to match bilayer thickness (Powl et al. 2003), and that the binding constants for lipids of varying acyl chain length are different for regions of the protein in the cytoplasmic leaflet of the lipid bilayer compared to the periplasmic side (Powl et al. 2007; Lee 2011).

The labelling of channels for FRET studies requires some consideration. One method of labelling involves the cloning of fluorescent fusion proteins whereby a protein such as *green fluorescent protein* (GFP) is attached to the host protein; this chimera can then be expressed in cells (Norman et al. 2005). Alternatively, proteins may be labelled via the attachment of organic fluorescent dyes to reactive amino acid residues such as cysteine. If not pre-existing, these residues may be inserted into a protein via mutagenesis, which is beneficial as it allows the labelling of specific sites which may be of structural or functional interest within the protein. Conversely, if unwanted reactive residues are present in the protein they may be altered by mutagenesis to prevent excess labelling. Numerous proteins also contain fluorescent amino acids such as tryptophan which may act as a donor fluorophore. In addition, artificial amino acids may be inserted into proteins to behave as acceptors (Summerer et al. 2006). An advantage of fluorescent dye labelling rather than the use of fusion proteins is that fluorescent dye molecules are small, which allows the labelling of channels at multiple loci and so minimise their effect on channel activity. Labelling of channels with lanthanide metals such as europium or terbium

can also be advantageous since their fluorescence decays are longer (0.5–3 ms). Thus the accuracy of the fluorescence readings are enhanced as background fluorescence (typically in the nanosecond range) can be excluded if the fluorescence is measured only after a lag period following a pulsed excitation. However lanthanides have a poor absorption profile and therefore they typically have to be used in conjunction with a chelator to enhance their overall fluorescence (Selvin and Hearst 1994; Lakowicz 2006).

1.10 Other Structural Techniques Recently Employed in Studies of Bacterial MS Channels

The great interest in understanding the structure and function relationship in ion channels and other membrane proteins whose function is closely linked to the bilayer lipid environment in which these proteins operate, has led to a revived interest in determining the structure of membrane proteins in their native membrane environment using a wide range of structural techniques. Towards this goal researchers have, in addition to the techniques described in this chapter, employed a range of other techniques, including NMR spectroscopy, small-angle neutron scattering (SANS), small-angle X-ray scattering (SAXS) and atomic force microscopy (AFM), to name a few.

Recently Abdine and colleagues reported the first solid-state NMR study of the MscL protein selectively labelled by using cell-free expression and reconstituted in a hydrated lipid bilayer (Abdine et al. 2010). As an alternative method to produce membrane proteins of both, prokaryotic and eukaryotic origins, cell-free expression facilitates not only expression of high amounts of proteins but also helps to eliminate toxicity problems, reduce proteolytic degradation, and can synthesize the membrane proteins directly into detergent micelles or lipid bilayers (Reckel 2010). The cell-free expression of MscL enabled preparation of NMR samples providing a significant reduction of the spectral crowding. This method should help to determine the secondary protein structure and dynamics, as well as distance constraints, that can further be used for computational modelling of MscL molecular dynamics, as it has previously been done by employing EPR and FRET spectroscopy (Perozo et al. 2002a; Corry et al. 2010).

Another recent study by Grage and colleagues employed small angle neutron scattering (SANS) and atomic force microscopy (AFM) in addition to fluorescence microscopy, patch-clamp recording and computational modelling to investigate clustering and functional interaction of MscL channels in lipid bilayers of different composition (Grage et al. 2011). The study indicated that MscL exhibited tendency to form clusters under a wide range of conditions, and, although closely packed, the channel still remained active and MS. The MscL channel activity was however modulated by the presence of neighbouring proteins in the clusters indicating the importance of the lipid bilayer for the interactions between MscL proteins. It is worth noting here that MscL as an ~80 kDa protein is amenable to these structural methods

and techniques because of its relatively small size. Similar approaches have thus far not been used for studies of MscS structure because of the limitations that the size of the MscS channel protein (∼210 kDa) may impose on these techniques.

1.11 Conclusion and Perspectives

The mechanisms that underlie how individual bacterial MS ion channels interact with their lipid environments need further investigation if we are to fully comprehend the mechanisms of mechanotransduction. Once we have a better knowledge of these mechanisms, not only will that knowledge contribute to a better understanding of the molecular principles underlying mechanosensory transduction in living cells, but the utility of these MS channels as nano-valves in various biomedical and engineering applications can also be optimally beneficially exploited.

Acknowledgments The work from our laboratory discussed in the manuscript was supported by the Australian Research Council (DP0769983), the National Health & Medical Research Council of Australia (635525), and the Yamada Science Foundation.

References

Abdine A, Verhoeven MA, Park K-H, Ghazi A, Guittet E, Berrier C, Van Heijenoort C, Warschawski DE (2010) Structural study of the membrane protein MscL using cell-free expression and solid-state NMR. J Magn Reson 204(1):155–159

Akitake B, Anishkin A, Liu N, Sukharev S (2007) Straightening and sequential buckling of the pore-lining helices define the gating cycle of MscS. Nat Struct Mol Biol 14(12):1141–1149

Anishkin A, Sukharev S (2004) Water dynamics and dewetting transitions in the small mechanosensitive channel MscS. Biophys J 86(5):2883–2895

Anishkin A, Akitake B, Sukharev S (2008a) Characterization of the Resting MscS: modeling and analysis of the closed bacterial mechanosensitive channel of small conductance. Biophys J 94(4):1252–1266

Anishkin A, Kamaraju K, Sukharev S (2008b) Mechanosensitive channel MscS in the open state: modeling of the transition, explicit simulations, and experimental measurements of conductance. J Gen Physiol 132(1):67–83

Anishkin A, Akitake B, Kamaraju K, Chiang CS, Sukharev S (2010) Hydration properties of mechanosensitive channel pores define the energetics of gating. J Physics: Condens Matter 22(45):454120

Ashcroft FM (2000) Life at the extremes: the science of survival. Harper Collins, London

Bartlett JL, Levin G, Blount P (2004) An in vivo assay identifies changes in residue accessibility on mechanosensitive channel gating. PNAS 101(27):10161–10165

Bartlett JL, Li Y, Blount P (2006) Mechanosensitive channel gating Transitions resolved by functional changes upon pore modification. Biophys J 91(10):3684–3691

Bass RB, Strop P, Barclay M, Rees D (2002) Crystal structure of Escherichia coli MscS, a voltage-modulated and mechanosensitive channel. Science 298:1582–1587

Batiza AF, Kuo MM-C, Yoshimura K, Kung C (2002) Gating the bacterial mechanosensitive channel MscL in vivo. PNAS 99(8):5643–5648

Battle AR, Petrov E, Pal P, Martinac B (2009) Rapid and improved reconstitution of bacterial mechanosensitive ion channel proteins MscS and MscL into liposomes using a modified sucrose method. FEBS Letters 583(2):407–412

Battle AR, Nomura T, Martinac B (2011) Understanding the role of cardiolipin on the gating behaviour of mechanosensitive ion channels. Biophys J 100(3 S1):1518

Belyy V, Anishkin A, Kamaraju K, Liu N, Sukharev S (2010) The tension-transmitting 'clutch' in the mechanosensitive channel MscS. Nat Struct Mol Biol 17(4):451–458

Betanzos M, Chiang CS, Guy HR, Sukharev S (2002) A large iris-like expansion of a mechanosensitive channel protein induced by membrane tension. Nat Struct Mol Biol 9(9):704–710

Bezanilla F, Perozo E (2002) Structural biology. Force and voltage sensors in one structure. Science 298(5598):1562–1563

Bilston LE, Mylvaganam K (2002) Molecular simulations of the large conductance mechanosensitive (MscL) channel under mechanical loading. FEBS Letters 512(1–3):185–190

Blount P, Sukharev SI, Moe PC, Schroeder MJ, Guy HR, Kung C (1996) Membrane topology and multimeric structure of a mechanosensitive channel protein of Escherichia coli. EMBO J 15(18):4798–4805

Blount P, Sukharev SI, Moe P, Martinac B, Kung C (1999) Mechanosensitive channels in bacteria. Methods Enzymol 294:458–482

Booth IR, Edwards MD, Murray E, Miller S (2005) The role of bacterial channels in cell physiology In: Kubalski A, Martinac B (eds) Bacterial ion channels and their eukaryotic homologs. ASM Press, Washington DC, pp 291–312

Booth IR, Rasmussen T, Edwards MD, Black S, Rasmussen A, Bartlett W, Miller S (2011) Sensing bilayer tension: bacterial mechanosensitive channels and their gating mechanisms. Biochem Soc Trans 39(3):733–740

Borisenko V, Lougheed T, Hesse J, Füreder-Kitzmüller E, Fertig N, Behrends JC, Woolley GA, Schütz GJ (2003) Simultaneous optical and electrical recording of single gramicidin channels. Biophys J 84(1):612–622

Braganza LF, Worcester DL (1986) Structural changes in lipid bilayers and biological membranes caused by hydrostatic pressure. Biochemistry 25(23):7484–7488

Brehm P, Kullberg R, Moody-Corbett F (1984) Properties of non-junctional acetylcholine receptor channels on innervated muscle of Xenopus laevis. J Physiol 350:631–648

Chalfie M (2009) Neurosensory mechanotransduction. Nat Rev Mol Cell Biol 10(1):44–52

Chang G, Spencer RH, Lee AT, Barclay MT, Rees DC (1998) Structure of the MscL homolog from Mycobacterium tuberculosis: a gated mechanosensitive ion channel. Science 282(5397):2220–2226

Chiang CS, Anishkin A, Sukharev S (2004) Gating of the large mechanosensitive channel in situ: estimation of the spatial scale of the transition from channel population responses. Biophys J 86(5):2846–2861

Colombo G, Marrink SJ, Mark AE (2003) Simulation of MscL gating in a bilayer under stress. Biophys J 84(4):2331–2337

Corry B, Hurst AC, Pal P, Nomura T, Rigby P, Martinac B (2010) An improved open-channel structure of MscL determined from FRET confocal microscopy and simulation. J Gen Physiol 136(4):483–494

Corry B, Martinac B (2008) Bacterial mechanosensitive channels: Experiment and theory. Biochim Et Biophys Acta-Biomembranes 1778(9):1859–1870

Corry B, Rigby P, Liu ZW, Martinac B (2005) Conformational changes involved in MscL channel gating measured using FRET spectroscopy. Biophys J 89(6):L49–51

Cranfield CG, Kloda A, Petrov E, Battle A, Nomura T, Rohde P, Cox C, Martinac B (2011) Techniques for investigating the mechanosensitivity of ion channels. Encycl Biophys: (In press)

Criado M, Keller BU (1987) A membrane fusion strategy for single-channel recordings of membranes usually non-accessible to patch-clamp pipette electrodes. FEBS Lett 224(1):172–176

Cruickshank CC, Minchin RF, Le Dain AC, Martinac B (1997) Estimation of the pore size of the large-conductance mechanosensitive ion channel of Escherichia coli. Biophys J 73(4):1925–1931

Cui C, Smith DO, Adler J (1995) Characterization of mechanosensitive channels in Escherichia coli cytoplasmic membrane by whole-cell patch clamp recording. J Membr Biol 144(1):31–42
Delcour AH, Martinac B, Adler J, Kung C (1989) Modified reconstitution method used in Patch-Clamp studies of Escherichia-Coli ion channels. Biophys J 56(3):631–636
Edwards MD, Bartlett W, Booth IR (2008) Pore mutations of the Escherichia coli MscS channel affect desensitization but not ionic preference. Biophys J 94(8):3003–3013
Elmore DE, Dougherty DA (2003) Investigating lipid composition effects on the mechanosensitive channel of large conductance (MscL) using molecular dynamics simulations. Biophys J 85(3):1512–1524
Foo AFW, Landsberg MJ, Battle AR, Marsh BJ, Hankamer B, Martinac B (2011) Mscl Channels as nanovales for the controlled release of Liposome-Encapsulated compounds. Biophys J 100(3, Suppl 1):277a–278a
Förster T (1959) Transfer mechanisms of electronic excitation. Discuss Faraday Soc 27(7):25
Gallet PF, Petit JM, Maftah A, Zachowski A, Julien R (1997) Asymmetrical distribution of cardiolipin in yeast inner mitochondrial membrane triggered by carbon catabolite repression. Biochem J 324(Pt 2):627–634
Gamini R, Sotomayor M, Chipot C, Schulten K (2011) Cytoplasmic domain filter function in the mechanosensitive channel of small conductance. Biophys J 101(1):80–89
Grage SL, Keleshian AM, Turdzeladze T, Battle AR, Tay WC, May RP, Holt SA, Antoranz Contera S, Haertlein M, Moulin M, Pal P, Rohde PR, Forsyth VT, Watts A, Huang KC, Ulrich AS, Martinac B (2011) Bilayer-mediated clustering and functional interaction of MscL channels. Biophys J 100:1252–1260
Grajkowski W, Kubalski A, Koprowski P (2005) Surface changes of the mechanosensitive channel MscS upon its activation, inactivation, and closing. Biophys J 88(4):3050–3059
Guharay F, Sachs F (1984) Stretch-activated single ion channel currents in tissue-cultured embryonic chick skeletal muscle. J Physiol 352:685–701
Gullingsrud J, Schulten K (2004) Lipid bilayer pressure profiles and mechanosensitive channel gating. Biophys J 86(6):3496–3509
Gullingsrud J, Kosztin D, Schulten K (2001) Structural determinants of MscL gating studied by molecular dynamics simulations. Biophys J 80(5):2074–2081
Gustin MC, Zhou XL, Martinac B, Kung C (1988) A mechanosensitive ion channel in the yeast plasma membrane. Science 242(4879):762–765
Hamill OP, Martinac B (2001) Molecular basis of mechanotransduction in living cells. Physiol Rev 81(2):685–740
Harms GS, Orr G, Montal M, Thrall BD, Colson SD, Lu HP (2003) Probing conformational changes of Gramicidin ion channels by single-molecule Patch-Clamp fluorescence microscopy. Biophys J 85(3):1826–1838
Häse CC, Le Dain AC, Martinac B (1995) Purification and functional reconstitution of the recombinant large mechanosensitive ion channel (MscL) of Escherichia coli. J Biol Chem 270(31):18329–18334
Heinemann SH, Conti F, Stühmer W, Neher E (1987) Effects of hydrostatic pressure on membrane processes. Sodium channels, calcium channels, and exocytosis. J Gen Physiol 90(6):765–778
Iscla I, Levin G, Wray R, Reynolds R, Blount P (2004) Defining the physical gate of a mechanosensitive channel, MscL, by engineering metal-binding sites. Biophys J 87(5):3172–3180
Iscla I, Levin G, Wray R, Blount P (2007) Disulfide trapping the mechanosensitive channel MscL into a gating-transition state. Biophys J 92(4):1224–1232
Kloda A, Martinac B (2001a) Molecular identification of a mechanosensitive channel in archaea. Biophys J 80(1):229–240
Kloda A, Martinac B (2001b) Structural and functional differences between two homologous mechanosensitive channels of Methanococcus jannaschii. EMBO J 20(8):1888–1896
Kloda A, Ghazi A, Martinac B (2006) C-terminal charged cluster of MscL, RKKEE, functions as a pH sensor. Biophys J 90(6):1992–1998
Koçer A, Walko M, Meijberg W, Feringa BL (2005) A light-actuated nanovalve derived from a channel protein. Science 309(5735):755–758

Koçer A, Walko M, Bulten E, Halza E, Feringa BL, Meijberg W (2006) Rationally designed chemical modulators convert a bacterial channel protein into a pH-sensory valve. Angew Chem Int Ed 45(19):3126–3130

Koeppe R, Anderson O (1996) Engineering the gramicidin channel. Annu Rev Biophys Biomol Struct 25(1):231–258

Kong YF, Shen YF, Warth TE, Ma JP (2002) Conformational pathways in the gating of Escherichia coli mechanosensitive channel. Proc Nat Acad Sci 99:5999–6004

Koprowski P, Grajkowski W, Isacoff EY, Kubalski A (2011) Genetic screen for potassium leaky small mechanosensitive channels (MscS) in Escherichia coli. J Biol Chem 286(1):877–888

Koprowski P, Kubalski A (2003) C termini of the Escherichia coli mechanosensitive ion channel (MscS) move apart upon the channel opening. J Biol Chem 278(13):11237–11245

Kubalski A, Martinac B (eds) (2005). Bacterial ion channels and their eukaryotic homologues. ASM Press, Washington, D.C.

Kung C, Martinac B, Sukharev S (2010) Mechanosensitive channels in microbes. Annu Rev Microbiol 64:313–329

Lakowicz JR (2006) Principles of fluorescence spectroscopy. Springer, New York

Le Dain AC, Saint N, Kloda A, Ghazi A, Martinac B (1998) Mechanosensitive ion channels of the archaeon Haloferax volcanii. J Biol Chem 273(20):12116–12119

Lee AG (2011) Lipid-protein interactions. Biochem Soc Transact 39:761–766

Levin G, Blount P (2004) Cysteine scanning of MscL transmembrane domains reveals residues critical for mechanosensitive channel gating. Biophys J 86(5):2862–2870

Levina N, Totemeyer S, Stokes NR, Louis P, Jones MA, Booth IR (1999) Protection of Escherichia coli cells against extreme turgor by activation of MscS and MscL mechanosensitive channels: identification of genes required for MscS activity. EMBO J 18(7):1730–1737

Li Y, Wray R, Eaton C, Blount P (2009) An open-pore structure of the mechanosensitive channel MscL derived by determining transmembrane domain interactions upon gating. FASEB J 23(7):2197–2204

Macdonald AG (1984) The effects of pressure on the molecular structure and physiological functions of cell membranes. Philos Trans R Soc London B Biol Sci 304(1118):47–68

Macdonald AG, Martinac B (2005) Effect of high hydrostatic pressure on the bacterial mechanosensitive channel MscS. Eur Biophys J 34(5):434–441

Machiyama H, Tatsumi H, Sokabe M (2009) Structural changes in the cytoplasmic domain of the mechanosensitive channel MscS during opening. Biophys J 97(4):1048–1057

Malcolm HR, Heo YY, Elmore DE, Maurer JA (2011) Defining the role of the tension sensor in the mechanosensitive channel of small conductance. Biophys J 101(2):345–352

Markin V, Shlyonsky V, Simon S, Benos D, Ismailov I (2006) Mechanosensitivity of gramicidin a channels in bulged bilayer membranes at constant tension. Biophysics 51(6):892–895

Martinac B (2004) Mechanosensitive ion channels: molecules of mechanotransduction. J Cell Sci 117(Pt 12):2449–2460

Martinac B (2007) 3.5 billion years of mechanosensory transduction: structure and function of mechanosensitive channels in prokaryotes. In: Hamill OP (ed) Current topics in membranes, vol 58. Elsevier Inc., San Diego, CA, pp 25–57

Martinac B, Cranfield C (2012) Shining a light on the structural dynamics of ion channels using Förster resonance energy transfer (FRET). IPSI BgD Transact Adv Res 8(1):19–24

Martinac B, Hamill OP (2002) Gramicidin a channels switch between stretch activation and stretch inactivation depending on bilayer thickness. Proc Nat Acad Sci 99(7):4308–4312

Martinac B, Buechner M, Delcour AH, Adler J, Kung C (1987) Pressure-sensitive ion channel in Escherichia coli. Proc Nat Acad Sci 84(8):2297–2301

Martinac B, Adler J, Kung C (1990) Mechanosensitive ion channels of E. coli activated by amphipaths. Nature 348(6298):261–263

Martinac B, Saimi Y, Kung C (2008) Ion channels in microbes. Physiol Rev 88(4):1449–1490

Martinac B, Corry B, Hurst AC, Pal P, Nomura T, Rigby P (2010) An improved open-channel structure of MscL determined from FRET confocal microscopy and simulation. J Gen Physiol 136(4):483–494

Maurer JA, Dougherty DA (2003) Generation and evaluation of a large mutational library from the Escherichia coli mechanosensitive channel of large conductance, MscL: implications for channel gating and evolutionary design. J Biol Chem 278(23):21076–21082

Mchaourab HS, Perozo E (2000) Determination of protein folds and conformational dynamics using spin-labeling EPR spectroscopy. In: Eaton SS, Eaton GE, Berliner L (eds) Biological magnetic resonance: Distance measurements in biological systems by EPR, vol 19. Kluwer Academic/Plenum Publishers, New York, pp 155–218

Meyer GR, Gullingsrud J, Schulten K, Martinac B (2006) Molecular dynamics study of MscL interactions with a curved lipid bilayer. Biophys J 91(5):1630–1637

Miller S, Bartlett W, Chandrasekaran S, Simpson S, Edwards M, Booth IR (2003a) Domain organization of the MscS mechanosensitive channel of Escherichia coli. EMBO J 22(1):36–46

Miller S, Edwards MD, Ozdemir C, Booth IR (2003b) The closed structure of the MscS mechanosensitive channel. Cross-linking of single cysteine mutants. J Biol Chem 278(34):32246–32250

Mitra K, Ubarretxena-Belandia I, Taguchi T, Warren G, Engelman DM (2004) Modulation of the bilayer thickness of exocytic pathway membranes by membrane proteins rather than cholesterol. Proc Nat Acad Sci 101(12):4083–4088

Moe P, Blount P (2005) Assessment of potential stimuli for mechano-dependent gating of MscL: effects of pressure, tension, and lipid headgroups. Biochemistry 44(36):12239–12244

Morris CE (1990) Mechanosensitive ion channels. J Membr Biol 113(2):93–107

Nomura T, Sokabe M, Yoshimura K (2006) Lipid-protein interaction of the MscS mechanosensitive channel examined by scanning mutagenesis. Biophys J 91(8):2874–2881

Nomura T, Sokabe M, Yoshimura K (2008) Interaction between the cytoplasmic and transmembrane domains of the mechanosensitive channel MscS. Biophys J 94(5):1638–1645

Nomura T, Battle AR, Martinac B (2011) Lipid and lyso-lipid effects on the mechanosensitivity of liposome co-reconstituted mscs and mscl. Biophys J 100(3, Supp. 1):278a

Norman C, Liu Z-W, Rigby P, Raso A, Petrov Y, Martinac B (2005) Visualisation of the mechanosensitive channel of large conductance in bacteria using confocal microscopy. Eur Biophys J 34(5):396–402

Ou X, Blount P, Hoffman RJ, Kung C (1998) One face of a transmembrane helix is crucial in mechanosensitive channel gating. Proc Nat Acad Sci 95(19):11471–11475

Perozo E (2006) Gating prokaryotic mechanosensitive channels. Nat Rev Mol Cell Biol 7(2):109–119

Perozo E, Kloda A, Cortes DM, Martinac B (2001) Site-directed spin-labeling analysis of reconstituted Mscl in the closed state. J Gen Physiol 118(2):193–206

Perozo E, Cortes DM, Sompornpisut P, Kloda A, Martinac B (2002a) Open channel structure of MscL and the gating mechanism of mechanosensitive channels. Nature 418(6901):942–948

Perozo E, Kloda A, Cortes DM, Martinac B (2002b) Physical principles underlying the transduction of bilayer deformation forces during mechanosensitive channel gating. Nat Struct Mol Biol 9(9):696–703

Petrov E, Rohde PR, Macdonald AG, Martinac B (2007) Effect of High Hydrostatic Pressure and Voltage on Gating of the Bacterial Mechanosensitive Channel of Small Conductance. Proc 4th Int Conf High Pressure Biosci Biotechnol 1:20–27

Petrov E, Rohde PR, Martinac B (2011) Flying-patch Patch-clamp study of G22E-MscL mutant under high hydrostatic pressure. Biophys J 100(7):1635–1641

Powl AM, Lee AG (2007) Lipid effects on mechanosensitive channels. In: Owen PH (ed) Current topics in membranes, vol 58. Academic Press, New York, pp 151–178

Powl AM, East JM, Lee AG (2003) Lipid−protein interactions studied by introduction of a tryptophan residue: the mechanosensitive channel MscL†. Biochemistry 42(48):14306–14317

Powl AM, East JM, Lee AG (2007) Different effects of lipid chain length on the two sides of a membrane and the lipid annulus of MscL. Biophys J 93(1):113–122

Powl AM, East JM, Lee AG (2008) Anionic phospholipids affect the rate and extent of flux through the mechanosensitive channel of large conductance MscL. Biochemistry 47(14):4317–4328

Reckel S, Sobhanifar S, Durst F, Löhr F, Shirokov VA, Dötsch V, Bernhard F (2010) Strategies for the cell-free expression of membrane proteins. In: Endo Y (ed) Cell-free protein production:

methods and protocols, methods in molecular biology, vol 607. Humana Press, New York, pp 187–212
Renner LD, Weibel DB (2011) Cardiolipin microdomains localize to negatively curved regions of Escherichia coli membranes. Proc Nat Acad Sci 108(15):6264–6269
Romantsov T, Battle AR, Hendel JL, Martinac B, Wood JM (2010) Protein localization in Escherichia coli cells: comparison of the cytoplasmic membrane proteins ProP, LacY, ProW, AqpZ, MscS, and MscL. J Bacteriol 192(4):912–924
Roy R, Hohng S, Ha T (2008) A practical guide to single-molecule FRET. Nat Methods 5(6):507–516
Ruthe HJ, Adler J (1985) Fusion of bacterial spheroplasts by electric fields. Biochimica et Biophysica Acta 819(1):105–113
Sachs F (2010) Stretch-activated ion channels: what are they? Physiology 25(1):50–56
Selvin PR, Hearst JE (1994) Luminescence energy transfer using a terbium chelate: improvements on fluorescence energy transfer. Proc Nat Acad Sci 91(21):10024–10028
Sheetz MP, Singer SJ (1974) Biological membranes as bilayer couples. A molecular mechanism of drug-erythrocyte interactions. Proc Nat Acad Sci 71(11):4457–4461
Sokabe M, Sachs F (1990) The structure and dynamics of patch-clamped membranes: a study using differential interference contrast light microscopy. J Cell Biol 111(2):599–606
Sokabe M, Sachs F, Jing ZQ (1991) Quantitative video microscopy of patch clamped membranes stress, strain, capacitance, and stretch channel activation. Biophys J 59(3):722–728
Sotomayor M, Schulten K (2004) Molecular dynamics study of gating in the mechanosensitive channel of small conductance MscS. Biophys J 87(5):3050–3065
Sotomayor M, Van Der Straaten TA, Ravaioli U, Schulten K (2006) Electrostatic properties of the mechanosensitive channel of small conductance MscS. Biophys J 90(10):3496–3510
Spronk SA, Elmore DE, Dougherty DA (2006) Voltage-dependent hydration and conduction properties of the hydrophobic pore of the mechanosensitive channel of small conductance. Biophys J 90(10):3555–3569
Stokes NR, Murray HD, Subramaniam C, Gourse RL, Louis P, Bartlett W, Miller S, Booth IR (2003) A role for mechanosensitive channels in survival of stationary phase: regulation of channel expression by RpoS. Proc Nat Acad Sci 100(26):15959–15964
Sukharev S (2002) Purification of the small mechanosensitive channel of Escherichia coli (MscS): the subunit structure, conduction, and gating characteristics in liposomes. Biophys J 83(1):290–298
Sukharev S, Betanzos M, Chiang CS, Guy HR (2001a) The gating mechanism of the large mechanosensitive channel MscL. Nature 409(6821):720–724
Sukharev S, Durell SR, Guy HR (2001b) Structural models of the MscL gating mechanism. Biophys J 81(2):917–936
Sukharev SI, Martinac B, Arshavsky VY, Kung C (1993) Two types of mechanosensitive channels in the Escherichia coli cell envelope: solubilization and functional reconstitution. Biophys J 65(1):177–183
Sukharev SI, Blount P, Martinac B, Blattner FR, Kung C (1994a) A large-conductance mechanosensitive channel in E. Coli encoded by Mscl alone. Nature 368(6468):265–268
Sukharev SI, Martinac B, Blount P, Kung C (1994b) Functional reconstitution as an assay for biochemical isolation of channel proteins: Application towards the molecular identification of a bacterial mechanosensitive channel. In: Montal M (ed) Methods: A companion to methods in enzymology, vol 6. Academic Press, New York, pp 51–59
Sukharev SI, Sigurdson WJ, Kung C, Sachs F (1999) Energetic and spatial parameters for gating of the bacterial large conductance mechanosensitive channel, MscL. J Gen Physiol 113(4):525–540
Summerer D, Chen S, Wu N, Deiters A, Chin JW, Schultz PG (2006) A genetically encoded fluorescent amino acid. Proc Nat Acad Sci 103(26):9785–9789
Urry DW, Goodall MC, Glickson JD, Mayers DF (1971) The gramicidin a transmembrane channel: characteristics of head-to-head dimerized π(L, D) Helices. Proc Nat Acad Sci 68(8):1907–1911
van den Bogaart G, Krasnikov V, Poolman B (2007a) Dual-color fluorescence-burst analysis to probe protein efflux through the mechanosensitive channel MscL. Biophys J 92(4):1233–1240

van den Bogaart G, Mika JT, Krasnikov V, Poolman B (2007b) The lipid dependence of melittin action investigated by dual-color fluorescence burst analysis. Biophys J 93(1):154–163
van Meer G, Voelker DR, Feigenson GW (2008) Membrane lipids: where they are and how they behave. Nat Rev Mol Cell Biol 9(2):112–124
Vásquez V, Cortes DM, Furukawa H, Perozo E (2007) An optimized purification and reconstitution method for the MscS channel: strategies for spectroscopical analysis. Biochemistry 46(23):6766–6773
Vásquez V, Sotomayor M, Cordero-Morales J, Schulten K, Perozo E (2008a) A structural mechanism for MscS gating in lipid bilayers. Science 321(5893):1210–1214
Vásquez V, Sotomayor M, Cortes DM, Roux B, Schulten K, Perozo E (2008b) Three-dimensional architecture of membrane-embedded MscS in the closed conformation. J Mol Biol 378(1):55–70
Vora T, Corry B, Chung SH (2006) Brownian dynamics investigation into the conductance state of the MscS channel crystal structure. Biochimica Et Biophysica Acta 1758(6):730–737
Wann K, Macdonald A (1980) The effects of pressure on excitable cells. Comparative biochemistry and physiology Part A: Physiology 66(1):1–12
Weiss S (2000) Measuring conformational dynamics of biomolecules by single molecule fluorescence spectroscopy. Nat Struct Biol 7(9):724
Yang L-M, Blount P (2011) Manipulating the permeation of charged compounds through the MscL nanovalve. FASEB J 25(1):428–434
Yoo J, Cui Q (2009) Curvature generation and pressure profile modulation in membrane by lysolipids: insights from coarse-grained simulations. Biophys J 97(8):2267–2276
Yoshimura K, Batiza A, Schroeder M, Blount P, Kung C (1999) Hydrophilicity of a single residue within MscL correlates with increased channel mechanosensitivity. Biophys J 77(4):1960–1972
Yoshimura K, Batiza A, Kung C (2001) Chemically charging the pore constriction opens the mechanosensitive channel MscL. Biophys J 80(5):2198–2206
Yoshimura K, Nomura T, Sokabe M (2004) Loss-of-function mutations at the rim of the funnel of mechanosensitive channel MscL. Biophys J 86(4):2113–2120
Yoshimura K, Sokabe M (2010) Mechanosensitivity of ion channels based on protein–lipid interactions. J Royal Soc Interface 7(Suppl 3):S307–S320

Chapter 2
Mechanosensitive K2P channels, TREKking through the autonomic nervous system

J. Antonio Lamas

2.1 Introduction

The TOK1/YORK channel from the yeast *Saccharomyces cerevisiae* was the first channel containing two-pore loop-forming domains to be cloned and sequenced (Ketchum et al. 1995; Lesage et al. 1996b). Although the TOK1/YORK channel comprises eight transmembrane segments (8TMS-2P), its discovery anticipated the flourishing of a new family of 4TMS mammalian potassium channels now known as the "two-pore domain potassium channels" (K2P, KCNK). The sequence of a family of 4TM channels containing two-pore domains (the CeK family) was obtained from the genome of the nematode *Caenorhabditis elegans* and it was also deposited in DNA databases in 1995 (Salkoff and Jegla 1995). One year later, the first member of the mammalian 4TMS-K2P family was described in human tissue and named TWIK-1 for "**T**andem of pore domains in a **W**eak **I**nward rectifying $\mathbf{K}^+$ channel" (Lesage et al. 1996a). Within less than 10 years 15 such channels had been categorized into six subfamilies: TWIK, TREK, TASK, TALK, THIK and TRESK (for extensive reviews on K2P channels see: Lesage and Lazdunski 2000; Lotshaw 2007; Enyedi and Czirják 2010).

The second member of the mammalian K2P family, TREK-1 (**T**WIK-1 **RE**lated $\mathbf{K}^+$ channel), was first isolated from mouse brain in 1996 (Fink et al. 1996). This channel was the first member of the TREK subfamily discovered, soon followed by the mouse TRAAK (TWIK-Related Arachidonic Acid-stimulated K+ channel: Fink et al. 1998) and finally by the rat (Bang et al. 2000) and human (Lesage et al. 2000b) TREK-2.

The members of the TREK subfamily are non-inactivating background potassium channels that can open at any membrane potential, thus playing an important role in the control of the resting membrane potential and in neuronal excitability. Moreover, their open rectification and slight voltage-dependency suggests a role in action potential repolarization, and consequently in repetitive firing (Goldstein et al. 2001).

J. A. Lamas (✉)
Laboratory of Neuroscience, CINBIO, Department of Functional Biology,
University of Vigo, 36310 Vigo, Spain
e-mail: antoniolamas@uvigo.es

A. Kamkin, I. Lozinsky (eds.), *Mechanically Gated Channels and their Regulation,*
Mechanosensitivity in Cells and Tissues 6,
DOI 10.1007/978-94-007-5073-9_2,

TREK channels are widely expressed throughout the nervous system, as well as in several non-neuronal tissues (Talley et al. 2001, 2003), indicating a broad and complex range of physiological and pathological roles, depending on the function of the cells, tissues and organs in which they are expressed.

All three members of the TREK subfamily share the distinctive characteristic of being activated by a mechanical membrane stretch (Patel et al. 1998; Maingret et al. 1999a; Bang et al. 2000). In addition, TREK channels are modulated via G protein-coupled receptors and by a extremely high number of physical and chemical physiological stimuli, including membrane deformation, temperature, pH, polyunsaturated fatty acids, lysophospholipids and neurotransmitters, (Lesage 2003; Kim 2003; Franks and Honore 2004; Mathie 2007; Mathie and Veale 2007; Lotshaw 2007; Huang and Yu 2008; Sabbadini and Yost 2009; Dedman et al. 2009; Noël et al. 2011). Non-physiological stimuli such as neuroprotective agents and volatile general anesthetics also potently regulate these channels. Indeed, their strong reactivity confers TREK channels with an additional complex set of putative cellular functions, apparently derived from the interaction of these factors with the C-terminus region of the protein.

2.2 Electrophysiological Properties

We usually think of leak channels as pores that produce non-rectifying ohmic currents, thereby producing a linear relationship between current and voltage (linear I–V) similar to that of an ohmic resistor in an electrical circuit. However, in theory, the current-voltage relationship (I–V) for a potassium-selective leak channel is expected to rectify in the outward direction, due to the difference in potassium concentration between the extracellular and intracellular fluids in physiological conditions. This behavior was already predicted by the constant field theory (GHK-current equation) and it is often referred to as "open channel rectification", meaning that K^+ ions travel more easily through an open channel when moving from a compartment with high K^+ concentration to one with low K^+ concentration, producing higher conductance in this direction (Goldman 1943; Hodgkin and Katz 1949; Lesage and Lazdunski 2000; Goldstein et al. 2001; Plant et al. 2005; Honore 2007). However, current passing through a single-channel is most commonly studied at equimolar (symmetrical) potassium concentrations (often 150 mM, both inside and outside of the membrane). In these ideal conditions the concentration gradient vanishes and the I-V becomes linear, at least for a perfect leak channel.

As classically hypothesized, a leak current should also be voltage-independent, meaning that the open probability of the channel should be the same at any membrane voltage and that channels should not undergo inactivation. This also implies that rapid changes in the voltage of the membrane result in instantaneous alterations in the macroscopic current (whole-cell current) with only negligible time course constants, simply depending on the driving force for potassium (V_m–E_K). In summary, in ideal conditions (*e.g.,* equimolar potassium concentrations) the current generated by leak

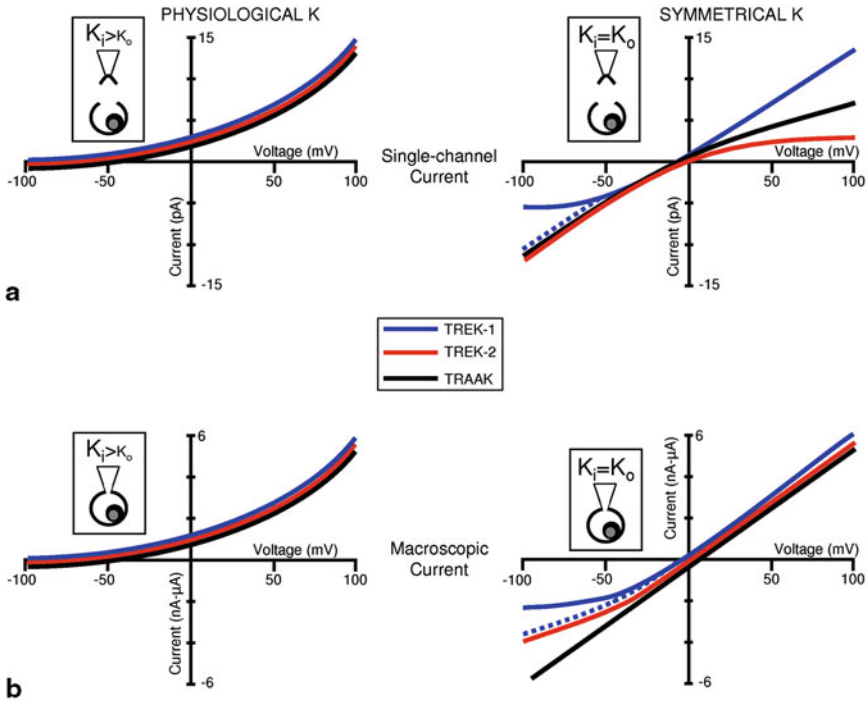

Fig. 2.1 Current-voltage relationships for TREK channels. At near physiological potassium concentrations, both single-channel (**a**, *left*) and macroscopic whole-cell currents (**b**, *left*) rectify strongly in the outward direction. This rule is applicable to all three members of the TREK subfamily. At high symmetrical potassium concentrations, TREK-1 single-channel currents still rectify in the outward direction (**a**, *right*; *blue*). This rectification essentially disappears when cations are removed (**a**, *right*; *dotted-blue*). TREK-2 and TRAAK single-channels exhibit inward rectification at symmetrical potassium concentrations (**a**, *right*; *red* and *black*). In the same conditions, TREK-1 and TREK-2 macroscopic whole-cell currents exhibit outward rectification (**b**, *right*; *blue* and *red*), although the stronger rectification of TREK-1 can be reduced by removing extracellular cations (**b**, *right*; *dotted blue*). TRAAK macroscopic I-Vs at high potassium concentrations are essentially linear (**b**, *right*; *black*). The data shown in this figure are not real but rather, they serve to summarize the cumulative findings of many authors (see text). "nA-μA" roughly refers to values obtained from experiments performed following heterologous expression in small cells or in oocytes, respectively

channels (macroscopic or single-channel) should follow Ohm's law, maintaining a linear relationship with the voltage (linear I–V), while at physiological potassium concentrations the I–V should exhibit a slight outward rectification, as predicted by the GHK equation (outwardly rectifying I–V). TREK channels are universally considered leak (or baseline, background or resting) channels, and although they generally conform to the rules outlined above, some important deviations from this ideal behavior occur (as discussed below and in Fig. 2.1).

2.2.1 TREK Single-Channel Properties

Heterologously expressed members of the TREK subfamily, TREK-1 (Fink et al. 1996), TREK-2 (Lesage et al. 2000b) and TRAAK (Fink et al. 1998; Maingret et al. 1999a; see also Lesage et al. 2000a), exhibit flickering-bursting behavior, and a strongly outwardly rectifying single-channel I-V when recorded at asymmetrical (close to physiological) potassium concentrations (Fig. 2.1a, left). In atrial myocytes (Terrenoire et al. 2001), recordings from native TREK-1-like single-channels also revealed outward rectification at asymmetrical potassium concentrations. Thus, it seems likely that TREK channels do not permit the passage of significant inward potassium current in physiological conditions.

By contrast, there are clear differences among TREK channels when single-channels are studied at symmetrical potassium concentrations (approximately 150 mM on each side; Fig. 2.1a, right). In these conditions TREK-1 single-channel currents still exhibit clear outward rectification and a conductance of about 100 pS at positive potentials (Patel et al. 1998; Kim et al. 2001a; Maingret et al. 2002; Li et al. 2006). This single-channel outward rectification disappears in the absence of extracellular divalent cations (Ca^{2+} and Mg^{2+}) and the single-channel I–V becomes linear (Fig. 2.1a, right; dotted blue line) or very slightly inwardly rectifying (Bockenhauer et al. 2001; Maingret et al. 2002; Han et al. 2003; Li et al. 2006). Native TREK-1-like channels showing high conductance (84–120 pS) at positive potentials have also been described in rat atrial (Terrenoire et al. 2001) and ventricular (Tan et al. 2002; Kang et al. 2005; Li et al. 2006) myocytes, as well as rat hippocampal (Bockenhauer et al. 2001), Dorsal Root Ganglia (DRG: Kang et al. 2005) and supraoptic (Han et al. 2003) neurons.

TREK-2 single-channels exhibit clear inward rectification at symmetrical potassium concentrations (Fig. 2.1a, right; red line), with much lower conductance at positive (approx. 65 pS at + 40 mV) than at negative (approx. 110 pS at -40 mV) voltages (Bang et al. 2000; Kim et al. 2001b; Han et al. 2002, 2003; Kang et al. 2004). Interestingly, human TREK-2 channels display much weaker rectification (Lesage et al. 2000b). Similar disparities in conductance at different membrane potentials have been reported for native TREK-2-like single-channel currents in cerebellar (Han et al. 2002; Kang et al. 2005), supraoptic (Han et al. 2003), pancreatic (Kang et al. 2004), DRG (Kang et al. 2005) and ganglionar sympathetic (Cadaveira-Mosquera et al. 2011) cells.

Heterologously expressed single TRAAK channels exhibit inward rectification at symmetrical potassium concentrations, although to a lesser degree than the TREK-2 channel (Fig. 2.1a, right; black line), showing a conductance of about 75 pS and > 100 pS at positive and negative membrane potentials respectively (Kim et al. 2001a; Han et al. 2003). Similar results were obtained for native TRAAK-like channels from supraoptic (Han et al. 2003) and DRG (Kang et al. 2005; Kang and Kim 2006) neurons.

In summary, the outward rectification induced by external divalent cations when single TREK channels are recorded at equimolar potassium concentrations appears to

be exclusive to TREK-1 (Enyedi and Czirják 2010). The single-channel rectification observed in divalent cation-free and symmetrical solutions is probably an intrinsic property of the channel produced by the structural characteristics of the channel pore. Interestingly, at least two different isoforms of TREK-1 (one of them permeable to sodium) and TREK-2, with clearly different conductances, can be expressed in heterologous systems by alternative translation initiation mechanisms (Thomas et al. 2008; Simkin et al. 2008). Several sub-conductance levels have also been reported (Li et al. 2006; Kang et al. 2007).

While leak channels are expected to be voltage-independent, the open probability of TREK-1 channels increases at positive membrane potentials, such that their voltage-dependency is not negligible (Maingret et al. 2002; Li et al. 2006). Interestingly, phosphorylation by Protein Kinase A (PKA) of TREK-1 and TREK-1-like channels expressed in hippocampal cells induces voltage-dependency in the otherwise leak-like channel (Bockenhauer et al. 2001; but see Maingret et al. 2002). The open probability of both human (Lesage et al. 2000b) and rat (Bang et al. 2000; Kang et al. 2007) TREK-2 channels also increases at positive potentials. This observation may explain the unexpected outward rectification of TREK-2 macroscopic currents at symmetrical K^+ concentrations, even when the single-channel I–V is clearly inwardly rectifying in the same conditions. Also TRAAK channels have been described as slightly voltage-dependent, with significant increases in P_o observed at positive membrane potentials (Maingret et al. 1999a; Kim et al. 2001a).

2.2.2 TREK Macroscopic-Current Properties

Unlike single-channel currents, macroscopic (whole-cell) currents are usually studied at physiological (asymmetrical) potassium concentrations. In these conditions the I-Vs for heterologously expressed TREK-1 (Fink et al. 1996; Meadows et al. 2000; Bockenhauer et al. 2001; Koh et al. 2001; Enyeart et al. 2002; Maingret et al. 2002; Kennard et al. 2005), TREK-2 (Bang et al. 2000; Lesage et al. 2000b) and TRAAK (Fink et al. 1998; Maingret et al. 1999a; Duprat et al. 2000; Lesage et al. 2000a; Meadows et al. 2001) currents are all strongly outwardly rectifying, with almost no inward current (Fig. 2.1b, left). This behavior appears to be independent of the subunit source (mouse, rat or human) and the heterologous system employed (oocyte (OO), COS or HEK), and rectification often exceeds that predicted by the constant field theory. Native TREK-1-like macroscopic currents from adrenocortical cells (Enyeart et al. 2002; Danthi et al. 2003) and TREK-2-like currents from cortical astrocytes and sympathetic neurons (Ferroni et al. 2003; Kucheryavykh et al. 2009; Cadaveira-Mosquera et al. 2011) are also predominantly outward, crossing the voltage axis near the Nernst equilibrium potential for potassium.

Although uncommon, analysis of TREK macroscopic currents in symmetrical conditions reveals that I–Vs can exhibit clear inward currents at negative potentials (Fig. 2.1b, right), indicating that the strong outward rectification observed at physiological concentrations (Fig. 2.1b, left) is not (or at least not completely) due

to voltage dependency. This phenomenon has been described in heterologously expressed TREK-1 (Patel et al. 1998; Koh et al. 2001; Maingret et al. 2002; Lopes et al. 2005; Sandoz et al. 2006; Cohen et al. 2008), TREK-2 (Lesage et al. 2000b) and TRAAK (Fink et al. 1998; Lesage et al. 2000a; Meadows et al. 2001) channels. Interestingly, TREK-1 and TREK-2 currents do not completely linearize at equimolar potassium concentrations and a clear outward rectification is still evident (Fig. 2.1b; right, blue and red lines). The macroscopic rectification of TREK-1 can be attenuated by removing divalent Mg^{2+} and Ca^{2+} cations and the residual outward rectification in these conditions has been ascribed to the intrinsic voltage-dependency of TREK-1 channels (Maingret et al. 2002; Sandoz et al. 2006; Li et al. 2006). However, this remaining rectification was recently attributed to voltage-dependent inhibition by protons as in the absence of Mg^{2+}, mutant TREK-1 channels that are insensitive to H^+ exhibit an essentially linear I-V at symmetrical K^+ concentrations (Cohen et al. 2008). Linear, or very slightly outwardly-rectifying I–Vs have been described for TRAAK, indicating a lack of intrinsic voltage dependency for this channel or possibly a compensation for the slight voltage dependency by inward single-channel rectification (Fink et al. 1998; Lesage et al. 2000a; Ozaita and Vega-Saenz de Miera 2002). At symmetrical K^+ concentrations, linear or weak outwardly-rectifying I–Vs have also been described for native TREK-1-like (Danthi et al. 2003) and TREK-2-like (Ferroni et al. 2003; Cadaveira-Mosquera et al. 2011) macroscopic currents.

While initial analyses of macroscopic currents evoked by voltage steps indicated no time dependency accompanying TREK-1 outward rectification (Meadows et al. 2000; Maingret et al. 2000a), clear time-dependent activation was reported subsequently (Bockenhauer et al. 2001; Maingret et al. 2002; Kennard et al. 2005). Thus, it has been proposed that two distinct populations of TREK-1 channels may coexist in physiological conditions, one phosphorylated and hence voltage-dependent, and the other dephosphorylated and voltage-independent. If true, step-activated macroscopic current should exhibit both instantaneous and time-dependent components, which indeed has been frequently reported (Enyeart et al. 2002; Kennard et al. 2005). Similarly, voltage changes result in rapid activation of human TREK-2 currents, exhibiting instantaneous and delayed components (Lesage et al. 2000b; Kim et al. 2005). By contrast, TRAAK channels appear to produce instantaneous non-inactivating currents when the membrane is voltage-stepped (Fink et al. 1998; Duprat et al. 2000; Lesage et al. 2000a; Ozaita and Vega-Saenz de Miera 2002).

A second and distinct form of voltage-dependence has been described for TREK-1 macroscopic currents expressed in oocytes. A slow, progressive increase in TREK-1 currents in response to membrane hyperpolarization has been reported, which declined when the membrane was depolarized (Segal-Hayoun et al. 2010). As a result, it was proposed that the resting membrane potential (or holding voltage) modulates the activity of Gq-coupled receptors in the absence of agonist, such that persistent membrane depolarization activates the Gq cascade, depleting PIP2 levels and thereby inhibiting TREK-1 activity.

Regulation of TREK-1 activity by extracellular sodium and potassium concentrations has been reported in heterologous systems (oocytes). A reduction in the $[Na]_o$ clearly inhibited macroscopic outward currents, whereas the outward current slope

conductance was augmented when the $[K]_o$ increased from 2–98 mM, indicating a potentiating effect of both extracellular Na^+ and K^+ (Fink et al. 1996; Meadows et al. 2000; Ma et al. 2011). TREK-2 outward currents are also larger than expected from the driving force at high external K^+ concentrations, and they are reduced when the Na^+ concentration drops (Lesage et al. 2000b), suggesting a stimulating effect of extracellular K^+ and Na^+ similar to that described for TREK-1 channels. The modulation of TREK channels by external K^+ may be important in pathologies involving large variations in extracellular potassium concentrations, such as epilepsy and brain or heart ischemia.

In summary, the strong outward rectification observed in TREK currents at physiological K^+ concentrations appears to result from the interplay of "open rectification" (for all three channel types), weak voltage-dependence (mainly TREK-1 and probably TREK-2) and blockage (exclusively TREK-1) by divalent cations (Enyedi and Czirják 2010). While TREK channels deviate from the classical definition of leak channels, they can still be considered resting channels, as they remain open across the physiological voltage range and do not inactivate, despite of their voltage-dependency. In addition, TREK channels lack the classical positively charged S4 transmembrane domain and their apparent "activation threshold" follows the potassium equilibrium potential rather than depending on the membrane voltage (Fink et al. 1996).

2.2.3 Resting Membrane Potential and Excitability

The heterologous expression of TREK channels in oocytes, COS or HEK cells clearly modifies the resting membrane potential by shifting its value (20–50 mV) towards the equilibrium potential for potassium, as described for TREK-1 (Fink et al. 1996; Gruss et al. 2004a; Thomas et al. 2008), TREK-2 (Kim et al. 2005) and TRAAK (Fink et al. 1998; Meadows et al. 2001; Ozaita and Vega-Saenz de Miera 2002). The influence of TREK channels on the resting membrane potential of real neurons is more difficult to determine, nevertheless, several authors have reported rather soft effects following pharmacological modulation or genetic deletion/overexpression of TREK channels (Ferroni et al. 2003; Heurteaux et al. 2004; Alloui et al. 2006; Yang and Jan 2008; Deng et al. 2009).

Modulation of TREK-2-like native currents mildly influences the resting membrane potential and excitability of mouse sympathetic neurons (Cadaveira-Mosquera et al. 2011). A depolarization of 10 mV is observed only when TREK channels are blocked strongly by fluoxetine (100 μM), while relatively high concentrations of riluzole (300 μM) induce a comparable hyperpolarization (Cadaveira-Mosquera et al. 2011). Fluoxetine also decreases the latency to the first action potential evoked by current-injections, but it fails to attenuate the adaptation of sympathetic neurons as expected (Cadaveira-Mosquera et al. 2011). This may seem a disappointing result for the channel touted as the long-awaited "leak channel". However, we should bear in mind that the sympathetic neurons of the superior cervical ganglion (SCG) are

endowed with a number of other voltage-dependent (potassium M-type, cationic H-type, sodium persistent) and voltage-independent (unidentified chloride and sodium) channels that will influence the resting membrane potential (Lamas 1998; Lamas et al. 2002; Romero et al. 2004; Lamas 2005; Lamas et al. 2009). Whether TREK channels are additional contributors or the main regulators of the resting membrane potential remains to be determined.

2.3 Pharmacology

The pharmacology of K2P channels is extremely complex (Lesage 2003). Traditionally, researchers have sought to identify the most selective channel blocker in order to study a given ion current. However, K2P channels in general, and the TREK subfamily in particular, have demonstrated the importance of channel enhancers as useful tools to study the channels themselves but also as putative useful tools in clinical pharmacology.

2.3.1 Channel Blockers

A distinctive characteristic of K2P channels is that they are not sensitive to most classic potassium channel blockers. It is generally agreed that all members of the TREK subfamily, TREK-1 (Fink et al. 1996; Patel et al. 1998; Meadows et al. 2000; Koh et al. 2001; Han et al. 2003; Moha ou Maati et al. 2011), TREK-2 (Bang et al. 2000; Lesage et al. 2000b; Han et al. 2002, 2003; Kang et al. 2007; Deng et al. 2009; Kucheryavykh et al. 2009; Xiao et al. 2009; Cadaveira-Mosquera et al. 2011) and TRAAK (Fink et al. 1998; Lesage et al. 2000a; Ozaita and Vega-Saenz de Miera 2002; Han et al. 2003) are insensitive to millimolar concentrations of TEA, 4-AP and Cs^+. TREK channels are also insensitive to blockers of the calcium-dependent potassium channels such as apamin, charybdotoxin, iberiotoxin and paxilline (Kang et al. 2007; Mazella et al. 2010; Cadaveira-Mosquera et al. 2011; Moha ou Maati et al. 2011), ATP-sensitive potassium channels like glibenclamide and tolbutamide (Kucheryavykh et al. 2009; Moha ou Maati et al. 2011), inward rectifier potassium channels like tertiapin (Deng et al. 2009), voltage-dependent sodium channel such as TTX and valproate (Cadaveira-Mosquera et al. 2011) and calcium channels such as Cd (Cadaveira-Mosquera et al. 2011). However, other calcium channel blockers such as mibefradil, penfluridol and pimozide do effectively inhibit heterologously expressed and native TREK-1 channels (Enyeart et al. 2002; Chemin et al. 2005a).

The effect of Ba^{2+} on TREK channels has originated some discrepancies (see Patel and Honore 2001). TREK-1 was found to be insensitive to or very slightly inhibited by low concentrations ($\leq$1 mM) of barium (Patel et al. 1998; Meadows et al. 2000; Zhou et al. 2009), although stronger inhibition had been described with equivalent and higher concentrations (Fink et al. 1996; Ma et al. 2011). Inhibition

of TREK-2 with $\geq$2 mM (Bang et al. 2000; Han et al. 2002; Ferroni et al. 2003; Kang et al. 2007; Xiao et al. 2009; Cadaveira-Mosquera et al. 2011) but not with $\leq$1 mM (Lesage et al. 2000b; Kim et al. 2005) has also been reported. Similarly Ba^{2+} was also found to block mouse (Fink et al. 1998) but not human (Lesage et al. 2000a; Ozaita and Vega-Saenz de Miera 2002) or rat (Han et al. 2003) TRAAK homologues. In summary, TREK channels can be inhibited by moderate millimolar concentrations of barium. However, complete dose-response relationships must be stablished to determine whether distinct TREK subunits or their orthologues exhibit different sensitivities. A putative competition between Ba^{2+} and extracellular K^+, recently reported, should also be taken into account (see Ma et al. 2011).

There is also conflicting data regarding the effects of quinine and quinidine. While these alkaloids have been reported to inhibit TREK-1 (Patel et al. 1998; Meadows et al. 2000; Zhou et al. 2009; Seifert et al. 2009) and TREK-2 (Lesage et al. 2000b; Ferroni et al. 2003; Kucheryavykh et al. 2009), other studies found no effects on TREK-1 (Fink et al. 1996; Koh et al. 2001), TREK-2 (Bang et al. 2000; Han et al. 2002; Cadaveira-Mosquera et al. 2011) and TRAAK channels (Lesage et al. 2000a; Ozaita and Vega-Saenz de Miera 2002).

The inorganic dye ruthenium red (RR) can interact with a large number of ion channels, including K2P. RR strongly blocks macroscopic currents via heterologously expressed TRAAK (Czirják and Enyedi 2002, 2006) but not TREK-1 channels (Czirják and Enyedi 2002). Besides, we recently reported that RR fails to block TREK-2-like native sympathetic currents (Cadaveira-Mosquera et al. 2011), suggesting RR as a useful tool with which to identify native TRAAK channels.

The antidepressant fluoxetine strongly inhibits TREK currents. Interestingly TREK-1-KO, but not TRAAK-KO, mice are much less sensitive to depression and stress than normal cohorts, and they exhibit a behavior similar to that of control mice treated with classical antidepressants (Heurteaux et al. 2006). As TREK-1-KO mice exhibit abnormally high dorsal raphe activity, the antidepressant phenotype has been attributed to the loss of this channel in serotonin-producing neurons (Bayliss and Barrett 2008). Fluoxetine and norfluoxetine strongly inhibit TREK-1 channels (Kennard et al. 2005; Heurteaux et al. 2006; Sandoz et al. 2011; Moha ou Maati et al. 2011; Eckert et al. 2011), while a range of serotonin reuptake inhibitors and antidepressants (including fluoxetine, paroxetine, sertraline, fluvoxamine, maprotiline, citalopram, mirtazapine and doxepin) block human TREK-1 currents at concentrations that do not affect TRAAK (Heurteaux et al. 2006; Eckert et al. 2011). TREK-2 channels are also inhibited by fluoxetine (Kang et al. 2008; Cadaveira-Mosquera et al. 2011), although clinically related drugs such as lamotrigine have no such effect (Kang et al. 2008). In summary, fluoxetine can be used to distinguish between TREK-1/2 and TRAAK channels. Furthermore, inhibiting TREK-1 may be a putative strategy to develop new antidepressants and other mood regulators (Gordon and Hen 2006) as recently demonstrated with the peptide spadin (Mazella et al. 2010; Moha ou Maati et al. 2011). In fact, it has been recently observed an association between human genetic variants in the TREK-1 locus and patient resistence to multiple antidepressant classes (Perlis et al. 2008).

Heterologously expressed human TREK-1 and TREK-2, but not TRAAK, macroscopic and inside-out currents have been reported to be inhibited by antipsychotic substances like fluphenacine, chlorpromazine, haloperidol, flupenthixol, loxapine, clozapine and pimozide but not by sulpiride and tiapride (Patel et al. 1998; Thümmler et al. 2007), suggesting that TREK-1 may also be related with other psychiatric disorders like schizophrenia.

2.3.2 Channel Enhancers

Volatile general anesthetics such as chloroform, cyclopropane, diethyl ether, halothane, isoflurane, nitrous oxide, sevoflurane and xenon reversibly activate currents (macroscopic or single-channel) via mouse and human TREK-1 channels, and they hyperpolarize COS cells expressing TREK-1 (Patel et al. 1998, 1999; Heurteaux et al. 2004; Franks and Honore 2004; Gruss et al. 2004a). Natively-expressed TREK-1-like channels in astrocytes and striatal neurons are also activated by halothane (Heurteaux et al. 2004; Seifert et al. 2009). The effect of volatile anesthetics has been attributed to their direct action, independent of second messengers (Patel et al. 1999). The strong resistance of TREK-1-KO mice to gaseous anesthetics such as chloroform, halothane, sevoflurane, desflurane and isofluorane may have important clinical relevance (Heurteaux et al. 2004) and indeed, TREK-1-KO and TRAAK-KO mice display thermal and mechanical hyperalgesia (Alloui et al. 2006; Noël et al. 2009). In contrast to general anesthetics, the barbiturate pentobarbital has no effect on macroscopic TREK-1 currents and it displays comparable anesthetic effects in KO and wt mice (Heurteaux et al. 2004). Macroscopic TREK-2 currents are also strongly activated by gaseous anesthetics such as chloroform, halothane and isofluorane (Lesage et al. 2000b; Gu et al. 2002) but not by bupivacaine or lidocaine (Bang et al. 2000; Han et al. 2002). On the contrary, TRAAK macroscopic currents from mouse and human are insensitive to volatile general anesthetics such as chloroform, diethyl ether, halothane and isoflurane (Patel et al. 1999; Lesage et al. 2000a). Taken together, these findings suggest that TREK channels may be potential targets for the development of new analgesics and anesthetics.

While macroscopic currents through heterologously expressed TREK-1 (Czirják and Enyedi 2006) and TREK-2 (Kim et al. 2005; Czirják and Enyedi 2006) channels are markedly enhanced by low micromolar concentrations (about 10 μM) of zinc (Zn^{2+}), human TREK-1 is inhibited by high (IC_{50} ca. 650 μM) Zn^{2+} concentrations (Gruss et al. 2004b). Species differences and in expression systems could underlie this discrepancy, although the concentrations used may also have contributed to the divergent outcomes. Macroscopic currents generated by the expression of TRAAK channels (Czirják and Enyedi 2006) are only slightly inhibited at much higher concentrations of Zn^{2+}. Moreover, activation by Zn^{2+} of native TREK-2-like macroscopic currents in sympathetic neurons has been recently demonstrated (Cadaveira-Mosquera et al. 2011). Zinc is an important component of a large number of proteins and it is also synaptically released from glutamatergic neurons (Freder-ickson

and Bush 2001). Thus, TREK channels have been proposed as possible targets for synaptically released zinc (Kim et al. 2005; Czirják and Enyedi 2006). A similar enhancement of TREK-1 and TREK-2 currents is induced by the mercuric ion (Hg^{2+}), having no effect on TRAAK currents (Czirják and Enyedi 2006). TREK-1 (Gruss et al. 2004b) and TREK-2 (Kim et al. 2005) macroscopic currents are also activated by low micromolar concentrations of copper (Cu^{2+}) applied to the extracellular side of the membrane. These divalent cations can be useful to distinguish native TRAAK from TREK-1/2 channels.

Initial studies suggested that macroscopic currents from TREK-1 channels were insensitive to intracellular acidification by CO_2 bubbling (Fink et al. 1996). However, intracellular acidification using extracellular HCO_3^- or dinitrophenol (DNP) strongly increases heterologously expressed TREK-1 macroscopic outward currents (Maingret et al. 1999b; Duprat et al. 2000). Single-channel TREK-1 (Maingret et al. 1999b; Honore et al. 2002; Chemin et al. 2005b; Sandoz et al. 2006; Moha ou Maati et al. 2011) and TREK-2 (Bang et al. 2000; Lesage et al. 2000b; Kim et al. 2001b; Kang et al. 2007) currents are also enhanced by low pH levels in cell-attached (extracellular application of CO_2, HCO_3^- or removal of NH_4Cl) and inside-out patches. Macroscopic and single-channel currents in natively expressed TREK-1-like channels from myocytes, supraoptic, DRG and striatal neurons (Enyeart et al. 2002; Tan et al. 2002; Han et al. 2003; Heurteaux et al. 2004; Kang et al. 2005; Chemin et al. 2005b; Alloui et al. 2006) and TREK-2-like channels from cerebellar, entorhinal, supraoptic and sympathetic neurons (Han et al. 2002, 2003; Kang et al. 2005, 2007; Deng et al. 2009; Cadaveira-Mosquera et al. 2011) are also strongly enhanced by intracellular acidification. Indeed, circumvallate and foliate taste buds express TREK-1 and TREK-2 channels, suggesting a role on the sour taste transduction (Richter et al. 2004).

Interestingly, extracellular acidification was recently proposed to strongly inhibit single-channels and macroscopic currents when human TREK-1 channels are expressed in oocytes, while the murine counterpart is much less sensitive (Cohen et al. 2008, 2009; Ma et al. 2011). This inhibition appears to involve two distinct temporal components, with an initial rapid inhibition (within seconds) due to direct protonation of the channel and a subsequent slower reduction (within minutes), probably involving proton-sensing G-protein receptors and a second messenger of the Gq-PLC pathway (Cohen et al. 2009). Note that both TREK-1 and TREK-2 channels have also been reported to be substantially insensitive to the acidification of the extracellular medium (Lesage et al. 2000b; Zhou et al. 2009).

Analysis of TRAAK currents has revealed an increase in macroscopic currents in response to alkalinization, however no effect is observed in response to either external or internal acidification (Fink et al. 1998; Maingret et al. 1999b). Recording of TRAAK channels in inside-out patches has further demonstrated the insensitivity of these channels to intracellular acidosis (Maingret et al. 1999b; Kim et al. 2001a), and their activation by intracellular alkalinization (Kim et al. 2001a; Han et al. 2003).

Coexpression of the A-kinase-anchoring protein (AKAP150) with TREK-1 and TREK-2, but not with TRAAK channels, strongly enhanced whole-cell macroscopic currents in COS cells (Sandoz et al. 2006). Whether this scaffolding protein interacts ubiquitously with TREK channels in native cells is still a matter of debate.

2.3.3 Neuroprotectors

In several heterologous systems (OO, COS, HEK, CHO), both single-channel and macroscopic currents from human and rodent TREK-1 are strongly and reversibly potentiated by arachidonic acid (AA) and other polyunsaturated free fatty acids (PUFAs), such as docosahexaenoate, oleate and linolenate (Patel et al. 1998; Maingret et al. 1999b, 2000b; Meadows et al. 2000; Honore et al. 2002; Sandoz et al. 2006; Mazella et al. 2010; Moha ou Maati et al. 2011). Natively expressed channels with properties resembling those of TREK-1 are also activated by AA in astrocytes (Seifert et al. 2009), myocytes (Kang et al. 2005; Li et al. 2006) and cerebellar (Lauritzen et al. 2000), supraoptic (Han et al. 2003), striatal (Heurteaux et al. 2004; Chemin et al. 2005a), hippocampal (Mazella et al. 2010) and DRG neurons (Alloui et al. 2006). By contrast, saturated fatty acids (SFA) such as arachidate, myristate, palmitate or stearate have no effect on macroscopic (Maingret et al. 2000b) or single-channel (Patel et al. 1998; see also Maingret et al. 2000a) TREK-1 currents. Notably, TREK-1-KO, but not TRAAK-KO, mice are extremely sensitive to kainic acid-induced epileptic seizures and to experimentally-induced global and spinal cord ischemia mortality (Heurteaux et al. 2004). Interestingly, expressed TREK-1 macroscopic currents are strongly activated by FCCP, an inductor of chemical ischemia (Honore et al. 2002) and moreover, the presence of TREK-1 channels in HEK cells protects them from OGD-induced ischemia (Moha ou Maati et al. 2011). Accordingly, enhancing TREK-1 currents by administration of PUFAs (linolenic) and lysophospholipids (lysophosphatidyl-choline), but not with saturated fatty acids (palmitic), elicits a strongly anti-ischemic effect in wild-type but not in TREK-1-KO mice (Lauritzen et al. 2000; Blondeau et al. 2002; Heurteaux et al. 2004). Based on these findings it is tempting to speculate that activation of TREK-1 channels may decrease neuronal excitability and enhance blood flow during cerebral ischemia, thereby diminishing brain damage (Blondeau et al. 2007; Bayliss and Barrett 2008).

Macroscopic (Lesage et al. 2000b; Gu et al. 2002) and single-channel (Bang et al. 2000; Kim et al. 2001b; Han et al. 2002; Kang et al. 2007) currents from heterologously expressed TREK-2 channels are also activated by low micromolar concentrations of unsaturated fatty acids (arachidonic, docosahexanoic, eicosapentaenoic, linolenic, linoleic, and oleic), yet not by saturated (elaidic, palmitic and stearic) fatty acids (Bang et al. 2000; Lesage et al. 2000b). Similarly, natively expressed TREK-2-like single-channels (in cerebellar granule and DRG neurons) and macroscopic currents (in sympathetic neurons and astrocytes) are activated by arachidonic and linolenic acids but not by the saturated AA-analog arachidic acid (Ferroni et al. 2003; Kang et al. 2005; Kucheryavykh et al. 2009; Cadaveira-Mosquera et al. 2011).

Significantly, the enhancement of mouse TRAAK currents by arachidonic acid (AA) and other unsaturated fatty acids led to the specific nomenclature of this channel. Micromolar concentrations of AA and other unsaturated fatty acids (docosahexaenoate, eicosapentaenoate, linoleate, oleate and linolenate) induce a strong, reversible and dose-dependent increase in the amplitude of the macroscopic and/or single-channel currents from heterologously expressed TRAAK channels (Fink et al.

1998; Maingret et al. 1999a, 1999b, 2000b; Lesage et al. 2000a; Meadows et al. 2001; Kim et al. 2001a; Han et al. 2003), while saturated fatty acids (myristate, palmitate, stearate and arachidate) again produce no such effects (Fink et al. 1998; Lesage et al. 2000a; Maingret et al. 2000b). TRAAK activation by AA develops slowly, resulting in an outwardly rectifying macroscopic current. Similar results have been reported for the mouse, rat and human orthologs. Members of the TREK subfamily are strongly activated by AA and other PUFAs in inside-out and outside-out patch configurations but not in cell-attached patches, suggesting a direct effect on the channel or on the lipid environment (for a review see Patel et al. 2001).

Lysophospholipids, such as lysophosphatidylcholine (LPC) and lysophosphatidylinositol (LPI), strongly enhance the heterologously expressed macroscopic TREK-1 (Maingret et al. 2000b), TREK-2 (Lesage et al. 2000b) and TRAAK (Maingret et al. 2000b) currents at low concentrations. Similar potentiation is induced by platelet-activating factor, but not by phosphatidylcholine, lysophosphatidic acid (LPA) or choline (Maingret et al. 2000b). The action of LPA seems to be complex, it has been reported to strongly inhibit macroscopic currents and to antagonize LPC-activated currents through TREK-1 channels expressed in oocytes (Cohen et al. 2009), but also to enhance expressed TREK-1, TREK-2 and TRAAK and native striatal TREK-1-like channels in inside-out patches but not in whole-cell, outside-out or cell-attached patches (Chemin et al. 2005a). Lysophospholipids, at least LPC, may influence TREK-1 channels via a second messenger, as LPC strongly activates the channel in cell-attached patches but not in excised-patches (Maingret et al. 2000b). A similar hypothesis (involving PLC) has been proposed for the inhibitory effect of LPA (Cohen et al. 2009).

The neuroprotective, anti-convulsive and anti-ischemic drug riluzole, currently used to treat amyotrophic lateral sclerosis (ALS), potentiates macroscopic currents through heterologously expressed mouse, rat and human TREK-1 (Duprat et al. 2000; Meadows et al. 2000; Moha ou Maati et al. 2011) and TREK-2 channels (Lesage et al. 2000b). This activating effect is transient, and is followed by current decline and ultimately, strong inhibition. Similar transient current activation has been described in natively expressed adrenocortical (Enyeart et al. 2002), sympathetic (Cadaveira-Mosquera et al. 2011) and nodose ganglion cells (Fernández-Fernández et al. 2011). Inclusion of riluzole in the pipette also increases the open probability of TREK-2 single-channels in cell-attached patches from SCG neurons (Cadaveira-Mosquera et al. 2011). Secondary TREK-1 inhibition has been attributed to the inhibition of PDA, which increases cAMP levels and provokes channel phosphorylation by PKA (Duprat et al. 2000). Interestingly, riluzole also induces a sustained increase in the open probability of single heterologous TREK-1 channels when recorded in excised outside-out channels, suggesting that the inhibition is through second messengers (Duprat et al. 2000). Macroscopic and single-channel currents from TRAAK channels are also strongly enhanced by riluzole (Fink et al. 1998; Duprat et al. 2000), but distinctively, the macroscopic current activation is sustained as long as the presence of riluzole is maintained (Duprat et al. 2000).

Notably, another neuroprotective agent, sipatrigine, but not lamotrigine, strongly inhibits hTREK-1 and hTRAAK currents in HEK cells (Meadows et al. 2001).

While the link between potassium channel inhibition and neuroprotection remains unclear, TREK-1 overexpression has recently been proposed as a marker for prostate cancer, and sipatrigine was shown to inhibit the proliferative effect of TREK-1 overexpression (Voloshyna et al. 2008).

In summary, several known nervous system protective factors strongly increase the activity of TREK channels, including the heterogeneous "neuroprotective agents", unsaturated fatty acids and lysophospholipids. TREK channels are also robustly activated by disturbances associated with tissue damage, such as cell swelling, intracellular acidification and increases in the concentration of free fatty acids. The hyperpolarization induced by the activation of TREK channels is thought to reduce calcium influx through voltage-gated calcium channels and NMDA receptors, thereby acting as a neuroprotective signal. The enhancement of TREK currents by a large number of neuroprotective agents singles out this K2P subfamily as a promising target for the development of new neuroprotective strategies and drugs.

2.4 Mechanosensitivity

It is generally accepted that TREK channels are selectively activated by the convex curvature of the membrane. Accordingly, a reversible increase in the open probability of these channels has been reported in response to negative pressure applied to the external surface (or positive pressure to the internal surface), osmotic changes that induce cell swelling, shear stress and the application of crenating compounds. Although cytoskeletal integrity is not necessary to maintain mechanosensitivity, it appears to repress mechanical activation of TREK channels, probably by opposing to membrane stretch (Lesage and Lazdunski 2000).

The open probability of heterologously expressed members of the TREK subfamily, TREK-1 (Patel et al. 1998; Maingret et al. 1999b, 2000a, 2002; Koh et al. 2001; Honore et al. 2002, 2006; Moha ou Maati et al. 2011), TREK-2 (Bang et al. 2000; Lesage et al. 2000b; Kim et al. 2001b; Kang et al. 2007) and TRAAK (Maingret et al. 1999a, 1999b; Lesage et al. 2000a; Kim et al. 2001a; Han et al. 2003) is gradually increased when negative pressure is applied to the recording pipette in cell-attached and inside-out patches (Fig. 2.2a). Consistently, TRAAK activity is only enhanced by positive pressure in outside-out patches (Maingret et al. 1999a; Honore et al. 2006). Although more commonly studied in heterologous systems, natively expressed TREK-1-like (Tan et al. 2002; Han et al. 2003; Heurteaux et al. 2004; Kang et al. 2005; Chemin et al. 2005a; Alloui et al. 2006), TREK-2-like (Han et al. 2003; Kang et al. 2005, 2007) and TRAAK-like (Han et al. 2003) channels also exhibit this behavior in myocytes, DRG, supraoptic, cerebellar and striatal neurons. In general the open probability of TREK channels is very low at atmospheric pressure (Fig. 2.2a) and it increases with negative pressure in a dose-dependent manner, with half-maximal activation between -20 and -60 mmHg (Patel et al. 1998; Maingret et al. 1999a, 1999b; Bang et al. 2000; Kim et al. 2001a; see also Han et al. 2003).

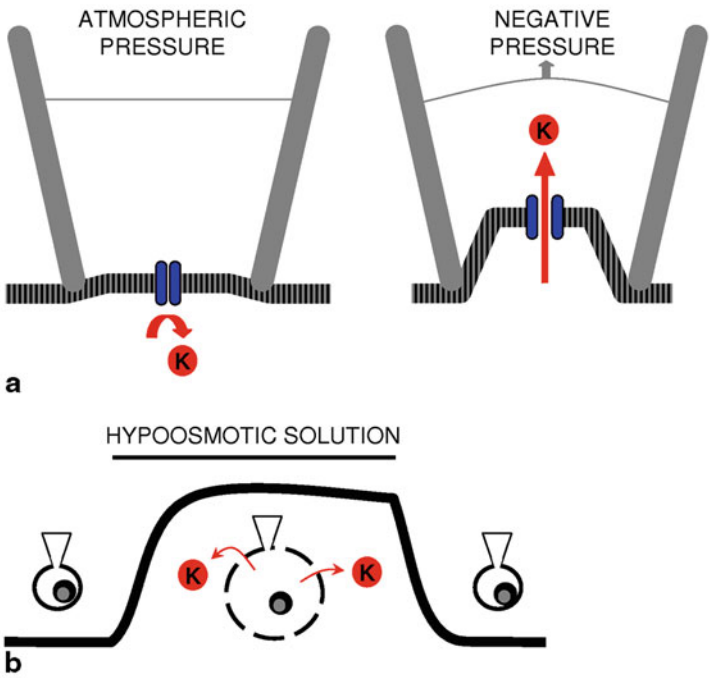

Fig. 2.2 TREK channels are mechanosensitive. In cell-attached or outside-out patches, the open probability of TREK channel is very low (**a**, *left*), while it increases greatly when negative pressure (suction) is applied to the recording pipette (**a**, *right*). Similarly, cell swelling induced by an extracellular solution of low osmolarity strongly increases the macroscopic whole-cell current through TREK channels (**b**). The data are not real but rather, they are based on our own experiments in sympathetic neurons where a change in osmolarity from 290–245 mOsm invoked an outward current of about 220 pA. (see Cadaveira-Mosquera et al. 2011)

Macroscopic currents through heterologously expressed TREK-1 channels are reversibly modulated by membrane stretching (Fig. 2.2b). When extracellular osmolarity is increased (cell shrinking) the amplitude is reduced, while decreases in osmolarity (cell swelling) increase current amplitude (Patel et al. 1998; see also Maingret et al. 2000a). TREK-1 macroscopic currents can also be activated by laminar shear stress induced by increasing the speed of bath perfusion (Patel et al. 1998) or by cell elongation using a micromanipulator (Koh et al. 2001). Similar effects have been described for native TREK-1-like (Li et al. 2006) and TREK-2-like (Ferroni et al. 2003; Cadaveira-Mosquera et al. 2011) macroscopic currents.

The degree of activation by negative pressure appears to be greater at positive potentials (Patel et al. 1998; Maingret et al. 1999a; Lesage et al. 2000b; Kim et al. 2001a). Moreover, a synergistic effect of mechanical activation combined with activation by variations in AA and pH has been described for TREK-1, TREK-2 and TRAAK channels (Maingret et al. 1999b; Kim et al. 2001a, 2001b; Honore et al. 2002). Interestingly, TREK-1 and TRAAK, but not TREK-2 currents

evoked by negative pressure undergo strong desensitization within a 100 ms time-frame, an effect prevented by acidic pH values or in the presence of AA (Honore et al. 2006).

Inhibition of macroscopic and single-channel TREK-1 (Maingret et al. 2000b), TREK-2-like (Ferroni et al. 2003) and TRAAK (Maingret et al. 1999a) currents evoked by mechanical stimuli and other activators has been described using stretch-sensitive channel blockers such as amiloride and gadolinium (Gd^{3+}). Surprisingly, insensitivity of both TREK-1 (Fink et al. 1996) and TREK-2 (Bang et al. 2000) channels to 100 μM Gd^{3+} has also been reported. While the reason for these conflicting results remains unclear, Gd^{3+} may more effectively block evoked rather than background TREK currents.

Crenators are anionic and neutral amphipathic molecules that insert preferentially into the external membrane leaflet, altering membrane curvature (Hao et al. 2009). Several such compounds, including trinitrophenol (TNP) and lysolecithin, can activate TREK-1 (Patel et al. 1998) and TRAAK (Maingret et al. 1999a) macroscopic currents. By contrast, TREK-1 and TREK-2 currents are inhibited by "cup-formers" such as chlorpromazine (CPZ) and tetracaine, cationic amphipathic molecules that insert preferentially into the internal membrane leaflet (Patel et al. 1998; Maingret et al. 2000b; Chemin et al. 2005a; Honore et al. 2006). These results suggest that TREK channels are activated by the expansion of the membrane, consistent with their strong activation by negative pressure applied through the recording pipette or upon induction of cell swelling.

An interesting question is whether mechanical stimulation acts via the cell cytoskeleton. Mechanical activation of TREK-1 and TRAAK channels persists when cytoskeleton-disrupting agents are applied to inside-out patches (e.g., colchicine, latrunculin A or cytochalasin D), and they even activate the channels in cell-attached patches (Patel et al. 1998; Maingret et al. 1999a; Lauritzen et al. 2005; Honore et al. 2006). Together with the enhanced activation by negative pressure in excised versus cell-attached patches (Maingret et al. 1999a; Bang et al. 2000; Lauritzen et al. 2005; Honore et al. 2006; Moha ou Maati et al. 2011), these findings suggest that the cytoskeleton exerts a continuous negative regulatory effect on TREK channels, even though mechanical stimulation seems to be directly transmitted by the deformation of the lipid bilayer.

Similarly, it remains unknown whether TREK channel mechanosensitivity plays a major role in neuronal function in the CNS, where they are widely expressed (Fink et al. 1998; Reyes et al. 2000; Meadows et al. 2000; Lesage et al. 2000b; Talley et al. 2001; Hervieu et al. 2001; Medhurst et al. 2001; Gu et al. 2002). However, this sensitivity is thought to play a general role in controlling cell shape and volume, as well as cone motility and elongation (Maingret et al. 1999a; Reyes et al. 2000; Lauritzen et al. 2005).

TREK channels expressed in somatosensory DRG neurons of the peripheral nervous system (PNS) (Talley et al. 2001; Medhurst et al. 2001; Kang and Kim 2006), and mechanosensitive neurons innervating the bladder and colon (La et al. 2011) are involved in the detection and transduction of skin and organ deformation, and even in mechanically-evoked painful stimuli (Maingret et al. 2000a; Kang and Kim 2006;

Yamamoto et al. 2009). In fact, TREK-1-KO, TRAAK-KO and TREK-1/TRAAK-KO mice all exhibit significant mechanical hypersensitivity to stimulation with von Frey hairs (Alloui et al. 2006; Noël et al. 2009).

To date, the expression of these channels in the autonomic nervous system has received little attention. However, we recently described strong expression of TREK-1 channels in the visceral afferents of the mouse nodose ganglion (Fernández-Fernández et al. 2011; Cadaveira-Mosquera et al. 2012) and TREK-2 in motor neurons of the mouse superior cervical ganglia (Cadaveira-Mosquera et al. 2011, 2012), although all three members were expressed in both ganglia. Expression of TREK-1 and TRAAK has also been reported in the rat nodose ganglion (Zhao et al. 2010) and a role for these channels has been proposed in gastrointestinal acid sensation (Holzer 2011). TRAAK channels were also recently identified in the terminals of mechanosensitive vagal afferents innervating the lungs (Lembrechts et al. 2011). Given the capacity of several internal organs to change size and form, these channels may play a key role in transmitting mechanical information from them to the central nervous system, but also in regulating some vagal reflexes.

Some TREK channels (mainly TREK-1 but not TRAAK) are also strongly expressed in the smooth muscle fibers of the visceral organs that are subjected to deformation, such as the lung, uterus, stomach, intestine, colon and bladder (Reyes et al. 1998; Koh et al. 2001). In fact, the stretch-activated potassium channels found in colonic myocytes may be TREK-1 channels (Koh et al. 2001). TREK-1 has also been described in the smooth muscle cells of pulmonary blood vessels (Lembrechts et al. 2011).

TREK-1 (Fink et al. 1996; Li et al. 2006) but not TREK-2 or TRAAK (Li et al. 2006) channels are well expressed in the heart (for a review see Gurney and Manoury 2009) and TREK-1 activation during heart contraction may contribute to cardiomyocyte repolarization and hyperpolarization, preventing the occurrence of ventricular extrasystoles (Patel et al. 1998; Tan et al. 2002; Li et al. 2006). Intracellular acidosis and cell swelling occurs during heart ischemia, which will activate TREK-1 channels and induce protective hyperpolarization. Finally, TREK-1 has been proposed to participate in the regulation of the heart by β-adrenergic stimulation (Terrenoire et al. 2001).

2.5 Thermosensitivity

TREK-1 channels are thought to act as cold-sensors at the level of peripheral sensory and central hypothalamic neurons, arguing that low temperature would close them and hence depolarize the neurons increasing their excitability (Maingret et al. 2000a; Viana et al. 2002). Nonetheless, all three members of the TREK subfamily exhibit a similar degree of sensitivity to temperature changes, suggesting that TREK channels may be involved in temperature regulation and thermonociception (Kang et al. 2005; Pongs 2009).

While heterologously expressed TREK-1 (Maingret et al. 2000a; Kang et al. 2005), TREK-2 (Kang et al. 2005) and TRAAK (Kang et al. 2005) single-channels show weak activity at room temperature when recorded in cell-attached patches, their open probability (NPo) strongly and progressively increases as bath temperatures are raised (approximately 10-fold/10 °C). Interestingly, activation of all three channels by increasing temperature is dependent on cell integrity and it disappears in excised patches, suggesting the participation of an intracellular second messenger in temperature transduction (Maingret et al. 2000a; Kang et al. 2005; Honore 2007). Similarly, all TREK channels are activated by negative pressure, AA and intracellular pH modifications when recorded at 37 °C in either cell-attached or inside-out patches (Kang et al. 2005). The increase in temperature strongly potentiates the response of TREK-1 channels to membrane stretching, again revealing a synergistic effect of several stimuli on TREK channel activity (Maingret et al. 2000a). Natively expressed TREK-1, TREK-2 and TRAAK-like channels are also temperature-dependent when recorded in myocytes, astrocytes, cerebellar, entorhinal and DRG neurons (Kang et al. 2005; Deng et al. 2009; Kucheryavykh et al. 2009).

Heterologously expressed TREK-1, TREK-2 and TRAAK channels generate small outwardly rectifying macroscopic potassium currents at room temperature (22–24 °C), which are quickly, strongly and reversibly enhanced by progressive increases in temperature to 37 °C (Maingret et al. 2000a; Kang et al. 2005). In fact, current through TREK-1 channels is essentially absent at 12 °C (Maingret et al. 2000a). Interestingly, the current enhancement coupled with increased temperature is strongly attenuated by increasing extracellular osmolarity and by cAMP administration (CPT-cAMP, 0.5 mM), probably via PKA activation (Maingret et al. 2000a).

In general TREK channels are often reported to have a low open probability at rest and in the absence of any stimulus, and hence only a mild contribution to maintain the resting membrane potential should be expected. However, as the majority of these studies were carried out at room temperature (22–24 °C), the role of TREK channels in cellular behavior was probably underestimated. For greater understanding of this role, further experiments should be carried out at temperatures closer to physiological body temperature (32–37 °C: (see Lotshaw 2007).

TREK channels are strongly expressed in a large number of sensory neurons involved in thermal and thermonociceptive sensory transduction, including the dorsal root ganglion (Maingret et al. 2000a; Meadows et al. 2001; Talley et al. 2001; Medhurst et al. 2001; Kang et al. 2005; Alloui et al. 2006), trigeminal (Hervieu et al. 2001; Yamamoto et al. 2009) and autonomic vagal (Zhao et al. 2010; Fernández-Fernández et al. 2011; Cadaveira-Mosquera et al. 2012) sensory neurons. In fact, TREK-1-KO and TREK-1/TRAAK-KO mice exhibit heat hyperalgesia, probably due to the increased sensitivity of small DRG neurons and C-fibers from KO mice to noxious heat (Alloui et al. 2006; Noël et al. 2009). Double but not single KO strains, also exhibit cold-hyperalgesia (Noël et al. 2009). Finally, TREK-1 channels are strongly expressed in hypothalamic regions classically involved in regulating body temperature (Maingret et al. 2000a).

2.6 G-Protein Modulation

The primary structure of TREK proteins reveals several potential phosphorylation sites for protein kinase C (PKC), PKA and protein kinase G (PKG) in the cytoplasmic C-terminus (Fink et al. 1996, 1998; Patel et al. 1998; Bang et al. 2000; Lesage et al. 2000b; Koh et al. 2001; Murbartian et al. 2005), suggesting putative modulation of TREK channels by the activation of G protein-coupled receptors (GPCRs). It was recently proposed that under most experimental conditions, basal G protein activity mediates the constant down regulation of TREK-1 (Cohen et al. 2009), and perhaps TREK-2, channels (Xiao et al. 2009).

Macroscopic currents from heterologously expressed TREK-1 (Fink et al. 1996; Patel et al. 1998; Duprat et al. 2000; Maingret et al. 2000b; Enyeart et al. 2002; Honore et al. 2002; Murbartian et al. 2005; Alloui et al. 2006) and TREK-2 (Bang et al. 2000; Lesage et al. 2000b; Gu et al. 2002), but not TRAAK (Fink et al. 1998) channels, are consistently inhibited by increasing intracellular cAMP levels with IBMX + forskolin, or CPT-cAMP. Stimulation of co-expressed Gs-coupled 5-HT_4 receptors also inhibits macroscopic TREK-1 (Patel et al. 1998) and TREK-2 (Lesage et al. 2000b) currents through the activation of adenylate cyclase (AC).

By contrast, activation of the co-expressed Gi-coupled mGluR2 and $GABA_B$ receptors augment TREK-2 currents (Lesage et al. 2000b; Deng et al. 2009). In fact, the hyperpolarization and associated decrease in neuronal excitability induced by norepinephrine and GABA in neurons from the entorhinal cortex has been attributed to the stimulation of native Gi-coupled receptors, and the consequent activation of TREK-2-like channels by inhibition of the AC-cAMP-PKA pathway (Deng et al. 2009; Xiao et al. 2009). The modulation of TREK-2 channels in the entorhinal cortex seems to be related with spatial learning in rats (Deng et al. 2009).

The role of the cGMP pathway is more complex, as stimulation of PKG using sodium nitroprusside (SNP) or 8-Br-cGMP only increases TREK-1 macroscopic currents when using the perforated (but not the ruptured) patch-clamp technique (Koh et al. 2001). However, both SNP and 8-Br-cGMP increase the open probability of TREK-1 channels in cell-attached patches (Koh et al. 2001).

Expressed TREK-1 and TREK-2 channel currents are also inhibited by activating co-expressed Gq-coupled group I glutamate mGluR1 (Lesage et al. 2000b; Chemin et al. 2003; Sandoz et al. 2011), 5HT2cR (Sandoz et al. 2011), THRH1 (Murbartian et al. 2005), Orx1R (Murbartian et al. 2005) and muscarinic M1 (Lopes et al. 2005) and M3 (Kang et al. 2006, 2008) receptors (see Fig. 2.3), in whole-cell and cell-attached patches but not in outside-out patches (Kang et al. 2006). This inhibition requires the activation of phospholipase C (PLC), and while it is insensitive to pertussis and cholera toxins, it is suppressed by the PLC inhibitor U73122 (Chemin et al. 2003; Kang et al. 2006). PLC inhibition also greatly increases human TREK-1 currents when these channels are expressed in oocytes (Segal-Hayoun et al. 2010). However, the next steps in this pathway remain unclear, with little agreement on the second messenger involved.

Macroscopic whole-cell TREK-1 currents are potently inhibited by ACh in oocytes co-expressing M1 receptors (Lopes et al. 2005). PIP2 applied to inside-out

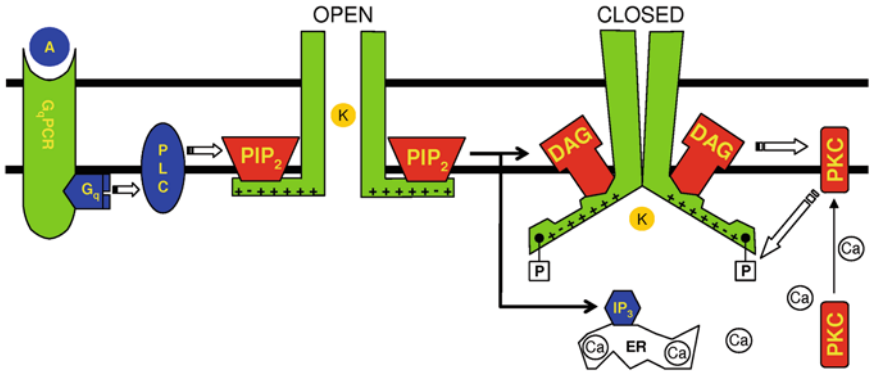

Fig. 2.3 TREK-1 and TREK-2 but not TRAAK are inhibited by the activation of Gq protein-coupled receptors. Agonists (*A*) of Gq protein-coupled receptors (*Gq-PCR*) activate Gq proteins, which in turn stimulate phospholipase C (*PLC*). PLC breaks down phosphatidylinositol-bisphosphate (PIP_2) to produce inositol-triphosphate (IP_3) and diacylglycerol (*DAG*). IP_3 migrates to the endoplasmic reticulum (*ER*) to induce calcium (Ca) release, while DAG activates protein kinase C (*PKC*), which in turn phosphorylates (-P) TREK channels. The identity of the elements in this cascade that directly mediate TREK channel inhibition remains unclear. Of the three mechanisms proposed (in red), detachment of PIP_2, direct interaction with DAG and/or phosphorylation by PKC, the first appears the most plausible

macropatches strongly enhances the activity of heterologously expressed TREK-1 channels, while poly-lysine (a competitor of PIP2) and wortmannin (a blocker of PI 4-kinases that impedes PIP2 replenishment) inhibit their activity, suggesting that PIP2 depletion by PLC underlies the agonist-induced inhibition of TREK-1 (Lopes et al. 2005; Chemin et al. 2005b, 2007). Findings from our laboratory show that native TREK-2-like channels expressed in sympathetic neurons are inhibited by agonists in a PIP2-dependent manner, via activation of Gq proteins (Reboreda et al. 2010; Rivas-Ramírez et al. 2011). However, addition of antibodies against PIP2, blockade of its replenishment with wortmannin, or the use of PIP2 depletion systems were also reported not to affect TREK1/2 macroscopic currents (Chemin et al. 2003; Kang et al. 2006; Sandoz et al. 2011). Confusingly, also PIP or even PI may interact with TREK channels so that PIP2 depletion may not be sufficient to see a strong current inhibition (Chemin et al. 2005b; Segal-Hayoun et al. 2010; Sandoz et al. 2011).

Administration of DOG, a membrane-permeable analog of DAG, rapidly inhibits TREK-1/2 macroscopic currents, while impermeable DAG-analogs (SAG and SLG) also inhibit AA-evoked single-channel TREK-1 and TREK-2 currents in inside-out patches. Hence, DAG may directly inhibit TREK channels without the participation of PKC (Chemin et al. 2003). However, DAG or its impermeable DAG-analogs also fail to substantially affect TREK-1 and TREK-2 currents in inside-out macropatches (Lopes et al. 2005; Kang et al. 2006).

Phosphorylation by PKC has been proposed to mediate the modulation of TREK channels by Gq proteins, based on the inhibition of TREK-1/2 currents by the PKC

activators PMA and PDBu (Fink et al. 1996; Maingret et al. 2000b; Gu et al. 2002; Murbartian et al. 2005; Kang et al. 2006). Moreover, the PKC inhibitor bisindolylmaleimide (BIS) reportedly attenuates the inhibition of TREK-1/2 by TRH, ACh and OrxA (Murbartian et al. 2005; Kang et al. 2006). However, elsewhere no such effect on TREK-1/2 currents was observed with the PKC activators PMA and PDBu or PKC inhibition with staurosporine, calphostin-C or a PKC peptide inhibitor (Bang et al. 2000; Lesage et al. 2000b; Chemin et al. 2003), or on their inhibition by glutamate, ACh or serotonin (Chemin et al. 2003; Lopes et al. 2005; Sandoz et al. 2011). Similarly, modulation of intracellular calcium and IP_3 levels has no effect on TREK1/2 currents (Lesage et al. 2000b; Chemin et al. 2003; Kang et al. 2006) or their inhibition by glutamate or ACh (Chemin et al. 2003; Lopes et al. 2005).

There is however a good agreement in that TRAAK channels are not modulated through Gq-protein coupled receptors, given the insensitivity of TRAAK expressed currents to the activation of co-expressed mGluR1 (Chemin et al. 2003) and M1 (Lopes et al. 2005) receptors. Neither changes in the internal calcium concentration (IP_3, EGTA) nor activation of PKC (PMA) affect TRAAK currents (Fink et al. 1998), yet application of PIP2 to inside-out macropatches does activate TRAAK channels, an effect dependent on prior mechanical stimulation (Lopes et al. 2005).

In summary, the modulation of TREK-1/2 channels by the activation of Gq-coupled receptors is far from being understood. While several elements of the PLC cascade (mainly PIP2, DAG and PKC; see Fig. 2.3) have been proposed to influence the activity of these channels, there is also evidence to the contrary. Currently, the PIP2 depletion theory appears to be the most attractive (see also Suh and Hille 2005; Lotshaw 2007; Suh and Hille 2007). Accordingly, it has been proposed that the final mechanism involves the dissociation of the TREK-1 polybasic C-terminal from the plasma membrane (see Fig. 2.3) when membrane PIP2 is broken down (Chemin 2005; Sandoz 2011; Honore 2007).

2.7 Distribution/Expression

A good number of the important functions ascribed to K2P channels come from the extensive distribution of these channels in the mammalian body. The widespread expression of TREK channels both in and beyond the nervous system has been described in the mouse (Fink et al. 1996, 1998; Reyes et al. 2000), rat (Bang et al. 2000; Talley et al. 2001; Hervieu et al. 2001; Gu et al. 2002) and human (Meadows et al. 2000; Lesage et al. 2000a, 2000b; Meadows et al. 2001; Medhurst et al. 2001). The expression of TREK channels (in the form of mRNA, protein or channel current) has been assessed using a wide variety of techniques including RT-PCR, qRT-PCR, immunocytochemistry, immunohistochemistry, *in situ* hybridisation, Northern blot, Western blot and electrophysiology.

The interpretation of expression data is hampered by several limitations. Firstly, not all techniques are equally appropriate for quantitative analysis and secondly, expression levels are generally represented in qualitative or comparative terms, limiting

comparison between studies. In addition, the levels of TREK channel expression may differ between species (see Table 2.1), although almost identical distributions have been reported for all TREK subfamily members in the mouse and rat CNS (Talley et al. 2001). Therefore, the data summarized below and in Table 2.1 should be regarded as orientative, and the reader is encouraged to read the original articles for specific details. To avoid unnecessary complexity, expression data is grouped into three main categories: strong (S), which includes medium, strong and very strong expression; weak (W), including what authors reported as weak or very weak expression; and absent (A), which refers to absence or failure to detect expression. Where discrepancies exist, more than one of these labels is assigned to a given region in Table 2.1, although it should be noted that some of these discrepancies may have arisen through my own interpretation of other authors' data.

2.7.1 Strong Expression

Since their initial identification, all three TREK channels (TREK-1, TREK-2 and TRAAK) have been seen to be strongly expressed in the brain of the three most commonly studied species (mouse, rat and human: see Table 2.1), specifically in the amygdala, basal ganglia, cortex, dorsal root ganglia and hippocampus. TREK-1 channels have been also reported to be well expressed in the brain, cortex, hippocampus, hypothalamus and DRG of all three species. It is notable that there is almost no expression data for TREK-2 in the mouse, (but see Aller and Wisden 2008). However, TREK-2 channels show a good level of expression in rat an human amygdala, brain, cerebellum, hippocampus, thalamus, DRG, pancreas, spleen and testis. Also in the three species, TRAAK has been shown to be well expressed in amygdala, brain, cortex and hippocampus (Fink et al. 1996, 1998; Patel et al. 1999; Bang et al. 2000; Reyes et al. 2000; Meadows et al. 2000, 2001; Lauritzen et al. 2000; Lesage et al. 2000a, 2000b; Maingret et al. 2000a; Talley et al. 2001; Hervieu et al. 2001; Medhurst et al. 2001; Kim et al. 2001a; Gu et al. 2002; Dobler et al. 2007; Putzke et al. 2007; Aller and Wisden 2008; La et al. 2011).

2.7.2 Weak Expression

Structures in which TREK-1 data have shown a weak expression in at least one of the species and strong expression has not been reported in any of them are: brain stem, globus palidus, habenula, pons, supraoptic, SCG, trigeminal ganglion, pancreas, pituitary gland, prostate, testis, thymus and uterus. The same type of weak expression was reported for TREK-2 in arcuate, interpeduncular, red nucleus, spinal cord, nodose ganglion, trigeminal ganglion, heart, liver, lung, pituitary gland, placenta, prostate, skeletal muscle, stomach, thymus and ventricle. For TRAAK in arcuate, astrocytes, colliculus, interpeduncular, medulla, solitary nucleus, substantia nigra,

Table 2.1 Tissue distribution of TREK channels. Data were compiled from studies that used any technical approach permitting the reasonable quantification of mRNA, protein or ionic current. The category labeled strong (**S**) refers to medium, strong and very strong expression levels, weak (**W**) refers to weak and very weak levels and absent (**A**) describes absent or undetectable expression

	TREK-1			TREK-2			TRAAK		
	m	r	h	m	r	h	m	r	h
Central nervous system									
Accumbens[12,14,23–25,34]		SA	SW		A	S		W	S
Amygdala[9,10,12,14,20,23–25,34,34]	W	S	SW		SW	SA	S	S	SW
Arcuate nucleus[12,14,34]		S			W			W	
Basal ganglia[9,10,12,14,20,23–25,29,34]	W	S	S			S	S		S
Brain[2,9,10,12,15,19,20,23,25,27,28,31]	S	S	SW	S	S	S	S	S	S
Brain stem[9,10,29]	W						SW		
Caudate[1,9,10,12,14,20,24,25,29]	W	SW	S	W	A	S	SW		S
Cerebellum[1,2,9,10,12,14,18,20,23–25,29,33,34]	SW	W	W	S	SA	S	SW	W	WA
Cerebellum (nuclei)[9,10,12,29]	W	A			A		S		
Cochlear nuclei[14,29,34]		SA			A		S	A	
Colliculus[1,14]		S					W		
Cortex[1,9,10,12,14,20,23,25,29,34]	S	SW	S		W	S	SW	S	S
Cortex (frontal)[14,20,24,25]		S	SW			SW			S
Cortex (temporal)[1,20,25]			SW			S	W		S
Cortex (occipital)[20,25]			SW			S			S
Cortex (parietal)[14]		S							
Cortex (enthorrinal)[1,6,10,38]		W			S		SW		
Cortex (piriform)[9,10,12,14,34]	S	S			S		S	S	
Dorsal motor vagus[12]		S			S				
Facial nucleus[12,14]		S			S				
Gigantocellular nuleus[12]		A			S				
Glia[5,10]	A	A							
Glia (astrocytes)[8,11,32,42]	S	WA			S		W	A	
Globus pallidus[9,12,14,24,34]	W	WA			A			A	S

Table 2.1 (continued)

	TREK-1			TREK-2			TRAAK		
	m	r	h	m	r	h	m	r	h
Habenula[9,10,12,34]	W	WA			SW		S	A	
Hippocampus[1,9,10,12,14,18,18,20,23–25,29,34]	SW	S	S	W	SWA	S	SW	S	S
Hypoglossus[12]		S			S				
Hypothalamus[9,10,12,14,22–25,29,33,34]	SW	S	SW		WA	S	SW	W	W
Interpeduncular nucleus[12,14,34]		S			WA			WA	
Locus coeruleus[12,24,34]		A			SA			A	SW
Medulla[2,9,10,20,24]	W		S		A	S	W		W
Midbrain[2,9,14]	W	S			A				
Oculomotor[14]		S							
Olfactory bulb[9,10,12,29,34]	S	SW			S		S	W	
Olive[14]		S							
Olive (inferior)[12]		S			A				
Pons[2,9,10,12,29,34]	W	A			SWA		SW		
Putamen[1,9,10,12,14,20,24,25,29]	W	SW	S	W	A	S	SW		S
Raphe[12,14,34]		S			SW			A	
Red nucleus[14,34]		SA			W			A	
Septum[14,34]		SA			A			A	
Solitary nucleus[12,34]		S			SWA			WA	
Spinal cord[2,10,14,20,21,23–25,29,34]		SW	S		WA	WA	S	W	WA
Striatum[24,29,34]		S			A		S	W	S
Subiculum[1,10,14,29]	S	S					S		
Subthalamic nucleus[14,34]		SA			A			W	
Substantia nigra[9,10,14,20,23–25,34]	W	SA	SW		A	S	W	A	W
Supraoptic[12,13,34]		W			SW			W	
Thalamus[1,2,9,10,12,14,20,23–25,29,34]	W	SW	S	W	SWA	S	SW	W	SW
Trigeminal N. (motor)[12]		S			S				
Tigeminal N. (spinal)[12,14,29,34]		SW			SW		S	W	
Trigeminal N. (principal)[14]		S							
Vestibular nuclei[14,29,34]		SWA			A		S	A	

Table 2.1 (continued)

	TREK-1			TREK-2			TRAAK		
	m	r	h	m	r	h	m	r	h
Periferal somatic and autonomic nervous system									
Carotid body[40]		S							
DRG[7,17,22,24,25,34]	S	S	S	S	S	S	SW	S	SW
Fibroblasts[26,40]	A	A							
Glia[26]	A	A							
Nodose ganglion[4,41]	S	W		W			W	W	
Retina[10,29]							S		
Satellite cells[4,5]	A			A			A		
Superior cervical ganglion[4,5]	W			S			W		
Trigeminal ganglion[33,39]		W			WA			W	
Vestibular ganglion[26]	S	S		A			A		
Non neuronal organs and tissues									
Adipose tissue[24]									A
Bladder[10]							A		
Bone[24]									A
Cartilage[24]									A
Colon[2,10,15,19,20]			A		A	S	A	A	A
Heart[2,9,10,12,15,19,20,23–25,28,35,36]	S	S	A		WA	WA	A	A	A
Heart (atrium)[2,10,15]					A		A	A	
Heart (ventricle)[2,10,15,28,35]		S			WA		A	A	
Intestine[2,10,15,19,20,23–25]			SW		A	SW	A	A	WA
Kidney[2,9,10,12,15,19,20,23–25]	S		SW		A	S	A	A	WA
Liver[2,9,10,12,15,19,20,23–25,25]	A		A		A	WA	A	S	A
Lung[2,9,10,12,15,19,20,23–25,25]	S		A		A	WA	A	W	A
Ovary[19,20]			S			A	A		A
Pancreas[2,12,15,19,20,23–25]			WA		S	SW		S	A
Pituitary gland[23–25]			W			W			WA
Placenta[2,10,12,19,20,23–25]			A		A	WA	A		SW

Table 2.1 (continued)

	TREK-1			TREK-2			TRAAK		
	m	r	h	m	r	h	m	r	h
Prostate[19,20,23–25,37]			WA			W			WA
Salivary gland[10]							A		
Skeletal muscle[2,9,10,12,15,19,20,23–25]	S		WA		A	WA	A	S	A
Smooth muscle (basilar artery)[3]	S	S							
Smooth muscle (bladder)[16]	S			A			A		
Smooth muscle (carotid artery)[3]	A	A							
Smooth muscle (intestine)[16]	S			A			A		
Smooth muscle (portal vein)[16]	S			A			A		
Smooth muscle (pulmonary artery)[16]	S			S			A		
Smooth muscle (stomach)[16]	S			S			A		
Smooth muscle (uterus)[16]	S			A			A		
Spleen[2,15,19,20,23–25]			A		S	SA		A	A
Stomach[2,10,15,23–25]			S		A	W	A	W	A
Taste buds[30]	S			S					
Testis[2,10,15,19,20,23,25]			W		S	SW	A	S	SA
Thymus[10,19,20]			W			W	A		WA
Uterus[10,23,25]			W			A	A		A

m = mouse, **r** = rat, **h** = human1. Aller and Wisden 2008; 2. Bang et al. 2000; 3. Blondeau et al. 2007; 4. Cadaveira-Mosquera et al. 2012; 5. Cadaveira-Mosquera et al. 2011; 6. Deng et al. 2009; 7. Dobler et al. 2007; 8. Ferroni et al. 2003; 9. Fink et al. 1996; 10. Fink et al. 1998; 11. Gnatenco et al. 2002; 12. Gu et al. 2002; 13. Han et al. 2003; 14. Hervieu et al. 2001; 15. Kim et al. 2001; 16. Koh et al. 2001; 17. La et al. 2011; 18. Lauritzen et al. 2000; 19. Lesage et al. 2000; 20. Lesage et al. 2000; 21. Maingret et al. 1999; 22. Maingret et al. 2000; 23. Meadows et al. 2000; 24. Meadows et al. 2001; 25. Medhurst et al. 2001; 26. Nicolas et al. 2004; 27. Patel et al. 1999; 28. Putzke et al. 2007; 29. Reyes et al. 2000; 30. Richter et al. 2004; 31. Richter et al. 2004; 32. Seifert et al. 2009; 33. Simkin et al. 2008; 34. Talley et al. 2001; 35. Tan et al. 2002; 36. Terrenoire et al. 2001; 37. Voloshyna et al. 2008; 38. Xiao et al. 2009; 39. Yamamoto et al. 2009; 40. Yamamoto and Taniguchi 2006; 41. Zhao et al. 2010; 42. Zhou et al. 2009

subthalamic, supraoptic, nodose ganglion, SCG, trigeminal ganglion, intestine, kidney, lung, piyuitary gland, prostate, stomach and thymus (Fink et al. 1996, 1998; Maingret et al. 1999a; Bang et al. 2000; Reyes et al. 2000; Meadows et al. 2000, 2001; Lauritzen et al. 2000; Lesage et al. 2000a, 2000b; Talley et al. 2001; Hervieu et al. 2001; Terrenoire et al. 2001; Medhurst et al. 2001; Kim et al. 2001a; Gu et al. 2002; Tan et al. 2002; Gnatenco et al. 2002; Han et al. 2003; Ferroni et al. 2003; Putzke et al. 2007; Voloshyna et al. 2008; Yamamoto et al. 2009; Zhou et al. 2009; Seifert et al. 2009; Zhao et al. 2010; Cadaveira-Mosquera et al. 2011, 2012).

2.7.3 No Expression

TREK-1 was reported to be absent in the gigantocellular nucleus, glial cells, locus coeruleus, fibroblasts, satellite cells, colon, liver, placenta and spleen. No TREK-2 expression has been reported in deep cerebellar nuclei, cochelar nuclei, globus pallidus, midbrain, inferior olive, septum, striatum, subthalamic nucleus, vestibular nuclei, satellite cells, vestibular ganglia, ovary and uterus. TRAAK is absent from the raphe, red nucleus, septum, satellite cells, vestibular ganglia, adipose tissue, bladder, bone, cartilage, colon, heart, ovary, salivary gland, smooth muscle, spleen and uterus (Fink et al. 1996, 1998; Bang et al. 2000; Reyes et al. 2000, 2001; Meadows et al. 2000; Lesage et al. 2000a, 2000b; Talley et al. 2001; Hervieu et al. 2001; Terrenoire et al. 2001; Medhurst et al. 2001; Koh et al. 2001; Kim et al. 2001a; Gu et al. 2002; Tan et al. 2002; Nicolas et al. 2004; Yamamoto and Taniguchi 2006; Putzke et al. 2007; Cadaveira-Mosquera et al. 2011, 2012).

2.8 Conclusion and Perspectives

TREK channels generate neuronal leak potassium currents throughout the nervous system and as such, these channels are well positioned to regulate the resting activity and excitability of the entire nervous system. Although considered background channels, they are modulated by a wide variety of physiological and pathological stimuli, including membrane potential, mechanical deformation and temperature. Together with their strong reactivity to clinically important drugs, including neuroprotectors, mood modulators, anesthetics and neurotransmitters, these properties have increased interest in TREK channels as putative targets for the development of new pharmacotherapeutic compounds. In addition, the study of TREK channels has taught us to approach leakage conductances with an open mind, as they do not always obey all the classical Hodgkin-Huxley rules. The discovery of more selective modulators of these channels should aid further understanding of their physiological and pathophysiological roles in the nervous system. Moreover, an improved and more consistent means of quantifying the distribution and expression of these channels would help clarify their true relevance in the organism.

Acknowledgments Our investigation is currently supported by grants from the Spanish Ministry of Science and Innovation (MICINN BFU2008-02952/BFI and CONSOLIDER-INGENIO CSD2008–00005) and the Galician Government (INBIOMED 2009/063) to JAL. Help from Antonio Reboreda and Alba Cadaveira is gratefully recognized.

References

Aller MI, Wisden W (2008) Changes in expression of some two-pore domain potassium channel genes (KCNK) in selected brain regions of developing mice. Neuroscience 151:1154–1172

Alloui A, Zimmermann K, Mamet J, Duprat F, Noel J, Chemin J, Guy N, Blondeau N, Voilley N, Rubat-Coudert C, Borsotto M, Romey G, Heurteaux C, Reeh P, Eschalier A, Lazdunski M (2006) TREK-1, a K^+ channel involved in polymodal pain perception. EMBO J 25:2368–2376

Bang H, Kim Y, Kim D (2000) TREK-2, a new member of the mechanosensitive tandem-pore K^+ channel family. J Biol Chem 275:17412–17419

Bayliss DA, Barrett PQ (2008) Emerging roles for two-pore-domain potassium channels and their potential therapeutic impact. Trends Pharmacol Sci 29:566–575

Blondeau N, Petrault O, Manta S, Giordanengo V, Gounon P, Bordet R, Lazdunski M, Heurteaux C (2007) Polyunsaturated fatty acids are cerebral vasodilators via the TREK-1 potassium channel. Circ Res 101:176–184

Blondeau N, Widmann C, Lazdunski M, Heurteaux C (2002) Polyunsaturated fatty acids induce ischemic and epileptic tolerance. Neuroscience 109:231–241

Bockenhauer D, Zilberberg N, Goldstein SAN (2001) KCNK2: reversible conversion of a hippocampal potassium leak into a voltage-dependent channel. Nat Neurosci 4:486–491

Cadaveira-Mosquera A, Pérez M, Reboreda A, Rivas-Ramírez P, Fernández-Fernández D, Lamas JA (2012) Expression of K2P channels in sensory and motor neurons of the autonomic nervous system. J Mol Neurosci 48:86–96

Cadaveira-Mosquera A, Ribeiro SJ, Reboreda A, Pérez M, Lamas JA (2011) Activation of TREK currents by the neuroprotective agent riluzole in mouse sympathetic neurons. J Neurosci 31:1375–1385

Chemin J, Girard C, Duprat F, Lesage F, Romey G, Lazdunski M (2003) Mechanisms underlying excitatory effects of group I metabotropic glutamate receptors via inhibition of 2P domain K^+ channels. EMBO J 22:5403–5411

Chemin J, Patel A, Duprat F, Zanzouri M, Lazdunski M, Honore E (2005a) Lysophosphatidic acid-operated K^+ channels. J Biol Chem 280:4415–4421

Chemin J, Patel AJ, Duprat F, Lauritzen I, Lazdunski M, Honore E (2005b) A phospholipid sensor controls mechanogating of the K^+ channel TREK-1. EMBO J 24:44–53

Chemin J, Patel AJ, Duprat F, Sachs F, Lazdunski M, Honore E (2007) Up- and down-regulation of the mechano-gated K(2P) channel TREK-1 by PIP (2) and other membrane phospholipids. Pflugers Arch -Eur J Physiol 455:97–103

Cohen A, Ben-Abu Y, Hen S, Zilberberg N (2008) A novel mechanism for human K2P2.1 channel gating. Facilitation of C-type gating by protonation of extracellular histidine residues. J Biol Chem 283:19448–19455

Cohen A, Sagron R, Somech E, Segal-Hayoun Y, Zilberberg N (2009) Pain-associated signals, acidosis and lysophosphatidic acid, modulate the neuronal K(2P)2.1 channel. Mol Cell Neurosci 40:382–389

Czirják G, Enyedi P (2002) TASK-3 dominates the background potassium conductance in rat adrenal glomerulosa cells. Mol Endocrinol 16:621–629

Czirják G, Enyedi P (2006) Zinc and mercuric ions distinguish TRESK from the other two-pore-domain K^+ channels. Mol Pharmacol 69:1024–1032

Danthi S, Enyeart JA, Enyeart JJ (2003) Modulation of native TREK-1 and Kv1.4 K^+ channels by polyunsaturated fatty acids and lysophospholipids. J Membr Biol 195:147–164

Dedman A, Sharif-Naeini R, Folgering JH, Duprat F, Patel A, Honore E (2009) The mechano-gated K(2P) channel TREK-1. Eur Biophys J 38:293–303

Deng PY, Xiao Z, Yang C, Rojanathammanee L, Grisanti L, Watt J, Geiger JD, Liu R, Porter JE, Lei S (2009) GABAB Receptor Activation Inhibits Neuronal Excitability and Spatial Learning in the Entorhinal Cortex by Activating TREK-2 K^+ Channels. Neuron 63:230–243

Dobler T, Springauf A, Tovornik S, Weber M, Schmitt A, Sedlmeier R, Wischmeyer E, Doring F (2007) TRESK two-pore-domain K^+ channels constitute a significant component of background potassium currents in murine dorsal root ganglion neurones. J Physiol 585:867–879

Duprat F, Lesage F, Patel AJ, Fink M, Romey G, Lazdunski M (2000) The neuroprotective agent riluzole activates the two P domain K^+ channels TREK-1 and TRAAK. Mol Pharmacol 57:906–912

Eckert M, Egenberger B, Doring F, Wischmeyer E (2011) TREK-1 isoforms generated by alternative translation initiation display different susceptibility to the antidepressant fluoxetine. Neuropharmacology 61:918–923

Enyeart JJ, Xu L, Danthi S, Enyeart JA (2002) An ACTH- and ATP-regulated background K^+ channel in adrenocortical cells is TREK-1. J Biol Chem 277:49186–49199

Enyedi P, Czirják G (2010) Molecular background of leak K^+ currents: two-pore domain potassium channels. Physiol Rev 90:559–605

Fernández-Fernández D, Cadaveira-Mosquera A, Reboreda A, Rivas-Ramírez P, Domínguez V, Lamas JA (2011) Expresión de canales K2P y estudio de la corriente activada por riluzol en el ganglio nodoso. SENC Abstracts, SII-P31 http://www.senc2011.com/,

Ferroni S, Valente P, Caprini M, Nobile M, Schubert P, Rapisarda C (2003) Arachidonic acid activates an open rectifier potassium channel in cultured rat cortical astrocytes. J Neurosci Res 72:363–372

Fink M, Duprat F, Lesage F, Reyes R, Romey G, Heurteaux C, Lazdunski M (1996) Cloning, functional expression and brain localization of a novel unconventional outward rectifier K^+ channel. EMBO J 15:6854–6862

Fink M, Lesage F, Duprat F, Heurteaux C, Reyes R, Fosset M, Lazdunski M (1998) A neuronal two P domain K^+ channel stimulated by arachidonic acid and polyunsaturated fatty acids. EMBO J 17:3297–3308

Franks NP, Honore E (2004) The TREK K2P channels and their role in general anaesthesia and neuroprotection. Trends Pharmacol Sci 25:601–608

Frederickson CJ, Bush AI (2001) Synaptically released zinc: physiological functions and pathological effects. Biometals 14:353–366

Gnatenco C, Han J, Snyder AK, Kim D (2002) Functional expression of TREK-2 K^+ channel in cultured rat brain astrocytes. Brain Res 931:56–67

Goldman DE (1943) Potential, impedance and rectification in membranes. J Gen Physiol 3760

Goldstein SAN, Bockenhauer D, O'Kelly I, Zilberberg N (2001) Potassium leak channels and the KCNK family of two-P-domain subunits. Nat Rev Neurosci 2:175–184

Gordon JA, Hen R (2006) TREKing toward new antidepressants. Nat Neurosci 9:1081–1083

Gruss M, Bushell TJ, Bright DP, Lieb WR, Mathie A, Franks NP (2004a) Two-pore-domain K^+ channels are a novel target for the anesthetic gases xenon, nitrous oxide, and cyclopropane. Mol Pharmacol 65:443–452

Gruss M, Mathie A, Lieb WR, Franks NP (2004b) The two-pore-domain K^+ Channels TREK-1 and TASK-3 are differentially modulated by copper and zinc. Mol Pharmacol 66:530–537

Gu W, Günter S, Jochen RH, Hartmut E, Chiristine KS, Andreas KS, Christian D, Ortrud KS, Jürgen D (2002) Expression pattern and functional characteristics of two novel splice variants of the two-pore-domain potassium channel TREK-2. J Physiol 539:657–668

Gurney A, Manoury B (2009) Two-pore potassium channels in the cardiovascular system. Eur Biophys J 38:305–318

Han J, Truell J, Gnatenco C, Kim D (2002) Characterization of four types of background potassium channels in rat cerebellar granule neurons. J Physiol 542:431–444

Han J, Gnatenco C, Sladek CD, Kim D (2003) Background and tandem-pore potassium channels in magnocellular neurosecretory cells of the rat supraoptic nucleus. J Physiol 546:625–639

Hao J, Raoux M, Azorin N, Despoix-Rodat L, Giamarchi A, Maingret F, Crest M, Coste B, Delmas P (2009) Mechanosensitive cation currents and their molecular counterparts in mammalian sensory neurons. In: Kamkin A, Kiseleva I (ed) Mechanosensitivity of the nervous system. Mechanosensitivity in cell and tissues series, vol. 2. Springer, pp 51–64

Hervieu GJ, Cluderay JE, Gray CW, Green PJ, Ranson JL, Randall AD, Meadows HJ (2001) Distribution and expression of TREK-1, a two-pore-domain potassium channel, in the adult rat CNS. Neuroscience 103:899–919

Heurteaux C, Guy N, Laigle C, Blondeau N, Duprat F, Mazzuca M, Lang-Lazdunski L, Widmann C, Zanzouri M, Romey G, Lazdunski M (2004) TREK-1, a K^+ channel involved in neuroprotection and general anesthesia. EMBO J 23:2684–2695

Heurteaux C, Lucas G, Guy N, El Yacoubi M, Thümmler S, Peng X-D, Noble F, Blondeau N, Widmann C, Borsotto M, Gobbi G, Vaugeois J-M, Debonnel G, Lazdunski M (2006) Deletion of the background potassium channel TREK-1 results in a depression-resistant phenotype. Nat Neurosci 9:1134–1144

Hodgkin AL, Katz B (1949) The effect of sodium ions on the electrical activity of the giant axon of the squid. J Physiol 108:37–77

Holzer P (2011) Acid sensing by visceral afferent neurones. Acta Physiol (Oxf) 201:63–75

Honore E (2007) The neuronal background K2P channels: focus on TREK1. Nat Rev Neurosci 8:251–261

Honore E, Maingret F, Lazdunski M, Patel AJ (2002) An intracellular proton sensor commands lipid- and mechano-gating of the K^+ channel TREK-1. EMBO J 21:2968–2976

Honore E, Patel AJ, Chemin J, Suchyna T, Sachs F (2006) Desensitization of mechano-gated K2P channels. Proc Natl Acad Sci USA 103:6859–6864

Huang D, Yu B (2008) Recent advance and possible future in TREK-2: a two-pore potassium channel may involved in the process of NPP, brain ischemia and memory impairment. Med Hypotheses 70:618–624

Kang D, Kim D (2006) TREK-2 (K2P10.1) and TRESK (K2P18.1) are major background K^+ channels in dorsal root ganglion neurons. Am J Physiol Cell Physiol 291:C138-C146

Kang D, Choe C, Kim D (2004) Functional expression of TREK-2 in insulin-secreting MIN6 cells. Biochem Biophys Res Commun 323:323–331

Kang D, Choe C, Kim D (2005) Thermosensitivity of the two-pore domain K^+ channels TREK-2 and TRAAK. J Physiol 564:103–116

Kang D, Han J, Kim D (2006) Mechanism of inhibition of TREK-2 (K2P10.1) by the Gq-coupled M3 muscarinic receptor. Am J Physiol Cell Physiol 291:C649-C656

Kang D, Choe C, Cavanaugh E, Kim D (2007) Properties of single two-pore domain TREK-2 channels expressed in mammalian cells. J Physiol 583:57–69

Kang D, Kim GT, Kim EJ, La JH, Lee JS, Lee ES, Park JY, Hong SG, Han J (2008) Lamotrigine inhibits TRESK regulated by G-protein coupled receptor agonists. Biochem Biophys Res Commun 367:609–615

Kennard LE, Chumbley JR, Ranatunga KM, Armstrong SJ, Veale EL, Mathie A (2005) Inhibition of the human two-pore domain potassium channel, TREK-1, by fluoxetine and its metabolite norfluoxetine. Br J Pharmacol 144:821–829

Ketchum KA, Joiner WJ, Sellers AJ, Kaczmarek LK, Goldstein SA (1995) A new family of outwardly rectifying potassium channel proteins with two pore domains in tandem. Nature 376:690–695

Kim D (2003) Fatty acid-sensitive two-pore domain K^+ channels. Trends Pharmacol Sci 24:648–654

Kim Y, Bang H, Gnatenco C, Kim D (2001a) Synergistic interaction and the role of C-terminus in the activation of TRAAK K^+ channels by pressure, free fatty acids and alkali. Pflugers Arch -Eur J Physiol 442:64–72

Kim Y, Gnatenco C, Bang H, Kim D (2001b) Localization of TREK-2 K^+ channel domains that regulate channel kinetics and sensitivity to pressure, fatty acids and pHi. Pflugers Arch -Eur J Physiol 442:952–960

Kim JS, Park JY, Kang HW, Lee EJ, Bang H, Lee JH (2005) Zinc activates TREK-2 potassium channel activity. J Pharmacol Exp Ther 314:618–625

Koh SD, Monaghan K, Sergeant GP, Ro S, Walker RL, Sanders KM, Horowitz B (2001) TREK-1 regulation by nitric oxide and cGMP-dependent protein kinase. An essential role in smooth muscle inhibitory neurotransmission. J Biol Chem 276:44338–44346

Kucheryavykh LY, Kucheryavykh YV, Inyushin M, Shuba YM, Sanabria P, Cubano LA, Skatchkov SN, Eaton MJ (2009) Ischemia increases TREK-2 channel expression in astrocytes: relevance to glutamate clearance. Open Neurosci J 2:40–47

La JH, Schwartz ES, Gebhart GF (2011) Differences in the expression of transient receptor potential channel V1, transient receptor potential channel A1 and mechanosensitive two pore-domain K^+ channels between the lumbar splanchnic and pelvic nerve innervations of mouse urinary bladder and colon. Neuroscience 186:179–187

Lamas JA (1998) A hyperpolarization-activated cation current (Ih) contributes to resting membrane potential in rat superior cervical sympathetic neurones. Pflugers Arch -Eur J Physiol 436: 429–435

Lamas JA (2005) The development of the concept of neuronal resting potential. Fundamental and clinical aspects. Rev Neurol 41:538–549

Lamas JA, Reboreda A, Codesido V (2002) Ionic basis of the resting membrane potential in cultured rat sympathetic neurons. Neuroreport 13:585–591

Lamas JA, Romero M, Reboreda A, Sanchez E, Ribeiro SJ (2009) A riluzole- and valproate-sensitive persistent sodium current contributes to the resting membrane potential and increases the excitability of sympathetic neurones. Pflugers Arch -Eur J Physiol 458:589–599

Lauritzen I, Blondeau N, Heurteaux C, Widmann C, Romey G, Lazdunski M (2000) Polyunsaturated fatty acids are potent neuroprotectors. EMBO J 19:1784–1793

Lauritzen I, Chemin J, Honore E, Jodar M, Guy N, Lazdunski M, Jane PA (2005) Cross-talk between the mechano-gated K2P channel TREK-1 and the actin cytoskeleton. EMBO Rep 6:642–648

Lembrechts R, Pintelon I, Schnorbusch K, Timmermans JP, Adriaensen D, Brouns I (2011) Expression of mechanogated two-pore domain potassium channels in mouse lungs: special reference to mechanosensory airway receptors. Histochem Cell Biol 136:371–85

Lesage F (2003) Pharmacology of neuronal background potassium channels. Neuropharmacology 44:1–7

Lesage F, Lazdunski M (2000) Molecular and functional properties of two-pore-domain potassium channels. Am J Physiol Renal Physiol 279:F793-F801

Lesage F, Guillemare E, Fink M, Duprat F, Lazdunski M, Romey G, Barhanin J (1996a) TWIK-1, a ubiquitous human weakly inward rectifying K^+ channel with a novel structure. EMBO J 15:1004–1011

Lesage F, Guillemare E, Fink M, Duprat F, Lazdunski M, Romey G, Barhanin J (1996b) A pH-sensitive yeast outward rectifier K^+ channel with two pore domains and novel gating properties. J Biol Chem 271:4183–4187

Lesage F, Maingret F, Lazdunski M (2000a) Cloning and expression of human TRAAK, a polyunsaturated fatty acids-activated and mechano-sensitive K^+ channel. FEBS Lett 471:137–140

Lesage F, Terrenoire C, Romey G, Lazdunski M (2000b) Human TREK2, a 2P domain mechano-sensitive K^+ channel with multiple regulations by polyunsaturated fatty acids, lysophospholipids, and Gs, Gi, and Gq protein-coupled receptors. J Biol Chem 275:28398–28405

Li XT, Dyachenko V, Zuzarte M, Putzke C, Preisig-Muller R, Isenberg G, Daut J (2006) The stretch-activated potassium channel TREK-1 in rat cardiac ventricular muscle. Cardiovasc Res 69:86–97

Lopes CM, Rohacs T, Czirják G, Balla T, Enyedi P, Logothetis DE (2005) PIP2 hydrolysis underlies agonist-induced inhibition and regulates voltage gating of two-pore domain K^+ channels. J Physiol 564:117–129

Lotshaw DP (2007) Biophysical, pharmacological, and functional characteristics of cloned and native mammalian two-pore domain K^+ channels. Cell Biochem Biophys 47:209–256

Ma XY, Yu JM, Zhang SZ, Liu XY, Wu BH, Wei XL, Yan JQ, Sun HL, Yan HT, Zheng JQ (2011) External Ba^{2+} block of the two-pore domain potassium channel TREK-1 defines conformational transition in its selectivity filter. J Biol Chem 286:39813–39822

Maingret F, Fosset M, Lesage F, Lazdunski M, Honore E (1999a) TRAAK is a mammalian neuronal mechano-gated K^+ channel. J Biol Chem 274:1381–1387

Maingret F, Patel AJ, Lesage F, Lazdunski M, Honoré E (1999b) Mechano- or acid stimulation, two interactive modes of activation of the TREK-1 potassium channel. J Biol Chem 274: 26691–26696

Maingret F, Lauritzen I, Patel AJ, Heurteaux C, Reyes R, Lesage F, Lazdunski M, Honore E (2000a) TREK-1 is a heat-activated background K^+ channel. EMBO J 19:2483–2491

Maingret F, Patel AJ, Lesage F, Lazdunski M, Honoré E (2000b) Lysophospholipids open the two-pore domain mechano-gated K^+ channels TREK-1 and TRAAK. J Biol Chem 275:10128–10133

Maingret F, Honore E, Lazdunski M, Patel AJ (2002) Molecular basis of the voltage-dependent gating of TREK-1, a mechano-sensitive K^+ channel. Biochem Biophys Res Commun 292: 339–346

Mathie A (2007) Neuronal two-pore-domain potassium channels and their regulation by G protein-coupled receptors. J Physiol 578:377–385

Mathie A, Veale EL (2007) Therapeutic potential of neuronal two-pore domain potassium-channel modulators. Curr Opin Investig Drugs 8:555–562

Mazella J, Petrault O, Lucas G, Deval E, Beraud-Dufour S, Gandin C, El-Yacoubi M, Widmann C, Guyon A, Chevet E, Taouji S, Conductier G, Corinus A, Coppola T, Gobbi G, Nahon JL, Heurteaux C, Borsotto M (2010) Spadin, a sortilin-derived peptide, targeting rodent TREK-1 channels: a new concept in the antidepressant drug design. PLoS Biol 8 e1000355

Meadows HJ, Benham CD, Cairns W, Gloger I, Jennings C, Medhurst AD, Murdock P, Chapman CG (2000) Cloning, localisation and functional expression of the human orthologue of the TREK-1 potassium channel. Pflugers Arch -Eur J Physiol 439:714–722

Meadows HJ, Chapman CG, Duckworth DM, Kelsell RE, Murdock PR, Nasir S, Rennie G, Randall AD (2001) The neuroprotective agent sipatrigine (BW619C89) potently inhibits the human tandem pore-domain K^+ channels TREK-1 and TRAAK. Brain Res 892:94–101

Medhurst AD, Rennie G, Chapman CG, Meadows H, Duckworth MD, Kelsell RE, Gloger II, Pangalos MN (2001) Distribution analysis of human two pore domain potassium channels in tissues of the central nervous system and periphery. Brain Res Mol Brain Res 86:101–114

Moha ou Maati H, Peyronnet R, Devader C, Veyssiere J, Labbal F, Gandin C, Mazella J, Heurteaux C, Borsotto M (2011) A human TREK-1/HEK cell line: a highly efficient screening tool for drug development in neurological diseases. PLoS One 6 e25602

Murbartian J, Lei Q, Sando JJ, Bayliss DA (2005) Sequential phosphorylation mediates receptor- and kinase-induced inhibition of TREK-1 background potassium channels. J Biol Chem 280: 30175–30184

Nicolas MT, Lesage F, Reyes R, Barhanin J, Dememes D (2004) Localization of TREK-1, a two-pore-domain K^+ channel in the peripheral vestibular system of mouse and rat. Brain Res 1017:46–52

Noël J, Zimmermann K, Busserolles J, Deval E, Alloui A, Diochot S, Guy N, Borsotto M, Reeh P, Eschalier A, Lazdunski M (2009) The mechano-activated K^+ channels TRAAK and TREK-1 control both warm and cold perception. EMBO J 28:1308–1318

Noël J, Sandoz G, Lesage F (2011) Molecular regulations governing TREK and TRAAK channel functions. Channels (Austin) 5:402–409

Ozaita A, Vega-Saenz de Miera E (2002) Cloning of two transcripts, HKT4.1a and HKT4.1b, from the human two-pore K^+ channel gene KCNK4: Chromosomal localization, tissue distribution and functional expression. Mol Brain Res 102:18–27

Patel AJ, Honore E (2001) Properties and modulation of mammalian 2P domain K^+ channels. Trends Neurosci 24:339–346

Patel AJ, Honore E, Maingret F, Lesage F, Fink M, Duprat F, Lazdunski M (1998) A mammalian two pore domain mechano-gated S-like K^+ channel. EMBO J 17:4283–4290

Patel AJ, Honore E, Lesage F, Fink M, Romey G, Lazdunski M (1999) Inhalational anesthetics activate two-pore-domain background K^+ channels. Nat Neurosci 2:422–426

Patel AJ, Lazdunski M, Honore E (2001) Lipid and mechano-gated 2P domain K^+ channels. Curr Opin Cell Biol 13:422–428

Perlis RH, Moorjani P, Fagerness J, Purcell S, Trivedi MH, Fava M, Rush AJ, Smoller JW (2008) Pharmacogenetic analysis of genes implicated in rodent models of antidepressant response: association of TREK1 and treatment resistance in the STAR*D study. Neuropsychopharmacology 33:2810–2819

Plant LD, Rajan S, Goldstein SA (2005) K2P channels and their protein partners. Curr Opin Neurobiol 15:326–333

Pongs O (2009) TREKing noxious thermosensation. EMBO J 28:1195–1196

Putzke C, Wemhoner K, Sachse FB, Rinne S, Schlichthorl G, Li XT, Jae L, Eckhardt I, Wischmeyer E, Wulf H, Preisig-Muller R, Daut J, Decher N (2007) The acid-sensitive potassium channel TASK-1 in rat cardiac muscle. Cardiovasc Res 75:59–68

Reboreda A, Cadaveira-Mosquera A, Rivas-Ramírez P, Fernández-Fernández D, Domínguez V, Lamas JA (2010) Muscarinic modulation of TREK currents in culture mouse superior cervical ganglion neurons. FENS Abstr 5:013–33

Reyes R, Duprat F, Lesage F, Fink M, Salinas M, Farman N, Lazdunski M (1998) Cloning and expression of a novel pH-sensitive two pore domain K^+ channel from human kidney. J Biol Chem 273:30863–30869

Reyes R, Lauritzen I, Lesage F, Ettaiche M, Fosset M, Lazdunski M (2000) Immunolocalization of the arachidonic acid and mechanosensitive baseline TRAAK potassium channel in the nervous system. Neuroscience 95:893–901

Richter TA, Dvoryanchikov GA, Chaudhari N, Roper SD (2004) Acid-sensitive two-pore domain potassium (K2P) channels in mouse taste buds. J Neurophysiol 92:1928–1936

Rivas-Ramírez P, Reboreda A, Cadaveira-Mosquera A, Fernández-Fernández D, Domínguez V, Lamas JA (2011) Caracterización de la vía de inhibición muscarínica de corrientes TREK en neuronas del ganglio cervical superior en cultivo. SENC Abstracts, SIII-P33, www senc2011 com

Romero M, Reboreda A, Sánchez E, Lamas JA (2004) Newly developed blockers of the M-current do not reduce spike frequency adaptation in cultured mouse sympathetic neurons. Eur J Neurosci 19:2693–2702

Sabbadini M, Yost CS (2009) Molecular biology of background K^+ channels: insights from K2P knockout mice. J Mol Biol 385:1331–1344

Salkoff L, Jegla T (1995) Surfing the DNA databases for K^+ channels nets yet more diversity. Neuron 15:489–492

Sandoz G, Thummler S, Duprat F, Feliciangeli S, Vinh J, Escoubas P, Guy N, Lazdunski M, Lesage F (2006) AKAP150, a switch to convert mechano-, pH- and arachidonic acid-sensitive TREK K^+ channels into open leak channels. EMBO J 25:5864–5872

Sandoz G, Bell SC, Isacoff EY (2011) Optical probing of a dynamic membrane interaction that regulates the TREK1 channel. Proc Natl Acad Sci USA 108:2605–2610

Segal-Hayoun Y, Cohen A, Zilberberg N (2010) Molecular mechanisms underlying membrane-potential-mediated regulation of neuronal K2P2.1 channels. Mol Cell Neurosci 43:117–126

Seifert G, Huttmann K, Binder DK, Hartmann C, Wyczynski A, Neusch C, Steinhauser C (2009) Analysis of astroglial K^+ channel expression in the developing hippocampus reveals a predominant role of the Kir4.1 subunit. J Neurosci 29:7474–7488

Simkin D, Cavanaugh EJ, Kim D (2008) Control of the single channel conductance of K2P10.1 (TREK-2) by the amino-terminus: role of alternative translation initiation. J Physiol 586: 5651–5663

Suh BC, Hille B (2005) Regulation of ion channels by phosphatidylinositol 4,5-bisphosphate. Curr Opin Neurobiol 15:370–378

Suh BC, Hille B (2007) Regulation of KCNQ channels by manipulation of phosphoinositides. J Physiol 582:911–916

Talley EM, Solorzano G, Lei Q, Kim D, Bayliss DA (2001) CNS distribution of members of the two-pore-domain (KCNK) potassium channel family. J Neurosci 21:7491–7505

Talley EM, Sirois JE, Lei Q, Bayliss DA (2003) Two-pore-domain (KCNK) potassium channels: dynamic roles in neuronal function. Neuroscientist 9:46–56

Tan JHC, Liu W, Saint DA (2002) Trek-like potassium channels in rat cardiac ventricular myocytes are activated by intracellular ATP. J Membr Biol 185:201–207

Terrenoire C, Lauritzen I, Lesage F, Romey G, Lazdunski M (2001) A TREK-1-like potassium channel in atrial cells inhibited by beta-adrenergic stimulation and activated by volatile anesthetics. Circ Res 89:336–342

Thomas D, Plant LD, Wilkens CM, McCrossan ZA, Goldstein SAN (2008) Alternative translation initiation in rat brain yields $K_2P2.1$ potassium channels permeable to sodium. Neuron 58: 859–870

Thümmler S, Duprat F, Lazdunski M (2007) Antipsychotics inhibit TREK but not TRAAK channels. Biochem Biophys Res Commun 354:284–289

Viana F, de la Peña E, Belmonte C (2002) Specificity of cold thermotransduction is determined by differential ionic channel expression. Nat Neurosci 5:254–260

Voloshyna I, Besana A, Castillo M, Matos T, Weinstein IB, Mansukhani M, Robinson RB, Cordon-Cardo C, Feinmark SJ (2008) TREK-1 is a novel molecular target in prostate cancer. Cancer Res 68:1197–1203

Xiao Z, Deng PY, Rojanathammanee L, Yang C, Grisanti L, Permpoonputtana K, Weinshenker D, Doze VA, Porter JE, Lei S (2009) Noradrenergic depression of neuronal excitability in the entorhinal cortex via activation of TREK-2 K^+ channels. J Biol Chem 284:10980–10991

Yamamoto Y, Taniguchi K (2006) Expression of tandem P domain K^+ channel, TREK-1, in the rat carotid body. J Histochem Cytochem 54:467–472

Yamamoto Y, Hatakeyama T, Taniguchi K (2009) Immunohistochemical colocalization of TREK-1, TREK-2 and TRAAK with TRP channels in the trigeminal ganglion cells. Neurosci Lett 454:129–133

Yang SB, Jan LY (2008) Thrilling moment of an inhibitory channel. Neuron 58:823–824

Zhao H, Sprunger LK, Simasko SM (2010) Expression of transient receptor potential channels and two-pore potassium channels in subtypes of vagal afferent neurons in rat. Am J Physiol Gastrointest Liver Physiol 298:G212-G221

Zhou M, Xu G, Xie M, Zhang X, Schools GP, Ma L, Kimelberg HK, Chen H (2009) TWIK-1 and TREK-1 are potassium channels contributing significantly to astrocyte passive conductance in rat hippocampal slices. J Neurosci 29:8551–8564

Chapter 3
TRPV1 in Cell Signaling: Molecular Mechanisms of Function and Modulation

Andrés Jara-Oseguera and Tamara Rosenbaum

3.1 Introduction

The first Transient Receptor Potential (TRP) channel was identified in a phototransduction mutant in *Drosophila melanogaster* that exhibited transient instead of sustained responses to light in the retina (Minke 1977; Montell and Rubin 1989). Since then, an avalanche of findings concerning this family of ion channels has been released (Montell 2011). Today, at least 28 members belonging to seven different subfamilies (TRPV, TRPM, TRPML, TRPA, TRPN, TRPC and TRPP) have been identified (Montell 2011; Venkatachalam and Montell 2007). TRPs have been found in mammals, birds, reptiles, worms, flies and even yeast, where they perform a myriad of different functions, influencing intracellular calcium concentration, vascular tone, neuronal excitability, ion transport across epithelia and sensory stimuli detection, among many others (see Venkatachalam and Montell 2007 for review).

A distinguished group of TRP channels that has received special experimental attention are the thermo-TRPs, which exhibit an outstanding temperature sensitivity as compared to the rest of the known proteins, with Q_{10}-values greater than 20, whereas voltage-dependent potassium channels (Kv) have a Q_{10} of around 2 (Rodriguez et al. 1998). Moreover, each thermo-TRP displays a different temperature threshold, covering the whole spectrum from noxious cold (TRPA1), cold (TRPM8), warm temperatures (TRPM2, TRPM4, TRPM5 and TRPV3 and TRPV4) to noxious heat (TRPV1 and TRPV2) (Vay et al. 2011), establishing them as the long sought molecular thermometers of the organism.

The first thermo-TRP channel to be identified, the TRPV1 (vanilloid 1), has resulted even more attractive since its activation by capsaicin constitutes the molecular

T. Rosenbaum (✉)
Departamento de Neurodesarrollo y Fisiología, División Neurociencias,
Instituto de Fisiología Celular, Universidad Nacional Autónoma de México,
México, D. F., México
e-mail: trosenba@ifc.unam.mx

A. Jara-Oseguera
Departamento de Fisiología, Facultad de Medicina, Universidad Nacional
Autónoma de México, D.F., México

A. Kamkin, I. Lozinsky (eds.), *Mechanically Gated Channels and their Regulation,*
Mechanosensitivity in Cells and Tissues 6,
DOI 10.1007/978-94-007-5073-9_3,

basis for the pungency of hot chili peppers (Caterina et al. 1997). But more to the point, it also indicates that its function is associated with pain.

We now know that the TRPV1 channel is a non-selective cation channel preferentially permeable to calcium ($P_{Ca} \approx 2\ P_{Mg} \approx 10\ P_{Na} \approx 10\ P_K$) (Caterina et al. 1997) that is thought to be structurally related to voltage-dependent potassium channels. Biochemical (Kedei et al. 2001; Kuzhikandathil et al. 2001) as well as biophysical evidence (Moiseenkova-Bell et al. 2008) suggests that the functional channel is a homotetramer, in which each subunit is formed by six transmembrane domains (S1-S6) with intracellular carboxyl (C-) and amino (N-) termini. The N-terminus contains six ankyrin repeat domains (Jin et al. 2006; Mccleverty et al. 2006), while the C-terminus is thought to contain the tetramerization domain of the channel (Valente et al. 2011; Zhang et al. 2011a; García-Sanz et al. 2004).

The available evidence indicates that the pore is formed by the S5 and S6 segments and the loop between them, which contains the putative selectivity filter, with a signature sequence similar to that of Kv channels, the turret and a putative pore helix (see Jara-Oseguera et al. 2010 for review). The channel's activation gate has been shown to be located at the S6 segment (Salazar et al. 2009), probably forming a broken alpha-helical structure (Susankova et al. 2007; Islas et al. 2009; Salazar et al. 2009) with two constrictions, one that hinders the passage of large ions (Oseguera et al. 2007; Jara-Oseguera et al. 2008; Salazar et al. 2009) and one that hinders small ion permeation, located at Tyr671 (Salazar et al. 2009). The gate constitutes the point of convergence of the signals that modulate channel function, as has been shown at least for capsaicin and temperature (Salazar et al. 2009).

Functionally, the TRPV1 channel is a polymodal receptor, directly activated by very different stimuli including, as said, temperature and capsaicin, but also voltage, low and high pH, lipids, cysteine-modifying agents, extracellular cations, toxins from plants and animals (see Jara-Oseguera et al. 2010 for review). In addition, its function can be modulated by several molecules involved in intra- and extracellular signaling (Fig. 3.1).

Its complex modulation is reflected in the intricacies of the physiological phenomena it is involved with. From the axons of neurons in the dorsal root and trigeminal ganglia in the spinal cord, namely C- and Aδ-fibers, it senses incoming stimuli from the environment and generates electrical signals that are transmitted to the brain and perceived as pain (Szallasi and Blumberg 1999). Moreover, it can become sensitized during inflammation or pathological conditions, leading to neuropathic pain and hyperalgesia (Davis et al. 2000; Caterina and Julius 2001). Furthermore, its activity in nerve terminals also triggers the release of transmitters such as substance-P and calcitonin-gene related peptide (CGRP) (Szallasi and Blumberg 1999), which then act on the innervated tissue.

Finally, the TRPV1 seems to be involved in other processes not entirely related to pain. An example is mechanotransduction. This chapter will explore the molecular mechanisms of TRPV1 channel modulation by several endogenous chemical and physical stimuli and give an overview of the evidence pertaining to TRPV1's function in mechanotransduction.

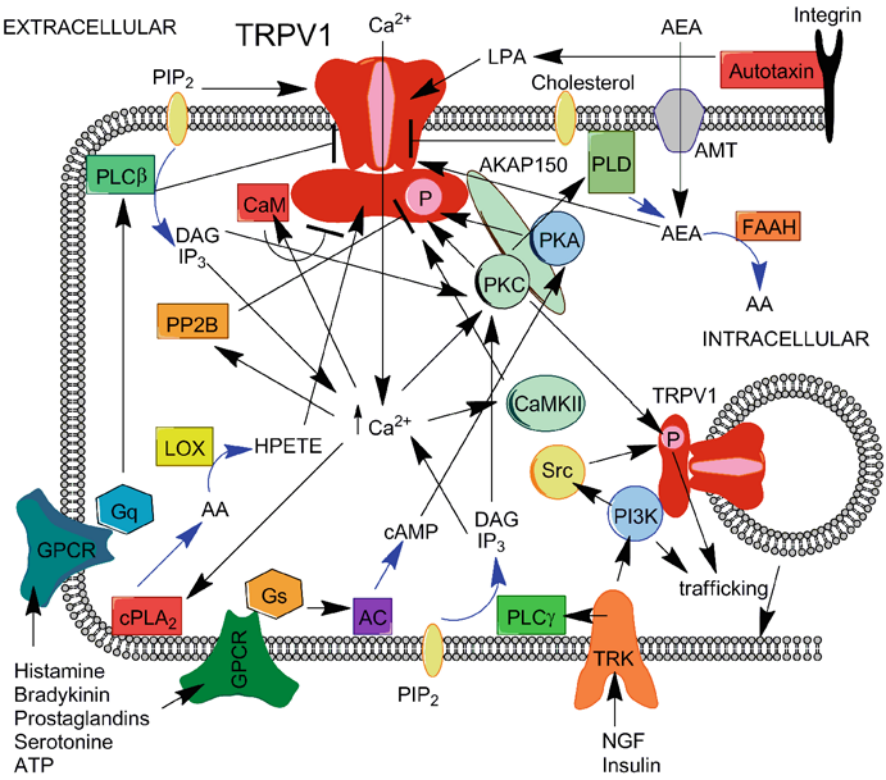

Fig. 3.1 Examples of signaling pathways associated with TRPV1 function and modulation. *Black* arrows denote positive modulation, while an orthogonal line at the end denotes inhibition. *Blue* arrows denote biosynthesis. TRPV1 is schematically depicted in *red*, with both its transmembrane and cytoplasmic domains. PKA, PKC, CaMKII sensitize TRPV1 through phosphorylation, denoted as a pink-encircled "*P*" in the channel. Calcineurin (PP2B) desensitizes the channel through dephosphorylation. Both G_q- and G_s-protein coupled receptors (GPCRs) are depicted with some of its agonists. AC denotes G_s-stimulated adenylate cyclase. Phospholipase Cβ and Cγ catalize the formation of 1,4,5-inositoltriphosphate (IP_3) and diacylglycerol (DAG) from PIP_2, depicted as a yellow oval, after their activation by a G_q protein or a receptor tyrosine kinase (TRK). Calcium-stimulated phospholipase A_2 (PLA_2) catalizes arachidonic acid (AA) formation, which is further converted into TRPV1-activating eicosanoids and leukotrienes such as HPETEs by the lipoxygenase enzymes (LOX). TRPV1 agonist anandamide (AEA) is shuttled into the cell by the anandamide membrane transporter (AMT), and is also synthesized from phospholipids by phospholipase D (PLD). AEA is transformed to AA by the fatty acid amide hydrolase (FAAH). TRK-stimulated phosphoinositide 3-kinase (PI3 K) stimulates TRPV1 trafficking to the membrane and Src-mediated channel phosphorylation, which also stimulates channel trafficking. Membrane cholesterol can directly inhibit channel function and lysophosphatidic acid (LPA), which is synthesized by the integrin-associated enzyme autotaxin, activates the channel after its translocation into the cell

3.2 Channel Activation by Voltage and Temperature

TRPV1 channels are weakly gated by voltage (Piper et al. 1999; Gunthorpe et al. 2000; Voets et al. 2004), with an apparent charge associated with gating of around 0.6 e_0, less than an elementary charge (e_0), whereas Kv channels have gating charges of about 12 and 13 e_0 per channel (Schoppa et al. 1992). The voltage-sensing domain (VSD) in Kv channels is formed by the S1-S4 transmembrane segments. The S4 contains a series of basic residues, termed gating charges, which interact with the transmembrane electric field and so allow the protein to translate changes in membrane potential into conformational transitions (see (Catterall 2010) for review). The S4-S5 linker is thought to be responsible for the coupling between the VSD and the pore domain in these channels, which is constituted by the S5 and S6 segments (Catterall 2010). Interestingly, charged residues in the S4 and S4-S5 linker in the TRPM8 channel have been proposed to contribute to the gating charge based on site-directed mutagenesis and limiting-slope analysis (Voets et al. 2007). However, the identified residues also have effects on the channel's temperature and menthol sensitivity, indicating that they are not solely involved in voltage-sensing (Voets et al. 2007).

The S4 and S4-S5 linker are highly conserved among TRPV channels (Boukalova et al. 2010) and contain a series of charged residues that could contribute to the gating charge. Notably, the charged residues are not located orderly along the S4 segment, like in Kv channels, but can be found in the lower S4 and mainly in the S4–S5 linker (Brauchi et al. 2007; Fernandez-Ballester and Ferrer-Montiel 2008). A recent study evaluated the effects on voltage- and capsaicin-sensitivity of amino acid substitutions in the TRPV1 S4 and S4-S5 linker (Boukalova et al. 2010). Several basic and acidic residues were found to have effects on the voltage of half-maximal activation ($V_{1/2}$) or the apparent gating charge measured from conductance to voltage relations. However, as with TRPM8, the mutations had also significant effects on the channel's sensitivity to capsaicin, 2-APB and temperature, so that it was not possible to assign the individual contribution of each residue to gating charge as has been done in Kv channels.

Even since the early studies in the cloned TRPV1 channel, a connection between voltage- and temperature-sensitivity was established, given that changes in temperature were found to result in changes in $V_{1/2}$ in measurements of channel activity in response to voltage pulses at different temperatures (Voets et al. 2004). Based on these results and on measurements of channel gating kinetics, a two-state model was proposed in which the high temperature-sensitivity of the channel arises from large changes in the entropy (ΔS) and enthalpy (ΔH) associated with channel activation and small changes in ΔS and ΔH associated with channel deactivation. This asymmetry in the thermodynamic parameters of the rate constants for channel gating in the two-state model, which is reversed in the cold-activated TRPM8 channel, determines the sign of the change in $V_{1/2}$ upon temperature changes, and is able to account for the opposing temperature sensitivities of TRPV1 and TRPM8 (Voets et al. 2004; Nilius et al. 2005). An important consequence of this model is that gating is obligatorily voltage-dependent.

Recently, by using an infrared laser-diode heating system that can generate temperature jumps with submillisecond time resolution (Yao et al. 2009), it was possible to directly measure channel activation and deactivation kinetics in response to temperature changes. Interestingly, the thermodynamic analysis of the data confirmed that the activation time constant is very temperature-dependent, while the closing time constant is practically temperature-independent. Surprisingly, the ΔH associated with activation is comparable with the potential energy of 43 e_0 under a 100 mV potential (Yao et al. 2010a), very large compared with the energy of translocating the $\sim$12 e_0 that gate a Kv channel. Yet, this large enthalpic change is precisely compensated by a change in entropy of comparable magnitude, resulting in a small free energy difference between the closed and open states (Nilius et al. 2005; Yao et al. 2010a). Another relevant finding in this study is that the channel exhibits a finite voltage-independent open probability, indicating that voltage-sensor activation is not necessary for channel opening (Yao et al. 2010a).

Other arguments against an obligatory voltage-dependent gating in TRPV1 come from observations that voltage is not a full agonist of the channel (Matta and Ahern 2007), and that it exhibits voltage-independent gating at saturating capsaicin concentrations (Matta and Ahern 2007; Boukalova et al. 2010). Furthermore, single-channel analysis indicates that the channel has more than one kinetically discernible open and closed states (Premkumar et al. 2002; Liu et al. 2003; Grandl et al. 2010). To account for these observations an allosteric Monod-Wyman-Changeux (MWC)-type of model has been proposed for TRPV1 and TRPM8, in which each stimulus (temperature, voltage, ligand binding) is independently sensed by distinct protein modules that are coupled to the pore module (Brauchi et al. 2004; Latorre et al. 2007; Matta and Ahern 2007).

The existence of an autonomous temperature-sensing domain in TRPV1 implies the possibility of it being a discrete structure within the channel that can be identified, as with other agonist-sensing domains. It has already been demonstrated that the temperature-sensitivity of TRPV1 does not arise from protein-membrane interactions, since changes in membrane rigidity do not interfere with the channel's thermosensitivity (Liu et al. 2003). Consistently with the existence of a discrete temperature-sensor, it has been shown that the temperature-sensitivities of TRPV1 and TRPM8 channels can be successfully swapped by transferring a portion of the pore-proximal C-terminus of one channel to the other (Brauchi et al. 2006). These results suggest that the temperature sensor may be located in the C-terminal region, and certainly establish that this region is important for temperature-mediated channel gating. Interestingly, splice variants of TRPV1 present in different bat species that differ in the distal C-terminus were found to exhibit different temperature sensitivities that are correlated with the physiological adaptation of each species to its environment (Gracheva et al. 2011). Consistently, the C-terminal TRP domain that contains the highly conserved TRP box has been shown to be important for channel gating, modulating the energy for channel opening and closing (García-Sanz et al. 2007; Valente et al. 2008). Deletions in the distal C-terminal region of the channel were also shown to have an effect in channel gating (Vlachova et al. 2003).

By constructing chimeras between the rat TRPV1 and TRPV2 channels, a region encompassing the last two N-terminal ankyrin repeat domains and the following segment before the first transmembrane domain (residues 358–434 in TRPV1) was shown to be responsible for the temperature-sensing properties of each channel (Yao et al. 2011). The crucial observation in the study was that the transfer of this N-terminal region from one channel to the other also transferred the change in enthalpy associated with temperature activation from the donor to the recipient channel, while swapping of other channel regions, including the whole transmembrane region or the C-terminus, did not cause any changes in activation enthalpy. The rate-limiting step influencing the time course of channel activation by temperature jumps at negative potentials is thought to be the activation of the temperature sensor. Therefore, the measured changes in activation enthalpy are thought to directly reflect a change in the enthalpy of temperature sensor activation (Yao et al. 2010a, 2011). Consistently, transfer of that region to the weakly temperature-sensitive TRPV4 channel or to the temperature-insensitive human TRPV2 conferred them with increased thermal sensitivity (Yao et al. 2011), suggesting that this region may indeed be the temperature sensor of the channel.

3.3 pH and Extracellular Cations

The modulation of TRPV1 activity by protons is perhaps the best understood as compared to other agonists. At mild extracellular acidification (pH<6) the channel's response to stimuli such as capsaicin and heat becomes potentiated (Petersen and LaMotte 1993; Tominaga et al. 1998), both through a stabilization of the open state and an increase in capsaicin binding (Ryu et al. 2003). At more intense acidification (pH<5) the channel can be directly activated by protons (Bevan and Yeats 1991; Tominaga et al. 1998). Interestingly, the titratable residues responsible for the activation and the potentiation are different: Glu600, located at the extracellular portion of the S5 is responsible for the potentiation, whereas Glu648, located in the linker between the selectivity filter and S6 mediates channel activation (Jordt et al. 2000). Both residues have been implicated in channel activation by extracellular cations, including Na^+, Mg^{2+}, Ca^{2+}(Ahern et al. 2005), Ni^{2+}(Luebbert et al. 2010) and Gd^{3+} (Tousova et al. 2005), and in channel inhibition by high extracellular sodium, possibly by competing with protons for their binding site (Ohta et al. 2008). More recently, residue Glu536 in the S3–S4 linker was demonstrated to also contribute to proton-mediated potentiation of the response to saturating capsaicin in the human TRPV1 (Wang et al. 2010).

Amino acid substitutions at Val538, in the S3–S4 linker, and Thr633, in the putative pore helix, selectively ablate channel activation by protons without interfering with the channel's sensitivity to capsaicin and heat and their potentiation by mild acidification (Ryu et al. 2007), indicating that channel potentiation or activation by protons occurs through different conformational pathways. Yet, different agonist-elicited conformational changes are expected to converge at the pore module to

influence gating (Latorre et al. 2007; Salazar et al. 2009). In the case of protons, a phenylalanine at position 660 in the S6 was suggested to be responsible for integrating proton-mediated activation and potentiation (Aneiros et al. 2011).

Apart from activating or potentiating the channel, protons also reduce the channel's unitary conductance (Baumann and Martenson 2000; Ryu et al. 2003; Liu et al. 2009). This effect is mediated by two acidic residues, Glu636 in the putative pore helix and Asp646 in the extracellular pore entrance (Liu et al. 2009). Although protons seem to be able to permeate through the channel (Hellwig et al. 2004), the reduction in unitary conductance does not arise from a pore-blocking mechanism (Liu et al. 2009). Instead, it has been proposed that it is mediated by proton-dependent conformational changes in the putative pore helix through a net of charged interacting residues, Glu636, Asp646 and Lys639 (Liu et al. 2009). Notably, these same residues have been shown to be implicated in several other phenomena related to permeability. For example, Asp646, Glu648 and Glu651 have been shown to influence calcium permeability in a pH-dependent manner (Samways et al. 2008), whereas Asp646 has been shown to determine channel's affinity to ruthenium red (Garcia-Martinez et al. 2000). Interestingly, calcium has been shown to reduce single channel conductance in a pH-independent manner through a site in the pore that does not involve Glu363 and Asp646 (Samways and Egan 2011).

Although the effect on the unitary currents is independent from the activation and potentiation effects mediated by protons, both Glu636 and Asp646 and other residues in the region have also been implicated in channel gating. For example, E636Q/D646N mutant channels exhibit substantially altered gating properties (Liu et al. 2009), Glu636, Asp646 and Glu648 have been demonstrated to influence capsaicin-dependent gating (Welch et al. 2000), Asp646 and Glu648 have been shown to be responsible for TRPV1 activation by polyamines (Ahern et al. 2006), the M644Y mutant in the putative selectivity filter influences capsaicin-dependent activation kinetics (Garcia-Martinez et al. 2000), the F640L mutant increases the channel's sensitivity to heat and capsaicin, possibly by mimicking proton-mediated potentiation (Myers et al. 2008) and tarantula toxins lock the channel in the open state by interacting with the extracellular pore (Bohlen et al. 2010). Moreover, the putative pore turret suffers conformational changes exclusively triggered by temperature (Yang et al. 2010), although its entire deletion does not interfere with temperature sensitivity (Ryu et al. 2007; Yao et al. 2010b). Likewise, positions N628, in the putative loop between S5 and the pore helix and N652 and Y653, in the extracellular loop between the filter and S6, have been shown to selectively affect temperature-activation of the channel (Grandl et al. 2010). Furthermore, agonist-specific changes in TRPV1 unitary conductance have been reported to occur (Chung et al. 2008). All these data demonstrate that the TRPV1 channel pore is a very dynamic structure that is tightly coupled to the gating mechanism of the channel.

Finally, it is worth mentioning that the TRPV1 channel has also been shown to be activated by ammonia and that a histidine at position 378 in the N-terminus is responsible for such effect (Dhaka et al. 2009).

3.4 Lipids

3.4.1 Cholesterol

Cholesterol is a component of the plasma membrane that affects membrane stiffness and thickness and has been also shown to interfere with the function of ion channels through specific interactions. With regards to TRPV1 channels, it has been shown that removal of cholesterol and other lipids, presumed to be enriched in membrane rafts from the plasma membranes of DRG (Liu et al. 2006) and trigeminal neurons and TRPV1-expressing HEK293 cells (Szoke et al. 2011), provokes a decrease in channel activity, which has been suggested to be caused by the perturbation of the putative membrane rafts where the channel is suggested to reside. Conversely, neither cholesterol enrichment nor cholesterol removal was found to have a dramatic effect on the channel's response to temperature when expressed in HEK293 cells (Liu et al. 2003).

In a recent study by our group performed in excised membrane patches from TRPV1-transfected HEK293 cells, it was found that cholesterol removal with MβCD has no effect on channel function and that TRPV1 is localized in the non-raft fraction of the plasma membrane (Picazo-Juarez et al. 2011). Additionally, cholesterol was found to progressively reduce channel activity in excised membrane patches, an effect that could be reversed by cholesterol removal with MβCD. Stationary noise analysis and single-channel recordings indicated that cholesterol reduces the number of agonist-responsive channels in the patch, suggesting that cholesterol-binding strongly destabilizes the channel's open state. It was also found that the rat TRPV1 channel contains a cholesterol-binding motif in the S5, and that amino acid substitutions in the region attenuate or completely eliminate the effects of cholesterol on the channel (Picazo-Juarez et al. 2011). A leucine to isoleucine substitution in the rat TRPV1 channel at position 585 in the cholesterol- binding motif, renders the channel insensitive to cholesterol, probably due to steric hindrance at the binding site. The human TRPV1 channel exhibits a very common polymorphism at precisely that position (Cantero-Recasens et al. 2010), with either a valine or an isoleucine instead of the leucine of the rat channel. As expected, the human TRPV1-I585 channel is unresponsive to cholesterol, whereas the hTRPV1-I585L is inhibited by cholesterol similarly to the rat TRPV1, and the hTRPV1-V585 exhibits an intermediate phenotype (Picazo-Juarez et al. 2011). Interestingly, the occurrence of this polymorphism at residue 585 correlates with physiological changes under certain pathological conditions (Cantero-Recasens et al. 2010; Valdes et al. 2011).

3.4.2 PIP_2, Acyl-Glycerols and Lysophosphatidic Acid

Phosphatidylinositol 4,5-bisphosphate (PIP_2) contributes little to the bulk of lipids that form the plasma membrane but has an extraordinarily important role as a signaling molecule (Gamper and Shapiro 2007). Early reports concerning the modulation

of TRPV1 by PIP_2 indicated that the lipid had inhibitory effects on the channel (Chuang et al. 2001), and a C-terminal region (from residue 777–820) was proposed to be responsible for the inhibition (Prescott and Julius 2003). Yet, the studies did not test the effects of PIP_2 on the channel directly, but relied on indirect evidence.

Soon, contradictory reports began to emerge. First, it was shown that PIP_2 depletion causes channel desensitization rather than inhibition, and that recovery from desensitization requires high concentrations of ATP and re-synthesis of PIP_2 by phosphatidylinositol 4-kinase (PI4K) (Liu et al. 2005). Moreover, it was found that PIP_2 potentiates the channel's response to capsaicin in inside-out membrane patches from transiently transfected F-11 cells and DRG neurons (Stein et al. 2006). Two subsequent studies indicated that PIP_2 and other PIP_2-related molecules potentiate the channel's response to capsaicin in excised membrane patches and whole-cell recordings without activating the channels by themselves (Lukacs et al. 2007; Lishko et al. 2007; Klein et al. 2008). Later, it was also found that PIP_2 depletion-associated channel desensitization does not render the channel non-functional, but shifts its response to capsaicin, most probably by reducing the channel's affinity for the agonist (Yao and Qin 2009). The inhibitory effects of PIP_2 might have resulted from the displacement of an endogenous lipidic TRPV1 agonist by the potentiating but not activating PIP_2.

A recent study provided evidence that the PIP_2-binding protein Pirt binds to TRPV1 and that it is responsible for the actions of PIP_2 on the channel (Kim et al. 2008). As opposed to these results, another study that combined electrophysiological, biochemical and fluorescence-spectroscopy data showed that the presence of Pirt is not essential for the PIP_2-dependent potentiation of the channel in heterologous expression systems and DRG neurons (Ufret-Vincenty et al. 2011). Additionally, it was shown that deletion of the fragment previously associated with PIP_2-dependent inhibition (777–820) does not interfere with the potentiating effects of PIP_2. Finally, a proximal region in the C-terminus (residues 682–725) was shown to interact with PIP_2 (Ufret-Vincenty et al. 2011), suggesting that this is the PIP_2-sensor in the channel.

Diacylglycerols (DAGs) are generated upon PIP_2 cleavage by phospholipase C (PLC). Interestingly, it has been reported that 1-oleoyl-2-acetyl-*sn*-glycerol (OAG), a DAG analogue (Fig. 3.2), directly activates the TRPV1 channel through the capsaicin binding site, since the Y511A mutation, which dramatically reduces capsaicin sensitivity (Jordt and Julius 2002), also abolishes the effects of OAG (Woo et al. 2008). Furthermore, the study showed that in cells cotransfected with muscarinic $G_{q/11}$-protein coupled receptor and TRPV1, activation of the first influenced activity of the later (Woo et al. 2008), suggesting that physiological DAG-generation by $G_{q/11}$-protein stimulation could affect TRPV1 channel function. It is intriguing that monoacylglycerols and other hydrophobic TRPV1 agonists (Iida et al. 2003; Iwasaki et al. 2006) activate the TRPV1 channel but are non-pungent (Iwasaki et al. 2008). It has been proposed that highly hydrophobic TRPV1 agonists are non-pungent since they do not reach the nerve terminals where the TRPV1 channel is expressed.

Lysophosphatidic acid (LPA, Fig. 3.2) is a bioactive lipid whose production is stimulated by activated platelets upon tissue damage (Lin et al. 2010) and has been shown to be involved in the development of neuropathic pain and hyperalgesia (Inoue

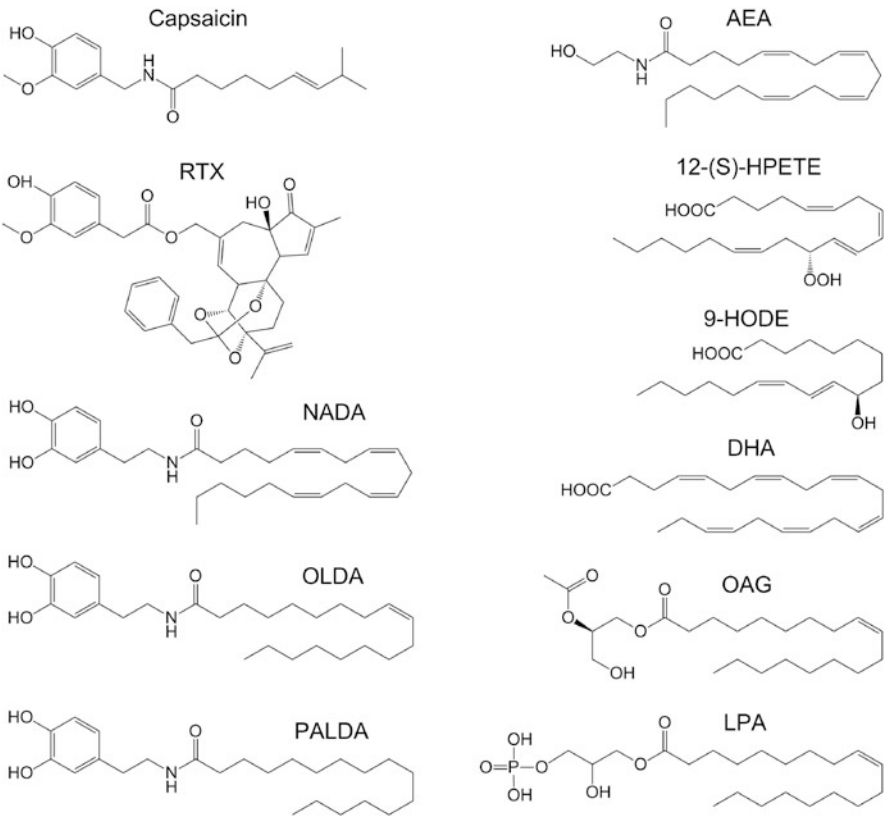

Fig. 3.2 Chemical structures of TRPV1 agonists. RTX, resiniferatoxin; NADA, N-arachydonoyl dopamine; OLDA, N-oleoyl-dopamine; PALDA, N-palmitoyl dopamine (entourage coumpound); AEA, anandamide; 12-(*S*)-HPETE, 12-(*S*)-hydroperoxyeicosatetraenoic acid (lipoxygenase 12 product); 9-HODE, 9-hydroxyoctadecadienoic acid; DHA, docosahexaenoic acid (omega-3 fatty acid); OAG, 1-oleoyl-2-acetyl-*sn*-glycerol (diacyl glycerol); LPA, lysophosphatidic acid

et al. 2004) by acting on specific G-protein coupled receptors (GPCRs). Recently, it was proposed that LPA causes hyperalgesia in a model of rat bone-cancer pain by sensitizing the TRPV1 channel through an LPA_1 receptor-PKCε-dependent pathway (Pan et al. 2010).

In the last few months a study by our group demonstrated that the TRPV1 can be directly activated by LPA with an apparent dissociation constant (K_D) of around 700 nM (Nieto-Posadas et al. 2011). Interestingly, the effects of LPA on the channel were independent of the specific LPA GPCRs, and were shown to be mediated by a direct interaction of the lipid with the carboxyl-terminus of the channel. Moreover, the activation of TRPV1 channel by LPA was found to be physiologically relevant, since it caused action potential firing in TRPV1-expressing DRG neurons that was absent in neurons from TRPV1-null mice, and its intra-plantar injection caused pain-related behaviors in WT mice that were attenuated in the TRPV1 knock-outs. Interestingly,

a lysine residue at position 710, previously identified as a putative PIP_2-binding site (Brauchi et al. 2007), was found to be largely responsible for the interaction of the channel with LPA. Consistently, PIP_2 and LPA were shown to compete for a binding site within the channel, with LPA being able to activate the channel in the absence of PIP_2, and PIP_2 displacing LPA from the site without causing channel activation (Nieto-Posadas et al. 2011). These results establish a new signaling pathway for channel modulation under acute pain-related states and offer a possible explanation for the previously observed inhibitory effects of PIP_2, in which this lipid inhibits the channel by displacing another endogenous agonist from its binding site.

3.4.3 Capsaicin, N-acyl-ethanolamines and N-acyl-dopamines

Capsaicin, the well known TRPV1 agonist that played an important role in the cloning of the receptor (Caterina et al. 1997), is a hydrophobic membrane-permeant compound that activates the channel from the intracellular side (Jung et al. 1999) with a K_D of around 200 nM and a Hill coefficient of near 2. The pharmacological properties of capsaicin-mediated activation of its receptor had already been characterized before the channel was even cloned (Szallasi and Blumberg 1991; Szallasi et al. 1993b).

By constructing chimeras between capsaicin-sensitive rat TRPV1 channels and vanilloid-insensitive chicken TRPV1, a region from S2-S4 was shown to be necessary for capsaicin activation (Jordt and Julius 2002). Moreover, through site-directed mutagenesis, essential residues for vanilloid sensitivity were identified: Tyr511 and Ser512, two conserved residues among TRPV1 channels from several species, were shown to be essential for high sensitivity to capsaicin (Jordt and Julius 2002), whereas a I550T mutation in the rabbit receptor, which is also capsaicin-insensitive, was necessary for conferring it with capsaicin-sensitivity as in the rat and human TRPV1, which have a threonine at that position (Gavva et al. 2004). Moreover, a methionine at position 547, present in rat and human but not rabbit TRPV1, was shown to be necessary for sensitivity to resiniferatoxin (RTX) (Chou et al. 2004; Gavva et al. 2004), a compound from the cactus *Euphorbia resinifera* that activates the channel with higher affinity than capsaicin (Szallasi and Blumberg 1989; Caterina et al. 1997). As of now, the precise nature of the interaction between vanilloids and the channel remains unanswered, although it is clear that interactions with the vanillylamine moiety and with an unsaturated acyl chain are required for channel activation (Walpole et al. 1993; De Petrocellis et al. 2000). Other residues and regions throughout the protein, including the N- and C-termini and the pore have been shown to affect vanilloid sensitivity (Welch et al. 2000; Kuzhikandathil et al. 2001; Jung et al. 2002; Vlachova et al. 2003; García-Sanz et al. 2007; Myers et al. 2008; Valente et al. 2008).

Interestingly, a series of endogenous compounds with structural similarities to capsaicin (Fig. 3.2), many of which are agonists of cannabinoid receptors (CB) and are therefore known as endocannabinoids, have been found to activate the TRPV1 channel.

N-acylethanolamides (NAEs) are a group of bioactive lipids whose production is catalyzed by phospholipase D-like enzymes (Di Marzo et al. 1994) and that have been shown to activate TRPV1 (Figs. 3.1 and 3.2). The first endovanilloid identified, *N*-arachidonoylethanolamide (AEA) or anandamide, was found to induce vasodilatation in rat hepatic mesenteric arteries by causing CGRP release from perivascular sensory nerves in a CB-independent manner, and that its effect could be inhibited by capsazepine (Zygmunt et al. 1999). Moreover, it was also found that anandamide could elicit rat and human TRPV1-mediated currents in heterologous expression systems, albeit with an affinity lower than capsaicin ($K_D \approx 5\ \mu M$) (Zygmunt et al. 1999; Smart et al. 2000). AEA was found to displace radioactively labeled RTX from its binding site (Ross et al. 2001), indicating that it probably binds to the same region as capsaicin and RTX, and activates the channel by a similar mechanism. Consistently, mutations at Tyr511, Ser512 and Thr550 have been found to interfere with channel activation by anandamide and other endovanilloids (Jordt and Julius 2002; Gavva et al. 2004; Sutton et al. 2005).

Oleoylethanolamide (OEA), another N-acylethanolamide, is released in the intestine where it acts as a satiety factor by acting on visceral nerve terminals (Rodriguez de Fonseca et al. 2001). It has been demonstrated that OEA directly activates the TRPV1 channel in heterologous expression systems with an affinity similar to AEA in a PKC-dependent fashion (Ahern 2003). Notably, TRPV1 activation by OEA in vagal sensory neurons has been shown to cause visceral pain, indicating that this mechanism might underlie the feeling of discomfort upon excessive feeding (Wang et al. 2005). Other endogenous unsaturated N-acylethanolamides also activate the channel with varying affinities, depending on the length of the acyl chains and the degree of saturation, with at least one unsaturation required to have agonistic effects (Movahed et al. 2005). Interestingly, although the anti-inflammatory lipid palmitoylethanolamide (PEA), which is co-synthesized with AEA in most cells (Petrosino et al. 2010), and N-lauroylethanolamide do not act as TRPV1 channel agonists, they have been shown to act as "entourage" compounds, potentiating the effects of other vanilloids for activating the channel (De Petrocellis et al. 2001a; Smart et al. 2002). Similar observations have been reported for two endogenous N-acyl-dopamines, N-palmitoyl- (PALDA) and N-stearoyl-dopamine (STEARDA) (Chu et al. 2003; De Petrocellis et al. 2004).

As opposed to PALDA, STEARDA and N-acylethanolamides, N-arachidonoyl-dopamine (NADA) and N-oleoyl-dopamine (OLDA), two endocannabinoids found in the central nervous system, activate the TRPV1 channel with an affinity similar to capsaicin (Huang et al. 2002; Chu et al. 2003), probably due to the fact that they contain the vanillyl-amine moiety and at least one unsaturation at the acyl chain.

3.4.4 Lipoxygenase Products, Polyunsaturated Fatty Acids and Nitrated Lipids

Lipoxigenase (LOX) products have been implicated in inflammatory processes since their production is stimulated during inflammation (Samuelsson 1983) and have also

been shown to cause hyperalgesia (Levine and Taiwo 1990; Di Marzo et al. 2002). Interestingly, 12-(*S*)-hydroperoxyeicosatetraenoic acid (12-(*S*)-HPETE) (Fig. 3.2) was shown to directly activate the TRPV1 channel in cultured DRG neurons and transiently transfected HEK293 cells with a K_D of around 8 μM (Hwang et al. 2000) and to inhibit [^{3}H]-RTX binding to the TRPV1 (Shin et al. 2002), likely by competing for the same binding site. Other lipoxygenase products including the eicosanoids 15-(*S*)-HPETE, 5-(*S*)-HETE, leukotriene B4 (LTB_4), and 15-(*S*)-HETE were effective in activating the TRPV1. On the contrary, other LOX products such as hepoxilins A_3 and B_3, 5-(*S*)-HPETE, 8-(*R*)-15-(*S*)-dihydroxyeicosatetraenoic acid, 12-(*S*)-HETE and LTC_4, were found to be rather poor TRPV1 agonists (Hwang et al. 2000). Interestingly, bradykinin was shown to be able to stimulate TRPV1 activity in sensory neurons by stimulating 12-(*S*)-HPETE production through phospholipase A_2 (PLA_2) activation, arachidonic acid production and its subsequent conversion to 12-(*S*)-HPETE by LOX-12 (Fig. 3.1) (Shin et al. 2002). Furthermore, histamine binding to the H1R GPCR was found to activate the TRPV1 channel also through PLA_2 activation and concomitant 12-HPETE production (Shim et al. 2007).

Oxidized metabolites of linoleic acid, which can also be generated by the lipoxygenase enzymes, are released under inflammatory conditions (Jira et al. 1997). Notably, 9- and 13-hydroxyoctadecadienoic acid (9-HODE and 13-HODE) (Fig. 3.2) and their metabolites 9-oxo-ODE and 13-oxo-ODE, all products of linoleic acid oxidation, were shown to be released from the spinal cord upon depolarization (Patwardhan et al. 2009) and from mouse skin upon heating (Patwardhan et al. 2011). More interestingly, it was found that these compounds directly activate the TRPV1 channel through a site different from the capsaicin-binding site, since point mutations at positions 511 and 512 did not eliminate the agonistic effects of the molecules (Patwardhan et al. 2011). TRPV1 channel activation by 9- and 13-HODEs generated by heat and inflammation has been proposed to be partly associated with the channel's thermosensitivity (Patwardhan et al. 2011) and to its participation in mechanical allodynia (Patwardhan et al. 2009).

Omega-3 polyunsaturated fatty acids (*n*-3 PUFAs) are essential dietary lipids that are highly concentrated in the brain and if absent in the diet cause significant neurological defects (Guesnet and Alessandri 2011). Additionally, they have been found to have analgesic properties and to compete with arachidonic acid for the cyclo- and lipoxygenase enzymes and therefore hinder the production of pro-inflammatory prostaglandins and eicosanoids (Lee et al. 1984). Interestingly, they also activate the TRPV1 channel when it is phosphorylated by PKC, but with an affinity significantly lower than capsaicin. This activation seems to also depend on the capsaicin-binding domain, since they displace [^{3}H]-RTX from its binding site and antagonize capsaicin, anandamide and NADA's actions at the receptor (Matta et al. 2007).

Nitroalkenyl fatty acids are electrophilic lipid derivatives that are formed under oxidative and inflammatory conditions (Khoo and Freeman 2011) and that can modulate the function of many proteins, including transcription factors, leading to anti-inflammatory responses. Nitro-oleic acid actives both the TRPV1 and TRPA1 channels in dorsal root ganglion neurons (Sculptoreanu et al. 2010) and

sensitive afferent nerves in the bladder (Artim et al. 2011). It has been proposed the nitro-oleic acid activates both channels by covalently modifying cysteines (Artim et al. 2011).

3.5 Post-Translational Modifications

3.5.1 Redox Modulation

Before its cloning, radio-ligand binding studies in sensory nerves indicated that [^{3}H]-RTX binding to the capsaicin receptor was diminished by oxidizing agents, establishing a link between the TRPV1 channel and redox modulation (Szallasi and Blumberg 1993; Szallasi et al. 1993b). Later studies with the cloned receptor indicated that its responses to capsaicin and heat can be potentiated by the reducing agent dithiothreitol (DTT) (Vyklicky et al. 2002). Consistently, the sulfhydryl oxidizing agent thimerosal and other oxidizing agents, when applied extracellularly, were shown to decrease the channel's response to capsaicin and heat, and that mutation of Cys621, located in the linker between the S5 and the putative p-loop, eliminates these effects (Jin et al. 2004; Susankova et al. 2006).

Other intracellular residues have been also demonstrated to participate in channel redox modulation: A cysteine at position 157 in the rat TRPV1 N-terminus was shown to be responsible for channel activation by certain cysteine modifying compounds through a covalent-modification mechanism (Salazar et al. 2008). More recently, the involvement of other intracellular cysteine residues in channel redox modulation was evaluated (Chuang and Lin 2009). By re-introducing combinations of different cysteine residues into a cysteineless chicken TRPV1 channel, several residues in the N- and C-termini were shown to be important for channel function. Specifically, Cys772 and Cys783 in the C-terminus were shown to form intersubunit disulfide bonds that sensitize the receptor. Conversely, Cys393 and Cys397 in the N-terminus were shown to form intrasubunit disulfide bonds that result in channel potentiation (Chuang and Lin 2009). The equivalent residues in the human TRPV1 receptor, Cys387 and Cys391, were shown to accomplish similar functions, whereas the conserved C-terminal cysteine Cys767 was demonstrated to take part in channel-potentiating intersubunit disulfide bond formation. Interestingly, oxidative modulation of TRPV1 channel was shown to be able to override Ca^{2+}-dependent channel desensitization.

3.5.2 Phosphorylation

Biochemical data has shown that the TRPV1 channel is heavily phosphorylated in the resting state (Bhave et al. 2002; Zhang et al. 2008). Consistently, channel responsiveness to capsaicin, but not to heat or low pH, has been shown to require

phosphorylation of either Ser502 or Thr704 by Ca^{2+}/calmodulin-dependent protein kinase II (CaMKII) (Jung et al. 2004; Novakova-Tousova et al. 2007). These sites have also been shown to be substrates for phosphorylation by cAMP-dependent protein kinase A (PKA) (Rathee et al. 2002; Mohapatra and Nau 2003) and the calcium-independent DAG-activated protein kinase Cε (PKCε) (Numazaki et al. 2002; Bhave et al. 2003), whose action causes channel sensitization to vanilloids, heat and acid, allowing the channel to open at normal body temperature (Premkumar and Ahern 2000; De Petrocellis et al. 2001b; Vellani et al. 2001; Rathee et al. 2002; Premkumar et al. 2004). PKA has been also shown to act on Ser116, Thr144, Thr370 and Ser502 (Rathee et al. 2002; Bhave et al. 2002; Mohapatra and Nau 2003). Interestingly, the previously characterized desensitization of TRPV1 by the Ca^{2+}- and calmodulin-dependent phosphatase 2B (calcineurin) that occurs after calcium entry due to channel activity (Docherty et al. 1996; Liu and Simon 1996; Koplas et al. 1997), has been found to be highly dependent on dephosphorylation of Thr370, since desensitization in the T370A mutant is insensitive to calcineurin inhibition (Mohapatra and Nau 2005), although other residues, including Ser116 and Thr144, are also calcineurin substrates (Bhave et al. 2002; Jeske et al. 2006). Moreover, phosphorylation of Ser116 by PKA prevents desensitization, indicating that the state of Ser116 functions as a PKA- and calcineurin-dependent switch between channel sensitization and desensitization, since dephosphorylation at this site must occur before desensitization (Bhave et al. 2002; Mohapatra and Nau 2003).

PKCε-dependent phosphorylation at Ser502, Thr704 and Ser800 causes receptor potentiation (Numazaki et al. 2002; Bhave et al. 2003) and has also been reported to blunt desensitization (Mandadi et al. 2004). The calcium- and DAG-sensitive PKCα (Olah et al. 2002) and the atypical PKD/PKCμ (Wang et al. 2004) also sensitize TRPV1, although the later acts on Ser116, while PKCγ and PKCδ do not affect the channel function (Olah et al. 2002; Amadesi et al. 2006). Interestingly, PKA and PKC-dependent actions on the channel depend on their association with the rodent scaffolding protein A-kinase anchoring protein 150 (AKAP150) or its human equivalent AKAP79 (Rathee et al. 2002; Schnizler et al. 2008; Zhang et al. 2008; Jeske et al. 2009b), which binds to a C-terminal region in the channel (Zhang et al. 2008). Calcineurin's actions have also been suggested to depend on AKAP150 (Zhang et al. 2008), although these data have been recently debated (Por et al. 2010). TRPV1 is also sensitized by extracellular-signal-regulated kinases 1 and 2 (ERK1/2) through an as yet uncharacterized mechanism that seems to involve an increase in intracellular calcium (Zhang et al. 2011b; Zhuang et al. 2004).

Several pro-inflammatory signaling molecules act on GPCRs whose activation leads to PKA or PKC stimulation, causing channel sensitization and hyperalgesia. Accordingly, bradykinin (BK) (Cesare and McNaughton 1996; Cesare et al. 1999), the pro-inflammatory chemokine CCL3 (Zhang et al. 2005a), substance P (Zhang et al. 2007a), serotonin (Ohta et al. 2006), ATP (Tominaga et al. 2001; Moriyama et al. 2003), hypoxia-inducible factor 1a (Ristoiu et al. 2011), prostaglandins E_2 and I_2 (Bhave et al. 2002; Moriyama et al. 2005), interleukin-1 (IL-1) (Obreja et al. 2002) and the inflammation-associated protease activated receptor 2 (Amadesi et al. 2006), among many others, have been found to cause channel sensitization though PKC

and PKA (Fig. 3.1). Conversely, cannabinoid receptors CB1 and CB1 can inhibit channel function by promoting calcineurin function (Jeske et al. 2006; Patwardhan et al. 2006).

Interestingly, PKCε-dependent phosphorylation of TRPV1, especially at Ser502 (Zhang et al. 2008), also stimulates rapid shuttling of TRPV1-, SytIX- and Snapin-containing vesicles to the membrane through a SNARE-dependent mechanism, increasing TRPV1 expression (Morenilla-Palao et al. 2004). Notably, NGF, insulin and insulin-like growth factor 1 (IGF-1) have been shown to potentiate channel function by stimulating channel trafficking (Van Buren et al. 2005; Zhang et al. 2005b; Stein et al. 2006; Lilja et al. 2007; Camprubi-Robles et al. 2009), whereas BK, artemin and IL-1 do not (Camprubi-Robles et al. 2009). Furthermore, NGF, IGF-1, insulin and the extracellular matrix protein fibronectin (Jeske et al. 2009a) also enhance TRPV1 expression levels though a PI3K dependent mechanism that seems to involve a direct interaction of PI3K with the N-terminus of the channel (Stein et al. 2006) and TRPV1 phosphorylation at Tyr200 by the non-receptor tyrosine kinase c-Src (Zhang et al. 2005b) through an AKAP150-independent mechanism (Zhang et al. 2008) (Fig. 3.1).

3.6 Ankyrin Repeat Domain, Sensitization and Ca^{2+}-CaM-Dependent Desensitization

Ankyrin repeat domains (ARD) are present in many proteins where they engage in protein-protein interactions and form modulatory ligand-binding sites (Gaudet 2008). The ankyrin motif consists of an anti-parallel helix-turn-helix motif followed by a β-hairpin "finger" loop, where the concave structure formed by the loop and helices forms a cradle for interaction with other proteins (Gaudet 2008). The TRPV1 channel has six ankyrin repeats at the N-terminus, whose structure has been determined at a resolution of 2.7 Å (Lishko et al. 2007).

Interestingly, the TRPV1 ARDs crystallized together with a bound ATP molecule between repeats 1–3 (Lishko et al. 2007). Biochemical as well as functional data with the WT and mutant channels with point mutations introduced into the putative ATP-binding site confirmed a direct interaction between the TRPV1 channel and ATP (Lishko et al. 2007), which has a sensitizing effect on the receptor, as had been previously shown at the functional level (Kwak et al. 2000). GTP was found to compete with ATP for binding to the channel whereas ADP, CTP and UTP bound poorly and AMP and cAMP did not show any binding at all (Lishko et al. 2007). Interestingly, adenosine has been shown to have an inhibitory effect on the channel also by means of a direct interaction, constituting a possible route for TRPV1 feedback inhibition (Puntambekar et al. 2004), since adenosine is released in response to TRPV1 channel activation (Sawynok and Liu 2003).

The ATP binding site overlaps with a previously characterized Ca^{2+}-CaM-binding site between residues 189–222 that mediates channel desensitization. This region was found to interact with CaM in a calcium-dependent manner, leading to a reduction

in channel open probability in spite of receptor stimulation (Rosenbaum et al. 2004), providing a molecular explanation for at least one type of channel desensitization. As expected from the overlap in binding sites, Ca^{2+}-CaM and ATP were shown to compete for binding to the channel and to either cause channel desensitization or potentiation. Moreover, point mutations that affected ATP binding to the receptor also interfered with Ca^{2+}-CaM binding and channel desensitization (Lishko et al. 2007).

Notably, Ca^{2+}-CaM-dependent channel desensitization has also been shown to depend on a C-terminal region encompassing residues 767–801. This region also interacts with CaM in a calcium-dependent manner, and its elimination severely impairs channel desensitization (Numazaki et al. 2003), while increasing AKAP150 binding and PKA-dependent channel potentiation (Chaudhury et al. 2011). Conversely, Ca^{2+}-CaM interferes with AKAP150 binding to its binding site in the C-terminus of the channel, suggesting that Ca^{2+}-CaM might desensitize the channel by inhibiting channel phosphorylation through an interference with the association AKAP150 (Chaudhury et al. 2011). Another possibility is that the C- and N-terminal CaM-binding sites interact and cause channel desensitization by inducing a conformational change (Lishko et al. 2007).

3.7 The Cytoskeleton

Interactions between the TRPV1 channel and the microtubule cytoskeleton, but not with actin and intermediate filaments, have been reported (Goswami et al. 2004). Studies performed in vitro (Goswami et al. 2004) and in living F-11 cells (Goswami et al. 2006) indicate that the C-terminus of TRPV1 interacts with and stabilizes microtubule filaments in a calcium-dependent manner. It was found that the channel interacts preferentially with β-tubulin in αβ-tubulin dimers and the sites of interaction were mapped to two regions in the channel's C-terminus (residues 710–730 and 770–797) that contain a high density of positively charged residues that likely interact with the C-terminal acidic region of tubulin (Goswami et al. 2007a). Moreover, the interaction with tubulin was found to be mutually exclusive with PKCε-dependent phosphorylation of Ser800 (Goswami et al. 2011). Furthermore, it was found that estrogen-dependent activation of PKCε was capable of interfering with the association of tubulin and TRPV1, which resulted in microtubule destabilization and neuronal growth cone retraction in F-11 cells and mouse DRG neurons (Goswami et al. 2011). These effects may play an important role in PKCε-dependent mechanical sensitization.

It was also found that activation of TRPV1 results in microtubule destabilization in F-11 cells within a minute, resulting in neuronal growth cone retraction and morphological changes attributable to tubulin destabilization (Goswami et al. 2006; Goswami et al. 2007b). Dynamic microtubules were found to be mainly affected, whereas stable microtubules and actin- and intermediate-filaments were unaffected by TRPV1 activity (Goswami et al. 2006).

3.8 Modulation of TRPV1 Activity by Mechanical and Osmotic Stimuli

To date it has not been possible to determine whether TRPV1 channel activity can be directly modulated by mechanical stimuli. Yet, a growing body of experimental evidence points to a role of the TRPV1 in many physiological processes related to mechanical and osmotic stimuli detection, which will be discussed in the following section.

3.8.1 The Vasculature

The myogenic response is the mechanism by which resistance arteries constrict in response to an elevation in blood flow in order to control the perfusion level of tissues and protect them from variations in systemic blood pressure. Recently, the myogenic response in rat mesenteric resistance arteries has been shown to be stimulated by activation of TRPV1-expressing C- and Aδ-fibers (Scotland et al. 2004). Moreover, this response was significantly attenuated by capsazepine application, suggesting a role for TRPV1 in sensory fiber activation by an increase in artery transmural pressure. However, the sensitivity of the myogenic constriction to inhibition by gadolinium was much larger than TRPV1's sensitivity to Gd^{3+}-block when expressed in CHO cells, arguing against a role for TRPV1 as a mechanoreceptor (Scotland et al. 2004). Instead, mechanotransduction-related TRPV1 activity was suggested to depend on its activation by 20-HETE, which has been previously shown to be important for the myogenic response (Inoue et al. 2009). Resistance artery smooth muscle cells are able to carry out a myogenic response by themselves through the action of other proteins such as mechanosensitive GPCRs (Mederos y Schnitzler et al. 2011), suggesting that TRPV1's role in this system is purely modulatory, and not essential for mechanosensing. A similar modulatory action of TRPV1-expressing sensory fibers might be operating in relation to the baroreflex system (Sun et al. 2009).

Surgical arteriovenous fistulae are connections between an artery and a vein that are routinely performed for hemodialysis. A disadvantage of the procedure is that the involved vein is subject to an abnormal increase in pressure, which is sensed by an unknown mechanosensor that triggers remodeling compensatory mechanisms that can ultimately occlude the fistula. In a recent study in rat fistulae it was shown that TRPV1 expression, but not TRPV4, was enhanced both at the protein and mRNA levels after fistula establishment (Chen et al. 2010). CaMKII and endothelial nitric oxide synthase (eNOS), two primary mediators of the remodeling process, were shown to be increased downstream of TRPV1 expression. Moreover, treatment with capsazepine considerably decreased fistula remodeling and CaMKII and eNOS activity, without affecting other hemodynamic changes. Interestingly, remodeling was found to be entirely dependent on the increase in pressure, since it was prevented by a decrease in blood flow to the fistula (Chen et al. 2010).

3.8.2 The Small Intestine and Colon

An involvement of TRPV1 in mechanotransduction in the colon and small intestine has also been demonstrated. By measuring in vitro sensory nerve activity in response to physical distention in the jejunum of WT and TRPV1 KO mice, it was found that the electrical responses of low threshold-activated sensory fibers were attenuated in TRPV1-null mice (Rong et al. 2004). In the case of the colon, it has been shown that the majority of mouse colon sensory neurons express TRPV1 (Matsumoto et al. 2011; Robinson et al. 2004; Tan et al. 2008) and can be stimulated by heat, low pH and capsaicin (Sugiuar et al. 2004; Spencer et al. 2008). Moreover, human patients with faecal urgency and rectal hypersensitivity display an increase in TRPV1 expression in colon sensory nerves (Chan et al. 2003). In a physiological and morphological study, it was found that visceral nociception upon colorectal distention is attenuated in both TRPV1 and acid sensing ion channel 3 (ASIC3) knock-out mice (Jones et al. 2005). Muscular/mucosal afferent fibers, which are the main stretch-sensitive fibers in the colon, displayed no anatomical abnormalities in the knock-outs, but evidenced a decreased response to circumferential stretch. WT fiber responses to stretch were also attenuated by capsazepine (Jones et al. 2005).

Results from several studies suggest that capsaicin-sensitive sensory fibers in the colon are responsible for pain sensation (Laird et al. 2001; Christoph et al. 2006; Miranda et al. 2007). However, as in the case of the jejunum (Rong et al. 2004), all capsaicin-responsive sensory nerves in mice colon identified until now have been shown to respond to circumferential stretch with a low threshold (Spencer et al. 2008). This is intriguing, since it would be expected for pain-related responses to be associated with fibers that respond with an elevated threshold. Consistently, there is evidence that indicates that TRPV1 is connected with mechanical acute hyperalgesia development but not in normal pain sensation, since selective TRPV1 antagonists blocked hyperalgesic responses without causing hypoalgesia (Ravnefjord et al. 2009).

3.8.3 The Bladder

The bladder is another organ in which TRPV1 has been proposed to be involved in mechanical stimuli detection. TRPV1 is not only expressed in sensory fibers innervating the bladder (Szallasi et al. 1993a; Avelino and Cruz 2006), but in the bladder urothelial cells themselves (Heng et al. 2011; Birder et al. 2001). Urothelial cells have intrinsic mechanosensory properties, which are important for triggering the micturition reflex, and release NO, acetylcholine and ATP. TRPV1-null mice exhibit some functional bladder abnormalities such as an increase in bladder capacity, a reduction in the frequency of bladder reflex contractions and a decrease in spinal cord c-fos induction, which is a marker of neural activity, upon bladder distention, but show no anatomical abnormalities (Birder et al. 2002). In the same study it was found that stretch-evoked ATP release is reduced in isolated bladders and cultured urothelial cells from TRPV1$^{-/-}$ mice (Birder et al. 2002). Conversely, capsaicin

application to cultured urothelial cells has been shown to result in an increase in ATP and NO release that can be blocked by capsazepine (Birder et al. 2001; Birder et al. 2002). This argues in favor of a direct role of TRPV1 in mechanosensation, since capsaicin mimics the effects of pressure-increase in regards to ATP release.

Recently the importance of TRPV1 for mechanotransduction in the bladder has been brought into question (Everaerts et al. 2010). A series of recent studies by different research groups have failed to detect TRPV1 channel expression in urothelial cell cultures at the mRNA, protein and functional levels (Everaerts et al. 2010; Yu et al. 2011; Mochizuki et al. 2009; Xu et al. 2009; Yamada et al. 2009). Whether expressed in the bladder or not, TRPV1 channels are certainly present in sensory nerves innervating the bladder (Szallasi et al. 1993a). By recording afferent electrical nerve activity *in vitro* in response to distention, the authors found that the sensitivity of low-treshold fibers was attenuated in TRPV1-null mice (Daly et al. 2007). In regards to the precise function of the channel, the authors argue that it could either act as a mechanosensor directly or could only be modulating the excitability of the nerve cells in order to lower the threshold for their activation upon mechanical stimulus arrival (Daly et al. 2007).

3.8.4 The Central Nervous System

Another system in mammalian physiology that involves mechanotransduction and where TRPV1 plays a role is the one that controls body fluid osmolality. Changes in blood osmolality are detected by neurons in blood-brain barrier-deficient nuclei of the lamina terminalis, namely the subfornical region, the median preoptic nucleus and the organum vasculosum (OV). These cells stimulate magnocellular (MNC) neurons in the hypothalamic paraventricular and supraoptic nuclei upon increases in blood osmolality. Magnocellular neurons, in turn, release from their axons in the pituitary gland the antidiuretic homone vasopressin (VP) to the blood stream, which ultimately signals the kidneys to retain water (Bourque 2008).

MNC neurons possess intrinsic osmosensitivity (Oliet and Bourque 1992, 1993), which is sufficient to trigger or inhibit VP release upon changes in extracellular fluid tonicity. The electrical responses of MNCs to tonicity are mediated by a stretch-inactivated non-selective cationic current (SIC) of unknown origin. Interestingly, hypertonic solution-elicited increases in MNC membrane conductance can be mimicked by equivalent negative changes in pressure applied by suction from a pipette in the whole-cell configuration of the patch clamp, and inhibited by applying a counterbalancing increase in pressure (Zhang et al. 2007b). These data establish that the SIC is equally sensitive to osmotic and mechanical stimuli.

Recently an interesting report provided evidence that an N-terminally truncated capsaicin-insensitive variant of TRPV1, but not the WT channel, is expressed in MNC neurons (Sharif Naeini et al. 2006). Furthermore, neurons from TRPV1-null mice displayed neither an increase in conductance nor depolarization and action potential firing upon exposure to hypertonic solutions. Moreover, VP-release as a

function of hyperosmolality was reduced 4-fold in the genetically modified mice (Yokoyama et al. 2010; Sharif Naeini et al. 2006). Notably, TRPV1-null mice OV neurons also display decreased electrical activity in response to hyperosmolality with respect to WT, and a reduction in water intake under systemic hyperosmolality (Ciura and Bourque 2006), although these data remain controversial (Taylor et al. 2008).

Another source of evidence that connects the TRPV1 channel with MNC neuron osmosensing comes from their thermosensitivity. Elevation of the temperature above 35°C has been shown to augment MNC neuron conductance and to increase action potential firing rate (Sharif-Naeini et al. 2008). Genetic TRPV1 ablation or acute specific inhibition with SB366791 results in a significant diminution of this response (Sharif-Naeini et al. 2008). Consistently, VP release upon hyperthermia is not increased in TRPV1-null mice (Sharif-Naeini et al. 2008). However, these results are in contradiction with the recently proposed temperature-sensing domain in the TRPV1 channel (Yao et al. 2011), which is located around the region that is altered in the MNC neurons' N-terminally truncated variant (Sharif Naeini et al. 2006).

Regarding the identity of the mechanosensory channel in this system, interesting information may come from pharmacological inhibition of signaling cascades: Angiotensin II (AngII) has been shown to potentiate MNC neuron's response to hypertonicity by increasing the frequency of action potential firing (Chakfe and Bourque 2000; Zhang and Bourque 2008). Based on results obtained by applying a series of pharmacological inhibitors, it has been suggested that the potentiating effects of AngII result from the sequential activation of PLC and a Ca^{2+}-dependent PKC, which in turn is proposed to increase cortical F-actin concentration by promoting polymerization (Zhang and Bourque 2008), which is essential not only for the potentiating effects of AngII but also for neuronal responsiveness to hypertonicity (Zhang et al. 2007b). Notably, the mechanosensitive (Mederos y Schnitzler et al. 2011) G_q protein-coupled angiotensin type 1 receptor (AT1R) has been shown to be responsible for the effects of AngII in MNC neurons (Hatae et al. 2001), putting it forward as a possible mechanosensor in this system.

What might the connection be between TRPV1, AngII and F-actin? Notably, genetic ablation of TRPV1 in mice also eliminates the stimulatory effects of AngII in MNC neurons (Sharif Naeini et al. 2006), indicating that there is, in fact a connection. Signaling molecules activated downstream of AT1R stimulation might be sensitizing the channel after mechanical stimulation. In this regard, a study performed in trigeminal ganglion cells reported that a transmembrane osmotic gradient, regardless of its orientation (extracellular hypo- or hypertonicity), potentiates the channel's response to capsaicin, suppresses tachyphylaxis and increases TRPV1 membrane expression (Liu et al. 2007). The observed effects were independent of other osmolality induced currents (e.g. mediated by TRPV4). A very interesting result came from the use of inhibitors of PKA, PKC, PI3K and PLC: the effects of hyper- or hypo-tonicity on channel activity were differentially affected by each inhibitor. In short, potentiation by hypertonic stimuli was more dependent on PKA and PI3K, while hypotonic potentiation was more severely affected by PKC inhibition (Liu et al. 2007). These results indicate that the effects of tonicity on the channel are mediated by different intracellular pathways depending on the direction of the osmolality gradient. A recent

Ca^{2+}-imaging study in TRPV1-transfected HEK293 cells found that hypertonicity, but not hypotonicity, potentiates the channel's response to elevated temperature, capsaicin and low pH (Nishihara et al. 2011).

3.9 Conclusion and Perspectives

As becomes evident from the data, mechanosensation seems to involve a plethora of different cell-signaling pathways that can interact with each other at many points along the signaling cascade. Notably, the TRPV1 channel is a formidable point of convergence. It becomes evident that a combination of several approaches will be necessary to gain a deeper insight into mechanosensory processes. Experimental settings that allow monitoring function, location and proximity to other molecules simultaneously will certainly aid in the advancement. Some useful techniques may include single-molecule fluorescence tracking, fluorescence correlation spectroscopy and FRET, together with electrophysiological recordings. In any case, it is likely that significant methodological improvements and innovations will be required to fully unravel the molecular mechanisms that underlie physiological processes such as mechanosensation.

Acknowledgments This work was supported by grants from PAPIIT IN204111, CONACyT CB-129474 and a Grant from Fundación Miguel Alemán to T.R.

References

Ahern GP (2003) Activation of TRPV1 by the satiety factor oleoylethanolamide. J Biol Chem 278:30429–30434

Ahern GP, Brooks IM, Miyares RL, Wang XB (2005) Extracellular cations sensitize and gate capsaicin receptor TRPV1 modulating pain signaling. J Neurosci 25:5109–5116

Ahern GP, Wang X, Miyares RL (2006) Polyamines are potent ligands for the capsaicin receptor TRPV1. J Biol Chem 281:8991–8995

Amadesi S, Cottrell GS, Divino L, Chapman K, Grady EF, Bautista F, Karanjia R, Barajas-Lopez C, Vanner S, Vergnolle N, Bunnett NW (2006) Protease-activated receptor 2 sensitizes TRPV1 by protein kinase Cepsilon- and A-dependent mechanisms in rats and mice. J Physiol 575:555–571

Aneiros E, Cao L, Papakosta M, Stevens EB, Phillips S, Grimm C (2011) The biophysical and molecular basis of TRPV1 proton gating. EMBO J 30:994–1002

Artim DE, Bazely F, Daugherty SL, Sculptoreanu A, Koronowski KB, Schopfer FJ, Woodcock SR, Freeman BA, de Groat WC (2011) Nitro-oleic acid targets transient receptor potential (TRP) channels in capsaicin sensitive afferent nerves of rat urinary bladder. Exp Neurol 232:90–99

Avelino A, Cruz F (2006) TRPV1 (vanilloid receptor) in the urinary tract: expression, function and clinical applications. Naunyn Schmiedebergs Arch Pharmacol 373:287–299

Baumann TK, Martenson ME (2000) Extracellular protons both increase the activity and reduce the conductance of capsaicin- gated channels. J Neurosci 20:RC80

Bevan S, Yeats J (1991) Protons activate a cation conductance in a sub-population of rat dorsal root ganglion neurones. J Physiol 433:145–161

Bhave G, Hu HJ, Glauner KS, Zhu W, Wang H, Brasier DJ, Oxford GS, Gereau R Wt (2003) Protein kinase C phosphorylation sensitizes but does not activate the capsaicin receptor transient receptor potential vanilloid 1 (TRPV1). Proc Natl Acad Sci U S A 100:12480–12485

Bhave G, Zhu W, Wang H, Brasier D, Oxford G, IV RG (2002) cAmp-Dependent protien kinase regulates desensitization of the capsaicin receptor (VR1) by direct phosphorylation. Neuron 35:721–731

Birder LA, Kanai AJ, de Groat WC, Kiss S, Nealen ML, Burke NE, Dineley KE, Watkins S, Reynolds IJ, Caterina MJ (2001) Vanilloid receptor expression suggests a sensory role for urinary bladder epithelial cells. Proc Natl Acad Sci USA 98:13396–13401

Birder LA, Nakamura Y, Kiss S, Nealen ML, Barrick S, Kanai AJ, Wang E, Ruiz G, De Groat WC, Apodaca G, Watkins S, Caterina MJ (2002) Altered urinary bladder function in mice lacking the vanilloid receptor TRPV1. Nat Neurosci 5:856–860

Bohlen C, Priel A, Zhou S, King D, Siemens J, Julius D (2010) A bivalent tarantula toxin activates the capsaicin receptor, TRPV1, by targeting the outer pore domain. Cell 141:834–845

Boukalova S, Marsakova L, Teisinger J, Vlachova V (2010) Conserved residues within the putative S4–S5 region serve distinct functions among thermosensitive vanilloid transient receptor potential (TRPV) channels. J Biol Chem 285:41455–41462

Bourque CW (2008) Central mechanisms of osmosensation and systemic osmoregulation. Nat Rev Neurosci 9:519–531

Brauchi S, Orio P, Latorre R (2004) Clues to understanding cold sensation: thermodynamics and electrophysiological analysis of the cold receptor TRPM8. Proc Natl Acad Sci USA 101:15494–15499

Brauchi S, Orta G, Salazar M, Rosenmann E, Latorre R (2006) A hot-sensing cold receptor: C-terminal domain determines thermosensation in transient receptor potential channels. J Neurosci 26:4835–4840

Brauchi S, Orta G, Mascayano C, Salazar M, Raddatz N, Urbina H, Rosenmann E, Gonzalez-Nilo F, Latorre R (2007) Dissection of the components for PIP2 activation and thermosensation in TRP channels. Proc Natl Acad Sci USA 104:10246–10251

Camprubi-Robles M, Planells-Cases R, Ferrer-Montiel A (2009) Differential contribution of SNARE-dependent exocytosis to inflammatory potentiation of TRPV1 in nociceptors. Faseb J 23:3722–3733

Cantero-Recasens G, Gonzalez JR, Fandos C, Duran-Tauleria E, Smit LA, Kauffmann F, Anto JM, Valverde MA (2010) Loss of function of transient receptor potential vanilloid 1 (TRPV1) genetic variant is associated with lower risk of active childhood asthma. J Biol Chem 285:27532–27535

Caterina MJ, Julius D (2001) The vanilloid receptor: a molecular gateway to the pain pathway. Annu Rev Neurosci 24:487–517

Caterina MJ, Schumacher MA, Tominaga M, Rosen TA, Levine JD, Julius D (1997) The capsaicin receptor: a heat-activated ion channel in the pain pathway. Nature 389:816–824

Catterall WA (2010) Ion channel voltage sensors: structure, function, and pathophysiology. Neuron 67:915–928

Cesare P, McNaughton P (1996) A novel heat-activated current in nociceptive neurons and its sensitization by bradykinin. Proc Natl Acad Sci USA 93:15435–15439

Cesare P, Dekker LV, Sardini A, Parker PJ, McNaughton PA (1999) Specific involvement of PKC-epsilon in sensitization of the neuronal response to painful heat. Neuron 23:617–624

Ciura S, Bourque C (2006) Transient receptor potential vanilloid 1 is required for intrinsic osmoreception in organum vasculosum lamina terminalis neurons and for normal thirst responses to systemic hyperosmolality. J Neurosci 26:9069–9075

Chakfe Y, Bourque CW (2000) Excitatory peptides and osmotic pressure modulate mechanosensitive cation channels in concert. Nat Neurosci 3:572–579

Chan CL, Facer P, Davis JB, Smith GD, Egerton J, Bountra C, Williams NS, Anand P (2003) Sensory fibres expressing capsaicin receptor TRPV1 in patients with rectal hypersensitivity and faecal urgency. Lancet 361:385–391

Chaudhury S, Bal M, Belugin S, Shapiro MS, Jeske NA (2011) AKAP150-mediated TRPV1 sensitization is disrupted by calcium/calmodulin. Mol Pain 7:34

Chen YS, Lu MJ, Huang HS, Ma MC (2010) Mechanosensitive transient receptor potential vanilloid type 1 channels contribute to vascular remodeling of rat fistula veins. J Vasc Surg 52:1310–1320

Chou MZ, Mtui T, Gao YD, Kohler M, Middleton RE (2004) Resiniferatoxin binds to the capsaicin receptor (TRPV1) near the extracellular side of the S4 transmembrane domain. Biochemistry 43:2501–2511

Christoph T, Grunweller A, Mika J, Schafer MK, Wade EJ, Weihe E, Erdmann VA, Frank R, Gillen C, Kurreck J (2006) Silencing of vanilloid receptor TRPV1 by RNAi reduces neuropathic and visceral pain in vivo. Biochem Biophys Res Commun 350:238–243

Chu CJ, Huang SM, De Petrocellis L, Bisogno T, Ewing SA, Miller JD, Zipkin RE, Daddario N, Appendino G, Di Marzo V, Walker JM (2003) N-oleoyldopamine, a novel endogenous capsaicin-like lipid that produces hyperalgesia. J Biol Chem 278:13633–13639

Chuang HH, Lin S (2009) Oxidative challenges sensitize the capsaicin receptor by covalent cysteine modification. Proc Natl Acad Sci USA 106:20097–20102

Chuang HH, Prescott ED, Kong H, Shields S, Jordt SE, Basbaum AI, Chao MV, Julius D (2001) Bradykinin and nerve growth factor release the capsaicin receptor from PtdIns(4,5)P2-mediated inhibition. Nature 411:957–962

Chung MK, Guler AD, Caterina MJ (2008) TRPV1 shows dynamic ionic selectivity during agonist stimulation. Nat Neurosci 11:555–564

Daly D, Rong W, Chess-Williams R, Chapple C, Grundy D (2007) Bladder afferent sensitivity in wild-type and TRPV1 knockout mice. J Physiol 583:663–674

Davis JB, Gray J, Gunthorpe MJ, Hatcher JP, Davey PT, Overend P, Harries MH, Latcham J, Clapham C, Atkinson K, Hughes SA, Rance K, Grau E, Harper A J, Pugh PL, Rogers DC, Bingham S, Randall A, Sheardown SA (2000) Vanilloid receptor-1 is essential for inflammatory thermal hyperalgesia. Nature 405:183–187

De Petrocellis L, Bisogno T, Davis JB, Pertwee RG, Di Marzo V (2000) Overlap between the ligand recognition properties of the anandamide transporter and the VR1 vanilloid receptor: inhibitors of anandamide uptake with negligible capsaicin-like activity. FEBS Lett 483:52–56

De Petrocellis L, Chu CJ, Moriello AS, Kellner JC, Walker JM, Di Marzo V (2004) Actions of two naturally occurring saturated N-acyldopamines on transient receptor potential vanilloid 1 (TRPV1) channels. Br J Pharmacol 143:251–256

De Petrocellis L, Davis JB, Di Marzo V (2001a) Palmitoylethanolamide enhances anandamide stimulation of human vanilloid VR1 receptors. FEBS Lett 506:253–256

De Petrocellis L, Harrison S, Bisogno T, Tognetto M, Brandi I, Smith GD, Creminon C, Davis JB, Geppetti P, Di Marzo V (2001b) The vanilloid receptor (VR1)-mediated effects of anandamide are potently enhanced by the cAMP-dependent protein kinase. J Neurochem 77:1660–1663

Dhaka A, Uzzell V, Dubin AE, Mathur J, Petrus M, Bandell M, Patapoutian A (2009) TRPV1 is activated by both acidic and basic pH. J Neurosci 29:153–158

Di Marzo V, Fontana A, Cadas H, Schinelli S, Cimino G, Schwartz JC, Piomelli D (1994) Formation and inactivation of endogenous cannabinoid anandamide in central neurons. Nature 372:686–691

Di Marzo V, Blumberg PM, Szallasi A (2002) Endovanilloid signaling in pain. Curr Opin Neurobiol 12:372–379

Docherty RJ, Yeats JC, Bevan S, Boddeke HW (1996) Inhibition of calcineurin inhibits the desensitization of capsaicin-evoked currents in cultured dorsal root ganglion neurones from adult rats. Pflugers Arch 431:828–837

Everaerts W, Vriens J, Owsianik G, Appendino G, Voets T, De Ridder D, Nilius B (2010) Functional characterization of transient receptor potential channels in mouse urothelial cells. Am J Physiol Renal Physiol 298:F692–701

Fernandez-Ballester G, Ferrer-Montiel A (2008) Molecular modeling of the full-length human TRPV1 channel in closed and desensitized states. J Membr Biol 223:161–172

Gamper N, Shapiro MS (2007) Regulation of ion transport proteins by membrane phosphoinositides. Nat Rev Neurosci 8:921–934

Garcia-Martinez C, Morenilla-Palao C, Planells-Cases R, Merino JM, Ferrer-Montiel A (2000) Identification of an aspartic residue in the P-loop of the vanilloid receptor that modulates pore properties. J Biol Chem 275:32552–32558

García-Sanz N, Fernández-Carvajal A, Morenilla-Palao C, Planells-Cases R, Fajardo-Sánchez E, Fernández-Ballester G, Ferrer-Montiel A (2004) Identification of a tetramerization domain in the C terminus of the Vanilloid receptor. J Neurosci 24:5307–5314

García-Sanz N, Valente P, Gomis A, Fernandez-Carvajal A, Fernandez-Ballester G, Viana F, Belmonte C, Ferrer-Montiel A (2007) A role of the transient receptor potential domain of vanilloid receptor I in channel gating. J Neurosci 27:11641–11650

Gaudet R (2008) A primer on ankyrin repeat function in Trp channels and beyond. Molecular BioSystems 4:372–379

Gavva NR, Klionsky L, Qu Y, Shi L, Tamir R, Edenson S, Zhang TJ, Viswanadhan V N, Toth A, Pearce LV, Vanderah TW, Porreca F, Blumberg PM, Lile J, Sun Y, Wild K, Louis JC, Treanor JJ (2004) Molecular determinants of vanilloid sensitivity in TRPV1. J Biol Chem 279:20283–20295

Goswami C, Dreger M, Jahnel R, Bogen O, Gillen C, Hucho F (2004) Identification and characterization of a Ca^{2+}-sensitive interaction of the vanilloid receptor TRPV1 with tubulin. J Neurochem 91:1092–1103

Goswami C, Dreger M, Otto H, Schwappach B, Hucho F (2006) Rapid disassembly of dynamic microtubules upon activation of the capsaicin receptor TRPV1. J Neurochem 96:254–266

Goswami C, Hucho TB, Hucho F (2007a) Identification and characterisation of novel tubulin-binding motifs located within the C-terminus of TRPV1. J Neurochem 101:250–262

Goswami C, Schmidt H, Hucho F (2007b) TRPV1 at nerve endings regulates growth cone morphology and movement through cytoskeleton reorganization. Febs J 274:760–772

Goswami C, Kuhn J, Dina OA, Fernandez-Ballester G, Levine JD, Ferrer-Montiel A, Hucho T (2011) Estrogen destabilizes microtubules through an ion-conductivity-independent TRPV1 pathway. J Neurochem 117:995–1008

Gracheva EO, Cordero-Morales JF, Gonzalez-Carcacia JA, Ingolia NT, Manno C, Aranguren CI, Weissman JS, Julius D (2011) Ganglion-specific splicing of TRPV1 underlies infrared sensation in vampire bats. Nature 476:88–91

Grandl J, Kim S, Uzzell V, Bursulaya B, Petrus M, Bandell M, Patapoutian A (2010) Temperature-induced opening of TRPV1 ion channel is stabilized by the pore domain. Nat Neurosci

Guesnet P, Alessandri J M (2011) Docosahexaenoic acid (DHA) and the developing central nervous system (CNS) – Implications for dietary recommendations. Biochimie 93:7–12

Gunthorpe MJ, Harries MH, Prinjha RK, Davis JB, Randall A (2000) Voltage- and time-dependent properties of the recombinant rat vanilloid receptor (rVR1). J Physiol 525 Pt 3:747–759

Hatae T, Kawano H, Karpitskiy V, Krause JE, Masuko S (2001) Arginine-vasopressin neurons in the rat hypothalamus produce neurokinin B and co-express the tachykinin NK-3 receptor and angiotensin II type 1 receptor. Arch Histol Cytol 64:37–44

Hellwig N, Plant TD, Janson W, Schafer M, Schultz G, Schaefer M (2004) TRPV1 acts as proton channel to induce acidification in nociceptive neurons. J Biol Chem 279:34553–34561

Heng YJ, Saunders CI, Kunde DA, Geraghty DP (2011) TRPV1, NK1 receptor and substance P immunoreactivity and gene expression in the rat lumbosacral spinal cord and urinary bladder after systemic, low dose vanilloid administration. Regul Pept 167:250–258

Huang SM, Bisogno T, Trevisani M, Al-Hayani A, De Petrocellis L, Fezza F, Tognetto M, Petros TJ, Krey JF, Chu CJ, Miller JD, Davies SN, Geppetti P, Walker JM, Di Marzo V (2002) An endogenous capsaicin-like substance with high potency at recombinant and native vanilloid VR1 receptors. Proc Natl Acad Sci USA 99:8400–8405

Hwang SW, Cho H, Kwak J, Lee SY, Kang CJ, Jung J, Cho S, Min KH, Suh YG, Kim D, Oh U (2000) Direct activation of capsaicin receptors by products of lipoxygenases: endogenous capsaicin-like substances. Proc Natl Acad Sci USA 97:6155–6160

Iida T, Moriyama T, Kobata K, Morita A, Murayama N, Hashizume S, Fushiki T, Yazawa S, Watanabe T, Tominaga M (2003) TRPV1 activation and induction of nociceptive response by a non-pungent capsaicin-like compound, capsiate. Neuropharmacology 44:958–967

Inoue M, Rashid M, Fujita R, Contos J, Chun J, Ueda H (2004) Initiation of neuropathic pain requires lysophosphatidic acid receptor signaling. Nat Med 10(7):712–718

Inoue R, Jensen LJ, Jian Z, Shi J, Hai L, Lurie AI, Henriksen FH, Salomonsson M, Morita H, Kawarabayashi Y, Mori M, Mori Y, Ito Y (2009) Synergistic activation of vascular TRPC6 channel by receptor and mechanical stimulation via phospholipase C/diacylglycerol and phospholipase A2/omega-hydroxylase/20-HETE pathways. Circ Res 104:1399–1409

Islas LD, Salazar H, Jara-Oseguera A, Nieto-Posadas A, Llorente I, Rangel-Yescas G, Rosenbaum T (2009) The helical character of the S6 segment of TRPV1 channels. Channels (Austin) 3:311–313

Iwasaki Y, Morita A, Iwasawa T, Kobata K, Sekiwa Y, Morimitsu Y, Kubota K, Watanabe T (2006) A nonpungent component of steamed ginger–[10]-shogaol–increases adrenaline secretion via the activation of TRPV1. Nutr Neurosci 9:169–178

Iwasaki Y, Saito O, Tanabe M, Inayoshi K, Kobata K, Uno S, Morita A, Watanabe T (2008) Monoacylglycerols activate capsaicin receptor, TRPV1. Lipids 43:471–483

Jara-Oseguera A, Llorente I, Rosenbaum T, Islas LD (2008) Properties of the inner pore region of TRPV1 channels revealed by block with quaternary ammoniums. J Gen Physiol 132:547–562

Jara-Oseguera A, Nieto-Posadas A, Szallasi A, Islas LD, Rosenbaum T (2010) Molecular Mechanisms of TRPV1 Channel Activation. The Open Pain Journal 3:68–81

Jeske NA, Patwardhan AM, Gamper N, Price TJ, Akopian AN, Hargreaves KM (2006) Cannabinoid WIN 55,212–2 regulates TRPV1 phosphorylation in sensory neurons. J Biol Chem 281:32879–32890

Jeske NA, Patwardhan AM, Henry MA, Milam SB (2009a) Fibronectin stimulates TRPV1 translocation in primary sensory neurons. J Neurochem 108:591–600

Jeske NA, Patwardhan AM, Ruparel NB, Akopian AN, Shapiro MS, Henry MA (2009b) A-kinase anchoring protein 150 controls protein kinase C-mediated phosphorylation and sensitization of TRPV1. Pain 146:301–307

Jin Y, Kim DK, Khil LY, Oh U, Kim J, Kwak J (2004) Thimerosal decreases TRPV1 activity by oxidation of extracellular sulfhydryl residues. Neurosci Lett 369:250–255

Jin X, Touhey J, Gaudet R (2006) Structure of the N-terminal ankyrin repeat domain of the TRPV2 ion channel. J Biol Chem 281(35):25006–25010

Jira W, Spiteller G, Richter A (1997) Increased levels of lipid oxidation products in low density lipoproteins of patients suffering from rheumatoid arthritis. Chem Phys Lipids 87:81–89

Jones RC, 3rd, Xu L, Gebhart GF (2005) The mechanosensitivity of mouse colon afferent fibers and their sensitization by inflammatory mediators require transient receptor potential vanilloid 1 and acid-sensing ion channel 3. J Neurosci 25:10981–10989

Jordt SE, Julius D (2002) Molecular basis for species-specific sensitivity to "hot" chili peppers. Cell 108:421–430

Jordt SE, Tominaga M, Julius D (2000) Acid potentiation of the capsaicin receptor determined by a key extracellular site. Proc Natl Acad Sci USA 97:8134–8139

Jung J, Hwang SW, Kwak J, Lee SY, Kang CJ, Kim WB, Kim D, Oh U (1999) Capsaicin binds to the intracellular domain of the capsaicin-activated ion channel. J Neurosci 19:529–538

Jung J, Lee SY, Hwang SW, Cho H, Shin J, Kang YS, Kim S, Oh U (2002) Agonist recognition sites in the cytosolic tails of vanilloid receptor 1. J Biol Chem 277:44448–44454

Jung J, Shin JS, Lee SY, Hwang SW, Koo J, Cho H, Oh U (2004) Phosphorylation of vanilloid receptor 1 by Ca^{2+}/calmodulin-dependent kinase II regulates its vanilloid binding. J Biol Chem 279:7048–7054

Kedei N, Szabo T, Lile JD, Treanor JJ, Olah Z, Iadarola MJ, Blumberg PM (2001) Analysis of the native quaternary structure of vanilloid receptor 1. J Biol Chem 276:28613–28619

Khoo NK, Freeman BA (2011) Electrophilic nitro-fatty acids: anti-inflammatory mediators in the vascular compartment. Curr Opin Pharmacol 10:179–184

Kim A, Tang Z, Liu Q, Patel K, Maag D, Geng Y, Dong X (2008) Pirt, a phosphoinositide-binding protein, functions as a regulatory subunit of TRPV1. Cell 133(3):475–485

Klein R, Ufret-Vincenty C, Hua L, Gordon S (2008) Determinants of molecular specificity in phosphoinositide regulation. J Biol Chem 283:26208–26216

Koplas PA, Rosenberg RL, Oxford GS (1997) The role of calcium in the desensitization of capsaicin responses in rat dorsal root ganglion neurons. J Neurosci 17:3525–3537

Kuzhikandathil EV, Wang H, Szabo T, Morozova N, Blumberg PM, Oxford GS (2001) Functional analysis of capsaicin receptor (vanilloid receptor subtype 1) multimerization and agonist responsiveness using a dominant negative mutation. J Neurosci 21:8697–8706

Kwak J, Wang MH, Hwang SW, Kim TY, Lee SY, Oh U (2000) Intracellular ATP increases capsaicin-activated channel activity by interacting with nucleotide-binding domains. J Neurosci 20:8298–8304

Laird JM, Martinez-Caro L, Garcia-Nicas E, Cervero F (2001) A new model of visceral pain and referred hyperalgesia in the mouse. Pain 92:335–342

Latorre R, Brauchi S, Orta G, Zaelzer C, Vargas G (2007) ThermoTRP channels as modular proteins with allosteric gating. Cell Calcium 42:427–438

Lee TH, Mencia-Huerta JM, Shih C, Corey EJ, Lewis RA, Austen KF (1984) Effects of exogenous arachidonic, eicosapentaenoic, and docosahexaenoic acids on the generation of 5-lipoxygenase pathway products by ionophore-activated human neutrophils. J Clin Invest 74:1922–1933

Levine JD, Taiwo YO (1990) Hyperalgesic pain: a review. Anesth Prog 37:133–135

Lilja J, Laulund F, Forsby A (2007) Insulin and insulin-like growth factor type-I up-regulate the vanilloid receptor-1 (TRPV1) in stably TRPV1-expressing SH-SY5Y neuroblastoma cells. J Neurosci Res 85:1413–1419

Lin ME, Herr DR, Chun J (2010) Lysophosphatidic acid (LPA) receptors: signaling properties and disease relevance. Prostaglandins Other Lipid Mediat 91:130–138

Lishko P, Procko E, Jin X, Phelps CRG (2007) The ankyrin repeats of TRPV1 bind multiple ligands and modulate channel sensitivity. Neuron 54:905–918

Liu L, Simon SA (1996) Capsaicin-induced currents with distinct desensitization and Ca^{2+} dependence in rat trigeminal ganglion cells. J Neurophysiol 75:1503–1514

Liu B, Hui K, Qin F (2003) Thermodynamics of heat activation of single capsaicin ion channels VR1. Biophys J 85:2988–3006

Liu B, Zhang C, Qin F (2005) Functional recovery from desensitization of vanilloid receptor TRPV1 requires resynthesis of phosphatidylinositol 4,5-bisphosphate. J Neurosci 25:4835–4843

Liu M, Huang W, Wu D, Priestley JV (2006) TRPV1, but not P2X, requires cholesterol for its function and membrane expression in rat nociceptors. Eur J Neurosci 24:1–6

Liu L, Chen L, Liedtke W, Simon S (2007) Changes in osmolality sensitize the response to capsaicin in trigeminal sensory neurons. J Neurophysiol 97:2001–2015

Liu B, Yao J, Wang Y, Li H, Qin F (2009) Proton inhibition of unitary currents of vanilloid receptors. J Gen Physiol 134:243–258

Luebbert M, Radtke D, Wodarski R, Damann N, Hatt H, Wetzel CH (2010) Direct activation of transient receptor potential V1 by nickel ions. Pflugers Arch 459:737–750

Lukacs V, Thyagarajan B, Varnai P, Balla A, Balla T, Rohacs T (2007) Dual regulation of TRPV1 by phosphoinositides. J Neurosci 27:7070–7080

Mandadi S, Numazaki M, Tominaga M, Bhat MB, Armati PJ, Roufogalis BD (2004) Activation of protein kinase C reverses capsaicin-induced calcium-dependent desensitization of TRPV1 ion channels. Cell Calcium 35:471–478

Matsumoto K, Hosoya T, Tashima K, Namiki T, Murayama T, Horie S (2011) Distribution of transient receptor potential vanilloid 1 channel-expressing nerve fibers in mouse rectal and colonic enteric nervous system: relationship to peptidergic and nitrergic neurons. Neuroscience 172:518–534

Matta JA, Ahern GP (2007) Voltage is a partial activator of thermo-sensitive TRP channels. J Physiol

Matta JA, Miyares RL, Ahern GP (2007) TRPV1 is a novel target for omega-3 polyunsaturated fatty acids. J Physiol 578:397–411

Mccleverty C, Koesema E, Patapoutian A, Lesley S, Kreusch A (2006) Crystal structure of the human TRPV2 channel ankyrin repeat domain. Protein Sci 2201–2206

Mederos y Schnitzler M, Storch U, Gudermann T (2011) AT1 receptors as mechanosensors. Curr Opin Pharmacol 11:112–116

Minke B (1977) Drosophila mutant with a transducer defect. Biophys Struct Mech 3:59–64

Miranda A, Nordstrom E, Mannem A, Smith C, Banerjee B, Sengupta JN (2007) The role of transient receptor potential vanilloid 1 in mechanical and chemical visceral hyperalgesia following experimental colitis. Neuroscience

Mochizuki T, Sokabe T, Araki I, Fujishita K, Shibasaki K, Uchida K, Naruse K, Koizumi S, Takeda M, Tominaga M (2009) The TRPV4 cation channel mediates stretch-evoked Ca^{2+} influx and ATP release in primary urothelial cell cultures. J Biol Chem 284:21257–21264

Mohapatra DP, Nau C (2003) Desensitization of capsaicin-activated currents in the vanilloid receptor TRPV1 is decreased by the cyclic AMP-dependent protein kinase pathway. J Biol Chem 278:50080–50090

Mohapatra DP, Nau C (2005) Regulation of Ca^{2+}-dependent desensitization in the vanilloid receptor TRPV1 by calcineurin and cAMP-dependent protein kinase. J Biol Chem 280:13424–13432

Moiseenkova-Bell VY, Stanciu LA, Serysheva, II, Tobe BJ, Wensel TG (2008) Structure of TRPV1 channel revealed by electron cryomicroscopy. Proc Natl Acad Sci USA 105:7451–7455

Montell C (2011) The history of TRP channels, a commentary and reflection. Pflugers Arch 461:499–506

Montell C, Rubin GM (1989) Molecular characterization of the Drosophila trp locus: a putative integral membrane protein required for phototransduction. Neuron 2:1313–1323

Moriyama T, Iida T, Kobayashi K, Higashi T, Fukuoka T, Tsumura H, Leon C, Suzuki N, Inoue K, Gachet C, Noguchi K, Tominaga M (2003) Possible involvement of P2Y2 metabotropic receptors in ATP-induced transient receptor potential vanilloid receptor 1-mediated thermal hypersensitivity. J Neurosci 23:6058–6062

Morenilla-Palao C, Planells-Cases R, García-Sanz N, Ferrer-Montiel A (2004) Regulated exocytosis contributes to protein kinase C potentiation of vanilloid receptor activity. J Biol Chem 279:25665–25672

Moriyama T, Higashi T, Togashi K, Iida T, Segi E, Sugimoto Y, Tominaga T, Narumiya S, Tominaga M (2005) Sensitization of TRPV1 by EP1 and IP reveals peripheral nociceptive mechanism of prostaglandins. Mol Pain 1:3

Movahed P, Jonsson BA, Birnir B, Wingstrand JA, Jorgensen TD, Ermund A, Sterner O, Zygmunt PM, Hogestatt ED (2005) Endogenous unsaturated C18 N-acylethanolamines are vanilloid receptor (TRPV1) agonists. J Biol Chem 280:38496–38504

Myers BR, Bohlen CJ, Julius D (2008) A yeast genetic screen reveals a critical role for the pore helix domain in TRP channel gating. Neuron 58:362–373

Nieto-Posadas A, Picazo-Juárez G, Llorente I, Jara-Oseguera A, Morales-Lázaro S, Escalante-Alcalde D, Islas LD, Rosenbaum T (2011) Lysophosphatidic acid directly activates TRPV1 through a C-terminal binding site. Nat Chem Biol 8: 78–85

Nilius B, Talavera K, Owsianik G, Prenen J, Droogmans G, Voets T (2005) Gating of TRP channels: a voltage connection? J Physiol 567:35–44.

Nishihara E, Hiyama TY, Noda M (2011) Osmosensitivity of transient receptor potential vanilloid 1 is synergistically enhanced by distinct activating stimuli such as temperature and protons. PLoS One 6:e22246

Novakova-Tousova K, Vyklicky L, Susankova K, Benedikt J, Samad A, Teisinger J, Vlachova V (2007) Functional changes in the vanilloid receptor subtype 1 channel during and after acute desensitization. J Neurosci 149:144–154

Numazaki M, Tominaga T, Toyooka H, Tominaga M (2002) Direct phosphorylation of capsaicin receptor VR1 by protein kinase Cepsilon and identification of two target serine residues. J Biol Chem 277:13375–13378

Numazaki M, Tominaga T, Takeuchi K, Murayama N, Toyooka H, Tominaga M (2003) Structural determinant of TRPV1 desensitization interacts with calmodulin. Proc Natl Acad Sci USA 100:8002–8006

Obreja O, Rathee PK, Lips KS, Distler C, Kress M (2002) IL-1 beta potentiates heat-activated currents in rat sensory neurons: involvement of IL-1RI, tyrosine kinase, and protein kinase C. Faseb J 16:1497–1503

Ohta T, Ikemi Y, Murakami M, Imagawa T, Otsuguro K, Ito S (2006) Potentiation of transient receptor potential V1 functions by the activation of metabotropic 5-HT receptors in rat primary sensory neurons. J Physiol 576:809–822

Ohta T, Imagawa T, Ito S (2008) Novel gating and sensitizing mechanism of capsaicin receptor (TRPV1): tonic inhibitory regulation of extracellular sodium through the external protonation sites on TRPV1. J Biol Chem 283:9377–9387

Olah Z, Karai L, Iadarola MJ (2002) Protein kinase C(alpha) is required for vanilloid receptor 1 activation. Evidence for multiple signaling pathways. J Biol Chem 277:35752–35759

Oliet SH, Bourque CW (1992) Properties of supraoptic magnocellular neurones isolated from the adult rat. J Physiol 455:291–306

Oliet SH, Bourque CW (1993) Mechanosensitive channels transduce osmosensitivity in supraoptic neurons. Nature 364:341–343

Oseguera AJ, Islas LD, Garcia-Villegas R, Rosenbaum T (2007) On the mechanism of TBA block of the TRPV1 channel. Biophys J 92:3901–3914

Pan HL, Zhang YQ, Zhao ZQ (2010) Involvement of lysophosphatidic acid in bone cancer pain by potentiation of TRPV1 via PKCepsilon pathway in dorsal root ganglion neurons. Mol Pain 6:85

Patwardhan AM, Jeske NA, Price TJ, Gamper N, Akopian AN, Hargreaves KM (2006) The cannabinoid WIN 55,212–2 inhibits transient receptor potential vanilloid 1 (TRPV1) and evokes peripheral antihyperalgesia via calcineurin. Proc Natl Acad Sci USA 103:11393–11398

Patwardhan AM, Scotland PE, Akopian AN, Hargreaves KM (2009) Activation of TRPV1 in the spinal cord by oxidized linoleic acid metabolites contributes to inflammatory hyperalgesia. Proc Natl Acad Sci USA 106:18820–18824

Patwardhan AM, Akopian AN, Ruparel NB, Diogenes A, Weintraub ST, Uhlson C, Murphy RC, Hargreaves KM (2011) Heat generates oxidized linoleic acid metabolites that activate TRPV1 and produce pain in rodents. J Clin Invest 120:1617–1626

Petersen M, LaMotte RH (1993) Effect of protons on the inward current evoked by capsaicin in isolated dorsal root ganglion cells. Pain 54:37–42

Petrosino S, Iuvone T, Di Marzo V (2010) N-palmitoyl-ethanolamine: Biochemistry and new therapeutic opportunities. Biochimie 92:724–727

Picazo-Juarez G, Romero-Suarez S, Nieto-Posadas A, Llorente I, Jara-Oseguera A, Briggs M, McIntosh TJ, Simon SA, Ladron-de-Guevara E, Islas LD, Rosenbaum T (2011) Identification of a binding motif in the S5 helix that confers cholesterol sensitivity to the TRPV1 ion channel. J Biol Chem 286:24966–24976

Piper AS, Yeats JC, Bevan S, Docherty RJ (1999) A study of the voltage dependence of capsaicin-activated membrane currents in rat sensory neurones before and after acute desensitization. J Physiol 518 (Pt 3):721–733

Por ED, Samelson BK, Belugin S, Akopian AN, Scott JD, Jeske NA (2010) PP2B/calcineurin-mediated desensitization of TRPV1 does not require AKAP150. Biochem J 432:549–556

Premkumar LS, Ahern GP (2000) Induction of vanilloid receptor channel activity by protein kinase C. Nature 408:985–990

Premkumar LS, Agarwal S, Steffen D (2002) Single-channel properties of native and cloned rat vanilloid receptors. J Physiol 545:107–117

Premkumar LS, Qi ZH, Van Buren J, Raisinghani M (2004) Enhancement of potency and efficacy of NADA by PKC-mediated phosphorylation of vanilloid receptor. J Neurophysiol 91:1442–1449

Prescott ED, Julius D (2003) A modular PIP2 binding site as a determinant of capsaicin receptor sensitivity. Science 300:1284–1288

Puntambekar P, Van Buren J, Raisinghani M, Premkumar LS, Ramkumar V (2004) Direct interaction of adenosine with the TRPV1 channel protein. J Neurosci 24:3663–3671

Rathee P, Distler C, Obreja O, Neuhuber W, Wang G, Wang S, Nau C, Kress M (2002) PKA/AKAP/VR-1 module: A common link of Gs-mediated signaling to thermal hyperalgesia. J Neurosci 22:4740–4745

Ravnefjord A, Brusberg M, Kang D, Bauer U, Larsson H, Lindstrom E, Martinez V (2009) Involvement of the transient receptor potential vanilloid 1 (TRPV1) in the development of acute visceral hyperalgesia during colorectal distension in rats. Eur J Pharmacol 611:85–91

Ristoiu V, Shibasaki K, Uchida K, Zhou Y, Ton BH, Flonta ML, Tominaga M (2011) Hypoxia-induced sensitization of transient receptor potential vanilloid 1 involves activation of hypoxia-inducible factor-1 alpha and PKC. Pain 152:936–945

Robinson DR, McNaughton PA, Evans ML, Hicks GA (2004) Characterization of the primary spinal afferent innervation of the mouse colon using retrograde labelling. Neurogastroenterol Motil 16:113–124

Rodriguez BM, Sigg D, Bezanilla F (1998) Voltage gating of Shaker K^+channels. The effect of temperature on ionic and gating currents. J Gen Physiol 112:223–242

Rodriguez de Fonseca F, Navarro M, Gomez R, Escuredo L, Nava F, Fu J, Murillo-Rodriguez E, Giuffrida A, LoVerme J, Gaetani S, Kathuria S, Gall C, Piomelli D (2001) An anorexic lipid mediator regulated by feeding. Nature 414:209–212

Rong W, Hillsley K, Davis JB, Hicks G, Winchester WJ, Grundy D (2004) Jejunal afferent nerve sensitivity in wild-type and TRPV1 knockout mice. J Physiol 560:867–881

Rosenbaum T, Gordon-Shaag A, Munari M, Gordon S E (2004) Ca^{2+}/calmodulin modulates TRPV1 activation by capsaicin. J Gen Physiol 123:53–62

Ross RA, Gibson TM, Brockie HC, Leslie M, Pashmi G, Craib SJ, Di Marzo V, Pertwee RG (2001) Structure-activity relationship for the endogenous cannabinoid, anandamide, and certain of its analogues at vanilloid receptors in transfected cells and vas deferens. Br J Pharmacol 132:631–640

Ryu S, Liu B, Qin F (2003) Low pH potentiates both capsaicin binding and channel gating of VR1 receptors. J Gen Physiol 122:45–61

Ryu S, Liu B, Yao J, Fu Q, Qin F (2007) Uncoupling proton activation of vanilloid receptor TRPV1. J Neurosci 27:12797–12807

Salazar H, Jara-Oseguera A, Hernandez-Garcia E, Llorente I, Arias O, II, Soriano-Garcia M, Islas LD, Rosenbaum T (2009) Structural determinants of gating in the TRPV1 channel. Nat Struct Mol Biol 16:704–710

Salazar H, Llorente I, Jara-Oseguera A, Garcia-Villegas R, Munari M, Gordon SE, Islas LD, Rosenbaum T (2008) A single N-terminal cysteine in TRPV1 determines activation by pungent compounds from onion and garlic. Nat Neurosci 11:255–261

Samuelsson B (1983) Leukotrienes: mediators of immediate hypersensitivity reactions and inflammation. Science 220:568–575

Samways DS, Egan TM (2011) Calcium-dependent decrease in the single-channel conductance of TRPV1. Pflugers Arch 62:681–691

Samways DS, Khakh BS, Egan TM (2008) Tunable calcium current through TRPV1 receptor channels. J Biol Chem 283:31274–31278

Sawynok J, Liu XJ (2003) Adenosine in the spinal cord and periphery: release and regulation of pain. Prog Neurobiol 69:313–340

Scotland RS, Chauhan S, Davis C, De Felipe C, Hunt S, Kabir J, Kotsonis P, Oh U, Ahluwalia A (2004) Vanilloid receptor TRPV1, sensory C-fibers, and vascular autoregulation: a novel mechanism involved in myogenic constriction. Circ Res 95:1027–1034

Sculptoreanu A, Kullmann FA, Artim DE, Bazley FA, Schopfer F, Woodcock S, Freeman BA, de Groat WC (2010) Nitro-oleic acid inhibits firing and activates TRPV1- and TRPA1-mediated inward currents in dorsal root ganglion neurons from adult male rats. J Pharmacol Exp Ther 333:883–895

Schnizler K, Shutov LP, Van Kanegan MJ, Merrill MA, Nichols B, McKnight GS, Strack S, Hell JW, Usachev YM (2008) Protein kinase A anchoring via AKAP150 is essential for TRPV1 modulation by forskolin and prostaglandin E2 in mouse sensory neurons. J Neurosci 28:4904–4917

Schoppa NE, McCormack K, Tanouye MA, Sigworth FJ (1992) The size of gating charge in wild-type and mutant Shaker potassium channels. Science 255:1712–1715

Sharif Naeini R, Witty MF, Seguela P, Bourque CW (2006) An N-terminal variant of Trpv1 channel is required for osmosensory transduction. Nat Neurosci 9:93–98

Sharif-Naeini R, Ciura S, Bourque CW (2008) TRPV1 gene required for thermosensory transduction and anticipatory secretion from vasopressin neurons during hyperthermia. Neuron 58:179–185

Shim WS, Tak MH, Lee MH, Kim M, Kim M, Koo JY, Lee CH, Kim M, Oh U (2007) TRPV1 mediates histamine-induced itching via the activation of phospholipase A2 and 12-lipoxygenase. J Neurosci 27:2331–2337

Shin J, Cho H, Hwang SW, Jung J, Shin CY, Lee SY, Kim SH, Lee MG, Choi YH, Kim J, Haber NA, Reichling DB, Khasar S, Levine JD, Oh U (2002) Bradykinin-12-lipoxygenase-VR1 signaling pathway for inflammatory hyperalgesia. Proc Natl Acad Sci USA 99:10150–10155

Smart D, Gunthorpe MJ, Jerman JC, Nasir S, Gray J, Muir AI, Chambers JK, Randall AD, Davis JB (2000) The endogenous lipid anandamide is a full agonist at the human vanilloid receptor (hVR1). Br J Pharmacol 129:227–230

Smart D, Jonsson KO, Vandevoorde S, Lambert DM, Fowler CJ (2002) 'Entourage' effects of N-acyl ethanolamines at human vanilloid receptors. Comparison of effects upon anandamide-induced vanilloid receptor activation and upon anandamide metabolism. Br J Pharmacol 136:452–458

Spencer NJ, Kerrin A, Singer CA, Hennig GW, Gerthoffer WT, McDonnell O (2008) Identification of capsaicin-sensitive rectal mechanoreceptors activated by rectal distension in mice. Neuroscience 153:518–534

Stein AT, Ufret-Vincenty CA, Hua L, Santana LF, Gordon SE (2006) Phosphoinositide 3-kinase binds to TRPV1 and mediates NGF-stimulated TRPV1 trafficking to the plasma membrane. J Gen Physiol 128:509–522

Sugiuar T, Bielefeldt K, Gebhart GF (2004) TRPV1 function in mouse colon sensory neurons is enhanced by metabotropic 5-hydroxytryptamine receptor activation. J Neurosci 24:9521–9530

Sun H, Li DP, Chen SR, Hittelman WN, Pan HL (2009) Sensing of blood pressure increase by transient receptor potential vanilloid 1 receptors on baroreceptors. J Pharmacol Exp Ther 331:851–859

Susankova K, Tousova K, Vyklicky L, Teisinger J, Vlachova V (2006) Reducing and oxidizing agents sensitize heat-activated vanilloid receptor (TRPV1) current. Mol Pharmacol 70:383–394

Susankova K, Ettrich R, Vyklicky L, Teisinger J, Vlachova V (2007) Contribution of the putative inner-pore region to the gating of the transient receptor potential vanilloid subtype 1 channel (TRPV1). J Neurosci 27:7578–7585

Sutton KG, Garrett EM, Rutter AR, Bonnert TP, Jarolimek W, Seabrook GR (2005) Functional characterisation of the S512Y mutant vanilloid human TRPV1 receptor. Br J Pharmacol 146:702–711

Szallasi A, Blumberg PM (1989) Resiniferatoxin, a phorbol-related diterpene, acts as an ultrapotent analog of capsaicin, the irritant constituent in red pepper. Neuroscience 30:515–520

Szallasi A, Blumberg PM (1991) Characterization of vanilloid receptors in the dorsal horn of pig spinal cord. Brain Res 547:335–338

Szallasi A, Blumberg PM (1993) [3H]resiniferatoxin binding by the vanilloid receptor: species-related differences, effects of temperature and sulfhydryl reagents. Naunyn Schmiedebergs Arch Pharmacol 347:84–91

Szallasi A, Blumberg PM (1999) Vanilloid (Capsaicin) receptors and mechanisms. Pharmacol Rev 51:159–212

Szallasi A, Conte B, Goso C, Blumberg PM, Manzini S (1993a) Characterization of a peripheral vanilloid (capsaicin) receptor in the urinary bladder of the rat. Life Sci 52:PL221–226

Szallasi A, Lewin NA, Blumberg PM (1993b) Vanilloid (capsaicin) receptor in the rat: positive cooperativity of resiniferatoxin binding and its modulation by reduction and oxidation. J Pharmacol Exp Ther 266:678–683

Szoke E, Borzsei R, Toth DM, Lengl O, Helyes Z, Sandor Z, Szolcsanyi J (2011) Effect of lipid raft disruption on TRPV1 receptor activation of trigeminal sensory neurons and transfected cell line. Eur J Pharmacol 628:67–74

Tan LL, Bornstein JC, Anderson CR (2008) Distinct chemical classes of medium-sized transient receptor potential channel vanilloid 1-immunoreactive dorsal root ganglion neurons innervate the adult mouse jejunum and colon. Neuroscience 156:334–343

Taylor AC, McCarthy JJ, Stocker SD (2008) Mice lacking the transient receptor vanilloid potential 1 channel display normal thirst responses and central Fos activation to hypernatremia. Am J Physiol Regul Integr Comp Physiol 294:R1285–1293

Tominaga M, Caterina MJ, Malmberg AB, Rosen TA, Gilbert H, Skinner K, Raumann BE, Basbaum AI, Julius D (1998) The cloned capsaicin receptor integrates multiple pain-producing stimuli. Neuron 21:531–543

Tominaga M, Wada M, Masu M (2001) Potentiation of capsaicin receptor activity by metabotropic ATP receptors as a possible mechanism for ATP-evoked pain and hyperalgesia. Proc Natl Acad Sci USA 98:6951–6956

Tousova K, Vyklicky L, Susankova K, Benedikt J, Vlachova V (2005) Gadolinium activates and sensitizes the vanilloid receptor TRPV1 through the external protonation sites. Mol Cell Neurosci 30:207–217

Ufret-Vincenty CA, Klein RM, Hua L, Angueyra J, Gordon SE (2011) Localization of the PIP2 sensor of TRPV1 ion channels. J Biol Chem 286:9688–9698

Valdes AM, De Wilde G, Doherty SA, Lories RJ, Vaughn FL, Laslett LL, Maciewicz RA, Soni A, Hart DJ, Zhang W, Muir KR, Dennison EM, Wheeler M, Leaverton P, Cooper C, Spector TD, Cicuttini FM, Chapman V, Jones G, Arden NK, Doherty M (2011) The Ile585Val TRPV1 variant is involved in risk of painful knee osteoarthritis. Ann Rheum Dis 70:1556–1561

Valente P, García-Sanz N, Gomis A, Fernandez-Carvajal A, Fernandez-Ballester G, Viana F, Belmonte C, Ferrer-Montiel A (2008) Identification of molecular determinants of channel gating in the transient receptor potential box of vanilloid receptor I. Faseb J 22:3298–3309

Valente P, Fernandez-Carvajal A, Camprubi-Robles M, Gomis A, Quirce S, Viana F, Fernandez-Ballester G, Gonzalez-Ros JM, Belmonte C, Planells-Cases R, Ferrer-Montiel A (2011) Membrane-tethered peptides patterned after the TRP domain (TRPducins) selectively inhibit TRPV1 channel activity. Faseb J 25:1628–1640

Van Buren JJ, Bhat S, Rotello R, Pauza ME, Premkumar LS (2005) Sensitization and translocation of TRPV1 by insulin and IGF-I. Mol Pain 1:17

Vay L, Gu C, McNaughton PA (2011) The thermo-TRP ion channel family: properties and therapeutic implications. Br J Pharmacol

Vellani V, Mapplebeck S, Moriondo A, Davis JB, McNaughton PA (2001) Protein kinase C activation potentiates gating of the vanilloid receptor VR1 by capsaicin, protons, heat and anandamide. J Physiol 534:813–825

Venkatachalam K, Montell C (2007) TRP channels. Annu Rev Biochem 76:387–417

Vlachova V, Teisinger J, Susankova K, Lyfenko A, Ettrich R, Vyklicky L (2003) Functional role of C-terminal cytoplasmic tail of rat vanilloid receptor 1. J Neurosci 23:1340–1350

Voets T, Droogmans G, Wissenbach U, Janssens A, Flockerzi V, Nilius B (2004) The principle of temperature-dependent gating in cold- and heat-sensitive TRP channels. Nature 430:748–754

Voets T, Owsianik G, Janssens A, Talavera K, Nilius B (2007) TRPM8 voltage sensor mutants reveal a mechanism for integrating thermal and chemical stimuli. Nat Chem Biol 3:174–182

Vyklicky L, Lyfenko A, Susankova K, Teisinger J, Vlachova V (2002) Reducing agent dithiothreitol facilitates activity of the capsaicin receptor VR-1. Neuroscience 111:435–441

Walpole CS, Wrigglesworth R, Bevan S, Campbell EA, Dray A, James IF, Masdin K J, Perkins MN, Winter J (1993) Analogues of capsaicin with agonist activity as novel analgesic agents;

structure-activity studies. 3. The hydrophobic side-chain "C-region". J Med Chem 36:2381–2389

Wang Y, Kedei N, Wang M, Wang QJ, Huppler AR, Toth A, Tran R, Blumberg PM (2004) Interaction between protein kinase Cmu and the vanilloid receptor type 1. J Biol Chem 279:53674–53682

Wang X, Miyares RL, Ahern GP (2005) Oleoylethanolamide excites vagal sensory neurones, induces visceral pain and reduces short-term food intake in mice via capsaicin receptor TRPV1. J Physiol 564:541–547

Wang S, Poon K, Oswald RE, Chuang HH (2010) Distinct modulations of human capsaicin receptor by protons and magnesium through different domains. J Biol Chem 285:11547–11556

Welch JM, Simon SA, Reinhart PH (2000) The activation mechanism of rat vanilloid receptor 1 by capsaicin involves the pore domain and differs from the activation by either acid or heat. Proc Natl Acad Sci USA 97:13889–13894

Woo D, Jung S, Zhu M, Park C, Kim Y, Oh S, Lee C (2008) Direct activation of transient receptor potential vanilloid 1(TRPV1) by diacylglycerol (DAG). Mol Pain. 1:4:42

Xu X, Gordon E, Lin Z, Lozinskaya I M, Chen Y, Thorneloe K S (2009) Functional TRPV4 channels and an absence of capsaicin-evoked currents in freshly-isolated, guinea-pig urothelial cells. Channels (Austin) 3:156–160

Yamada T, Ugawa S, Ueda T, Ishida Y, Kajita K, Shimada S (2009) Differential localizations of the transient receptor potential channels TRPV4 and TRPV1 in the mouse urinary bladder. J Histochem Cytochem 57:277–287

Yang F, Cui Y, Wang K, Zheng J (2010) Thermosensitive TRP channel pore turret is part of the temperature activation pathway. Proc Natl Acad Sci USA 107(15):7083–7088

Yao J, Qin F (2009) Interaction with phosphoinositides confers adaptation onto the TRPV1 pain receptor. PLoS Biol 7:e46

Yao J, Liu B, Qin F (2009) Rapid temperature jump by infrared diode laser irradiation for patch-clamp studies. Biophys J 96:3611–3619

Yao J, Liu B, Qin F (2010a) Kinetic and energetic analysis of thermally activated TRPV1 channels. Biophys J 99:1743–1753

Yao J, Liu B, Qin F (2010b) Pore turret of thermal TRP channels is not essential for temperature sensing. Proc Natl Acad Sci USA 107:E125; author reply E126–127

Yao J, Liu B, Qin F (2011) Modular thermal sensors in temperature-gated transient receptor potential (TRP) channels. Proc Natl Acad Sci USA 108:11109–11114

Yokoyama T, Saito T, Ohbuchi T, Hashimoto H, Suzuki H, Otsubo H, Fujihara H, Nagatomo T, Ueta Y (2010) TRPV1 gene deficiency attenuates miniature EPSC potentiation induced by mannitol and angiotensin II in supraoptic magnocellular neurons. J Neurosci 30:876–884

Yu W, Hill WG, Apodaca G, Zeidel ML (2011) Expression and distribution of transient receptor potential (TRP) channels in bladder epithelium. Am J Physiol Renal Physiol 300:F49–59

Zhang Z, Bourque CW (2008) Amplification of transducer gain by angiotensin II-mediated enhancement of cortical actin density in osmosensory neurons. J Neurosci 28:9536–9544

Zhang N, Inan S, Cowan A, Sun R, Wang JM, Rogers TJ, Caterina M, Oppenheim J J (2005a) A proinflammatory chemokine, CCL3, sensitizes the heat- and capsaicin-gated ion channel TRPV1. Proc Natl Acad Sci USA 102:4536–4541

Zhang X, Huang J, McNaughton PA (2005b) NGF rapidly increases membrane expression of TRPV1 heat-gated ion channels. Embo J 24:4211–4223

Zhang H, Cang CL, Kawasaki Y, Liang LL, Zhang YQ, Ji RR, Zhao ZQ (2007a) Neurokinin-1 receptor enhances TRPV1 activity in primary sensory neurons via PKCepsilon: a novel pathway for heat hyperalgesia. J Neurosci 27:12067–12077

Zhang Z, Kindrat AN, Sharif-Naeini R, Bourque CW (2007b) Actin filaments mediate mechanical gating during osmosensory transduction in rat supraoptic nucleus neurons. J Neurosci 27:4008–4013

Zhang X, Li L, McNaughton PA (2008) Proinflammatory mediators modulate the heat-activated ion channel TRPV1 via the scaffolding protein AKAP79/150. Neuron 59:450–461

Zhang F, Liu S, Yang F, Zheng J, Wang K (2011a) Identification of a tetrameric assembly domain in the C terminus of heat-activated TRPV1 channels. J Biol Chem 286:15308–15316

Zhang X, Daugherty SL, de Groat WC (2011b) Activation of CaMKII and ERK1/2 contributes to the time-dependent potentiation of Ca^{2+}response elicited by repeated application of capsaicin in rat DRG neurons. Am J Physiol Regul Integr Comp Physiol 300:R644–654

Zhuang ZY, Xu H, Clapham D E, Ji RR (2004) Phosphatidylinositol 3-kinase activates ERK in primary sensory neurons and mediates inflammatory heat hyperalgesia through TRPV1 sensitization. J Neurosci 24:8300–8309

Zygmunt PM, Petersson J, Andersson DA, Chuang H, Sorgard M, Di Marzo V, Julius D, Hogestatt ED (1999) Vanilloid receptors on sensory nerves mediate the vasodilator action of anandamide. Nature 400:452–457

Chapter 4
The Molecular Mechanism of Multifunctional Mechano-Gated Channel TRPV4

Makoto Suzuki and Astuko Mizuno

4.1 Introduction

A rise in intracellular free calcium ($[Ca^{2+}]_i$) is an important regulator of numerous cellular functions triggered by ligand-gated non-selective cation channels. Since the identification of the gene responsible for a *Drosophila* mutation that exhibited a transient receptor potential (TRP), in comparison with the control, and a sustained receptor potential in the eye, several novel Ca^{2+} entry channels belonging to the TRP superfamily of cation channels have been discovered (Clapham 2001; Montell et al. 2002). Numerous TRP genes have been identified, encoding membrane proteins with six transmembrane segments (TM1–TM6) and a putative pore region formed by a short hydrophobic stretch between TM5 and TM6. On the basis of homology, mammalian TRP proteins are classified into subfamilies: TRPC, TRPV, TRPM, TRPN, TRPP, TRPA and TRPML.

TRPV1 (capsaicin receptor) was isolated by Caterina et al. in 1997 by expression cloning and was the first channel to be identified that could convert physical input, hot temperature, into electrical current driven by Ca^{2+}. An ion channel capable of converting pressure, or anisoosmolarity, into electrical stimuli was conjectured to be part of this family. A clue to its identity came from the discovery of *Osm-9* in a genetic screen of high-osmolarity-insensitive *Caenorhabditis elegans* mutants (Colbert et al. 1997). TRPV4 was a candidate mammalian homologue of *Osm-9* and was thus investigated.

TRPV4 (transient receptor potential vanilloid 4, also formerly called OTRPC4, VR-OAC, VRL2 and TRP12), a member of the TRPV subfamily, was first identified as an osmo-sensing channel (Strotmann et al. 2000; Liedtke et al. 2000). *TRPV4* mRNA is widely expressed, and is present in neurons, kidney, lung, skin,

M. Suzuki (✉)
Edogawabashi clinic, 348 Yamabuki, Shinjyuku, Tokyo, Japan
e-mail: msuzuki@edogawabashi-clinic.com

A. Mizuno
Department of Molecular Pharmacology, Jichi Medical university,
Yakushiji 3311-1, Tochigi, Japan

A. Kamkin, I. Lozinsky (eds.), *Mechanically Gated Channels and their Regulation,*
Mechanosensitivity in Cells and Tissues 6,
DOI 10.1007/978-94-007-5073-9_4,

vascular endothelium and other tissues (Strotmann et al. 2000; Liedtke et al. 2000; Suzuki et al. 2003c). A growing body of experiments has revealed that cells expressing TRPV4 display a swell-activated current (demonstrated by electrophysiology) and Ca^{2+} influx (demonstrated by Ca^{2+}-sensitive fluorescence detection), while those from TRPV4-deficient (*Trpv4*$^{-/-}$) mice do not exhibit these. We previously found that TRPV4 is activated by inflation of the cell, i.e., a gain of cell volume in a whole cell configuration (Suzuki 2003a). More recently, accumulating evidence for a direct association between the cytoskeleton and TRPV4 has revealed that the channel is a direct pressure sensor. TRPV4 can also be activated by acids and moderate heat, playing a role in inflammatory nociception (Watanabe et al. 2002a, 2002b; Suzuki et al. 2003a, Vriens et al. 2004). TRPV4 activation induces cells to release ATP, transmitting signals towards nerve endings in the bladder (Andersson et al. 2010), the skin (Sokabe et al. 2010), or the newly discovered osmosensor, the liver (Lechner et al. 2011).

Our early studies using *Trpv4*$^{-/-}$ mice suggested that TRPV4 functions as a nociceptor for pressure (Suzuki et al. 2003a), warmth (Chung et al. 2004; Lee et al. 2005), noxious compounds (Todaka et al. 2004), and noxious sound (Tabuchi et al. 2005). Our work also indicated that it functions as a flow-sensor (Taniguchi 2007) and, in addition, is capable of acting as a trigger for the differentiation of cells, such as chondrocytes, in various systems. Physiological data from *Trpv4*$^{-/-}$ mice further suggested that TRPV4 is necessary for normal osmotic regulation (Mizuno et al. 2003; Liedtke and Friedman 2003a, b). In view of these observations, TRPV4 can be legitimately considered a "multi-micromachine", capable of sensing diverse physical stimuli and converting them to Ca^{2+} signals in the various tissues of the body.

A number of recent reports on human TRPV4 mutations have demonstrated the importance of the channel in humans. TRPV4 mutations affect bone development (Rock et al. 2008; Verma et al. 2010; Dai et al. 2010), cause neuromuscular abnormalities (Auer-Grumach et al. 2010; Deng et al. 2010; Landoure et al. 2010) and produce electrolyte imbalance (Tian et al. 2009). Both gain-of-function and loss-of-function mutations cause disease. The phenotypes of human and animal TRPV4 mutations have begun to provide a clearer understanding of the mechanistic processes that link channel stimulation with physiological outcome.

4.2 Channel Physical Properties

4.2.1 Channel Structure (Fig. 4.1)

TRPV4 consists of 871 amino acids, with 6 transmembrane segments^{TM} and 6 ankyrin (ANK) repeats in the NH2 terminus. Species differences in TRPV4 sequence are minimal (human/mouse, 95.2/96.9 %; human/rat, 94.8/97.0 %; mouse/rat, 98.9/99.2 % [identity/similarity]).

ANK repeats are 33-amino acid motifs that are involved in protein-protein interactions ((Denker and Barber 2002; Sedgwick and Smerdon 1999). These ANK

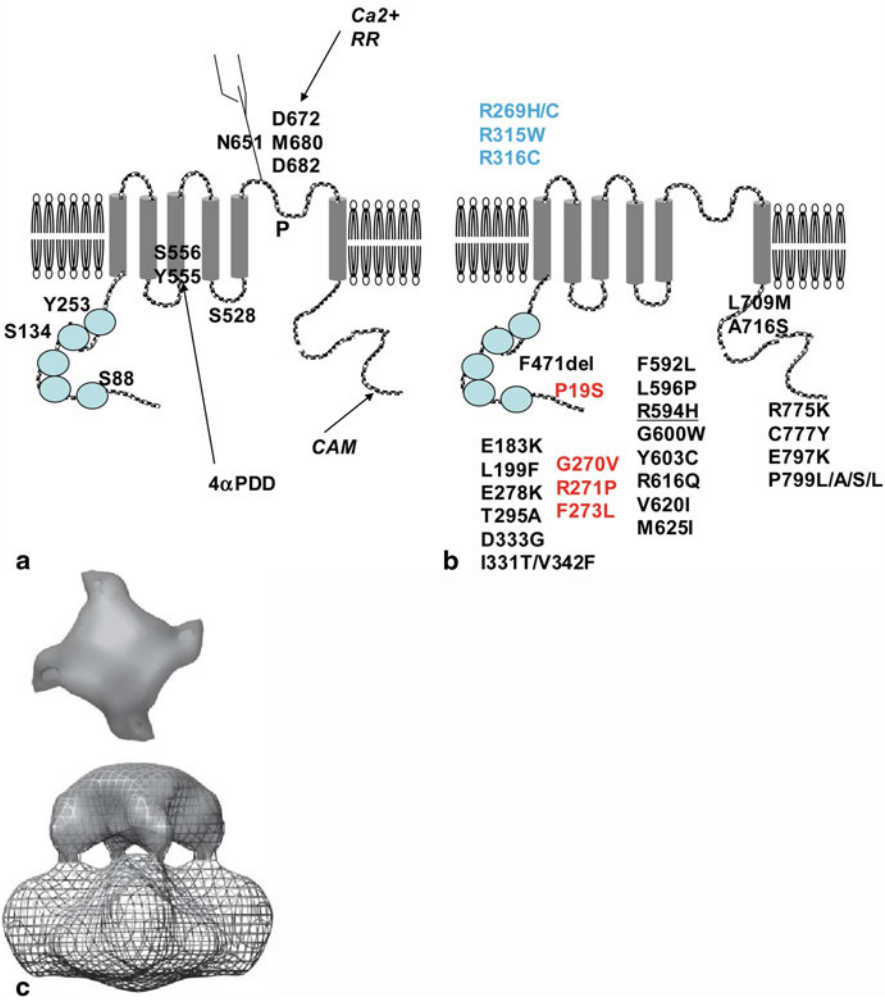

Fig. 4.1 **a** Putative TRPV4 structure and the regulatory alignments. A. TRPV4 is supposed to have six ankyrin repeats (blue circle), and six putative transmembrane segments with pore (P), followed by Ca^{2+} (or Ca-calmodulin) binding C-terminal domain. Deletion before 410 or after 741 looses ability in response to mechanical stress. Putative protein kinase C phosphorylation sites are s88, S134, and S528. D672, M680, and D682 are important in Ca^{2+} permeability and RR inhibition. N 651 is the site of glycosylation. **b** Representative mutations found in human diseases. The upper mutations marked in blue cause peripheral sensory motor neuron disease. The lower mutations are found in abnormal skeletal disorders. Most of them show a gain-of-function. P19 marked in red is found in hyponatremia. G270, R271 and F273 L in red are found in arthropathy. These show a-loss-of-function mutations. **c** Representative structure of TRPV4 by cryoelectrone microscopy. This show the tetrameric channel with upper membrane surface area, middle transmembrane portions and with lower larger N- and C-terminal complex. The ion permeating pore is predicted in the center and phorbol binding site in beneath the pore region. (With permission by the author Shigematsu et al. 2010)

repeats self-associate at the N termini to form a tetrameric structure (Gaudet 2008). The putative domain structure of TRPV4 includes six ANK repeats, PKC and PKA phosphorylation sites (S88, S134, T175, S162, S189, S528, S824), the six transmembrane region (TM1–TM6), a glycosylation site close to the pore (N651), the pore region (P), a Ca^{2+}/calmodulin (CAM)-binding site and a tyrosine kinase phosphorylation site (Y253).

The structure of Osm-9 is similar to the vanilloid receptive channel, TRPV1(Caterina et al. 1997), as well as to TRPV4 (VRl2, OTRPC4 (Strotmann et al. 2000), VR-OAC (Liedtke et al. 2000), TRP12 (Nilius et al. 2001) and TRPV2 (Caterina et al. 1999). Therefore, TRPV4 structure is thought to be similar to that of TRPV1. Sigematsu et al. (2010) revealed the 3-dimensional structure of rat TRPV4 by cryoelectron microscopy (Fig. 4.1c). This revealed that the channel is a tetramer and the overall structure comprises two distinct regions: a larger dense component, likely corresponding to the cytoplasmic N and C-terminal regions, and a smaller component, likely corresponding to the transmembrane region. The structure is quite similar to that of TRPV1 (Moiseenkova-Bell et al. 2008), and has a 4α-phorbol 12,13-didecanoate (4αPDD)-binding pocket in the center. The 4αPDD-binding sites Y555/S556 correspond to the capsaicin-binding sites (Y511/S512) in TRPV1. Compared with TRPV1, which is not a mechanosensitive channel, a vacant cavity in the larger dense component is not obvious in the TRPV4 structure. This may reflect a different arrangement of the C and N-termini, affecting their interaction with the various partners. It is predicted that the C and N-termini are located just under the mouth of the ion permeation pore—this would imply that mutations at either termini should affect ion permeation as well as plasma membrane expression. Higher resolution 3D imaging should enhance our knowledge of the molecular structure of the channel and provide insight into the mechanisms of mechanosensitivity and how mutations cause disease.

Exogenously expressed TRPV4 in Chinese hamster ovary (CHO) or human embryonic kidney (HEK) cells exhibits a robust outward-rectified current when activated by hypotonic stress or by the agonist 4αPDD (Watanabe et al. 2002b; Nilius et al. 2003). Without any stimuli, the current is inactive when measured at room temperature. Gao et al. (2003) revealed that the basal level of Ca^{2+} at body temperature (37 °C) is significantly higher than at room temperature and that warm temperature is essential for the activation of TRPV4 by phorbol ester (PMA), hypotonic stress, 4αPDD and shear stress. Thus, TRPV4 is constitutively active in cells expressing the protein at body temperature. Single channel conductance is 90–110 pS for outward currents and 50–70 pS for inward currents (Liedtke et al. 2000; Watanabe et al. 2002).

4.2.2 Structural Variants

Genomic sequence analysis revealed that TRPV4 maps to 12q24.1. Five human TRPV4 splice variants, TRPV4-A–E, have been identified (Liedtke et al. 2000;

Arniges et al. 2006). All of these vary in the cytoplasmic N-terminal region, affecting (except for TRPV4-D) the ANK domains. TRPV4 undergoes glycosylation and oligomerization in the endoplasmic reticulum followed by transfer to the Golgi apparatus. The ANK domains are necessary for the oligomerization of TRPV4, and the lack of TRPV4 oligomerization (in TRPV4-B, C, and E) affects its accumulation in the endoplasmic reticulum. Thus, the amount of each of the splice variants may determine the quantity of the functional TRPV4 channel in the plasma membrane.

TRP channels may constitute homomeric or heteromeric complexes. The multimerization was examined with fluorescence resonance energy transfer and coimmunoprecipitation in TRPV1–6. Except for TRPV5 and TRPV6, TRPV channel subunits preferentially assemble into homomeric pore complexes (Hellwig et al. 2005).

4.2.3 Pore Selectivity

TRPV4 channel permeation is essentially non-selective for the cation. Permeability values relative to Na^+ are 6–10 for Ca^{2+} and 2–3 for Mg^{2+} (Liedtke et al. 2000; Nilius et al. 2001; Strotmann et al. 2000, 2003; Watanabe et al. 2002a). The magnitude of the current can be diminished by external Ca^{2+}, and the removal of Ca^{2+} by EGTA or citrate potentiates the amplitude.

Aspartate residues play a critical role in cation selectivity (García-Martínez et al. 2000; Nilius et al. 2001, 2004; Liedtke et al. 2003b; Voets et al. 2002) (Fig. 4.1a). Aspartate to alanine mutations (D→A) between TM5 and TM6 has revealed valuable information on pore characteristics of the TRPV4 channel. Ca^{2+} permeability is moderately influenced by the D672A mutation without significantly altering monovalent permeability. A further change in permeability (involving monovalent permeability), rectification and sensitivity to ruthenium red (RR) is achieved by the D682A mutation. The mutation of M680 also reduces the whole-cell current amplitude and impairs Ca^{2+} permeability. Thus, these three amino acids (D672, M680, D682) in the pore are essential for TRPV4 permeation, selectivity, RR sensitivity, and outward rectification. The TRPV4 current can be slowly blocked by Gd^{3+} at μM concentrations (Liedtke et al. 2000; Strotmann et al. 2000). Unlike RR, Gd^{3+} blocks both the inward and the outward current. The blockers RR and Gd^{3+}, although non-specific for the TRPV4 channel, may be specific for other TRP channels. Although we (Suzuki et al. 2003a) suggested that low pH may sensitize TRPV4, data on the responsible amino acids are lacking. Acidosis represents synergic stimulation to TRPV4 in osteoclast differentiation (Kato and Morita 2011) while acidosis inhibits TRPV4 mediated Ca^{2+} influx in esophageal epithelia (Shikano et al. 2011).

Recent findings of human mutations have shed light on the pore-closing mechanism around TM6. The amino acids W733, R616, L619, and L623 may be important for closing since the mutations produce constitutively open channels (see Sect. 4.5.5).

4.2.4 Modulation by Ca^{2+}

An increase in intracellular Ca^{2+} by ionomycin in the whole-cell configuration was shown to stimulate TRPV4, and TRPV4 currents stimulated by hypotonic solutions were strongly reduced in the absence of extracellular Ca^{2+} (Strotmann et al. 2003). The proposed CAM-binding site at 809–832 is responsible for this Ca^{2+}-dependent potentiation. V814 seems essential for the spontaneous opening of TRPV4 channels, and appears to be responsible for the observed elevated Ca^{2+} levels in non-stimulated TRPV4-expressing cells (Watanabe et al. 2003a). However, recent work revealed another possibility—that the primary site of Ca^{2+}-dependent potentiation was not in the C-terminal, but in the N-terminal. ATP and CAM may bind to N-terminal ANK common in TRPV1, TRPV3 and TRPV4 (Phelps et al. 2010). A unique study (Strotmann et al. 2010) using fluorescence for geometric molecular analysis demonstrated that the activation of TRPV4 by CAM is, in fact, a dis-inhibition process where CAM displaces a regulatory domain that is bound in the resting state. CAM displaces the N-terminal, but not the C-terminal, high affinity domain and relaxes the autoinhibitory binding (N and C-termini are self bridged) to facilitate homodimerization.

An increase in Ca^{2+} to very high levels inhibits the TRPV4 current; a TRPV4 with a single mutation of E797 was constitutively open, suggesting that this site may interfere with Ca^{2+} binding at the neighboring CAM-binding motif. The repeated application of hypotonic stress or 4αPDD causes the ensuing activation to rapidly decay in the presence of Ca^{2+} in a bath solution. (Watanabe et al. 2002a; Nilius et al. 2004). This self-desensitization occurs in currents mediated by TRPV4 but not by TRPV3 (Moqrich et al. 2005). In the absence of Ca^{2+}, desensitization is much slower, indicating that the Ca^{2+}-dependentinhibition of this channel is involved in the mechanism of desensitization.

4.2.5 Glycosylation

The glycosylation of TRPV4 has been examined in detail (Xu et al. 2006). A single high-probability N-linked glycosylation site in TRPV4 that faces the extracellular milieu is phylogenetically conserved. From a structural perspective, this site (N651) is adjacent to the hydrophobic hairpin of the pore-forming loop. Mutation of this residue results in loss of glycosylation and promotes the trafficking of the channel to the plasma membrane. Thus, glycosylation affects membrane trafficking of the TRPV4 protein and the functional expression of this channel.

4.2.6 C-Terminal Domain

The C-terminal domain of TRPV4 is functionally important (Liedtke et al. 2003b) and essential for plasma membrane localization (Becker et al. 2008). The sorting of

TRPV4 from the ER appears to require the C-terminal residues. Truncations of the final C-terminal amino acids (D844 or D828) result in partial retention in the ER, whereas all deletions upstream of amino acid 828 result in complete ER retention. The insertion of TRPV4 into the plasma membrane is regulated by a member of the ubiquitin-ligase family, atrophin-interacting protein 4 (AIP4), which decreases surface expression of TRPV4. AIP4 facilitates the ubiquitination of the channel and thus renders it available for endocytosis. Overexpression of AIP4 promotes the endocytosis of TRPV4, thereby decreasing expression of the protein on the plasma membrane (Wegierski et al. 2006). Arrestin1 is an adaptor for AIP4 that also plays a role in TRPV4 localization (Shukla et al. 2010).

The C-terminal of TRPV4 directly binds to cytoskeletal proteins, including actin, tubulin and neurofilament, and interacts with regulatory proteins such as protein kinase Cε and CAM kinase II. Pull-down assays of cytoskeletal extracts by the TRPV4 C-terminus suggest that it interacts with cytoskeletal components to a level similar to that of the N-terminus (Goswami et al. 2010). We searched for proteins that potentially bind the C-terminal and found that candidate proteins include the microtubule-associated protein 7 (MAP7 = E-MAP-115), which is a tubulin-binding heat shock protein that contains an EH domain (Suzuki et al. 2003b), indicating indirect binding of the C-terminal to tubulin. The importance of tubulin is demonstrated by the fact that taxol is the most potent blocker of TRPV4 function in TRPV4-overexpressing cells (Suzuki et al. 2003b) and dorsal root ganglion (DRG) neurons (Goswami et al. 2010). The interaction of TRPV4 with the cytoskeleton is mutual. TRPV4 signaling induces striking morphologic changes, resulting in a decrease in migratory behavior in many cell types, including the retraction of lamellipodia, growth cones and neurites in neurons (Zaninetti et al. 2011). Although speculation at present, rho is activated by an increase in Ca^{2+} by TRPV4 and may initiate changes in the cytoskeleton and in adhesion molecules.

Coimmunoprecipitation assays also suggested an interaction between the C terminus of TRPV4 and the inositol (1,4,5) triphosphate (Ins(1,4,5)P3) receptor type 3 (Fernandes et al. 2008). This interaction results in the sensitization of the channel to epoxyeicosatrienoic acids (EETs) and mechanical stimuli via the CAM-binding site (Garcia-Elias et al. 2008).

4.2.7 N-Terminal Domain

The N-terminal intracellular domain is important for thermo-sensation by TRPV4 and for its ability to respond to swelling. It is also involved in the translocation of the protein within the cell. TRPV4 activation by hypotonic swelling is delayed if the ANK repeats are lacking (Liedtke et al. 2000).

The ANK repeats of human TRPV4 are affected by alternative splicing—the TRPV4-B (Δ384–444), TRPV4-C (Δ237–284) and TRPV4-E (Δ237–284 and Δ384–444) variants are not carried toward the plasma membrane (Arniges et al. 2004). In contrast, TRPV4-D (Δ27–61) variants, in which splicing does not affect

ANK, are expressed on the plasma membrane, as in wild-type TRPV4. Thus, the N-terminal of TRPV4 is crucial for plasma membrane expression.

PACSIN (protein kinase C and casein kinase substrate in neuron protein) 3, but not PACSINs 1 and 2, increase the plasma membrane/cytosolic ratio of TRPV4 expression, in a process mediated by dynamin (Cuajungco et al. 2006). PACSIN 3 has been identified as a protein that binds the N-terminal of TRPV4, and it specifically affects the endocytosis of TRPV4, thereby modulating its subcellular localization. Substitution of proline for leucine, P415L, almost completely blocks their binding. In particular, co-immunostaining of PACSIN3 and TRPV4 reveals that they are localized to the luminal membrane of renal tubules. Thus, the interaction of the binding protein affects not only the membrane surface expression of TRPV4 but also the polarity of expression in epithelia. PACSIN3 inhibits the basal activity of TRPV4, including the ability to be activated by warmth and cell swelling, but does not affect activation by 4αPDD (D'hoedt et al. 2008). However, arachidonate was still able to increase intracellular Ca^{2+} in TRPV4/PACSIN3 co-expressing cells, although swelling triggered the formation of arachidonate that activated TRPV4. These results indicate that PACSIN3 affects the translocation of the channel protein and modifies channel properties as well.

The recent discoveries of TRPV4 mutations in neuronal disease have uncovered a new role of the N-terminal in channel gating. R269, R315 and R361 mutations shift the channel to a more open state, but do not influence intracellular distribution. The positions of these amino acids, although not near the mouth of the permeation pore, modify gating kinetics, and do not influence channel recycling. One can hypothesize that the N-terminal binds to another protein that may modify the mouth of the channel.

Additionally, new mutations around this thirst loop of AKN domain, G270V, R271P and F273L endows the crucial in polymerization and resultant poor membrane expression. This loss of function mutation in human reveals arthrophathy (Lamandé et al. 2011). Interestingly, the analysis of Ca^{2+} images indicates that the mutants were unable to respond completely to hypotonicity while less to agonists. The swell-activated mechanism requires the N-terminal dependent polymerization or the interaction of this loop to AQP water channel (see below).

4.2.8 Modulation by Phosphorylation

The classic protein kinase C (PKC) activator, phorbol 12-myristate 13-acetate (PMA), a known activator of PKC, activates TRPV4 (Gao et al. 2003; Xu et al. 2003a, b). The activation by PMA at room temperature is not noticeable, but becomes obvious at warm temperature (37 °C) (Gao et al. 2003). There are a number of possible phosphorylation sites. Among these, S162, S189, T175 and S824 are important for PKC-dependent functional enhancement (Peng et al. 2010; Fan et al. 2009). PKA phosphorylation of S824 is dependent on the scaffolding protein AKAP79, and results in the enhancement of channel function (Fan et al. 2009). cGMP inactivates

the TRPV4 current in lung endothelial cells (Yin et al. 2008) and in DRG neurons (Ding et al. 2010) that play an important role in the negative feedback loop.

Src family tyrosine kinases are involved in mediating activation due to swelling (Xu et al. 2003a, b). Whether the phosphorylation is essential for hypoosmolality-induced channel activation is controversial, however, Xu et al. (2003b) reported that hypotonic stress resulted in the genistein-sensitive phosphorylation of TRPV4 at residue Y253, and that cells expressing the Y253F mutant were incapable of responding to hypotonic cell swelling. However, these results could not be reproduced by another group (Vriens et al. 2004). In contrast, irritable chemical-triggered, and hypotonic and hypertonic solution-induced hyperalgesia are TRPV4-mediated and dependent on integrin/Src tyrosine kinase signaling in sensory cells *in vitro* and in the rat *in vivo* (Alessandri-Haber et al. 2004, 2005, 2006)), and this process is potentiated by the prostaglandin E pathway (Alessandri-Haber et al. 2003). Therefore, tyrosine phosphorylation appears to be involved in the sensitization of TRPV4 to other stimuli (Wegierski et al. 2009), and not in the activation of the channel *per se*.

The WNK family of kinases was described by Wilson et al. (2001) in a screen for novel mitogen-activated protein (MAP)/extracellular signal-regulated protein kinase (ERK) kinase (MEK) family members in the rat brain. Human hypertension (pseudohypoaldosteronism type II, PHAII) is, in some cases, caused by mutations in WNK kinases. WNK kinases are activated by a variety of stimuli, including hypertonicity and hypotonicity (Lenertz et al. 2005). Interestingly, WNK4 down-regulates TRPV4 membrane expression, although no direct coupling of WNK4 and TRPV4 has been demonstrated (Fu et al. 2006). The N-terminal deletion mutant (Δ2–147) is unable to interact with WNK4, suggesting that an unknown protein(s) regulates the membrane expression of TRPV4 under the influence of WNK kinases. Studies using gain of WNK4 function demonstrate that the protein has an inhibitory role in PHAII, revealing the involvement of TRPV4 in the pathogenesis of hypercalcemia and hypertension (Gamba 2006). Because loss of function of WNK4 leads to PHAII, where renal distal tubule cell-cell junctions are abnormally leaky, the WNK4 signaling cascade may play a role in the regulation by TRPV4 of cell barrier function.

4.2.9 Lipids

During pharmacological studies of endothelial Ca^{2+} channels, researchers observed that TRPV4 was activated by arachidonic acid (AA) (Nilius et al. 2004). Subsequently, electrophysiological studies revealed the molecular mechanisms behind hypoosmolality-activation of TRPV4. Exposure of cells to hypoosmolality activates TRPV4 by the PLA2-dependent formation of AA (Basavappa et al. 1998) and its subsequent metabolization to 5,6-EET through a cytochrome P450 epoxygenase-dependent pathway. Consequently, hypoosmolality-activated currents driven by TRPV4 can be completely blocked by PLA2 inhibitors, such as methylarachidonyl fluorophosphate (MAFP), arachidonyl trifluoromethyl ketone (AACOCF3), 3-[(4-octadecyl) benzoyl]acrylic acid (OBAA, 100 μM), *N*-(*p*-amylcinnamoyl)

anthranilic acid (ACA, 80 μM) and p-bromophenacyl bromide (BPB, 100 μM) in TRPV4-expressing HEK cells (Watanabe et al. 2003b; Vriens et al. 2004). PLA2 can be divided into two groups—cytosolic PLA2 (cPLA2) in the cell interior and secretory PLA2 (sPLA2) in the plasma. The effect of inhibitors on each PLA subclass varies: MAFP, AACOCF3 and OBAA are inhibitors of cPLA2, while BPB is a specific inhibitor of sPLA2 (Hernández et al. 1998). Furthermore, the inhibition of the cytochrome P-450 epoxygenase pathway by 5,8,11,13-eicosatetraynoic acid, miconazole, 17-octadecynoic acid (all at 10 μM) (Vriens et al. 2004) and sulfaphenazole (for CYP2C9) (Vriens et al. 2005) blocks the hypoosmolality activation of TRPV4. The amino acid motif in TRPV4 responsible for the effect of 5.6-EET remains unclear. Although not substantiated, BPB at 100 μM might be non-specific and might block other currents (Loukin et al. 2010a).

AA is derived from various fatty acids of the plasma membrane. Hydrolysis of the endocannabinoids, anandamide (AEA) and 2-arachidonoylglycerol (2-AG), which are endogenous ligands of the CB1 and CB2 metabotropic cannabinoid receptors, is one mechanism resulting in the formation of AA. AEA and 2-AG activate TRPV4 in an AA-dependent pathway (Watanabe et al. 2003b).

Bisandrographolide (BAA), a compound derived from plants, was found to activate TRPV4 (Smith et al. 2006), but not TRPV1–3. BAA also functions in cell-free inside-out patches indicating a membrane-delimited action. The mutations L584M and W586A were fully unresponsive to BAA (Vriens et al. 2007).

4α-Phorbol-12,13-didecanoate (4αPDD; EC50, 200–400 nM), a phorbol ester analogue, is a potent activator of TRPV4 (Watanabe et al. 2002a). The tyrosine-serine (YS) motif in the TM2-TM3 loop domain is important for the activation of TRPV1 by capsaicin (Jordt and Julius 2002). In an experiment based on analogy, Vriens et al. (2004) mutated a Y residue (Y-555) or the YS sequence (Y555 and S556) in the N-terminal part of TM3 to alanine (A)—this strongly impaired the activation of TRPV4 by 4αPDD and warmth, but had no effect on activation mediated by cell swelling or AA. 4α-phorbol 12,13-dihexanoate (4α-PDH) shows a very high efficacy for TRPV4 activation (EC50 70 nM), being 5 times more potent than 4αPDD (Klausen et al. 2009). A number of different TRPV4 agonists are currently available, including 4α-PDD and GSK1016790A, which are 300- to 1000-fold more potent than 4αPDD. Another fully synthetic TRPV4 agonist was identified by screening small molecule libraries (Thorneloe et al. 2008; Willette et al. 2008). Unfortunately, the most potent compound, GSK1016790A, is also an efficient activator of TRPV1 (EC50, 50 nM) (Jin et al. 2011).

Vincent et al. (2009) found that the antagonists RN-1734 and RN-1747 were able to completely inhibit both ligand and hypotonicity-activation of TRPV4. In addition, RN-1734 was found to be selective for TRPV4. Everaerts et al. (2010) found that HC-067047 (EC50 of 22 nM for 4αPDD activated Ca^{2+} fluorescence) was a potent antagonist of TRPV4-induced currents and fluo-4 fluorescence. HC-067047 increased functional bladder capacity and reduced micturitional frequency; consequently, it might be useful for treating cyclophosphamide-induced cystitis or neurogenic bladder. We sought a specific blocker in a 16,804 chemical compound library by using human TRPV4 expressing HEK cells and found that a sulfonamide

derivative, in the micromolar range, blocked the 4αPDD-induced rise (but not the ATP-induced rise) in intracellular Ca^{2+} (unpublished observation).

4.2.10 Trafficking

As demonstrated by reduced surface expression of spliced variants and by the phenotype of human mutations, as mentioned above, the N-terminal ANK domains and the C-terminal domains are essential for homotetramerization and sorting. The TRPV4 monomer is synthesized in the ER. Human OS-9 is a ubiquitously-expressed protein that is localized to the ER and plays an important role in the selection of substrates for ER-associated degradation. OS-9 binds to the N-terminal of TRPV4, preventing its polyubiquitination and subsequent proteosomal degradation (Wang et al. 2007). After homotetramerization, TRPV4 was transported to the plasma membrane. Caveolin in endothelial cells induced TRPV4 to preferentially localize to cholesterol-rich caveolae (lipid rafts). The absence of caveolin-1 in knockout mice led to decreased TRPV4 activity, observed as a reduction in nitric oxide (NO) and endothelial-derived-hyperpolarizing factor (EDHF)-mediated relaxation (Saliez et al. 2008; Rath et al. 2009). TRPV4 and other proteins that are required for cell volume regulation are colocalized to form a functional unit and lipid rafts are important for promoting the assembly of fully functional channel complexes.

TRPV4 in the plasma membrane can be sequestered by ubiquitination performed by atrophin-1-interacting protein. Monoubiquitinated TRPV4 can enter the ER pathway to be recycled. The possible mechanisms mediated the recycling of mutated TRPV4 variants have been discussed in detail (Dai et al. 2010). Trafficking of TRPV4 may be important for future understanding of the mechanism of TRPV4 channelopathies (Dai et al. 2010), since most mutational hotspots are located in the N and C-termini, where interaction with other molecules frequently occurs. However, some mutations do not affect recycling, but rather alter channel kinetics (see Sect. 4.4).

4.3 Distribution of TRPV4

TRPV4 mRNA is widely distributed. While the presence of a functional TRPV4 channel has been demonstrated in some tissues, the presence of functional TRPV4 remains to be established for others. TRPV4 mRNA is detected at high levels in the lung and the kidney. Northern blot analysis revealed that TRPV4 transcripts are present at the highest levels in the trachea, followed by the kidney, prostate, pancreas, placenta (Liedtke et al. 2000; Wissenbach et al. 2002b), liver and heart (Strotmann et al. 2000).

In the brain, *in situ* hybridization revealed that the lamina terminalis, the subfornical organ, and the median preoptic area in the hypothalamus express TRPV4 transcripts. The ependymal cells in the choroid plexus of the third and lateral

ventricles also express TRPV4 transcripts (Liedtke et al. 2000). All of these structures are involved in regulating body fluid osmolality.

The trigeminal ganglion is positively stained by *in situ* hybridization and by an anti-C-terminal antibody (Liedtke et al. 2000; Suzuki et al. 2003a, c). In the murine cochlea, TPV4 is expressed in most cells lining the endolymphatic duct of the mouse ear, including the hair cells and the marginal cells of the stria vascularis (Liedtke et al. 2000; Shen et al. 2006; Kumagami et al. 2009).

DRG neurons and primary sensory neurons express TRPV4 (Alessandri-Haber et al. 2003) in the mouse, but not in humans (Delany et al. 2001). Interestingly, TRPV4 mRNA, but not the protein, could be detected in the soma of DRG neurons, suggesting that there might be a mechanism for the transport of the TRPV4 protein from the neuronal bodies to the sensory terminals (Guler et al. 2002). Human sympathetic ganglia have been reported to possess TRPV4 immunoreactivity (Delany et al. 2001). Human and mouse motor neurons also express TRPV4 (Facer 2007), but at low levels compared with the trachea. Adrenal and sweat glands are other sites thought to express TRPV4 mRNA, although immunolocalization data is not available. Vagal afferent nerves may also express TRPV4.

In the skin, keratinocytes in deep layers, rather than the surface, express TRPV4. Merkel bodies (Liedtke et al. 2000) and other mechanosensitive terminals with Merkel endings (Suzuki et al. 2003c) may express TRPV4. Both white and brown adipocytes in rodents strongly express TRPV4. Endothelial cells in mouse aorta show robust positive signals for TRPV4 by Northern blot and histochemical analyses, but cells in small vessels, such as in the lung, show negative signals. In contrast, human endothelial cells in the lung, but not in the aorta, were shown to contain TRPV4 transcripts by RT-PCR. Thus, a species difference in the expression of TRPV4 in endothelial cells may exist. Vascular smooth muscle cells in the aorta and pulmonary arteries of rodents also express TRPV4.

In the kidney, the basolateral membrane, from the proximal to the connecting tubules, is positively stained by an anti-C-terminal antibody. The water-permeant cells of the macula densa are, however, unstained. Moderate TRPV4 expression is noted in all collecting duct portions and in the papillary epithelium, including intercalated cells (Tian et al. 2004). Luminal localization has also been demonstrated using an anti-N-terminal antibody (Cuajungco et al. 2006).

Liver expresses TRPV4 mRNA by Northern blot analysis (Strotmann et al. 2000), and human hepatoblastoma cells show TRPV4 mRNA by RT-PCR; these also exhibit a 4αPDD-induced Ca^{2+} increase (Vriens et al. 2004; Gradilone et al. 2007). Human synoviocytes also show mRNA as well as increases in Ca^{2+} (Kochukov et al. 2006, 2009; Itoh et al. 2009). It is not known whether heart muscles express functional TRPV4 channels, although an early report suggested the presence of mRNA by Northern blotting (Strotmann et al. 2000). Coronary vessels may express TRPV4. TRPV4 mRNA is detected in chondrocytes, osteoblasts and osteoclasts. TRPV4 is also found in urinary bladder epithelium (Yu et al. 2011; Everaerts et al. 2010). The cornea (Pan et al. 2008; Mergler et al. 2010) and retinal gangion neurons (Ryskamp et al. 2011) expresses TRPV4 that may be important in vision. Details of TRPV4 expression in the various tissues and the proposed role of the protein are summarized in Table 4.1.

Table 4.1 Summary of TRPV4 pathophysiology: The human diseases with abnormal function of TRPV4 clearly indicate most frequent abnormality of TRPV4 seen in bone development. Additionally, HMSN2C's symptoms show axonal degeneration with skeletal abnormality, peripheral muscle atrophy, weakness of mechanical sensation, a significant weakness of thermal sensation, bladder incontinence and hearing loss. Based on the signs and symptom in these human diseases TRPV4 dysfunction is clearly found and summarized in Table 4.1 summary 1. However, more roles are suggested, though not prominent phenotypes in human disease, in animal models and experiments in summary 2. Summary TRPV4 is detected and functionally active in summary 3. Summary 1 includes important phenotypes for human model tissues for understanding the pathophysiology. Summary 2 includes vivid evidences for the contribution of TRPV4, although phenotypes or symptoms are not clarified. A kind of stress such as salt-overloading may reveal the phenotypes where TRPV4 underlies the pathogenesis of a disorder. Summary 3 shows tissues expressing TRPV4 that are functionally active.

Summary 1 TRPV4-channelopathy reported with human mutations
Impaired bone development
Motor dysfunction
Sensory loss where touch sensation is affected more than thermal and pain sensation
Abnormal sensation of osmolarity, hyponatremis
Hearing impairment
Bladder dysfunction
Airway dysfunction
Summary 2 TRPV4 underlies a disorder until not clarified by human mutations
Skin barrier and skin sensatio
Mechanosensitivity in blood vessels
Mechano-and osmo-sensitivity in renal function
Insulin secretion
Liver function
Pressure sensing in esophagus
Summary 3
Group 1. Localization where TRPV4 is closely related to human disease phenotype, *Bone*; chondrocytes, osteoblast, osteoclast, *Brain*; circumventricular organ, choroid plexus, hippocampus, substantia nigra, trigeminal ganglion, hypothalamus, *Ear*; (inner) and outer hair cell, vestibular gangion Peripheral neurons; DRG, dorsal horn, lateral root, Merkel body, *Lung*; epithelial cells, smooth muscle cells, endothelium, *Urinary bladder*; epithelium, *Skin*; keratinocyte
Group 2. Localization where TRPV4 is functionally active. Pathophysiologic roles in diseases are still unknown *Heart*; cardiomyocytes, coronary artery *Blood vessels*; aorta, carotid artery, celleberal artery, mesenteric artery, endothelium, smooth muscle, *Kidney* (Cohen 2007a, b); thick ascending limb, distal tubules (connecting, distal convoluted collecting tubules), collecting tubules, *Liver*: Hepatocyte,
Group 3. Localization where TRPV4 may be active
Cornea
Adipocytes; brown, white fat, (Wang et al. 2009)
Skeletal muscle
Pancreas β-cell (Casas et al. 2008; Islam 2011)
Adrenal
Uterus
Testis
Odontblast (Sole-Magdalena et al. 2011; Son et al. 2009)
Esophagus; epithelium (Mihara et al. 2011; Ueda et al. 2011)
Olfactory (Ahmed et al. 2009)
Basophilic cells (Yang et al. 2009)
Salivary (Aure et al. 2010)
Mast cell line (Kim et al. 2010)

Table 4.1 (continued)

Leukocytes (Spinsanti et al. 2008)
Larynx (Hamamoto et al. 2008, 2009)
Female reproductive organ; ciliated epithelia in the amplulla and isthmus (Teilmann et al. 2005)

Attention should be given to the antibody used, since localization is dependent on the specific antibody. For example, an anti-C-terminal peptide antibody detected TRPV4 in the basolateral membrane of renal tubules (Tian et al. 2004), while an anti-N-terminal antibody detected it in the luminal membrane of renal tubules (Cuajungco et al. 2006). Both antibodies detect a 98 kDa signal in exogenous channel-expressing cells by Western blot analysis. Thus, controversy remains regarding the precise immunohistological localization of TRPV4 *in situ*. The precise localization of TRPV4 protein will not be known until the generation of marker tagged TRPV4 or the production of highly specific antibodies.

4.4 Molecular Mechanisms Converting Physical Stimuli into Channel Opening

4.4.1 Mechanical Force

4.4.1.1 Variables in Mechanical Force (Fig. 4.2)

A number of studies have been performed to elucidate the molecular mechanisms that convert mechanical stress into channel opening, since the first observation of single channel activity by patch-clamping. Cations are conveyed through their respective channels opened by direct membrane stretch applied with a pipette (in so-called stretch-activated Na^+, K^+ and Ca^{2+} -permeable cation channels). Other mechanical stimuli, such as direct touching of the cell, swelling by hypotonic solution, liquid flow on the cell surface and noxious pressure, were previously all considered to be transduced by the same membrane stretch mechanism. However, the molecular identification of ion channels that were proposed to be sensitive to mechanical force revealed that several different mechanisms are required for mechano-gated channel opening. In other words, the nature of the mechano-gating is not uniform, but varies for different cells and channels. TRPV4 was first considered to be activated by cell-swelling, but not by direct stretch of the patch membrane (Strotoman et al. 2000). However, inflation of the cell, induced by applying positive pressure into the patch pipette in the whole cell configuration, activated TRPV4 in CHO cells expressing exogenous channel (Suzuki et al. 2003a). Subsequent investigations *in vivo* suggested that TRPV4 sensed pressure directly in neurons (Liedtke et al. 2003; Suzuki et al. 2003a) and bladder (Andersson et al. 2010). A sensory inability to detect vibration is found in humans with a TRPV4 mutation (hereditary motor and sensory neuropathy, type 2 C; HMSN2C). These data led us to examine in detail the various direct mechanical forces on the TRPV4 protein. We may subdivide

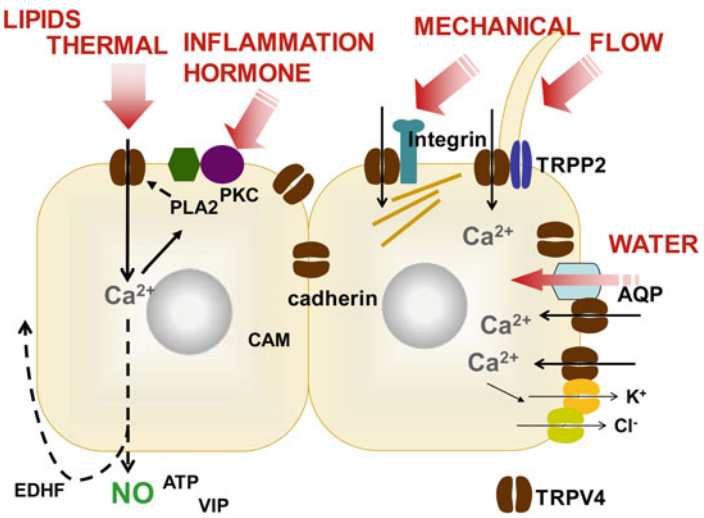

Fig. 4.2 Molecular mechanisms of TRPV4 signal transduction. Right cell shows direct mechanisms of TRPV4 signals. Mechanical pressure/stretch activates TRPV4 with cytoskeletal elements including tubulin, actin and integrin. Flow moves primary cilium that activates TRPP2 (or other TRPs) with TRPV4 complex resulting in TRPV4 activation. Hypotonic solution lets water drive through AQPs that may increase the surface expression of TRPV4 and potentiate TRPV4 activation. TRPV4 and K and/or Cl channels construct a functional channel complex unit located together in caveolae that effluxes the ions and decreases cellular volume. Left shows indirect regulatory mechanisms of TRPV4 activation. The increase in the intracellular Ca driven by TRPV4 activated PLA2 and PLC that activates TRPV4. The increase would couple with adhesion molecule such as cadherin to tighten the cell-junction. The increase would release NO, EDHF (PLA2 products) and ATP that transmit the signal around the cells, such as vascular smooth muscle or peripheral neurons

mechanical stimuli into (1) membrane stretch, (2) membrane pressing/pulling, (3) shear stress, and (4) swelling in hypotonic solutions, as discussed below.

Cytoskeletal elements are crucial in sensing the mechanical force in cells. Experiments using fluorescence-tagged TRPV4 and F-actin revealed that TRPV4 and actin colocalize (Becker et al. 2009). Single photon counting methods predict the minimum of 4 nm between actin and TRPV4 (Ramadass et al. 2007). Biochemical screening also successfully showed that actin and tubulin were colocalized with TRPV4 (Goswami et al. 2010; Matthews et al. 2010). Integrin is a receptor that mediates attachment between a cell and the substrate surrounding it, and it was considered to be a TRPV4-binding protein. Polycyctin is also a probable binding protein for TRPV4 and has an ankyrin-like extracellular domain.

4.4.1.2 Membrane Stretch

The most well-known mechanism is the direct coupling of membrane stretch and channel opening, due to alterations in the lipid bilayer caused by a direct physical force. Stretch energy changes the composition of phospholipids and phosphoinositides, resulting in alterations in membrane fluidity that induces topological changes

in the TM domains of the channels. This mechanism was first established for the Na^+ selective MEC channel and the K^+ selective TREK channel. Because most TRP channels are sensitive to lipids, it was hypothesized that one of them might be a stretch-activated cation channel. Indeed, TRPC1 and TRPC6 expressed in *Xenopus* oocytes and in artificial membranes appear to be stretch-activated channels (Maroto et al. 2005; Spassova et al. 2006); however, this is controversial (Gottlieb et al. 2007).

The effects of negative and positive pressure, as applied to the patch pipette, on channel activity in the cell-attached mode were examined, but no significant effect on TRPV4 activation was observed in an early report (Strotmann et al. 2000). However, in DRG neurons, TRPC1 and TRPC6 cooperate with TRPV4 to mediate mechanical hyperalgesia and nociceptor sensitization, although direct coupling of these molecules has not been demonstrated (Alessandri-Haber et al. 2009).

Recently TRPV4 and a gain-of-function mutant, expressed in *Xenopus* oocytes, exhibited stretch-activated channel activity (activation at -20–30 mmHg) even in the presence of PLA2 blockers. The activation of direct stretch, from 0–60 mmHg, was observed in detached membranes in the presence of PLA2 blockers (Loukin et al. 2010a, b). We had examined stretch activity in CHO cells transfected with TRPV4 and found a few channels with characteristics of stretch-activated channels (4–5/100 trials). Loukin et al. (2010b) observed patch-to-patch heterogeneity but showed a statistically significant probability that TRPV4 was the stretch-activated channel. This may reflect differences in patch elasticity or other geometric and mechanical complexities of the membrane and its subtending cytoskeleton. Thus, stretch-mediated TRPV4 activation might also be detectable in neuronal, bone and urothelium cells *in situ*, since TRPV4 appears to be able to sense direct mechanical pressure in these tissues (see Sect. 4.4).

4.4.1.3 Pressing/Pulling of the Membrane

We (Suzuki et al. 2003a) early on proposed that inflation of the cell, by positive pressure in the whole cell patch configuration, can induce TRPV4 activation more efficiently than by hypotonic swelling in CHO cells at room temperature. Inflation is different from swelling since measured capacitance is increased by inflation, but not by hypotonicity (220–250 mOsm) and water is not transferred across the membrane. Matthews et al. (2010) developed a unique method of directly pulling the plasma membrane using magnetic beads while performing fluo-4 Ca^{2+} imaging in endothelial cells. Using a specific antibody against integrin β1, they showed that TRPV4 was rapidly activated (within 4 ms) by local forces over 450 pN. The displacement of the plasma membrane *per se*, rather than the adhesion of the beads, was required, indicating that TRPV4 opening was not due to generalized deformation of the plasma membrane, membrane stretch, or structural changes in the submembranous cytoskeleton alone. Cytochalasin D potentiated the TRPV4-induced Ca^{2+} influx following bead pulling, suggesting that actin, though thought to be colocalized with TRPV4, did not transmit the pulling force required to activate the channel. In contrast, the distal portion of integrin β1 was found to play an important role in transmitting the pulling force. TRPV2, proposed to be another stretch-activated channel, could not be opened

by this method. The authors concluded that the mechanical force, transmitted via integrin, opened the mouth of the TRPV4 channel. Indeed, the microtubule stabilizing agent, taxol, potently inhibited TRPV4 activation in this model and by the inflation.

In another report for presumably intermediate strength of mechanical force, stretch was applied to the basal side of cells by a specific designed stretchable dish. Cultured cells were grown on the dishes and stretched by this device. TRPV4 in exogenously expressed cells and bladder epithelial cells endowed direct stretch-sensitive Ca^{2+} influx with fluo-4 that was disrupted by actin modifying agents (Mochizuki et al. 2009).

4.4.1.4 Shear Stress

Shear stress arises from fluid flow, which observes Poiseuille's equation, where velocity and viscosity are critical parameters. Although not precisely defined by physical parameters, shear stress in the aorta is thought to be much higher than shear stress in renal tubules. Higher magnitude shear stress, due to rapid fluid flow, opens TRPV4 even in cells in which the channel is artificially overexpressed (O'Neil and Heller 2005). High magnitude shear stress, that occurs for example, in the aorta (Fian et al. 2007; Tanaka et al. 2008), arteries (Kohler et al. 2006) and airways lined with thick viscous fluid, stimulate PLA2, leading to the activation of TRPV4. Airway ciliary beat frequency, achieved by varying viscosity, was related to TRPV4 activity and was dependent on the activation of PLA2 (Andrade et al. 2005, 2007). PBP completely blocked, but AACOCF3 only partially inhibited, the 20 % dextrose-activated Ca^{2+} influx in ciliary cells. These data indicate that shear stress activates PLA2, resulting in the activation of TRPV4, which causes Ca^{2+} influx. However, the association of PLA2 with primary mechanical sensors, such as cytoskeletal elements, was not elucidated in detail.

Lower magnitude shear stress, such as urinary flow in renal microtubules, also activates TRPV4. Polycystin is a well-known glycoprotein that plays a role in renal tubular development, and mutations in this gene have been associated with autosomal dominant polycystic kidney disease. Polycystin may function as an integral membrane protein involved in cell-matrix interactions, and might modulate intracellular calcium homoeostasis in response to urinary flow. Polycystin-2 (TRPP2), in mammals and in zebrafish, is a TRPV4 coupling protein located in the primary cilium of renal epithelia where integrin is also located (Kottgen et al. 2008). The primary cilium is a sensory structure that decorates renal epithelial cells and possibly all other cell types. Because TRPP2 homo-multimers lack mechanosensitivity, we hypothesized that TRPP2 may require and bind TRPV4. Using fluorescence, researchers showed that TRPP2 and TRPV4 colocalized. In addition, TRPP2 and TRPV4 could be co-immunoprecipitated. Furthermore, co-transfection of TRPP2 and TRPV4 into *Xenopus* oocytes resulted in higher magnitude currents than in oocytes transfected with TRPP2 or TRPV4 alone. Flow-dependent Ca^{2+} transients in MDCK cells, a kidney epithelial cell line, were diminished by siRNA against TRPV4. TRPV4 and TRPP2/TRPP1 also colocalized in oviduct cilium (Spinsanti et al. 2008). TRPP2 formed heterotetramers with TRPV4 as well as TRPC1 (Stewart et al. 2010; O'Neil

and Heller 2005). Lower magnitude flow in tubular cells, therefore, might move cilia sufficiently to magnify the integrin-based mechanical force, thereby activating TRPP2/TRPV4.

Heteromeric TRPV4 and TRPC1 channels mediate flow-induced Ca^{2+} influx in vascular endothelial cells (Ma et al. 2010a, b). Administration of dominant-negative TRPC1 inhibited TRPV4-dependent flow-induced $[Ca^{2+}]_i$ increase in human umbilical vein and rat mesenteric artery. The authors also emphasized that heteromerization enabled it be negatively inhibited by protein kinase G. Whether the response of this heteromer to shear stress is dependent on PLA2 products was not examined.

4.4.1.5 Swelling Due to Hypoosmolarity

Most cells in hypotonic solution swell due to an excess of water passing through aquaporin channels. The cells recover their volume by exiting solutes, such as K^+ and Cl^- ions, through channels, which helps to maintain isoosmolarity between the cell exterior and interior. This recovery is termed regulatory volume decrease (RVD). A functional RVD-molecular complex forms when K^+, Cl- and Ca^{2+} channels associate. The TRPV4 Ca^{2+} channel, the Ca^{2+} -activated K^+ channel and the CFTR Cl^- channel may work together. It is known that TRPV4 in many mammalian cells plays a central role in Ca^{2+} influx during RVD (Liedtke 2005; Liedtke et al. 2000; Nilius et al. 2004; Strotmann et al. 2000; Becker et al. 2005). Nevertheless, effects on TRPV4 seem to be indirect since activation by cell-swelling is relatively slow. Swelling may be sensed by phospholipase A2 (PLA2), leading to production of arachidonic acid, which is in turn metabolized to epoxyeicosatrienoic acids (EETs) which activate TRPV4 (Watanabe et al. 2003b). Ca^{2+}-activated K^+ channels (K(Ca)) are active during RVD and might be coupled with TRPV4, forming a K^+ secreting complex. Swelling-activated Ca^{2+} entry via TRPV4 is defective in cystic fibrosis airway epithelia (Arniges et al. 2004). Patients' airway epithelia lack PLA2 activity, thus TRPV4 may not respond to hypotonicity. Although not demonstrated in epithelial tissues, lipid rafts and caveolae in smooth muscle contain a tripartite functional unit involving TRPV4, K(Ca)s, calcium regulatory proteins and connexin 43, a molecular component of gap junctions. Thus cells swollen in hypotonic media may directly or indirectly activate the RVD-molecular complex to recover their original volume.

The pathway from swelling to TRPV4 channel opening by the PLA2 cascade is fascinating but may only be a part of the story. TRPV4 activation during hypotonic cell swelling might occur in the absence of PLA2 in the yeast (Loukin et al. 2009). Yeast swelling still activates TRPV4, resulting in an increase in Ca^{2+} from intracellular stores. Activation of TRPV4 by swelling might be cell-dependent, as HEK cells showed better expression of swelling-induced TRPV4 currents than did CHO cells. When treated with an actin disrupting agent, hypotonic stress no longer activated TRPV4 in CHO cells (Becker et al. 2009). N and C-terminal deletion mutants of TRPV4 are unresponsive to swell-activation. Therefore, it appears that, in addition to the lipid-dependent mechanism, swelling involves translocation of TRPV4, interaction with the cytoskeleton and/or requires additional proteins.

Aquaporin 5 (AQP5) is expressed in lung epithelia and various secretory glands, where it is required for water permeability and cell volume regulation. In airway epithelial cells, the amount of AQP5 surface expression is reduced in the hypotonic state required for TRPV4 activation (Sidhaye et al. 2006; Liu et al. 2006). Further studies indicated that AQP5 and TRPV4 cooperate to recover cell volume in hypotonic media and to enable barrier function against shear stress (Sidhaye et al. 2008). Importantly, an N-terminal deletion of AQP5 did not inhibit cell swelling in hypotonic solution, but it suppressed TRPV4-mediated Ca^{2+} influx, indicating the involvement of a PLA2-independent mechanism. AQP5 might pull TRPV4 toward the plasma membrane when water permeates through itself. Subsequently, Ca^{2+} influx might reduce the abundance of the AQP5/TRPV4 complex. Consequently, TRPV4 might be activated by hypotonic solutions only when colocalized with aquaporin (Liu et al. 2006). Presumably, N-terminal of AQP and N-terminal of TRPV4 are required for the mechanism under swelling although further studies are needed to substantiate.

The other aquaporins, such as AQP4 in astrocytes (Benfenati et al. 2011) and possibly AQP2 in renal collecting tubules, can interact with TRPV4. Human endolymphatic sac showed intimate colocalization of AQP2 with TRPV4 in the luminal membrane (Taguchi et al. 2007).

4.4.2 Temperature

In cells expressing exogenous TRPV4 (Watanabe et al. 2002b) or in primary cultured cells (Chung et al. 2003; Chung et al. 2004), warm temperature (> 33 °C) induced the characteristic outward-rectified current or a rise in $[Ca^{2+}]_i$. As suggested by Gao et al. (2003), warm temperature (37 °C) amplifies the magnitude of other stimuli that activate TRPV4, such as shear stress, phorbols and hypoosmolality, and integrates them.

Based on analogy to TRPV1, thermo-sensitive amino-acid residues were initially proposed to be located in the TM segments. The mechanism behind the activation of TRPV4 by warmth would involve a ligand-dependent conformational change of TM3 (Y555); thus, heat and 4αPDD would share similar molecular mechanisms (Vriens et al. 2004). However, the opening of TRPV4 in cell-attached patches by warming was abolished by detaching the membrane from TRPV4-expressing HEK cells (Watanabe et al. 2002) or from 308 keratinocytes (Chung et al. 2003). In this regard, TRPV4 was not behaving in the same manner as thermo-TRPs, such as TRPM8, TRPA1, TRPV1, TRPV2 or TRPV3, because thermo-TRP activity could be observed in cell free membranes. A vast effort has been made to elucidate the molecular mechanism of temperature sensing in the first thermo-TRP channel identified, TRPV1 (Grandl et al. 2010; Salazar et al. 2009). Patch clamp recordings of single channels showed that thermal stimuli mainly produce changes in the open probability rather than in unitary currents. C-terminal domains were considered to be sensitive to hot temperature (Vlachová et al. 2003; Brauchi et al. 2006); however,

research has shown that mutations near the ion permeation pathway (pore, loop and TM5,6) resulted in diminished temperature activation by heat (> 42 °C).

At present, warmth activation of TRPV4 is considered to require the N-terminal domain, and the mechanism is thought to be quite different from that involved in the opening of thermo-TRPs. But a structure based explanation for the thermosensitivity of TRPV4 requires further study.

4.4.3 Nociception and Inflammation

Several signal transduction pathways were investigated to uncover the mechanisms of pain sensation by TRPV4. Alessandri-Haber et al. (2003, 2004, 2005, 2006, 2008, 2009) investigated, in a series of studies, the role of TRPV4 in nociception in peripheral DRG neurons. They suggested that hypoosmolality, mechanical stress and chemical irritants induce TRPV4 dependent pain sensation. Administration of 4αPDD promoted the release of substance P and calcitonin gene related peptide from central terminals of primary afferent neurons (Grant et al. 2007). The release of these peptides in the central nervous system mediated pain sensation. Studies on *Trpv4*$-/-$ mice revealed that TRPV4 has a significant role in the development of acute inflammatory mechanical and osmotic hyperalgesia (Levine 2007). *Trpv4*$-/-$ mice also showed marked reduction of C-fiber sensitization to mechanical and hypotonic stimuli induced by inflammatory mediators (Chen et al. 2007). Capsaicin and carrageenan could reduce inflammatory and thermal hyperalgesia in TRPV4-null mice (Todaka et al. 2004). The anti-cancer drug, paclitaxel, induces pain. Administration of TRPV4 antisense oligonucleotides reversed paclitaxel-induced mechanical hyperalgesia (Alessandri-Haber et al. 2004). The authors suggested the involvement of PKA, PKC (Cao et al. 2009) and integrin/Src kinase in nociception mediated by TRPV4. TRPV4 has also been implicated in visceral nociception in response to colorectal distension (Brierley et al. 2008; Cenac et al. 2008), colitis (D'Aldebert et al. 2011) and pancreatitis (Ceppa et al. 2010; Vergnolle et al. 2010).

TRPV4 is co-expressed with PAR2 (Grant et al. 2007), a G protein-coupled receptor and inflammatory mediator, in a subset of primary sensory neurons. Activation of PAR2 induced sensitization of TRPV4-expressing cells to mechanical and osmotic stimuli via activation of phospholipase C and protein kinase A, C and D (Alessandri-Haber et al. 2006; Cenac et al. 2008; Grant et al. 2007; Sipe et al. 2008; Akopian et al. 2009). In contrast, PAR4 negatively modulated TRPV4 activation. Visceral inflammation, where PAR4 was involved (Auge et al. 2009), including colonic pain and pancreatitis, was also considered to be mediated in conjunction with TRPV4 in mice (Bradesi 2009). The interaction of TRPV4, integrin and SRC tyrosine kinase in mechanical hyperalgesia was also reported (Alessandri-Haber et al. 2008; Wegierski et al. 2009). The role of TRPV4 in nociception was considered not only for DRG neuronal cell bodies, but also for nerve endings mediating dental pain (Magloire et al. 2010) and for trigeminal neurons (Chen et al. 2008, 2009a, b; Li et al. 2009). In fact, a new antagonist against TRPV4 mitigated pain sensation due to drug-induced

cystitis (Everaerts et al. 2010). All of these studies lead to the conclusion that reagents blocking TRPV4 are potential drug candidates for pain relief in TRPV4-expressing tissues.

Oxidative stress plays an important role in various physiological and pathophysiological process, including aging, cancer, diabetes mellitus, atherosclerosis and so on. The TRP channel was originally discovered in a study of anoxic cell death in *Drosophila*. Oxidative stress activates TRP and TRPL, inducing Ca^{2+} influx in photoreceptor cells (Agam et al. 2000). Oxidative stress appears to directly increase TRPV1 activation via several cysteine residues (Chuang and Lin 2009). In turn, activation of TRPV4 may produce oxidative stress in the hippocampus (Bai and Lipski 2010) and in the bladder. Activation of TRPV4-dependent Ca^{2+} influx is crucial for the production of H_2O_2 via NADPH oxidase, which promotes inflammation in mouse urothelium (DonKo et al. 2010).

4.4.4 Signals Mediating TRPV4 Activation

Since second messengers, such as IP3 (Garcia-Elias et al. 2008, Fernandes et al. 2008), PLA2, PKC, etc., modulate TRPV4 sensitivity, various molecules were investigated as candidates that enhance Ca^{2+} influx by activating TRPV4 or altering channel sensitivity. Acetylcholine (Ach) in mesenteric endothelial cells activates TRPV4 followed by Ca^{2+} influx, leading to vasodilatation. Ach-induced vasodilatation, decreased blood pressure, and Ca^{2+} signal transduction are absent in *Trpv4*$^{-/-}$ mice *in vivo* and *in vitro* (Zhang et al. 2009). Ach stimulates TRPV4 activity via PKCα in vascular endothelium (Adapala et al. 2011).

Histamine and serotonin in DRG neurons (Cenac et al. 2010) sensitize TRPV4 and play a role in visceral hyperalgesia. The PKC, PLA2, PLCβ and MAPKK pathways may contribute to signal transduction (Cenac et al. 2010). In oral mucosa, TRPV4, sensitized by serotonin, mediates nociceptive hyperalgesia (Nakatsuka et al. 2009).

4.4.5 Signaling Cascades Downstream of TRPV4 Activation

4.4.5.1 Cell Shape

Activation of TRPV4 in individual tissues may induce not only Ca^{2+} influx, but also activate specific signaling cascades, such as SOX9, cytoskeleton-associated proteins, such as rho, and paracrine factors that affect cell shape/orientation/regeneration, cell junction formation or the release of ATP.

TRPV4 activation is associated with SOX9, a transcription factor that plays a major role in chondrocyte differentiation. Interestingly, SOX9 is regulated partly by the activation of rho (Haudenschild et al. 2010). As noted, the C-terminal of TRPV4 interacts with the cytoskeleton and the TRPV4 signal may trigger cytoskeletal

reorganization. As a result, neuronal cell shape, cell differentiation, and epithelial polarity may be effected and neo-vascularization or the development of collateral vessels may develop (Troidl et al. 2009). However, the molecular mechanisms underlying these changes remain obscure.

4.4.5.2 Cell Barrier Function

Activation of TRPV4 tightens cell-cell junctions; it is found in airway epithelia (Alvarez et al. 2006), endothelial cells (Willette et al. 2008), keratinocytes (Sokabe et al. 2010), renal tubules (Taniguchi et al. 2007) and mammary epithelia (Reiter et al. 2006). After the Ca^{2+} burst by TRPV4, specified signal transduction cascades other than Ca^{2+}-dependent signaling may be triggered. The integrity of cell-cell junctions is dependent on TRPV4. We found that the transepithelial voltage difference of renal collecting cells was nearly zero in *Trpv4*$-/-$ mice compared to the −10 mV difference in wild-type mice, suggesting that the absence of TRPV4 makes cell-cell junctions leaky. In keratinocytes, TRPV4, but not TRPV3, bound to β-catenin, forming complexes with adhesion molecules such as cadherin and actin fibers. Rho was activated by the TRPV4 mediated-Ca^{2+} influx induced by warmth (33 °C). Cytoskeletal reorganization involving the participation of adhesion molecules then occurred, forming cell-cell junctions (Sokabe et al. 2010). Keratinocytes are unable to form apical cell-cell junctions without extracellular Ca^{2+}, at low temperature (24 °C) or without TRPV4 (i.e., in *Trpv4*$-/-$ keratinocytes). In lung endothelium, pressure causes TRPV4 activation in lung capillary endothelial cells, leading to an increased vascular permeability via NO formation and activation of myosin light chain kinase (Hamanaka et al. 2010; Yin et al. 2008). Administration of a large amount of the TRPV4 stimulant, GSK1016790A, into the body induced low blood pressure (BP) and vascular collapse that could be prevented by blocking NO synthesis or by using *Trpv4*$-/-$ vessels (Willette et al. 2008).

All of these observations reveal an intimate association between TRPV4 and cell-cell junction formation and integrity, although a common mechanism for all tissues has not been demonstrated yet.

4.4.5.3 Release of ATP

ATP is released by cells when TRPV4 is activated resulting in the transmission of mechanical signals via the ATP-receptor (purinergic receptor). It is observed in renal medullary thick ascending tubules (Silva et al. 2008), keratinocytes (Sokabe et al. 2010), bladder urothelium (Mochizuki et al. 2009; Andersson et al. 2010; Birder et al. 2007) and lung epithelia (Seminario-Vidal et al. 2011). Renal medullary ATP may regulate Na^{+} reabsorption following the activation of TRPV4 by hypoosmolality. Keratinocytes release ATP, following TRPV4 activation, which directly stimulates purinergic receptors of C-fibers that transmit warm temperature sensation. Inflation of the bladder by filling or by stretching the urothelium releases ATP, which

activates purinergic receptors on sensory afferents to transmit bladder volume sensation. Lung epithelia also release ATP; this release is regulated by rho-dependent pannexin 1 opening, which is triggered by stretch activation of TRPV4 (Seminario-Vidal et al. 2011). Activation of purinergic receptor in airway epithelia is important for mucocilliary clearance. Vasoactive intestinal peptide is released from Merkel cells via activation of TRPV4 (Boulais et al. 2009).

4.5 TRPV4 Channelopathies

Figure 4.1b shows mutational hot spots in the TRPV4 amino acid sequence. Three hot spots have been identified: N-terminal, C-terminal and the TM5 pore regions. Representative mutations in these three sites result in channel gain-of-function. TM5 may be related to channel inactivation, with the R616 mutation resulting in a constitutively open channel. N-terminal representative mutants (R269, R315 and R361) prolong open time probability of the channel. P19S is likely phosphorylated and provides a loss of function. More recently, G270, R271 and F273 are related to a loss of function because of unable to polymerize. The functional analyses of other mutations have not yet been performed.

A skeletal mutation involves the abolition of C-terminal P799 and substitution with a stretch of 63 missense amino acids (Nishimura et al. 2010). The authors state (Dai et al. 2010) that it is difficult to hypothesize that it is a gain-of-function mutation, because the truncation of the C-terminal from amino acid 828 leads to accumulation in the ER (Becker et al. 2008). However, V814, located between amino acids 799 and 828, is a site of calmodulin-dependent inhibition, and thus deletion from P799 might abolish this inhibition and be a gain-of-function mutation. Further mutational analysis *in vitro* is required to confirm this notion.

4.5.1 Gain-of-Function Mutations

A striking finding by Rock et al. (2008) was that missense mutations in the TRPV4 gene in 2 families segregated with autosomal dominant brachyolmia type 3. Expression of the R616Q mutation in HEK cells resulted in a large constitutively active current before agonist application at room temperature. The shape of the IV curve and the reversal potentials were unchanged. The gain of function mutation was found to be due to a V620I substitution, with a significantly increased constitutive current at + 100 mV (although somewhat smaller than for the R616Q mutant). The authors suggested that TRPV4 was an important regulator of bone growth at the growth plate.

In addition to brachyolmia, spondylometaphyseal dysplasia, Kozalowski type and metatropic dysplasia (Krakow et al. 2009) are caused by gain-of-function mutations, D333G and R594H, in TRPV4. While brachyolmia is characterized by short stature,

a short trunk and scoliosis, Kozlowski type shows additional skeletal dysplasias involving the spine, as well as metaphyses of the long bones. A mild form of metatropic dysplasia has also been shown to be a TRPV4 channelopathy (Andreucci et al. 2011). Additional mutations have been found, increasing the range of abnormalities between metatropic dysplasia and Kozalowski type (Dai et al 2010), and these should be helpful for the diagnosis of the various channelopathies. Although functional analysis of these mutants awaits further study, the patients commonly exhibit metaphyseal involvement. Different mutations (approximately 30) have been found in skeletal dysplasias, as shown in Fig. 4.1b.

Most mutations in the various skeletal disorders are of the missense type and are widely found in the N-terminal ANK domain, the pore domain and the C-terminal modulation domain. A representative pore mutant, R616Q, displayed a higher density of channel currents without an alteration of single channel characteristics (Loukin et al. 2010a, b). Furthermore, the W733R, L619P and L623P mutations produce a constitutively open channel that is no longer activated by 4αPDD or hypotonic swelling (Loukin et al. 2011). The sites of the different mutations affect the closing mechanism, although independent of Ca^{2+} blocking. Interestingly, gating still possessed outward rectification and voltage-dependence, suggesting the presence of multiple pores in the mouth of the TRPV4 channel.

Three prominent research articles (Auer-Grumbach, et al. 2010; Deng et al. 2010; Landoure et al. 2010) described the identification of TRPV4 mutants in a spectrum of neuromuscular diseases, including congenital distal spinal muscular atrophy (SMA) and hereditary motor and sensory neuropathy type IIC (HMSN2C or Charcot-Marie-Tooth disease type 2). Most mutations in the neuromuscular type disorder were found in the N-terminal ANK domain. The mutations, R269H, R315W and R361C, resulted in loss of function due to reduced surface expression in HeLa cells (Auer-Grumach et al. 2010), while mutations R269C and R269H caused marked cellular toxicity and increased constitutive TRPV4 currents in *Xenopus* oocytes and HEK cells. A follow-up expression study revealed that the mutations at these three sites are gain of function (Fecto et al. 2011; Klein et al. 2011). Expression of these three mutants in cells demonstrated that they were constitutively active, possessing a higher open probability than wild-type TRPV4. The amount of plasma membrane expression of the mutants was not altered, and the R269H mutation did not affect the ability of the channel to interact with calmodulin or PACSIN3 (Fecto et al. 2011).

The affected family members exhibited short stature (Chen et al. 2010) and progressive motor paralysis in dorsal muscles. These were more prominent than the loss of temperature, pain and vibration sensation. Bilateral sensorineuronal hearing loss and impairment in bladder voiding were reported. To determine the role of the various mutations in generating the associated phenotypes, animal models with tissue specific overexpression of these TRPV4 mutants is required.

4.5.2 Loss of Function Mutation

The unique P19S mutation results in clinical hyponatremia. Tian et al. (2009) demonstrated that the SNP in the TRPV4 gene was significantly associated with serum

sodium concentration and hyponatremia (< 135mEq/l) in non-Hispanic Caucasian male populations. Confocal microscopy revealed that the intracellular distribution of the channel was not affected by the P19S mutation. The amount of the mutant in the plasma membrane was almost equal to that of the wild type. The P19S mutant channel exhibited a much diminished response to hypotonic stress, but a similar response to 4αPDD compared with the wild-type channel in whole cell currents. The serine may be modified by phosphorylation, resulting in the loss of function.

Recently, Lamandé et al. (2011) report that dominantly inherited arthropathy, familial digital arthrophathy-brachyodactyly (FDAB) in three independent families causes from TRPV4 mutations in N-terminal. The mutations, G270V, R271P and F273L expressed in HEK cells show poor membrane surface expression and the activation of TRPV4 in response to agonists and hypotonicity is diminished. They also show that amount of expression of TRPV4 changes during arthritis model mouse suggesting that age-and injury-related osteoarthritis may be also involved in the TRPV4 channelopaties.

Chronic obstructive pulmonary disease (COPD) may also be caused by mutations in TRPV4, as revealed by SNP analysis (Zhu et al. 2009). The authors genotyped 2 independent Caucasian populations at 20 SNPs in the TRPV4 gene on chromosome 12q24.1 and found a statistically significant correlation with COPD. However, no functional correlation was proposed or reproduced *in vitro*.

As pointed out (Dai et al. 2010), simple loss or gain of function mutations in TRPV4 are not strictly correlated with phenotype in HMSN2C. There are several possible explanations in addition to differences in experimental conditions. Variable phenotypes are observed even among a single family carrying the same mutation. Reduced penetrance is a possible genetic cause (Berciano et al. 2011; Zimon et al. 2010). Expression of spliced variants may be another reason among different species. In addition, negative feedback makes the phenotype more complex—TRPV4 leads to Ca^{2+} influx, and Ca^{2+}, in turn, inhibits TRPV4 function. Furthermore, associated proteins, including aquaporins and cytoskeletal components, modulate TRPV4 function, and the extent of modulation may depend on the expression levels of the various regulators. Finally, activation of TRPV4 influences neuronal growth and cytoskeletal reorganization. The small, but significantly larger currents in the TRPV4 mutants may affect neuronal phenotype, making them refractory to stimuli that normally activate TRPV4. This might explain why some features of HMSN2C patients are similar to those of TRPV4-null mice.

4.6 Physiology and Pathophysiology of TRPV4

4.6.1 Bone

Most mutations in TRPV4 have been reported in diseases showing abnormalities of bone development involving chondrocytes. Cartilage is a connective tissue that is comprised of matrix containing a relatively sparse population of chondrocytes, which produce and maintain the matrix. Chondrogenesis begins with the aggregation and

condensation of loose mesenchyme to form the chondrocytes (Cameron et al. 2009). Expression of the key protein SOX9 follows. Various types of chondrogenesis occur, forming hyaline, fibrous and elastic cartilage. Hyaline cartilage is found in craniofacial structures, bronchial tubules and the growth plate of long bones. This type of bone growth involves the process of endochondral ossification and is affected by mechanical stress. As proposed in the human disease possessing the gain of function TRPV4 mutation (Rock et al. 2008), endochondral ossification is a process where TRPV4 is able to transmit signals to chondrocytes leading them to produce various matrix proteins. Possible mechanisms of how TRPV4 modulates bone morphogenesis and enchondral ossification have been considered. The mechanical signal is believed to involve integrin receptors. Integrin receptor complexes bind extracellular matrix and transmit the mechanical perturbations to the cytoplasm of chondrocytes (Shakibaei et al. 1997). The TRPV4/integrin complex may be a primary sensor of the mechanical force. Otherwise, the ten-fold volumetric increase in hypertrophic chondrocytes contributes to the formation of the long bone growth plate (Hunziker 1994). This volumetric change may stimulate TRPV4. Finally TRPP2 (and TRPP1) have been shown to be located in the primary cilium of osteoblasts and osteoclasts. TRPP1-null mice develop articular cartilage and growth plate defects (Lu et al. 2001; Xiao et al. 2006). Thus the TRPV4/TRPP2 complex may transduce the mechanical signal in the primary cilium of bone cells.

It is believed that chondrocytes generally grow in synovial fluid, a source rich in anionic substrates. When mechanical stress is applied, water moves to the interstitium with the remaining cationic ions, resulting in a hypertonic synovial fluid. The hyperosmolality diminishes over time or when the mechanical stress is removed. Porcine TRPV4 in cartilage plays a role in hypoosmolality, but not in hyperosmolality (Phan et al. 2009). TRPV4 may respond to a change in osmolality rather than directly to mechanical stress (Hung 2010). TRPV4 may be a particularly important player in arthritis, where the changes in osmolality are larger and the release of inflammatory substrates, such as arachidonate, is enhanced.

Human disease: Gain of function mutations in TRPV4 are responsible for autosomal dominant skeletal dysplasias as described above. In particular, the development of axial bone is impaired, suggesting that chondrocyte and osteocyte-dependent ossification is mediated, at least in part, by TRPV4-mediated signal transduction. Metatropic dysplasia, characterized by short extremities, a short trunk with progressive kyphoscoliosis, and craniofacial abnormalities, is due to a gain of function mutation in TRPV4. Histological studies in two cases of lethal metatropic dysplasia revealed markedly disrupted endochondral ossification, with reduced numbers of hypertrophic chondrocytes and the presence of islands of cartilage within the zone of primary mineralization. These findings suggest a common TRPV4 mutation in these two cases alters chondrocyte differentiation in the growth plate, leading to the observed clinical findings (Camacho et al. 2010).

Recently, a loss of function mutations in TRPV4 is found in FDAB (Lamandé et al. 2011). FDAB is distinct to metatropic dysplasia where FDAB includes deformity in the fingers and toes but not includes that in the spine, knee, hip and other joints. This fact implies that a loss of function of TRPV4 does not influence the normal

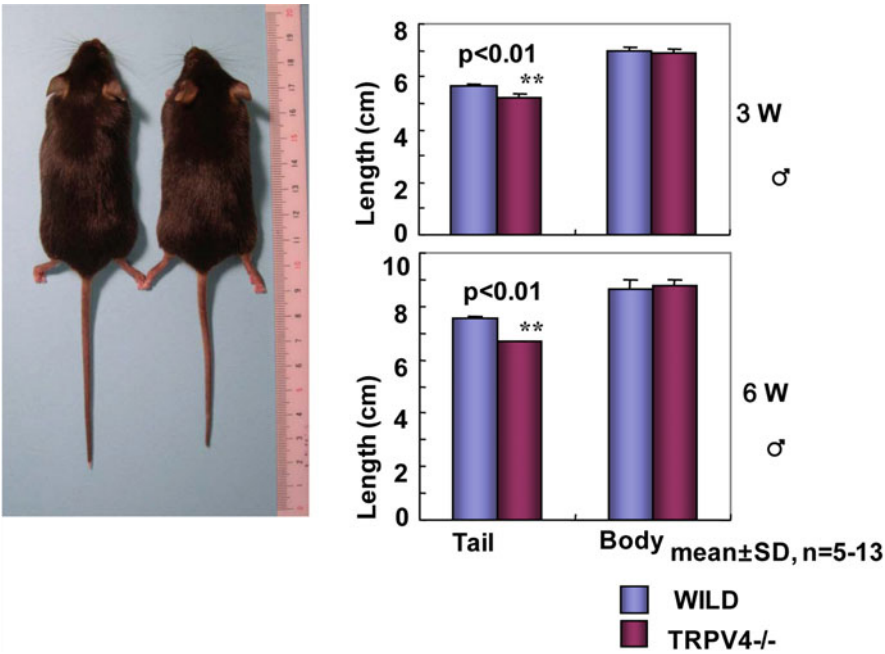

Fig. 4.3 **a** Gross appearance of 8-week-old *Trpv4*−/− male mouse (*right*) and the sex-matched wild type littermate (*left*). Note the shorter tail of *Trpv4*−/−. **b** Tail and body lengths in mutant and wild types. *, $p < 0.05$, by student t. **c** RT-PCR analysis for mRNA expression of TRPVs in primary cultured murine chondrocytes, osteoblasts, and osteoclasts. GAPDH were as positive control. **d** Schematic speculation of growth plate between in normal and TRPV4 mutants. In the normal endochondral ossification of prepuberty, resting chondrocytes differentiate unidirectionally to proliferative and hypertrophic chondrocytes and die by apoptosis. TRPV4 senses mechanical stress and the signal transmits to OS-9 contributing to the development. TRPV4 may present in the early process of this development; in proliferating chondrocytes. The column derived from this process is organized synchronously along the longitudinal axis. In Trpv4 mutants, the chondrocyte lineage often aligns in a disrupted order. TRPV4 channel on the proliferative chondrocytes is responsible for growth of and correct orientation of the chondrocyte alignment and matrix formation by sensing the mechanical force.

development of joints and cartilage but influence the healing process of the minor joints. They suggest that age- and injury related recovery of arthritis are TRPV4-related, although the details in the mechanism remained obscure.

Animal models: Although TRPV4 overexpression in mammals has not been studied yet, Zebrafish oocytes have been injected with the channel to examine its role *in vivo* (Wang et al. 2007). The overexpression of TRPV4 in Zebrafish leads to numerous abnormalities, including curved or shortened body axis, edema, as well as malformation of the eyes and brain. OS-9 rescued these abnormalities by promoting the retention of TRPV4 in the ER.

When we generated *Trpv4*−/− mice, we found that they had a significantly shorter tail compared with wild-type mice (Fig. 4.3). However, the long bones are of normal length and skull size appears normal as well. Histological observations revealed a slight abnormality in enchondoral ossification. Mild osteopetrosis, which may

indicate osteoclast dysfunction, is observed (Masuyama et al. 2008). Chondrocytes were collected from the ribs of new-born mice and cultured. Patch clamp experiments showed that the swelling-activated outward rectified cation currents could be blocked by gadolinium, but no activation was found in hypotonic solution in *Trpv4*−/− chondrocytes, revealing the importance of swelling-activated TRPV4 in chondrocytes. In addition to the PLA2 inhibitor, chemical disruption of the cilium with chloral hydrate, which disrupts microtubules, prevents the swelling-activated Ca^{2+} influx in porcine chondrocytes (Phan et al. 2009). Thus, mechanical stress may activate TRPV4 via signaling from microtubules.

In cartilage, SOX9 is a well-established chondrocyte transcription factor that regulates the expression of cartilage specific extracellular matrix proteins and controls chondrocyte differentiation and bone formation. Muramatsu et al. (2007) described, using a unique approach, that TRPV4 stimulated SOX9-dependent reporter activity in mesenchymal stem cells via a Ca^{2+}-CAM dependent mechanism. However, the signal transduction mechanisms between TRPV4 activation and SOX9 induction remain unknown. Rho activation may play a role in the signaling cascade since it is a demonstrated regulator of SOX9 and is activated by Ca^{2+} influx.

Speculation on the lack of mechanosensation in bone cells led us to perform hind limb unloading. Mechanical hind limb unloading induces osteopenia, reduces the rate of bone formation and stimulates bone resorption by increasing the number of osteoclasts. These effects are suppressed in *Trpv4*−/− mice (Mizoguchi et al. 2008). Recently, increased trabecular bone mineral density and increased cortical thickness, resulting from reduced bone resorption, was found to be a consequence of disrupted osteoclast differentiation (Masuyama et al. 2008). Activation of functional TRPV4 in acidosis and a role for the channel in osteoclast differentiation in mice and humans was suggested (Kato and Morita 2011). TRPV4 mRNA is detected in human and murine osteoblast line cells (Abed et al. 2009). However, the role of TRPV4 in isolated osteoblasts has not been examined yet (Fig. 4.4).

Synovial fluid becomes hypotonic during the onset of arthritis. Inflammation may also involve PLA2 activation, releasing AA, which activates TRPV4. Thus, TRPV4 is conjectured to be activated in inflammatory arthritis. However, Clark et al. showed that *Trpv4*−/− mice exhibit severe osteoarthritic joint degeneration, indicating that TRPV4 plays an important role in maintaining the health of bone and joints (Clark et al. 2010). Lamandé et al. indicate that TRPV4 mRNA is reduced in the late healing process of arthritis model in mouse. The contribution of TRPV4 to the process and development of joint is now focused in human disease and will be clarified in the near future.

4.6.2 Central Nervous System

TRPV4 and Osm9 are similar and both have been proposed to play a role in osmo-sensation in the brain. The osmolality of the extracellular fluid is maintained near 290 mOsm by thirst and antidiuresis when hypertonic liquid is administered.

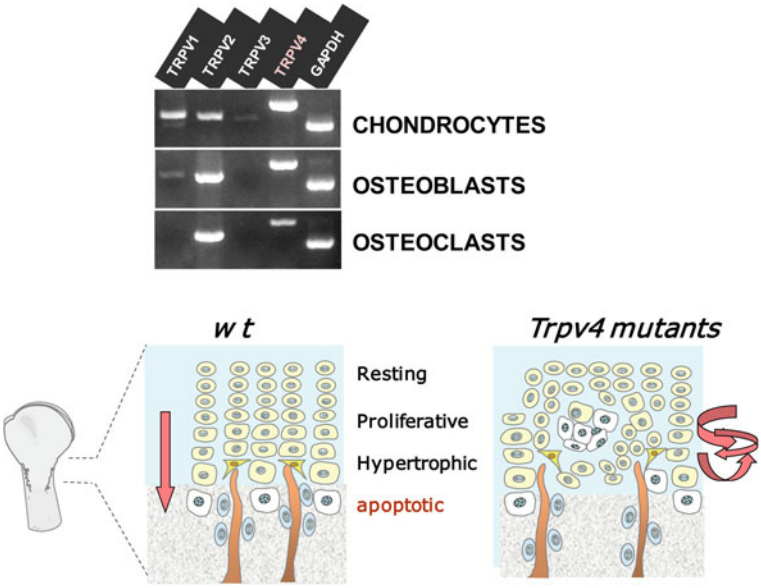

Fig. 4.4 RT-PCR detection of TRPV4 was performed on bone cells. Positive signal was detected in chondrocytes, osteoblast and osteoclasts. Thus TRPV4 may directly sense mechanical pressure and influence their development. We hypothesized the signal in chondrocytes showing schematic comparison of growth plate between in normal *wt* and *Trpv4*−/− mice. In the normal 'endochondral ossification' of prepuberty *wt*, resting chondrocytes differentiate unidirectionaly to proliferative and hypertrophic chondrocytes, and die by apoptosis (*left*). The column derived from this process is organized synchronously along the longitudinal axis. In *Trpv4*−/−, focal disordered column because of unable to detect the spatial orientation, like as 'cell nest', are shown (*right*). The chondrocyte lineage often aligns in disorder. TRPV4 channel on the proliferative chondrocytes is responsible for decision of orientation of the cell alignment and matrix formation by sensing the mechanical force (bottom).

In contrast, osmolality is maintained by diuresis and salt craving when animals are administered hypotonic liquid. This homeostatic control is believed to be mediated by osmosensory neurons in the organum vasculosum lamina terminalis (OVLT), which synaptically regulates the electrical activity of effector neurons in the supraoptic nucleus (SON), which release hormones (Bourque et al. 2007). The neurons express stretch-activated and stretch-inactivated cation channels and are believed to play a crucial role in sensing body osmolality. TRPV4 was first believed to be involved in these channels (Liedtke et al. 2003a, b, Mizuno et al. 2000) but controversy was emerged in the *Trpv4*−/− mouse model. On the other hand, a truncated form of TRPV1 was then involved in the hyperosmolality sensitive channel (Sharif Naeini et al. 2006) and *Trpv1*−/− showed the phenotype similar to diabetes insipedes (Ciura et al. 2006). Direct measurement of OVLT neurons suggests that TRPV1 but not TRPV4 contribute the hyperosmolality sensitive channel (Ciura et al. 2011). However, contribution of TRPV1 to this mechanism *in vivo* remained obscured (Taylor et al. 2008). More complex mechanisms should also be considered (May and Jordan 2011).

Human disease: Hyponatremia was observed in loss of function mutations of TRPV4. Mutations may enable the N-terminal of TRPV4 to be inactivated by phosphorylation. It is hypothesized that the mutant channel is less responsive to hypotonicity *in vitro*; decreased sensitivity of a hypotonicity sensor *in vivo* would permit water excess. An exaggerated vasopressin response was considered to contribute to the hyponatremia.

Mouse model: Trpv4$-/-$ mice are expected to show lack of thirst sensation leading to a diabetes insipidus-like phenotype (Liedtke et al. 2003a, b). However, we (Mizuno et al. 2003) examined drinking behavior and the effects of intensive water intake, salt overloading and a low salt diet, and failed to find a difference compared with wild-type mice. We concluded that *Trpv4*$-/-$ mice exhibited a phenotype similar to that due to disrupted ADH secretion. Figure 4.3 shows the vasopressin level in various serum sodium concentrations in wild-type and *Trpv4*$-/-$ mice. An overall higher concentration of vasopressin is present in *Trpv4*$-/-$ animals. An exaggerated vasopressin response to hyperosmolality was found in perfused *Trpv4*$-/-$ mouse brain slices. Presumably, TRPV4 suppresses vasopressin secretion when stimulated. The findings are similar to those observed in asymptomatic hyponatremia in humans with loss of TRPV4 function. Hyponatremia is observed in liver cirrhosis where an exaggerated vasopressin response is thought to contribute to the pathogenesis. The amount of TRPV4 in SON neurons was decreased in a rat cirrhosis model while vasopressin and renin activity were increased (Carreno et al. 2009).

More recently, TRPV4 has been shown to sense hypoosmolality in mouse liver neurons connecting to thoracic DRGs, and it is thought to play a role in the maintenance of isoosmolality and extracellular fluid volume. When hypotonic, but not isotonic, solution was ingested, TRPV4 was activated and thought to transmit the signal from the liver to the CNS (Lechner et al. 2011). This transmission may regulate BP. After portal hpoosmolality was achieved by water ingestion, wild-type, but not *Trpv4*$-/-$ mice, exhibited an increase in BP (McHugh et al. 2010).

Based on the above findings, chronic water intake or a restricted-salt diet for a long duration may produce serum hypotonicity, resulting in hyponatremia that was maintained by the relatively higher level of vasopressin in *Trpv4*$-/-$ animals.

Direct injection of 4αPDD (Tsushima 2006) or ghrelin (Hashimoto et al. 2010; Tsushima 2006) inhibited angiotensinII-induced dipsogenic behavior after 24 hours of water deprivation in the rat. TRPV4 activation in choroid plexus may thus prevent excessive thirst.

Taken together, the mechanisms that maintain body osmolality appear more complex than previously thought (that it was only regulated by stretch-sensitive channels in the SON). The mechanisms likely involve peripheral afferent signals in addition to central signals, and TRPV4 may contribute to both signaling pathways.

In addition to osmosensing neurons, TRPV4 can be found in other CNS structures. Functional TRPV4 is detected in the choroid plexus (Millar et al. 2007), substantia nigra (Guatteo et al. 2005), hippocampal CA1 (Lipski et al. 2006; Shibasaki et al. 2007), thermo-regulatory neurons (Shibasaki et al. 2007), astrocytes (Benfenati et al. 2007) and retinal cells (Benfenati et al. 2007). However, the physiological role of TRPV4 in these regions is unknown. For instance, TRPV4 was thought

to play a role in thermoregulatory neurons in the brain because of its localization in the hippocampus (Guler et al. 2002). It is hypothesized that a thermosensitive population of serotonergic neurons plays an important role in stress-related neuropsychiatric disorders, including anxiety and affective disorders (Lowry et al. 2009). The hypothalamus is thought to play a role in locomotor and metabolic circadian rhythms. IL15 regulates the rhythm, including heat dissipation and locomotion, and concomitantly activates TRPV4 in the hypothalamus (He et al. 2010). Interestingly, TRPV4 mRNA levels were dependent on circadian rhythms. Using *Trpv4*−/− mice, we examined the regulation of body temperature, memory and mood, but we failed to detect notable differences. The analysis may have been not detailed enough to permit detection of small differences.

4.6.3 Auditory System

TRP channels that mediate mechanosensation are proposed to contribute to normal hearing (Corey 2006; Cuajungco et al. 2007). TRPV4 is expressed in the auditory system in hair cells and nerve endings (Tabuchi et al. 2005; Takumida et al. 2005). RT-PCR revealed that mRNA expression of TRPA1, TRPP3 and TRPC5.2, but not TRPV4, changed with development, suggesting that these three TRP channels are important in the formation of the cochlea and in hearing impairment (Asai et al. 2010). Nonetheless, a TRPV4 channelopathy, HMSNII, involved a patient with progressive sensorineuronal hearing loss (Zimon et al. 2010). Because HMSNII appears to be due to a toxic gain of function in TRPV4, it is reasonable that the affected members should exhibit hearing loss. Gain of function TRPV4 may damage the nerve endings in the inner ear by causing excessive Ca^{2+} influx into the cells. In the absence of extracellular Ca^{2+}, TRPV4 was permeable to aminoglucoside antibiotics, leading to their uptake and toxicity in hair cells (Karasawa et al. 2008, Steyger and Karasawa 2008; Ishibashi et al. 2009; Kitahara et al. 2005).

We isolated outer hair cells from wild-type and *Trpv4*−/− mice and found that the swelling-activated rise in intracellular Ca^{2+} was absent in *Trpv4*−/− cells. Takeda-Nakazawa et al. (2007) also found that hypotonic swelling activated TRPV4 and released NO in guinea pig outer hair cells. Because outer hair cells are surrounded by lymphatic fluid, isotonic to serum, swelling of outer hair cells may occur in inflammation of the auditory system, such as in Meniere's disease. Although TRPV4 may be related to the pathogenesis of hearing loss, no direct measurement of functional TRPV4 has been performed in inner hair cells. On the other hand, *Trpv4*−/− mice did not present with congenital deafness, but these mice were more vulnerable to acoustic injury and developed late-onset hearing loss (Tabuchi et al. 2005). TRPV4 was not needed for normal development of the cochlear system.

4.6.4 Peripheral Nervous System

Peripheral sensation, including mechanical, thermal and nociceptive sensation, is transduced by specific nerve endings, such as Merkel bodies and is transmitted

through unmyelinated C-fibers and myelinated Aγ fibers. TRPV4 was found in sensory systems in skin, keratinocytes, specific nerve endings, DRG neurons and central neurons. Thus, TRPV4 is considered to play cardinal roles in sensing osmolality, pressure, temperature and noxious stimuli. Accordingly, a loss of TRPV4 function is expected to result in a loss of mechanosensation and nociception. A gain of function is toxic to the channel-expressing neurons, leading to axonal degeneration and resulting in the loss of mechanosensation, thermosensation and nociception. Because TRPV4 is expressed, though little, in motor neurons, the toxic TRPV4 results in late-onset motor paralysis. In zebrafish, TRPV4 is expressed in neurons involved in mechanosensation, thermosensation, hearing, vision and taste (Amato et al. 2011; Mangos et al. 2007).

Human disease: TRPV4 mutants are found in HMSN2. HMSN consists of two subtypes—HMSN1 (myelin type) and HMSN2 (axonal type)—which present with similar clinical features. The onset of clinical symptoms is in the first or second decade of life. Weakness starts distally in the feet and progresses proximally in an ascending pattern. Neuropathic bone deformities develop, including pes cavus and hammer toes. Muscle stretch reflexes disappear early in the ankles and later in the patella and upper limbs. Mild sensory loss to pain, temperature or vibration in the legs is observed. Patients also complain of allodynia, numbness and tingling, but paresthesias are not as common as in acquired neuropathies (Gemignani et al. 1999). Human TRPV4 is expressed in motor neurons, in the ventral and lateral roots, and in DRG neurons (Facer et al. 2007). The amount of TRPV4 protein expression is low, and less than 5 % of the signal found in the trachea was detected in mouse dorsal and lateral horn, primarily in motor and sensory neurons (Landoure et al. 2010). Following the onset of symptoms, the distribution of TRPV4 in peripheral neurons paralleled the clinical features in HMSN2.

Movement: The *Trpv4*$^{-/-}$ mice underwent the standard mouse behavior/locomotion test but did not show a significant weakness of movement. Body weight and lifespan were not different until 2 years of age from wild-type mice. TRPV4, TRPV2, TRPC1, C3, C4 and C6 are detected in skeletal muscle (Brinkmeier 2011). Because of faint expression in motor neurons, the role of TRPV4 in motor neurons has not yet been examined.

Mechanosensation: We (Suzuki et al. 2003c) and others (Liedtke et al. 2003a, b) reported that tail pressure sensation, but not gentle touch sensation in the hind paw, was impaired in *Trpv4*$^{-/-}$ mice. Stretch and pressure sensation, i.e., a harmful mechanical force, but not gentle mechanical touch sensation, was impaired in the *Trpv4*$^{-/-}$ mice.

TRPV4 contributes to mechanical allodynia following chronic compression of the dorsal root ganglion in rats (Zhang et al. 2008). After chronic compression of the DRG, mechanical hyperalgesia occurs in rats as well as in HMSN2 patients. These effects are at least in part mediated by an upregulation of TRPV4 expression 1–4 weeks after the compression.

Merkel bodies, specialized nerve endings located under the skin that sense mechanical force, express TRPV4. They appear to be activated in response to hypoosmolality, but not directly to mechanical force (Boulais et al. 2009).

Cultured peripheral neuronal cell lines also express TRPV4. Nociceptive signals were reproduced in these cells. Notably, activation of TRPV4 by mechanical stress not only induced Ca^{2+} influx, but concomitantly induced cytoskeletal reorganization (Goswami et al. 2010) and migration (Zaninetti et al. 2011) of neurons. Thus, gain of function of TRPV4 in human HMSN peripheral neurons may induce abnormalities in cytoskeletal organization, leading to axonal degeneration in addition to the Ca^{2+} toxicity.

Thermosensation: In human gain of function and in mouse loss of function TRPV4 mutations, a mild, but significant, abnormality was reported in thermosensation. Mild impairment in temperature sensation and thermotaxis was observed in the mouse model (Todaka et al. 2004). In addition to peripheral nerves, skin and central neurons also contribute to thermosensation. It was thought that heat sensitive TRPV1 and cold sensitive TRPA1 were sufficient to permit normal thermosensation (Voets et al. 2004). Nonetheless, TRPV4 certainly played a role in warmth sensation. A precise analysis of thermosensation in human mutants of these channels will be informative since, in contrast to mice, humans are capable of providing verbal feedback regarding the feeling of temperature.

TRPV4 is present in the sarcolemma of mouse muscle (Kruger et al. 2008). The application of an agonist increases resting Ca^{2+} influx in mouse muscles (Pritschow et al. 2011); however, little is known about the physiological significance of TRPV4 in skeletal muscle.

4.6.5 Bladder

Sensations from the bladder are conveyed by pelvic and hypogastric nerve afferents—Aγ and C fibers. There are two different mechanosensory information signaling pathways—direct, at nerve terminals, and indirect, mediated by chemical transmitters. Furthermore, two different magnitudes of mechanical stimuli are involved; a high threshold painful one and a low threshold physiological one that controls micturition.

The urothelium has recently been shown to play a major role in low threshold mechansensory transduction (Birder 2005). In response to mechanical and chemical stimuli, various neuromediators, such as ATP, ACh, NO and prostaglandins, are released from urothelial cells (Ferguson et al. 1997; Birder et al. 2002). Bladder epithelium expresses functional TRPV4 that was proposed to play a role in stretch sensing, and in inflammation and warmth sensation (Everaerts et al. 2008; Gevaert et al. 2007; Kullmann et al. 2009; Thorneloe et al. 2008; Yamada et al. 2009; Combrisson et al. 2007, Xu et al. 2009). Mochizuki used cultured urothelium on stretchable dishes and demonstrated that TRPV4 was actually a stretch-sensitive Ca^{2+} influx channel and that activation was followed by the release of ATP. TRPV4 is hypothesized to sense the filling of the bladder, promoting ATP release, which activates ATP/purinergic receptors to signal to sensory nerve endings. HMSN2 symptoms include bladder incontinence or neurogenic bladder. In contrast, TRPV4-deficient mice

exhibit abnormal voiding frequencies and non-voiding contractions in cystometric experiments (Andersson et al. 2010). All of these findings parallel the importance of TRPV4 in bladder mechanosensitivity.

At present, pharmacological agents targeting TRPV4 are used for the treatment of inflammatory and neuropathic pain, urinary incontinence, painful bladder syndrome, and even certain types of prostate cancer (Eid 2011; Boudes et al. 2011).

4.6.6 Respiratory System

TRPV4 is abundant in the lung where it has a vital role in airway epithelial volume regulation, smooth muscle contraction, mucociliary transport, and epithelial and endothelial permeability. However, *Trpv4*$^{-/-}$ mice do not show a prominent phenotype in respiratory function. The respiratory phenotype in human patients with TRPV4 mutations is still controversial.

Human disease: Zhu et al. (2009) genotyped 2 independent Caucasian populations at 20 SNPs in the TRPV4 gene and tested qualitative COPD and quantitative FEV1 and FEV1/FVC phenotypes. TRPV4 is supposed to play a role in the development of asthma (Liedtke et al. 2004). In a family-based study of 606 families and 1,891 patients, 7 of 20 SNPs tested were associated with COPD, and 6 SNPs were associated with FEV1/FVC. On the other hand, this association is not found in more wide population study (Obeidat et al. 2011). In contrast, the loss of function TRPV4 (P19S) was not associated with these lung diseases, but a loss of function TRPV1 variant was associated with a lower risk of childhood asthma (Cantero-Recasens et al. 2010). However, no lung abnormality has been described in the TRPV4 channelopathies, HMSN2 and brachyolmia.

Airway smooth muscle: Airway smooth muscle cells express TRPV4, which could be activated by hypotonic swelling (Jia et al. 2004). Activation of TRPV4 (Townsley et al. 2006) by pressure or by serotonin (Ducret et al. 2008) induced pulmonary hypertension, the mechanism of which may involve not only smooth muscle contraction, but proliferation induced by Ca^{2+} influx as well.

Mucociliary transport: Ciliated tracheal epithelial cells express TRPV4, which is activated by the flow of viscous fluid. This flow-triggered activation of TRPV4 involves receptor-mediated Ca^{2+} influx followed by ATP dependent ciliary beat frequency (Lorenzo et al. 2008). Thus, TRPV4 plays a role in mucociliary transport. TRPV4-mediated dysfunctions in mucociliary transport and mucus homeostasis may also contribute to the development of chronic rhinosinusitis (Bhargave et al. 2008).

Lung endothelial cells: Activation of TRPV4 by high lung pressure causes disruptions in the alveolar septal barrier and leads to alveolar flooding and hypoxemia (Jian et al. 2008; Alvarez et al. 2006; Curry and Glass 2006). Inflation of the lung activates endothelial TRPV4—this occurs through a mechanism involving myosin light chain kinase—and NO synthesis. This process makes the endothelium permeable, possibly leading to lung edema. Subsequently, NO likely inhibits TRPV4 function via the cGMP pathway (Yin et al. 2008). Alterations of TRPV4 function may further lead to

different pathological processes in the respiratory system (Li et al. 2011; Hamanaka et al. 2007, 2010).

4.6.7 Cardiovascular System

TRPV4 mRNA was abundant in aortic endothelial cells; therefore, mechanical stress, blood pressure and shear stress were early candidate stimulatory signals (Nilius 2003). Injection of the TRPV4 agonist, 4αPDD, rapidly decreased BP *in vivo*. Vascular tone is regulated by the endothelium through multiple mechanical signals via a rise in $[Ca^{2+}]_i$. Two pathways that elevate $[Ca^{2+}]_i$ are known: the so-called "receptor-stimulated Ca^{2+} influx" (RSC) pathway and the "store-operated Ca^{2+} influx" (SOC) pathway. The former mechanism is largely impaired in *Trpc4*$-/-$ endothelium (Freichel et al. 2004) and the latter is impaired in *Trpv4*$-/-$ mice (Zhang et al. 2009). Although TRPV4 may play a role in RSC, heteromers of TRPV4 and TRPC1 appear to play a role in SOC. When the Ca^{2+} store was depleted, the heteromer moved toward the plasma membrane (Ma et al. 2008). Two important mediators released after the rise in $[Ca^{2+}]_i$ are NO and endothelium-derived hyperpolarization factor (EDHF), both of which act on smooth muscle to cause relaxation. NO diffuses into smooth muscle cells and stimulates guanylyl cyclase to inhibit myosin kinase. In smooth muscle, EDHF stimulates TRPV4 coupled to the K(Ca) channel. K channel opening hyperpolarizes the membrane potential leading to cellular relaxation.

Vascular endothelium: TRPV4 mRNA is present in the endothelium of numerous organs and tissues, including bovine adrenal cortex capillaries (Thodeti et al. 2009), human cerebral cortex (Brayden et al. 2008), dermis, lungs, submucosal umbilical veins (Willette et al. 2008; Loot et al. 2008), mouse aorta (Zhang et al. 2009) and cerebral cortex (Ma et al. 2008), mesenteric arteries (Mendoza et al. 2010; Gao and Wang 2010), rat carotid artery (Kohler et al. 2006), rat cerebral cortex (Marrelli et al. 2007) and femurs (Troidl et al. 2009). TRPV4 mRNA is not detected in renal microvasculature in any species. TRPV4 mediated shear-stress induces release of NO via Ca^{2+} influx and NO synthase activation in the endothelium (Gao et al. 2010; Kohler and Hoyer 2007; Hartmannsgruber et al. 2007). Shear stress activates PLA_2 and AA products, which in turn activates TRPV4 ((Loot et al. 2008; Hartmannsgruber et al. 2007). In isolated carotid, cerebral, pulmonary, aortic (Yang et al. 2006) and mesenteric arteries, shear stress-induced TRPV4 activation and NO production were determined to be mediated by the PLA2 cascade (Loot et al. 2008).

Endothelium is composed of a monolayer of cells tightly adherent to each other. The paracellular pathway relies on the integrity of cell-cell junctions, which is maintained by a balance between the force applied by blood pressure at the junctions and the adhesive force applied by contractile molecules. As described above, activation of TRPV4 by lung pressure or agonists, such as EETs and 4aPDD, produced blebs or breaks in the epithelial wall in the airway endothelium. Administration of GSK1016790A decreased BP, followed by profound vascular collapse and hemorrhaging in the lungs, intestines and kidneys. This damage could not be prevented

by NOS inhibition in wild-type animals and was not observed in *Trpv4*−/− mice (Willette et al. 2008).

Smooth muscle: In smooth muscle, a predicted factor, released by the endothelium and that induced vasodilatation via the activation of K^+ channels, had not been identified and was termed the "endothelium-derived hyperpolarization factor" (EDHF). H_2 O_2, K^+ ions and the cytochrome P450 product, EETs, were candidates for the EDHF. As noted, the epoxygenase product, 11,12 EET, activates TRPV4, resulting in Ca^{2+} bursts. Earley et al. (2005) suggested that EET induced Ca^{2+} bursts via TRPV4 and the ryanodine receptor in sarcoplasmic reticulum, and that the activation of the Ca^{2+} activated K(Ca) nearby caused a transient hyperpolarisation of smooth muscle cells that led to arterial vasodilatation. In bronchial epithelial cells, Ca^{2+} influx trough TRPV4 directly activates BKCa channels without the help of ryanodine receptors (Fernandez-Fernandez et al. 2008). This was the initial evidence that EET was, in fact, the EDHF that induced vasodilatation (Kotlikoff 2005). NO-induced cGMP then decreased the activity of TRPV4, probably via the CAMII cascade, completing the negative feedback loop. This feedback system was theoretically linked to the cyclic dilatation and constriction of the vasculature—*myogenic autoregulation*—after an increase in shear stress or flow. This cyclic movement was weak or absent in *Trpv4*−/− mice (Kohler et al. 2006; Kohler 2007).

TRPV4 acts as a mechanosensor that regulates neovascularization in small arterial endothelial cells. Pulsatile mechanical stimuli induce cytoskeletal reorganization, forming new blood vessels via Ca^{2+} signal transduction. TRPV4 was shown to be the main sensor transducing the mechanical signals into Ca^{2+} influx. (Thodeti et al. 2009). Shear stress stimulated collateral growth in arterial occlusions, in which TRPV4 was also an important player (Troidl et al. 2009; Schierling et al. 2011).

Stimulation of the acetylcholine receptor via protein kinase C activates TRPV4 in endothelial cells, resulting in vasodilatation (Adapala et al. 2011). 5-hydroxytryptamine activates TRPV4 in pulmonary arteries, resulting in vasoconstriction; this mechanism probably also leads to smooth muscle proliferation and might cause pulmonary hypertension (Ducret et al. 2008).

TRPV4 mRNA was detected in heart muscle (Strotmann et al. 2003), but its functional role in cardiomyocytes remains to be clarified (Li et al. 2008; Hu et al. 2009). Fibroblasts possess functional TRPV4 (Hatano et al. 2009).

Basal BP in *Trpv4*−/− mice is not different from wild-type mice. Acetylcholine-induced hyperpolarization and vasodilation were reduced by approximately 75 % in mesenteric resistance arteries from *Trpv4*−/− mice, compared with wild-type mice (Zhang et al. 2009). Injection of L-NAME, a NO synthase inhibitor, produced an increase in BP in *Trpv4*−/− mice that was greater than the increase induced in wild-type animals (Earley et al. 2009). Activation of TRPV4 decreased BP in rats fed a normal-salt diet. Furthermore, the TRPV4 channel blocker, which increased BP in animals on a normal-salt diet, had a greater effect on rats fed a high-salt diet (Gao et al. 2009). Salt intake unmasked a difference in blood pressure in the Dahl salt-sensitive hypertensive rat. Salt-sensitive rats develop hypertension due to a decrease in TRPV4 in the kidneys and in the DRGs, compared to salt-resistant rats (Gao and Wang 2010; Armando and Jose 2009). Even in normal mice (Earley et al. 2009),

hypertension by salt overloading can be intensified by inhibiting TRPV4 activity. These experiments have shed light on the apparently normal, sub-clinical condition of hypertension and have provided the foundation for future research. The known human TRPV4 mutations exhibit no obvious phenotype in blood pressure or heart function.

4.6.8 Kidney

Abundant expression of TRPV4 channels has been detected in the kidney. However, the *Trpv4*$-/-$ mouse model and patients with TRPV4 mutations do not exhibit a prominent disturbance of renal function. Tian et al. (2004) found basolateral expression of TRPV4, using a sensitive antibody, in all the nephron segments following the ascending thin limb, except for the macula densa in rat and mouse kidney. Low, but significant, expression can be observed in luminal membranes.

Flow sensor: Several experiments have demonstrated that TRPV4 is an apical/luminal flow sensor in a renal tubular cell line overexpressing the protein (Kottgen et al. 2008) and in freshly isolated renal tubules (Taniguchi et al. 2007). TRPV4 is a sensor of luminal flow/shear stress in the collecting duct, functioning to open and enhance K excretion, possibly via the BKCa channel. TRPP2 is known to be another flow-sensor (Nauli et al. 2003) and plays a role in polycystic kidney disease. A defect of the flow-sensing mechanism was considered to be pathogenetic of cyst formation. Interestingly, both TRP channels are colocalized in the primary cilium, forming a functional flow-sensing complex (Kottgen et al. 2008). However, renal cysts were never observed in *Trpv4*$-/-$ mice. This indicates that the loss of TRPV4 function does not induce cyst formation and that a defect in the flow-sensing mechanism was not involved in cyst development. Nonetheless, activation of TRPV4 might help prevent cyst formation in renal tubules, but not in liver cysts, which are made of cholangiocytes (Gradilone et al. 2010).

Calcium metabolism: TRPV4 is phosphorylated by WNK4, reducing membrane expression of the channel. Gamba (2006) and Fu et al. (2006) proposed that patients with a gain of function mutation in WNK4 with lowered TRPV4 activity may develop a PHAII-like syndrome where enhanced Na reabsorption in cortical collecting ducts leads to salt sensitive hypertension. Calcium reabsorption is also proposed to be enhanced in *Trpv4*$-/-$ mice. Leaky epithelia may potentiate Ca^{2+} reabsorption in cortical collecting ducts or in the thick ascending limb. In contrast, high blood Ca^{2+} concentrations stimulate PLA2 via the Ca^{2+}-sensing receptor in the thick ascending limb to inhibit Ca^{2+} reabsorption through the paracellular pathway. If TRPV4 contributes to this mechanism, *Trpv4*$-/-$ mice should develop hypercalciuria.

Sodium metabolism: Hyperosmolality is maintained in renal medulla by a countercurrent mechanism. When free water is ingested, medullary hyperosmolality is decreased to dilute urine to keep body osmolality within the normal range. TRPV4 in the medullary thick ascending limb and cortical collecting ducts has been proposed to play a role in this process (Chen 2007). Reduction of osmolality in the thick

ascending limb releases ATP, which regulates Na excretion—this is not observed in TRPV4-deficient mice (Silva and Garvin 2008). Flow or swell induces the sustained rise in DCT and CCD that is required for P2Y2 receptor and TRPV4 (Mamenko et al. 2011). ATP is here again coupled with TRPV4 activation since isolated tubules from P2Y2 or TRPV4 null mice provoke much less Ca^{2+} influx from lumen in response to ATP. ATP stimulates rather than is stimulated by the activation of TRPV4.

Humans: No obvious phenotype in electrolyte metabolism or renal function has been reported yet in gain of function TRPV4 channelopathies.

Mouse model: No obvious renal defect has been reported in TRPV4 null mice. We maintained wild-type and *Trpv4*$-/-$ mice for 2 years and found no difference in renal weight. No cysts were detected in either group of mice. Volume overloading was performed by removing of one kidney, but no functional difference was found in the remaining one.

Taken together of the data regarding electrolytes and osmotic fluctuation, one can at least propose that (1) TRPV4 contribute osmotic, thus, sodium homeostasis that is amplified and become detectable by an alteration of extracellular tonicity (or volume) and that (2) TRPV4 is natriuretic rather than sodium retensive player in various organs contributing to sodium homeostatis, in the kidney, in the brain and in peripheral nerves spread in the liver.

4.6.9 Skin

As discussed above, TRPV4 in keratinocytes plays a role in thermosensation (Chung et al. 2003, 2004, Denda et al. 2007). A range of temperatures, roughly from room temperature to body temperature, activates TRPV4 in keratinocytes. The resulting Ca^{2+} influx releases ATP, leading to stimulation of purinergic receptors on sensory nerve endings. TRPV4 also plays a role in cell-cell junctions—the barrier of the skin—and in keratinocytes during development. Mechanical stimulation of keratinocytes might similarly be involved in the activation of TRPV4, but this possibility has not been investigated yet. ATP and the purinergic P2Y2 receptor were also shown to be important for the transmission of mechanical stimuli to nerve endings ((Lumpkin and Caterina 2007).

4.7 Conclusion and Perspectives

With a wide distribution, number of molecular studies and human diseases, TRPV4 is critically established as a mechanosensitive Ca^{2+} permeable channel that thereby is central for understanding the molecular mechanism of the conversion of physical force to ion permeation. Presumably, the mechanical force can directly pull the channel via cytoskeletal elements and also indirectly amplifies the activation by chemical cascade and local endocrines. Another protein adds an additional function:

Aquaporin adds TRPV4 to the sensing of water flux and polycystin adds TRPV4 to a flow sensing on primary cilium. Mutations of TRPV4 induced abnormalities in bone development, motor paralysis and mild loss of variable sensation. Analysis of the mutations will have own merit for understanding how mechanical sensation plays in normal and in disease.

Acknowledgements This work was supported by grants-in-aid for scientific research (22590291). We would like to thank Shigematsu for helpful comment and photo.

References

Abed E, Labelle D, Martineau C, Loghin A, Moreau R (2009) Expression of transient receptor potential (TRP) channels in human and murine osteoblast-like cells. Mol Membr Biol 26: 146–158

Adapala RK, Talasila PK, Bratz IN, Zhang DX, Suzuki M, Meszaros JG, Thodeti CK (2011) PKC{alpha} mediates acetylcholine-induced activation of TRPV4-dependent calcium influx in endothelial cells. Am J Physiol Heart Circ Physiol 301:H757–765

Agam K, von Campenhausen M, Levy S, Ben-Ami HC, Cook B, Kirschfeld K, Minke B (2000) Metabolic stress reversibly activates the Drosophila light-sensitive channels TRP and TRPL in vivo. J Neurosci 20:5748–55

Ahmed MK, Takumida M, Ishibashi T, Hamamoto T, Hirakawa K (2009) Expression of transient receptor potential vanilloid (TRPV) families 1, 2, 3 and 4 in the mouse olfactory epithelium. Rhinology 47:242–247

Akopian AN, Ruparel NB, Jeske NA, Patwardhan A, Hargreaves KM (2009) Role of ionotropic cannabinoid receptors in peripheral antinociception and antihyperalgesia. Trends Pharmacol Sci 30:79–84

Alessandri-Haber N, Yeh JJ, Boyd AE, Parada CA, Chen X, Reichling DB, Levine JD (2003) Hypotonicity induces TRPV4-mediated nociception in rat. Neuron 39:497–511

Alessandri-Haber N, Dina OA, Yeh JJ, Parada CA, Reichling DB, Levine JD (2004) Transient receptor potential vanilloid 4 is essential in chemotherapy-induced neuropathic pain in the rat. J Neurosci 24:4444–4452

Alessandri-Haber N, Joseph E, Dina OA, Liedtke W, Levine JD (2005) TRPV4 mediates pain-related behavior induced by mild hypertonic stimuli in the presence of inflammatory mediator. Pain 118:70–79

Alessandri-Haber N, Dina OA, Joseph EK, Reichling D, Levine JD (2006) A transient receptor potential vanilloid 4-dependent mechanism of hyperalgesia is engaged by concerted action of inflammatory mediators. J Neurosci 26:3864–3874

Alessandri-Haber N, Dina OA, Joseph EK, Reichling DB, Levine JD (2008) Interaction of transient receptor potential vanilloid 4, integrin, and SRC tyrosine kinase in mechanical hyperalgesia. J Neurosci 28:1046–1057

Alessandri-Haber N, Dina OA, Chen X, Levine JD (2009) TRPC1 and TRPC6 channels cooperate with TRPV4 to mediate mechanical hyperalgesia and nociceptor sensitization. J Neurosci 29:6217–6228

Alvarez DF, King JA, Weber D, Addison E, Liedtke W, Townsley MI (2006) Transient receptor potential vanilloid 4-mediated disruption of the alveolar septal barrier: a novel mechanism of acute lung injury. Circ Res 99:988–995

Amato V, Vina E, Calavia MG, Guerrera MC, Laura R, Navarro M, De Carlos F, Cobo J, Germana A, Vega JA (2011) TRPV4 in the sensory organs of adult zebrafish. Microsc Res Tech: 2011 Jun 15. doi: 10.1002/jemt.21029

Andersson KE, Gratzke C, Hedlund P (2010) The role of the transient receptor potential (TRP) superfamily of cation-selective channels in the management of the overactive bladder. BJU Int 106:1114–1127

Andrade YN, Fernandes J, Vazquez E, Fernandez-Fernandez JM, Arniges M, Sanchez TM, Villalon M, Valverde MA (2005) TRPV4 channel is involved in the coupling of fluid viscosity changes to epithelial ciliary activity. J Cell Biol 168:869–874

Andrade YN, Fernandes J, Lorenzo IM, Arniges M, Valverde MA (2007) The TRPV4 Channel in Ciliated Epithelia

Andreucci E, Aftimos S, Alcausin M, Haan E, Hunter W, Kannu P, Kerr B, McGillivray G, Gardner RJ, Patricelli MG, Sillence D, Thompson E, Zacharin M, Zankl A, Lamande SR, Savarirayan R (2011) TRPV4 related skeletal dysplasias: a phenotypic spectrum highlighted by clinical, radiographic, and molecular studies in 21 new families. Orphanet J Rare Dis 6:37

Armando I, Jose PA (2009) Sensing salt intake. Hypertension 53:118–119

Arniges M, Vazquez E, Fernandez-Fernandez JM, Valverde MA (2004) Swelling-activated $Ca2^{+}$ entry via TRPV4 channel is defective in cystic fibrosis airway epithelia. J Biol Chem 279:54062–54068

Arniges M, Fernandez-Fernandez JM, Albrecht N, Schaefer M, Valverde MA (2006) Human TRPV4 channel splice variants revealed a key role of ankyrin domains in multimerization and trafficking. J Biol Chem 281:1580–1586

Asai Y, Holt JR, Geleoc GS (2010) A quantitative analysis of the spatiotemporal pattern of transient receptor potential gene expression in the developing mouse cochlea. J Assoc Res Otolaryngol 11:27–37

Auer-Grumbach M, Olschewski A, Papic L, Kremer H, McEntagart ME, Uhrig S, Fischer C, Frohlich E, Balint Z, Tang B, Strohmaier H, Lochmuller H, Schlotter-Weigel B, Senderek J, Krebs A, Dick KJ, Petty R, Longman C, Anderson NE, Padberg GW, Schelhaas HJ, van Ravenswaaij-Arts CM, Pieber TR, Crosby AH, Guelly C (2010) Alterations in the ankyrin domain of TRPV4 cause congenital distal SMA, scapuloperoneal SMA and HMSN2C. Nat Genet 42:160–164

Auge C, Balz-Hara D, Steinhoff M, Vergnolle N, Cenac N (2009) Protease-activated receptor-4 (PAR 4): a role as inhibitor of visceral pain and hypersensitivity. Neurogastroenterol Motil 21:1189-e1107

Aure MH, Roed A, Galtung HK (2010) Intracellular C^{2+} responses and cell volume regulation upon cholinergic and purinergic stimulation in an immortalized salivary cell line. Eur J Oral Sci 118:237–244

Bai JZ, Lipski J (2010) Differential expression of TRPM2 and TRPV4 channels and their potential role in oxidative stress-induced cell death in organotypic hippocampal culture. Neurotoxicology 31:204–214

Basavappa S, Pedersen SF, Jørgensen NK, Ellory JC, Hoffmann EK (1998) Swelling-induced arachidonic acid release via the 85-kDa cPLA2 in human neuroblastoma cells. J Neurophysiol 79:1441–1449

Becker D, Blase C, Bereiter-Hahn J, Jendrach M (2005) TRPV4 exhibits a functional role in cell-volume regulation. J Cell Sci 118:2435–2440

Becker D, Muller M, Leuner K, Jendrach M (2008) The C-terminal domain of TRPV4 is essential for plasma membrane localization. Mol Membr Biol 25:139–151

Becker D, Bereiter-Hahn J, Jendrach M (2009) Functional interaction of the cation channel transient receptor potential vanilloid 4 (TRPV4) and actin in volume regulation. Eur J Cell Biol 88: 141–152

Benfenati V, Amiry-Moghaddam M, Caprini M, Mylonakou MN, Rapisarda C, Ottersen OP, Ferroni S (2007) Expression and functional characterization of transient receptor potential vanilloid-related channel 4 (TRPV4) in rat cortical astrocytes. Neuroscience 148: 876–892

Benfenati V, Caprini M, Dovizio M, Mylonakou MN, Ferroni S, Ottersen OP, Amiry-Moghaddam M (2011) An aquaporin-4/transient receptor potential vanilloid 4 (AQP4/TRPV4) complex is essential for cell-volume control in astrocytes. Proc Natl Acad Sci USA 108: 2563–2568

Berciano J, Baets J, Gallardo E, Zimon M, Garcia A, Lopez-Laso E, Combarros O, Infante J, Timmerman V, Jordanova A, De Jonghe P (2011) Reduced penetrance in hereditary motor neuropathy caused by TRPV4 Arg269Cys mutation. J Neurol 258:1413–1421

Bhargave G, Woodworth BA, Xiong G, Wolfe SG, Antunes MB, Cohen NA (2008) Transient receptor potential vanilloid type 4 channel expression in chronic rhinosinusitis. Am J Rhinol 22:7–12

Birder LA (2005) More than just a barrier: urothelium as a drug target for urinary bladder pain. Am J Physiol Renal Physiol 289:F489–495

Birder LA, Nakamura Y, Kiss S, Nealen ML, Barrick S, Kanai AJ, Wang E, Ruiz G, De Groat WC, Apodaca G, Watkins S, Caterina MJ (2002) Altered urinary bladder function in mice lacking the vanilloid receptor TRPV1. Nat Neurosci 5:856–860

Birder L, Kullmann FA, Lee H, Barrick S, de Groat W, Kanai A, Caterina M (2007) Activation of urothelial transient receptor potential vanilloid 4 by 4alpha-phorbol 12,13-didecanoate contributes to altered bladder reflexes in the rat. J Pharmacol Exp Ther 323:227–235

Brauchi S, Orta G, Salazar M, Rosenmann E, Latorre R (2006) A hot-sensing cold receptor: C-terminal domain determines thermosensation in transient receptor potential channels. J Neurosci 26:4835–4840

Brinkmeier H (2011) TRP channels in skeletal muscle: gene expression, function and implications for disease. Adv Exp Med Biol 704:749–758

Boudes M, Uvin P, De Ridder D (2011) TRPV4, new therapeutic target for urinary problems. Med Sci (Paris) 27:232–234

Boulais N, Pennec JP, Lebonvallet N, Pereira U, Rougier N, Dorange G, Chesne C, Misery L (2009) Rat Merkel cells are mechanoreceptors and osmoreceptors. PLoS One 4:e7759

Boulais N, Pereira U, Lebonvallet N, Gobin E, Dorange G, Rougier N, Chesne C, Misery L (2009) Merkel cells as putative regulatory cells in skin disorders: an in vitro study. PLoS One 4:e6528

Bourque CW, Ciura S, Trudel E, Stachniak TJ, Sharif-Naeini R (2007) Neurophysiological characterization of mammalian osmosensitive neurones. Exp Physiol 92:499–505

Bradesi S (2009) PAR4: a new role in the modulation of visceral nociception. Neurogastroenterol Motil 21:1129–1132

Brayden JE, Earley S, Nelson MT, Reading S (2008) Transient receptor potential (TRP) channels, vascular tone and autoregulation of cerebral blood flow. Clin Exp Pharmacol Physiol 35: 1116–1120

Brierley SM, Page AJ, Hughes PA, Adam B, Liebregts T, Cooper NJ, Holtmann G, Liedtke W, Blackshaw LA (2008) Selective role for TRPV4 ion channels in Brayden sensory pathways. Gastroenterology 134:2059–2069

Camacho N, Krakow D, Johnykutty S, Katzman PJ, Pepkowitz S, Vriens J, Nilius B, Boyce BF, Cohn DH (2010) Dominant TRPV4 mutations in nonlethal and lethal metatropic dysplasia. Am J Med Genet A 152A:1169–1177

Cameron TL, Belluoccio D, Farlie PG, Brachvogel B, Bateman JF (2009) Global comparative transcriptome analysis of cartilage formation in vivo. BMC Dev Biol 9:20

Cantero-Recasens G, Gonzalez JR, Fandos C, Duran-Tauleria E, Smit LA, Kauffmann F, Anto JM, Valverde MA (2010) Loss of function of transient receptor potential vanilloid 1 (TRPV1) genetic variant is associated with lower risk of active childhood asthma. J Biol Chem 285:27532–27535

Cao DS, Yu SQ, Premkumar LS (2009) Modulation of transient receptor potential Vanilloid 4-mediated membrane currents and synaptic transmission by protein kinase C. Mol Pain 5:5

Caterina MJ, Schumacher MA, Tominaga M, Rosen TA, Levine JD, Julius D (1997) The capsaicin receptor: a heat-activated ion channel in the pain pathway. Nature 389:816–824

Caterina MJ, Rosen TA, Tominaga M, Brake AJ, Julius D (1999) A capsaicin-receptor homologue with a high threshold for noxious heat. Nature 398:436–441

Carreno FR, Ji LL, Cunningham JT (2009) Altered central TRPV4 expression and lipid raft association related to inappropriate vasopressin secretion in cirrhotic rats. Am J Physiol Regul Integr Comp Physiol 296:R454–466

Casas S, Novials A, Reimann F, Gomis R, Gribble FM (2008) Calcium elevation in mouse pancreatic beta cells evoked by extracellular human islet amyloid polypeptide involves activation of the mechanosensitive ion channel TRPV4. Diabetologia 51:2252–2262

Cenac N, Altier C, Chapman K, Liedtke W, Zamponi G, Vergnolle N (2008) Transient receptor potential vanilloid-4 has a major role in visceral hypersensitivity symptoms. Gastroenterology 135:937–946, 946 e931–932

Cenac N, Altier C, Motta JP, d'Aldebert E, Galeano S, Zamponi GW, Vergnolle N (2010) Potentiation of TRPV4 signalling by histamine and serotonin: an important mechanism for visceral hypersensitivity. Gut 59:481–488

Ceppa E, Cattaruzza F, Lyo V, Amadesi S, Pelayo JC, Poole DP, Vaksman N, Liedtke W, Cohen DM, Grady EF, Bunnett NW, Kirkwood KS Transient receptor potential ion channels V4 and A1 contribute to pancreatitis pain in mice (2010) Am J Physiol Gastrointest Liver Physiol 299:G556–571

Chen X, Alessandri-Haber N, Levine JD (2007) Marked attenuation of inflammatory mediator-induced C-fiber sensitization for mechanical and hypotonic stimuli in TRPV4-/- mice. Mol Pain 3:31

Chen L, Liu C, Liu L (2008) Changes in osmolality modulate voltage-gated calcium channels in trigeminal ganglion neurons. Brain Res 1208:56–66

Chen L, Liu C, Liu L (2009a) Osmolality-induced tuning of action potentials in trigeminal ganglion neurons. Neurosci Lett 452:79–83

Chen L, Liu C, Liu L, Cao X (2009b) Changes in osmolality modulate voltage-gated sodium channels in trigeminal ganglion neurons. Neurosci Res 64:199–207

Chen DH, Sul Y, Weiss M, Hillel A, Lipe H, Wolff J, Matsushita M, Raskind W, Bird T (2010) CMT2C with vocal cord paresis associated with short stature and mutations in the TRPV4 gene. Neurology 75:1968–1975

Chuang HH, Lin S (2009) Oxidative challenges sensitize the capsaicin receptor by covalent cysteine modification. Proc Natl Acad Sci USA 106:20097–20102

Chung MK, Lee H, Caterina MJ (2003) Warm temperatures activate TRPV4 in mouse 308 keratinocytes. J Biol Chem 278:32037–32046

Chung MK, Lee H, Mizuno A, Suzuki M, Caterina MJ (2004) 2-aminoethoxydiphenyl borate activates and sensitizes the heat-gated ion channel TRPV3. J Neurosci 24:5177–5182

Chung MK, Lee H, Mizuno A, Suzuki M, Caterina MJ (2004) TRPV3 and TRPV4 mediate warmth-evoked currents in primary mouse keratinocytes. J Biol Chem 279:21569–21575

Ciura S, Bourque CW (2006) Transient receptor potential vanilloid 1 is required for intrinsic osmoreception in organum vasculosum lamina terminalis neurons and for normal thirst responses to systemic hyperosmolality. J Neurosci 26:9069–75

Ciura S, Liedtke W, Bourque CW (2011) Hypertonicity Sensing in Organum Vasculosum Lamina Terminalis Neurons: A Mechanical Process Involving TRPV1 But Not TRPV4. J Neurosci 31:14669–14676

Clapham DE, Runnels LW, Strubing C (2001) The trp ion channel family. Nat Rev Neurosci 2:387–396

Clark AL, Votta BJ, Kumar S, Liedtke W, Guilak F (2010) Chondroprotective role of the osmotically sensitive ion channel transient receptor potential vanilloid 4: age- and sex-dependent progression of osteoarthritis in Trpv4-deficient mice. Arthritis Rheum 62:2973–2983

Cohen DM (2007a) The Role of TRPV4 in the Kidney. In: Liedtke WB, Heller S, editors. TRP Ion Channel Function in Sensory Transduction and Cellular Signaling Cascades. Boca Raton (FL): CRC Press; Chapter 29

Cohen DM (2007b) The transient receptor potential vanilloid-responsive 1 and 4 cation channels: role in neuronal osmosensing and renal physiology. Curr Opin Nephrol Hypertens 16:451–458

Colbert HA, Smith TL, Bargmann CI (1997) OSM-9, a novel protein with structural similarity to channels, is required for olfaction, mechanosensation, and olfactory adaptation in Caenorhabditis elegans. J Neurosci 17:8259–8269

Combrisson H, Allix S, Robain G (2007) Influence of temperature on urethra to bladder micturition reflex in the awake ewe. Neurourol Urodyn 26:290–295

Corey DP (2006) What is the hair cell transduction channel?. J Physiol 576:23–28

Cuajungco MP, Grimm C, Oshima K, D'Hoedt D, Nilius B, Mensenkamp AR, Bindels RJ, Plomann M, Heller S (2006) PACSINs bind to the TRPV4 cation channel. PACSIN 3 modulates the subcellular localization of TRPV4. J Biol Chem 281:18753–18762

Curry FR, Glass CA (2006) TRP channels and the regulation of vascular permeability: new insights from the lung microvasculature. Circ Res 99:915–917

Cuajungco MP, Grimm C, Heller S (2007) TRP channels as candidates for hearing and balance abnormalities in vertebrates. Biochim Biophys Acta 1772:1022–1027

Dai J, Cho TJ, Unger S, Lausch E, Nishimura G, Kim OH, Superti-Furga A, Ikegawa S (2010) TRPV4-pathy, a novel channelopathy affecting diverse systems. J Hum Genet 55:400–402

Dai J, Kim OH, Cho TJ, Schmidt-Rimpler M, Tonoki H, Takikawa K, Haga N, Miyoshi K, Kitoh H, Yoo WJ, Choi IH, Song HR, Jin DK, Kim HT, Kamasaki H, Bianchi P, Grigelioniene G, Nampoothiri S, Minagawa M, Miyagawa SI, Fukao T, Marcelis C, Jansweijer MC, Hennekam RC, Bedeschi F, Mustonen A, Jiang Q, Ohashi H, Furuichi T, Unger S, Zabel B, Lausch E, Superti-Furga A, Nishimura G, Ikegawa S (2010) Novel and recurrent TRPV4 mutations and their association with distinct phenotypes within the TRPV4 dysplasia family. J Med Genet 47:704–709

D'Aldebert E, Cenac N, Rousset P, Martin L, Rolland C, Chapman K, Selves J, Alric L, Vinel JP, Vergnolle N (2011) Transient receptor potential vanilloid 4 activated inflammatory signals by intestinal epithelial cells and colitis in mice. Gastroenterology 140:275–285

Delany NS, Hurle M, Facer P, Alnadaf T, Plumpton C, Kinghorn I, See CG, Costigan M, Anand P, Woolf CJ, Crowther D, Sanseau P, Tate SN (2001) Identification and characterization of a novel human vanilloid receptor-like protein, VRL-2. Physiol Genomics 4:165–174

Denda M, Sokabe T, Fukumi-Tominaga T, Tominaga M (2007) Effects of skin surface temperature on epidermal permeability barrier homeostasis. J Invest Dermatol 127:654–659

Deng HX, Klein CJ, Yan J, Shi Y, Wu Y, Fecto F, Yau HJ, Yang Y, Zhai H, Siddique N, Hedley-Whyte ET, Delong R, Martina M, Dyck PJ, Siddique T (2010) Scapuloperoneal spinal muscular atrophy and CMT2C are allelic disorders caused by alterations in TRPV4. Nat Genet 42:165–169

Denker SP, Barber DL (2002) Ion transport proteins anchor and regulate the cytoskeleton. Curr Opin Cell Biol 14:214–220

D'Hoedt D, Owsianik G, Prenen J, Cuajungco MP, Grimm C, Heller S, Voets T, Nilius B (2008) Stimulus-specific modulation of the cation channel TRPV4 by PACSIN 3. J Biol Chem 283:6272–6280

Ding XL, Wang YH, Ning LP, Zhang Y, Ge HY, Jiang H, Wang R, Yue SW (2010) Involvement of TRPV4-NO-cGMP-PKG pathways in the development of thermal hyperalgesia following chronic compression of the dorsal root ganglion in rats. Behav Brain Res 208:194–201

Donko A, Ruisanchez E, Orient A, Enyedi B, Kapui R, Peterfi Z, de Deken X, Benyo Z, Geiszt M (2010) Urothelial cells produce hydrogen peroxide through the activation of Duox1. Free Radic Biol Med 49:2040–2048

Ducret T, Guibert C, Marthan R, Savineau JP (2008) Serotonin-induced activation of TRPV4-like current in rat intrapulmonary arterial smooth muscle cells. Cell Calcium 43:315–323

Earley S, Heppner TJ, Nelson MT, Brayden JE (2005) TRPV4 forms a novel $Ca2^{+}$ signaling complex with ryanodine receptors and BKCa channels. Circ Res 97:1270–1279

Earley S, Pauyo T, Drapp R, Tavares MJ, Liedtke W, Brayden JE (2009) TRPV4-dependent dilation of peripheral resistance arteries influences arterial pressure. Am J Physiol Heart Circ Physiol 297:H1096–1102

Eid SR (2011) Therapeutic Targeting of TRP Channels—The TR(i)P to Pain Relief. Curr Top Med Chem 11:2118–2130

Everaerts W, Gevaert T, Nilius B, De Ridder D (2008) On the origin of bladder sensing: Tr(i)ps in urology. Neurourol Urodyn 27:264–273

Everaerts W, Nilius B, Owsianik G (2010) The vanilloid transient receptor potential channel TRPV4: from structure to disease. Prog Biophys Mol Biol 103:2–17

Everaerts W, Vriens J, Owsianik G, Appendino G, Voets T, De Ridder D, Nilius B (2010) Functional characterization of transient receptor potential channels in mouse urothelial cells. Am J Physiol Renal Physiol 298:F692–701

Everaerts W, Zhen X, Ghosh D, Vriens J, Gevaert T, Gilbert JP, Hayward NJ, McNamara CR, Xue F, Moran MM, Strassmaier T, Uykal E, Owsianik G, Vennekens R, De Ridder D, Nilius B, Fanger CM, Voets T (2010) Inhibition of the cation channel TRPV4 improves bladder function in mice and rats with cyclophosphamide-induced cystitis. Proc Natl Acad Sci USA 107:19084–19089

Facer P, Casula MA, Smith GD, Benham CD, Chessell IP, Bountra C, Sinisi M, Birch R, Anand P (2007) Differential expression of the capsaicin receptor TRPV1 and related novel receptors TRPV3, TRPV4 and TRPM8 in normal human tissues and changes in traumatic and diabetic neuropathy. BMC Neurol 7:11

Fan HC, Zhang X, McNaughton PA (2009) Activation of the TRPV4 ion channel is enhanced by phosphorylation. J Biol Chem 284:27884–27891

Fecto F, Shi Y, Huda R, Martina M, Siddique T, Deng HX (2011) Mutant TRPV4-mediated Toxicity Is Linked to Increased Constitutive Function in Axonal Neuropathies. J Biol Chem 286: 17281–17291

Ferguson DR, Kennedy I, Burton TJ (1997) ATP is released from rabbit urinary bladder epithelial cells by hydrostatic pressure changes–a possible sensory mechanism?. J Physiol 505:503–11

Fernandes J, Lorenzo IM, Andrade YN, Garcia-Elias A, Serra SA, Fernandez-Fernandez JM, Valverde MA (2008) IP3 sensitizes TRPV4 channel to the mechano- and osmotransducing messenger 5'-6'-epoxyeicosatrienoic acid. J Gen Physiol 131:i2 J Cell Biol 181:143–155

Fernandez-Fernandez JM, Andrade YN, Arniges M, Fernandes J, Plata C, Rubio-Moscardo F, Vazquez E, Valverde MA (2008) Functional coupling of TRPV4 cationic channel and large conductance, calcium-dependent potassium channel in human bronchial epithelial cell lines. Pflugers Arch 457:149–159

Fian R, Grasser E, Treiber F, Schmidt R, Niederl P, Rosker C (2007) The contribution of TRPV4-mediated calcium signaling to calcium homeostasis in endothelial cells. J Recept Signal Transduct Res 27:113–124

Freichel M, Philipp S, Cavalie A, Flockerzi V (2004) TRPC4 and TRPC4-deficient mice. Novartis Found Symp 258:189–199; discussion 199–203, 263–186

Fu Y, Subramanya A, Rozansky D, Cohen DM (2006) WNK kinases influence TRPV4 channel function and localization. Am J Physiol Renal Physiol 290:F1305–1314

Gamba G (2006) TRPV4: a new target for the hypertension-related kinases WNK1 and WNK4. Am J Physiol Renal Physiol 290:F1303–1304

Gaudet R (2008) A primer on ankyrin repeat function in TRP channels and beyond. Mol Biosyst 4:372–9

Gao F, Wang DH (2010) Hypotension induced by activation of the transient receptor potential vanilloid 4 channels: role of $Ca2^{+}$ -activated K^{+} channels and sensory nerves. J Hypertens 28:102–110

Gao F, Wang DH (2010) Impairment in function and expression of transient receptor potential vanilloid type 4 in Dahl salt-sensitive rats: significance and mechanism. Hypertension 55: 1018–1025

Gao X, Wu L, O'Neil RG (2003) Temperature-modulated diversity of TRPV4 channel gating: activation by physical stresses and phorbol ester derivatives through protein kinase C-dependent and -independent pathways. J Biol Chem 278:27129–27137

Gao F, Sui D, Garavito RM, Worden RM, Wang DH (2009) Salt intake augments hypotensive effects of transient receptor potential vanilloid 4: functional significance and implication. Hypertension 53:228–235

García-Martínez C, Morenilla-Palao C, Planells-Cases R, Merino JM, Ferrer-Montiel A (2000) Identification of an aspartic residue in the P-loop of the vanilloid receptor that modulates pore properties. J Biol Chem 275:32552–32558

Garcia-Elias A, Lorenzo IM, Vicente R, Valverde MA (2008) IP3 receptor binds to and sensitizes TRPV4 channel to osmotic stimuli via a calmodulin-binding site. J Biol Chem 283:31284–31288

Gemignani F, Marbini A, Di Giovanni G, Salih S, Terzano MG (1999) Charcot-Marie-Tooth disease type 2 with restless legs syndrome. Neurology 52:1064–1066

Gevaert T, Vriens J, Segal A, Everaerts W, Roskams T, Talavera K, Owsianik G, Liedtke W, Daelemans D, Dewachter I, Van Leuven F, Voets T, De Ridder D, Nilius B (2007) Deletion of the transient receptor potential cation channel TRPV4 impairs murine bladder voiding. J Clin Invest 117:3453–3462

Goswami C, Kuhn J, Heppenstall PA, Hucho T (2010) Importance of non-selective cation channel TRPV4 interaction with cytoskeleton and their reciprocal regulations in cultured cells. PLoS One 5:e11654

Gottlieb P, Folgering J, Maroto R, Raso A, Wood TG, Kurosky A, Bowman C, Bichet D, Patel A, Sachs F, Martinac B, Hamill OP, Honoré E (2007) Revisiting TRPC1 and TRPC6 mechanosensitivity. Pflugers Arch 455:1097–103

Gradilone SA, Masyuk AI, Splinter PL, Banales JM, Huang BQ, Tietz PS, Masyuk TV, Larusso NF (2007) Cholangiocyte cilia express TRPV4 and detect changes in luminal tonicity inducing bicarbonate secretion. Proc Natl Acad Sci USA 104:19138–19143

Gradilone SA, Masyuk TV, Huang BQ, Banales JM, Lehmann GL, Radtke BN, Stroope A, Masyuk AI, Splinter PL, LaRusso NF (2010) Activation of Trpv4 reduces the hyperproliferative phenotype of cystic cholangiocytes from an animal model of ARPKD. Gastroenterology 139: 304–314 e302

Grant AD, Cottrell GS, Amadesi S, Trevisani M, Nicoletti P, Materazzi S, Altier C, Cenac N, Zamponi GW, Bautista-Cruz F, Lopez CB, Joseph EK, Levine JD, Liedtke W, Vanner S, Vergnolle N, Geppetti P, Bunnett NW (2007) Protease-activated receptor 2 sensitizes the transient receptor potential vanilloid 4 ion channel to cause mechanical hyperalgesia in mice. J Physiol 578: 715–733

Guatteo E, Chung KK, Bowala TK, Bernardi G, Mercuri NB, Lipski J (2005) Temperature sensitivity of dopaminergic neurons of the substantia nigra pars compacta: involvement of transient receptor potential channels. J Neurophysiol 94:3069–3080

Guler AD, Lee H, Iida T, Shimizu I, Tominaga M, Caterina M (2002) Heat-evoked activation of the ion channel, TRPV4. J Neurosci 22:6408–6414

Grandl J, Kim SE, Uzzell V, Bursulaya B, Petrus M, Bandell M, Patapoutian A (2010) Temperature-induced opening of TRPV1 ion channel is stabilized by the pore domain. Nat Neurosci 13: 708–714

Hamamoto T, Takumida M, Hirakawa K, Takeno S, Tatsukawa T (2008) Localization of transient receptor potential channel vanilloid subfamilies in the mouse larynx. Acta Otolaryngol 128: 685–693

Hamamoto T, Takumida M, Hirakawa K, Tatsukawa T, Ishibashi T (2009) Localization of transient receptor potential vanilloid (TRPV) in the human larynx. Acta Otolaryngol 129:560–568

Hamanaka K, Jian MY, Weber DS, Alvarez DF, Townsley MI, Al-Mehdi AB, King JA, Liedtke W, Parker JC (2007) TRPV4 initiates the acute calcium-dependent permeability increase during ventilator-induced lung injury in isolated mouse lungs. Am J Physiol Lung Cell Mol Physiol 293:L923–932

Hamanaka K, Jian MY, Townsley MI, King JA, Liedtke W, Weber DS, Eyal FG, Clapp MM, Parker JC (2010) TRPV4 channels augment macrophage activation and ventilator-induced lung injury. Am J Physiol Lung Cell Mol Physiol 299:L353–362

Hartmannsgruber V, Heyken WT, Kacik M, Kaistha A, Grgic I, Harteneck C, Liedtke W, Hoyer J, Kohler R (2007) Arterial response to shear stress critically depends on endothelial TRPV4 expression. PLoS One 2:e827

Hashimoto H, Otsubo H, Fujihara H, Suzuki H, Ohbuchi T, Yokoyama T, Takei Y, Ueta Y (2010) Centrally administered ghrelin potently inhibits water intake induced by angiotensin II and hypovolemia in rats. J Physiol Sci 60:19–25

Hatano N, Itoh Y, Muraki K (2009) Cardiac fibroblasts have functional TRPV4 activated by 4alpha-phorbol 12,13-didecanoate. Life Sci 85:808–814

Haudenschild DR, Chen J, Pang N, Lotz MK, D'Lima DD (2010) Rho kinase-dependent activation of SOX9 in chondrocytes. Arthritis Rheum 62:191–200

He Y, Wu X, Khan RS, Kastin AJ, Cornelissen-Guillaume GG, Hsuchou H, Robert B, Halberg F, Pan W (2010) IL-15 receptor deletion results in circadian changes of locomotor and metabolic activity. J Mol Neurosci 41:315–321

Hellwig N, Albrecht N, Harteneck C, Schultz G, Schaefer M (2005) Homo- and heteromeric assembly of TRPV channel subunits. J Cell Sci 118:917–928

Hernández M, Burillo SL, Crespo MS, Nieto ML (1998) Secretory phospholipase A2 activates the cascade of mitogen-activated protein kinases and cytosolic phospholipase A2 in the human astrocytoma cell line 1321N1. J Biol Chem 273:606–612

Hu L, Ma J, Zhang P, Zheng J (2009) Extracellular hypotonicity induces disturbance of sodium currents in rat ventricular myocytes. Physiol Res 58:807–815

Hung CT (2010) Transient receptor potential vanilloid 4 channel as an important modulator of chondrocyte mechanotransduction of osmotic loading. Arthritis Rheum 62:2850–2851

Hunziker EB (1994) Mechanism of longitudinal bone growth and its regulation by growth plate chondrocytes. Microsc Res Tech 28:505–519

Ishibashi T, Takumida M, Akagi N, Hirakawa K, Anniko M (2009) Changes in transient receptor potential vanilloid (TRPV) 1, 2, 3 and 4 expression in mouse inner ear following gentamicin challenge. Acta Otolaryngol 129:116–126

Islam MS (2011) TRP Channels of Islets. Adv Exp Med Biol 704:811–830

Itoh Y, Hatano N, Hayashi H, Onozaki K, Miyazawa K, Muraki K (2009) An environmental sensor, TRPV4 is a novel regulator of intracellular $Ca2^{+}$ in human synoviocytes. Am J Physiol Cell Physiol 297:C1082–1090

Jia Y, Wang X, Varty L, Rizzo CA, Yang R, Correll CC, Phelps PT, Egan RW, Hey JA (2004) Functional TRPV4 channels are expressed in human airway smooth muscle cells. Am J Physiol Lung Cell Mol Physiol 287:L272–278

Jian MY, King JA, Al-Mehdi AB, Liedtke W, Townsley MI (2008) High vascular pressure-induced lung injury requires P450 epoxygenase-dependent activation of TRPV4. Am J Respir Cell Mol Biol 38:386–392

Jin M, Wu Z, Chen L, Jaimes J, Collins D, Walters ET, O'Neil RG (2011) Determinants of TRPV4 activity following selective activation by small molecule agonist GSK1016790A. PLoS One 6:e16713

Jordt SE, Julius D (2002) Molecular basis for species-specific sensitivity to "hot" chili peppers. Cell 108:421–430

Karasawa T, Wang Q, Fu Y, Cohen DM, Steyger PS (2008) TRPV4 enhances the cellular uptake of aminoglycoside antibiotics. J Cell Sci 121:2871–2879

Karlsson U, Sundgren-Andersson AK, Johansson S, Krupp JJ (2005) Capsaicin augments synaptic transmission in the rat medial preoptic nucleus. Brain Res 1043:1–11

Kato K, Morita I (2011) Acidosis environment promotes osteoclast formation by acting on the last phase of preosteoclast differentiation: A study to elucidate the action points of acidosis and search for putative target molecules. Eur J Pharmacol 663:27–39

Kim KS, Shin DH, Nam JH, Park KS, Zhang YH, Kim WK, Kim SJ (2010) Functional Expression of TRPV4 Cation Channels in Human Mast Cell Line (HMC-1). Korean J Physiol Pharmacol 14:419–425

Kitahara T, Li HS, Balaban CD (2005) Changes in transient receptor potential cation channel superfamily V (TRPV) mRNA expression in the mouse inner ear ganglia after kanamycin challenge. Hear Res 201:132–144

Klausen TK, Pagani A, Minassi A, Ech-Chahad A, Prenen J, Owsianik G, Hoffmann EK, Pedersen SF, Appendino G, Nilius B (2009) Modulation of the transient receptor potential vanilloid channel TRPV4 by 4alpha-phorbol esters: a structure-activity study. J Med Chem 52: 2933–2939

Klein CJ, Shi Y, Fecto F, Donaghy M, Nicholson G, McEntagart ME, Crosby AH, Wu Y, Lou H, McEvoy KM, Siddique T, Deng HX, Dyck PJ (2011) TRPV4 mutations and cytotoxic hypercalcemia in axonal Charcot-Marie-Tooth neuropathies. Neurology 76:887–894

Kochukov MY, McNearney TA, Fu Y, Westlund KN (2006) Thermosensitive TRP ion channels mediate cytosolic calcium response in human synoviocytes. Am J Physiol Cell Physiol 291:C424–432

Kochukov MY, McNearney TA, Yin H, Zhang L, Ma F, Ponomareva L, Abshire S, Westlund KN (2009) Tumor necrosis factor-alpha (TNF-alpha) enhances functional thermal and chemical responses of TRP cation channels in human synoviocytes. Mol Pain 5:49

Kohler R, Heyken WT, Heinau P, Schubert R, Si H, Kacik M, Busch C, Grgic I, Maier T, Hoyer J (2006) Evidence for a functional role of endothelial transient receptor potential V4 in shear stress-induced vasodilatation. Arterioscler Thromb Vasc Biol 26:1495–1502

Kohler R, Hoyer J (2007) Role of TRPV4 in the Mechanotransduction of Shear Stress in Endothelial Cells. In: Liedtke WB, Heller S (ed) TRP Ion Channel Function in Sensory Transduction and Cellular Signaling Cascades. CRC Press, Boca Raton (FL). Chapter 27

Kotlikoff MI (2005) EDHF redux: EETs, TRPV4, and $Ca2^{+}$ sparks. Circ Res 97:1209–1210

Kottgen M, Buchholz B, Garcia-Gonzalez MA, Kotsis F, Fu X, Doerken M, Boehlke C, Steffl D, Tauber R, Wegierski T, Nitschke R, Suzuki M, Kramer-Zucker A, Germino GG, Watnick T, Prenen J, Nilius B, Kuehn EW, Walz G (2008) TRPP2 and TRPV4 form a polymodal sensory channel complex. J Cell Biol 182:437–447

Krakow D, Vriens J, Camacho N, Luong P, Deixler H, Funari TL, Bacino CA, Irons MB, Holm IA, Sadler L, Okenfuss EB, Janssens A, Voets T, Rimoin DL, Lachman RS, Nilius B, Cohn DH (2009) Mutations in the gene encoding the calcium-permeable ion channel TRPV4 produce spondylometaphyseal dysplasia, Kozlowski type and metatropic dysplasia. Am J Hum Genet 84:307–315

Kruger J, Kunert-Keil C, Bisping F, Brinkmeier H (2008) Transient receptor potential cation channels in normal and dystrophic mdx muscle. Neuromuscul Disord 18:501–513

Kullmann FA, Shah MA, Birder LA, de Groat WC (2009) Functional TRP and ASIC-like channels in cultured urothelial cells from the rat. Am J Physiol Renal Physiol 296:F892–901

Kumagami H, Terakado M, Sainoo Y, Baba A, Fujiyama D, Fukuda T, Takasaki K, Takahashi H (2009) Expression of the osmotically responsive cationic channel TRPV4 in the endolymphatic sac. Audiol Neurootol 14:190–197

Landoure G, Zdebik AA, Martinez TL, Burnett BG, Stanescu HC, Inada H, Shi Y, Taye AA, Kong L, Munns CH, Choo SS, Phelps CB, Paudel R, Houlden H, Ludlow CL, Caterina MJ, Gaudet R, Kleta R, Fischbeck KH, Sumner CJ (2010) Mutations in TRPV4 cause Charcot-Marie-Tooth disease type 2C. Nat Genet 42:170–174

Lamandé SR, Yuan Y, Gresshoff IL, Rowley L, Belluoccio D, Kaluarachchi K, Little CB, Botzenhart E, Zerres K, Amor DJ, Cole WG, Savarirayan R, McIntyre P, Bateman JF (2011) Mutations in TRPV4 cause an inherited arthropathy of hands and feet. Nat Genet 10.1038/ng.945

Lechner SG, Markworth S, Poole K, Smith ES, Lapatsina L, Frahm S, May M, Pischke S, Suzuki M, Ibanez-Tallon I, Luft FC, Jordan J, Lewin GR (2011) The molecular and cellular identity of peripheral osmoreceptors. Neuron 69:332–344

Lee H, Iida T, Mizuno A, Suzuki M, Caterina MJ (2005) Altered thermal selection behavior in mice lacking transient receptor potential vanilloid 4. J Neurosci 25:1304–1310

Lenertz LY, Lee BH, Min X, Xu BE, Wedin K, Earnest S, Goldsmith EJ, Cobb MH (2005) Properties of WNK1 and implications for other family members. J Biol Chem 280:26653–26658

Li J, Wang MH, Wang L, Tian Y, Duan YQ, Luo HY, Hu XW, Hescheler J, Tang M (2008) Role of transient receptor potential vanilloid 4 in the effect of osmotic pressure on myocardial contractility in rat. Sheng Li Xue Bao 60:181–188

Li L, Liu C, Chen L, Chen L (2009) Hypotonicity modulates tetrodotoxin-sensitive sodium current in trigeminal ganglion neurons. Mol Pain 7:27

Li J, Kanju P, Patterson M, Chew WL, Cho SH, Gilmour I, Oliver T, Yasuda R, Ghio A, Simon SA, Liedtke W (2011) TRPV4-Mediated Calcium Influx into Human Bronchial Epithelia upon Exposure to Diesel Exhaust Particles. Environ Health Perspect 119:784–793

Liedtke W, Choe Y, Marti-Renom MA, Bell AM, Denis CS, Sali A, Hudspeth AJ, Friedman JM, Heller S (2000) Vanilloid receptor-related osmotically activated channel (VR-OAC), a candidate vertebrate osmoreceptor. Cell 103:525–535

Liedtke W, Friedman JM (2003a) Abnormal osmotic regulation in trpv4-/- mice. Proc Natl Acad Sci USA 100:13698–13703

Liedtke W, Tobin DM, Bargmann CI, Friedman JM (2003b) Mammalian TRPV4 (VR-OAC) directs behavioral responses to osmotic and mechanical stimuli in Caenorhabditis elegans. Proc Natl Acad Sci USA 100(2):14531–14536

Liedtke W, Simon SA (2004) A possible role for TRPV4 receptors in asthma. Am J Physiol Lung Cell Mol Physiol 287:L269–L271

Lipski J, Park TI, Li D, Lee SC, Trevarton AJ, Chung KK, Freestone PS, Bai JZ (2006) Involvement of TRP-like channels in the acute ischemic response of hippocampal CA1 neurons in brain slices. Brain Res 1077:187–199

Liu X, Bandyopadhyay BC, Nakamoto T, Singh B, Liedtke W, Melvin JE, Ambudkar I (2006) A role for AQP5 in activation of TRPV4 by hypotonicity: concerted involvement of AQP5 and TRPV4 in regulation of cell volume recovery. J Biol Chem 281:15485–15495

Loot AE, Popp R, Fisslthaler B, Vriens J, Nilius B, Fleming I (2008) Role of cytochrome P450-dependent transient receptor potential V4 activation in flow-induced vasodilatation. Cardiovasc Res 80:445–452

Lorenzo IM, Liedtke W, Sanderson MJ, Valverde MA (2008) TRPV4 channel participates in receptor-operated calcium entry and ciliary beat frequency regulation in mouse airway epithelial cells. Proc Natl Acad Sci USA 105:12611–12616

Loukin SH, Su Z, Kung C (2009) Hypotonic shocks activate rat TRPV4 in yeast in the absence of polyunsaturated fatty acids. FEBS Lett 583:754–758

Loukin S, Su Z, Zhou X, Kung C (2010a) Forward genetic analysis reveals multiple gating mechanisms of TRPV4. J Biol Chem 285:19884–19890

Loukin S, Zhou X, Su Z, Saimi Y, Kung C (2010b) Wild-type and brachyolmia-causing mutant TRPV4 channels respond directly to stretch force. J Biol Chem 285:27176–27181

Loukin S, Su Z, Kung C (2011) Increased Basal Activity Is a Key Determinant in the Severity of Human Skeletal Dysplasia Caused by TRPV4 Mutations. PLoS One 6:e19533

Lowry CA, Lightman SL, Nutt DJ (2009) That warm fuzzy feeling: brain serotonergic neurons and the regulation of emotion. J Psychopharmacol 23:392–400

Lu W, Shen X, Pavlova A, Lakkis M, Ward CJ, Pritchard L, Harris PC, Genest DR, Perez-Atayde AR, Zhou J (2001) Comparison of Pkd1-targeted mutants reveals that loss of polycystin-1 causes cystogenesis and bone defects. Hum Mol Genet 10:2385–2396

Lumpkin EA, Caterina MJ (2007) Mechanisms of sensory transduction in the skin. Nature 445: 858–865

Ma YY, Huo HR, Li CH, Zhao BS, Li LF, Sui F, Guo SY, Jiang TL (2008) Effects of cinnamaldehyde on PGE2 release and TRPV4 expression in mouse cerebral microvascular endothelial cells induced by interleukin-1beta. Biol Pharm Bull 31:426–430

Ma X, Cao J, Luo J, Nilius B, Huang Y, Ambudkar IS, Yao X (2010a) Depletion of intracellular $Ca2^{+}$stores stimulates the translocation of vanilloid transient receptor potential 4-c1 heteromeric channels to the plasma membrane. Arterioscler Thromb Vasc Biol 30:2249–2255

Ma X, Qiu S, Luo J, Ma Y, Ngai CY, Shen B, Wong CO, Huang Y, Yao X (2010b) Functional role of vanilloid transient receptor potential 4-canonical transient receptor potential 1 complex in flow-induced $Ca2^{+}$ influx. Arterioscler Thromb Vasc Biol 30:851–858

Ma X, Cheng KT, Wong CO, O'Neil RG, Birnbaumer L, Ambudkar IS, Yao X (2011) Heteromeric TRPV4-C1 channels contribute to store-operated Ca(2+) entry in vascular endothelial cells. Cell Calcium 50:502–509

Mamenko M, Zaika O, Jin M, O'Neil RG, Pochynyuk O (2011) Purinergic Activation of Ca-Permeable TRPV4 Channels Is Essential for Mechano-Sensitivity in the Aldosterone-Sensitive Distal Nephron. PLoS One 6:e22824

Magloire H, Maurin JC, Couble ML, Shibukawa Y, Tsumura M, Thivichon-Prince B, Bleicher F (2010) Topical review. Dental pain and odontoblasts: facts and hypotheses. J Orofac Pain 24:335–349

Mangos S, Liu Y, Drummond IA (2007) Dynamic expression of the osmosensory channel trpv4 in multiple developing organs in zebrafish. Gene Expr Patterns 7:480–484

Marrelli SP, O'Neil RG, Brown RC, Bryan RM, Jr. (2007) PLA2 and TRPV4 channels regulate endothelial calcium in cerebral arteries. Am J Physiol Heart Circ Physiol 292:H1390–1397

Maroto R, Raso A, Wood TG, Kurosky A, Martinac B, Hamill OP (2005) TRPC1 forms the stretch-activated cation channel in vertebrate cells. Nat Cell Biol 7:179–185

Masuyama R, Vriens J, Voets T, Karashima Y, Owsianik G, Vennekens R, Lieben L, Torrekens S, Moermans K, Vanden Bosch A, Bouillon R, Nilius B, Carmeliet G (2008) TRPV4-mediated calcium influx regulates terminal differentiation of osteoclasts. Cell Metab 8:257–265

Matthews BD, Thodeti CK, Tytell JD, Mammoto A, Overby DR, Ingber DE (2010) Ultra-rapid activation of TRPV4 ion channels by mechanical forces applied to cell surface beta1 integrins. Integr Biol (Camb) 2:435–442

May M, Jordan J (2011) The osmopressor response to water drinking. Am J Physiol Regul Integr Comp Physiol 300:R40–46

McHugh J, Keller NR, Appalsamy M, Thomas SA, Raj SR, Diedrich A, Biaggioni I, Jordan J, Robertson D (2010) Portal osmopressor mechanism linked to transient receptor potential vanilloid 4 and blood pressure control. Hypertension 55:1438–1443

Mendoza SA, Fang J, Gutterman DD, Wilcox DA, Bubolz AH, Li R, Suzuki M, Zhang DX (2010) TRPV4-mediated endothelial Ca2+ influx and vasodilation in response to shear stress. Am J Physiol Heart Circ Physiol 298:H466–476

Mergler S, Garreis F, Sahlmuller M, Reinach PS, Paulsen F, Pleyer U (2010) Thermosensitive transient receptor potential channels in human corneal epithelial cells. J Cell Physiol 226: 1828–1842

Mihara H, Boudaka A, Sugiyama T, Moriyama Y, Tominaga M (2011) Transient Receptor Potential Vanilloid 4 (TRPV4)-dependent calcium influx and ATP release in mouse esophageal keratinocytes. J Physiol 589:3471–3482

Millar ID, Bruce J, Brown PD (2007) Ion channel diversity, channel expression and function in the choroid plexuses. Cerebrospinal Fluid Res 4:8

Mizoguchi F, Mizuno A, Hayata T, Nakashima K, Heller S, Ushida T, Sokabe M, Miyasaka N, Suzuki M, Ezura Y, Noda M (2008) Transient receptor potential vanilloid 4 deficiency suppresses unloading-induced bone loss. J Cell Physiol 216:47–53

Mizuno A, Matsumoto N, Imai M, Suzuki M (2003) Impaired osmotic sensation in mice lacking TRPV4. Am J Physiol Cell Physiol 285:C96–101

Mochizuki T, Sokabe T, Araki I, Fujishita K, Shibasaki K, Uchida K, Naruse K, Koizumi S, Takeda M, Tominaga M (2009) The TRPV4 cation channel mediates stretch-evoked $Ca2^+$ influx and ATP release in primary urothelial cell cultures. J Biol Chem 284:21257–21264

Moiseenkova-Bell VY, Stanciu LA, Serysheva II, Tobe BJ, Wensel TG (2008) Structure of TRPV1 channel revealed by electron cryomicroscopy. Proc Natl Acad Sci USA 105:7451–7455

Moqrich A, Hwang SW, Earley TJ, Petrus MJ, Murray AN, Spencer KS, Andahazy M, Story GM, Patapoutian A (2005) Impaired thermosensation in mice lacking TRPV3, a heat and camphor sensor in the skin. Science 307:1468–1472

Montell C, Birnbaumer L, Flockerzi V, Bindels RJ, Bruford EA, Caterina MJ, Clapham D, Harteneck C, Heller S, Julius D, Kojima I, Mori Y, Penner R, Prawitt D, Scharenberg AM, Schultz G, Shimizu S, Zhu MX (2002) A unified nomenclature for the superfamily of TRP cation channels. Mol Cell 9:229–231

Muramatsu S, Wakabayashi M, Ohno T, Amano K, Ooishi R, Sugahara T, Shiojiri S, Tashiro K, Suzuki Y, Nishimura R, Kuhara S, Sugano S, Yoneda T, Matsuda A (2007) Functional gene screening system identified TRPV4 as a regulator of chondrogenic differentiation. J Biol Chem 282:32158–32167

Nakatsuka M, Iwai Y (2009) Expression of TRPV4 in the stimulated rat oral mucous membrane–nociceptive mechanisms of lingual conical papillae. Okajimas Folia Anat Jpn 86:45–54

Nauli SM, Alenghat FJ, Luo Y, Williams E, Vassilev P, Li X, Elia AE, Lu W, Brown EM, Quinn SJ, Ingber DE, Zhou J (2003) Polycystins 1 and 2 mediate mechanosensation in the primary cilium of kidney cells. Nat Genet 33:129–137

Nilius B, Prenen J, Wissenbach U, Bodding M, Droogmans G (2001) Differential activation of the volume-sensitive cation channel TRP12 (OTRPC4) and volume-regulated anion currents in HEK-293 cells. Pflügers Arch 443:227–233

Nilius B, Watanabe H, Vriens J (2003) The TRPV4 channel: structure-function relationship and promiscuous gating behaviour. Pflügers Arch 446:298–303

Nilius B, Droogmans G, Wondergem R (2003) Transient receptor potential channels in endothelium: solving the calcium entry puzzle?. Endothelium 10:5–15

Nilius B, Vriens J, Prenen J, Droogmans G, Voets T (2004) TRPV4 calcium entry channel: a paradigm for gating diversity. Am J Physiol Cell Physiol 286:C195–205

Nishimura G, Dai J, Lausch E, Unger S, Megarbane A, Kitoh H, Kim OH, Cho TJ, Bedeschi F, Benedicenti F, Mendoza-Londono R, Silengo M, Schmidt-Rimpler M, Spranger J, Zabel B, Ikegawa S, Superti-Furga A (2010) Spondylo-epiphyseal dysplasia, Maroteaux type (pseudo-Morquio syndrome type 2), and parastremmatic dysplasia are caused by TRPV4 mutations. Am J Med Genet A 152A:1443–1449

Obeidat M, Wain LV, Shrine N, Kalsheker N, Artigas MS, Repapi E, Burton PR, Johnson T, Ramasamy A, Zhao JH, Zhai G, Huffman JE, Vitart V, Albrecht E, Igl W, Hartikainen AL, Pouta A, Cadby G, Hui J, Palmer LJ, Hadley D, McArdle WL, Rudnicka AR, Barroso I, Loos RJ, Wareham NJ, Mangino M, Soranzo N, Spector TD, Glaser S, Homuth G, Volzke H, Deloukas P, Granell R, Henderson J, Grkovic I, Jankovic S, Zgaga L, Polasek O, Rudan I, Wright AF, Campbell H, Wild SH, Wilson JF, Heinrich J, Imboden M, Probst-Hensch NM, Gyllensten U, Johansson A, Zaboli G, Mustelin L, Rantanen T, Surakka I, Kaprio J, Jarvelin MR, Hayward C, Evans DM, Koch B, Musk AW, Elliott P, Strachan DP, Tobin MD, Sayers I, Hall IP, Consortium S (2011) A Comprehensive evaluation of potential lung function associated genes in the spirometa general population sample. PLoS One 6:e19382

O'Neil RG, Heller S (2005) The mechanosensitive nature of TRPV channels. Pflügers Arch 451:193–203

Pan Z, Yang H, Mergler S, Liu H, Tachado SD, Zhang F, Kao WW, Koziel H, Pleyer U, Reinach PS (2008) Dependence of regulatory volume decrease on transient receptor potential vanilloid 4 (TRPV4) expression in human corneal epithelial cells. Cell Calcium 44:374–385

Peng H, Lewandrowski U, Muller B, Sickmann A, Walz G, Wegierski T (2010) Identification of a Protein Kinase C-dependent phosphorylation site involved in sensitization of TRPV4 channel. Biochem Biophys Res Commun 391:1721–1725

Phan MN, Leddy HA, Votta BJ, Kumar S, Levy DS, Lipshutz DB, Lee SH, Liedtke W, Guilak F (2009) Functional characterization of TRPV4 as an osmotically sensitive ion channel in porcine articular chondrocytes. Arthritis Rheum 60:3028–3037

Phelps CB, Wang RR, Choo SS, Gaudet R (2010) Differential regulation of TRPV1, TRPV3, and TRPV4 sensitivity through a conserved binding site on the ankyrin repeat domain. J Biol Chem 285:731–740

Pritschow BW, Lange T, Kasch J, Kunert-Keil C, Liedtke W, Brinkmeier H (2011) Functional TRPV4 channels are expressed in mouse skeletal muscle and can modulate resting $Ca2^{+}$ influx and muscle fatigue. Pflügers Arch 461:115–122

Ramadass R, Becker D, Jendrach M, Bereiter-Hahn J (2007) Spectrally and spatially resolved fluorescence lifetime imaging in living cells: TRPV4-microfilament interactions. Arch Biochem Biophys 463:27–36

Rath G, Dessy C, Feron O (2009) Caveolae, caveolin and control of vascular tone: nitric oxide (NO) and endothelium derived hyperpolarizing factor (EDHF) regulation. J Physiol Pharmacol 60(4):105–109

Reiter B, Kraft R, Gunzel D, Zeissig S, Schulzke JD, Fromm M, Harteneck C (2006) TRPV4-mediated regulation of epithelial permeability. Faseb J 20:1802–1812

Rock MJ, Prenen J, Funari VA, Funari TL, Merriman B, Nelson SF, Lachman RS, Wilcox WR, Reyno S, Quadrelli R, Vaglio A, Owsianik G, Janssens A, Voets T, Ikegawa S, Nagai T, Rimoin DL, Nilius B, Cohn DH (2008) Gain-of-function mutations in TRPV4 cause autosomal dominant brachyolmia. Nat Genet 40:999–1003

Ryskamp DA, Witkovsky P, Barabas P, Huang W, Koehler C, Akimov NP, Lee SH, Chauhan S, Xing W, Renteria RC, Liedtke W, Krizaj D (2011) The polymodal Ion channel transient receptor potential vanilloid 4 modulates calcium flux, spiking rate, and apoptosis of mouse retinal ganglion cells. J Neurosci 31:7089–7101

Salazar H, Jara-Oseguera A, Hernández-García E, Llorente I, Arias-Olguín II, Soriano-García M, Islas LD, Rosenbaum T (2009) Structural determinants of gating in the TRPV1 channel. Nat Struct Mol Biol 16:704–710

Saliez J, Bouzin C, Rath G, Ghisdal P, Desjardins F, Rezzani R, Rodella LF, Vriens J, Nilius B, Feron O, Balligand JL, Dessy C (2008) Role of caveolar compartmentation in endothelium-derived hyperpolarizing factor-mediated relaxation: $Ca2^{+}$ signals and gap junction function are regulated by caveolin in endothelial cells. Circulation 117:1065–1074

Schierling W, Troidl K, Apfelbeck H, Troidl C, Kasprzak PM, Schaper W, Schmitz-Rixen T (2011) Cerebral arteriogenesis is enhanced by pharmacological as well as fluid-shear-stress activation of the Trpv4 calcium channel. Eur J Vasc Endovasc Surg 41:589–596

Seminario-Vidal L, Okada SF, Sesma JI, Kreda SM, van Heusden CA, Zhu Y, Jones LC, O'Neal WK, Penuela S, Laird DW, Boucher RC, Lazarowski ER (2011) RHO signaling regulates pannexin 1-mediated ATP release from airway epithelia. J Biol Chem 286:26277–26286

Sedgwick SG, Smerdon SJ (1999) The ankyrin repeat: a diversity of interactions on a common structural framework. Trends Biochem 24(8):311–316

Sharif Naeini R, Witty MF, Séguéla P, Bourque CW (2006) An N-terminal variant of Trpv1 channel is required for osmosensory transduction. Nat Neurosci 9:93–8

Shakibaei M, De Souza P, Merker HJ (1997) Integrin expression and collagen type II implicated in maintenance of chondrocyte shape in monolayer culture: an immunomorphological study. Cell Biol Int 21:115–125

Shen J, Harada N, Kubo N, Liu B, Mizuno A, Suzuki M, Yamashita T (2006) Functional expression of transient receptor potential vanilloid 4 in the mouse cochlea. Neuroreport 17:135–139

Shibasaki K, Suzuki M, Mizuno A, Tominaga M (2007) Effects of body temperature on neural activity in the hippocampus: regulation of resting membrane potentials by transient receptor potential vanilloid 4. J Neurosci 27:1566–1575

Shigematsu H, Sokabe T, Danev R, Tominaga M, Nagayama K (2010) A 3.5-nm structure of rat TRPV4 cation channel revealed by Zernike phase-contrast cryoelectron microscopy. J Biol Chem 285:11210–11218

Shikano M, Ueda T, Kamiya T, Ishida Y, Yamada T, Mizushima T, Shimura T, Mizoshita T, Tanida S, Kataoka H, Shimada S, Ugawa S, Joh T. (2011) Acid inhibits TRPV4-mediated $Ca2^{+}$ influx in mouse esophageal epithelial cells. Neurogastroenterol Motil. 1111/j.1365–2982

Shukla AK, Kim J, Ahn S, Xiao K, Shenoy SK, Liedtke W, Lefkowitz RJ (2010) Arresting a transient receptor potential (TRP) channel: beta-arrestin 1 mediates ubiquitination and functional down-regulation of TRPV4. J Biol Chem 285:30115–30125

Sidhaye VK, Guler AD, Schweitzer KS, D'Alessio F, Caterina MJ, King LS (2006) Transient receptor potential vanilloid 4 regulates aquaporin-5 abundance under hypotonic conditions. Proc Natl Acad Sci USA 103:4747–4752

Sidhaye VK, Schweitzer KS, Caterina MJ, Shimoda L, King LS (2008) Shear stress regulates aquaporin-5 and airway epithelial barrier function. Proc Natl Acad Sci USA 105:3345–3350

Silva GB, Garvin JL (2008) TRPV4 mediates hypotonicity-induced ATP release by the thick ascending limb. Am J Physiol Renal Physiol 295:F1090–1095

Sipe WE, Brierley SM, Martin CM, Phillis BD, Cruz FB, Grady EF, Liedtke W, Cohen DM, Vanner S, Blackshaw LA, Bunnett NW (2008) Transient receptor potential vanilloid 4 mediates protease activated receptor 2-induced sensitization of colonic afferent nerves and visceral hyperalgesia. Am J Physiol Gastrointest Liver Physiol 294:G1288–1298

Smith PL, Maloney KN, Pothen RG, Clardy J, Clapham DE (2006) Bisandrographolide from Andrographis paniculata activates TRPV4 channels. J Biol Chem 281:29897–29904

Sokabe T, Fukumi-Tominaga T, Yonemura S, Mizuno A, Tominaga M (2010) The TRPV4 channel contributes to intercellular junction formation in keratinocytes. J Biol Chem 285:18749–18758

Sole-Magdalena A, Revuelta EG, Menenez-Diaz I, Calavia MG, Cobo T, Garcia-Suarez O, Perez-Pinera P, De Carlos F, Cobo J, Vega JA (2011) Human odontoblasts express transient receptor protein and acid-sensing ion channel mechanosensor proteins. Microsc Res Tech 74:457–463

Son AR, Yang YM, Hong JH, Lee SI, Shibukawa Y, Shin DM (2009) Odontoblast TRP channels and thermo/mechanical transmission. J Dent Res 88:1014–1019

Spassova MA, Hewavitharana T, Xu W, Soboloff J, Gill DL (2006) A common mechanism underlies stretch activation and receptor activation of TRPC6 channels. Proc Natl Acad Sci USA 103:16586–165891

Spinsanti G, Zannolli R, Panti C, Ceccarelli I, Marsili L, Bachiocco V, Frati F, Aloisi AM (2008) Quantitative Real-Time PCR detection of TRPV1–4 gene expression in human leukocytes from healthy and hyposensitive subjects. Mol Pain 4:51

Stewart AP, Smith GD, Sandford RN, Edwardson JM (2010) Atomic force microscopy reveals the alternating subunit arrangement of the TRPP2-TRPV4 heterotetramer. Biophys J 99:790–797

Steyger PS, Karasawa T (2008) Intra-cochlear trafficking of aminoglycosides. Commun Integr Biol 1:140–142

Strotmann R, Harteneck C, Nunnenmacher K, Schultz G, Plant TD (2000) OTRPC4, a nonselective cation channel that confers sensitivity to extracellular osmolarity. Nat Cell Biol 2:695–702

Strotmann R, Schultz G, Plant TD (2003) $Ca2^{+}$ -dependent potentiation of the nonselective cation channel TRPV4 is mediated by a C-terminal calmodulin binding site. J Biol Chem 278: 26541–26549

Strotmann R, Semtner M, Kepura F, Plant TD, Schoneberg T (2010) Interdomain interactions control $Ca2^{+}$ -dependent potentiation in the cation channel TRPV4. PLoS One 5:e10580

Suzuki M, Mizuno A, Kodaira K, Imai M (2003a) Impaired pressure sensation in mice lacking TRPV4. J Biol Chem 278:22664–22668

Suzuki M, Hirao A, Mizuno A (2003b) Microtubule-associated [corrected] protein 7 increases the membrane expression of transient receptor potential vanilloid 4 (TRPV4). J Biol Chem 278:51448–51453

Suzuki M, Watanabe Y, Oyama Y, Mizuno A, Kusano E, Hirao A, Ookawara S (2003c) Localization of mechanosensitive channel TRPV4 in mouse skin. Neurosci Lett 353:189–192

Tabuchi K, Suzuki M, Mizuno A, Hara A (2005) Hearing impairment in TRPV4 knockout mice. Neurosci Lett 382:304–308

Taguchi D, Takeda T, Kakigi A, Takumida M, Nishioka R, Kitano H (2007) Expressions of aquaporin-2, vasopressin type 2 receptor, transient receptor potential channel vanilloid (TRPV)1, and TRPV4 in the human endolymphatic sac. Laryngoscope 117:695–698

Takeda-Nakazawa H, Harada N, Shen J, Kubo N, Zenner HP, Yamashita T (2007) Hyposmotic stimulation-induced nitric oxide production in outer hair cells of the guinea pig cochlea. Hear Res 230:93–104

Takumida M, Kubo N, Ohtani M, Suzuka Y, Anniko M (2005) Transient receptor potential channels in the inner ear: presence of transient receptor potential channel subfamily 1 and 4 in the guinea pig inner ear. Acta Otolaryngol 125:929–934

Tanaka R, Muraki K, Ohya S, Yamamura H, Hatano N, Itoh Y, Imaizumi Y (2008) TRPV4-like non-selective cation currents in cultured aortic myocytes. J Pharmacol Sci 108:179–189

Taniguchi J, Tsuruoka S, Mizuno A, Sato J, Fujimura A, Suzuki M (2007) TRPV4 as a flow sensor in flow-dependent K^{+} secretion from the cortical collecting duct. Am J Physiol Renal Physiol 292:F667–673

Taylor AC, McCarthy JJ, Stocker SD (2008) Mice lacking the transient receptor vanilloid potential 1 channel display normal thirst responses and central Fos activation to hypernatremia. Am J Physiol Regul Integr Comp Physiol 294 R1285–1293

Teilmann SC, Byskov AG, Pedersen PA, Wheatley DN, Pazour GJ, Christensen ST (2005) Localization of transient receptor potential ion channels in primary and motile cilia of the female murine reproductive organs. Mol Reprod Dev 71:444–452

Thodeti CK, Matthews B, Ravi A, Mammoto A, Ghosh K, Bracha AL, Ingber DE (2009) TRPV4 channels mediate cyclic strain-induced endothelial cell reorientation through integrin-to-integrin signaling. Circ Res 104:1123–1130

Thorneloe KS, Sulpizio AC, Lin Z, Figueroa DJ, Clouse AK, McCafferty GP, Chendrimada TP, Lashinger ES, Gordon E, Evans L, Misajet BA, Demarini DJ, Nation JH, Casillas LN, Marquis RW, Votta BJ, Sheardown SA, Xu X, Brooks DP, Laping NJ, Westfall TD (2008) N-((1 S)-1-{[4-((2 S)-2-{[(2,4-dichlorophenyl)sulfonyl]amino}- 3- hydroxypropanoyl)-1-piperazinyl]carbonyl}-3-methylbutyl)-1-benzothiophene-2-carboxamid e (GSK1016790 A), a novel and potent transient receptor potential vanilloid 4 channel agonist induces urinary bladder contraction and hyperactivity: Part I. J Pharmacol Exp Ther 326:432–442

Tian W, Salanova M, Xu H, Lindsley JN, Oyama TT, Anderson S, Bachmann S, Cohen DM (2004) Renal expression of osmotically responsive cation channel TRPV4 is restricted to water-impermeant nephron segments. Am J Physiol Renal Physiol 287:F17–24

Tian W, Fu Y, Garcia-Elias A, Fernandez-Fernandez JM, Vicente R, Kramer PL, Klein RF, Hitzemann R, Orwoll ES, Wilmot B, McWeeney S, Valverde MA, Cohen DM (2009) A loss-of-function nonsynonymous polymorphism in the osmoregulatory TRPV4 gene is associated with human hyponatremia. Proc Natl Acad Sci USA 106:14034–14039

Troidl C, Troidl K, Schierling W, Cai WJ, Nef H, Möllmann H, Kostin S, Schimanski S, Hammer L, Elsässer A, Schmitz-Rixen T, Schaper W (2009) Trpv4 induces collateral vessel growth during regeneration of the arterial circulation. J Cell Mol Med 13:2613–2621

Todaka H, Taniguchi J, Satoh J, Mizuno A, Suzuki M (2004) Warm temperature-sensitive transient receptor potential vanilloid 4 (TRPV4) plays an essential role in thermal hyperalgesia. J Biol Chem 279:35133–35138

Townsley MI, King JA, Alvarez DF (2006) $Ca2^{+}$ channels and pulmonary endothelial permeability: insights from study of intact lung and chronic pulmonary hypertension. Microcirculation 13:725–739

Tsushima H, Mori M (2006) Antidipsogenic effects of a TRPV4 agonist, 4alpha-phorbol 12,13-didecanoate, injected into the cerebroventricle. Am J Physiol Regul Integr Comp Physiol 290:R1736–1741

Ueda T, Shikano M, Kamiya T, Joh T, Ugawa S (2011) The TRPV4 channel is a novel regulator of intracellular $Ca2^{+}$ in human esophageal epithelial cells. Am J Physiol Gastrointest Liver Physiol 301:G138–147

Vergnolle N, Cenac N, Altier C, Cellars L, Chapman K, Zamponi GW, Materazzi S, Nassini R, Liedtke W, Cattaruzza F, Grady EF, Geppetti P, Bunnett NW (2010) A role for transient receptor potential vanilloid 4 in tonicity-induced neurogenic inflammation. Br J Pharmacol 159:1161–1173

Verma P, Kumar A, Goswami C (2010) TRPV4-mediated channelopathies. Channels (Austin) 4:319–328

Vincent F, Acevedo A, Nguyen MT, Dourado M, DeFalco J, Gustafson A, Spiro P, Emerling DE, Kelly MG, Duncton MA (2009) Identification and characterization of novel TRPV4 modulators. Biochem Biophys Res Commun 389:490–494

Vlachová V, Teisinger J, Susánková K, Lyfenko A, Ettrich R, Vyklický L (2003) Functional role of C-terminal cytoplasmic tail of rat vanilloid receptor 1. J Neurosci 23:1340–1350

Voets T, Prenen J, Vriens J, Watanabe H, Janssens A, Wissenbach U, Bodding M, Droogmans G, Nilius B (2002) Molecular determinants of permeation through the cation channel TRPV4. J Biol Chem 277:33704–33710

Voets T, Droogmans G, Wissenbach U, Janssens A, Flockerzi V, Nilius B (2004) The principle of temperature-dependent gating in cold- and heat-sensitive TRP channels. Nature 430:748–754

Vriens J, Watanabe H, Janssens A, Droogmans G, Voets T, Nilius B (2004) Cell swelling, heat, and chemical agonists use distinct pathways for the activation of the cation channel TRPV4. Proc Natl Acad Sci USA 101:396–401

Vriens J, Janssens A, Prenen J, Nilius B, Wondergem R (2004) TRPV channels and modulation by hepatocyte growth factor/scatter factor in human hepatoblastoma (HepG2) cells. Cell Calcium 36:19–28

Vriens J, Owsianik G, Fisslthaler B, Suzuki M, Janssens A, Voets T, Morisseau C, Hammock BD, Fleming I, Busse R, Nilius B (2005) Modulation of the Ca2 permeable cation channel TRPV4 by cytochrome P450 epoxygenases in vascular endothelium. Circ Res 97:908–915

Vriens J, Owsianik G, Janssens A, Voets T, Nilius B (2007) Determinants of 4 alpha-phorbol sensitivity in transmembrane domains 3 and 4 of the cation channel TRPV4. J Biol Chem 282:12796–1280

Wang T, Wang Y, Yamashita H (2009) Evodiamine inhibits adipogenesis via the EGFR-PKCalpha-ERK signaling pathway. FEBS Lett 583:3655–3659

Wang Y, Fu X, Gaiser S, Kottgen M, Kramer-Zucker A, Walz G, Wegierski T (2007) OS-9 regulates the transit and polyubiquitination of TRPV4 in the endoplasmic reticulum. J Biol Chem 282:36561–36570

Watanabe H, Vriens J, Suh SH, Benham CD, Droogmans G, Nilius B (2002a) Heat-evoked activation of TRPV4 channels in a HEK293 cell expression system and in native mouse aorta endothelial cells. J Biol Chem 277:47044–47051

Watanabe H, Davis JB, Smart D, Jerman JC, Smith GD, Hayes P, Vriens J, Cairns W, Wissenbach U, Prenen J, Flockerzi V, Droogmans G, Benham CD, Nilius B (2002b) Activation of TRPV4 channels (hVRL-2/mTRP12) by phorbol derivatives. J Biol Chem 277:13569–13577

Watanabe H, Vriens J, Janssens A, Wondergem R, Droogmans G, Nilius B (2003a) Modulation of TRPV4 gating by intra- and extracellular $Ca2^{+}$. Cell Calcium 33:489–495

Watanabe H, Vriens J, Prenen J, Droogmans G, Voets T, Nilius B (2003b) Anandamide and arachidonic acid use epoxyeicosatrienoic acids to activate TRPV4 channels. Nature 424:434–438

Wegierski T, Hill K, Schaefer M, Walz G (2006) The HECT ubiquitin ligase AIP4 regulates the cell surface expression of select TRP channels. Embo J 25:5659–5669

Wegierski T, Lewandrowski U, Muller B, Sickmann A, Walz G (2009) Tyrosine phosphorylation modulates the activity of TRPV4 in response to defined stimuli. J Biol Chem 284:2923–2933

Willette RN, Bao W, Nerurkar S, Yue TL, Doe CP, Stankus G, Turner GH, Ju H, Thomas H, Fishman CE, Sulpizio A, Behm DJ, Hoffman S, Lin Z, Lozinskaya I, Casillas LN, Lin M, Trout RE, Votta BJ, Thorneloe K, Lashinger ES, Figueroa DJ, Marquis R, Xu X (2008) Systemic activation of the transient receptor potential vanilloid subtype 4 channel causes endothelial failure and circulatory collapse: Part 2. J Pharmacol Exp Ther 326:443–452

Wilson FH, Disse-Nicodème S, Choate KA, Ishikawa K, Nelson-Williams C, Desitter I, Gunel M, Milford DV, Lipkin GW, Achard JM, Feely MP, Dussol B, Berland Y, Unwin RJ, Mayan H, Simon DB, Farfel Z, Jeunemaitre X, Lifton RP (2001) Human hypertension caused by mutations in WNK kinases. Science 293:1107–1112

Xiao Z, Zhang S, Mahlios J, Zhou G, Magenheimer BS, Guo D, Dallas SL, Maser R, Calvet JP, Bonewald L, Quarles LD (2006) Cilia-like structures and polycystin-1 in osteoblasts/osteocytes and associated abnormalities in skeletogenesis and Runx2 expression. J Biol Chem 281: 30884–30895

Xu F, Satoh E, Iijima T (2003a) Protein kinase C-mediated $Ca2^{+}$ entry in HEK 293 cells transiently expressing human TRPV4. Br J Pharmacol 140:413–421

Xu H, Zhao H, Tian W, Yoshida K, Roullet JB, Cohen DM (2003b) Regulation of a transient receptor potential (TRP) channel by tyrosine phosphorylation. SRC family kinase-dependent tyrosine phosphorylation of TRPV4 on TYR-253 mediates its response to hypotonic stress. J Biol Chem 278:11520–11527

Xu H, Fu Y, Tian W, Cohen DM (2006) Glycosylation of the osmoresponsive transient receptor potential channel TRPV4 on Asn-651 influences membrane trafficking. Am J Physiol Renal Physiol 290:F1103–1109

Xu X, Gordon E, Lin Z, Lozinskaya IM, Chen Y, Thorneloe KS (2009) Functional TRPV4 channels and an absence of capsaicin-evoked currents in freshly-isolated, guinea-pig urothelial cells. Channels (Austin) 3:156–160

Yamada T, Ugawa S, Ueda T, Ishida Y, Kajita K, Shimada S (2009) Differential localizations of the transient receptor potential channels TRPV4 and TRPV1 in the mouse urinary bladder. J Histochem Cytochem 57:277–287

Yang W, Chen J, Zhou L (2009) Effects of shear stress on intracellular calcium change and histamine release in rat basophilic leukemia (RBL-2H3) cells. J Environ Pathol Toxicol Oncol 28:223–230

Yang XR, Lin MJ, McIntosh LS, Sham JS (2006) Functional expression of transient receptor potential melastatin- and vanilloid-related channels in pulmonary arterial and aortic smooth muscle. Am J Physiol Lung Cell Mol Physiol 290:L1267–1276

Yin J, Hoffmann J, Kaestle SM, Neye N, Wang L, Baeurle J, Liedtke W, Wu S, Kuppe H, Pries AR, Kuebler WM (2008) Negative-feedback loop attenuates hydrostatic lung edema via a cGMP-dependent regulation of transient receptor potential vanilloid 4. Circ Res 102:966–974

Yu W, Hill WG, Apodaca G, Zeidel ML (2011) Expression and distribution of transient receptor potential (TRP) channels in bladder epithelium. Am J Physiol Renal Physiol 300:F49–59

Zaninetti R, Fornarelli A, Ciarletta M, Lim D, Caldarelli A, Pirali T, Cariboni A, Owsianik G, Nilius B, Canonico PL, Distasi C, Genazzani AA (2011) Activation of TRPV4 channels reduces migration of immortalized neuroendocrine cells. J Neurochem 116:606–615

Zhang DX, Mendoza SA, Bubolz AH, Mizuno A, Ge ZD, Li R, Warltier DC, Suzuki M, Gutterman DD (2009) Transient receptor potential vanilloid type 4-deficient mice exhibit impaired endothelium-dependent relaxation induced by acetylcholine in vitro and in vivo. Hypertension 53:532–538

Zhang Y, Wang YH, Ge HY, Arendt-Nielsen L, Wang R, Yue SW (2008) A transient receptor potential vanilloid 4 contributes to mechanical allodynia following chronic compression of dorsal root ganglion in rats. Neurosci Lett 432:222–227

Zhu G, Gulsvik A, Bakke P, Ghatta S, Anderson W, Lomas DA, Silverman EK, Pillai SG (2009) Association of TRPV4 gene polymorphisms with chronic obstructive pulmonary disease. Hum Mol Genet 18:2053–2062

Zimon M, Baets J, Auer-Grumbach M, Berciano J, Garcia A, Lopez-Laso E, Merlini L, Hilton-Jones D, McEntagart M, Crosby AH, Barisic N, Boltshauser E, Shaw CE, Landoure G, Ludlow CL, Gaudet R, Houlden H, Reilly MM, Fischbeck KH, Sumner CJ, Timmerman V, Jordanova A, Jonghe PD (2010) Dominant mutations in the cation channel gene transient receptor potential vanilloid 4 cause an unusual spectrum of neuropathies. Brain 133:1798–1809

Chapter 5
Mechanical Stretch and Intermediate-Conductance Ca^{2+}-Activated K^+ Channels in Arterial Smooth Muscle Cells

Yasunobu Hayabuchi, Miho Sakata, Tatsuya Ohnishi and Shoji Kagami

5.1 Introduction

Ion channels are important transmembrane proteins that, through their ability to alter membrane potential and intracellular ion levels and cell volume, impact multiple functions of vascular smooth muscle cells, including contractile state, size, and rates of proliferation and apoptosis. Although K^+ channels are classically recognized as regulators of vascular tone, through their effects on membrane potential they secondarily regulate K^+ and Ca^{2+} concentrations and thereby regulate cell migration, proliferation, and apoptosis (McMurtry et al. 2004; Remillard and Yuan 2004).

K^+ channels contribute to the regulation of the membrane potential in electrically excitable cells, including those found in smooth muscle. Membrane hyperpolarization due to an efflux of K^+ results from the opening of K^+ channels in vascular smooth muscle. This effect is followed by the closure of voltage-dependent Ca^{2+} channels, leading to a reduction in Ca^{2+} entry, and vasodilation (Nelson and Quayle 1995). In contrast, inhibition of K^+ channels function leads to membrane depolarization and vasoconstriction. K^+ channel activity is known to be linked to cell cycle progression in a variety of cell types (Ouadid-Ahidouch et al. 2001; Wonderlin and Strobl 1996; Wonderlin et al. 1995; Woodfork et al. 1995). Wonderlin et al suggested that the hyperpolarization during the transition through G0/G1 and into the S phase probably results from an increase in the relative permeability of the plasma membrane to K^+ (Wonderlin et al. 1995).

The intermediate-conductance Ca^{2+}-activated K^+ (IK_{Ca}) channel was first described by Gardos in erythrocytes (Gardos 1958). More recently, IK_{ca} channels are expressed in many different cell types such as secretory epithelial cells, endothelial cells, fibroblasts, T lymphocytes, melanoma cells, granulocytes, macrophages, erythrocytes, and cultured cell lines (Schwab 2001; Fioretti et al. 2005; Ouadid-Ahidouch et al. 2004). Since its discovery it has held numerous names,

Y. Hayabuchi (✉) · M. Sakata · T. Ohnishi · S. Kagami
Department of Pediatrics, University of Tokushima, Kuramoto-cho-3-18-15,
Tokushima 770-8503, Japan
e-mail: hayabuchi@clin.med.tokushima-u.ac.jp

A. Kamkin, I. Lozinsky (eds.), *Mechanically Gated Channels and their Regulation,*
Mechanosensitivity in Cells and Tissues 6,
DOI 10.1007/978-94-007-5073-9_5,

including IK, IK1, $IK_{ca}1$, SMIK, ImK, fIK, hIK, mIK, KCa3.1, and SK4. The gene encoding KCa3.1 is known as KCNN4 or IK1 (Neylon et al. 1999). Thus, IK_{ca} channels are required for a wide variety of physiologic functions ranging from transepithelial secretion to T cell activation. Many of the nonepithelial cells expressing IK_{ca} channels have the ability to migrate. Previous studies demonstrate that cell migration is modulated by the activity of IK_{ca} channels (Schwab 2001). Furthermore, in vascular smooth muscle cells, IK_{ca} channels contribute to muscle plasticity (Neylon et al. 1999). Köhler et al demonstrated that blockade of IK_{ca} channels results in inhibition of epidermal growth factor (EGF)-stimulated smooth muscle cell proliferation in vitro and in reduced neointima formation in vivo (Köhler et al. 2003). The human IK_{ca} channel (hIK1 or hSK4) has been cloned from placenta and pancreas (Ishii et al. 1997; Joiner et al. 1997).

In this review, we will discuss the role and regulation of IK_{ca} channel in arterial smooth muscle cells during physiological and pathophysiological conditions.

5.2 Calcium-Activated Potassium Channels

Potassium channels are the largest and most diverse subgroup of ion channels and are classified in four subgroups according to their membrane topology (Gutman et al. 2003; Alexander et al. 2008). Voltage-dependent K^+ (K_V) channels open upon depolarization of the plasma membrane in vascular smooth muscle cells. The subsequent efflux of K^+ through the channels induces repolarization to the resting membrane potential. Changes in the intracellular Ca^{2+} concentration and membrane depolarization stimulate large-conductance Ca^{2+}-activated K^+ (MaxiK or BK_{Ca}) channels, which are thought to play an important role in maintaining the membrane potential. ATP-sensitive K^+ (K_{ATP}) channels underscore the functional bond between cellular metabolism and membrane excitability. The blockade of K_{ATP} channel function results in vasoconstriction and depolarization in various types of vascular smooth muscle. Inward rectifier K^+ (Kir) channels, which are expressed in smooth muscle of the small-diameter arteries, contribute to the resting membrane potential and basal tone. Kir channel activation has been shown to raise the extracellular K^+ concentration to 10–15 mM, resulting in vasodilation. Each of K^+ channels listed above is responsive to a number of vasoconstrictors and vasodilators, which act through protein kinase C (PKC) and protein kinase A (PKA), respectively. Impaired these channel functions has been linked to a number of pathological conditions, which may lead to vasoconstriction.

The Ca^{2+}-activated K^+ channel family is divided into two subfamilies, the small (SK_{Ca}) and intermediate (IK_{Ca}) conductance K_{Ca} subfamily including $K_{Ca}2.1$–$K_{Ca}2.3$ (also known as SK1–SK3) and $K_{Ca}3.1$ (also known as IK1 or SK4) subunits and the large conductance (MaxiK or BK_{Ca}) K_{Ca} subfamily including the $K_{Ca}1.1$ a subunit (also known as *Slo1*α).

5.2.1 SK_{Ca} and IK_{Ca} Channels

SK_{Ca} and IK_{Ca} channels are voltage-independent and their calcium sensitivity is ascribed to the association with calmodulin (Köhler et al. 1996; Joiner et al. 1997; Xia et al. 1998; Fanger et al. 1999). Tetraethylammonium and tetrabutylammonium are non-specific blockers of K_{Ca}. SK_{Ca} channels are specially blocked by the bee toxin apamin and by some scorpion toxins such as scyllatoxin (also named leiurotoxin I from Leiurus quinquestriatus), tamapin (Mesobuthus tamulus) and BmSKTx1 (Buthus martensi) (Xu et al. 2004). The plant alkaloid tubocurarine and the synthetic compound UCL-1684 (Campos et al. 2000) are also potent and reasonably specific blockers of SK_{Ca} channels (Castle 1999; Dunn 1999; Strøbaek et al. 2000; Liegeois et al. 2003). Tamapin appears to be selective towards SK2 over SK1 and to a lesser extent over SK3 (Pedarzini et al. 2002). Non-specific blockers of IK_{Ca} channels include the scorpion toxins charybdotoxin (Leiurus quinquestriatus) and maurotoxin (Maurus palmatus) as well as clotrimazole, a non-peptide inhibitor of cytochrome P450 monooxygenase. The analogues of clotrimazole, TRAM-34 and TRAM-39, are devoid of cytochrome P450 epoxygenase inhibitory properties and are considered as specific blockers of IK_{Ca} (Wulff et al. 2000), although the former is also a blocker of non-selective cation channels (Schilling and Eder 2007). 1-EBIO (1-ethyl-2-benzimidazolinone), its more potent analogue DCEBIO (dichloro-1-ethyl-2-benzimidazolinone), chlorzoxazone-related compounds and riluzole are weak and non-specific activators of IK_{Ca} and SK_{Ca} (Cao et al. 2001; Wulff et al. 2007). Another derivative of 1-EBIO, NS-309, is a much more potent opener of both IK_{Ca} and SK_{Ca}, with a preferential selectivity for the former (Strøbaek et al. 2004; Leuranguer et al. 2008). CyPPA [cyclohexyl-[2-(3,5-dimethylpyrazol-1-yl)-6-methyl-pyrimidin-4-yl]-amine] is a preferential positive modulator of SK2 and SK3 over SK1 but is less potent than NS-309 and possesses inhibitory properties versus BK_{Ca} and some Na^+ channels (Hougaard et al. 2007; Wulff et al. 2007).

5.2.2 BK_{Ca} Channels

BK_{Ca} channels are characterized by a high unitary conductance and are both voltage- and calcium-regulated potassium channels. Numerous isoforms of the *Slo1α* subunit are generated by alternative splicing (Meera et al. 2001; Latorre and Brauchi 2006). In addition, the expression of accessory β subunits (β1 to β4) can lead to channel diversity (Shieh et al. 2000). BK_{Ca} channels are also blocked by charybdotoxin and low concentrations of tetraethylammonium. Another scorpion toxin, iberiotoxin (Buthus tamulus), and mycotoxins such as paxilline and penitrem A as well as the synthetic and nonpeptide compound 1-[1-hexyl-6-(methyloxy)-1H-indazol-3-yl]-2-methyl-1-propanone (HMIMP) (Zeng et al. 2008), are potent and selective inhibitors of this channel. They are activated by synthetic compounds such as NS-11021 the benzimidazolone derivatives, NS-1619 and NS-004, and naturally occurring compounds

such as pimaric acid (Gribkoff et al. 2001; Meera et al. 2001; Bentzen et al. 2007; Nardi and Olesen 2008).

5.3 Calcium-Activated Potassium Channels and Vascular Smooth Muscle Cells

5.3.1 IK_{Ca} Channels in Vascular Smooth Muscle Cells

IK_{Ca} channel is found predominantly in peripheral tissues such as blood cells, epithelia, and smooth muscle cells where it functions to couple alterations in cytosolic Ca^{2+} to K^+ flux (Bond et al. 1999; Jensen et al. 2001; Wulff et al. 2003). IK_{Ca} channels thereby play an important physiological role to set the membrane potential at negative values close to the K^+ equilibrium potential (Bond et al. 1999; Jensen et al. 2001; Wulff et al. 2003; Stocker 2004). This effect on membrane potential can have diverse physiological responses in a variety of cell types, including water movement and volume regulation in red blood cells, mitogen activation of T-lymphocytes, Cl^- secretion of exocrine epithelial cells, and control of proliferation by a variety of cells such as T and B-lymphocytes, vascular smooth muscle cells, keratinocytes, and some cancer cell lines (Khanna et al. 1999; Ghanshani et al. 2000; Fanger et al. 2001; Koegel and Alzheimer 2001; Köhler et al. 2003; Maher and Kuchel 2003; Ouadid-Ahidouch et al. 2004; Wulff et al. 2004). Based on these activities, pharmacological modulation of IK_{Ca} channels has been proposed to treat proliferative diseases such as restenosis after angioplasty and cancer, transplant rejection as well as secretory diarrheas, sickle cell anemia, and cystic fibrosis (Rufo et al. 1997; Jensen et al. 2001; Maher and Kuchel 2003; Wulff et al. 2003).

In contrast to intestinal smooth muscle, there is little evidence for a functional role of SK_{Ca} channels in vascular smooth muscle cells, although a non-identified apamin sensitive and voltage-dependent conductance has been reported (Gebremedhin et al. 1996; Quignard et al. 2000; Gauthier et al. 2004; 2008). Similarly, in healthy and freshly isolated vascular smooth muscle cells IK_{Ca} channels are not or very poorly expressed. However, in proliferating cells, as seen in culture or after vascular injury, the expression of this channel increases dramatically (Neylon et al. 1999; Köhler et al. 2003; Tharp et al. 2006; 2008). Up-regulation of IK_{Ca} is necessary for mitogen-induced suppression of smooth muscle-specific marker genes, that is, differentiation of vascular smooth muscle cells, as well for their proliferation and migration (Tharp et al. 2006). Selective blockade of IK_{Ca} with TRAM-34 (Wulff et al. 2000) prevents smooth muscle phenotypic changes and coronary artery neointimal formation in two different models of post-angioplasty restenosis (Köhler et al. 2003; Tharp et al. 2008). Similarly, coronary arteriolar remodelling in L-arginine-methylester (L-NAME)-treated rats and post-ischaemic cardiovascular remodelling in rats subjected to coronary artery ligation are associated with an increase in IK_{Ca} channel expression in vascular smooth muscle cells. A treatment with a statin in the

former model and with an AT1 receptor antagonist in the latter prevented both the up-regulation of IK_{Ca} expression and the structural alterations (Saito et al. 2002; Terata et al. 2003).

5.3.2 *Effect of Mechanical Stretch on IK_{ca} Channel*

Blood vessels in vivo are continuously exposed to hemodynamic forces. These include shear stresses on the luminal surface generated by blood flow, cyclic distension due to the vascular wave caused by the pulsatility of the blood flow, and endocrine and local factors including angiotensin II (Ang II) and endothelin-1 (Williams B 1998; Fernandes-Santos et al. 2009). The luminal surface of blood vessels is lined with endothelial cells so that shear stress is sensed predominantly by endothelial cells. However, both endothelial and vascular smooth muscle cells are subjected to cyclic stretch. Under normal conditions, vascular smooth muscle cells are quiescent and contractile (Williams 1998; Davis and Hill 1999; Wu and Davis 2001). In response to pathologic stress, however, vascular smooth muscle cells develop a proliferative, hypertrophic, and secretory phenotype (Williams 1998; Davis and Hill 1999; Wu and Davis 2001). These alterations result in vascular remodeling characterized by cellular hyperplasia, hypertrophy, apoptosis, enhanced protein synthesis, and extracellular matrix reorganization.

Mechanical stretch stimulates the migration and proliferation of vascular smooth muscle cells. Recent studies indicate that Ca^{2+}-activated K^+ channels, specifically IK_{Ca} channels, have an important role in cell migration and proliferation. Therefore, we investigated whether the cell membrane stretch is linked to IK_{Ca} channel regulation.

5.3.3 *Effect of Angiotension II on IK_{ca} Channel*

Ang II is one of the most potent and physiologically important endogenous vasoconstrictors that acts to increase intracellular Ca^{2+} and the contractile force of vascular smooth muscle cells. It also has an important pathophysiologic role in cardiovascular disease, including cardiac hypertrophy, myocardial infarction, hypertension, and atherosclerosis (Gurantz 2005; Matsusaka and Ichikawa 1997). Furthermore, Ang II promotes migration and proliferation of vascular smooth muscle cells, leading to neointima formation (Wilson 1999). Proliferating vascular smooth muscle cells are characterized by alterations in functional plasticity as they switch from a contractile phenotype to a de-differentiated phenotype.

The actions of Ang II have been widely studied in several vascular tissues. Ang II induces an increase in Ca^{2+} currents, blockade of K^+ currents, and depolarization of the plasma membrane (Toro 1990; Hayabuchi et al. 2001a, b). K^+ channels have an important role in controlling vascular tone by altering the resting membrane

potential and thereby Ca^{2+} entry (Nelson and Quayle 1995). BK_{Ca} channels (Toro 1990), voltage-dependent K^+ channels (Hayabuchi et al. b), and ATP-sensitive K^+ channels (Hayabuchi et al. 2001a) in vascular smooth muscle cells are inhibited by Ang II.

Mature smooth muscle cells predominantly express BKca channels (Neylon 1999), a product of the *S/o* gene (Atkinson 1991), which have a pivotal role in vascular smooth muscle cell relaxation by dampening depolarization-dependent activation of Ca^{2+} channels and Ca^{2+} influx through membrane hyperpolarization (Latorre R 1989). In contrast to the vasodilatory function of BKca channel, the role of SKca and IK_{ca} channels in vascular smooth muscle cells is not completely understood. IK_{ca} channels are required for many physiologic functions such as proliferation, epithelial transport, and cell migration (Schwab 2001; Fioretti 2005; Ouadid-Ahidouch 2004). They are regulated by the intracellular Ca^{2+} concentration and by phosphorylation (Neylon 1999; Wulf and Schwab 2002; Zhou et al. 1996; Gerlach 2000, 2001; Hayashi et al. 2004).

We therefore investigated whether Ang II regulates the activity of IK_{ca} channels in arterial smooth muscle cells using patch-clamp techniques. Furthermore, we studied the signal transduction of these effects on IK_{ca} channels.

5.4 Property and Regulation of IK_{ca} Channels in Vascular Smooth Muscle Cells

5.4.1 IK_{ca} Channels are Predominantly Expressed in Cultured Smooth Muscle Cells

The electrophysiologic properties of the Kca channels expressed on cultured smooth muscle cells were studied by whole-cell and single-channel recordings. First, we performed whole-cell patch-clamp experiments on cultured smooth muscle cells to measure functional Kca channel expression. Whole-cell recording was performed with a holding potential of −60 mV. The selective BKca channel blocker iberiotoxin (IbTX) inhibited the current by only 17±3 %. The subsequent addition of charybdotoxin (ChTX), the blocker of BKca and IK_{ca} channel, caused a large decline in the current (Fig. 5.1a). Next, we examined the effect of clotrimazole (CLT), a selective blocker of IK_{ca} channels. CLT-sensitive current was predominantly expressed in cultured smooth muscle cells (Fig. 5.1b).

Furthermore, in inside-out patches, BK_{Ca} currents, as characterized by their large amplitude and voltage-dependent open probability, were rarely observed in cultured smooth muscle cells. BK_{Ca}-like activity was observed in 1 of 22 membrane patches excised from smooth muscle cells. The predominant K^+ current in these cells had a smaller unitary conductance than BK_{Ca} channels, and 1–4 of these channels were recorded in 20 of 22 excised patches. Single-channel openings were recorded from

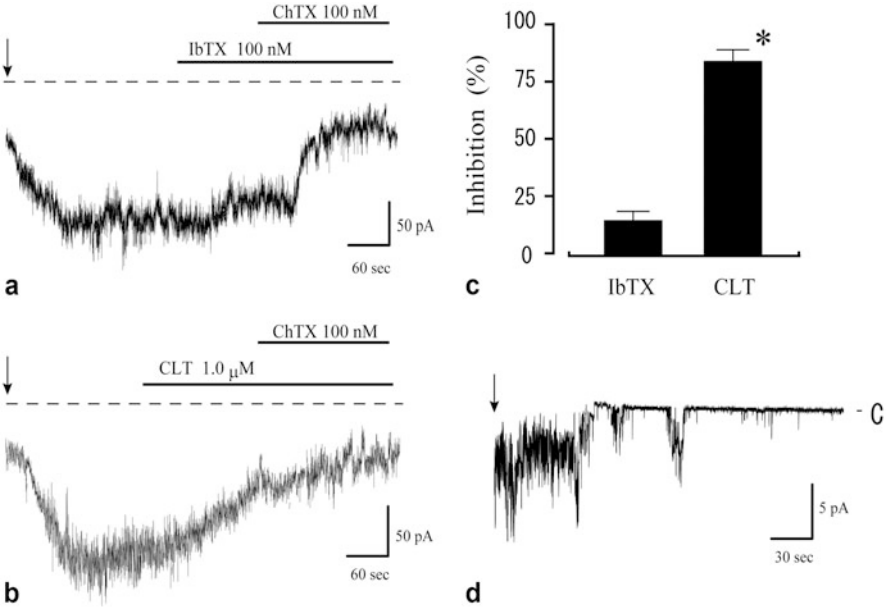

Fig. 5.1 Cultured smooth muscle cells predominantly express IK_{ca} channels. **a** Representative recording of whole-cell current from a smooth muscle cell held at − 60 mV. The current shows iberiotoxin (IbTX)-insensitive and charybdotoxin (ChTX)-sensitive K^+ currents. The vertical arrow indicates when the whole-cell configuration was established, and the dashed line shows the zero current level. The cell was dialysed with a solution containing 140 mM K^+, and the extracellular K^+ concentration was 140 mM. IbTX and ChTX were added as indicated. IbTX inhibited the ChTX-sensitive currents by 14 % in this cell. **b** Representative tracing of whole-cell current. The current shows clotrimazole (CLT)-sensitive K^+ current. CLT inhibited the current by 79 % in this cell, and ChTX inhibited the remaining current. **c** Percentage inhibition of ChTX-sensitive K^+ current by IbTX or CTL in experiments like those illustrated in A and B (n = 7 and 6 cells, respectively). The bars show mean ±SEM. $*p < 0.0001$. **d** The effect of CLT (1.0 μM) on the channel activity in a cultured smooth muscle cell. The trace is a record of an inside-out patch exposed to symmetrical 140 mM K^+ solutions, and the intracellular solution contained 1.0 μMf ree Ca^{2+}. The pipette solution contained CLT. Control channel activity was recorded before diffusion of CLT to the extracellular surface of the patch. The channel activity was absent after exposure to CLT. The membrane potential was − 40 mV. Closed state is represented by C. (Reproduced from Hayabuchi et al. 2006 with permission from Journal of Molecular and Cellular Cardiology and Elsevier Limited via Copyright Clearance Center)

inside-out excised membrane patches in which the pipette was back-filled with 1.0 μM CLT (Fig. 5.1d). Initially, K^+ channel openings were recorded immediately after formation of the high-resistance seal. Channel activity disappeared within 2–3 min, however, because of diffusion of the CLT to the membrane patch. In control patches (no CLT included in the pipette solution), the small K^+ currents were recorded for greater than 20 min at potentials both positive and negative of 0 mV.

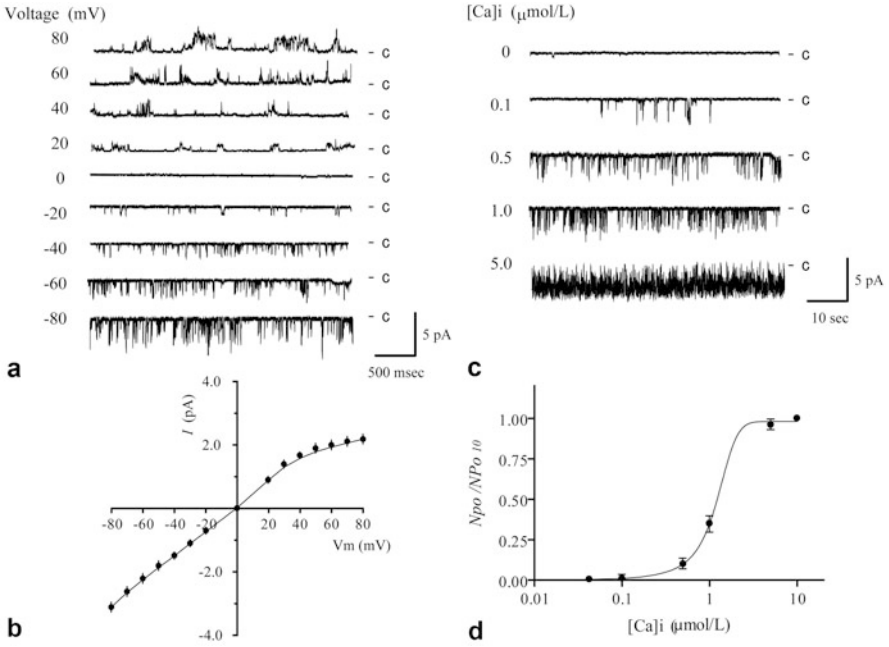

Fig. 5.2 Single channel properties of IK_{ca} channels expressed in smooth muscle cells. **a** IK_{ca} single-channel currents from an inside-out patch exposed to symmetrical (140 mM) K^+ solutions. Intracellular free Ca^{2+} concentration = 300 nM. Membrane potential was stepped from −80 to +80 mV in10 mV increments. **b** Single-channel current–voltage (I–V) curve obtained in symmetrical K^+ solutions. **c** Intracellular Ca^{2+} activation of IK_{ca} channels. Representative traces show single-channel activity of inside-out patches exposed to 0, 0.1, 0.5, 1.0, and 5.0 μmol/L free Ca^{2+}. Channel openings are shown as downward deflections. Voltage was −80 mV, and K^+ concentration was symmetrical at 140 mM. **d** Normalized mean current at a constant membrane potential of − 80mV from six different experiments plotted as a function the internal Ca^{2+} concentrations. Current at each Ca^{2+} concentration was normalized against the current in 10 μM Ca^{2+} solution (NPo-10). The sigmoid curve was computed according to a Hill equation with ED50 = 1.17 ± 0.06 μM and a Hill coefficient of 2.40 ± 0.07. (Reproduced from Hayabuchi et al. 2006 with permission from Journal of Molecular and Cellular Cardiology and Elsevier Limited via Copyright Clearance Center)

5.4.2 *Characterization of IK_{ca} Channels*

The IK_{ca} channel was characterized in a series of inside-out patch-clamp experiments. The single channel current-voltage relationship measured in symmetrical 140 mM K^+ solution is presented in Fig. 5.2a. The channel showed clear inwardly rectifying behavior. The mean values of six independent experiments were 3.1±0.2 and 2.1±0.1 pA at −80 and +80mV, respectively, corresponding to chord conductances of 37±2 and 26±1 pS, respectively. The single-channel current-voltage (I-V) relation

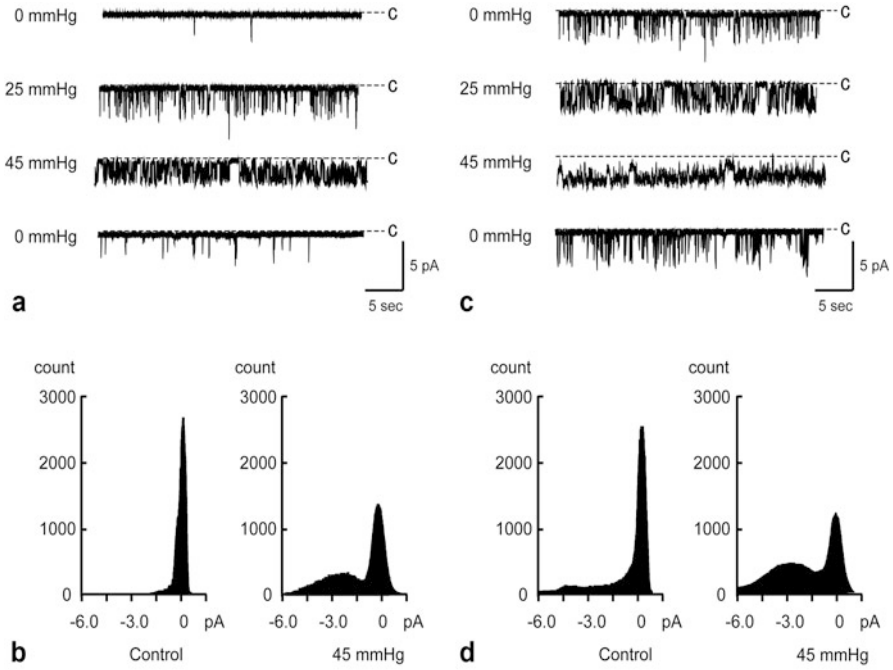

Fig. 5.3 Effect of cell membrane stretching on IK_{ca} channels. **a** Representative recordings showing the effect of membrane stretching on IK_{ca} channels in cultured smooth muscle cells. IK_{ca} channel currents are recorded from cell-attached patches at a pipette voltage of + 40 mV. **b** Amplitude histograms showing the activation of IK_{ca} channels in the same experiments as those of A. **c** Representative recordings showing the effect of membrane stretching on IK_{ca} channels in inside-out patch configuration. IK_{ca} channel currents are recorded at an intracellular Ca^{2+} concentration of 215 nM, and at a pipette voltage of − 80 mV. **d** Amplitude histograms showing the activation of IK_{ca} channels in the same experiments as those of C. (Reproduced from Hayabuchi et al. 2011 with permission from Heart and Vessels and Springer Science + Business Media Limited via Copyright Clearance Center)

is plotted in Fig. 5.2b. Inside-out single channel recordings measured in symmetrical 140 mM K^+ conditions for internal Ca^{2+} concentrations ranging from 0–10 μM are present in Fig. 5.2c. In these experiments, the membrane voltage was maintained at − 80 mV. Raising the internal Ca^{2+} concentration from 0–10 μM significantly increased the single channel activity (Fig. 5.2d). The sigmoidal curve in Fig. 5.2d was computed using the Hill equation with an ED50 of 1.17±0.06 μM and a Hill coefficient of 2.40±0.07. There was no obvious voltage dependence of the channel because *NPo* remained unchanged when the holding potential was varied between − 80 mV (*NPo* = 0.11 ± 0.03) and + 80 mV (*NPo* = 0.12 ± 0.05). These properties are consistent with IK_{ca} channels expressed in immature and de-differentiated smooth muscle cells (Neylon et al. 1999).

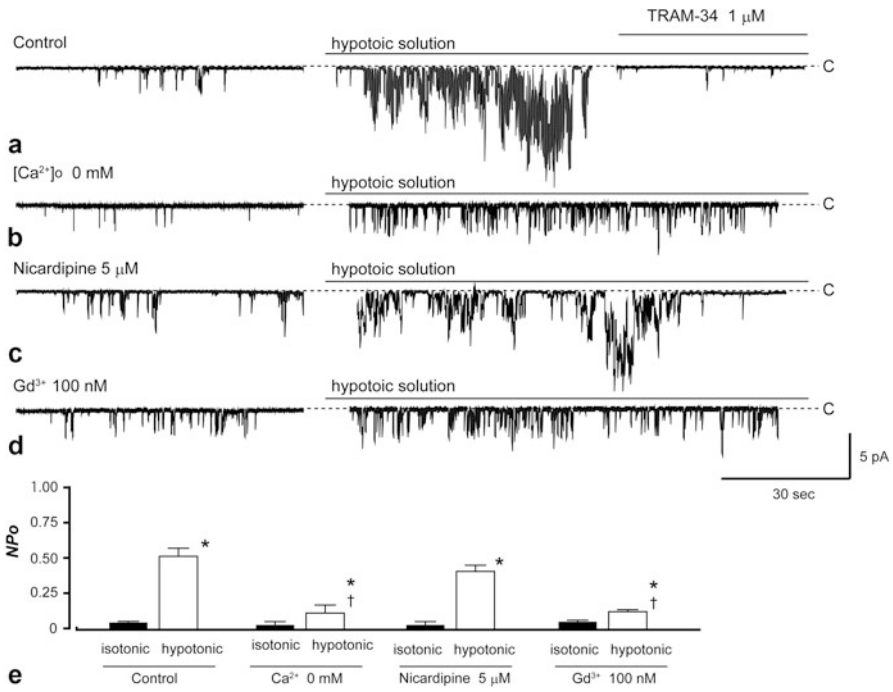

Fig. 5.4 Effect of hyposmotic stretching on IK_{ca} channels. **a** Representative recordings showing the effect of hyposmotic stretching on IK_{ca} channels. IK_{ca} channel currents are recorded from cell-attached patches at a pipette voltage of + 40 mV. Hyposmotic solution was added as indicated. The dashed line shows zero current level. **b** Effect of extracellular Ca^{2+} on the activation of IK_{ca} current. The trace shows a recording of cell-attached patch. Ca^{2+}-free isosmotic solution was replaced with Ca^{2+}-free hyposmotic solution. The activation of IK_{ca} channels was attenuated under this condition. **c** Effect of nicardipine on the activation of IK_{ca} current. The trace shows a recording of cell-attached patch that had been pretreated with nicardipine (5 μM). Hyposmotic stress activated IK_{ca} channels under this condition. **d** Effect of Gadolinium (Gd^{3+}) on the activation of IK_{ca} current. The trace shows a current recording pretreated with Gd^{3+} (100 nM). Gd^{3+} attenuated the activation of IK_{ca} channels. **e** Effect of extracellular Ca^{2+}, nicardipine, and Gd^{3+} on IK_{ca} channel activation by hyposmotic swelling. The bars show mean *NPo* (+ SEM) of IK_{ca} current before (filled bars) and after the hyposmotic stress (open bars) under these pretreatment conditions. *, $p < 0.01$ vs isotonic condition of each pretreatment.†, $p < 0.01$ vs hypotonic stress under the control (without the pretreatment) condition. (Reproduced from Hayabuchi et al. 2011 with permission from Heart and Vessels and Springer Science + Business Media Limited via Copyright Clearance Center)

5.4.3 Effect of Mechanical Stress on IK_{ca} Channels

5.4.3.1 Effect of Membrane Stretching on IK_{ca} Channels

Stretch-induced activation of IK_{ca} channels was observed in cultured smooth muscle cells. The effect of suction application of 25 and 45 mmHg was tested at + 40 mV in cell-attached mode. Figure 5.3a shows a sample recording from one of the patches

containing one channel that are activated during the application of negative pressure and subsequently inactivated after removal of the pressure.

To determine if IK_{ca} channel activity is enhanced by release of Ca^{2+} from intracellular stores or entrance of Ca^{2+} through the plasma membrane by stretch stimulus application, we performed experiments in the inside-out mode. At constant Ca^{2+} concentration (100 nM), application of pressure increased the member of channel openings at 25 and 45 mmHg (Fig. 5.3b). Application of negative pressure to the pipette caused activation of channels that produced outward unitary currents. The *NPo* without the negative pressure was 0.135 ± 0.027. The *NPo* after application of 25 and 45 mmHg were 0.281 ± 0.041 and 0.440 ± 0.101, respectively, which were significantly higher than the control condition. After restoring atmospheric pressure to the pipette, open probability returned to the control level. Fig. 5.3c, d display the amplitude histograms showing the effect of the negative pressure on IK_{ca} channel activity in the cell-attached and in the inside-out configuration, respectively.

5.4.3.2 Effect of Hyposmotic Stretching on IK_{ca} Channels

Hypotonic shock has been used in other many cell types to stretch the cell membrane. This procedure increases cell membrane tension due to cell swelling. We evaluated the effect of a hypotonic stimulus on the cell-attached mode. IK_{ca} currents were first recorded in isotonic medium (control; 310 mOsm/kg H_2O) and afterward, the bath solution was replaced by hypotonic medium (223 mOsm/kg H_2O).

Figure 5.4a is a typical recording showing the effects of hyposmotic stress on the IK_{Ca} channel in cultured smooth muscle cells. The superfusion with hyposmotic solution significantly stimulated IK_{Ca} channel activity. The mean open probability increased from 0.009 ± 0.006 in control solution to 0.480 ± 0.012 at 5 min of hypotonic stress. Subsequent application of TRAM-34 induced a significant inhibition in IK_{ca} channel current. Channel activity usually decreased when the hypotonic solution was removed and the cells were again bathed in control solution.

5.4.3.3 Effect of Extracellular Ca^{2+} on the Activation of IK_{Ca} Current Induced by Hyposmotic Swelling

It is well known that IK_{Ca} channel is activated by intracellular free Ca^{2+} and that extracellular Ca^{2+} is necessary for efficient control of Ca^{2+} homeostasis. To determine if Ca^{2+} influx is involved in the hyposmotic stretch-induced activation of the current, we removed extracellular Ca^{2+} and observed the effect of hyposmotic swelling on IK_{Ca} channels. When Ca^{2+}-free isosmotic solution was replaced with Ca^{2+}-free hyposmotic solution, the activation of IK_{ca} was attenuated significantly compared with the recordings using physiological Ca^{2+} solution (Fig. 5.4b). Although the mean open probability increased from 0.009 ± 0.005 in control solution to 0.120 ± 0.006 at 5 min of hypotonic stress, it was significantly lower than the *NPo* with the physiological Ca^{2+} hyposmotic solution.

5.4.3.4 L-type Ca^{2+} Channel is not Involved in the Pathway

To assess the contribution of L-type Ca^{2+} channels to the hyposmotic stretch-induced activation of IK_{Ca} channels, we tested the effect of hyposmotic solution on the IK_{Ca} current in the presence of nicardipine, an L-type Ca^{2+} channel blocker (Fig. 5.4c). Nicardipine was added to the extracellular solution for 10 min before the application of hyposmotic solution. The *NPo* after pretreatment with nicardipine was 0.007 ± 0.005, which was not significantly different from the *NPo* without the pretreatment. The *NPo* of IK_{ca} channels was significantly increased by hyposmotic solution after nicardipine treatment. The *NPo* in hyposmotic stress was 0.401 ± 0.109, which was not significantly different from the *NPo* without the pretreatment. This result indicates that L-type Ca channel is not involved in this pathway.

5.4.3.5 Gadolinium Blocks Hyposmotic Swelling-Induced Activation

Next, we examined the effect of the pretreatment of 100 nM Gadolinium (Gd^{3+}), a stretch-activated non-selective cation (SA) channel blocker. As shown in Fig. 5.4d, Gd^{3+} attenuated the activation of IK_{ca} channels induced by hyposmotic swelling. These results suggested that the influx of extracellular Ca^{2+} is through the SA channel and not the L-type calcium channel and that it is involved in the activation of IK_{Ca} channels.

5.4.3.6 PKC and F-actin are Involved in the Pathway

Although Ca^{2+}-free extracellular solution or the presence of Gd^{3+} attenuated the activation, the IK_{ca} current was still enhanced in those conditions. Furthermore, in the experiments of inside-out patch configuration, membrane stretch activated the IK_{ca} channel current at constant Ca^{2+} concentration. Therefore, other signal pathways may exist besides those that depend upon an increase in intracellular Ca^{2+}.

In order to test the involvement of PKC in hyposmotic swelling-induced IK_{Ca} channel activation, the effect of GF109203X, a PKC inhibitor, was examined in the experiments using Ca^{2+}-free extracellular solution. Pretreatment of smooth muscle cells with 10 μM GF109203X for 20 min abolished the effect of hyposmotic shock (Fig. 5.5a). Subsequent application of 10 μM A23187 induced a significant increase in IK_{Ca} channel current.

Another possibility involves a possible role played by the actin cytoskeleton in cell membrane stretch-dependent regulation of IK_{ca} channels. We therefore examined the effect of treatment with cytochalasin D. To disrupt the F-actin cytoskeleton in some experiments, smooth muscle cells were pre-incubated for 3 h in 3 μM cytochalasin D before being subjected to membrane stretch experiments. This treatment almost completely eliminated the response of IK_{ca} channels to cell swelling (Fig. 5.5b).

The GF109203X application data suggested that PKC is involved in the pathway of swelling-induced IK_{ca} channel activation. Therefore, we tested the effect of 1,2-dioctanoyl-sn-glycerol (DOG), a membrane permeable analog of 1,2-diacylglycerol

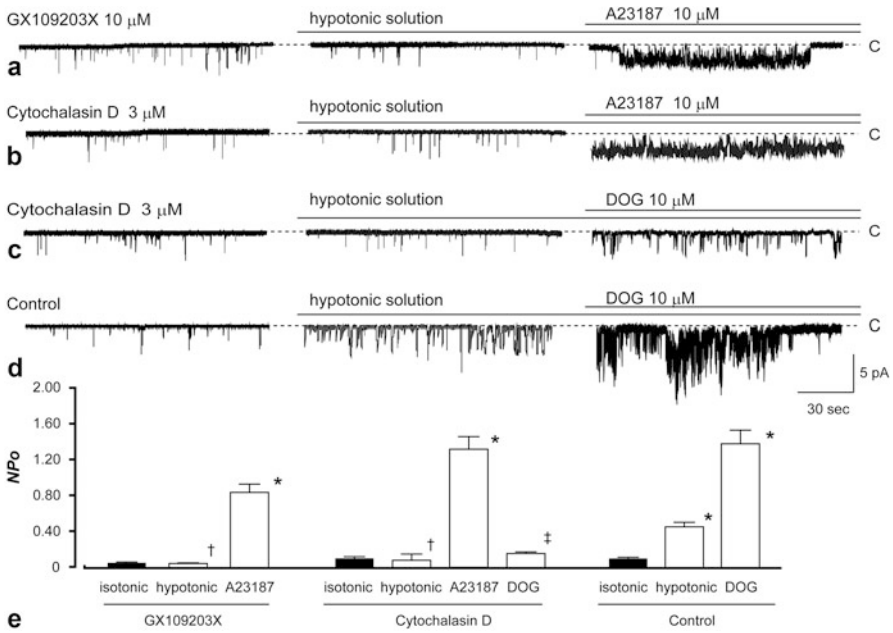

Fig. 5.5 Effects of PKC and F-actin on IK_{ca} channel activation induced by hyposmotic stress. **a** Representative recordings showing the effect of GF109203X (10 μM) on the activation of IK_{ca} current induced by hyposmotic stretching. Hyposmotic solution did not activate IK_{ca} channels under this condition, while subsequent application of the calcium-ionophore A23187 (10 μM) was effective. The pipette and bath solutions were the same as in Fig. 5.4. The pipette voltage was + 40 mV. The dashed line shows the zero current level. **b** Effect of cytochalasin D (3 μM) on the activation of IK_{ca} current. The trace shows a recording of cell-attached patch. Hyposmotic stress did not activate IK_{ca} channels under this pretreatment. Subsequent application of A23187 was effective. **c** Effect of 1,2-dioctyanoyl-sn-glycerol (DOG) on the activation of IK_{ca} current under the pretreatment with cytochalasin D. The trace shows a recording of cell-attached patch that had been pretreated with cytochalasin D (3 μM). Neither hyposmotic solution nor DOG (10 μM) activated IK_{ca} currents. **d** Effect of DOG on the activation of IK_{ca} current in the absence of cytochalasin D. DOG activated IK_{ca} channels under this condition. **e** Effect of GX109203X and cytochalasin D on IK_{ca} channel activation by hyposmotic swelling. The bars show mean *NPo* (+ SEM) of IK_{ca} current before (filled bars) and after the hyposmotic stress (open bars). *, $p < 0.01$ vs isotonic condition of each pretreatment.†, $p < 0.01$ vs hypotonic stress under the control (without the pretreatment) condition.‡, $p < 0.01$ vs DOG under the control (without the pretreatment) condition. (Reproduced from Hayabuchi et al. 2011 with permission from Heart and Vessels and Springer Science + Business Media Limited via Copyright Clearance Center)

(DAG) on IK_{ca} channel activity in the presence of cytochalasin D. In cells pretreated with GF109203X, DOG failed to activate the IK_{ca} current, whereas DOG increased *NPo* from 0.470 ± 0.101 to 1.380 ± 0.112 without the presence of cytochalasin D.

5.4.3.7 Effect of PKC and F-actin on the Experiments of Negative Pressure

In order to confirm the signal transduction of the mechanical stretch demonstrated in the hyposmotic stretch experiments, we tested the effect of GF109203X and

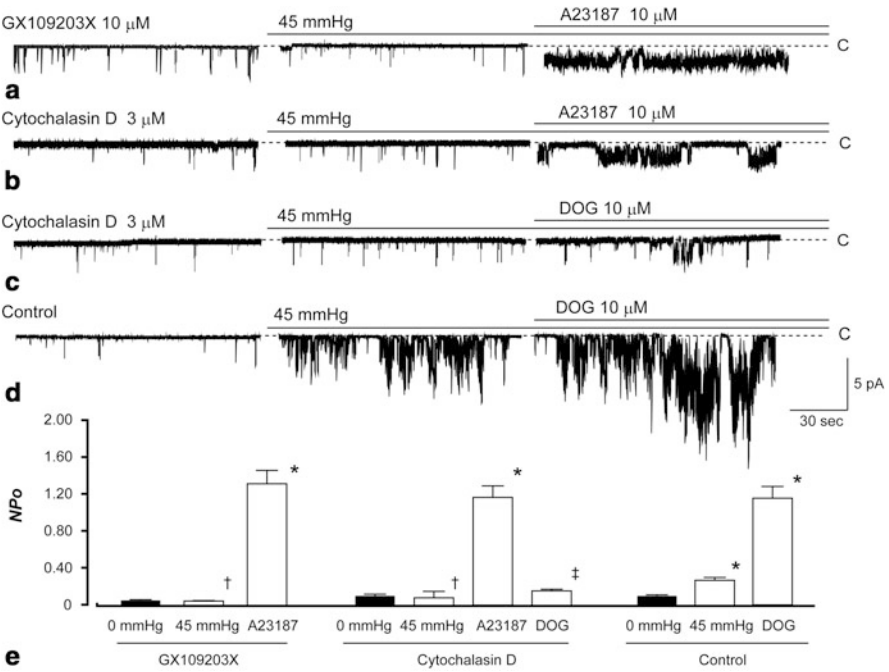

Fig. 5.6 Effect of PKC and F-actin on IK_{ca} channel activation induced by negative pressure. **a** Representative recordings showing the effect of GF109203X (10 μM) on the activation of IK_{ca} current induced by membrane stretching. Negative pressure of 45 mmHg did not activate IK_{ca} channels under this condition, while subsequent application of A23187 (10 μM) was effective. The pipette and bath solutions were the same as in Fig. 5.3a. The pipette voltage was + 40 mV. The dashed line shows the zero current level. **b** Effect of cytochalasin D (3 μM) on the activation of IK_{ca} current. The trace shows a recording of cell-attached patch. Membrane stretching did not activate IK_{ca} channels under this pretreatment. Subsequent application of A23187 was effective. **c** Effect of DOG on the activation of IK_{ca} current under the pretreatment with cytochalasin D. Negative pressure did not activate IK_{ca} current, and subsequent application of DOG was also ineffective. **d** Effect of DOG on the activation of IK_{ca} current in the absence of cytochalasin D. DOG activated IK_{ca} channels under this condition. **e** Effect of GX109203X and cytochalasin D on IK_{ca} channel activation by membrane stretching. The bars show mean *NPo* (+ SEM) of IK_{ca} current before (filled bars) and after the addition of negative pressure (open bars). *, $p < 0.01$ vs 0 mmHg of each pretreatment.†, $p < 0.01$ vs 45 mmHg under the control (without the pretreatment) condition.‡, $p < 0.01$ vs DOG under the control (without the pretreatment) condition. (Reproduced from Hayabuchi et al. 2011 with permission from Heart and Vessels and Springer Science + Business Media Limited via Copyright Clearance Center)

cytochalasin D in the cell-attached patch configuration. These examinations were performed in Ca^{2+}-free extracellular solution. Pretreatment with GF109203X abolished the stretch-induced IK_{ca} channel activation (Fig. 5.6a). Cytochalasin D also inhibited the effect of stretch on IK_{ca} current (Fig. 5.6b). Although DOG activated IK_{Ca} channels in the control condition, the pretreatment with cytochalasin D abolished the effect of DOG (Fig. 5.6c).

5.4.3.8 Mechanical Stretch and IK_{ca} Channels

Our study demonstrated that membrane stretch and hyposmotic swelling activates IK_{Ca} channels in cultured artery smooth muscle cells. In cell membrane stretch condition, extracellular Ca^{2+} influx through SA channels activated IK_{ca} channels. Furthermore, our results demonstrate clearly that PKC and F-actin are important factors in the cell membrane stretching-induced activation of IK_{Ca} channels. Unitary conductance was not modified by suction or swelling.

The arterial wall is continuously exposed to mechanical stimulation such as shear stress and luminal pressure. It is well known that such mechanical strain plays a pivotal role in the development of vascular remodeling in hypertension (Setoguchi et al. 1997; Folkow 1995). However, its exact mechanism remains unknown. Mitogen-activated protein kinases (MAPKs), members of a family of serine/threonine-specific protein kinases (Kosako et al. 1992) are believed to be involved in the pathway of cell proliferation and, therefore, in vascular structural remodeling (Alvarez et al. 1991; Pulverer et al. 1991; Sturgill et al. 1988). Kubo et al have reported that increases in perfusion pressure in isolated perfused rat aortae caused a pressure-dependent increase in the activity of MAPKs (Kubo et al. 2000). They also demonstrated that pressure loading of the vascular wall of rat aorta can activate p42 and p44 MAPKs and that MAPK activation is mediated at least in part by the vascular angiotensin system (Hosokawa et al. 2002). The regulation of MAPK is dependent upon changes in intracellular Ca^{2+} (Lucchesi et al. 1996). Furthermore, it is reported that activation of IK_{Ca} channels enhances Ca^{2+} influx by increasing its transmembrane electrical gradient (Lepple-Wienhues et al. 1996; Verheugen et al. 1997). The increase in Ca^{2+} influx, caused by activation of IK_{Ca}, stimulates distinct cellular mechanisms associated with smooth muscle growth and proliferation (Hayabuchi et al. 2006; Neylon et al. 1999), which can be mediated via MAPK activation. These previous studies suggest that the activation of IK_{Ca} channels is linked to the activation of MAPK.

5.4.3.9 Signal Transduction of Cell Membrane Stretch on IK_{Ca} Channels

Regulation of ion channel activity by changes in the organization of the F-actin cytoskeleton has been suggested for the epithelial Na^+ channel (Berdiev et al. 1996), the cystic fibrosis transmembrane regulator, CFTR (Cantiello 1996), Kv channels, and cardiac K_{ATP} channels (Furukawa et al. 1996). Changes in the structure of the F-actin cytoskeleton may also play an important role as a cell volume regulator. Generally, cell swelling is reported to cause a decrease in cellular F-actin content. Stretch has been shown to enhance vascular smooth muscle cell migration as a result of the translocation of PKCδ to the cytoskeleton (Li et al. 2003).

The pathway of signal transduction of IK_{ca} channel activation is still unknown. Our results show that PKC and F-actin are both involved in the activation of IK_{ca} channels in cultured smooth muscle cells. In order to study the relationship between PKC and F-actin in the activation pathway, we examined the effect of DOG together with cytochalasin D on the activation of IK_{ca} current under hyposmotic and stretched condition. The results showed that no significant current was activated as compared

with the control, which was different from the activation effect of DOG alone. This suggests that activation of PKC by DOG under the condition of depolymerization of F-actin cannot elicit IK_{ca} current any longer. This implies that the role of F-actin for regulation of IK_{ca} channel in the signal pathway would be downstream site related to the role of PKC. For stress-activated or mechanically gated channels, several studies have shown that the cytoskeleton directly interacts with the channel protein and can intrinsically sense the cell stretch (Hamill and Martinac 2001; Ingber and Tensegrity 1997). Stretch-activated IK_{ca} channels may act similarly. IK_{ca} channel activation by cell-membrane stretching contributes to Ca^{2+} entry in smooth muscle cells and therefore affects migration and proliferation in some pathophysiologic conditions. So far there have been few functional studies of the regulation of IK_{ca} channels by mechanical stress, though the IK_{ca} channel is required for de-differentiation, proliferation, and migration (Hayabuchi et al. 2006; Neylon 1999; Köhler et al. 2003). There is a clear need for future functional studies of the role of IK_{ca} channel activation by cell membrane stretch in cardiovascular disease, especially hypertension.

5.4.4 Activation of IK_{Ca} Channels by Ang II

5.4.4.1 AngII Activates IK_{Ca} Current

Figure 5.7a is a typical recording showing the effects of Ang II on the IK_{Ca} channel in cultured smooth muscle cells. Figure 5.7b displays the amplitude histogram showing the effect of Ang II on IK_{ca} channels. The addition of Ang II significantly stimulated IK_{ca} channel activity in a concentration-dependent manner. The ED50, the concentration required for stimulation of channel activity to 50 % of the maximal value, was 92 ± 3 nM. The Hill coefficient was 1.06 ± 0.14 (Fig. 5.7c).

5.4.4.2 PKC inhibitors block Ang II-induced activation

In addition to intracellular Ca^{2+} (Latorre et al. 1989; Neylon et al. 1999), phosphorylation modulates IK_{ca} channel gating (Wulf and Schwab 2002; Zhou et al. 1996; Gerlach et al. 2000, 2001; Hayashi et al. 2004). Recently, it was demonstrated that PKA enhances IK_{ca} channel activity (Gerlach et al. 2000, 2001), and cGMP, by activating cGMP-dependent protein kinase (PKG), produces the same effect (Zhou et al. 1996). Some reports demonstrate that IK_{ca} current is regulated by PKC (Wulf and Schwab 2002).

First, to assess the contribution of PKC activation to the Ang II-induced activation of IK_{ca} channels, we pretreated smooth muscle cells with 100 μM PKC-IP 20–28. PKC-IP 20–28 was applied in the extracellular solution for 10 min before the application of Ang II. The *NPo* after pretreatment with PKC-IP 20–28 was 0.014 ± 0.009, which was not significantly different from the *NPo* without the pretreatment ($NPo = 0.010 \pm 0.003$). In the presence of the PKC-IP 20–28, Ang II failed to induce a change in the current activity ($NPo = 0.032 \pm 0.010$) (Fig. 5.8a).

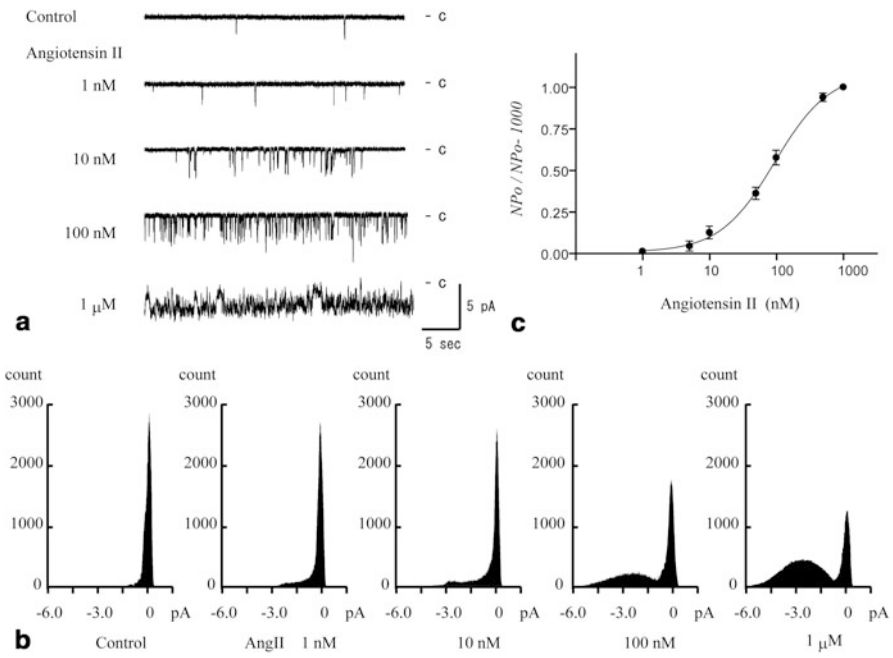

Fig. 5.7 Effect of Ang II on IK_{ca} channels in A10 cells. **a** Representative recordings showing the effect of Ang II on IK_{ca} channels in cultured smooth muscle cells. IK_{ca} channel currents are recorded from cell-attached patches at a pipette voltage of + 40 mV. Ang II-activated IK_{ca} channels in a concentration-dependent manner. **b** Amplitude histograms showing the concentration-dependent effect of Ang II on IK_{ca} channels in the same experiments as those of panel A. **c** Normalized concentration-response relationship for the effect of Ang II. The data were fitted with the Hill equation, yielding an EC50 of 92 ± 3 nM and a Hill coefficient of 1.06 ± 0.14. (Reproduced from Hayabuchi et al. 2006 with permission from Journal of Molecular and Cellular Cardiology and Elsevier Limited via Copyright Clearance Center)

Next, in order to confirm that PKC is involved in Ang II-induced IK_{ca} channel activation, the effect of GF109203X, a PKC inhibitor, were examined. Pretreatment of A10 cells with 10 μM GF109203X for 20 min abolished the effect of Ang II (Fig. 8b).

5.4.4.3 PKA and PKG are not Involved in the Pathway

We tested the effect of Ang II on the IK_{ca} current in the presence of Rp-cAMPS, a PKA inhibitor (Fig. 5.8c). The *NPo* of IK_{ca} channels was significantly increased by Ang II after Rp-cAMPS pretreatment. This result indicates that the PKA system is not involved in this pathway. Next, we examined the effect of the pretreatment of 1.0 μM KT-5823, a PKG inhibitor. The effect of Ang II was not affected by the presence of KT-5823 (Fig. 5.8d). The *NPo* after pretreatment with either Rp-cAMPS or KT-5823 was not significantly different from the *NPo* without pretreatments both before and after the addition of Ang II (Fig. 5.8e).

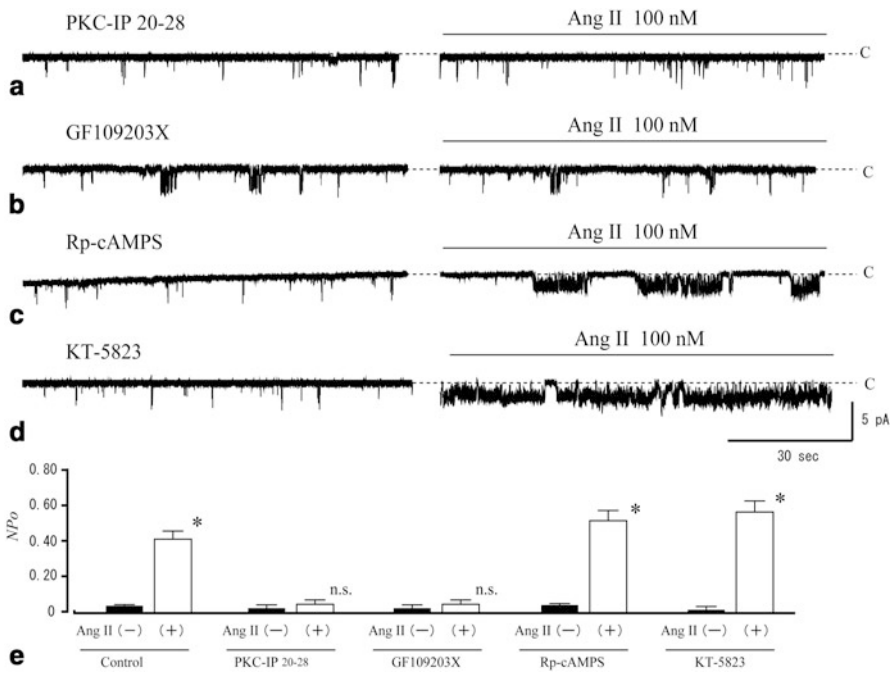

Fig. 5.8 PKC inhibitors prevent the current activation by Ang II. **a** Effect of PKC-IP 20–28. The trace shows a recording of cell-attached patch made from a smooth muscle cell that had been pretreated with PKC-IP 20–28 (100 μM). Ang II did not activate IK_{ca} channels under this condition. The dashed line shows the zero current level. **b** Effect of GF109203X. The trace shows a recording of cell-attached patch made from an A10 cell that had been pretreated with GF109203X (10 μM). Ang II did not activate IK_{ca} channels under this condition. **c** Effect of Rp-cyclic 3′,5′-hydrogen phosphothiate adenosine triethylammonium (Rp-cAMPS). The trace shows a current from a smooth muscle cell that had been pretreated for 10 min with Rp-cAMPS (100 μM). Ang II still activated IK_{ca} channels under this condition. **d** Effect of KT-5823. The trace shows a current recording pretreated with 1.0 μM KT-5823. Ang II was added as indicated. KT-5823 did not abolish the effect of Ang II. **e** Effect of PKC-IP 20–28, GF109203X, Rp-cAMPS, and KT-5823 on IK_{ca} channel activation by Ang II. The bars show mean NPo (+ SEM) of IK_{ca} current before (filled bars) and after adding Ang II (open bars) under these pretreatment conditions. $*p < 0.0001$ vs. before adding Ang II. n.s., not significant. (Reproduced from Hayabuchi et al. 2006 with permission from Journal of Molecular and Cellular Cardiology and Elsevier Limited via Copyright Clearance Center)

5.4.4.4 Losartan Inhibits the Action of Ang II

Ang II receptors can be divided into AT1 and AT2 subtypes (Guo et al. 2001). The AT1 receptor is coupled to phospholipase C through Gq/G11 G-proteins and is negatively coupled to adenylyl cyclase (Guo et al. 2001). To investigate the type of receptor involved in IK_{ca} channel activation, we tested the effect of Ang II in the presence of losartan (1.0 μM), an AT1 selective antagonist. Figure 5.9a is a representative recording from a cell-attached patch, and shows that Ang II did not activate IK_{ca} current in the cells after 10 min pretreatment with losartan. Subsequent application

of the calcium ionophore A23187 (10 μM) induced a significant increase in IK_{ca} currents.

5.4.4.5 Kca Current is Activated by DOG

The PKC-IP 20–28 application data suggested the involvement of PKC in the pathway of Ang II action. Therefore, we tested the effect of DOG, a membrane-permeant analog of DAG on IK_{ca} channel activity. In six cells pretreated with losartan, Ang II failed to activate the IK_{ca} current. Subsequent application of 10 μM DOG induced a significant increase in the IK_{ca} current (Fig. 5.9b).

5.4.4.6 Effect of AngII on IK_{ca} Channels

Our study demonstrated that Ang II activates IK_{ca} channels in cultured artery smooth muscle cells. The results provide evidence that Ang II increases these currents by interacting with the AT1 receptor, a mechanism that is involved in the activation of PKC.

The major bioactive peptide of the renin-angiotensin system, Ang II, has a fundamental role not only in controlling cardiovascular and renal homeostasis, but also contributes to various cardiovascular diseases such as hypertension, atherosclerosis, and heart failure. It is likely that the growth promoting activity of the AT1 receptor is involved in the progression of cardiovascular remodeling (Gurantz et al. 2005; Matsusaka et al. 1997; Wilson et al. 1999). In this respect, Ang II is recognized as a growth-promoting factor contributing to structural alteration in an endocrine and autocrine manner in various organs (Matsusaka et al 1997; Wilson et al. 1999).

Ang II regulates various types of K^+ channels (Toro et al. 1990; Hayabuchi et al. 2001a, b). We therefore tested the hypothesis that Ang II regulates IK_{ca} channels in smooth muscle cells. This is the first report that demonstrates Ang II regulation of IK_{ca} channels.

We previously reported that Ang II inhibits Kv channels and K_{ATP} channels in enzymatically isolated rat mesenteric artery smooth muscle cells (Hayabuchi et al. 2001a, b). Ang II inhibits these channels through the activation of PKC and inhibition of PKA. Furthermore, Ang II activated IK_{ca} channels in proliferative smooth muscle cells. It is reported that activation of IK_{ca} channels enhance Ca^{2+} influx by increasing its transmembrane electrical gradient (Lepple-Wienhues et al. 1996; Verheugen et al. 1997). The increase in Ca^{2+} influx, caused by activation of IK_{ca}, stimulates distinct cellular mechanisms associated with smooth muscle growth and proliferation (Hazelton et al. 1979; Cory et al. 1987; Nilius and Wohlrab 1992). Changes in the cytosolic Ca^{2+} concentration provide important regulatory signals during the cell cycle. Ca^{2+} is required for progression through G1 and for the G1/S transition in several cell types, including human embryonic lung fibroblasts (Hazelton et al. 1979) and L1210 leukemic cells (Cory et al. 1987). A link between intracellular Ca^{2+} and membrane potential was first reported in melanoma cells, where membrane

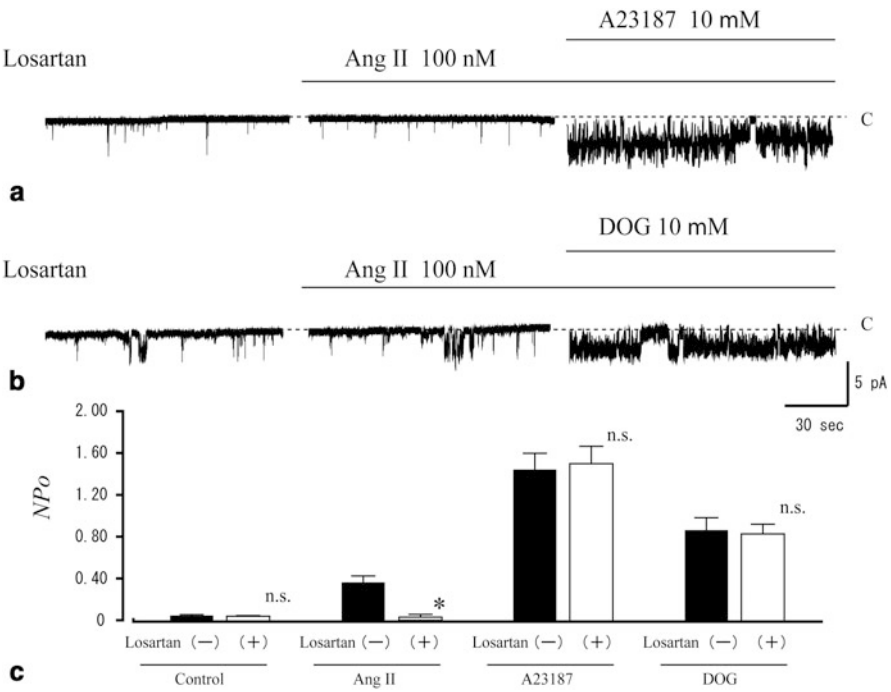

Fig. 5.9 Ang II is ineffective in the presence of losartan. **a** Recording of cell-attached patch current made from a smooth muscle cell pretreated with 1.0 μM losartan. Ang II did not activate IK_{ca} channels under this condition, while subsequent application of the calcium ionophore A23187 (10 μM) was effective. The pipette and bath solutions were the same as in Fig. 5.7. The pipette voltage was + 40 mV. **b** Recording of cell-attached patch current pretreated with 1.0 μM losartan. Ang II did not affect IK_{ca} channel activity. Subsequent application of 1,2-dioctyanoyl-sn-glycerol (DOG) was still effective. **c** Mean NPo (+ SEM) of IK_{ca} channel in cells without (filled bars) and with pretreatment of losartan (open bars). *Results significantly different from the value without pretreatment ($p < 0.0001$). n.s., not significant. (Reproduced from Hayabuchi et al., 2006 with permission from Journal of Molecular and Cellular Cardiology and Elsevier Limited via Copyright Clearance Center)

hyperpolarization increased intracellular Ca^{2+} by controlling the electrochemical gradient for Ca^{2+} entry into the cell (Nilius et al. 1992). This increase in Ca^{2+} might, in turn, induce the activation of IK_{ca} channels, thus providing a positive feedback mechanism.

The mechanisms of action of Ang II have been studied in several vascular tissues (Toro et al. 1990; Hayabuchi et al. 2001a, b). The signal transduction of the regulation of IK_{ca} channels, however, has not been elucidated. Our results using losartan indicate that the binding of Ang II to AT1 receptors leads to the activation of IK_{ca} current. Furthermore, the present study indicated that PKC activation is involved in this Ang II action. Activation of AT1 receptors in the plasma membrane leads to the formation of inositol 1,4,5, triphosphate and DAG through G-protein-mediated activation of phospholipase C (Guo et al. 2001). DAG activates PKC, which in turn stimulates

protein phosphorylation and ionic channel activation (Toro et al. 1990; Hayabuchi et al. 2001a, b). On the other hand, the AT1 receptor is negatively coupled to adenylyl cyclase G-proteins (Guo et al. 2001). Moreover, previous reports indicated that PKA and PKG modulate IK_{ca} current activity (Zhou et al. 1996; Gerlach et al. 2000; Gerlach et al. 2001). However, the present results suggest that PKA and PKG are not involved in the action of Ang II on IK_{ca} channels.

IK_{ca} channel activation by Ang II is expected to contribute to Ca^{2+} entry in smooth muscle cells and therefore affect migration and proliferation in some pathophysiologic conditions. IK_{ca} channel is required for de-differentiation, proliferation, and migration (Nelson and Quayle 1995; Neylon et al. 1999). There is a clear need for future functional studies of the role of IK_{ca} channel activation by Ang II and other endogenous growth factors in cardiovascular disease, including hypertension, atherosclerosis, and restenosis after balloon angioplasty.

5.5 Role of IK_{ca} Channels in Smooth Muscle Cells

IK_{ca} channels have an important role in cell migration and proliferation. Previous reports suggest that proliferative smooth muscle cells predominantly express IK_{ca} channels (Neylon et al. 1999; Köhler et al. 2003) and that cell migration is also modulated by the activity of IK_{ca} channels (Schwab 2001).

Functional plasticity is a fundamental property of vascular smooth muscle, important for regulating blood pressure and controlling vascular growth and repair during development, in response to disease states, and after mechanical injury (Owens 1995; Sartore et al. 1997; Frid et al. 1997). Plasticity is dependent on extensive diversity in the properties, distribution, and function of individual smooth muscle cell populations, arising from both phenotypic modulation between contractile and de-differentiated states and the establishment of smooth muscle cell lineages early in embryonic life, which have the potential to become major cell populations in pathological conditions (Sartore et al. 1997; Frid et al. 1997).

Several studies suggest that differential expression of ion channels contributes to smooth muscle plasticity (Neylon et al. 1994a, Archer et al. 1996; Reeve et al. 1998). Morphologically distinct smooth muscle cell types exhibit marked differences in ion channel expression, giving rise to differences in electrical properties and responsiveness to vasoactive substances (Neylon et al. 1994a). Much of the variation in contractile reactivity between different arterial segments, vessels, and physiological and pathophysiological states can be explained, at least in part, by differences in the expression and/or activity of ion channels on functionally distinct smooth muscle cell types (Neylon et al. 1994a; Archer et al. 1996). Because calcium ions (Ca^{2+}) play a pivotal role in the control of many smooth muscle cell functions, ion channels that regulate Ca^{2+} are clearly of functional importance. A class of ion channels known to modulate intracellular Ca^{2+} are the Ca^{2+}-activated K^+ channels (Vergara et al. 1998). Activation of these channels produces membrane hyperpolarization which reduces vascular contractility by limiting Ca^{2+} influx through voltage-gated

Ca^{2+} channels (Brayden et al. 1992; Nelson et al. 1995). It is reported a marked contrast in the magnitude of a Ca^{2+}-activated K^+ channels current between smooth muscle cell types that differ in their morphology and proliferative capacity (Neylon et al. 1994b). This finding indicated that the functional properties of smooth muscle may be dependent in part on the expression and activity of Ca^{2+}-activated K^+ channels.

Köhler et al. demonstrated that growth factor stimulation of A7r5 rat aortic smooth muscle cell proliferation was blocked by TRAM-34 (Köhler et al. 2003), while Neylon and colleagues (Shepherd et al. 2007) demonstrated that blockade of IK_{Ca} channels with clotrimazole and TRAM-34 prevented growth factor induced proliferation of airway smooth muscle cells. Tharp et al. demonstrated that IK_{ca} channel was upregulated by PDGF-BB, and that TRAM-34 blocked PDGF-BB induced downregulation of smooth muscle specific marker genes, and thus smooth muscle cell phenotypic modulation in vitro (Tharp et al. 2006). Furthermore, they observed increased KCa3.1 (IK_{ca} channel) mRNA expression in proliferating porcine coronary medial cells taken from swine demonstrating signs of early atherosclerosis induced by a hypercholesterolemic diet (Tharp et al. 2006). TRAM-34 prevented IK_{Ca} channel upregulation 2 h post-angioplasty, downregulation of SMMHC 2 days post-angioplasty, and reduced restenosis 14 and 28 days post-angioplasty (Tharp et al. 2008). These data demonstrate IK_{Ca} channel upregulation is necessary for smooth muscle cell dedifferentiation, proliferation, and migration, which contributes to arterial lesion development. Therefore, investigating the pathways responsible for IK_{Ca} channel upregulation is vital to understanding the progression of vessel disease. Blockade of IK_{Ca} channel, or inhibition of the pathway(s) responsible for its upregulation, represents a potential treatment for reducing post-angioplasty restenosis

Upregulation of IK_{Ca} channel by growth factors appears to be mediated largely *via* activation of the traditional MEK/ERK kinase cascade. Basic fibroblast growth factor (FGF) increases IK_{Ca} channel expression *via* the ERK pathway in fibroblasts (Pena et al. 2000), as well as in human umbilical vein endothelial cells (Grgic et al. 2005), which leads to increased cell proliferation. In A7r5 cells, PDGF-BB induced upregulation of IK_{Ca} channel was found to be dependent on the phosphorylation of ERK1/2 as well as Ca^{2+} mobilization (Si 2006). Ghanshani et al described the role of IK_{Ca} channel in Tcell activation, and demonstrated that IK_{Ca} channel activation and mRNA expression was increased with PKC (Ghanshani et al. 2000). Interestingly, both ERK and PKC can activate *c-jun* and *c-fos*, which bind to AP-1 promoter response elements. The KCa3.1 promoter region contains 7 putative activator protein-1 (AP-1) motifs, and mutations in the 5′-AP-1 motif abolished induction of KCa3.1 with T-cell activation (Ghanshani et al. 2000). AP-1 as a common end point for signaling cascades regulating IK_{Ca} channel expression.

Evidence in the literature to date strongly supports a significant role for IK_{Ca} channels in the vasculature in both physiological and pathophysiological conditions. Upregulation of IK_{Ca} channel has been demonstrated to be an early and necessary step in smooth muscle cell phenotypic modulation, proliferation, and migration, which

will impact the onset and development of numerous vasculoproliferative diseases, such as atherosclerotic and post-angioplasty restenotic lesions. Therefore, IK_{Ca} channel holds significant promise as a therapeutic target for vascular disease.

5.6 Conclusion and Perspectives

IK_{ca} channels play important roles in physiological and pathophysiological conditions. The regulation of IK_{ca} channel modulation and expression can be a strong therapeutic tool in various vascular diseases.

References

Alexander SPH, Mathie A, Peters JA (2008) Guide to receptors and Channels (GRAC), 3rd edition (2008 revision). Br J Pharmacol 153(Suppl. 2):S1–S209

Alvarez E, Northwood IC, Gonzalez FA, Latour DA, Seth A, Abate C, Curran T, Davis RJ (1991) Pro-Leu-Ser/Thr-Pro us consensus primary sequence for substrate protein phosphorylation. Characterization of the phosphorylation of c-myc and c-jun proteins by an epidermal growth factor receptor threonine 669 protein kinase. J Biol Chem 266:15277–15285

Archer S, Huang J, Reeve H, Hampl V, Tolarova S, Michelakis E, Weir E (1996) Differential distribution of electrophysiologically distinct myocytes in conduit and resistance arteries determines their response to nitric oxide and hypoxia. Circ Res 78:431–442

Atkinson NS, Robertson GA, Ganetzky B (1991) A component of calcium-activated potassium channels encoded by the Drosophila slo locus. Science 253:551–555

Bentzen BH, Nardi A, Calloe K, Madsen LS, Olesen SP, Grunnet M (2007) The small molecule NS11021 is a potent and specific activator of Ca^{2+}-activated big-conductance K^+ channels. Mol Pharmacol 72:1033–1044

Berdiev BK, Prat AG, Cantiello HF, Ausiello DA, Fuller CM, Jovov B, Benos DJ, Ismailov II (1996) Regulation of epithelial sodium channels by short actin filaments. J Biol Chem 271:17704–17710

Bond CT, Maylie J, Adelman JP (1999) Small-conductance calcium-activated potassium channels. Ann N Y Acad Sci 868:370–378

Brayden J, Nelson M (1992) Regulation of arterial tone by activation of calcium-dependent potassium channels. Science 256:532–535

Campos Rosa J, Galanakis D, Piergentili A, Bhandari K, Ganellin CR, Dunn PM, Jenkinson DH (2000) Synthesis, molecular modeling, and pharmacological testing of bis-quinolinium cyclophanes: potent, nonpeptidic blockers of the apamin-sensitive Ca^{2+}-activated K^+ channel. J Med Chem 43: 420–431

Cantiello HF (1996) Role of the actin cytoskeleton in the regulation of the cystic fibrosis transmembrane conductance regulator. Exp Physiol 81:505–514

Cao Y, Dreixler JC, Roizen JD, Roberts MT, Houamed KM (2001) Modulation of recombinant small-conductance Ca^{2+}-activated K^+ channels by the muscle relaxant chlorzoxazone and structurally related compounds. J Pharacol Exp Ther 296: 683–689

Castle NA (1999) Recent advances in the biology of small conductance calcium-activated potassium channels. Perspect Drug Discov Design 15(16):131–154

Cory JG, Carter GL, Karl RC (1987) Calcium ion-dependent proliferation of L1210 cells in culture. Biochem Biophys Res Commun 145:556–62

Davis MJ, Hill MA (1999) Signaling mechanisms underlying the vascular myogenic response. Physiol Rev 79:387–423

Dunn PM (1999) UCL 1684: a potent blocker of Ca^{2+}-activated K^+ channel in rat adrenal chromaffin cells in culture. Eur J Pharmacol 368:119–123

Fanger CM, Ghanshani S, Logsdon NJ, Rauer H, Kalman K, Zhou J, Beckingham K, Chandy KG, Cahalan MD, Aiyar J (1999) Calmodulin mediates calcium-dependent activation of the intermediate conductance KCa channel, $IK_{ca}1$. J Biol Chem 274:5746–5754

Fanger CM, Rauer H, Neben AL, Miller MJ, Rauer H, Wulff H, Rosa JC, Ganellin CR, Chandy KG, Cahalan MD (2001) Calcium-activated potassium channels sustain calcium signaling in T lymphocytes. Selective blockers and manipulated channel expression levels. J Biol Chem 276(15):12249–12256

Fernandes-Santos C, de Souza Mendonça L, Mandarim-de-Lacerda CA (2009) Favorable cardiac and aortic remodeling in olmesartan-treated spontaneously hypertensive rats. Heart Vessels 24:219–227

Fioretti B, Pietrangelo T, Catacuzzeno L, Franciolini F (2005) Intermediate-conductance Ca^{2+}-activated K^+ channel is expressed in C2C12 myoblsts and is downregulated during myogenesis. Am J Physiol 289:C89-C96

Folkow B (1995) Integration of hypertension research in the era of molecular biology. J Hypertens 13:5–18

Frid MG, Dempsey EC, Durmowicz AG, Stenmark KR (1997) Smooth muscle cell heterogeneity in pulmonary and systemic vessels. Importance in vascular disease. Arterioscler Thromb Vasc Biol 17:1203–1209

Furukawa T, Yamane T, Terai T, Katayama Y, Hirakoka M (1996) Functional linkage of the cardiac ATP-sensitive K^+ channel to the actin cytoskeleton. Pflügers Arch 431:504–512

Gardos G (1958) The function of calcium in the potassium permeability of human erythrocytes. Biochim Biophys Acta 30(3):653–654

Gauthier KM, Spitzbarth N, Edwards EM, Campbell WB (2004) Apamin-sensitive K^+ currents mediate arachidonic acid-induced relaxations of rabbit aorta. Hypertension 43:413–419

Gauthier KM, Chawengsub Y, Goldman DH, Conrow RE, Anjaiah S, Falck JR, Campbell WB (2008) 1(R),12(S),15(S)-trihydroxyeicosa-5(Z),8(Z),13(E)-trienoic acid: an endothelium-derived 15-lipoxygenase metabolite that relaxes rabbit aorta. Am J Physiol Heart Circ Physiol 294**:**H1467–H1472

Gebremedhin D, Kaldunski M, Jacobs ER, Harder DR, Roman RJ (1996) Coexistence of two types of calcium activated potassium channels in rat renal arterioles. Am J Physiol 270:F69–F81

Gerlach AC, Gangopadhyay NN, Devor DC (2000) Kinase-dependent regulation of the intermediate conductance, calcium-dependent potassium channel, hIK1. J Biol Chem 275:585–598

Gerlach AC, Syme CA, Giltinan L, Adelman JP, Devors DC (2001) ATP-dependent activation of the intermediate conductance, Ca^{2+}-activated K^+ channel, hIK1, is conferred by a C-terminal domain. J Biol Chem 276:10963–10970

Ghanshani S, Wulff H, Miller MJ, Rohm H, Neben A, Gutman GA, Cahalan MD, Chandy KG (2000) Up-regulation of the $IK_{ca}1$ potassium channel during T-cell activation. Molecular mechanism and functional consequences. J Biol Chem 275: 37137–37149

Grgic I, Eichler I, Heinau P, Si H, Brakemeier S, Hoyer J, Kohler R (2005) Selective blockade of the intermediate-conductance Ca^{2+}-activated K^+ channel suppresses proliferation of microvascular and macrovascular endothelial cells and angiogenesis In vivo. Arterioscler Thromb Vasc Biol 25:704–709

Gribkoff VK, Starett JE, Jr, Dworetzky SI (2001) Maxi-K potassium channels: form, function and modulation of a class of endogenous regulators of intracellular calcium. Neuroscientist 7:166–177

Guo DF, Sun YL, Hamet P, Inagami T (2001) The angiotensin II type 1 receptor and receptor-associated proteins. Cell Res 11:165–180

Gurantz D, Cowling RT, Varki N, Frikovsky E, Moore CD, Greenberg BH (2005) IL-1b and TNF-a upregulate angiotensin II type 1 (AT1) receptors on cardiac fibroblasts and are associated with increased AT1 density in the post-MI heart. J Mol Cell Cardiol 38:505–515

Gutman GA, Chandy GK, Adelman JP, Aiyar J, Bayliss DA, Clapham DE, Covarriubias M, Desir GV, Furuichi K, Ganetzky B, Garcia ML, Grissmer S, Jan LY, Karschin A, Kim D, Kuperschmidt S, Kurachi Y, Lazdunski M, Lesage F, Lester HA, McKinnon D, Nichols CG, O'Kelly I, Robbins J, Robertson GA, Rudy B, Sanguinetti M, Seino S, Stuehmer W, Tamkun MM, Vandenberg CA, Wei A, Wulff H, Wymore RS; International Union of Pharmacology (2003) International Union of Pharmacology. XLI. Compendium of Voltage-Gated Ion Channels: Potassium Channels. Pharmacol Rev 55: 583–586

Hamill OP, Martinac B (2001) Molecular basis of mechanotransduction in living cells. Physiol Rev 81:685–740

Hayabuchi Y, Davies NW, Standen NB (2001a) Angiotensin II inhibits rat arterial KATP channels by inhibiting steady-state protein kinase A activity and activating protein kinase Ce. J Physiol 530:193–205

Hayabuchi Y, Standen NB, Davies NW (2001b) Angiotensin II inhibits and alters kinetics of voltage-gated K^+ channels of rat arterial smooth muscle. Am J Physiol 281:H2480–2489

Hayabuchi Y, Nakaya Y, Yasui S, Mawatari K, Mori K, Suzuki M, Kagami S (2006) Angiotensin II activates intermediate-conductance Ca^{2+}-activated K^+ channels in arterial smooth muscle cells. J Mol Cell Cardiol 41:972–979

Hayabuchi Y, Nakaya Y, Mawatari K, Inoue M, Sakata M, Kagami S (2011) Cell membrane stretch activates intermediate-conductance Ca^{2+}-activated K^+ channels in arterial smooth muscle cells. Heart Vessels 26:91–100

Hayashi M, Kunii C, Takahata T, Ishikawa T (2004) ATP-dependent regulation of SK4/IK1-like currents in rat submandibular acinar cells: possible role of cAMP-dependent protein kinase. Am J Physiol 286:C635–646

Hazelton B, Mitchell B, Tupper J (1979) Calcium, magnesium, and growth control in the WI-38 human fibroblast cell. J Cell Biol 83:487–498

Hosokawa H, Aiuchi S, Kambe T, Hagiwara Y, Kubo T (2002) Mechanical stretch-induced mitogen-activated protein kinase activation is mediated via angiotensin and endothelin systems in vascular smooth muscle cells. Biol Pharm Bull 25:1588–1592

Hougaard C, Eriksen BL, Jørgensen S, Johansen TH, Dyhring T, Madsen LS,, Strøbaek D, Christophersen P (2007) Selective positive modulation of the SK3 and SK2 subtypes of small conductance Ca^{2+}-activated K^+ channels. Br J Pharmacol 151:655–665

Ingber DE. Tensegrity (1997) The architectural basis of cellular mechanotransduction. Annu Rev Physiol 59:575–599

Ishii TM, Silvia C, Hirschberg B, Bond CT, Adelman JP, Maylie J (1997) A human intermediate conductance calcium-activated potassium channel. Proc Natl Acad Sci USA 94:11651–11656

Jensen BS, Strøbaek D, Olesen SP, Christophersen P (2001) The Ca^{2+}-activated K^+ channel of intermediate conductance: a molecular target for novel treatments? Curr Drug Targets 2(4):401–422

Joiner WJ, Wang LY, Tang MD, Kaczmarek LK (1997) hSK4, a member of a novel subfamily of calcium-activated potassium channels. Proc Natl Acad Sci USA 94:11013–11018

Khanna R, Chang MC, Joiner WJ, Kaczmarek LK, Schlichter LC (1999) hSK4/hIK1, a calmodulin-binding KCa channel in human T lymphocytes. Roles in proliferation and volume regulation. J Biol Chem 274:14838–14849

Koegel H, Alzheimer C (2001) Expression and biological significance of Ca^{2+}-activated ion channels in human keratinocytes. FASEB J 15(1):145–154

Köhler M, Hirschberg B, Bond CT, Kinzie JM, Marrion NV, Maylie J, Adelman JP (1996). Small-conductance calcium-activated K^+ channels from mammalian brain. Science 273:1709–1714

Köhler R, Wulff H, Eichler I, Kneifel M, Neumann D, Knorr A, Grgic I, Kämpfe D, Si H, Wibawa J, Real R, Borner K, Brakemeier S, Orzechowski HD, Reusch HP, Paul M, Chandy KG, Hoyer J (2003) Blockade of the intermediate-conductance calcium-activated potassium channel as a new therapeutic strategy for restenosis. Circulation 108:1119–1125

Kosako H, Gotoh Y, Matsuda S, Ishikawa M, Nishida E (1992) Xenopus MAP kinase activator is a serine/threonine/tyrosine kinase activated by threonine phosphorylation. EMBO J 11:2903–2908

Kubo T, Hosokawa H, Kambe T, Fukumori R (2000) Angiotensin II mediates pressure loading – induced mitogen-activated protein kinase activation in isolated rat aorta. Eur Pharmacol 391:281–287

Latorre R, Brauchi S (2006). Large conductance Ca^{2+}-activated K^+ (BK) channel: activation by Ca^{2+} and voltage. Biol Res 39:385–401

Latorre R, Oberhauser A, Labarca P, Alvarez O (1989) Varieties of calcium-activated potassium channels. Annu Rev Physiol 51:385–99

Lepple-Wienhues A, Berweck S, Böhmig M, Leo CP, Meyling B, Garbe C, Wiederholt M (1996) K^+ channels and the intracellular calcium signal in human melanoma cell proliferation. J Membr Biol 151:149–157

Leuranguer V, Gluais P, Vanhoutte PM, Verbeuren TJ, Félétou M (2008) Openers of calcium-activated potassium channels and endothelium-dependent hyperpolarizations in the guinea pig carotid artery. Naunyn Schmiedebergs Arch Pharmacol 377:101–109

Li C, Wernig F, Leitges M, Hu Y, Xu Q (2003) Mechanical stress-activated PKCdelta regulates smooth muscle cell migration. FASEB J 17:2106–2108

Liegeois JF, Mercier F, Graulich A, Graulich-Lorge F, Scuvee-Moreau J, Setin V (2003) Modulation of small conductance calcium-activated potassium (SK) channels: a new challenge in medicinal chemistry. Curr Med Chem 10:625–647

Lucchesi PA, Bell JM, Willis LS, Byron KL, Corson MA, Berk BC (1996) Ca^{2+}-dependent mitogen-activated protein kinase activation in spontaneously hypertensive rat vascular smooth muscle defines a hypertensive signal transduction phenotype. Circ Res 78:962–970

Maher AD, Kuchel PW (2003) The Gárdos channel: a review of the Ca^{2+}-activated K^+ channel in human erythrocytes. Int J Biochem Cell Biol 35(8):1182–97

Matsusaka T, Ichikawa I (1997) Biological functions of angiotensin and its receptors. Annu Rev Physiol 59:395–412

McMurtry MS, Bonnet S, Wu X, Dyck JR, Haromy A, Hashimoto K, Michelakis ED (2004) Dichloroacetate prevents and reverses pulmonary hypertension by inducing pulmonary artery smooth muscle cell apoptosis. Circ Res 95:830–40

Meera P, Wallner M, Toro L (2001) Molecular biology of highconductance, Ca^{2+}-activated potassium channels. In: Archer S, Rush N (eds). Potassium Channels in Cardiovascular Biology. Kluwer Academic/Plenium Publishers: New York, pp 49–70

Nardi A, Olesen SP (2008) BK channel modulators: a comprehensive overview. Curr Med Chem 15:1126–1146

Nelson MT, Quayle JM (1995) Physiological roles and properties of potassium channels in arterial smooth muscle. Am J Physiol 268:C799–822

Nelson M, Cheng H, Rubart M, Santana L, Bonev A, Knot H, Lederer W (1995) Relaxation of arterial smooth muscle by calcium sparks. Science 270:633–637

Neylon CB, Avdonin PV, Dilley RJ, Larsen MA, Tkachuk VA, Bobik A (1994a) Different electrical responses to vasoactive agonists in morphologically distinct smooth muscle cell types. Circ Res 75:733–741

Neylon CB, Avdonin PV, Larsen MA, Bobik A (1994b) Rat aortic smooth muscle cells expressing charybdotoxin-sensitive potassium channels exhibit enhanced proliferative responses. Clin Exp Pharmacol Physiol 21:117–120

Neylon CB, Lang RJ, Fu Y, Bobik A, Reinhart PH (1999) Molecular cloning and characterization of the intermediate-conductance Ca^{2+}-activated K^+ channel in vascular smooth muscle: relationship between Kca channel diversity and smooth muscle cell function. Circ Res 85:e33–43

Nilius B, Wohlrab W (1992) Potassium channels and regulation of proliferation of human melanoma cells. J Physiol 445:537–548

Ouadid-Ahidouch H, Le Bourhis X, Roudbaraki M, Toillon RA, Delcourt P, Prevarskaya N (2001) Changes in the K^+ current-density of MCF-7 cells during progression through the cell cycle: possible involvement of a h-ether.a-gogo K^+ channel. Receptors Channels 7(5):345–56

Ouadid-Ahidouch H, Roudbaraki M, Delcourt P, Ahidouch A, Joury N, Prevarskaya N (2004) Functional and molecular identification of intermediate-conductance Ca^{2+}-activated K^+channels in breast cancer cells: association with cell cycle progression. Am J Physiol 287:C125-C134

Owens GK (1995) Regulation of differentiation of vascular smooth muscle cells. Physiol Rev 75:487–517

Pedarzini P, D'hoedt D, Doorty KB, Wadsworth JDF, Joseph JS, Jeyaseelan K, Kini RM, Gadre SV, Sapatnekar SM, Stocker M, Strong PN (2002) Tapamin, a venom peptide from the Indian red scorpion (Mesobuthus tamulus) that targets small conductance Ca^{2+}-activated K^+ channels and afterhyperpolarization currents in central neurons. J Biol Chem 277:46101–46109

Pena TL, Chen SH, Konieczny SF, Rane SG (2000) Ras/MEK/ERK Up-regulation of the fibroblast KCa channel FIK Is a common mechanism for basic fibroblast growth factor and transforming growth factor-beta suppression of myogenesis. J Biol Chem 275:13677–13682

Pulverer BJ, Kyriakis JM, Avruch J, Nikolakaki E, Woodqett JR (1991) Phosphorylation of c-jun mediated by MAP kinases. Nature 353:670–674

Quignard JF, Félétou M, Edwards G, Duhault J, Weston AH, Vanhoutte PM (2000) Role of endothelial cell hyperpolarization in EDHFmediated responses in the guinea-pig carotid artery. Br J Pharmacol 129:1103–1112

Reeve HL, Weir EK, Archer SL, Cornfield DN (1998) A maturational shift in pulmonary K1 channels, from Ca^{2+} sensitive to voltage dependent. Am J Physiol 275:L1019–1025

Remillard CV, Yuan JX (2004) Activation of K^+ channels: an essential pathway in programmed cell death. Am J Physiol Lung Cell Mol Physiol 286(1):L49–67

Rufo PA, Merlin D, Riegler M, Ferguson-Maltzman MH, Dickinson BL, Brugnara C, Alper SL, Lencer WI (1997) The antifungal antibiotic, clotrimazole, inhibits chloride secretion by human intestinal T84 cells via blockade of distinct basolateral K^+ conductances. Demonstration of efficacy in intact rabbit colon and in an in vivo mouse model of cholera. J Clin Invest 100(12):3111–3120

Saito T, Fujiwara Y, Fujiwara R, Hasegawa H, Kibira S, Miura H, Miura M (2002) Role of augmented expression of intermediate-conductance Ca^{2+}-activated K^+ channels in postischaemic heart. Clin Exp Pharmacol Physiol 29:324–329

Sartore S, Chiavegato A, Franch R, Faggin E, Pauletto P (1997) Myosin gene expression and cell phenotypes in vascular smooth muscle during development, in experimental models, and in vascular disease. ArteriosclerThromb Vasc Biol 17:1210–1215

Schilling T, Eder C (2007) TRAM-34 inhibits nonselective cation channels. Pflugers Arch 454: 559–563

Schwab A (2001) Function and spatial distribution of ion channels and transporters in cell migration. Am J Physiol 28:F739-F747

Setoguchi M, Ohya Y, Abe I, Fujishima M (1997) Stretch-activated whole-cell currents in smooth muscle cells from mesenteric resistance artery of guinea-pig. J Physiol 501:343–353

Shepherd MC, Duffy SM, Harris T, Cruse G, Schuliga M, Brightling CE, Neylon CB, Bradding P, Stewart AG (2007) KCa3.1 Ca^{2+}activated K^+ channels regulate human airway smooth muscle proliferation. Am J Respir Cell Mol Biol 37(5):525–531

Shieh C-C, Coghlan M, Sullivan JP, Gopalakrishnan M (2000) Potassium channels: molecular defects, diseases and therapeutic opportunities. Pharmacol Rev 52: 557–593

Si H, Grgic I, Heyken WT, Maier T, Hoyer J, Reusch HP, Kohler R (2006) Mitogenic modulation of Ca^{2+}-activated K^+ channels in proliferating A7r5 vascular smooth muscle cells. Br J Pharmacol 148:909–917

Stocker M (2004) Ca^{2+}-activated K^+ channels: molecular determinants and function of the SK family. Nat Rev Neurosci 5(10):758–770

Strøbaek D, Joergensen TD, Christophersen P, Ahring PK, Olesen SP (2000) Pharmacological characterization of small-conductance Ca^{2+}-activated K^+ channels stably expressed in HEK 293 cells. Br J Pharmacol 129:627–630

Strøbaek D, Teuber L, Jørgensen TD, Ahring PK, Kjaer K, Hansen RS, Olesen SP, Christophersen P, Skaaning-Jensen B (2004) Activation of human IK and SK Ca^{2+}-activated K^+ channels by NS309 (6,7-dichloro-1H-indole-2,3-dione 3-oxime). Biochim Biophys Acta 1665:1–5

Sturgill TW, Ray LB, Erikson E, Maller JL (1988) Insulin-stimulated MAP-2 kinase phosphorylates and activates ribosomal protein S6 kinase II. Nature 334:715–718

Terata Y, Saito T, Fujiwara Y, Hasegawa H, Miura H, Watanabe H, Chiba Y, Kibira S, Miura M (2003) Pitavastatin inhibits upregulation of intermediate conductance calcium-activated potassium channels and coronary arteriolar remodeling induced by long-term blockade of nitric oxide synthesis. Pharmacology 68:169–176

Tharp DL, Wamhoff BR, Turk JR, Bowles DK (2006) Upregulation of intermediate-conductance Ca^{2+}-activated K^+ channel ($IK_{ca}1$) mediates phenotypic modulation of coronary smooth muscle. Am J Physiol Heart Circ Physiol 291:H2493–H2503

Tharp DL, Wamhoff BR, Wulff H, Raman G, Cheong A, Bowles DK (2008) Local delivery of the KCa3.1 blocker, TRAM-34, prevents acute angioplasty-induced coronary smooth muscle phenotypic modulation and limits stenosis. Arterioscler Thromb Vasc Biol 28:1084–1089

Toro L, Amador M, Staefani E (1990) ANG II inhibits calcium-activated potassium channels from coronary smooth muscle in lipid bilayers. Am J Physiol 258:H912–H915

Vergara C, Latorre R, Marrion NV, Adelman JP (1998) Calcium-activated potassium channels. Curr Opin Neurobiol 8:321–329

Verheugen JA, Le Deist F, Devignot V, Korn H (1997) Enhancement of calcium signaling and proliferation responses in activated human T lymphocytes. Inhibitory effects of K^+ channel block by charybdotoxin depend on the T cell activation state. Cell Calcium 21:1–17

Williams B (1998) Mechanical influences on vascular smooth muscle cell function. J Hypertens 16:1921–1926

Wilson DP, Saward L, Zahradka P, Cheung PK (1999) Angiotensin II receptor antagonists prevent neointimal proliferation in a porcine coronary artery organ culture model. Cardiovasc Res 42:761–772

Wonderlin WF, Strobl JS (1996) Potassium channels, proliferation and G1 progression. J Membr Biol 154(2):91–107

Wonderlin WF, Woodfork KA, Strobl JS (1995) Changes in membrane potential during the progression of MCF-7 human mammary tumor cells through the cell cycle. J Cell Physiol 165(1):177–185

Woodfork KA, Wonderlin WF, Peterson VA, Strobl JS (1995) Inhibition of ATP-sensitive potassium channels causes reversible cell-cycle arrest of human breast cancer cells in tissue culture. J Cell Physiol 162(2):163–171

Wulf A, Schwab A (2002) Regulation of a calcium-sensitive K^+ channel (cIK1) by protein kinase C. J Membr Biol 187:71–79

Wulff H, Miller MJ, Haensel W, Grissner S, Cahalan MD, Chandy KG (2000) Design of potent and selective inhibitor of the intermediate-conductance Ca^{2+}-activated K^+ channel, $IK_{ca}1$: a potential immunosuppressant. Proc Natl Acad Sci USA 97:8151–8156

Wulff H, Beeton C, Chandy KG (2003) Potassium channels as therapeutic targets for autoimmune disorders. Curr Opin Drug Discov Devel 6(5):640–647

Wulff H, Knaus HG, Pennington M, Chandy KG (2004) K^+ Channel expression during B cell differentiation: Implications for immunomodulation and autoimmunity. J Immunol 173:776–786

Wulff H, Kolski-Andreaco A, Sankaranarayanan A, Sabatier JM, Shakkottai V (2007) Modulators of small- and intermediateconductance calcium-activated potassium channels and their therapeutic indications. Curr Med Chem 14:1437–1457

Wu X, Davis MJ (2001) Characterization of stretch-activated cation current in coronary smooth muscle cells. Am J Physiol Heart Circ Physiol 280:H1751–H1761

Xia XM, Fakler B, Rivard A, Wayman G, Johnson-Pais T, Keen JE, Ishii T, Hirschberg B, Bond CT, Lutsenko S, Maylie J, Adelman JP (1998) Mechanism of calcium-gating in small-conductance calcium-activated potassium channels. Nature 395:503–507

Xu CQ, Brône B, Wicher D, Bozkurt O, Lu WY, Huys I, Han YH, Tytgat J, Van Kerkhove E, Chi CW (2004) BmBKTx1, a novel Ca^{2+}-activated K^+ channel blocker purified from the Asian scorpion Buthus martensi Karsch. J Biol Chem 279:34562–34569

Zeng H, Gordon EA, Lin Z, Lozinskaya IM, Willette RN, Xu X (2008) 1-[1-hexyl-6-(methyloxy)-1H-indazol-3-yl]-2-methyl-1-propanone (HMIMP), a potent and highly selective small molecule blocker of the large-conductance voltage-gated and calcium-dependent K^+ channel. J Pharmacol Exp Ther 327:168–177

Zhou XB, Ruth P, Schlossmann J, Hofmann F, Korth M (1996) Protein phosphatase 2 A is essential for the activation of Ca^{2+}-activated K^+ currents by cGMP-dependent protein kinase in tracheal smooth muscle and Chinese hamster ovary cells. J Biol Chem 271:19760–19767

Chapter 6
Sensing Mechanism of Stretch Activated Ion Channels

Naomi Niisato and Yoshinori Marunaka

6.1 Introduction

Physical stresses/mechanical force such as expansile force (membrane tension), osmotic pressure, hydrostatic pressure, shear stress, and gravity are crucial stimuli for cells in various tissues to control their proliferation, differentiation, development and cell death. For instance, the transpulmonary pressure balance produced by appropriate lung fluid is crucial for normal lung growth and development in the fetal late stages (Hooper et al. 2006). The airways and alveoli of the fetal lung are filled with fluid. Tracheal ligation, which impedes the outflow of fluid from the trachea, produces large fluid-filled lungs (Alcorn et al. 1997; Carmel et al. 1965), and increases hydrostatic pressure to expand the lung. In contrast, tracheal drainage reduces the hydrostatic pressure by excreting the fluid from the inside of lung to the outside. Previous studies with fetal lamb have indicated that lung growth and development is stimulated by tracheal ligation-increased expansion of lung (Alcorn et al. 1997; Fewell et al. 1983), and is inhibited by tracheal drainage (Alcorn et al. 1997). So far, various *in vivo* and *in vitro* model systems have been developed to investigate the mechanotransduction process. In the lung epithelial cells and fibroblasts, mechanical force is mainly recognized by membrane proteins such as stretch-activated cation (SAC) channels and receptor tyrosine kinases that transduce the mechanical force into intracellular signal molecules associated with their proliferation and differentiation (Liu et al. 1995, 1999). For the cardiovascular systems, endothelial cells, smooth muscle cells and cardiac myocytes are the major cells that face mechanical force including vessel stretch and cardiac stretch. Blood pressure is the major determinant of vessel stretch, and blood volume and pressure are the major determinants of cardiac stretch. Mechanical forces in the cardiovascular systems have been categorized into at least three elements; magnitude, frequency and duration in cyclic stretch. Although cells in cardiovascular systems are exposed to a dynamic mechanical environment

N. Niisato (✉) · Y. Marunaka
Department of Molecular Cell Physiology, Graduate School of Medical Sciences,
Kyoto Prefectural University of Medicine, Kyoto 602-8566, Japan
e-mail: naomi@koto.kpu-m.ac.jp

A. Kamkin, I. Lozinsky (eds.), *Mechanically Gated Channels and their Regulation,*
Mechanosensitivity in Cells and Tissues 6,
DOI 10.1007/978-94-007-5073-9_6,

modified by pulsatile pressure and oscillatory shear forces, they should have mechanisms sensing these mechanical stimuli. Endothelial cells are mainly exposed to shear stress produced by flowing blood that is known to cause stress fibers aligned perpendicular to the stretch direction for bearing less tension and remodeling of endothelial cells (Chien 2007; Taber 1998). Mechanical stretch in vascular smooth muscle cells *in vitro* can cause a uniform alignment almost perpendicular to stretch vector (Lehoux et al. 2000; Standly et al. 2002). These phenomena show that cells in vascular system sense both magnitude and direction of mechanical force, and that cytosckelton and extracellular matrix molecules complementarily support the basic sensing mechanism through membrane tension. Further, shear stress, osmotic pressure and hydrostatic pressure are also important stimuli for Na^+ reabsorption to control extracellular fluid volume and blood pressure in renal tubule. When epithelial cells in cortical collecting duct (CCD) are exposed to the decreased plasma osmolality, epithelial Na^+ channel (ENaC)-mediated Na^+ reabsorption in CCD is stimulated to recover normal plasma osmolality, suggesting that epithelial cells in CCD have ability to sense changes in extracellular osmolality and precisely respond to it by increasing both translocation and gene expression of ENaC (Niisato et al. 2000; Taruno et al. 2007). On the other hand, weightlessness and being bedridden accelerate bone resorption, indicating that physical stress/mechanical force by gravity and exercise is necessary for osteogenesis (Carmeliet et al. 2001; LeBlanc et al. 2007).

As described above, it is well known that physical stress/mechanical force is a crucial signal for diverse cellular functions likely chemical stimuli. In previous studies, the existence of mechanosensitive ion (MS) channels have been recognized in various cells and tissues, and MS channels are considered to be involved in sensing physical stress/mechanical force (Arnadóttir et al. 2010; Yoshimura et al. 2010). Currently, MS channels are believed to play central roles in mechanotrasduction and to convert physical stress/mechanical force into intracellular signals that contribute to physiological functions in their expressed cells and tissues.

6.2 MS Channels in Bacteria for Sensing Osmotic Pressure

6.2.1 Physiological Importance of MS Channels

Prokaryotic cells possess MS channels that sense mechanical force to survive and adjust to a new environment. When bacteria cells are exposed to hypotonic environments (for example, exposure to rain), the cells protect themselves against the hypotonicity-caused lysis by activating MscS (mechanosensitive channel with small conductance) and MscL (mechanosensitive channel with large conductance) (Kung et al. 2010; Levina et al. 1999; Batiza et al. 2002) that release cytosolic components for reduction of intracellular osmotic pressure adapting to extracellular hypotonic environments. Especially, in bacteria cell as monad, the action of MS channel to avoid hypotonic lysis is closely related to a matter of life and death. In bacteria cells,

MS channels are considered to be activated by an increase of membrane tension due to cell swelling (Levina et al. 1999) in response to hypotonic stress and serve as 'emergency valves'. Notably, for bacteria cells, sensing magnitudes of changes in extracellular osmolality is essential to determine amounts of cytosolic components to be released for adaptation to reduction of extracellular hypotonic pressure. Therefore, these two MS channels with different conductance, MscS and MscL, are activated at different tension thresholds and control amounts of cytosolic components to be released through MscS and MscL. Hypotonic stress is converted to cell swelling (i.e., the changes in cell volume) through osmotic pressure-dependent water influx, which in turn produces membrane tension as mechanical force. Namely, magnitudes of hypotonic stress are transduced to magnitudes of membrane tension. This means that bacteria cells can sense changes in extracellular osmolality as magnitudes of membrane tension. The MscS and MscL channels open, when the membrane tension is larger than their thresholds. If hypotonic stress is weak or moderate, only MscS with small conductance is activated, because the amount of cytosolic component to be released in response to the hypotonic stress is relatively small. On the contrary, if hypotonic stress is strong, both MscS and MscL should be activated for releasing large amounts of cytosolic component. These regulatory mechanisms of two MS channels physiologically seem to be reasonable and similar to regulatory volume decrease (RVD) as regulatory mechanisms of cell volume observed in higher organisms.

6.2.2 MscL (Mechanosensitive Channel with large Conductance)

MscL in *Escherichia coli* (EcMscL) and *Mycobacterium tuberculosis* (TbMscL) is one of the most studied MS channels in prokaryotic cells. MscL is a homo-pentamer (Fig. 6.1a) and each subunit has two transmembrane domains, TM1 and TM2 (Sukharev et al. 1994, 1999) (Fig. 6.1b). The sequence at amino-terminus and carboxy-terminus forms S1 and cytoplasmic helixes (CP), respectively (Fig. 6.1b). The channel pore is lined with TM1 and the gate is probably formed between two residues, A20 and G26 (Fig. 6.1c). The region facing to the membrane (lipid bilayer) comprises the whole length of TM2 and the periplasmic end of TM1. EcMscL has a conductance of 3 nS and passes low molecular substances such as inorganic ions (Ajouz et al. 1998). It is supposed that exposure of hydrophobic surface of the gate in TM1 to aqueous environments is an energy barrier for channel gating (Fig. 6.1d). Hydrophobic lock of the gate via this energy barrier stabilizes the closed structure of EcMscL. In MS channels, membrane tension is generally an energy source for activation of channel getting over the barrier (Sokabe et al. 1991; Hamill et al. 2001). Mutants in the pore-lining residues substituted with a more hydrophilic amino acid lower the gating threshold. Substitution of Gly-22 in the gate with all other 19 amino acids reveals that hydrophilicity determines the ease of gating (Fig. 6.1c). The diameter of the open pore is estimated to be as large as 3–4 nm. This large pore is formed by an iris-like rotation of the transmembrane helices: the helices tilt, while

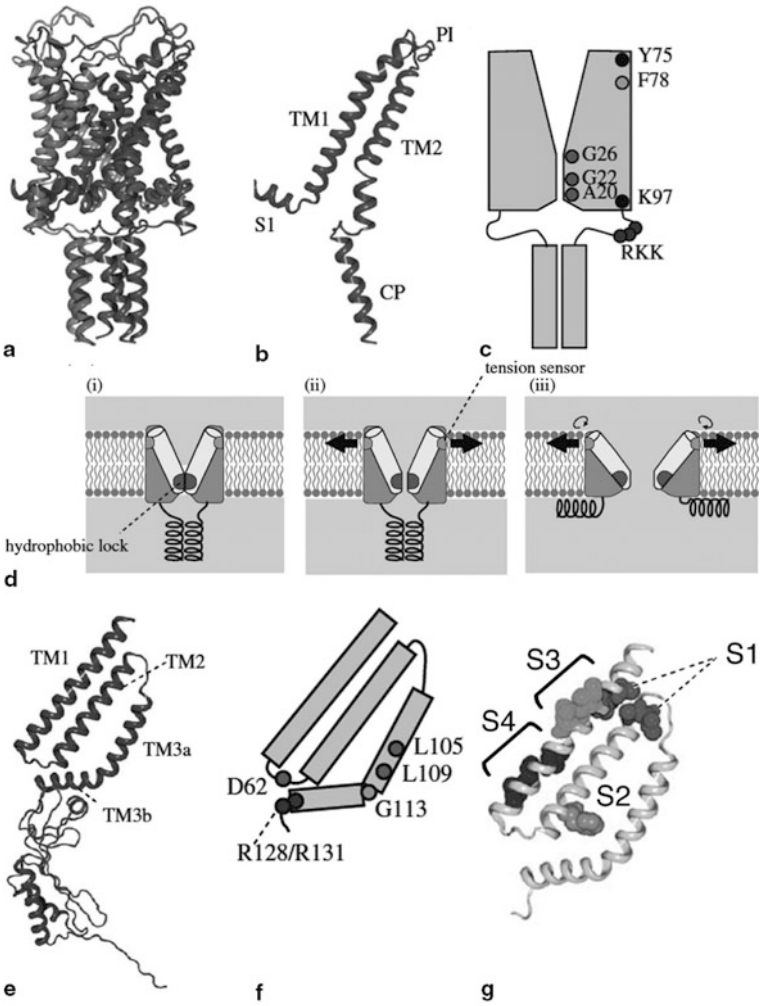

Fig. 6.1 Structure and gating model of MscL and MscS channel. **a** Crystal structure of *M. tuberculosis* MscL channel. **b** Structure of single subunit of Tb MscL. S1; N-terminal helix, TM1; the first transmembrane helix, TM2; the second transmembrane helix, PL; periplasmic loop, CP; cytoplasmic helix. **c** Positions of important residues in the schematic EcMscL. The pore is constricted between A20 and G26. Gating threshold depends upon the hydrophilicity of G22 and mechanosensitivity is lost on hydrophilic substitution of Y78. **d** Gating model of MscL. (i) The closed structure is stabilized by the hydrophobic lock of the gate. (ii) Membrane tension perceived by the tension sensor opens the gate that results in the exposure of hydrophobic lock to water. (iii) On full opening, cytoplasmic helices are disassembled. **e** Structure of single subunit MscS. TM1; the first transmembrane helix, TM2; the second transmembrane helix, TM3; the third transmembrane helix, which is separated by a kink at G113 (TM3a and TM3b). **f** Important residues for MscS function. L105 and L109 form a pore of MscS. **g** The gating threshold increases on asparagine substitution at the residues indicated by S1 (A34, I37, A85, L86), S4 (I48, A51, L55) and S2 (F68). Conversely, the threshold decreases on mutation at I39, V40 and V43 (S3). (Reproduced from Yoshimura et al. 2010 with copyright permission, Royal Society Publishing)

sliding between neighboring TM1 helices occurs (Fig. 6.1d). Further, expansion in the transmembrane domain dissociates the CP helices that probably causes association between TM2 and CP. Previous studies critically indicate that MscL opens by directly sensing changes in membrane tension, since MscL keeps mechanosensing ability in its purified and reconstituted form in liposomes (Sukharev et al. 1993; Häse et al. 1995). Notably, it is revealed that the identified 21 residues in M1 and M2 domains contribute to interaction with membrane lipid (Yoshimura et al. 2004), and that this lipid-protein interaction plays a central role in sensing membrane lipid tension directly. Especially, mapping by asparagine scanning mutagenesis in the lipid-protein interface region indicates that high-impact residues (Leu-36, Ile-40 and Ile-41 in M1 domain and Phe-78, Ile-79, Phe83 and Ile-87 in M2 domain) form clusters in the lipid-protein interface probably receiving the membrane tension (stretch) from membrane lipid through hydrophobic interaction. Further, roles of the periplasmic loop are not fully understood although a number of loss-of-function mutations are detected in this region (Li et al. 2004; Yoshimura et al. 2004). Proteolysis of the periplasmic loop in MscL markedly increases its sensitivity to membrane tension by decreasing the gating threshold, suggesting that periplasmic loop might be involved in holding MscL in the closed state (Ajouz et al. 2000; Yoshimura et al. 2004). Thus, the gating of MscL is regulated in a balance between the expansible force of MscL by membrane tension and the strength of intramolecular interaction for holding the closed conformation.

6.2.3 MscS (Mechanosensitive Channel with Small Conductance)

MscS is also a major component for adaptation of bacteria to hypotonic stress in addition to MscL (Blount et al. 1999; Levina et al. 1999). MscS is gated by both membrane tension and voltage (Martinac et al. 1987). Bass et al. have revealed that the MscS with 1 nS conductance is composed of homo-heptameric complex with three transmembrane helices in a subunit and a large cytoplasmic C-terminal domain by presenting crystallographic analysis of the 3D MscS structure (Bass et al. 2002) (Fig. 6.1e). The transmembrane domains TM1 and TM2 are thought to constitute to sensing membrane tension and voltage (Bass et al. 2002), whereas TM3, a pore lining helix, has a distinctive kink at G113, which divides TM3 into amino-terminal helix TM3a and carboxy-terminal helix TM3b (Fig. 6.1f). TM3a helices fit each other to form a tightly closed gate by inserting knobs of alanine residues into holes of glycine residues as a highly conserved region in the membrane domain (Edwards et al. 2005). The cytoplasmic domain forms a large cage. TM3b covers the upper surface of the cytoplasmic cage (Fig. 6.1e). A study by using electron paramagnetic resonance (EPR) spectroscopy indicates that one side of TM1 is exposed to membrane lipid and another side faces to other domain of the channel protein (Vasquez et al. 2008), and that TM2 is mostly buried in the protein. The gating threshold is increased by substituting four hydrophobic residues (A34, I37, A85, L86) in the periplasmic ends of TM1 and TM2 with asparagine (Fig. 6.1g; S1). Loss of hydrophobic contact between TM1

and TM2 at these ends possibly interrupts transmission of membrane tension to the channel. The mutants (I48, A51, L55) on one side of TM1 close to the cytoplasmic end also have decreased sensitivity to mechanotransduction (Fig. 6.1g; S4), leading a distorted TM1 conformation. Hydrophobic residues at border between membrane lipid and channel protein maintain the tension-sensitive conformation. Phe-68 is considered to play a crucial role in transmitting membrane tension to the gate through hydrophobic contact between TM2 and TM3a (Fig. 6.1g; S2), as Phe-68 points towards TM3 (Belyy et al. 2010). Conversely, three mutants (I39N, V40N and I43N) on the TM1 facing to lipid decrease the threshold (Fig. 6.1g; S3) (Nomura et al. 2006). Interestingly, introduction of asparagine into the most hydrophobic residues in the middle of transmembrane domains does not interrupt the mechanosensitivity. In contrast, mutations that increase the gating threshold are only at the ends of transmembrane domains. These observations suggest that residues close to the surface of the lipid bilayer are essential parts for MscS function. In previous studies, it is considered that membrane proteins are subject to a negative lateral pressure from the lipid just beneath the surface of the membrane. Therefore, proper intramolecular interactions at the level of water-lipid interface are important for the MscS function. MscS shares the same characteristics as MscL in which the interaction with lipid near the polar-apolar boundary is essential to the function.

During transition from the closed to the open state, MscS drastically changes its conformation (Miller et al. 2003, Edwards et al. 2004). TM3 is considered to be involved in the channel opening by slight iris-like rotations and tilting by expansile force (Edwards et al. 2005) likely to MscL. Further, MscS is inhibited by submillimolar concentrations of gadolinium (Gd^{3+}) likely to other MS channels (Hamill et al. 2001). Notably, Gd^{3+} is thought to affect mechanical properties of lipid bilayer surrounding the MS channels, due to its high affinity to negatively charged lipid head groups (Ermakov et al. 1998), rather than directly acting on the MS channels. Numerous compounds are discovered to activate MS channels by modifying membrane curvature after asymmetrical insertion into the membrane, thereby changing the pressure profile in lipid bilayer (Kung 2005). Among the compounds, chlorpromazine (CPZ) and trinitrophenol (TNP) can activate the MS channel in the absence of pressure (Martinac et al. 1990). Lysolipids as conical lipids also modify membrane shape and affect MS channel gating by causing hydrophobic mismatches and/or curvature at the critical protein–lipid interphase (Martinac et al. 1990). Recently, parabens (*p*-hydroxybenzoic acid) has been found to activate MscS and MscL of *E. coli* by directly binding the gate of these channels without membrane stretch (Nguyen et al. 2005). The discovery of these compounds is expected to characterize the gating of MS channels.

As described above, MscS and MscL are channels to sense the membrane tension directly and be activated by conformational changes. The subunits of these channels tilt depending upon expancile forces of membrane through hypotonic cell swelling by iris-like rotation, resulting in opening of the MS channels. When bacteria adapts to the changes in extracellular osmolality for survival, they need to sense magnitudes of the changes in extracellular osmolality to release the proper amount of cytosolic components through MS channels. A physiological role of MscS and MscL channels

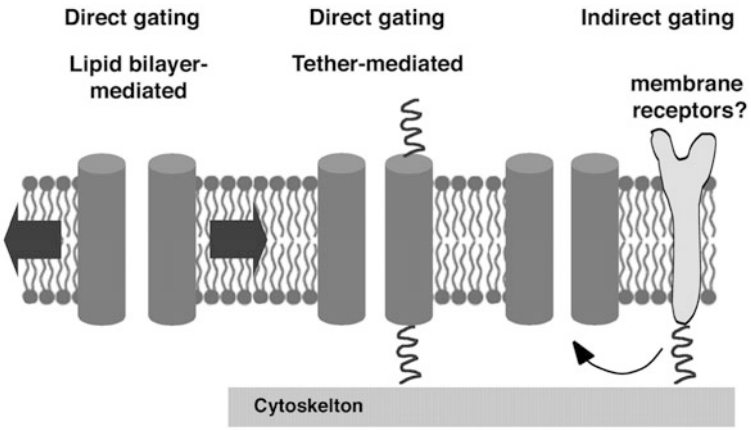

Fig. 6.2 Models for mechanosensitive ion channels gating

is to convert the expansile force caused by changes in osmotic pressure into survival ability to release cytoplasmic components leading to reduction of cytoplamic osmotic pressure for adaptation of cytoplasmic osmolality to extracellular hypotonic one.

6.3 MSCs in Eukaryotes

We can sense physical contact, gravity, sound waves, muscle stretch, fluid flow, and blood pressure via conversion of these stimuli interacting with specific sensory cells into electrical signals through MS channels. At the present, several types of MS channels in eukaryotes are recognized as candidates for transmission of mechanical force. MS channels can be gated directly with membrane tension coming from lipid bilayers themselves or from tethered extracellular matrixes and/or cytoskeletons (Fig. 6.2). An alternative indirect model involves another primary mechanosensor(s), such as a membrane receptor and associated second messenger(s) (Fig. 6.2). In recent studies, most focused MS channels in eukaryotes belong to transient receptor potential (TRP) ion channel superfamily, nonselective cation channels to permeate Ca^{2+}. The mechanotransduction for sensing mechanical forces through MS channels are mostly mediated to regulate cytosolic Ca^{2+} concentration that in turn activates downstream signal molecules to respond to the mechanical forces. Noteworthy, eukaryotic cells have extensive cytoskelton near the lipid bilayer and contact to extracellular matrix through focal adhesion. The cytoskeletons and/or extracellular matrixes as tethers enable to sense the magnitude, direction and duration of mechanical forces and to transmit the elements of mechanical forces to various intracellular signal molecules for achievement of complicated and precise responses to diverse stimuli. In this section, we summarize the mechanical gating of the MS channels in eukaryotes and discuss physiological importance of these channels.

6.3.1 TRP Channels as MSCs

Transient receptor potential (TRP) ion channel superfamily is known to contribute to sensing and transduction of various external and internal stimuli including pain, temperature, pH, mechanical force, osmotic pressure, and chemical stimuli. Most of TRP channels are Ca^{2+} permeable, non-selective cation channels. They are composed of four homomeric or heteromeric TRP subunits. TRP channels in mammals are divided into several groups (TRPA, TRPC, TRPN, TRPV, TRPM, TRPP and TRPML) on basis of similarity of their amino-acid sequences. TRP channels are considered to have a common topological structure with six transmembrane domains and intracellular amino- and carboxyl-termini. Numerous evidences have recently revealed that members of TRP ion channel superfamily are potential candidates for cellular mechanosensing and mechanotransduction.

6.3.1.1 TRPV Channels

Transient receptor potential vanilloid (TRPV) channels (TRPV1–6 have been identified) are widely expressed in both sensory and nonsensory cells, and are activated by various chemical and physical stimuli. TRPV4 displays significantly a stronger homology with TRPV1-TRPV3 than with TRPV5 or TRPV6. TRPV4 (OTRPC4, VRL-2, VR-OAC, and TRP12) was first described as a channel activated by hypotonicity-induced cell swelling (Liedtke et al. 2000; Nilius et al. 2001). Genetic analysis in *Caenorhabditis elegans* has revealed that OSM-9 and OCR-2 are essential for both osmosensory and mechanosensory (nose-touch) behaviors (Colbert et al. 1997; Tobin et al. 2002; Sokolchik et al. 2005). In particular, the rescue of OSM-9 and PCR-2 functions with mammalian TRPV4 and TRPV2 respectively has indicated that these two channel proteins are a central component of the sensor channel in *C. elegans*. It is now recognized that TRPV2 (Muraki et al. 2003) and TRPV4 (Strotmann et al. 2000) are sensitive to hypotonic cell swelling, shear stress/fluid flow (TRPV4), and membrane stretch (TRPV2). In the study of osmotic metabolism in $TRPV4^{-/-}$ mice, TRPV4 in the brain may transmit a negative signal to AVP secretion similar to an inhibitory pass through the baroregulatory system (Mizuno et al. 2003). Therefore, TRPV4 may be the hypothalamic osmoreceptor, or a component of the osmoreceptor, which controls water balance by releasing vasopressin from the posterior pituitary (Liedtke et al. 2003; Mizuno et al. 2003; Suzuki et al. 2003). Further, functional characterization of the TRPV4 has progressed owing to discovery of synthetic 4alpha-phorbol as a direct channel activator. The mechanism to activate TRPV4 channel by cell swelling is not due to a direct sensing to mechanical stimuli, whereas it may be activated indirectly through arachidonic acid metabolic pathways. Cell swelling has been shown to activate phospholipase A_2 (PLA_2), producing arachidonic acid and cytochrome P450 metabolite, 5′, 6′-epoxyeicosatrienoic acid (5′6′-EET) that would be signals to activate TRPV4 (Basavappa et al. 1998, Thoroed et al. 1997). Moreover, abolishment of the arachidonic acid and 5′6′-EET production by preventing PLA_2 and cytochrome

P450 epoxygenase respectively strongly inhibited the hypotonicity-induced TRPV4 Ca^{2+} influx and TRPV4 channel current (Vriens et al. 2004). Accordingly, hypotonic activation of TRPV4 channel would be mediated via indirect pathways.

6.3.1.2 TRPM Channels

The melastatin-related transient receptor potential (TRPM) subfamily is named based on the first discovered member, melastatin (TRPM1), which has identified in the study of melanomas. Some members of TRPM channels have been shown to relate to human tumors. Expression of TRPM8 increases in prostate carcinomas (Tsavaler et al. 2001), TRPM5 may be found in Wilms' tumours and rhabdomyosarcomas (Prawitt et al. 2000), and reduction of TRPM1 expression is linked to more-malignant melanomas (Duncan et al. 1998; Deeds et al. 2000). It is proposed that TRPM channels play a role in tumourigenesis, proliferation and differentiation, while members of TRPM channels, TRPM3, TRPM4 and TRPM7, are activated with mechanical stimuli such as hypotonic cell swelling and membrane stretch. TRPM7 is initially characterized as a Ca^{2+}-permeable, non-selective cation channel. Oancea et al. have previously indicated that shear stress activates TRPM7 channel by increasing exocytotic incorporation of TRPM7 into plasma membrane in vascular smooth muscle cells and recombinant TRPM7-overexpressing HEK293T cells (Oancea et al. 2006). On the other hand, Numata et al. have demonstrated that endogenously expressed TRPM7-like channel in HeLa cells is directly activated by membrane expansion induced by membrane stretch or osmotic cell swelling (Numata et al. 2007a). Further, Numata et al. have revealed that membrane stretch directly activates TRPM7 by increasing open probability of heterologous TRPM7 expressed in HEK 293 cells (Numata et al. 2007b). Consequently, it is considered that mechanical forces activate TRPM 7 channel by increasing both number and open probability of the channel in a cell type- and tissue-dependent manner. On the other hands, TRPM4-like channels can be activated by membrane stretch, possibly through ryanodine receptor (RyR) activation in rat cerebral artery myocytes and TRPM4B-overexpressing HEK cells. Activation of TRPM4 channel in response to membrane stretch is mostly abolished by a putative RyR antagonist in cell-attached mode patch clamp, whereas inhibitors for PLC-dependent cascade failed to suppress the effect of membrane stretch on TRPM4 channels (Morita et al. 2007). TRPM3 is also characterized as a cation channel activated by extracellular hypotonic stress (Harteneck et al. 2007). Although the mechanism of TRPM3 activation by hypotonic stress is at the present unclear, sphingosine is a possible candidate to activate TRPM3 channel. It is well known that hypotonic stress and cell swelling activate receptors for growth factors and coupled to G proteins (Franco et al. 2004; Niisato et al. 2000; Sadoshima et al. 1996; Taruno et al. 2007). Production of sphingosine is dependent upon activity of enzymes such as sphingomyelinase and ceramidase following activation by growth factors (Coroneos et al. 1995; Jacobs et al. 1993). Therefore, cell swelling and hypotonic stress might activate TRPM3 by up-regulating the sphingomyelinase/ceramidase pathway through activation of receptor tyrosine kinase for growth factors (Kraft et al. 2005).

As describe above, TRPM7 channel increases its activity by sensing membrane tension, meanwhile TRPM3 and TRPM4 is might be indirectly activated through sphongosine- and ryanosine-dependent pathway respectively. However, even in TRPM7, exocytotic insertion of TRPM7 channel to the plasma membrane induced by hypotonic stress might be regulated by intracellular signal molecules. Therefore, it is supposed that TRPM channel is likely to be indirectly regulated by hypotonic cell swelling and membrane stretch through intracellular signal cascades.

6.3.1.3 TRPC Channels

The subfamily of TRP channels; canonical TRP channels (TRPC) have seven members. TRPC1 and TRPC6 are non-selective Ca^{2+} permeable channels that have been recently claimed to be stretch-activated cation channels (SACs) (Maroto et al. 2005; Spassova et al. 2006). Further, these channels are related to inherited and acquired pathologies including familial focal segmental glomerulosclerosis, Duchenne muscular dystrophy (DMD), and cardiac hypertrophy (Pagnamenta et al. 2011; Ward et al. 2008; Winn et al. 2005). TRPC1 is widely expressed, and is a non-selective "store-operated ion channel" (SOC) involved in Ca^{2+} entry following Ca^{2+} depletion of the endoplasmic reticulum (ER). Maroto et al. have indicated that TRPC1 is a component of vertebrate mechanosensitive cation channels that are gated by tension in reconstituted lipid bilayers (Maroto et al. 2005). TRPC6 is another Ca^{2+}-permeable non-selective cation channel, and is activated in response to PIP_2 receptors, thus called a "receptor-operated channel" (ROC). When TRPC6 is coexpressed with angiotension II type 1 receptor (AT_1R), TRPC6 would gain ability of mechanosensitivity without any ligands in vascular smooth muscle cells (Mederos et al. 2008). TRPC6 activation by stretch or swelling is blocked by PLC inhibition or by GDPβs that suppresses G protein activation (Mederos et al. 2008; Park et al. 2003). Consequently, membrane stretch causes an agonist-independent conformational change of AT_1R thereby activating the downstream Gq_{11}/PLC/DAG/TRPC6 signaling cascade. As mentioned above, activation of TRPC6 is mediated through an indirect pathway and a G protein-coupled receptor (GPCR) might be a sensor of membrane tension.

6.3.1.4 TRPP Channels

TRPP subunits are abundantly expressed in the kidney and the cardiovascular system (Bichet et al. 2006). TRPP1 (PKD1, PC1) is a large transmembrane glycoprotein with an extended N-terminal extracellular domain, 11 transmembrane domains and a short intracellular C-terminal domain (Bichet et al. 2006). TRPP channel subfamily has four members including TRPP1 and TRPP2 (PKD2, PC2) (Giamarchi et al. 2006). Surfaces of the primary cilium in renal epithelial and endothelial cells express the TRPP1/TRPP2 complex. Shear stress causes an increase in intracellular Ca^{2+} concentration in primary cilia and this response disappears in cells lacking TRPP1 or TRPP2 (Nauli et al. 2003, 2008; Praetorius et al. 2003). Sharif-Naeini et al.

have indicated that TRPP2 alone inhibits stretch-activated ion channels (SACs) (Sharif et al. 2009). This inhibitory effect is reversed by coexpression with TRPP1. On the other hand, the actin cytoskeleton is indeed implicated in SAC inhibition by TRPP2, as this effect is abolished by F-actin disruption (Sharif et al. 2009). Further, filamin A (FLNa) is a novel cytoskeletal element interacting with TRPP2 (Stossel et al. 2001). FLNa stiffens cell cortexes by virtue of its ability to crosslink adjacent actin filaments and increases actin polymerization/gelation rates in vitro (Stossel et al. 2001). Activity of nonselective SACs is reduced in the presence of FLNa, and the inhibitory effect of TRPP2 on SACs is abolished when FLNa is absent. Thus, it is now recognized that the TRPP1/TRPP2 ratio controls SAC mechanosensitivity through coupling of FLNa to the actin cytoskeleton, and affects the conversion of intraluminal pressure to local bilayer tension for modulating the arterial myogenic response to intraluminal pressure (Giamarchi et al. 2006; McGrath et al. 2003; Nauli et al. 2003; Sharif et al. 2009).

6.4 Degenerin/Epithelial Na^+ Channel (DEG/ENaC) Superfamily

C. elegans degenerins were named due to phenotypes of some touch-defective mutants that cause neuronal degeneration. Degenerin/epithelial Na^+ channel (DEG/ENaC) family is generally characterized as being selective for Na^+ and blocked by amiloride. DEG/ENaC subunits have two transmembrane domains with intracellular amino- and carboxyl- termini and a large extracellular loop. Channels of DEG/ ENaC family are multimeric (both homomeric and heteromeric) and appear to be gated by diverse stimuli including hormones (Marunaka et al. 1991; Rossier 2002), mechanical force, low extracellular pH (Krishtal et al. 1981). Genes required for mechano (touch) sensitivity are first identified in *C. elegans* by screening mutants defective in response to gentle touch. Screened genes are named *mec* for mechanosensory abnormal and expressed in touch receptor neurons. Four *mec* genes are coded proteins involved in mechanosensory channel complex. Electrophysiological studies in live animals have revealed that touching the animal actually increases amiloride-sensitive Na^+ inward current that probably transduces the mechanical stress into electrical signals through mechanosensitive channels such as degenerins. However, it is still unclear how gentle touch activates the mechnosensory channel in *C. elegans*.

6.4.1 ASIC: Acid-Sensing Ion Channel

In 1981, Krishtal and Pidoplichko have provided the first evidence to indicate a receptor for H^+ that carries inward Na^+ currents, that is ASIC (acid-sensing ion

channel), in mammalian sensory neurons (Krishtal et al. 1981). Currently, ASIC proteins have 4 members (ASIC1, ASIC2, ASIC3, and ASIC4) and closely related to ENaC. ASIC can form homomultimeric and heteromultimeric channels. The structure of ASIC in the chicken has been revealed by X-ray crystallography, and the crystallized ASIC is composed of a homotrimer (Jasti et al. 2007). Although ASIC is also sensitive to amiloride, they need higher doses than ENaC (10- to 100-fold) to be blocked. A decrease in extracellular pH opens most of ASICs. ASIC has also been proposed as a mechanosensor. ASICs among the DEG/ENaC superfamily are identified in neuronal and neuroepithelial tissues, where they may be involved in acid taste, acid sensation, learning, and mechanosensation. Further, recent evidences suggest that ASICs are also expressed in vascular smooth muscle cells and involved in cardiovascular homeostasis through actions as mechanoreceptors in arterial baroreceptor neurons and vascular smooth muscle cells. For example, ASIC/ENaC blocker (amiloride) suppresses responses in baroreceptor neurons to mechanical stimulation (Drummond et al. 1998). In addition, mechanosensory dorsal root ganglion cells are found to express ASIC subunits (Garcia-Anoveros et al. 2001). Investigations in ASIC knock-out mice have revealed that these channels may indeed be required for touch sensitivity (Price et al. 2000, 2001). Furthermore, ASIC3 expression in transgenic mice leads to an increased sensitivity to mechanical stimuli (Mogil et al. 2005). On the contrary, more recent reports have failed to demonstrate a significant role of ASICs in mechano-sensory function (Drew et al. 2004; Roza et al. 2004). Therefore, involvements of ASICs in mechanotransduction remain controversial.

6.4.2 ENaC: Epithelial Na^+ Channel

ENaC plays a key role in maintenance of Na^+ balance and regulation of blood pressure. Generally, entry of Na^+ through ENaC in the apical membrane is the rate limiting step for transcellular Na^+ absorption in epithelium. ENaC belong to the DEG/ ENaC superfamily (Kellenberger et al. 2002; Mano et al. 1999) and is characterized to be sensitive to amiloride and its derivatives. Three homologous ENaC subunits (α, β and γ), which has two transmembrane domains (Canessa et al. 1994) with intracellular amino- and carboxyl- termini and a large extracellular loop, assemble to form a highly Na^+ selective channel. Firsov et al. (Firsov et al. 1998) have indicated that ENaC stoichiometry (four subunits) is two α, one β and one γ and that the channel pore consists of two α subunits (Berdiev et al. 1998). The conformational analysis of ENaC by mutagenesis reveals that the region of G/SXS; G587–S589 in α-ENaC forms the narrowest part of the pore, which determines ionic selectivity and unitary conductance (Kellenberger et al. 1999a, b, 2001). The binding site of amiloride, a pore blocker, is located at four residues upstream of the selectivity filter, as identified by mutations of residues, αS583 and homologous βG525/γG537 that obstruct amiloride binding (Schild et al. 1997).

It is well known that activity of ENaC is generally regulated by various factors such as hormones (Marunaka et al. 1991; Rossier 2002), kinases (Diakov et al. 2004; Nilius et al. 2001), intrinsic Na^+-dependent mechanisms (Garty et al. 1997; Turnheim 1991) and proteases (Caldwell et al. 2003; Knight et al. 2006; Rossier 2004; Vallet et al. 1997). So far, evidences implicating responses of ENaC to mechanical force including osmotic stress (Awayda et al. 1998; Ji et al. 1998; Taruno et al. 2007), hydrostatic pressure (Awayda et al. 1995; Palmer et al. 1996), and laminar shear stress (Carattino et al. 2004; Satlin et al. 2001) have been provided. When alpha-bENaC (bovine ENaC) alone is inserted into artificial planar lipid bilayers without β- and γ-subunits, the reconstituted ion channel with a single-channel conductance of 40 pS exhibits characteristics very similar to those of stretch-activated nonselective cation channel observed in several types of tissues (Awayda et al. 1995) and is activated due to increasing open probability by exposure to a hydrostatic pressure gradient. Kizer et al. have also indicated (Kizer et al. 1997) that stretch-activated, nonselective cation channels were observed in α-ENaC alone expressed in LM (mouse fibroblast cell line) cell, that the channels are activated by negative pressure applied to the cell attached patches, cell swelling, or patch excision. However, it is still controversial, because some studies have failed to indicate mechanosensitivity of ENaC (Awayda et al. 1998). Possibilities of ENaC to have mechanosensitivity are explained by reasons why some kinds of epithelia expressing ENaC are constantly exposed to mechanical forces; that is airway epithelia by air flow during breathings (Sidhaye et al. 2008; Tarran et al. 2005) and the cortical collecting duct epithelium by the tubular flows (Liu et al. 2003; Satlin et al. 2001). Shear stress such as air and fluid flows is one of possible mechanical stresses for ENaC physiologically relevant to ENaC functions in various cells. Althaus et al. have clearly indicated that laminar shear stress (LSS) significantly increases open probabilities (*Po*) of rENaC (rat ENaC) and xENaC (*Xenopus* ENaC) after LSS exposure by using single-channel recordings. Increased *Po* is associated with either a significant increase of mean open time or a decrease of mean closed time. There is no significant increase in the number of active ENaCs in exposure to LSS. On the other hand, shear force also activates hENaC (human ENaC) cloned from human lung tissue that is expressed in *Xenopus* oocytes. In outside-out single channel recording experiments, it is proved that ENaC is directly activated by shear force with increases in *NPo* (number of channels × *Po*) (Froniusa et al. 2010). This observation suggests that hENaC has a crucial role in regulation of pulmonary Na^+ absorption and pulmonary fluid homeostasis by directly sensing shear force. Further, ENaC subunits are revealed to be expressed in vascular tissues (Drummond et al. 2001, 2004; Jernigan et al. 2005) and sensory nerve endings (Drummond et al. 2000). ENaC expressed in vascular tissues might contribute to mechano-sensory systems that are involved in control of blood pressure (Drummond et al. 2001, 2004). These studies strongly support the possibilities that ENaC responds to some kinds of mechanical forces and plays a crucial role as a mechanosensor.

6.5 MS Channels in Renal Tubules

6.5.1 Sensing Renal Fluid Flow

It has previously reported (Engbretson et al. 1987; Malnic et al. 1989; Satlin 1994, 2001; Stokes 1993) that elevation in tubular fluid flow rate upregulates net Na^+ reabsorption in the mammalian cortical collecting duct (CCD). On the other hand, we and others have indicated that ENaC and/or non-selective stretch-activated cation (SAC) channel as a Na^+ permeable ion channel exist in CCD and contribute to Na^+ reabsorption (Butterworth 2010; Marunaka et al. 1994, 1997; Niisato et al. 2001). Therefore, it is expected that at least either of ENaC or SAC channel in CCD should be activated in response to shear stress caused by tubular fluid flow. A flow-induced increase in net Na^+ absorption in CCD or I_{Na} in oocytes expressing ENaC is supposed to be caused by increasing the number of apical channels and/or channel open probability. LSS does not enhance mutant ENaC channels ($\alpha\beta$S518Kγ or αS580C$\beta\gamma$) that have a high intrinsic open probability, suggesting that LSS activates ENaC by increasing channel open probability (Carattino et al. 2004). A previous study has indicated that LSS alters the channel gating, especially the open probability, without affecting other parameters including amiloride binding kinetics, single-channel conductance, or ion selectivity (Carattino et al. 2005). Nevertheless, it is postulated mechanosensors might be located at the extracellular region of the channel. Namely, mechanosensors might either be parts of, or associated with, the large extracellular loops of ENaC molecules which must be coupled to the gating of the channel. This hypothesis, the large extracellular loop is a mechanosensor, is further supported by a recent study indicating that ENaC activation by LSS (fluid flow) is independent of membrane trafficking (Morimoto et al. 2006). However, additional experimental data are necessary to identify mechanosensors and to clarify this issue.

6.5.2 NSC Channel in Xenopus Laevis A6 Cells

In a model of CCD cell (A6 cells) to study ENaC-mediated Na^+ reabsorption, our and other laboratories have shown that A6 cells have stretch activated non-selective cation (NSC) channels that are activated by negative pressure applied to patch pipettes (Marunaka et al. 1994, 1997; Nakahari et al. 1996; Niisato et al. 2001; Urbach et al. 1999; Yu et al. 1997). In our previous reports, NSC channels have 28–29 pS conductance and Na^+/K^+ permeability. Although most of SACs can permeate Ca^{2+} in addition to Na^+ and K^+, 28 pS NSC channel in A6 cells hardly permeate Ca^{2+} (Nakahari et al. 1996; Marunaka et al. 1997). The NSC channel is also activated by compounds to increase cytosolic cAMP concentration. After the NSC channel is once fully activated by cAMP, negative pressure can no longer activate it and vice versa (Fig. 6.3). At the present, it is considered that cAMP and negative pressure is involved in a common mechanism for activation of NSC channels. By using

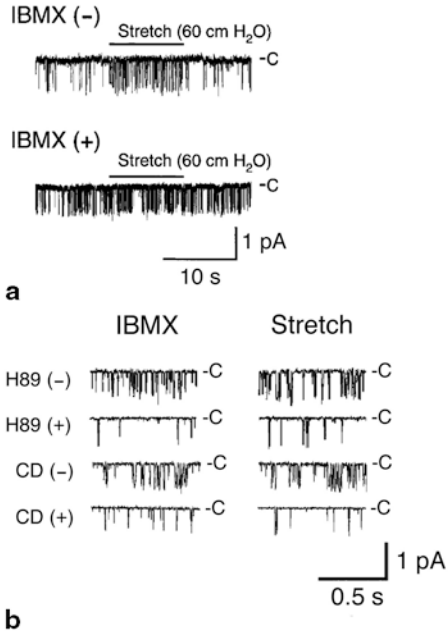

Fig. 6.3 Single channel recording of NSC channel stimulated with IBMX and stretch in the presence or absence of H89 and cytochalasin D. **a** Effects of negative pressure (stretch) on open probability (*P*o) of NSC channels obtained from cell-attached patches formed on the apical membrane at no applied potential (the resting membrane potential) in IBMX-untreated and -treated cells. Representative traces of single channel currents with and without negative pressure of 60 cm H_2O (stretch) in IBMX -untreated and -treated cells. **b** Effects of H89 (a PKA inhibitor) and cytochalasin D (CD) on *P*o of NSC channels obtained in cell-attached patches of A6 cells treated with IBMX or subjected to negative pressure as stretch. (Modified from Marunaka et al. 1997)

open and closed time-interval histograms obtained from cell-attached patches, single channel kinetics in the NSC channel in the presence and absence of 3-isobutyl-1-methylxanthine (IBMX, an inhibitor of phosphodiesterase used to increase cytosolic cAMP) and negative pressure is analyzed. The open time-interval histogram obtained from an NSC channel is fitted by one exponential function. In contrast, the closed time-interval histogram is fitted by two exponential functions. The mean values of open or closed times do not change significantly with application of IBMX, although IBMX increases the open probability (*P*o) as NSC channel activity. To clarify how IBMX could increase the *P*o without any detectable changes in open and closed times, the frequency of events staying at each state is compared. IBMX increased the frequency of the short closed events and decreased the frequency of the long closed events leading to an increase in *P*o of the channel. In A6 cells, the NSC channel has one open and two closed states, and a linear gating kinetic model "$C_L \leftrightarrow C_S \leftrightarrow O$" (the long closed state, C_L; the short closed state, C_S,the open state, O) is the most suitable one to explain observed channel behaviors. According to the Model "$C_L \leftrightarrow C_S \leftrightarrow O$" only the leaving rate of the channel for C_L from C_S is

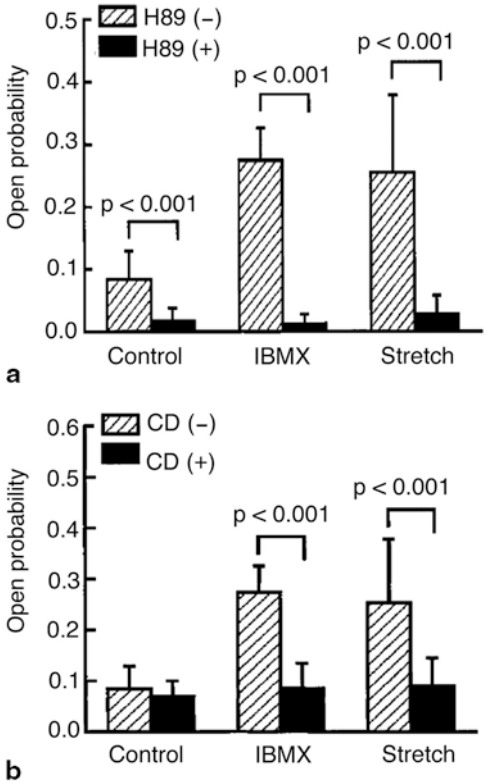

Fig. 6.4 Statistical results of the effects of H89 and cytochalasin D (CD) on *P*o of basal, IBMX-, and stretch-activated channels. (Modified from Marunaka et al. 1997)

decreased by application of IBMX or stretch, resulting in an increase in the *P*o of the channel.

On the other hand, the actin cytoskeleton is known to contribute to sensing mechanical force and regulation of MSCs activities (Prat et al. 1993a, b). In NSC channels of A6 cells, treatment with cytochalasin D, which depolymerizes actin filaments, decreases the *P*o of the IBMX- or stretch-activated channel to the basal level (Figs. 6.3 and 6.4). H89 (a PKA inhibitor) also markedly decreased the *P*o of the NSC channel and abolished the response of the NSC channel to IBMX or stretch (Figs. 6.3 and 6.4). On the other hand, a PKA catalytic subunit significantly increases *P*o, which is abolished by cytochalasin D (Fig. 6.5). The observations indicate that both activation of PKA and existence of polymerized actin filaments are essential for activation of NSC channels in A6 cells by IBMX and stretch.

In excised inside-out patches, catalytic subunits of PKA significantly increased Po of NSC channels and single channel kinetics are changes to "$C \leftrightarrow O$" (one closed state and one open state). It is supposed that PKA may influence only the communication between the short and long closed states without affecting the communication between C_S and O. There are two possibilities to explain this phenomenon: (i) the long closed state really disappeared (in other words, the channel does not have

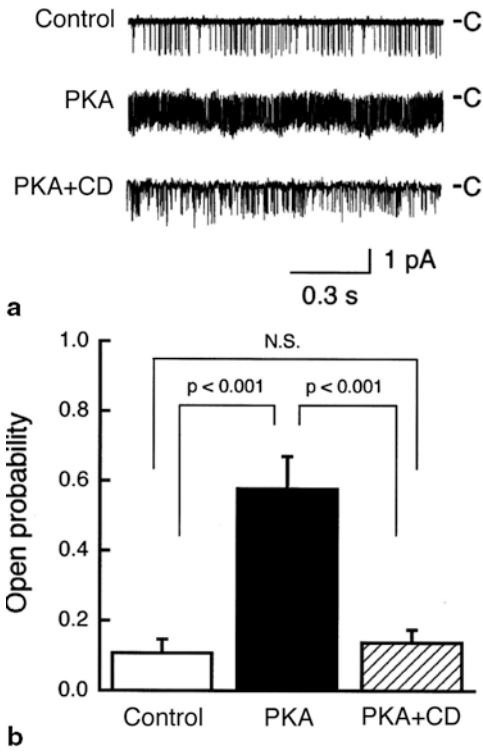

Fig. 6.5 Effects of PKA catalytic subunit and cytochalasin D (CD) on *P*o of NSC channels obtained from excised inside-out patches formed on the apical membrane at a membrane potential of −40 mV in the presence of 2 mM ATP. **a** Representative traces of single-channel currents before treatment (Control), 10 min after application of PKA (10 μg/mL) (PKA), and 10 min after PKA application with CD pretreatment (5 μM, 10 min) (PKA + CD) to the cytosolic surface of the patch membrane. The closed level is marked by a horizontal bar and "C." **b** Statistical results of effects of PKA catalytic subunit and CD on the *P*o. (Modified from Niisato et al. 2001)

access to the long closed state and has only one closed state), or (ii) the mean time of the channel staying at the long closed state becomes identical to that of the short closed state (in other words, based upon only the mean times the long closed state cannot be distinguished from the short closed state, hence giving an impression that the channel has only one closed state). Consequently, application of PKA catalytic subunit affects the transition rate of the channel from the short closed state to the long closed state, and that PKA action on this rate is abolished by treatment with cytochalasin D. Communication of the channel between the short and long closed states is affected by PKA-induced phosphorylation of polymerized actin filaments. These observations and our previous study (Marunaka et al. 1997) indicate that phosphorylation of polymerized actin filaments mimics the action of stretch, suggesting that phosphorylation might produce some stretch-like mechanical phenomenon.

It is generally considered that mechanical force initiates signal transduction via stretch-activated ion channels in the cell membrane (Gillespie et al. 2001). However, cellular mechanotransduction may involve numerous molecular mechanisms other than ion channels, such as force initiated signal transduction via changes in cytoskeletal-ECM linkages (Sawada et al. 2002; Tamada et al. 2004). In this study, negative pressure as mechanical force might be converted to chemical signals activating PKA. As reported in studies on mechanosensitivity of TRPC6 channel (Mederos

et al. 2008; Park et al. 2003), membrane tension possibly activates G protein-coupled receptor (GPCR) associated with adenylate cyclase without ligand, and the increased cAMP by membrane tension activates PKA in A6 cells. Therefore, a sensor of membrane tension in A6 cells might be GPCR but not NSC channel. However, it is still unclear that a role of the polymerized actin filament especially in excised inside-out patches. One possibility is that existence of actin filaments nearby cell membrane is essentially required but not transmit the mechanical force through cytoskelton network to the channels. It is seemed that gating of NSC channels is "indirect gating" rather than "tether model" shown in Fig. 6.2, although further studies are needed.

6.6 Conclusion and Perspectives

Physical force including osmotic pressure, hydrostatic pressure, gravity, shear stress and expansile force (membrane tension) is a crucial signal to control cellular functions such as proliferation, differentiation, development and cell death. In prokaryotic cell as monad, physical stress such as osmotic pressure directly connects to life and death. In bacteria cells, MS channels simply and directly sense the magnitude of membrane tension as the osmotic pressure activating MS channels if the membrane tension is larger than its gating threshold. MscL and MscS in lipid bilayers are physically expanded by membrane tension, which in turn causes conformational changes for gating. Recent progress of crystallographic analysis and computing modeling have revealed gating mechanisms of MscL and MscS; tiling of transmembrane domains in lipid bilayer by iris-like rotations that enlarges the channel pore size through transition from the closed state to the open state. The gating of MscL and MscS seems to be simple, because bacteria cells only need to recognize the magnitude of membrane tension as osmotic pressure that determines the amount of releasing cytosolic components. In contrast, eukaryotic cells, more complex mechanisms are involved in sensing mechanical force. Mechanical force contains some kinds of elements; magnitude, direction, cycle, duration. To precisely sense mechanical force including elements, MS channels recognize the mechanical force not only through membrane tension itself but also through cytoskeltal networks, adhesion between cell and extracellular matrix and mechanosensitive membrane proteins associated with MS channels (Fig. 6.2). Basically, channel gating is tightly related to the conformation of the channel in the plasma membrane. On the other hand, cytoskeletons backup the plasma membrane by connecting to proteins in the plasma membrane. This means that modification of cytoskeletons is an alternative way to affect MS channels in the plasma membrane. Thus, indirect transmission of mechanical force via cytoskeletons might enable more fine control of activity of MS channels. One of the most interesting examples is a response to shear stress in endothelial cells. They align perpendicular to the stretch for bearing less tension. This phenomenon indicates that endothelial cell can recognize the direction of blood flow as shear stress through stress fiber reconstitution. In eukaryotic cell, cytoskelton contributes

to recognition of the direction of mechanical force. As an indirect gating of MS channels, mechanosensitive proteins in the plasma membrane are also involved in the mechanotransduction. MS channels such as TRPC6 channel and NSC channel in A6 cells might be regulated by GPCR-dependent signal molecules and GPCR converts the mechanical force to production of its second messengers without its ligand. This means that mechanical force is a physical ligand to activate receptors located in the plasma membrane instead of chemical ligands. Based on previous numerous studies, the plasma membrane itself might be a special complex to sense physical stress and lipid bilayer is a transmitter of mechanical stress to MS channels. Further studies are necessary to reveal the complete understanding of MS channel gating.

References

Alcorn D, Adamson TM, Lambert TF, Maloney JE, Ritchie BC, Robinson PM (1997) Morphological effects of chronic tracheal ligation and drainage in the fetal lamb lung. J Anal 123:649–660

Ajouz B, Berrier C, Garrigues A, Besnard M, Ghazi A (1998) Release of thioredoxin via the mechanosensitive channel MscL during osmotic downshock of Escherichia coli cells. J Biol Chem 273(26):670–26 674

Ajouz B, Berrier C, Besnard M, Martinac B Ghazi A (2000) Contributions of the different extramembranous domains of the mechanosensitive ion channel MscL to its response to membrane tension. J Biol Chem 275:1015–1022

Althaus M, Bogdan R, Clauss WG, Fronius M (2007) Mechano-sensitivity of epithelial sodium channels (ENaCs): laminar shear stress increases ion channel open probability. FASEB 21:2389–2399

Arnadóttir J, Chalfie M (2010) Eukaryotic mechanosensitive channels. Annu Rev Biophys 39:111–137

Awayda MS, Ismailov II, Berdiev BK, Benos DJ (1995) A cloned renal epithelial Na^+ channel protein displays stretch activation in planar lipid bilayers. Am J Physio 268:C1450–C1459

Awayda MS, and Subramanyam M (1998) Regulation of the epithelial Na^+ channel by membrane tension. J Gen Physiol 112:97–111

Basavappa S, Pedersen SF, Jorgensen NK, Ellory JC, Hoffmann EK (1998) Swelling-induced arachidonic acid release via the 85-kDa cPLA2 in human neuroblastoma cells. J Neurophysiol 79:1441–1449

Bass RB, Strop P, Baeclay M, Rees DC (2002) Crystal structure of Escherichia coli MscS, a voltage-modulated and mechanosensitive channel. Science 298:1582–1587

Batiza AF, Kuo MM, Yoshimura K, Kung C (2002) Gating the bacterial mechanosensitive channel MscL in vivo. Proc Natl Acad Sci USA 99:5643–5648

Belyy V, Anishkin A, Kamaraju K, Liu N, Sukharev S (2010) The tension-transmitting 'clutch' in the mechanosensitive channel MscS. Nat Struct Mol Biol 17:451–458

Berdiev BK, Karlson KH, Jovov B, Ripoll PJ, Morris R, Loffing-Cueni D, Halpin P, Stanton BA, Kleyman TR, Ismailov II (1998) Subunit stoichiometry of a core conduction element in a cloned epithelial amiloride-sensitive Na^+ Channel. Biophys 75:2292–301

Bershadsky AD, Ballestrem C, Carramusa L, Zilberman Y, Gilquin S, Khochbin S Alexandrova AY, Verkhovsky AB, Shemesh T, Kozlov MM (2006) Assembly and mechanosensory function of focal adhesions: Experiments and models. Eur J Cell Biol 85:165–173

Bichet D, Peters D, Patel A, Delmas P, Honoré E (2006) The cardiovascular polycystins: insights from autosomal dominant polycystic kidney disease and transgenic animal models. Trends Cardiovasc Med 16:292–298

Blount P, Moe PC (1999) Bacterial mechanosensitive channels: integrating physiology, structure and function. Trends Microbiol 7:420–424
Butterworth MB (2010) Regulation of the epithelial sodium channel (ENaC) by membrane trafficking. Biochim Biophys Acta 1802 (12):1166–1177
Caldwell RA, Boucher RC, Stutts MJ (2003) Serine protease activation of near-silent epithelial Na^+ channels. Am J Physiol Cell Physiol 286:C190–C194
Canessa CM, Merillat AM, Rossier BC (1994) Membrane topology of the epithelial sodium channel in intact cells. Am J Physiol Cell Physiol 267:C1682–1690
Carattino MD, Sheng S, Kleyman TR (2004) Epithelial Na^+ channels are activated by laminar shear stress. J Biol Chem 279:4120–4126
Carattino MD, Sheng S, Kleyman TR (2005) Mutations in the pore region modify epithelial sodium channel gating by shear stress. J Biol Chem 280:4393–4401
Carmel JA, Friedman F, Adams FH (1965) Fetal tracheal lgation and lung development. Am J Dis Child 109:452–456
Carmeliet G, Vico L, Bouillon R (2001) Space flight: a challenge for normal bone homeostasis. Crit Rev Eukaryot Gene Expr 11:131–144
Chien S (2007) Mechanotransduction and endothelial cell homeostasis: the wisdom of the cell. Am J Physiol Heart Circ Physiol 292:H1209–H1224
Colbert HA, Smith TL, Bargmann CI (1997) OSM-9, a novel protein with structural similarity to channels, is required for olfaction, mechanosensation, and olfactory adaptation in Caenorhabditis elegans. J Neurosci 17:8259–8269
Coroneos E, Martinez M, McKenna S, Kester M (1995) Differential regulation of sphingomyelinase and ceramidase activities by growth factors and cytokines. Implications for cellular proliferation and differentiation. J Biol Chem 270:23305–23309
Deeds J, Cronin F, Duncan LM (2000) Patterns of melastatin mRNA expression in melanocytic tumors. Hum Pathol 31:1346–1356
Diakov A, Korbmacher C (2004) A novel pathway of epithelial sodium channel activation involves a serum- and glucocorticoid-inducible kinase consensus motif in the C terminus of the channel's alpha-subunit. J Biol Chem 279:38134–38142
Drew LJ, Rohrer DK, Price MP, Blaver KE, Cockayne DA, Cesare P, Wood JN (2004) Acid-sensing ion channels ASIC2 and ASIC3 do not contribute to mechanically activated currents in mammalian sensory neurones. J Physiol 556:691–710
Drummond HA, Price MP, Welsh MJ, Abboud FM (1998) A molecular component of the arterial baroreceptor mechanotransducer. Neuron 21:1435–1441
Drummond HA, Abboud FM, Welsh MJ (2000) Localization of β and γ subunits of ENaC in sensory nerve endings in the rat foot pad. Brain Res 884:1–12
Drummond HA, Welsh MJ, Abboud FM (2001) ENaC subunits are molecular components of the arterial baroreceptor complex. Ann N Y Acad Sci 940:42–47
Drummond HA, Gebremedhin D, Harder DR (2004) Degenerin/epithelial Na^+ channel proteins: components of a vascular mechanosensor. Hypertension 44:643–648
Duncan LM, Deeds J, Hunter J, Shao J, Holmgren LM, Woolf EA, Tepper RI, Shyjan AW (1998) Down-regulation of the novel gene melastatin correlates with potential for melanoma metastasis. Cancer Res 58:1515–1520
Edwards MD, Booth IR, Miller S (2004) Gating the mechanosensitive channels: MscS a new paradigm? Curr Opin Microbiol 7:163–167
Edwards MD, Li Y, Kim S, Miller S, Bartlett W, Black S, Dennison S, Iscla I, Blount P, Bowie JU, Booth IR (2005) Pivotal role of the glycine-rich TM3 helix in gating the MscS mechanosensitive channel. Nat Struct Mol Biol 12:113–119
Engbretson BG, Stoner LC (1987) Flow-dependent potassium secretion by rabbit cortical collecting tubule in vitro. Am J Physiol Renal Physiol 253:F896–F903
Ermakov YA, Averbakh AZ, Arbuzova AB, Sukharev SI (1998) Lipid and cell membranes in the presence of gadolinium and other ions with high affinity to lipids. 2. A dipole component of the boundary potential on membranes with different surface charge. Membr Cell Biol 12:411–426

Fewell JE, Hislop AA, Kitterman JA, Johnson P (1983) Effect of tracheostomy on lung development in fetal lambs. Appl Physiol 55:1103–1108
Firsov D, Gautschi I, Merillat AM, Rossier BC, Schild L (1998) The heterotetrameric architecture of the epithelial sodium channel (ENaC). EMBO J 17:344–352
Franco R, Lezama R, Ordaz B, Pasantes-Morales H (2004) Epidermal growth factor receptor is activated by hypoosmolarity and is an early signal modulating osmolyte efflux path- ways in Swiss 3T3 fibroblasts. Pflugers Arch – Eur J Physiol 447:830–839
Froniusa M, Bogdana R, Althausa M, Morty RE, Clauss WG (2010) Epithelial Na^+ channels derived from human lung are activated by shear force. Respir Physiol Neurobiol 170:113–119
Garcia-Anoveros J, Samad TA, Zuvela-Jelaska L, Woolf CJ, Corey DP (2001) Transport and localization of the DEG/ENaC ion channel BNaC1α to peripheral mechanosensory terminals of dorsal root ganglia neurons. J Neurosci 21:2678–2686
Garty H, Palmer LG (1997) Epithelial sodium channels: function, structure, and regulation. Physiol Rev 77:359–396
Giamarchi A, Padilla F, Coste B, Raoux M, Crest M, Honoré E, Delmas P (2006) The versatile nature of the calcium-permeable cation channel TRPP2. EMBO Rep 7:787–793
Gillespie PG, Walker RG (2001) Molecular basis of mechanosensory transduction. Nature 413:194–202
Hamill OP, Martinac B (2001) Molecular basis of mechanotransduction in living cells. Physiol Rev 81:685–740
Harteneck C, Schultz G (2007) TRPV4 and TRPM3 as Volume-Regulated Cation Channels. In: Liedtke WB, Heller S, editors. TRP Ion Channel Function in Sensory Transduction and Cellular Signaling Cascas. Bocade Raton (FL): CRC Press: Chap. 10
Häse CC, Le Dain AC, Martinac B (1995) Purification and functional reconstitution of the recombinant large mechanosensitive ion channel (MscL) of Escherichia coli. J Biol Chem 270:18329–18334
Hooper SB, Wallace MJ (2006) Role of the physicochemical environment in lung development. Clin Exp Pharmacol Physiol 33:273–279
Jacobs LS, Kester M (1993) Sphingolipids as mediators of effects of platelet-derived growth factor in vascular smooth muscle cells. Am J Physiol Cell Physiol 265:C740–C747
Jasti J, Furukawa H, Gonzales EB, Gouaux E (2007) Structure of acid-sensing ion channel 1 at 1.9 A resolution and low pH. Nature 449:316–323
Jernigan NL, Drummond HA (2005) Vascular ENaC proteins are required for renal myogenic constriction. Am J Physiol Renal Physiol 289:F891–F901
Ji, HL, Fuller, CM, Benos, DJ (1998) Osmotic pressure regulates α-rENaC expressed in *Xenopus* oocytes. Am J Physiol Cell Physiol 275:C1182–C1190
Kellenberger S, Schild L (2002) Epithelial sodium channel/degenerin family of ion channels: a variety of functions for a shared structure. Physiol Rev 82:735–767
Kellenberger S, Gautschi I, Schild L (1999a) A single point mutation in the pore region of the epithelial Na^+ channel changes ion selectivity by modifying molecular sieving. Proc Natl Acad Sci USA 96:4170–4175
Kellenberger S, Hoffmann-Pochon N, Gautschi I, Schneeberger E, Schild L (1999b) On the molecular basis of ion permeation in the epithelial Na^+ channel. J Gen Physiol 114:13–30
Kellenberger S, Auberson M, Gautschi I, Schneeberger E, Schild L (2001) Permeability properties of ENaC selectivity filter mutants. J Gen Physiol 118:679–692
Kizer N, Guo XL, Hriska K (1997) Reconstitution of stretch-activated cation channels by expression of the a-subunit of the epithelial sodium channel cloned from osteoblasts. Proc Natl Acad Sci USA 94:1013–1018
Knight KK, Olson DR, Zhou R, Snyder PM (2006) Liddle's syndrome mutations increase Na^+ transport through dual effects on epithelial Na^+ channel surface expression and proteolytic cleavage. Proc Natl Acad Sci USA 103:2805–2808
Kraft R, Harteneck C (2005) The mammalian melastatin-related transient receptor potential cation channels: an overview. Pflugers Arch—Eur J Physiol 451:204–211

Krishtal OA, Pidoplichko VI (1981) Receptor for protons in the membrane of sensory neurons. Brain Res 214:150–154

Kung C (2005) A possible unifying principle for mechanosensation. Nature 436:647–654

Kung C, Martinac B, Sukharev S (2010) Mechanosensitive channels in microbes. Annu Rev Microbiol 64:313–329

LeBlanc AD, Spector ER, Evans HJ, Sibonga JD (2007) Skeletal responses to space flight and the bed rest analog: a review. J Musculoskelet Neuronal Interact 7:33–47

Lehoux S, Esposito B, Merval R, Loufrani L, Tedgui A (2000) Pulsatile stretch-induced extracellular signal-regulated kinase 1/2 activation in organ culture of rabbit aorta involves reactive oxygen species. Arterioscler Thromb Vasc Biol 20:2366–2372

Levina N, Tötemeyer S, Stokes NR, Louis P, Jones MA, Booth IR (1999) Protection of Escherichia coli cells against extreme turgor by activation of MscS and MscL mechanosensitive channels: Identification of genes required for MscS activity. EMBO J 18:1730–1737

Li Y, Wray R, Blount P (2004) Intragenic suppression of gain-of-function mutations in the Escherichia coli mechanosensitive channel, MscL. Mol Microbiol 53:485–495

Liedtke W, Friedman JM (2003) Abnormal osmotic regulation in trpv4$^{-/-}$ mice. Proc Natl Acad Sci USA 100:13698–13703

Liedtke W, Choe Y, Marti-Renom MA, Bell AM, Denis CS, Sali A, Hudspeth AJ, Friedman JM, Heller S (2000) Vanilloid receptor-related osmotically activated channel (VR-OAC), a candidate vertebrate osmoreceptor. Cell 103:525–535

Liu M, Xu J, Liu J, Kraw ME, Tanswell AK, and Post M (1995) Mechanical strain-enhanced fetal lung cell proliferation is mediated by phospholipase C and D and protein kinase C. Am J Physiol Lung Cell Mol Physiol 268:L729–L738

Liu M, Tanswell AK, and Post M (1999) Mechanical force-induced signal transduction in lung cells. Am J Physiol Lung Cell Mol Physiol 277:L667–L683

Liu W, Xu S, Woda C, Kim P, Weinbaum S, Satlin LM (2003) Effect of flow and stretch on the [Ca^{2+}]i response of principal and intercalated cells in cortical collecting duct. Am J Physiol Renal Physiol 285:F998–F1012

Malnic G, Berliner RW, Giebisch G (1989) Flow dependence of K^+ secretion in cortical distal tubules of the rat. Am J Physiol Renal Physiol 256:F932–F941

Mano I, Driscoll M (1999) DEG/ENaC channels: a touchy superfamily that watches the salt. Bioessays 21:568–578

Maroto R, Raso A, Wood TG, Kurosky A, Martinac B, Hamill OP (2005) TRPC1 forms the stretch-activated cation channel in vertebrate cells. Nat Cell Biol 7:179–185

Martinac B, Buechner M, Delcour AH, Adler J, Kung C (1987) Pressure-sensitive ion channel in *Escherichia coli*. Proc Natl Acad Sci USA 84:2297–2301

Martinac B, Adler J, Kung C (1990) Mechanosensitive ion channels of *E. coli* activated by amphipaths. Nature 348:261–263

Marunaka Y, Eaton DC (1991) Effects of vasopressin and cAMP on single amiloride-blockable Na channels. Am J Physiol Cell Physiol 260:C1071–C1084

Marunaka Y, Tohda H, Hagiwara N, Nakahari T (1994) Antidiuretic hormone-responding non-selective cation channel in distal nephron epithelium (A6). Am J Physiol Cell Physiol 266:C1513–C1522

Marunaka Y, Shintani Y, Downey GP, Niisato N (1997) Activation of Na^+-permeant cation channel by stretch and cyclic AMP-dependent phosphorylation in renal epithelial A6 Cells. J Gen Physiol 110:327–336

McGrath J, Somlo S, Makova S, Tian X, Brueckner M (2003) Two populations of node monocilia initiate left-right asymmetry in the mouse. Cell 114:61–73

Mederos Y, Schnitzler M, Storch U, Meibers S, Nurwakagari P, Breit A, Essin K, Gollasch M, Gudermann T (2008) Gq-coupled receptors as mechanosensors mediating myogenic vasoconstriction. EMBO J 27:3092–3103

Miller S, Edwards MD, Ozdemir C, Booth IR (2003) The closed structure of the MscSmechanosensitive channel. Cross-linking of single cysteine mutants. J Biol Chem 278:32246–32250

Mizuno A, Matsumoto N, Imai M, Suzuki M (2003) Impaired osmotic sensation in mice lacking TRPV4. Am J Physiol Cell Physiol 285:C96–C101

Mogil JS, Breese NM, Witty MF, Ritchie J, Rainville ML, Ase A, Abbadi N, Stucky CL, Seguela P (2005) Transgenic expression of a dominant- negative ASIC3 subunit leads to increased sensitivity to mechanical and inflammatory stimuli. J Neurosci 25:9893–9901

Morimoto T, Liu W, Woda C, Carattino M, Wei Y, Hughey R, Apodaca G, Satlin LM, Kleyman TR (2006) Mechanism underlying flow-stimulation of sodium absorption in the mammalian collecting duct. Am J Physiol Renal Physiol 291:F663–F669

Morita H, Honda A, Inoue R, Ito Y, Abe K, Nelson MT, Brayden JE (2007) Membrane stretch-induced activation of a TRPM4-like nonselective cation channel in cerebral artery myocytes. J Pharmacol Sci 103:417–426

Muraki K, Iwata Y, Katanosaka Y, Ito T, Ohya S, Shigekawa M, Imaizumi Y (2003) TRPV2 is a component of osmotically sensitive cation channels in murine aortic myocytes. Circ Res 93:829–838

Nakahari T, Marunaka Y (1996) ADH action on whole-cell currents by cytosolic Ca^{2+}-dependent pathways in aldosterone-treated A6 cells. J Membr Biol 154:35–44

Nauli SM, Alenghat FJ, Luo Y, Williams E, Vassilev P, Li X, Elia AE, Lu W, Brown EM, Quinn SJ, Ingber DE, Zhou J (2003) Polycystins 1 and 2 mediate mechanosensation in the primary cilium of kidney cells. Nat Genet 33:129–137

Nauli SM, Kawanabe Y, Kaminski JJ, Pearce WJ, Ingber DE, Zhou J (2008) Endothelial cilia are fluid shear sensors that regulate calcium signaling and nitric oxide production through polycystin-1. Circulation 117:1161–1171

Nguyen T, Clare B, Guo W, Martinac B (2005) The effects of parabens on the mechanosensitive channels of *E. coli.* Eur Biophys J 34:389–396

Niisato N, Marunaka Y (2001) Blocking action of cytochalasin D on protein kinase A stimulation of a stretch-activated cation channel in renal epithelial A6 cells. Biochem Pharmacol 61:761–765

Niisato N, Van Driessche W, Liu M, Marunaka Y (2000) Involvement of protein tyrosine kinase in osmoregulation of Na^+ transport and membrane capacitance in renal A6 cells. J Membr Biol 175:63–77

Nilius B, Prenen J, Wissenbach U, Bodding M, and Droogmans G (2001) Differential activation of the volume-sensitive cation channel TRP12 (OTRPC4) and volume-regulated anion currents in HEK-293 cells. Pflugers Arch—Eur J Physiol 443:227–233

Nomura T, Sokabe M, Yoshimura K (2006) Lipid-protein interaction of the MscS mechanosensitive channel examined by scanning mutagenesis. Biophys J 91:2874–2881

Numata T, Shimizu T, Okada Y (2007a) TRPM7 is a stretch- and swelling-activated cation channel involved in volume regulation in human epithelial cells. Am J Physiol Cell Physiol 292:C460–C467

Numata T, Shimizu T, Okada Y (2007b) Direct Mechano-Stress Sensitivity of TRPM7 Channel. Cell Physiol Biochem 19:01–08

Oancea E, Wolfe JT, Clapham DE (2006) Functional TRPM7 channels accumulate at the plasma membrane in response to fluid flow. Circ Res 98:245–253

Pagnamenta AT, Holt R, Yusuf M, Pinto D, Wing K, Betancur C, Scherer SW, Volpi EV, Monaco AP (2011) A family with autism and rare copy number variants disrupting the Duchenne/Becker muscular dystrophy gene DMD and TRPM3. J Neurodevelop Disord 3:124–131

Palmer LG, Frindt G (1996) Gating of Na^+ channels in the rat cortical collecting tubule: effects of voltage and membrane stretch. J Gen Physiol 107:35–45

Park KS, Kim Y, Lee YH, Earm YE, Ho WK (2003) Mechanosensitive cation channels in arterial smooth muscle cells are activated by diacylglycerol and inhibited by phospholipase C inhibitor. Circ Res 93:557–564

Praetorius HA, Spring KR (2003) The renal cell primary cilium functions as a flow sensor. Curr Opin Nephrol Hypertens 12:517–520

Prat AG, Ausiello DA, Cantiello HF (1993a) Vasopressin and protein kinase A activate G protein-sensitive epithelial Na^+ channels. Am J Physiol Cell Physiol 265:C218–C223

Prat AG, Bertorello AM, Ausiello DA, Cantiello HF (1993b) Activation of epithelial Na^+ channels by protein kinase A requires actin filaments. Am J Physiol Cell Physiol 265:C224–C333

Prawitt D, Enklaar T, Klemm G, Gartner B, Spangenberg C, Winterpacht A, Higgins M, Pelletier J, Zabel B (2000) Identification and characterization of MTR1, a novel gene with homology to melastatin (MLSN1) and the trp gene family located in the BWS-WT2 critical region on chromosome 11p15.5 and showing allele-specific expression. Hum Mol Genet 22:203–216

Price MP, Lewin GR, McIlwrath SL, Cheng C, Xie J, Heppenstall PA, Stucky CL, Mannsfeldt AG, Brennan TJ, Drummond HA, Qiao J, Benson CJ, Tarr DE, Hrstka RF, Yang, B, Williamson RA, Welsh MJ (2000) The mammalian sodium channel BNC1 is required for normal touch sensation. Nature 407:1007–1011

Price MP, McIlwrath SL, Xie J, Cheng C, Qiao J, Tarr DE, Sluka KA, Brennan TJ, Lewin GR, Welsh MJ (2001) The DRASIC cation channel contributes to the detection of cutaneous touch and acid stimuli in mice. Neuron 32:1071–1083

Rossier BC (2002) Hormonal regulation of the epithelial sodium channel ENaC: N or Po? J Gen Physiol 120:67–70

Rossier BC (2004) The epithelial sodium channel: activation by membrane-bound serine proteases. Proc Am Thorac So. 1:4–9

Rotin D, Bar-Sagi D, O'Brodovich H, Merilainen J, Lehto VP, Canessa CM, Rossier BC, Downey GP (1994) An SH3 binding region in the epithelial Na^+ channel (alpha rENaC) mediates its localization at the apical membrane. EMBO J 13:4440–4450

Roza C, Puel JL, Kress M, Baron A, Diochot S, Lazdunski M, Waldmann R (2004) Knock-out of the ASIC2 channel in mice does not impair cutaneous mechanosensation, visceral mechanonociception and hearing. J Physiol 558:659–669

Sadoshima J, Qiu Z, Morgan JP, Izumo S (1996) Tyrosine kinase activation is an immediate and essential step in hypotonic cell swelling-induced ERK activation and c-fos gene expression in cardiac myocytes. EMBO J 15:5535–5546

Satlin LM (1994) Postnatal maturation of potassium transport in rabbit cortical collecting duct. Am J Physiol Renal Physiol 266:F57–F65

Satlin LM, Sheng S, Woda CB, Kleyman TR (2001) Epithelial Na^+ channels are regulated by flow. Am J Physiol Renal Physiol 280:F1010–F1018

Sawada Y, Sheetz MP (2002) Force transduction by Triton cytoskeletons. J Cell Biol 156:609–615

Schild L, Schneeberger E, Gautschi I, Firsov D (1997) Identification of amino acid residues in the α, β, γ subunits of the epithelial sodium channel (ENaC) involved in amiloride block and ion permeation. J Gen Physiol 109:15–26

Sharif Naeini R, Folgering J, Bichet D, Duprat F, Lauritzen I, Arhatte M, Jodar M, Dedman A, Chatelain FC, Schulte U, Retailleau K, Loufrani L, Patel A, Sachs F, Delmas P, Peters DJ, Honoré E (2009) Polycystin-1 and -2 dosage regulates pressure sensing. Cell 139:587–596

Sidhaye VK, Schweitzer KS, Caterina MJ, Shimoda L, King LS (2008) Shear stress regulates aquaporin-5 and airway epithelial barrier function. Proc Natl Acad Sci USA 105:3345–3350

Sokabe M, Sachs F, Jing ZQ (1991) Quantitative video microscopy of patch clamped membranes stress, strain, capacitance, and stretch channel activation. Biophys J 59:722–728

Sokolchik I, Tanabe T, Baldi PF, Sze JY (2005) Polymodal sensory function of the *Caenorhabditis elegans* OCR-2 channel arises from distinct intrinsic determinants within the protein and is selectively conserved in mammalian TRPV proteins. J Neurosci 25:1015–1023

Spassova MA, Hewavitharana T, Xu W, Soboloff J, Gill DL (2006) A common mechanism underlies stretch activation and receptor activation of TRPC6 channels. Proc Natl Acad Sci USA 103:16586–16591

Standly PR, Cammarata A, Nolan BP, Purgason CT, Stanley MA (2002) Cyclic stretch induces vascular smooth muscle cell alignment via NO signaling. Am J Physiol Heart Circ Physiol 283:H1907–H1914

Stokes JB (1993) Ion transport by the collecting duct. Semin Nephrol 13:202–212

Stossel TP, Condeelis J, Cooley L, Hartwig JH, Noegel A, Schleicher M, Shapiro SS (2001) Filamins as integrators of cell mechanics and signalling. Nat Rev Mol Cell Biol 2:138–145

Strotmann R, Harteneck C, Nunnenmacher K, Schultz G, Plant TD (2000) OTRPC4, a nonselective cation channel that confers sensitivity to extracellular osmolarity. Nat Cell Biol 2:695–772

Sukharev SI, Martinac B, Arshavsky VY, Kung C (1993) Two types of mechanosensitive channels in the Escherichia coli cell envelope: solubilization and functional reconstitution. Biophys J 65:177–183

Sukharev SI, Blount P, Martinac B, Blattner FR, Kung C (1994) A large-conductance mechanosensitive channel in E. coli encoded by mscL alone. Nature 368:265–268

Sukharev SI, Schroeder MJ, McCaslin DR (1999) Stoichiometry of the large conductance bacterial mechanosensitive channel of *E. coli.* A biochemical study. J Membr Biol 171:183–193

Suzuki M, Mizuno A, Kodaira K, Imai M (2003) Impaired Pressure Sensation in Mice Lacking TRPV4. J Biol Chem 278:22664–22668

Taber LA (1998) A model for aortic growth based on fluid shear and fiber stresses. J Biomech Eng 120:348–354

Tamada M, Sheetz MP, Sawada Y (2004) Activation of a signaling cascade by cytoskeleton stretch. Dev Cell 7:709–718

Tarran R, Button B, Picher M, Paradiso AM, Ribeiro CM, Lazarowski ER, Zhang L, Collins PL, Pickles RJ, Fredberg JJ, Boucher RC (2005) Normal and cystic fibrosis airway surface liquid homeostasis: the effects of phasic shear stress and viral infections. J Biol Chem 280:35751–35759

Taruno A, Niisato N, Marunaka Y (2007) Hypotonicity stimulates renal epithelial sodium transport by activating JNK via receptor tyrosine kinases. Am J Physiol Renal Physiol 293:F128–138

Thoroed SM, Lauritzen L, Lambert IH, Hansen HS, Hoffmann EK (1997) Cell swelling activates phospholipase A2 in Ehrlich ascites tumor cells. J Membr Biol 160:47–58

Tobin D, Madsen D, Kahn-Kirby A, Peckol E, Moulder G, Barstead R, Maricq A, Bargmann C (2002) Combinatorial expression of TRPV channel proteins defines their sensory functions and subcellular localization in *C. elegans* neurons. Neuron 35:307–318

Tsavaler L, Shapero MH, Morkowski S, Laus R (2001) Trp-p8, a novel prostate-specific gene, is up-regulated in prostate cancer and other malignancies and shares high homology with transient receptor potential calcium channel proteins. Cancer Res 61:3760–3769

Turnheim K (1991) Intrinsic regulation of apical sodium entry in epithelia. Physiol Rev 71:429–445

Urbach V, Leguen I, O'Kelly I, Harvey BJ (1999) Mechanosensitive calcium entry and mobilization in renal A6 cells. J Membr Biol 168:23–37

Vallet V, Chraibi A, Gaeggeler HP, Horisberger JD, Rossier BC (1997) An epithelial serine protease activates the amiloride-sensitive sodium channel. Nature 389:607–610

Vasquez V, Sotomayor M, Cortes DM, Roux B, Schulten K, Perozo E (2008) Three-dimensional architecture of membrane-embedded MscS in the closed conformation. J Mol Biol 378:55–70

Vriens J, Watanabe H, Janssens A, Droogmans G, Voets T, Nilius B (2004) Cell swelling, heat, and chemical agonists use distinct pathways for the activation of the cation channel TRPV4. Proc Natl Acad Sci USA 101:396–401

Ward ML, Williams IA, Chu Y, Cooper PJ, Ju YK, Allen DG (2008) Stretch-activated channels in the heart: contributions to length-dependence and to cardiomyopathy. Prog Biophys Mol Biol 97:232–249

Winn MP, Conlon PJ, Lynn KL, Farrington MK, Creazzo T, Hawkins AF, Daskalakis N, Kwan SY, Ebersviller S, Burchette JL, Pericak-Vance MA, Howell DN, Vance JM, Rosenberg PB (2005) A mutation in the TRPC6 cation channel causes familial focal segmental glomerulosclerosis. Science 308:1801–1804

Yoshimura K, Sokabe M (2010) Mechanosensitivity of ion channels based on protein-lipid interactions. J R Soc Interface 7(Suppl 3):S307–S320

Yoshimura K, Nomura T, Sokabe M (2004) Loss-of-Function Mutations at the Rim of the Funnel of Mechanosensitive Channel MscL. Biophys J 86:2113–2120

Yu WG, Sokabe M (1997) Hypotonically induced whole-cell currents in A6 cells: relationship with cell volume and cytoplasmic Ca^{2+}. Jpn J Physiol 47:553–565

Chapter 7
Ion Channels in Cardiac Fibroblasts: Link to Mechanically Gated Channels and their Regulation

Denis V. Abramochkin, Ilya Lozinsky and Andre Kamkin

7.1 Introduction

For many years the question of cardiac functioning was boiled down mainly to the functioning of cardiomyocytes and their interaction. However, though cardiomyocytes occupy approximately 75 % of normal myocardial tissue volume, they account for only 30–40 % of cell numbers (Vliegen et al. 1991). The majority of the remaining non-muscular cells are fibroblasts. Other cell types, such as endothelial or vascular smooth muscle cells, represent comparatively small populations (Adler et al. 1981). In several regions of the heart, such as sinoatrial node, the density of fibroblasts is particularly high. Along with the extracellular matrix (ECM) these cells occupy more than half of the sinoatrial tissue volume (Boyett et al. 2000; Kohl et al. 2005). Throughout the myocardium fibroblasts form the surroundings of cardiomyocytes, so that every cardiomyocyte is closely related to a fibroblast in normal cardiac tissue (Camelliti et al. 2005). Thus, the great importance of fibroblasts for development of myocardial structure is beyond dispute. However, during the last two decades the growing evidence of their contribution to the electro-mechanical function of myocardium was reported.

It is generally accepted that cardiac fibroblasts can affect electrophysiological properties of myocardium passively, for example by acting as obstacles to the orderly spread of electrical excitation (Camelliti et al. 2005). For example, fibroblasts, separating the sinoatrial node from the interatrial septum, reduce direct electrical coupling between these regions and form unique anisotropic pattern of impulse propagation from the sinoatrial node (Boyett et al. 2000; Oren and Clancy 2010). Moreover, interstitial fibrosis and collagen accumulation correspond as an important source of local anisotropy in myocardial ischaemia and hypertrophy, enhancing predisposition to cardiac arrhythmogenesis (Spach and Boineau 1997; Wolk et al. 1999). However,

A. Kamkin (✉) · I. Lozinsky · D. V. Abramochkin
Department of Fundamental and Applied Physiology, Laboratory of Electrophysiology, Russian State Medical University, Ostrovitjanova 1, Moscow 117997, Russia
e-mail: Kamkin.A@g23.relcom.ru

A. Kamkin, I. Lozinsky (eds.), *Mechanically Gated Channels and their Regulation,* Mechanosensitivity in Cells and Tissues 6,
DOI 10.1007/978-94-007-5073-9_7,

the possibility that fibroblasts may actively contribute to cardiac electrophysiology has been considered only recently (Kamkin et al. 2003a, b).

Early investigations on cultured cell lines have shown that fibroblasts posess resting membrane potential (E_m) between −10 mV and −40 mV (Tsuchiya et al. 1981; Okada et al. 1984). However, the fibroblasts within the cardiac tissue are not isolated at all. The subsequent studies demonstrated abundant presence of gap junction channels between cardiomyocytes and fibroblasts (Rook et al. 1992; Kohl et al. 2005). The electrical coupling between cardiomyocytes and fibroblasts is so effective that action potential propagates between two cardiomyocytes interconnected through a fibroblast with no apparent delay. In fibroblasts, which were co-cultured with cardiomyocytes, the changes of membrane potential, synchronized with the contractions of cardiomyocytes, have been detected (Goshima and Tonomura 1969; Goshima 1970). Therefore, the electrophysiological properties of cardiac fibroblasts should be studied to the possible extent in intact myocardium.

In 1986 these properties were determined for the first time in our lab by means of floating glass microelectrode technique and subsequently studied in detail (Kiseleva et al. 1987; Kamkin et al. 1988). Fibroblasts in rat atrial tissue had a mean resting membrane potential (E_m) of approximately −22 mV with a distribution range between −5 mV and −70 mV, and input resistances of ≈0.5 GΩ (Kiseleva et al. 1998; Kamkin et al. 2002). The wide range of recorded E_m points to the possibility that fibroblasts are exposed to variable mechanical forces in their normal tissue environment. A step-by-step increase of applied stretch gradually hyperpolarized E_m of the fibroblasts (Kamkin et al. 1999; 2003b, c) (Fig. 7.1). On the other hand, mechanical compression depolarized the membrane potential in the majority of fibroblasts and elicited so-called "mechanically induced potentials" (MIPs) (Kiseleva et al. 1996).

The present review is focused on properties and function of ionic currents described in the cardiac fibroblasts. At the present time several types of potassium ionic channels, as well as sodium and chloride voltage-gated channels, proton channels and non-voltage gated non-selective cation TRP channels are found in cardiac fibroblasts (Table. 7.1). As long as these cells demonstrate drastic susceptibility to mechanical stimuli, special attention is given to the mechanosensitive currents and mechanically gated ion channels. The reported electrophysiological findings were obtained in isolated fibroblasts, and considering the possible physiological role of each current one should take into account that fibroblasts, which are incorporated into the cardiac tissue differ from freshly isolated or cultured cells.

7.2 Voltage-Gated K^+ Currents

The typical potassium voltage-gated channels (K_V channels) contain six transmembrane segments and one pore-forming region (Tamargo et al. 2004). Immediately after depolarization K_V channels move from the closed to the open state (activation), leading to onset of related potassium current. After the activation many channels enter into a nonconducting state (inactivation), leading to a decline in activated

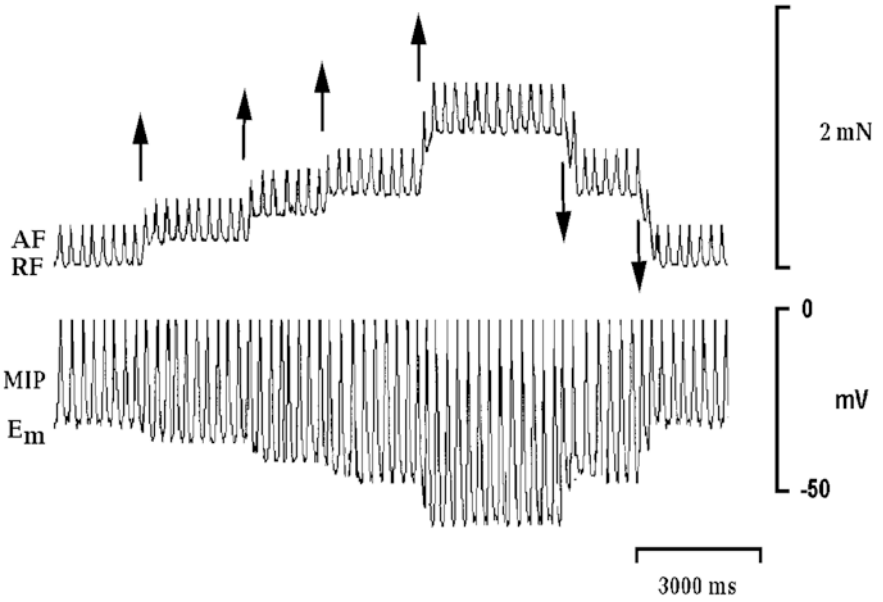

Fig. 7.1 Typical membrane potential changes of a rat atrial fibroblast and mechanically induced potentials (MIPs) in response to mechanical stretch of the tissue. Synchronous registration of the active force and resting force (*top* curve) and MIPs of the fibroblast (*bottom* curve). The symbol (↑) indicates the time point of stretch application, whereas ↓ marks the release of applied stretch. AF—active force, RF—resting force, MIP—mechanically induced potential of the fibroblast, E_m—resting potential of the fibroblast. Modified from Kiseleva et al. (1998) with permission of Elsevier

current. During the repolarization of the membrane channels recover from the inactivated state and are once again capable of opening in response to membrane depolarization. Two major types of inactivation are distinguished (Yellen 2002). The fast N-type inactivation results from the blocking of the intracellular mouth of the channel pore by a "ball and chain" mechanism when the channel opens. The relatively slow C-type inactivation appears to involve a rearrangement of residues in the external mouth of the channel that becomes occluded consequently.

The delayed rectifier potassium current (I_K) is carried through channels formed from four identical α-subunits (homotetramers) or combinations of different subunits (heterotetrameres). These subunits are $K_V1.1$, $K_V1.2$, $K_V1.3$, $K_V1.5$, and $K_V1.6$ (Tamargo et al. 2004). It is widely recognized that I_K is present in all cardiomyocytes and crucial for the repolarisation stage of action potential. In the human cardiomyocytes, I_K can be separated into at least three different components, the ultrarapid (I_{Kur}), rapid (I_{Kr}) and slow (I_{Ks}) delayed rectifier current (Roden and Balser 2002). These currents exhibit different kinetics and pharmacological properties, are regulated by different intracellular signaling pathways and are encoded by separate genes.

In cardiac fibroblasts the presence of I_K is beyond any doubt. The first detailed characterization of the time- and voltage-dependent properties of I_K in freshly

Table 7.1 Ionic currents found in the different types of cardiac fibroblasts

Current	Molecular components	Type of cardiac fibroblasts	References
Delayed rectifier potassium current (I_K)	K_V1.1, K_V1.2, K_V1.3, K_V1.6	Freshly isolated from adult rat	Shibukawa et al. 2005
	K_V1.5, K_V2.1	Freshly isolated from neonatal rat	Walsh and Zhang 2008
	K_V1.5, K_V1.6	Cultured from human	Li et al. 2009
Transient potassium current (I_{to})	K_V1.4	Freshly isolated from neonatal rat	Walsh and Zhang 2008
	K_V4.3, K_V4.2	Cultured from human	Li et al. 2009
Inward rectifier potassium current (I_{Kir})	K_{ir}2.1	Freshly isolated from adult rat	Chilton et al. 2005
	K_{ir}2.1, K_{ir}2.3	Cultured from human	Li et al. 2009
	K_{ir}6.1	Cultured from mouse	Benamer et al. 2009
Ca^{2+}-activated K^+currents ($I_{K(Ca)}$)	KCa1.1	Cultured from human	Wang et al. 2006; Li et al. 2009
TTX-sensitive sodium voltage-gated current ($I_{Na.TTX}$)	–	Freshly isolated from neonatal rat	Walsh and Zhang 2008 (the current was not characterized)
	Na_V1.2, Na_V1.3, Na_V1.6, Na_V1.7	Cultured from human	Li et al. 2009
TTX-resistant sodium voltage-gated current ($I_{Na.TTXR}$)	Na_V1.5	Cultured from human	Li et al. 2009
Volume-sensitive chloride current ($I_{Cl.vol}$)	Clcn3	Cultured from human	El Chemaly et al. 2006; Li et al. 2009
Voltage gated proton current(I_{Hv})	H_V1	Cultured from human	El Chemaly et al. 2006
Non-selective cation currents through TRP (I_{ns})	TRPC2, TRPC3, TRPC5, TRPV2, TRPV4, TRPV6, TRPM4, TRPM7	Freshly isolated from adult rat	Rose at al. 2007; Hatano et al. 2009
Mechanosensitive current	–	Freshly isolated from adult rat	Kamkin et al. 2003a, c; 2010a, b

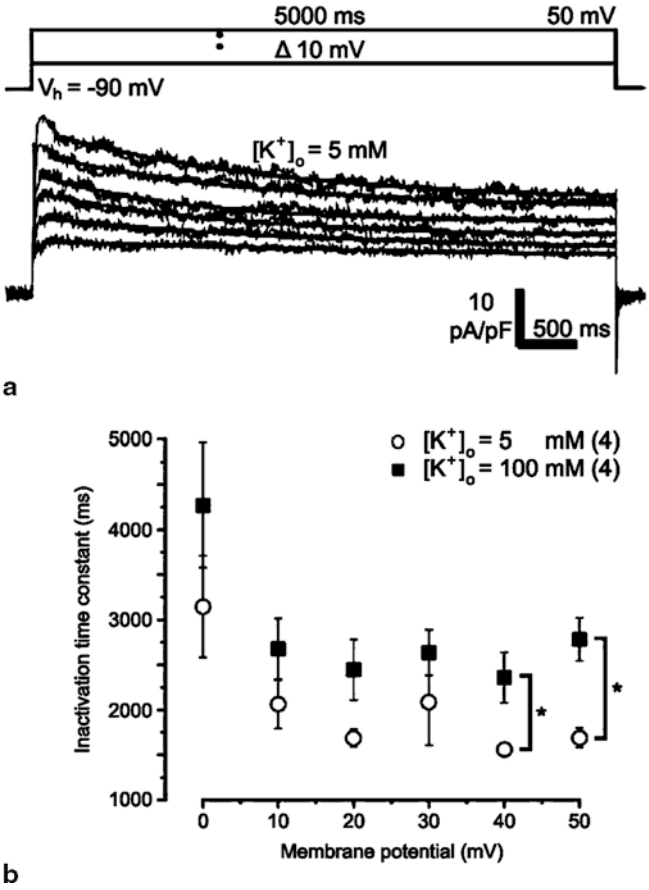

Fig. 7.2 Inactivation kinetics of the cardiac fibroblast K^+ current. **a** An example of the outward currents obtained at selected membrane potentials between +10 and +50 mV from a V_h of −90 mV (*gray* lines) in 5 mM $[K^+]_o$. The superimposed heavy lines denote best fit of a single exponential function. This analysis yielded inactivation time constants (τ) ranging from 2461 ms at a membrane potential of +10 mV to 1894 ms at a membrane potential of +50 mV. **b** Mean values of the time constants (τ) of activation versus membrane potentials from 0 mV to +50 mV in 5 mM (○) and 100 mM (■) $[K^+]_o$ are shown. Statistically significant differences between these values of inactivation time constants are indicated by asterisks: *P < 0.05. (From Shibukawa et al. (2005) with permission of Elsevier)

isolated adult rat ventricular fibroblasts was provided by Shibukawa et al. (2005). Their biophysical and pharmacological results showed that rat ventricular fibroblasts express a slowly activating and slowly inactivating K^+ current, which appears to exhibit C-type inactivation (Fig. 7.2), which activated with a time constant (τ) of 19 ms at +50 mV and underwent steady-state inactivation with a half-maximal voltage ($V_{1/2}$), required for inactivation, of −24 mV in physiological external solution. This current is sensitive to dendrotoxin-I (Shibukawa et al. 2005), which

selectively blocks $K_V1.1$, 1.2, 1.3 and 1.6 (Coetzee et al. 1999) and rTityustoxin-Kα, K_V 1.3 blocker (Rodrigues et al. 2003). Therefore authors supposed that the fibroblast potassium current resembling the properties of I_K is generated by channels consisting of subunits from the $K_V1.x$ family.

In neonatal rat ventricular fibroblasts two types of kinetically distinct I_K currents, different from those described in adult rat fibroblasts, were found (Walsh and Zhang 2008). The first current, defined as the fast delayed rectifier (I_{Kf}), activated with a T of 2.4 ± 1 ms at +50 mV. It was resistant to tetraethylammonium (TEA), but sensitive to 4-aminopyrydine (4-AP). The second, slow inward rectifier current (I_{Ks}) was, nevertheless much faster than I_K in adult fibroblasts (T – 6 ± 1 ms at +50 mV). Unlike I_{Kf} it was sensitive to TEA, but, in contrast to I_K of adult rat fibroblasts, it was completely insensitive to dendrotoxin. Authors propose $K_V1.5$ as a molecular basis for I_{Kf} and $K_V2.1$– for I_{Ks}. It is wholesome to note that I_{Kf} was present only in 22 % and I_{Ks} – in 19 % of neonatal fibroblast, while I_K was found in ~90 % of adult rat fibroblasts.

While speculating about possible clinical implications of cardiac fibroblast ionic currents, we should note that to the present moment there are no electrophysiological studies conducted on freshly isolated human cardiac fibroblasts. However, the properties of cultured cells were studied by Li et al. (2009). According to their findings, I_K, sensitive to 4-AP, is present in cultured human cardiac fibroblasts, although this current was not characterized in detail. Authors have also demonstrated significant gene expression of $K_V1.5$ and $K_V1.6$ and proposed their participation in generation of I_K.

Another important voltage-gated current is I_{to}. This current is rapidly activated and inactivated in response to depolarization. In cardiomyocytes I_{to} is usually considered to be a sum of a voltage-dependent, calcium-independent K^+ current sensitive to 4-AP and Ca^{2+}-activated 4-AP insensitive Cl^- or K^+ current (Tamargo et al. 2004; Oudit et al. 2001). However, the latter one is questionable and is not found in fibroblasts, so we are going to discuss only the former current, which has completely potassium nature. In cardiomyocytes I_{to} is responsible for early rapid repolarization phase of action potential and therefore determines the height of the early plateau. The $K_V1.4$, $K_V4.1$, $K_V4.2$ and $K_V4.3$ α-subunits, which can combine into homo- or heterotetrameres represent the molecular basis of I_{to} (Tamargo et al. 2004).

While I_{to} was not found in cardiac fibroblasts of adult rats (Shibukawa et al. 2005; Chilton et al. 2005), it is abundant in neonatal rat ventricular fibroblasts (was present in 58 % of studied cells) (Walsh and Zhang 2008). The current activated during voltage steps applied to potentials positive to −40 mV (Fig. 7.3) and inactivated during depolarizing steps to more positive potentials. The time constant of inactivation of I_{to}, measured during a 100-ms voltage step to −50 mV, was 29 ± 2 ms in average, $V_{1/2}$, required for inactivation was −58 mV, whereas the $V_{1/2}$for activation was −1 mV (Walsh and Zhang 2008). The results of immunoblot analysis indicated that I_{to} in these fibroblasts is generated by the channels composed of $K_V1.4$ only, unlike the cardiomyocytes, where $K_V4.x$ are predominant (Kaab et al. 1998). Such difference in molecular composition may be the possible explanation of surprising complete insensitivity of the fibroblast I_{to} to 4-AP.

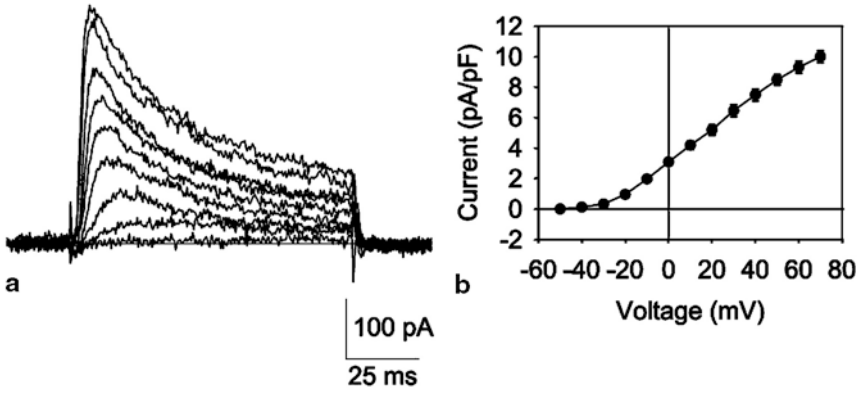

Fig. 7.3 Measurement of a transient outward K^+ current (I_{to}) in neonatal rat ventricular fibroblasts. **a** Currents recorded during voltage steps, given in 10-mV increments, to potentials ranging from −30 to + 50 mV. **b** Peak current vs. voltage relationship for I_{to} (n = 20 cells). Currents were normalized to cell membrane capacity. (From Walsh and Zhang (2008) with permission from The American Physiological Society)

In contrast to rat fibroblasts, human cultured cardiac fibroblasts express I_{to} very similar to those present in cardiomyocytes (Li et al. 2009). It is sensitive to 4-AP and depends on $K_V4.3$ and $K_V4.2$ α-subunits, instead of $K_V1.4$. The $V_{1/2}$for activation of this current was 11.2 ± 0.4 mV.

Interestingly, I_{to} can be regulated by PKC phosphorylation at least in fibroblasts of newborn rats (Walsh and Zhang 2008). Activation of PKC with phorbol esters leads to substantial decrease in I_{to}, indicating the potential role of this current as a target for various agents activating the phosphoinositide signaling cascade.

7.3 Inward Rectifying K^+ Currents

Inward rectifier K^+ channels (K_{irs}), which are responsible for inward rectifier current (I_{K1}), potassium ATP-dependent current (I_{KATP}) and potassium acetylcholine-dependent current (I_{KACh}), differ from K_V channels in their structure and functions. These channels contain two transmembrane domains connected by a pore region and intracellular N- and C-termini (Shieh et al. 2000; Lopatin and Nichols 2001). They can conduct K^+ currents in the inward direction easier than in the outward. In cardiomyocytes these currents play an important role in setting the resting potential close to the potassium equilibrium potential and in repolarization.

The latter statement is especially true for I_{K1}. At negative potentials I_{K1} conductance is many times larger than that of any other current, therefore it clamps the membrane potential of cardiomyocytes close to the potassium equilibrium potential (Lopatin and Nichols 2001; Schram et al. 2002). The K1 channels are formed by

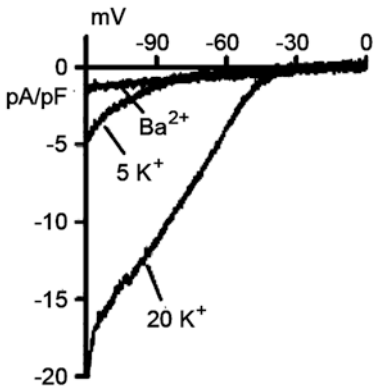

Fig. 7.4 Effect of Ba^{2+} on I_{K1} in human cardiac fibroblasts: I–V relationships of membrane currents recorded in a representative cell with a 2-s ramp protocol (−120 to 0 mV from a holding potential of −40 mV) in 5 mM K^+_o, 20 mM K^+_o, and after application of 0.5 mM Ba^{2+}. (From Li et al. (2009))

$K_{ir}2.1$, $K_{ir}2.2$ and $K_{ir}2.3$ subunits, among which the $K_{ir}2.1$ is predominant (Lopatin and Nichols 2001).

I_{K1} was found and characterized in adult rat ventricular fibroblasts by Chilton et al. (2005). Approximately 70 % of studied fibroblasts expressed a measurable inwardly rectifying current. This current is sensitive to Ba^{2+}, which is a potent blocker of I_{K1} (Wible et al. 1995), and depends greatly on changes in extracellular potassium concentration ($[K^+]_o$). Increase in $[K^+]_o$ caused shift in the reversal potential of I_{K1} to the less negative potentials. Authors claim the crucial role of I_{K1} in maintenance of resting membrane potential in fibroblasts, which is usually close to the potassium equilibrium potential. Such low membrane potential is required, in turn, for survival and proliferation of fibroblasts (Chilton et al. 2005). Basing on discovered significant expression of $K_{ir}2.1$ mRNA they propose that in fibroblasts I_{K1} is conducted by $K_{ir}2.1$ channels similarly to the cardiomyocytes.

Experiments on cultured human fibroblasts provided quite similar results to those obtained in rat fibroblasts (Li et al. 2009). In these cells I_{K1} also depends on $[K^+]_o$ and can be abolished by Ba^{2+} (Fig. 7.4). $K_{ir}2.1$ and $K_{ir}2.3$ are substantially expressed in human fibroblasts.

Novel inwardly rectifying K^+ channels, which are not present in cardiomyocytes, have been described recently by Benamer et al. (2009) in mouse ventricular fibroblasts. In many ways these channels resemble ATP-dependent channels, however, they are not sensitive to intracellular ATP at all and consist of $K_{ir}6.1$ α-subunits and SUR2 regulatory β-subunits, while normal ATP-dependent channels have $K_{ir}6.2$ with ATP-binding site instead of $K_{ir}6.1$. Similarly to I_{KATP} this current can be stimulated by pinacidil and blocked by glibenclamide (Fig. 7.5). Sphingosine-1-phosphate (S1P), a sphingolipid which is secreted by macrophages and platelets in response to cell damage stimulates this current via the third type of S1P receptors (Benamer et al. 2011). It leads to increased cell proliferation and decreased secretion of IL-6 (pro-hypertrophic cytokine) and collagen by fibroblasts, therefore these current might be involved in cardioprotection and postinfarct recovery of the heart.

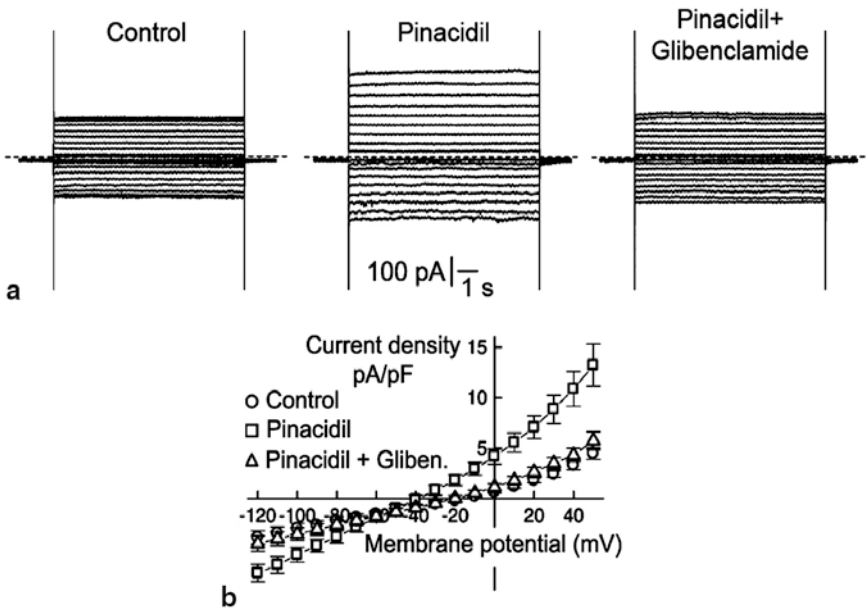

Fig. 7.5 Effects of pinacidil (100 μM) and glibenclamide (10 μM) on whole-cell currents. **a** Currents elicited by membrane depolarizations from −120 to +50 mV in control conditions (*left*), in the presence of 100 μM pinacidil (*middle*), and in the presence of pinacidil + glibenclamide 10 μM (*right*). Holding potential: −50 mV. **b** Mean I/V relationships obtained under control conditions, in the presence of pinacidil and in the presence of pinacidil+glibenclamide ($n = 12$). (From Benamer et al. (2009) with permission of Elsevier)

7.4 Ca^{2+}-Activated K^+ Currents

The large-conductance Ca^{2+}-activated channels (BK_{Ca}), which are formed by α-subunit ($K_{Ca}1.1$) homotetramers (Vergara et al. 1998), differ from most of other K+ channels, because their activation is allosterically switched on either by membrane depolarization or by increased intracellular Ca^{2+}. While these channels are abundant in vascular smooth muscle cells and participate in the regulation of vascular tone (Saito et al. 2002), they are absent in cardiomyocytes' plasmatic membrane. However, cardiomyocytes express another type, small conductance Ca^{2+}-activated K^+ channels (SK) (Xu et al. 2003). Along with I_K, I_{to} and I_{K1}, I_{SK} was shown to play an important role in the repolarization phase of the action potential.

Among cardiac fibroblasts of different species, the presence of BK_{Ca}channels was demonstrated only in cultured human fibroblasts. The pioneering findings of Wang et al. (2006) were subsequently confirmed by two other studies (Li et al. 2009; He et al. 2011). In human cardiac fibroblasts $I_{K(Ca)}$ is a large, noisy outward current with a pronounced outward rectification and reversal potential of −75 mV (Fig. 7.6). In patch-clamp experiments it can be greatly reduced by removal of extracellular Ca^{2+} or completely abolished by increase in the intracellular EGTA concentration.

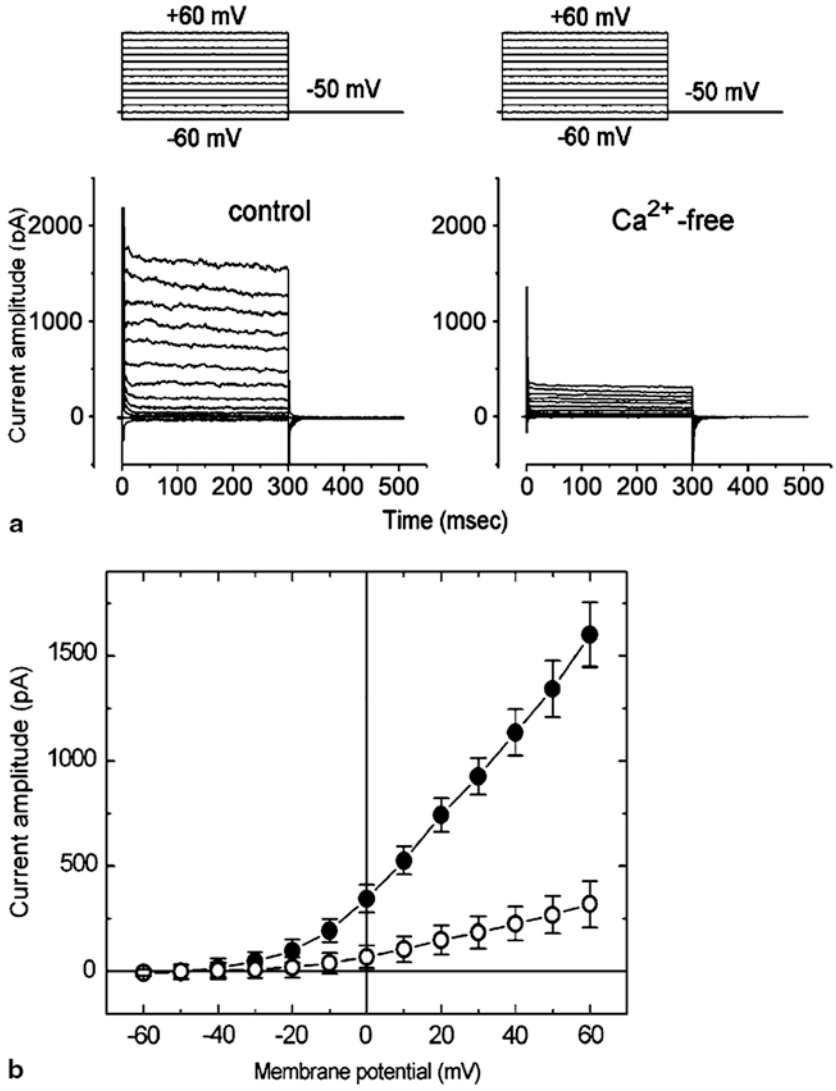

Fig. 7.6 Effect of removal of extracellular Ca^{2+} on $I_{K(Ca)}$recorded from human cardiac fibroblasts. The cells were bathed in normal Tyrode's solution containing 1.8 mM $CaCl_2$. The cell was held at −50 mV, and voltage pulses ranging from −60 to +60 mV in 10-mV increments were applied with a duration of 300 ms. The patch solution contained 0.1 mM EGTA. **a** Superimposed current traces obtained in the control (*left*) and during exposure (*right*) to Ca^{2+}-free solution. The upper parts shown in each current record indicate the voltage protocol examined. **b** I–V relationships of I_K measured at the end of voltage pulses in the absence (o) and presence (•) of extracellular Ca^{2+} (1.8 mM). Each point represents the mean ± SE (n = 7–10). (From Wang et al. (2006) with permission of Springer)

$I_{K(ca)}$ could be easily blocked by paxilline and iberiotoxin, typical blockers of BK_{Ca} channels, while it was almost insensitive to apamine (SK channels blocker) and glibenclamide (K_{ATP} blocker) (Wang et al. 2006). Thus, in contrast to cardiomyocytes, expressing SK, but not BK_{Ca}, channels, cultured human cardiac fibroblasts express prominent $I_{K(ca)}$, mediated by BK_{Ca} channels and composed of KCa1.1 α-subunits (Li et al. 2009).

The authors have also shown that $I_{K(Ca)}$ can be elicited by simulated cardiomyocyte action potential waveform. Therefore, the activity of BK_{Ca} channels in fibroblasts can be elicited by action potential from cardiomyocyte, if these two types of cells are functionally linked by gap junctions. On the other hand, the K^+ outward current to which BK_{Ca} channel activity seen in cardiac fibroblasts contributes, tends to have an impact on electrical activity of cardiomyocytes (Wang et al. 2006). Another physiological function of BK_{Ca} in cardiac fibroblasts is their recently shown involvement in the regulation of proliferation in cultured human cardiac fibroblasts by promoting cell cycle progression via modulating cyclin D1 and cyclin E expression (He et al. 2011).

7.5 Na^+ Voltage-Gated Currents

For a long time it was believed that no depolarizing inward currents, like those conducted by calcium and sodium voltage-sensitive channels in cardiomyocytes, can be present in nonexcitable cells such as fibroblasts. However, voltage-gated sodium currents were found in cardiac fibroblast just recently (Li et al. 2009). Calcium voltage-gated current are still not described in fibroblasts, although an auxiliary β subunit ($Ca_V\beta 2$) is expressed in murine cardiac fibroblasts (Meissner et al. 2011).

The first observation of sodium inward current in cardiac fibroblasts was made by Walsh and Zhang (2008) in their electrophysiological investigation of neonatal rat ventricular fibroblasts. The current, which was sensitive to tetrodotoxin (TTX) was detected in 36 % of studied cells, however, the authors didn't characterize it.

The only detailed study of fibroblast sodium voltage-gated currents was performed using cultured human cardiac fibroblasts (Li et al. 2009). Two distinct currents were described. The first exhibited an incomplete inactivation during 50 ms depolarization, similarly to I_{CaL} in cardiomyocytes. Nevertheless, it was carried by Na^+ cations and was insensitive to I_{CaL} blocker nifedepine, but could be abolished by nanomolar concentrations of TTX. This TTX-sensitive sodium current ($I_{Na,TTX}$) had a threshold potential of −40 mV and peaked at +10 mV (Fig. 7.7). Another sodium current was resistant to TTX ($I_{Na,TTXR}$), but was sensitive to nifedipine, although it was carried by Na^+. $I_{Na,TTXR}$ had a threshold potential of −50 mV and peaked at 0 mV. The inactivation process of $I_{Na,TTXR}$ was faster than that of $I_{Na,TTXR}$, at the same time the recovery from inactivation was slower for $I_{Na,TTXR}$ than for $I_{Na,TTXR}$.

Thus, the $I_{Na,TTX}$ in cultured human cardiac fibroblasts shares some properties with typical neuronal I_{Na}, e.g. a transient inward current followed by a persistent component, sensitive to inhibition by nanomolar TTX, and is likely to be encoded by $Na_V1.2$, $Na_V1.3$, $Na_V1.6$, and $Na_V1.7$, since mRNAs of these α-subunits are expressed in human cardiac fibroblasts. The $I_{Na,TTXR}$ in human cardiac fibroblasts

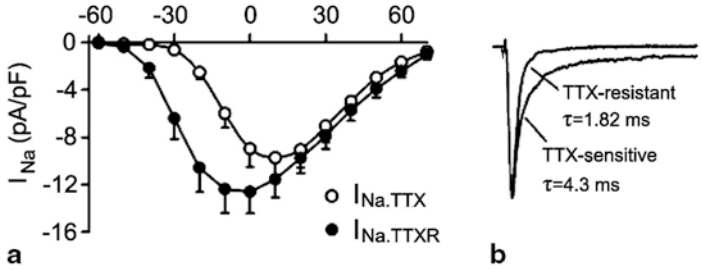

Fig. 7.7 Two types of sodium currents in human cultured cardiac fibroblasts. **a** Mean values of I–V relationships of $I_{Na.TTX}$ and $I_{Na.TTXR}$. **b** Inactivation time course of representative I_{Na} traces (at 0 mV) was fitted to a monoexponential function with time constant (τ) shown, 4.3 ms for $I_{Na.TTX}$ and 1.82 ms for $I_{Na.TTXR}$. (From Li et al. (2009))

shares some features with I_{Na} in cardiomyocytes, e.g. can be inhibited by micromolar TTX and it is encoded by $Na_V1.5$, although it is not completely the same.

To the present moment there are no sensible hypothesis concerning the functional role of I_{Na} in cardiac fibroblast. The possible participation of this current in regulation of fibroblasts proliferation was excluded in the recent study (He et al. 2011).

7.6 Volume-Sensitive Chloride Current

A volume-sensitive chloride current ($I_{Cl.vol}$) is found in mammalian cardiomyocytes, including human ones (Hiraoka et al. 1998; Baumgarten and Clemo 2003; Du et al. 2004). In normal myocytes this current is negligibly small, however, it is activated by cell swelling and/or membrane deformation. In the myocardium $I_{Cl.vol}$ participates in the cell volume regulation, shortens cardiac action potential and depolarizes resting membrane potential (Hiraoka et al. 1998). $I_{Cl.vol}$ is believed to be conducted by so-called volume regulated anion channels, although molecular basis of these channels is still not defined clearly.

Recently, $I_{Cl.vol}$ was found in cultured human cardiac fibroblasts by El Chemaly et al. (2006) and studied in detail by Li et al. (2009). In contrast to cardiomyocytes, 7 % of studied fibroblasts exhibited $I_{Cl.vol}$ without any hypotonic exposure or any other manipulations. During the hypotonic exposure this current was extensively activated in almost all fibroblasts. The current was sensitive to specific Cl^- channel inhibitor 4,49-diisothiocyanostilbene-2,29-disulfonic acid (DIDS). The I–V relationship (Fig. 7.8) of the DIDS-sensitive current obtained by subtracting control currents from the current recorded after DIDS application displayed outward rectification and had a reversal potential of −35 mV, which is close to Cl^- equilibrium potential (E_{Cl}, −46.8 mV).

Clcn3 channel was proposed as a major candidate for $I_{Cl.vol}$ channels. The presence of Clcn3 and to the lesser extent of Clcn2 in the cultured human cardiac fibroblasts was shown in the latter study (Li et al. 2009).

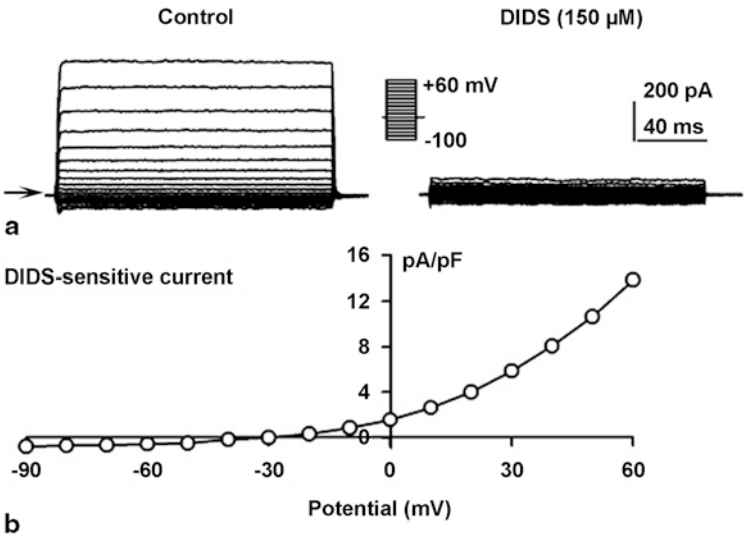

Fig. 7.8 I_{Cl} in human cardiac fibroblasts. **a** Voltage-dependent current was inhibited by the Cl^- channel blocker DIDS (150 μM). Current was elicited by the voltage steps ranging from −100 to +60 mV as shown in the inset (0.2 Hz). **b** I–V relation curve of DIDS-sensitive current obtained by subtracting currents before and after DIDS application in A

According to the recent study, along with obvious role of $I_{Cl.vol}$ in control of cell volume, one of the possible functions of this current is mediation of the cell cycle progression (He et al. 2011).

7.7 Voltage-Gated Proton Current

A voltage-gated current carried by protons has been described for many types of mammalian cells, although it was not found in cardiomyocytes to our knowledge (Decoursey 2003; El Chemaly et al. 2006). It is conducted via special voltage-gated channels H_V1, which are selectively permeable for protons. In contrast to typical voltage-gated channels (K_V, e.t.c.), where ions go through a single pore located between membrane-spanning pore domains from each of four subunits, Hv1 channel is a dimer, in which each subunit contains its own pore and gate, which is controlled by its own voltage sensor (Tombola et al. 2008). The pore is likely to be situated in the heart of voltage sensing domain of the subunit (Fig. 7.9).

Among cardiac fibroblasts voltage gated proton current (I_{Hv}) was found only in the cultured cells from humans (El Chemaly et al. 2006), where it is quite abundant (detected in 86 % of studied fibroblasts). This current is activated by depolarization and during normal extracellular pH it can be registered only in the case of intracellular acidification, because pH transmembrane gradient is needed as a driving force for this current. Changing the pH gradient by one unit leads to a 51 mV shift in the

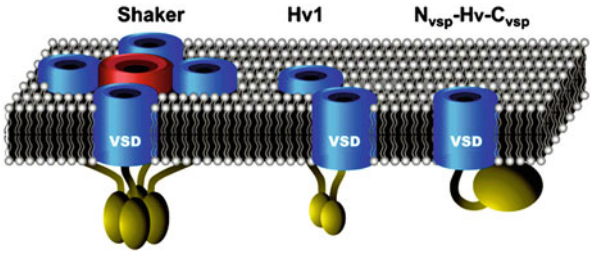

Fig. 7.9 Tetrameric omega-conducting shaker potassium channel compared to the dimeric Hv1 channel and the monomeric chimera N_{VSP}-Hv-C_{VSP}. Voltage-sensitive domains are *blue*, and the pore domain of Shaker is *pink*. Intracellular domains are dark *yellow*. In Hv1 and Shaker, the intracellular domains are important for oligomerization. The intracellular domain of Ci-VSP is a lipid phosphatase. The ability of the voltage-sensitive domains of Shaker and Hv1 to conduct ions or protons depends on the presence of neutral residues at key positions in the S4 segment. Wild type Ci-VSP does not conduct protons or solution ions, but the N_{VSP}-Hv-C_{VSP} chimera conducts protons. (From Tombola et al. (2009) with permission of Elsevier)

reversal potential of I_{Hv} (Fig. 7.10), demonstrating a high selectivity of Hv channels for protons. I_{Hv} can be completely blocked by 100 μM Zn^{2+} (Fig. 7.10), while Cd^{2+} promotes only moderate reduction in the current amplitude. The authors propose the important role of I_{Hv} in control of the membrane potential in the case of intracellular acidosis, which may appear at least due to the ischemic conditions. The augmentation of pH gradient facilitates the outward current by shifting its activation threshold to more negative potentials, thereby polarizing the cell membrane.

7.8 Non-Selective Cation Currents

During the last five years the presence of non-selective cation currents (NSCC), conducted via transient receptor potential (TRP) channels, in cardiac fibroblast was discovered and confirmed in several studies (Rose et al. 2007; Rose and Giles 2008; Yue et al. 2011). TRP channels represent a large family of non-selective cation channels permeable at least for Na^+ and Ca^{2+} (Clapham et al. 2001; Nilius et al. 2005; Owsianik et al. 2006). There are 6 subfamilies of TRP channels, among which TRPC (canonical) subfamily with 7 members, TRPM (melastatin) subfamily with 8 members and TRPV (vanilloid) subfamily including 6 channel types are the most widely distributed in the organism. All TRP channels consist of putative six transmembrane polypeptide subunits assembling as homo- or heterotetramers to form cation permeable pore (Montell 2005). However, they demonstrate only weak voltage sensitivity. Some TRP channels are constitutively open, while others open upon G_q-linked receptor activation. TRPC1–6, TRPV2 and 4 and TRPM3, 4 and 6 were found in mammalian cardiomyocytes, although their functions are still not understood clearly (Yue et al. 2011).

In cardiac fibroblasts NSCC mediated by TRP channels were described for the first time by Rose et al. (2007) using rat ventricular fibroblasts. In K^+-free conditions

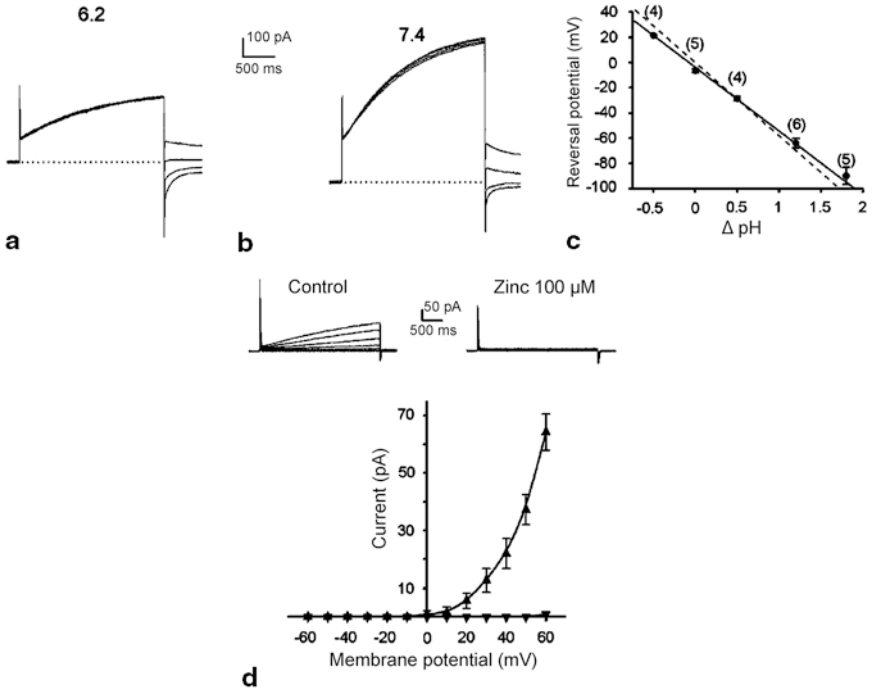

Fig. 7.10 Ionic characterization, inhibition and function of the H^+ current in human cultured cardiac fibroblasts. The bath solution contained 100 μM NPPB. Tail currents at −40 to +20 mV **a** and −80 to −20 mV **b** after depolarizing prepulses to +70 mV (duration 2.2 s) from a holding potential of −60 mV. pH_i was 6.2 while pH_o was 6.2 and 7.4 in (**a**, **b**), respectively. **c** Reversal potentials plotted against the pH gradient ($\delta pH = pH_o - pH_i$). Data were fitted by a continuous line with a slope of −51 mV/pH unit. Data are means ± SEM with the number of cells tested given in parentheses. **d** Current–voltage curve in the absence (▲) or presence (▼) of 100 μM Zn^{2+}. H^+ currents evoked by 3 s voltage steps from −60 to +60 mV in 20 mV increments from a holding potential of −70 mV in control and in the presence of 100 μM Zn^{2+} ($pH_i/pH_o = 6.2/7.4$) (example in inset). (From El Chemaly et al. (2006) with permission of Elsevier)

the authors observed small inward and outward currents with weak outwardly rectifying properties and reversal potential near 0 mV (Fig. 7.11). Removing external Na^+ markedly decreased inward currents without affecting outward currents (Fig. 7.11a). Removing Ca^{2+} substantially increased both inward and outward currents, indicating possible block of monovalent cation permeation by divalent cations (Fig. 7.11b). These currents could be strikingly increased by application of C-type natriuretic peptide or carbachol, which are both acting via G_i-proteins. Basing on RT-PCR data the authors assumed the possible role of TRPC2, TRPC3, TRPC5, TRPV2, TRPV6, TRPM4 and TRPM7 in conduction of these NSCC.

In cultured rat cardiac fibroblasts the presence of functional TRPV4 channels was also demonstrated (Hatano et al. 2009). The NSCC generated by TRPV4 had properties very similar to NSCC in the former study (Fig. 7.12). It could be stimulated by selective TRPV4 agonist 4αPDD or blocked with ruthenium red.

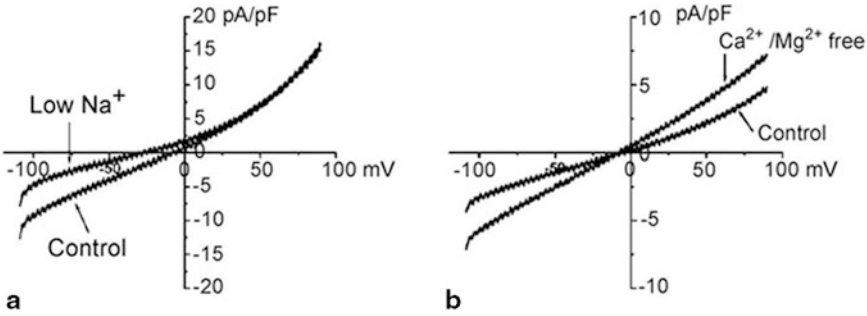

Fig. 7.11 Properties of a weakly outwardly rectifying ionic current identified using voltage ramps in acutely isolated rat cardiac fibroblasts. The voltage-clamp protocol consisted of a 1 s ramp from −100 to +100 mV from a holding potential of 0 mV. Under these conditions, and in the absence of any external pharmacological compounds, a small weakly outwardly rectifying current was identified. **a** representative recordings of the effects of replacing external Na^+ with $NMDG^+$. Replacement of external Na^+ with $NMDG^+$ significantly decreased inward current at −100 mV without altering outward current at +100 mV. **b** Representative recordings of the effects of divalent cation removal, which significantly increased both inward and outward currents and linearized the current–voltage (I–V) curve. (From Rose et al. (2007) with permission of John Wiley and Sons)

As long as TRP channels seem to be the only way for extracellular Ca^{2+} to enter the cardiac fibroblasts, they might play an important physiological role for these cells, mediating variety of Ca^{2+}-dependent processes.

7.9 Mechanosensitive Ionic Currents

Mechanically induced non-selective cation currents were described for the first time in freshly isolated rat cardiac fibroblasts and cultured rat cardiac fibroblasts by our group. The membrane currents of freshly isolated rat atrial and ventricular fibroblasts were studied by means of the patch-clamp technique in whole-cell configuration (Kamkin et al. 2003a, b). These cells had E_m of −37 ± 3 mV, an

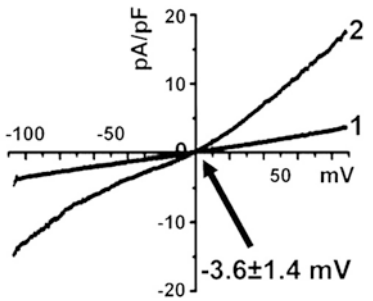

Fig. 7.12 I–V relationships of non-selective cation current carried by TRPV4 channels in the acutely isolated rat cardiac fibroblasts. The first I–V curve was obtained in control conditions and the second—during the application of selective TRPV4 agonist 4αPDD. (From Hatano et al. (2009) with permission of Elsevier)

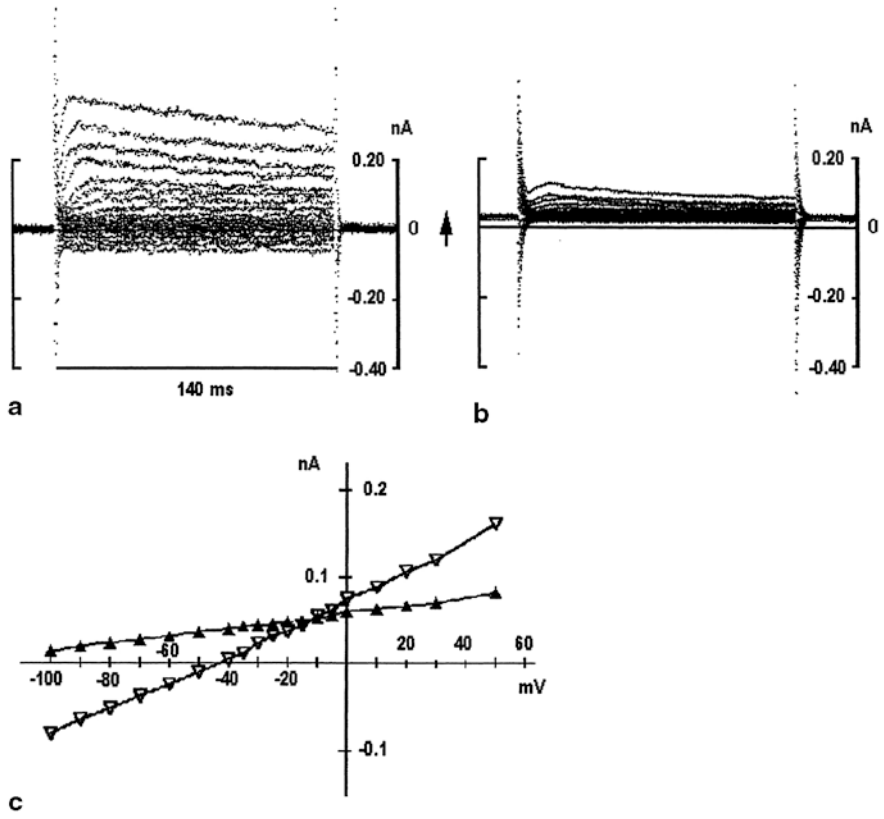

Fig. 7.13 Examples of electrophysiological characteristics of acute isolated fibroblast during "resting compression" by patch-pipettes. **a** Whole-cell currents from cardiac fibroblast in control. Starting from a holding potential of −45 mV, pulses of 140 ms duration were applied at 0.5 Hz. **b** Whole-cell currents after addition of 8 μM Gd^{3+}. **c** The I–V curves of the I_L in control (*open triangles*, $E_0 = 40$ mV) and after application of 8 μM Gd^{3+} (*filled triangles*, $E_0 > -100$ mV). Note: pCa = 7; K_{in}/K_{out} solution configuration. (From Kamkin et al. (2003) with permission of Oxford University Press)

input resistance of 514 ± 11 MΩ and a membrane capacity of 18 ± 3 pF. Thus, E_m in the isolated fibroblasts significantly differs from $E_m \approx -22$ mV, which was registered in the fibroblasts within the cardiac tissue. Cultured rat fibroblasts had resting potential of −32 ± 3 mV, a membrane resistance of 531 ± 32 MΩ, and a membrane capacity of 18 ± 3 pF (Kamkin et al. 2010b).

In the further patch-clamp experiments we have used original system of two patch-pipettes: first for registration and second for stretch or compression of the cell. Examples of electrophysiological characteristics of acute isolated cardiac fibroblast during "resting compression" by two patch-pipettes are presented in the Figs. 7.13a, c (open triangles, $E_0 = 40$ mV). The amplitude of the currents during both depolarizing and hyperpolarizing clamp steps are demonstrated in Fig. 7.13a. Addition of

8 μM Gd^{3+} shifted E_0 to −90 ± 5 mV during the first 7 min (Fig. 7.13b, c (filled triangles, $E_0 > -100$ mV). Gd^{3+} shifted the holding current into the positive direction (beginning of the traces in Fig. 7.13b) and decreased current amplitudes during depolarizing and hyperpolarizing clamp steps (Fig. 7.13b).

Currents at the end of the 140 ms long voltage-pulses were assembled to obtain the current-voltage relations (*I–V* curves). We were concerned that the different values of E_0 had resulted from a "resting compression" of the cell by the two patch-pipettes. Without artificial compression or stretch, 8 μM Gd^{3+} shifted the intercept of the *I–V* curve (I_L) with the voltage axis leftward indicating hyperpolarization, and E_0 shifted from −34 ± 4 to −98 ± 5 mV. Figure 7.13c (open triangles) demonstrates the effect, when two patch-pipettes are attached to the cell: PP in whole-cell configuration and SP in cell-attached mode. In this case E_0 was −40 mV. Addition of 8 μM Gd^{3+} (Fig. 7.13c; filled triangles) shifted E_0 during the first 7 min to −92 ± 4 mV. During the following time (15 min) Gd^{3+} further hyperpolarized E_0 toward values more negative than −100 mV (−120 mV by linear approximation). Figure 7.13 may suggest a "resting compression" by two patch-pipettes even in the absence of lateral displacement. This possibility was tested by comparing currents measured with a single patch-pipette. Under these conditions, E_0 was −35 ± 5 mV. Addition of 8 μM Gd^{3+} shifted E_0 to −90 ± 5 mV during the first 7 min. Since these values did not differ from those measured with two patch-pipettes it has been postulated that activation of G_{ns} by the second cell attached patch-pipette was negligible. These results suggested that a Gd^{3+}-sensitive non-selective membrane conductance G_{ns} is active in atrial fibroblasts under "normal recording conditions", and that this G_{ns} moves the resting potential away from the E_K (Kamkin et al. 2003a).

In freshly isolated rat cardiac fibroblasts we have observed modulation of net membrane currents by mechanical forces in a way that results in a shift of the holding current at −45 mV to more negative values during the slight (2 μm) compression of the cells with an attached glass stylus (Fig. 7.14a). Compression also increased the current amplitudes during the depolarizing clamp steps without changing their time course. At negative potentials, the currents were more negative than under resting conditions without compression. Hence, mechanical compression increases the membrane conductance of the cardiac fibroblasts, and this effect may be blocked by Gd^{3+} (Fig. 7.14a) suggesting that mechanical compression activates a mechanosensitive ion conductance in cardiac fibroblasts (Kamkin et al. 2003a, b).

Conversely, application of mechanical stretch (2 μm) to isolated cardiac fibroblasts shifted the holding current at −45 mV to more positive values (Fig. 7.14b). Furthermore, stretch application almost blocked the inward currents at negative potentials and lowered the outward currents at positive potentials, indicating a reduction of the membrane conductance (Fig. 7.14b). Gd^{3+} further reduced the currents during sustained stretch (Fig. 7.14b). These observations indicate that MGCs in cardiac fibroblasts are activated by mechanical compression and inhibited by physical stretch (Kamkin et al. 2003a).

In the absence of mechanical stimulation, the I–V curves intersected the voltage axis at −37 mV denoting the normal resting membrane potential E_m (=V_m) of a non-clamped fibroblast (Fig. 7.15a—empty triangles). Mechanical compression of the

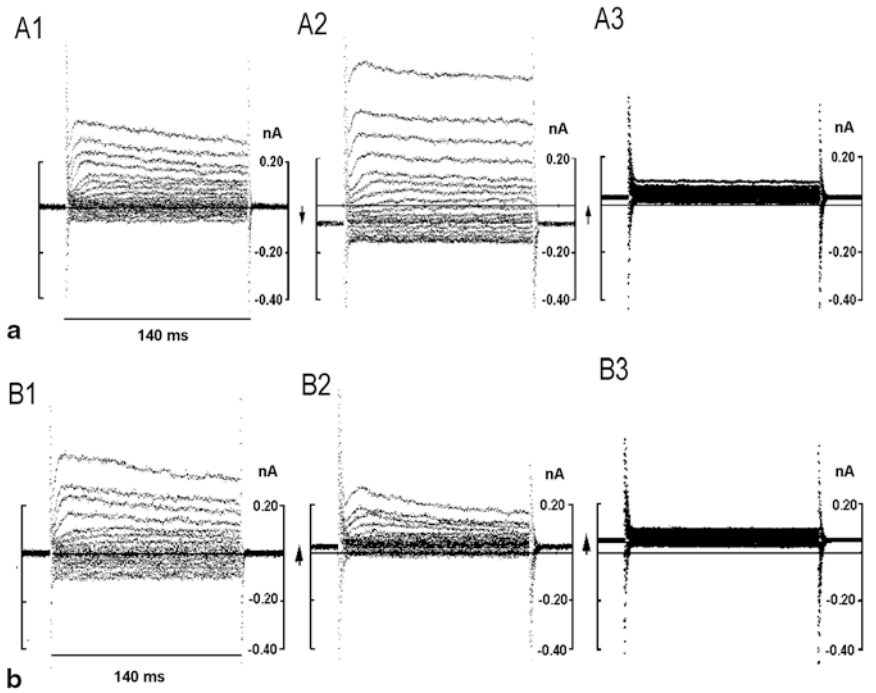

Fig. 7.14 Membrane currents in freshly isolated rat cardiac fibroblasts. **a** Whole-cell currents in cardiac fibroblasts in the absence (*A*1) and presence (*A*2) of mechanical compression (2 μm). Effect of 8 μM $Gd3^{+}$ on the whole-cell currents during sustained compression (*A*3). Note, that compression increased transmembrane ion currents in cardiac fibroblasts, and this effect was sensitive to inhibition with gadolinium. **b** Whole-cell currents in cardiac fibroblasts in the absence (*B*1) and presence (*B*2) of physical stretch (2 μm). Effect of 8 μM Gd^{3+} on the whole-cell currents during sustained stretch (*B*3). Changes of the holding current are marked by arrows. (From Kamkin et al. (2003) with permission of Oxford University Press)

cells increased the steepness of the I–V curve and shifted E_m to more positive values (Fig. 7.15a—filled triangles). In contrast, when cardiac fibroblasts were stretched, the steepness of the I–V curve was reduced and the intersection with the voltage axis shifted to a more negative E_m (Fig. 7.15c-filled triangles after stretch versus empty triangles in control). Currents during compression and stretch reversed their polarity close to 0 mV as would be expected for non-selective cation MGCs that conduct Na^{+}, K^{+} and Cs^{+} ions. In summary, the voltage-dependence and the Gd^{3+}-sensitivity of the compression-induced currents resembled the mechanosensitive currents in cardiomyocytes (Isenberg et al. 2003; Kamkin et al. 2000, 2003a; Zhang et al. 2000) and other cell types (for review about stretch-activated, non-selective cation channels (SACs) see Sachs and Morris 1998). Hence, we may conclude that modulation of MGCs is responsible at least in part for the mechanosensitivity of cardiac fibroblasts.

In addition to the experiments with freshly isolated fibroblasts, cardiac fibroblasts, which were cultured up to 5 days, were used for voltage-clamp analysis of ionic

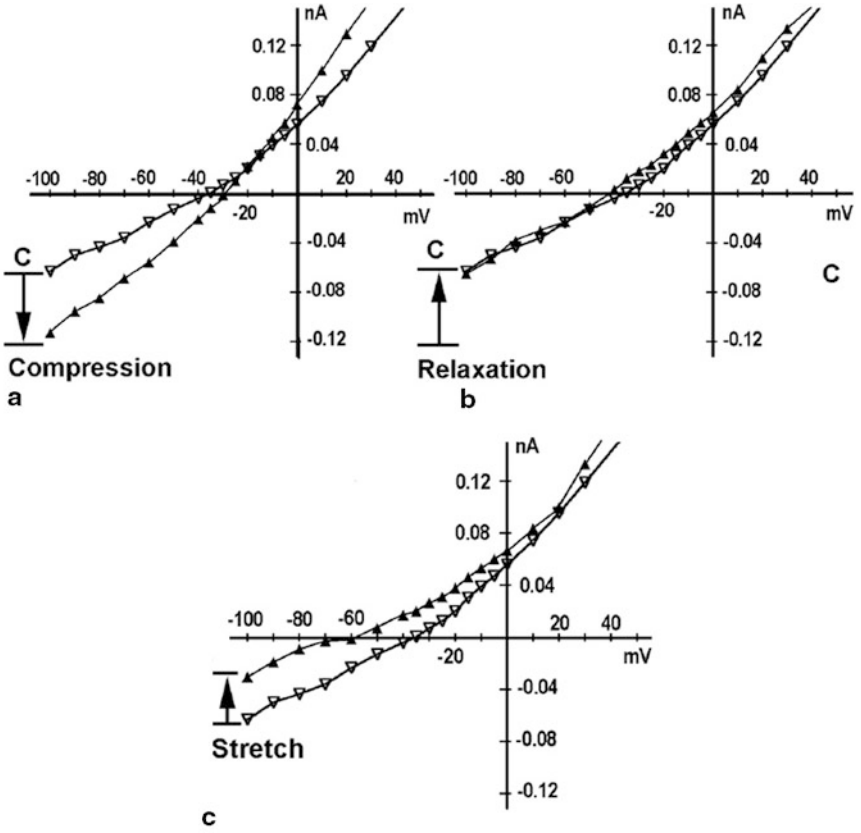

Fig. 7.15 Mechanosensitivity of membrane currents in freshly isolated rat atrial fibroblasts. **a** Current-voltage relations (I–V curves) before (*empty triangles*) and during 2 μm compression (*filled triangles*). Note the shift of the zero-current potential from E_m −37 mV to −28 mV. **b** Reversibility of the compression-induced changes (empty triangles before, filled triangles 2 min after stretch). **c** I–V curves before (*empty triangles*) and during 2 μm stretch (*filled triangles*). Note the shift of Em from −37 mV to −60 mV. I–V curves A, B, C were recorded from the same cell. Control curves in the absence of externally applied force are indicated as "C". (From Kamkin et al. (2003) with permission of Oxford University Press)

currents responsible for generation of mechanically-induced potentials (Kamkin et al. 2010b). Cultured cardiac fibroblasts responded to mechanical deformation similarly to the freshly isolated cells. Axial compression of the cultured cardiac fibroblasts by 2, 3 and 4 μm caused increase in depolarization by activating inward currents through a non-selective cation conductance. On the contrary, axial stretch of similar extent depressed inward currents and led to marked hyperpolarization. The changes in membrane currents continued as long as stretch (or compression) was sustained, i.e. there were no signs of adaptation (tested up to 15 min). Alterations in membrane potential and net current induced by compression or stretch were independent of the pCa indicating their dependence on non-selective Gd^{3+}-sensitive cation conductance.

The mechanosensitive currents were carried by Na^+, K^+ and Cs^+, and can be blocked by application of Gd^{3+} (Kamkin et al. 2010b). These data suggest that cultured cardiac fibroblasts preserve MGCs up to 5 days without special flexible substrates, which allow application of the stretch and compression, and do not change their conductance during direct axial compression or stretch of the cells.

The next stage of mechanosensitive channels study in cardiac fibroblasts required the registration of single channels activity. Mechanically stimulated single MGCs and whole-cell currents were simultaneously recorded from isolated cardiac fibroblasts using the cell-attached and whole-cell patch-clamp configurations or first cell-attached pipette (CAP) and second whole-cell pipette (WCP), respectively (Kamkin et al. 2010a). It was the first successful attempt to record activity of single MGCs caused by mechanical deformation of the whole cell, not by changing the pressure in the patch pipette, as earlier investigators used to do (Hamill and Martinac 2001; Sachs and Morris 1998).

Under "resting compression" by two patch-pipettes occasional typical "resting" whole-cell currents (Fig. 7.16A1) were observed, the single channel activity was registered simultaneously. This activity represented the short openings of two types of MGCs: one with the amplitude of single channel current of 1.95 ± 0.18 pA and the other with the amplitude of 3.9 ± 0.20 pA under the control conditions (Fig. 7.16A2), i.e. without any applied mechanical deformation. The conductances of these two MGC types were 43 pS and 87 pS, respectively. Application of 8 μM Gd^{3+} via cell attached pipette abolished openings of MGCs in control condition.

Small (1 μm) mechanical deformations affected neither MGCs nor whole-cell MG-currents. Higher levels of compression (by 2, 3 and 4 μm) increased the membrane conductance and increased the frequency and duration of single MGC openings (Fig. 7.16b for 2 μm of compression), while just a moderate (2 μm) stretch was enough to block the MGC activity completely.

In particular, compression of the cell by 2 μm shifted the holding current at −45 mV to the negative direction (beginning of the traces in Fig. 7.16B1 in comparison with the beginning of the traces in Fig. 7.16A1) and increased the currents during the depolarizing clamp steps without changing their time course. Stretch shifted the holding current at −45 mV to more positive values (beginning of the traces in Fig. 7.16C1 in comparison with the beginning of the traces in Fig. 7.16A1). It reduced the amplitude of the currents during the pulses during both depolarizing and hyperpolarizing steps, suggesting that stretch reduced the membrane conductance (Fig. 7.16C1). Cellular compression by 2 μm drastically increased the frequency of MGC openings (Fig. 7.16B3), while cellular stretch by 2 μm abolished channel activity (Fig. 7.16C2). Please note that termination of compression resulted in a decrease in MGC activity (Fig. 7.16B3). Interestingly, in contrast to the whole-cell mechanosensitive currents, single MGC activity was eliminated by a 2 μm stretch abruptly and completely (Fig. 7.16C2).

Compression of cells by 3 μm also significantly increased membrane conductance and the frequency of MGC openings. A 4 μm compression shifted the holding current to the negative direction (cf. Fig. 7.17A1 with Fig. 7.17A2) very significantly and raised the membrane conductance (Fig. 7.17A2). It strongly increased the frequency

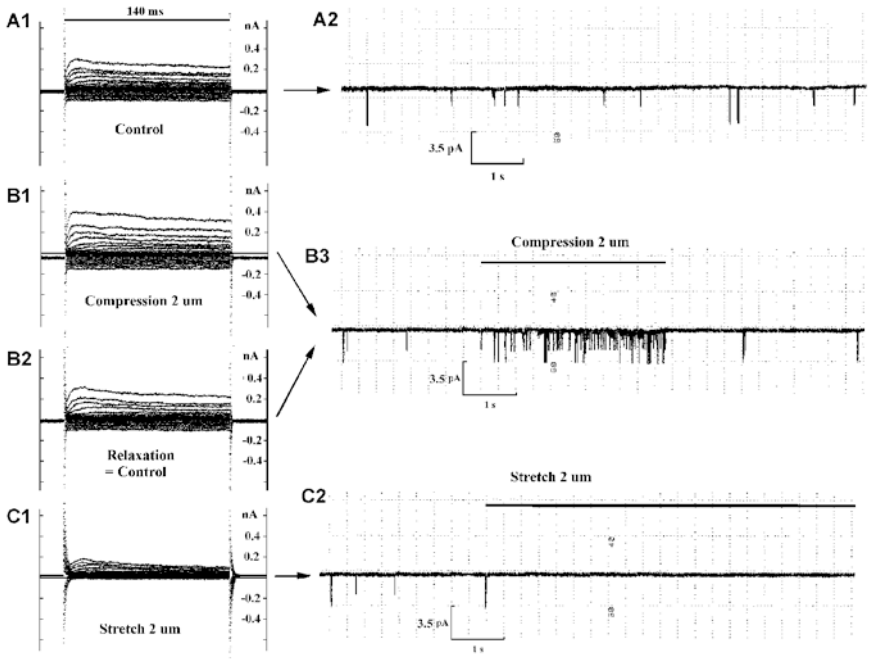

Fig. 7.16 Compression and stretch of cardiac fibroblast by 2 μm. *A*1 Whole-cell currents during control. *A*2 Single MGC activity recorded in the cell-attached mode. Sample traces show the activity of single MGCs in control ('resting compression'). *B*1 Whole-cell currents during a 2 μm cell compression. *B*2 Whole-cell currents after the release of mechanical stress (cf. *A*1). *B*3 Single MGC activity during compression. Returning to the control length decreases MGC activity to the control level. *C*1 Whole-cell currents during a 2 μm cell stretch. *C*2 Single MGC activity during stretch. Bars show the duration of applied stimuli. (From Kamkin et al. (2010) with permission of John Wiley and Sons)

of MGC openings (Fig. 7.17A3, B3, for the two types of MGCs). The effect of compression was also reversible (Fig. 7.17A3, B3). It is important to mention that the compression-induced changes in membrane currents continued as long as the compression was sustained, i.e. there was no sign of adaptation (tested for up to 15 min). Figure 7.17 shows that MGCs remain in the open state after a 3 min break in recording.

In general, cell compression shifted E_0 to more positive values. During 2, 3 and 4 μm compression E_0 shifted to -27 ± 3, -14 ± 3 and -8 ± 2 mV respectively (Fig. 7.18B1). Thus, lateral compression of the isolated cell caused depolarization via activation of inward current through MGCs. Cell stretch shifted E_0 to more negative values (-42 ± 6), -50 ± 4, and -81 ± 7 mV during 2, 3 and 4 μm stretch respectively; Fig. 7.18C1). Compression-induced difference currents reversed at approx. 0 ± 2 mV (Fig. 7.18B2). It is important to note the high degree of rectification in the whole-cell currents and high degree of rectification in difference current during mechanical stimulation (Fig. 7.18).

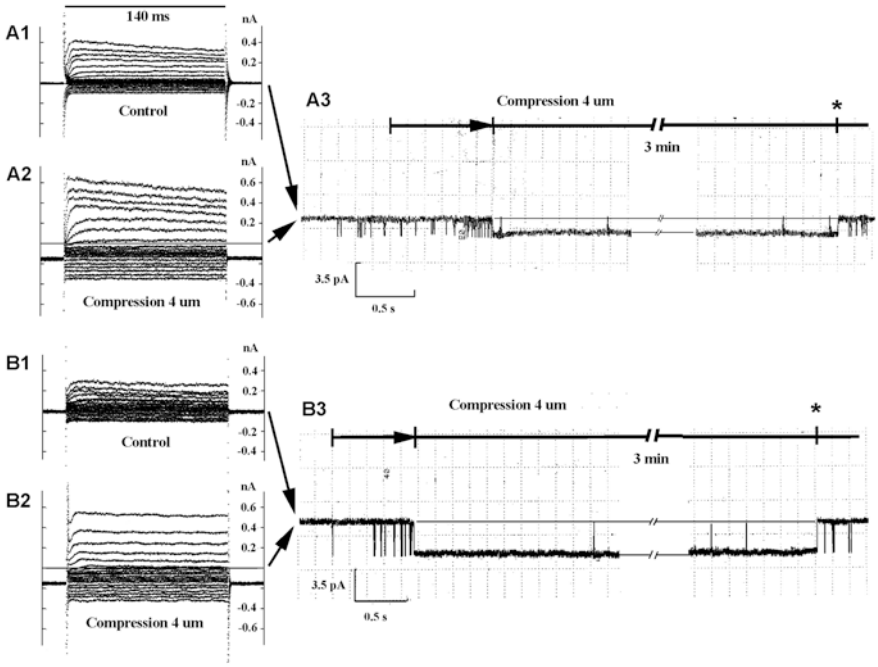

Fig. 7.17 Compression of cardiac fibroblast by 4 μm. *A*1, *A*2 Whole-cell currents during control *A*1 and a 4 μm compression *A*2. (*A*3) Single MGC activity induced by a 4 μm compression. Sample traces show the activity of small conductance MGCs elicited by compression. (*B*1) Whole-cell currents during control. *B*2 Whole-cell currents during compression. *B*3 Sample traces show the activity of large conductance MGCs elicited by compression. To prevent a possible seal disruption, a 4 μm compression was applied relatively slowly. The arrow shows the development of compression. Duration of 4 μm compression is indicated by the solid line. Asterisk shows the beginning of compression removal and return of the cell to its original condition. Note that both MGCs demonstrate no adaptation to mechanical stimulus. (From Kamkin et al. (2010) with permission of John Wiley and Sons)

Cell compression increased both the mechanosensitive whole-cell currents and the activity of single MGCs. At the holding potential of −45 mV, a 2 μm compression induced I_{ci} of -0.03 ± 0.01 nA and increased the probability of MGC opening (P_0) to 0.20 ± 0.04 and 0.19 ± 0.05 for small and large conductance MGCs respectively (Fig. 7.18a). A 3 μm compression caused I_{ci} of -0.18 ± 0.05 nA and increased the MGC P_0 to 0.52 ± 0.05 and 0.51 ± 0.09 for small and large conductance MGCs respectively (Fig. 7.18a). A 4 μm compression induced I_{ci} of -0.35 ± 0.08 nA and increased P_0 of MGCs to 0.98 ± 0.01 and 0.97 ± 0.02 for small and large conductance MGCs respectively (Fig. 7.18a). As P_0 values at this level of compression are close to 1, one can say that during 4 μm compression MGCs stay almost permanently in the open state, suggesting the saturation of compression-mediated response of cardiac fibroblasts.

The single-channel current–voltage relationships for both types of MGCs were acquired during application of 3 μm compression and shown in Fig. 7.19. Both channels

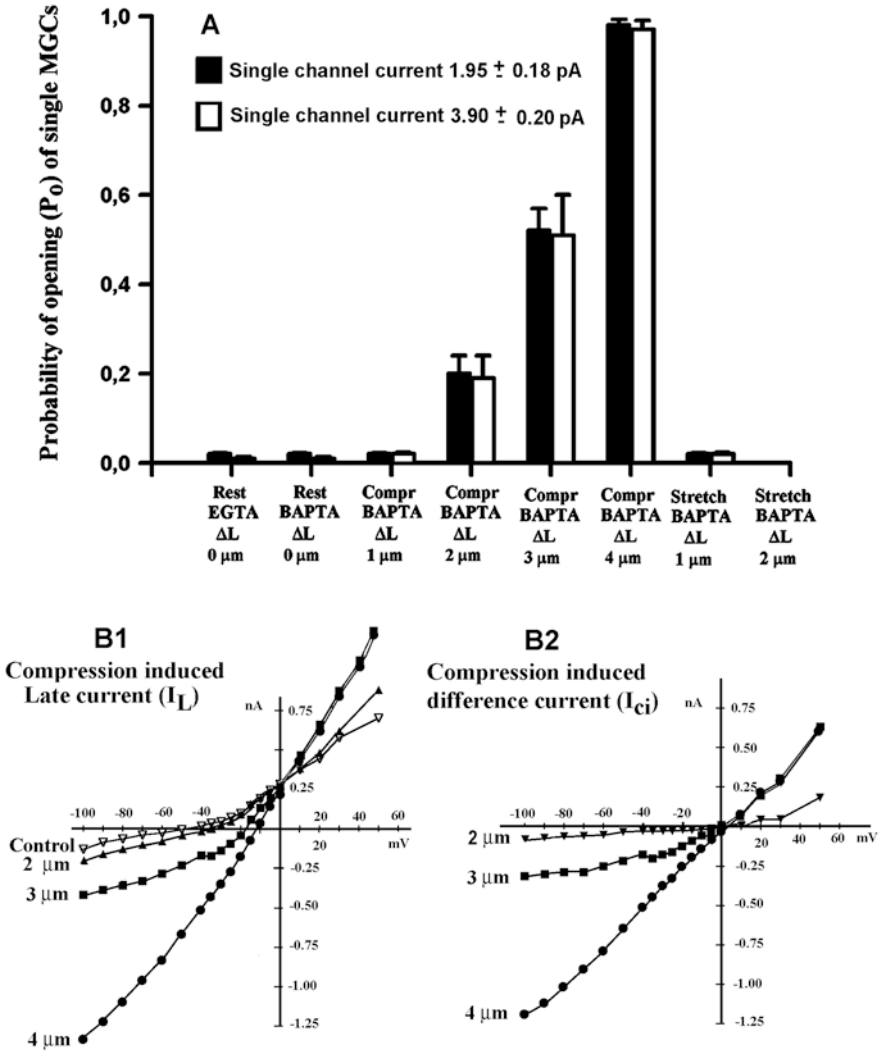

Fig. 7.18 Probability of opening (P_0) of single MGCs *A* and whole-cell MG currents induced by mechanical compression of acutely isolated cardiac fibroblasts *B*. *A* P_0, probability of opening for small conductance (*filled column*) and large conductance (*empty column*) MGCs. *B* Mechanical compression increases the whole-cell net membrane current and shifts the resting potential to more positive values. *B*1 Corresponding current–voltage relationships. Under 'resting compression' $E_0 = -45$ mV (control: *empty triangles*). The figure depicts the increase in later currents during 2 μm compression (*filled triangles*, $E_0 = -35$ mV), 3 μm compression (*filled squares*, $E_0 = -18$ mV) and 4 μm compression (*filled circles*, $E_0 = -12$ mV). *B*2 Current–voltage relationships of differential currents induced by different degrees of compression: 2 μm (*filled triangles*; $I_{ci} = -0.03$ nA at -45 mV; $E_{rev} = 0$ mV), 3 μm (*filled squares*; $I_{ci} = -0.19$ nA at -45 mV; $E_{rev} = 0$ mV), 4 μm (*filled circles*; $I_{ci} = -0.55$ nA at -45 mV; $E_{rev} = 0$ mV). (From Kamkin et al. (2010) with permission of John Wiley and Sons)

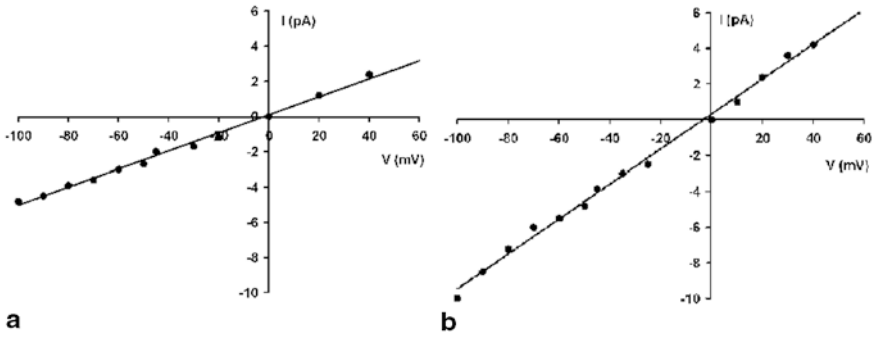

Fig. 7.19 The current–voltage relationship of small **a** and large **b** conductance MGCs, obtained from the single-channel data. Recordings were performed during a 3 μm compression. (From Kamkin et al. (2010) with permission of John Wiley and Sons)

display linear current–voltage relationships. The reversal potential was close to 0 mV. Single channel conductance determined as a slope of the current–voltage relationship was 43 and 87 pS for small and large conductance MGCs respectively. Please note the absence of rectification in the single-channel I–V curves (Figs. 7.19a, b), although the mechanosensitive whole-cell currents demonstrate rectification (Fig. 7.18b).

Thus, we conclude that fibroblasts are able to sense the directionality of the applied stress. The mechanisms of this sensitivity still require clarification. Nevertheless, several facts point to the possible important role of cytoskeleton in the translation of mechanical energy from the place of deformation to the mechanically gated channel protein (Sachs and Morris 1998; Lammerding et al. 2004). According to our own data, disruption of cytoskeletal proteins by cytochalasin D (which dissembles the microfilaments) and colchicine (which dissembles the microtubules) suppresses mechanically induced potentials of fibroblasts in the multicellular preparations (Kamkin et al. 2001) and completely blocks the whole-cell mechanosensitive currents and single-channel activity (Fig. 7.20) in the isolated cardiac fibroblasts (Kamkin et al. 2010a). Hence, mechanically gated channels and their putative cytoskeletal attachments, represent a vectorial sensor in cardiac fibroblasts.

Since MGCs are activated by cell compression and are inactivated by cell stretch, the transfer of mechanical energy seems to be rather asymmetrical. In cardiac fibroblasts incorporated into the myocardium, mechanical stress-induced response may be defined by several cellular components including extracellular matrix, integrins, the cytoskeleton and stretch-activated ion channels. The linkage between these cellular components undoubtedly plays a critical role (for reviews, see Thampatty and Wang 2008; Carver and Fuseler 2010). While the importance of cytoskeletal proteins in the transfer of mechanical energy seems to be confirmed, the role of integrins and extracellular matrix should be investigated in future experiments. Thus, further investigation will be important to reveal the elements responsible for the sensing of mechanical stimuli direction.

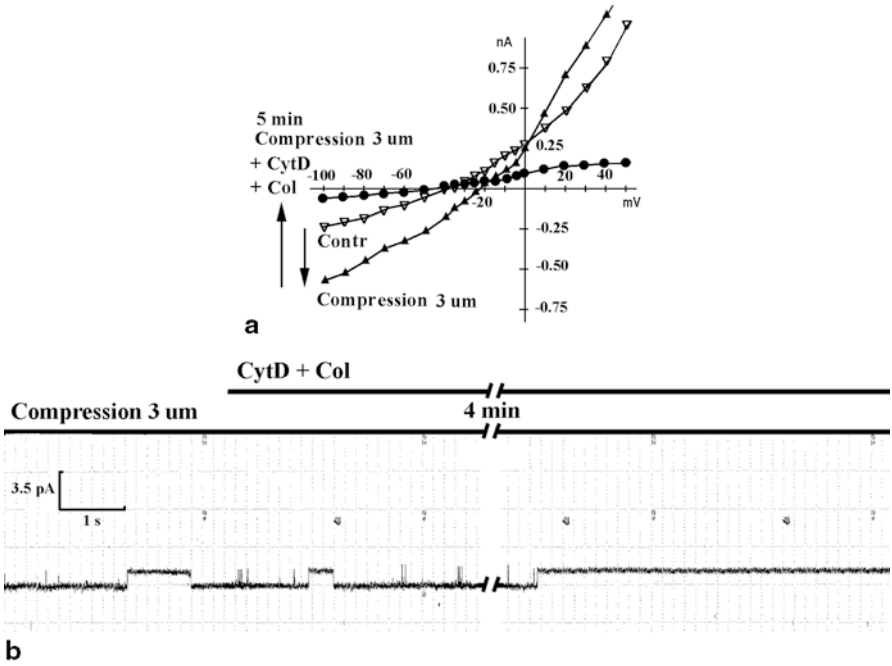

Fig. 7.20 Cytochalasin D and colchicine inhibit both the whole-cell mechanosensitive currents and single MGC activity after 5 min of application. **a** Current–voltage relationships of whole-cell currents recorded in control (*open triangles*), during a 3 μm compression (*filled triangles*), and during a 3 μm compression in the presence of cytochalasin D (100 μm) and colchicine (100 μm, *filled circles*) after 5 min of application. **b** Single MGC activity induced by a 3 μm compression was inhibited by cytochalasin D (100 μm) and colchicine (100 μm) after 4 min of application. (From Kamkin et al. (2010) with permission of John Wiley and Sons)

7.10 Conclusion and Perspectives

In the present review we have demonstrated the growing evidence that cardiac fibroblasts participate in the mechanical and electrical function of the heart. One of the most intriguing aspects of cardiac fibroblasts physiology is their ability to function as mechanoelectrical signal transducers in the heart. Transformation of mechanical forces into an electrical signal involves the activation of mechanically gated ion channels in response to cell compression that occurs during spontaneous contractions of the heart. Transmembrane influx of cations through gadolinium-sensitive, mechanically gated channels gives rise to mechanically induced potentials (MIPs). As long as fibroblasts are connected with cardiomyocytes via gap junctions, the repolarization of the MIPs may potentially extend the action potential duration in cardiomyocytes thereby predisposing the heart to arrhythmia. Since cardiac fibroblasts express various cation channels, including voltage-dependent potassium K_V channels and Ca^{2+}-activated K^+ channels, the role of these channels in the modulation

of cardiac fibroblasts mechanosensitivity seems to represent an important field for future investigations. Further research should also be dedicated to the physiological mechanisms of regulation of mechanosensitive currents in cardiac fibroblasts. Successful studies may eventually allow one to develop new strategies for the treatment of cardiac arrhythmias.

Acknowledgments This work was supported by the Russian Foundation for Basic Research (grant no. 09–04-01277-a). Department of Fundamental and Applied Physiology (Professor and Chairman – Andre Kamkin) was supported by Ministry of Education and Science of the Russian Federation. The Order of Ministry of Education and Science of the Russian Federation No. 743 from 01 July 2010, Supplement, Event 4.4, the Period of Financing 2010–2019.

References

Adler CP, Ringlage WP, Bohm N (1981) DNS-Gehalt und Zellzahl in Herz und Leber von Kindern. Pathol Res Pract 172:25–41

Baumgarten CM, Clemo HF (2003) Swelling-activated chloride channels in cardiac physiology and pathophysiology. Prog Biophys Mol Biol 82:25–42

Benamer N, Maati HMO, Demolombe S, Cantereau A, Delwail A, Bois P, Bescond J, Faivre J (2009) Molecular and functional characterization of a new potassium conductance in mouse ventricular fibroblasts. J Mol Cell Cardiol 46:508–517

Benamer N, Fares N, Bois P, Faivre J (2011) Electrophysiological and functional effects of sphingosine-1-phosphate in mouse ventricular fibroblasts. Biochem Biophys Res Commun 408:6–11

Boyett MR, Honjo H, Kodama I (2000) The sinoatrial node, a heterogenous pacemaker structure. Cardiovasc Res 47:658–687

Camelliti P, Borg TK, Kohl P (2005) Structural and functional characterization of cardiac fibroblasts. Cardiovasc Res 65:40–51

Carver W, Fuseler JW (2010) Mechanical stretch-induced reorganization of the cytoskeleton and the small GTPase Rac in cardiac fibroblasts. In: Mechanosensitivity in Cells and Tissues 3. Mechanosensitivity of the Heart. Andre Kamkin and Irina Kiseleva (eds.). Springer, Berlin, pp 35–54

Chilton L, Ohya S, Freed D, George E, Drobic V, Shibukawa Y, MacCannell KA, Imaizumi Y, Clark RB, Dixon IMC, Giles WR (2005) K^+ currents regulate the resting membrane potential, proliferation, and contractile responses in ventricular fibroblasts and myofibroblasts. Am J Physiol Heart Circ Physiol 288:H2931-H2939

Clapham DE, Runnels LW, Strubing C (2001) The TRP ion channel family. Nat Rev Neurosci 2:387–396

Coetzee WA, Amarillo Y, Chiu J, Chow A, Lau D, McCormack T, Moreno H, Nadal MS, Ozaita A, Pountney D, Saganich M, Vega-Saenz de Miera E, Rudy B (1999) Molecular diversity of K1 channels. Ann N Y Acad Sci 868:233–285

Decoursey TE (2003) Voltage-gated proton channels and other proton transfer pathways. Physiol Rev 83:475–579

Du X, Gao Z, Lau C, Chiu S, Tse H, Baumgarten CM, Li G (2004) Differential effects of tyrosine kinase inhibitors on volume-sensitive chloride current in human atrial myocytes: evidence for dual regulation by Src and EGFR kinases. J Gen Physiol 123:427–439

El Chemaly A, Guinamard R, Demion M, Fares N, Jebara V, Faivre JF, Bois P (2006) A voltage-activated proton current in human cardiac fibroblasts. Biochem Biophys Res Commun 340(2):512–516

Goshima K (1970) Formation of nexuses and electrotonic transmission between myocardial and FL cells in monolayer culture. Exp Cell Res 63(1):124–130

Goshima K, Tonomura Y (1969) Synchronized beating of embryonic mouse myocardial cells mediated by FL cells in monolayer culture. Exp Cell Res 56(2):387–392

Hamill OP, Martinac B (2001) Molecular basis of mechanotransduction in living cells. Physiol Rev 81(2):685–740

Hatano N, Itoh Y, Muraki K (2009) Cardiac fibroblasts have functional TRPV4 activated by 4α-phorbol 12,13-didecanoate. Life Sci 85:808–814

He M, Liu W, Sun H, Wu W, Liu J, Tse H, Lau C, Li G (2011) Effects of ion channels on proliferation in cultured human cardiac fibroblasts. J Mol Cell Cardiol 51:198–206

Hiraoka M, Kawano S, Hirano Y, Furukawa T (1998) Role of cardiac chloride currents in changes in action potential characteristics and arrhythmias. Cardiovasc Res 40:23–33

Isenberg G, Kazanski V, Kondratev D, Gallitelli MF, Kiseleva I, Kamkin A (2003) Differential effects of stretch and compression on membrane currents and $[Na^+]c$ in ventricular myocytes. Prog Biophys Mol Biol 82(1–3):43–56

Kaab S, Dixon J, Duc J, Ashen D, Näbauer M, Beuckelmann DJ, Steinbeck G, McKinnon D, Tomaselli GF (1998) Molecular basis of transient outward potassium current downregulation in human heart failure: a decrease in Kv4.3 mRNA correlates with a reduction in current density. Circulation 98:1383–1393

Kamkin A, Kiseleva I, Kircheis R, Kositzky G (1988) Abhandlungen der Akademie der Wissenschaften der DDR (Abteilung Mathematik – Naturwissenschaft – Technik) 1:103

Kamkin A, Kiseleva I, Wagner KD, Lammerich A, Bohm J, Persson PB, Günther J (1999) Mechanically induced potentials in fibroblasts from human right atrium. Exp Physiol 84:347–356

Kamkin A, Kiseleva I, Isenberg G (2000) Stretch-activated currents in ventricular myocytes: amplitude and arrhythmogenic effects increase with hypertrophy. Cardiovasc Res 48(3):409–420

Kamkin A, Kiseleva I, Wagner KD, Scholz H, Theres H, Kazanski V, Lozinsky I, Gunther J, Isenberg G (2001) Mechanically induced potentials in rat atrial fibroblasts depend on actin and tubulin polymerisation. Pflugers Arch 442:487–497

Kamkin A, Kiseleva I, Wagner KD, Pylaev A, Leiterer KP, Theres H, Scholz H, Günther J, Isenberg G (2002) A possible role for atrial fibroblasts in postinfarction bradycardia. Am J Physiol 282:H842-H849

Kamkin A, Kiseleva I, Isenberg G (2003a) Activation and inactivation of a non-selective cation conductance by local mechanical deformation of acutely isolated cardiac fibroblasts. Cardiovasc Res 57:793–803

Kamkin A, Kiseleva I, Isenberg G, Wagner KD, Günther J, Theres H, Scholz H (2003b) Cardiac fibroblasts and the mechano-electric feedback mechanism in healthy and diseased hearts. Prog Biophys Mol Biol 82:111–120

Kamkin A, Kiseleva I, Wagner KD, Lozinsky I, Günther J, Scholz H (2003c) Mechanically induced potentials in atrial fibroblasts from rat hearts are sensitive to hypoxia/reoxygenation. Pflügers Arch 446:169–174

Kamkin A, Kirischuk S, Kiseleva I (2010a) Single mechano-gated channels activated by mechanical deformation of acutely isolated cardiac fibroblasts from rats. Acta Physiol 199:277–292

Kamkin A, Kiseleva I, Lozinsky I (2010b) The role of mechanosensitive fibroblasts in the heart: evidence from acutely isolated single cells, cultured cells and from intracellular microelectrode recordings on multicellular preparations from healthy and diseased cardiac tissue. In: Mechanosensitivity in Cells and Tissues 3. Mechanosensitivity of the Heart. Andre Kamkin and Irina Kiseleva (eds.) Springer, Berlin, pp 239–266

Kamkin A, Scholz H, Kiseleva I (2011) Cardiac fibroblasts in normal and diseased heart: single mechanically-gated ion channels, mechanosensitive currents and mechanically induced potentials in isolated cells and tissue. In: Turner NA (ed) The cardiac fibroblast. Research Signpost, Kerala, pp 1–16

Kiseleva IS, Kamkin AG, Kircheis R, Kositski GI (1987) Intercellular electrotonic interactions in the cardiac sinus node in the frog. Dokl Akad Nauk SSSR, 292(6):1502–1505

Kiseleva I, Kamkin A, Kohl P, Lab M (1996) Calcium and mechanically induced potentials in fibroblasts of rat atrium. Cardiovasc Res 32:98–111

Kiseleva I, Kamkin A, Pylaev A, Kondratjev D, Leiterer KP, Theres H, Wagner KD, Persson PB, Günther J (1998) Electrophysiological properties of mechanosensitive atrial fibroblasts from chronic infarcted rat heart. J Mol Cell Cardiol 30:1083–1093

Kohl P, Camelliti P, Burton FL, Smith GL (2005) Electrical coupling of fibroblasts and myocytes: relevance for cardiac propagation. J Electrocardiol 38:45–50

Lammerding J, Kamm PD, Lee RT (2004) Mechanotransduction in cardiac myocytes. Ann N Y Acad Sci 1015:53–70

Li G, Sun H, Chen J, Zhou Y, Tse H, Lau C (2009) Characterization of Multiple Ion Channels in Cultured Human Cardiac Fibroblasts. PLoS ONE 4(10):e7307. doi:10.1371/journal.pone.0007307

Lopatin AN, Nichols CG (2001) Inward rectifiers in the heart: an update on IK1. J Mol Cell Cardiol 33:625–638

Meissner M, Weissgerber P, Londono JEC, Prenen J, Link S, Ruppenthal S, Molkentin JD, Lipp P, Nilius B, Freichel M, Flockerzi V (2011) Moderate calcium channel dysfunction in adult mice with inducible cardiomyocyte-specific excision of the cacnb2 gene. J Biol Chem 286(18):15875–15882

Montell C (2005) The TRP superfamily of cation channels. Sci STKE 2005:1–24

Nilius B, Talavera K, Owsianik G, Prenen J, Droogmans G, Voets T (2005) Gating of TRP channels: a voltage connection? J Physiol 567:35–44

Okada Y, Yada T, Ohno-Shosaku T, Oiki S, Ueda S, Machida K (1984) Exogenous ATP induces electrical membrane responses in fibroblasts. Exp Cell Res 152:552–557

Oren RV, Clancy CE (2010) Determinants of heterogeneity, excitation and conduction in the sinoatrial node: a model study. PLOS Comp Biol 6(12):e1001041. doi:10.1371/journal.pcbi.1001041

Oudit GY, Kassiri Z, Sah R, Ramirez RJ, Zobel C, Backx PH (2001) The molecular physiology of the cardiac transient outward potassium current Ito in normal and diseased myocardium. J Mol Cell Cardiol 33:851–872

Owsianik G, Talavera K, Voets T, Nilius B (2006) Permeation and selectivity of TRP channels. Annu Rev Physiol 68:685–717

Roden DM, Balser JR, George AL Jr (2002) Cardiac ion channels. Annu Rev Physiol 64:431–475

Rodrigues AR, Arantes EC, Monje F, Stuhmer W, Varanda WA (2003) Tityustoxin-K(alpha) blockade of the voltage-gated potassium channel Kv1.3. Br J Pharmacol 139:1180–1186

Rook MB, van Ginneken ACG, De Jonge B, El Aoumari A, Gros D, Jongsma HJ (1992) Differences in gap junction channels between cardiac myocytes, fibroblasts, and heterologous pairs. Cell Physiol 32:C959-C977

Rose RA, Giles WR (2008) Natriuretic peptide C receptor signaling in the heart and vasculature. J Physiol 586(2):353–366

Rose RA, Hatano N, Ohya S, Imaizumi Y, Giles WR (2007) C-type natriuretic peptide activates a non-selective cation current in acutely isolated rat cardiac fibroblasts via natriuretic peptide C receptor-mediated signaling. J Physiol 580(1):255–274

Sachs F, Morris CE (1998) Mechanosensitive ion channels in nonspecialized cells. Rev Physiol Biochem Pharmacol 132:1–77

Saito T, Fujiwara Y, Fujiwara R, Hasegawa H, Kibira S, Miura H, Miura M (2002) Role of augmented expression of intermediate conductance $Ca2^{+}$-activated K^{+} channels in postischaemic heart. Clin Exp Pharmacol Physiol 29:324–329

Schram G, Pourrier M, Nattel S (2002) Differential distribution of cardiac ion channel expression as a basis for regional specialization in electrical function. Circ Res 90:939–950

Shibukawa Y, Chilton EL, MacCannell KA, Clark RB, Giles WR (2005) K^{+} currents activated by depolarization in cardiac fibroblasts. Biophys J 88:3924–3935

Shieh C-C, Coghlan M, Sullivan JP, Gopalakrishnan M (2000) Potassium channels: molecular defects, diseases, and therapeutic opportunities. Pharmacol Rev 52:557–594

Spach MS, Boineau JP (1997) Microfibrosis produces electrical load variations due to loss of side-to-side cell connections: a major mechanism of structural heart disease arrhythmias. Pacing Clin Electrophysiol 20:397–413

Tamargo J, Caballero R, Gomez R, Valenzuela C, Delpon E (2004) Pharmacology of cardiac potassium channels. Cardiovasc Res 62:9–33

Thampatty B, Wang J (2008) Mechanobiology of fibroblasts. In: Mechanosensitivity in Cells and Tissues 1. Mechanosensitive ion channels. Andre Kamkin and Irina Kiseleva (eds.) Springer, Berlin, pp 351–378

Tombola F, Ulbrich MH, Isacoff EY (2008) The voltage-gated proton channel Hv1 has two pores, each controlled by one voltage sensor. Neuron 58:546–556

Tsuchiya W, Okada Y, Yano J, Inouye A, Sasaki S, Doida Y (1981) Effects of cytochalasin B and local anesthetics on electrical and morphological properties in L cells. Exp Cell Res 133:83–92

Vergara C, Latorre R, Marrion NV, Adelman JP (1998) Calcium-activated potassium channels. Curr Opin Neurobiol 8(3):321–329

Vliegen HW, Van Der Laarse A, Cornelisse CJ, Eulderink F (1991) Myocardial changes in pressure overload-induced left ventricular hypertrophy. A study on tissue composition, polyploidization and multinucleation. Eur Heart J 12:488–494

Walsh KB, Zhang J (2008) Neonatal rat cardiac fibroblasts express three types of voltage-gated K^+ channels: regulation of a transient outward current by protein kinase C. Am J Physiol Heart Circ Physiol 294:H1010–H1017

Wang Y, Sung RJ, Lin M, Wu S (2006) Contribution of BK_{ca}-channel activity in human cardiac fibroblasts to electrical coupling of cardiomyocytes-fibroblasts. J Membr Biol 213:175–185

Wible BA, De Biasi M, Majumder K, Taglialatela M, Brown AM (1995) Cloning and functional expression of an inwardly rectifying K^+ channel from human atrium. Circ Res 76:343–350

Wolk R, Cobbe SM, Hicks MN, Kane KA (1999) Functional, structural, and dynamic basis of electrical heterogeneity in healthy and diseased cardiac muscle: implications for arrhythmogenesis and anti-arrhythmic drug therapy. Pharmacol Ther 84:207–231

Xu Y, Tuteja D, Zhang Z, Xu D, Zhang Y, Rodriguez J, Nie L, Tuxson HR, Young JN, Glatter KA, Vasquez J, Yamoah EN, Chiamvimonvat N (2003) Molecular identification and functional roles of a Ca^{2+}-activated K^+ channel in human and mouse hearts. J Biol Chem 278(49):49085–49094

Yellen G (2002) The voltage-gated potassium channels and their relatives. Nature 419:35–42

Yue L, Xie J, Nattel S (2011) Molecular determinants of cardiac fibroblast electrical function and therapeutic implications for atrial fibrillation. Cardiovasc Res 89:744–753

Zhang Y, Gao F, Popov VL, Wen JW, Hamill OP (2000) Mechanically gated channel activity in cytoskeleton-deficient plasma membrane blebs and vesicles from Xenopus oocytes. J Physiol 523:117–130

Chapter 8
The Role of Nitric Oxide in the Regulation of Ion Channels in the Cardiomyocytes: Link to Mechanically Gated Channels

Ekaterina Yu. Makarenko, Ilya Lozinsky and Andre Kamkin

8.1 Introduction

Nitric oxide is an important regulator of the cardiac function under normal conditions and in different pathologies. During recent years our group described the impact of this endogenous low molecular agent on activity of mechanosensitive channels (MGCs) of cardiomyocytes (Kazanski et al. 2010a, b, 2011; Abramochkin et al. 2012), which play the key role in generation of mechanically induced arrhythmias, which frequently lead to fibrillation (Kamkin et al. 2000, 2003). However on tissue and organ level it would be misleading to consider NO influence on MGCs of cardiomyocytes without taking into account its impact on other cardiac cells.

According to literature nitric oxide affects almost every transport system of cardiomyocytes, modulating ionic currents and changing functional activity of cells of the cardiac muscle (briefly reviewed in Tamargo et al. 2010). In this manuscript we will not address widely discussed NO effects on calcium-activated potassium channels (Bang et al. 1999; Wang et al. 2004), sarcoplasmic reticulum Ca^{2+} release channels—ryanodine receptors (Stoyanovsky 1997; Lim 2008; Wang 2010; Donoso 2011), mitochondrial ATP-sensitive potassium channels (Sasaki et al. 2000; Han et al. 2002; Cuong et al. 2006; Ljubkovic et al. 2007), chloride channels (Chiang et al. 2004; Nishimura et al. 2010) and other cellular channels of cardiac cells. It will focus on description of the NO mediated alterations of the activity of ion channels of cardiomyocytes (Na^+, Ca^{2+}, K^+), which play the major role in formation and modulation of the action potential and its form under normal and pathological conditions. We will pay special attention to recent findings related to NO effects on cardiomyocyte mechanosensitive channels.

A. Kamkin (✉) · E. Yu. Makarenko · I. Lozinsky
Department of Fundamental and Applied Physiology, Laboratory of Electrophysiology, Russian State Medical University, Ostrovitjanova 1, Moscow 117997, Russia
e-mail: Kamkin.A@g23.relcom.ru

A. Kamkin, I. Lozinsky (eds.), *Mechanically Gated Channels and their Regulation,* Mechanosensitivity in Cells and Tissues 6,
DOI 10.1007/978-94-007-5073-9_8,

Table 8.1 Effect of nitric oxide on Na^+ channels of cardiomyocytes

Currents	Objects	Effects	References
I_{Na}	hH1 channels expressed in *Xenopus* oocytes	No effects (non significant inhibition)	Hu et al. 1997
	Isolated guinea pig and mice ventricular myocytes	Inhibition (Fig. 8.1a)	Ahmmed et al. 2001
I_{NaL}	Isolated rat ventricular myocytes	Activation (Fig. 8.1b)	Ahern et al. 2000
I_f	Isolated rabbit sinoatrial node cells	Activation (Fig. 8.2)	Musialek et al. 1997; Yoo et al. 1998

8.2 Effect of Nitric Oxide on Sodium Channels

8.2.1 Na^+ Channels of the Ventricular Myocytes

Currently data regarding NO effects on voltage sensitive sodium channels is scarce. We summarize it in Table 8.1 and Fig. 8.1.

According to Hu and colleagues (1997), nitrogen oxide does not significantly alter single Na^+ channels, expressed in cell culture. So, NO-donor SNAP (600 mkmol/l) does not change current through human cardiac tetrodotoxin-resistant Na^+ channels (hH1), expressed in oocytes from *Xenopus laevis*. Reported moderate inhibition of whole-cell current authors interpret as absence of pronounced effect. Moreover similar absence of effect is shown for rat skeletal muscle Na^+ channels (μ1) expressed in human embryonic kidney cells (Hu et al. 1997).

Other groups report pronounced modulatory effect of nitrogen oxide on cardiomyocyte sodium channels. Ahmmed et al. (2001) showed that NO statistically significantly reduces peak whole-cell Na^+ current (I_{Na}) in isolated guinea pig and mouse myocytes in a dose dependent manner (Fig. 8.1a). The same paper shows that sodium oxide does not affect steady-state activation or inactivation kinetics, as well as conductance of single Na^+ channels. Modulatory effect of NO authors attribute to significant reduction of open probabilities and/or channel number.

Ahern et al. (2000) demonstrated that nitrogen oxide activates late Na^+ current (I_{NaL}) in isolated ventricular rat myocytes (Fig. 8.1b). Photo-induced release of NO from NO-caged solutions leads to incomplete inactivation of Na^+ channels during action potential along with prolongation of the AP plato phase in cardiomyocytes. NO donor diethylamineNONOate (1–2 mM) induces appearance of persistent Na^+ current. Besides that Ca^{2+}-dependant activation of NO-syntases by ionomycin (5 mkM) leads to triple increase of persistent Na^+ current. Therefore stimulation of endogeneous synthesis of NO as well as exogeneous application of it leads to appearance and increase of late sodium current in ventricular myocytes.

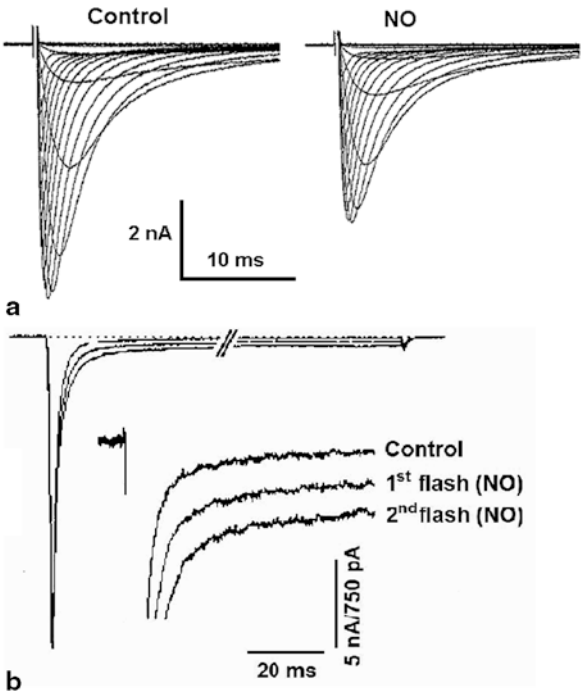

Fig. 8.1 Effect of nitric oxide on ventricular cardiomyocyte Na^+ channels. **a** Examples of families of whole-cell I_{Na} elicited by a series of voltage-clamp steps from a holding potential of −100 mV obtained from a guinea pig ventricular myocyte in control (*left*) and after application of NO (*right*). From Ahmmed et al. 2001 with permission Wolters Kluwer Health via Copyright Clearance Center. **b** Superimposed Na^+ currents before and after photorelease of NO in rat ventricular myocytes. Insets show enlargements of the same traces. Currents were evoked by voltage steps from −65 to −35 mV (200 ms). (From Ahern et al. 2000 with permission of American Society for Biochemistry and Molecular Biology via Copyright Clearance Center)

8.2.2 Na^+ Channels of the Pacemaker Cardiomyocytes

Nitrogen oxide demonstrates a pronounced effect on Na^+ channels activity of cardiac pace maker cells. There are reports that NO modulates hyperpolarization-activated inward current (I_f) in sinoatrial node myocytes (Table 8.1 and Fig. 8.2).

B. Casadei showed that I_f blockers CsCl (2 mmol/L) and ZD7288 (1 mkmol/L) attenuate positive chronotropic effect, triggered by NO-donors sodium nitroprusside (SNP, 10 mkmol/L) and 3-morpholinosydnonimine (SIN-1, 50 mkmol/L) in isolated guinea pig spontaneously beating sinoatrial node/atrial preparations. Direct effect of NO on hyperpolarization-activated inward current was investigated by the same group in rabbit isolated patch-clamped sinoatrial node cells. They found that SNP and SIN-1 (5 mkmol/L) significantly increase Cs^+-sensitive I_f in pacemaker cells (Musialek et al. 1997).

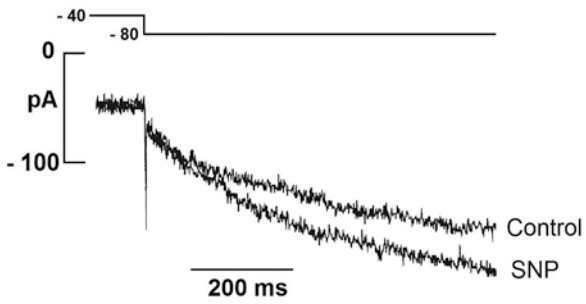

Fig. 8.2 Effect of nitric oxide on pacemaker cardiomyocyte Na^+ channels. Present effect of NO-donor on basal hyperpolarization-activated inward current. (From Yoo et al. 1998 with permission of Elsevier via Copyright Clearance Center)

Yoo and colleagues (1998) reported similar findings. They showed that sodium nitroprusside (80 mkmol/L) increases basal I_f in single sinoatrial node cells of the rabbit (Fig. 8.2). It is interesting to note that in the same preparation SNP significantly decreases stimulation of hyperpolarization-activated inward current, triggered by β-adrenergic agonist isoproterenol (1 mkmol/L). Different effects of NO on hyperpolarization-activated inward current in pacemaker cardiac cells in absence and presence of pre-stimulation of I_f authors attribute to existence of different intracellular NO mediated pathways.

8.3 Effect of Nitric Oxide on Calcium Channels

L-type of calcium channels (I_{CaL}) play the key role in formation of the plato phase of the action potential of cardiac myocytes. During last decades there were numerous reports of activating (Kumar et al. 1997; Vandecasteele et al. 1998; Wang et al. 2000), inhibiting (Han et al. 1994, 1995, 1996; Gallo et al. 1998, 2001; Levi RC et al. 1994; Vulcu et al. 2000; Abi-Gerges et al. 2001; Dittrich et al. 2001; Schröder et al. 2003), dual (Wahler and Dollinger 1995; Campbell et al. 1996) or biphasic (Méry et al. 1993; Kirstein et al. 1995) effects of NO on crdiomyocyte calcium channels. Summary of NO effects on Ca^{2+} channels is shown in Table 8.2.

Several papers report direct activating effect of NO on I_{CaL}. According to Vandecasteele and colleagues (1998), SNAP (100 nM) increases basal calcium current in isolated human atrial myocytes. This effect is completely blocked by application of NO-syntase inhibitor L-NMMA (1 mM), which proves direct involvement of NO-mediated mechanisms. This report goes in hand with findings of Kumar and colleagues, who showed that another NO-donor nitrosoglutathione (GSNO, 10–100 mkM) increases basal I_{Ca} (Fig. 8.3a) in rabbit newborn ventricular and adult atrial cells (Kumar et al. 1997; Wang et al. 2000).

Currently there are plenty of reports regarding inhibitory effects of NO on calcium current in cardiac cardiomyocytes. SNAP (100 mkM) inhibits I_{CaL} (Fig. 8.3b) in neonatal rat cardiac ventricular myocytes (Vulcu et al. 2000), and another NO-donor DEA-NO (1 mkM/L). It has similar effect in mouse ventricular myocytes (Schröder et al. 2003). According to Gallo and colleagues (1998, 2001), NO-syntases inhibitor

Table 8.2 Effect of nitric oxide on L-Ca^+ channels of cardiomyocytes

Currents	Objects	Effects	References
I_{CaL}	Isolated human atrial myocytes	Activation	Vandecasteele et al. 1998
	Isolated rabbit atrial and ventricular myocytes	Activation (Fig. 8.3a)	Kumar et al. 1997; Wang et al. 2000
	Isolated guinea pig ventricular myocytes	Inhibition	Gallo et al. 1998, 2001; Levi RC et al. 1994
	Neonatal rat cardiac ventricular strips	Inhibition (Fig. 8.3b)	Vulcu et al. 2000
	Mouse ventricular myocytes	Inhibition	Schröder et al. 2003
	Isolated frog ventricular myocytes	Biphasic effect (Fig. 8.3c)	Méry et al. 1993
	Isolated human atrial myocytes	Biphasic effect	Kirstein et al. 1995
	Isolated guinea pig ventricular myocytes	Dual effect	Wahler and Dollinger 1995
	Isolated ferret ventricular myocytes	Dual effect	Campbell et al. 1996

L-NMMA (1 mM) and L-NNA (1 mM), as well as NO scavenger PTIO (0.5 mM) triggered fast pronounced stimulation of calcium current in isolated guinea pig ventricular myocytes. Other authors showed that different NO-donors inhibit calcium current, which is prestimulated by β-adrenergic agonist in rat ventricular myocytes (Abi-Gerges et al. 2001) and rabbit sinoatrial cells (Han et al. 1994, 1995, 1996).

There are also reports of biphasic effects of NO on cardiomyocyte calcium currents. Kirstein and colleagues (1995) showed that NO-donor 3-morpholino-sydnonymine (SIN-1) has pronounced stimulatory effect on I_{Ca} in isolated human atrial myocytes, starting from 1 pM concentration. It reaches maximum stimulatory effect (doubling of the current amplitude) at 1 nM, while increasing NO-donor concentration to 1–100 mkM abruptly decreases it stimulatory effect on I_{Ca}. More over at 10 nM SIN-1 demonstrates pronounced simulatory effect on basal I_{Ca}. This data goes in hand with other reports. So, Méry and colleagues (1993) showed that at low concentrations (0.1 nM) SIN-1 has moderate activating effect on calcium current, which was prestimulated by application of β-adrenergic agonist, in isolated frog ventricular myocytes. At high concentrations (10 nM–100 mkM) NO-donor leads to pronounced dose dependant increase in β-adrenergic-stimulated I_{Ca} (Fig. 8.3c).

Several authors reported dual effects of NO on Ca^{2+} channels. Campbell and colleagues (1996) on isolated ferret ventricular myocytes showed that SIN-1 (1 mM) under the same experimental conditions in approximately 40 % of cases has stimulatory, in 40 %—inhibitory and in 20 %—biphasic effect on basal calcium current. Similar data was acquired by Wahler and Dollinger (1995) in isolated guinea pig ventricular myocytes: SIN-1 (10 mkM) in some experiments showed inhibitory effect, while in some stimulatory effect on calcium current, which is prestimulated by application of β-adrenergic agonist. At 100 mkM NO-donor has pronounced inhibitory effect on this current (Wahler and Dollinger 1995).

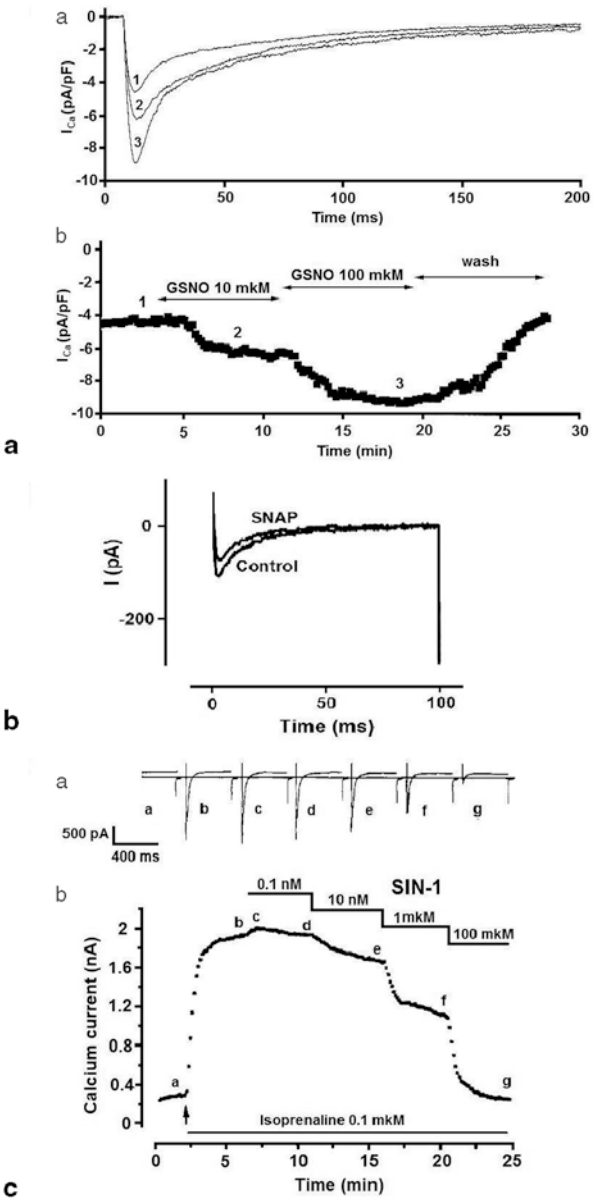

Fig. 8.3 Effect of nitric oxide on ventricular cardiomyocyte Ca^{2+} channels. **a** Increase of I_{CaL} by NO in rabbit atrial myocytes: time course of I (pA/pF) (a) and the superimposed current recordings where current traces (b) labeled as 1, 2 and 3 were obtained at the times marked by the corresponding letters in (a). From Wang et al. 2000 with permission of Oxford University Press via Copyright Clearance Center. **b** Decrease of I_{CaL} by NO in neonatal rat ventricular myocytes. Present effect of NO-donor. From Vulcu et al. 2000 with permission of Elsevier via Copyright Clearance Center. **c** Biphasic effect of NO-donor on isoprenaline-stimulated I_{Ca} (a) and current traces were obtained at the times indicated by the corresponding letters on the lower part (b). From Méry et al. 1993 with permission of American Society for Biochemistry and Molecular Biology via Copyright Clearance Center

Therefore it is possible to suppose that contradictory reports regarding NO effects on cardiomyocyte calcium channels can be explained by biphasic concentration dependence of the physiological effect of this endogenious regulator.

Physiological role of T-type Ca^{2+} channels, which are expressed in fetal and early neonatal cardiac cells, under normal conditions in adult organism is not clear yet.

Table 8.3 Effect of nitric oxide on K^+ channels of cardiomyocytes

Currents	Objects	Effects	References
I_{to1}	Kv4.1 channels expressed in *Xenopus* oocytes	Inhibition (Fig. 8.4)	Wang et al. 2007
	Kv4.3 channels expressed in Chinese hamster ovary cells	Inhibition	Gómez et al. 2008
	Isolated human atrial and mouse ventricular myocytes		
I_{Kur}	hKv1.5 channels expressed in mouse fibroblasts	Inhibition (Fig. 8.5)	Núñez et al. 2006
	Isolated mouse ventricular myocytes		
I_{Kr}	Kv11.1 channels (hERG1) expressed in *Xenopus* oocytes	Inhibition	Taglialatela et al. 1999
I_{Ks}	Isolated guinea pig ventricular myocytes	Activation (Fig. 8.6)	Bai et al. 2004
I_{K1}	Kir2.1 channels expressed in Chinese hamster ovary cells	Activation (Fig. 8.7)	Gómez et al. 2009
	Isolated human atrial myocytes		

However there are reports of abrupt increase in their expression in adult ventricular myocytes during pathological hypertrophy (Nuss and Houser 1993). There are no reports regarding NO effects on T-Ca^{2+} channels. However Nakayama and colleagues (2009) showed that transgenic mice with overexpression of channels, which generated $Ca_V1.3$ current (I_{CaT}), do not demonstrate pathological miocardium hypertrophy and NOS3 inhibitor abrogates antihipertrophic effect of overexpression. Therefore NO-mediated mechanisms are participating in modulation of I_{CaT} in adult cardiomyocytes.

8.4 Effect of Nitric Oxide on Potassium Channels

Effects of NO on different subtypes of potassium channels in cardiomyocites were investigated during recent decades relatively well. NO effects on main types of K^+ currents in cardiac cells are summarized in Table 8.3.

There is a number of reports that testify that NO inhibits activity of cardiac potassium Kv4 channels (Table 8.3 and Fig. 8.4), which participate in formation of the Ca^{2+}-independent transient outward potassium current (I_{to1}) (Tamargo et al. 2004). Also, fast NO-donor MAHMA-NONOate (100 mkmol/L) rapidly and significantly inhibits outward K^+ current in $K_V4.1$ channels expressed in *Xenopus* oocytes (Fig. 8.4). Slower NO-donor DEA-NO has similar effect (Wang et al. 2007).

Paper by Gómez et al. (2008) reports similar findings, showing that NO inhibits Kv4.3 channels. So, NO-donor SNAP (200 mkmol/L) reduces the peak $I_{Kv4.3}$ of channels, expressed in Chinese hamster ovary cells. DEA-NO (3 mkmol/L) and NO-saturated solution demonstrate similar effect. This study also showed that NO inhibits transient outward potassium current in human atrial myocytes. In presence of 4-AP

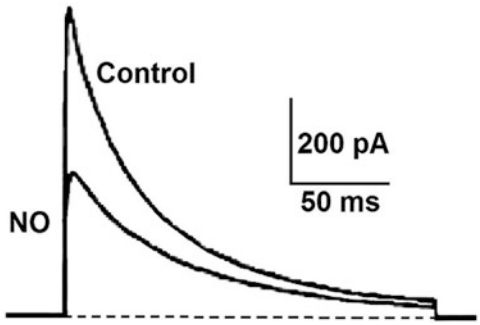

Fig. 8.4 Effect of nitric oxide on cardiomyocyte $K_V4.3$ channels. $I_{Kv4.1}$ recorded in *Xenopus* oocytes in the absence and presence of NO-donor. (From Wang et al. 2007 with permission of American Society for Biochemistry and Molecular Biology via Copyright Clearance Center)

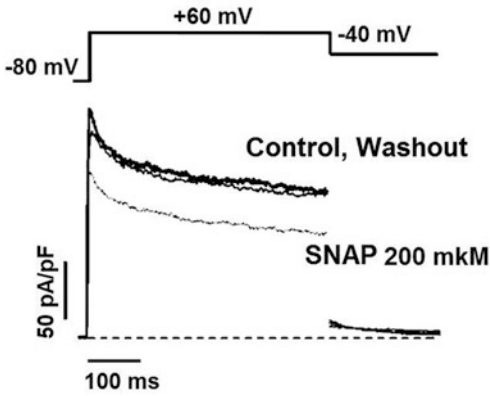

Fig. 8.5 Effect of nitric oxide on cardiomyocyte Kv1.5 channels. $hK_V1.5$ currents elicited in Ltk – cells by 500 ms-pulses from −80 to +60 mV and in the absence, presence and after washout of NO-donor. (From Núñez et al. 2006 with permission of Oxford University Press via Copyright Clearance Center)

(I_{Kur} blocker, 50 mkmol) SNAP (200 mkmol/L) decreases I_{to1} amplitude without alterations in time course of current decay. Authors propose, that NO-induced I_{to1} inhibition, which leads to prolongation of the plato phase of the action potential, can contribute to prevention or elimination of such severe pathology as ventricular fibrillation (Gómez et al. 2008).

NO inhibits activity of potassium $K_V1.5$ channels (Núñez et al. 2006), which generate ultrarapid delayed rectifier current (I_{Kur}) that determines the height and duration of atrial action potentials (Tamargo et al. 2004). It was show for $hK_V1.5$ channels expressed in mouse fibroblasts that SNAP (200 mkmol/L) significantly reduces the current amplitude (Fig. 8.5). Under such experimental conditions NO-donor does not affect the time course of current inactivation and kinetics of tail currents. Another NO-donor SNP (100 mkmol/L), NO-saturated solutions and NO precursor L-Arginine also depress $I_{Kv1.5}$. The same study reported that SNAP significantly reduces native I_{Kur} in isolated mouse ventricular myocytes (Núñez et al. 2006).

NO affects different components of delayed rectifier current in different ways, inhibiting its fast component – I_{Kr} (Taglialatela et al. 1999) and increasing its slow component – I_{Ks} (Bai et al. 2004, 2005).

Investigation by (Taglialatela et al. 1999) showed that NO depresses currents through human ether-a-gogo-related gene-1 (hERG1) K^+ channels. This type of channels, classified as $K_V11.1$, is responsible for rapidly activating delayed rectifier

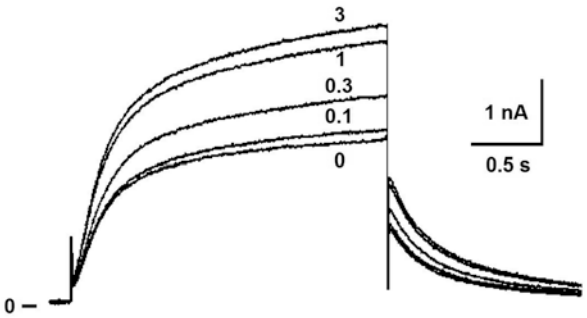

Fig. 8.6 Effect of nitric oxide on I_{Ks}. Present effects of NO-donor SNP. Representative superimposed current traces in the drug-free condition or in the presence of SNP at concentrations of 0.1, 0.3, 1, or 3 mM. (From Bai et al. 2004 with permission of John Wiley and Sons via Copyright Clearance Center)

current – I_{Kr} (Tamargo et al. 2004). An investigation of hERG1 channels expressed in *Xenopus* oocytes showed that NO source *L*-arginine (0.03–10 mM) inhibits outward current in a dose dependant manner. Different in their chemical origin NO-donors–sodium nitroprusside (SNP, 1–1000 mM), 3-morpholino-sydnonimine (SIN-1, 100–1000 mM), (Z)-1-[*N*-(2-aminoethyl)-*N*-(2-ammonioethyl)amino]diazen-1-ium-1,2-diolate (NOC-18; 1–300 mM), and *S*-nitroso *N*-acetylpenicillamine (SNAP, 1–300 mM)—inhibit current through hERG1 channels in a dose dependant manner as well (Taglialatela et al. 1999).

T. Furukawa et al. reported that NO activates slowly activating component of the delayed rectifier potassium current (I_{Ks}). NO-donor sodium nitroprusside (SNP, 1 mM) significantly increases this current in isolated guinea pig ventricular myocytes (Fig. 8.6). Under their experimental conditions an inhibitor of nitric oxide NO-synthases *S*-methylisothiourea (1 mM) and NO scavenger *N*-acetyl-*L*-cystein (1 mM) significantly depress I_{Ks} (Bai et al. 2004). Following publications of this research group show that NO plays a crucial role in Ca^{2+} mediated regulation of channels underlying I_{Ks} (Bai et al. 2005).

Investigation of Gómez et al. (2009) showed that NO increases the activity of $K_{ir}2$ channels, which generate inwardly rectifying K^+ current (I_{K1}), which plays a critical role in terminal repolarization phase of cardiac action potential (Tamargo et al. 2004). SNAP (200 mkmol/L) significantly increases current through $K_{ir}2.1$ channels expressed in Chinese hamster ovary cells (Fig. 8.7). Similar data was reported in case of application of DEA-NO (3 mkmol/L) and NO-saturated solution. It is also shown that SNAP increases both inward and outward I_{K1} in isolated human atrial myocytes. Authors suggest that NO facilitates the close-to-open transition and accelerates the channel closing kinetics (Gómez et al. 2009).

8.5 Effect of Nitric Oxide on Leak Channels (Two-Pore Potassium Channels)

Currently in literature there is only one report of NO effects on leak channels. According to Lu et al. (2007), in case of ischemic preconditioning, triggered by sodium cyanide (NaCN), NO modulates activity of K_{2P} channels in single guinea

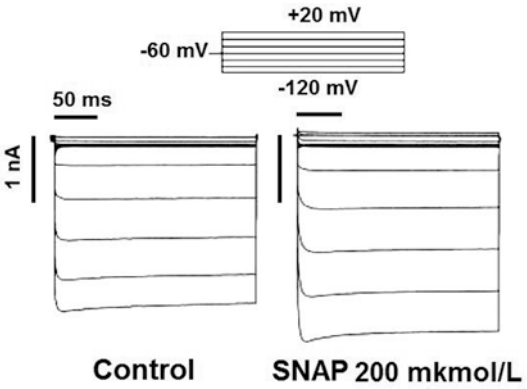

Fig. 8.7 Effect of nitric oxide on cardiomyocyte Kir2.1 channels expressed in Chinese hamster ovary cells. Presents $I_{Kir2.1}$ traces recorded by applying 250-ms pulses in the absence and presence of NO-donor. (From Gómez et al. 2009 with permission of Wolters Kluwer Health via Copyright Clearance Center)

pig ventricular cardiomyocytes. Increase of NO level via application of *L*-arginine increases NaCN-induced current via TALK-1 ($K_{2P}16.1$) and TALK-2 ($K_{2P}17.1$) channels, while inhibitor of NO-synthases L-NAME significantly deceases current through those channels. Authors propose that such modulatory effect of NO plays an important role in protection of cardiac cells during long lasting eschemia.

8.6 Effect of Nitric Oxide on Mechanically Gated Ion Channels

NO effects on mechanosensitive currents and cardiomyocyte channels as well as possible underlying mechanisms are discussed in detail (Kazanski et al. 2011). Investigations of mechanisms of action of NO on mechanically gated currents (MG-currents), which were performed at the same time by groups of G. Isenberg and A. Kamkin convincingly testify that NO is involved in regulation of MGCs in cardiomyocytes.

According to reports of the first and second groups of authors (Dyachenko et al. 2008; Dyachenko et al. 2009; Kazanski et al. 2011) application of NO-scavenger 2-(4-carboxyphenyl)-4,4,5,5-tetramethylimidazoline-1–1-oxy-3-oxide (PTIO, 100 mkmol/L and 500 mkmol/l) blocks MG-currents in isolated cardiomyocytes (Fig. 8.8). Besides that application of the blocker of NO-synthases *N*ω-Methyl-*L*-arginine acetate (*L*-NMMA, 200 mkmol/L) led to complete abolishment of MG-currents (Dyachenko et al. 2008). It is important to note that in the same investigation authors made an attempt to evaluate the contribution of NO-synthases (NOS) to modulatory effects of NO on activity of mechanosensitive channels of cardiomyocytes. It is shown that knockout of NOS1 does not lead to alterations of the MG-current, while in cardiomyocites from NOS3 knockout mice MG-currents can not be triggered at all (Dyachenko et al. 2008).

Investigations of A. Kamkin research group showed that NO-donors affect MG-currents (Fig. 8.9), registered in isolated mice, rat and guinea pig ventricular myocytes (Kazanski et al. 2010a, 2011). So, SNAP (100 mkmol/L) and DEA-NO (250 mkmol/L) in undeformed myocytes trigger appearance of current, which is similar to that appearing in response to cellular stretch by 10 μm. During mechanical

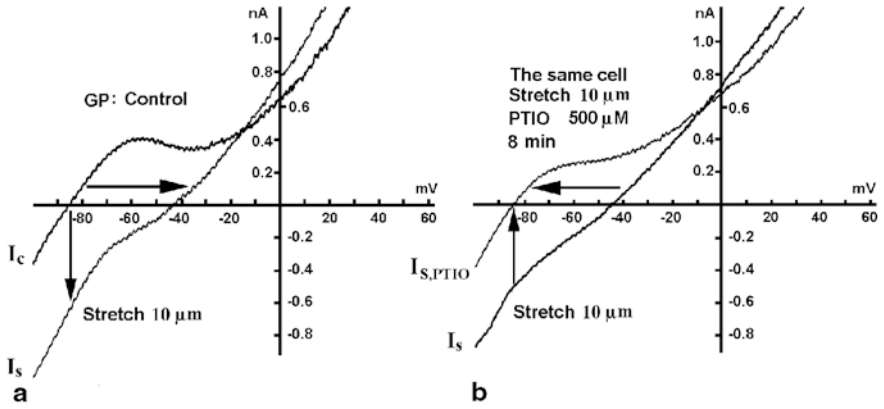

Fig. 8.8 Voltage dependence of membrane currents in ventricular myocyte from guinea-pig under PTIO perfusion on the background of the cell stretch. **a** *I–V* curve measured before stretch (I_C) and during 10 μm stretch (I_S). The arrows show the direction of the *I–V* curve shift. **b** *I–V* curves modifications under PTIO perfusion with continued stretch for 8 min ($I_{S,\ PTIO}$). The arrows show the direction of *I–V* curve shift at the given cell stretch under PTIO perfusion. It is obvious that during the PTIO perfusion the activity of MGCs is inhibited. (Modified from Kazanski et al. 2011 with permission from Springer)

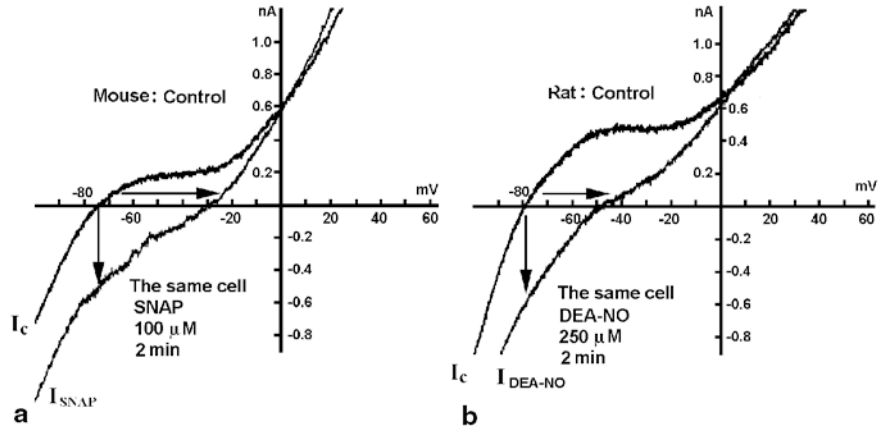

Fig. 8.9 NO-donors affect MG-currents. **a** Voltage dependence of membrane currents in ventricular cardiomyocytes from mouse under the SNAP perfusion of unstratched cell. *I–V* curve measured in control (I_C) and after 2 min SNAP perfusion (I_{SNAP}). **b** Voltage dependence of membrane currents in ventricular cardiomyocytes from rat under DEA-NO perfusion of unstretched cell. *I–V* curve measured in control (I_C) and after 2 min DEA-NO perfusion ($I_{DEA\text{-}NO}$). (Modified from Kazanski et al., 2011 with permission from Springer)

deformation of cardiomyocytes, which according to a number of reports leads to an increase of endogeneous concentration of NO (Pinsky et al. 1997; Petroff et al. 2001), effect of NO-donors is opposite (Kazanski et al. 2010a, 2011): perfusion

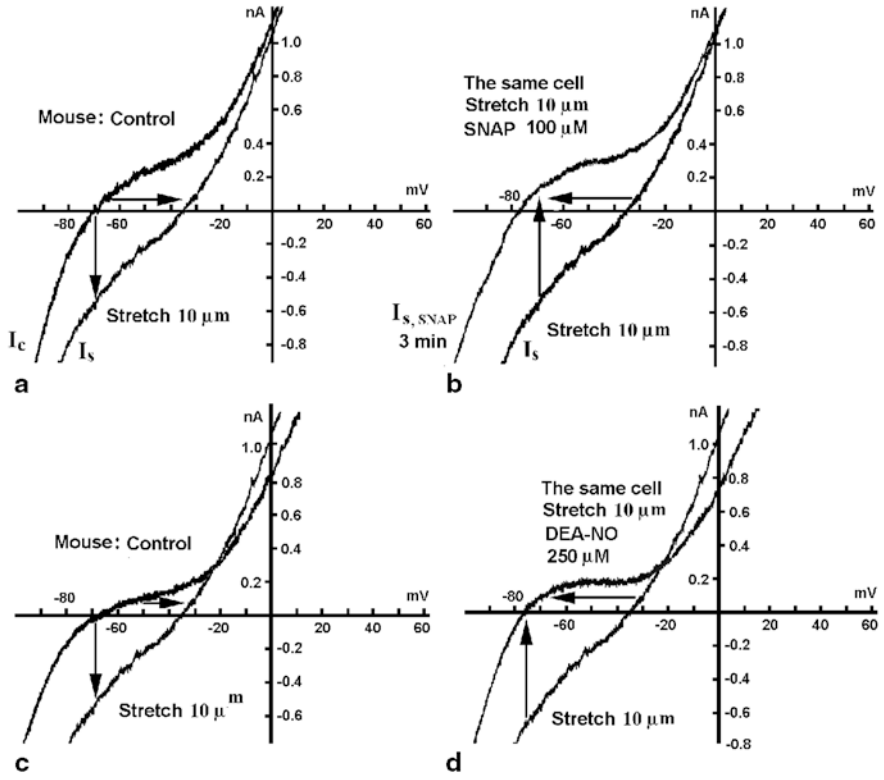

Fig. 8.10 Voltage dependence of membrane currents in ventricular cardiomyocyte under SNAP and DEA-NO perfusion on the background of the cell stretch. **a** Current-voltage relation (*I–V* curve) measured before stretch (I_C) and during 10 μm stretch (I_S). The arrows show the direction of the *I–V* curve shift at the given cell stretch. **b** modified *I–V* curves on the background of SNAP perfusion at continuous stretch during 3 min ($I_{S,\,SNAP}$). The arrows show the direction of the *I–V* curve shift at the given cell stretch under SNAP perfusion. It is obvious that during SNAP perfusion the activity of MGCs is inhibited. **c** *I–V* curve measured before stretch (I_C) and during 10 μm stretch (I_S). The arrows show the direction of the *I–V* curve shift at the given cell stretch. **d** modified *I–V* curves on the background of DEA-NO perfusion under continuous stretch during 3 min accordingly ($I_{S,\,DEA\text{-}NO}$). The arrows show the direction of the *I–V* curve shift at the given cell stretch on the background of its DEA-NO perfusion. It is obvious that in the process of DEA-NO perfusion the activity of MGCs is inhibited. (Modified from Kazanski et al. 2011 with permission from Springer)

with SNAP and DEA-NO during cellular stretch leads to inhibition of MG-currents (Fig. 8.9). Such dual effect of nitric oxide authors explain by the proposition that during perfusion with NO-donors as well as during cellular stretching there is a moderate elevation of NO concentration, which leads to activation of MGC of cardiomyocytes. However in case of perfusion with NO-donors during application of cellular stretch total concentration of NO significantly increases which in turn leads to inhibition of MGC. Since data regarding structure of mechanosensitive channels of cardiomyocytes is currently missing this assumption is based on analogy with concentration dependence of NO-donors effects on I_{CaL} (Kelly et al. 1996) (Fig. 8.10).

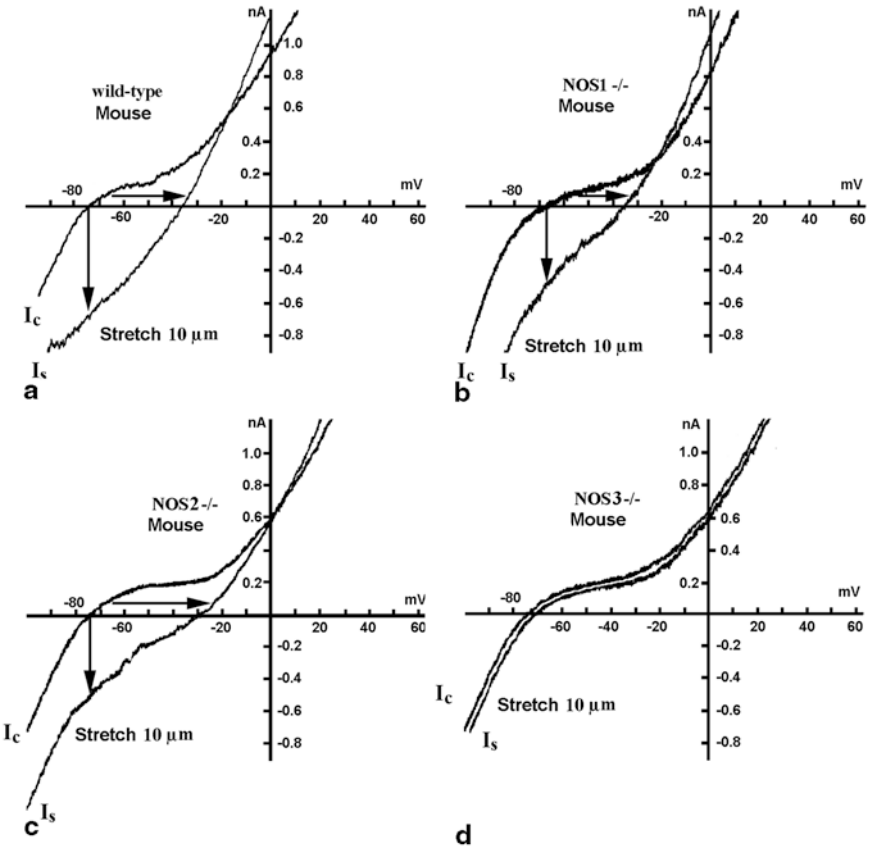

Fig. 8.11 Effects of NOS elimination on MG-currents in cardiomyocytes. **a** I–V curve for wild type mouse cardiomyocyte in control (I_C) and during stretching (I_S). **b** currents in cardiomyocytes from NOS1–/– mice in the control (I_C) and during stretching (I_S). **c** currents in cardiomyocytes from NOS2–/– mice in the control (I_C) and during stretching (I_S). **d** cardiomyocyte isolated from a NOS3–/– mice. 10-µm stretch of the myocyte does not induce MS currents in NOS3–/– mice cardiomyocytes in the control (I_C) and during stretching (I_S). Arrows show direction of curve shift during cell stretching. (Modified from Kazanski et al. 2011 with permission from Springer)

Other investigations of the same group reported that NO-scavenger PTIO (500 mkmol/L) blocks background MG-currents (Fig. 8.8) of not stretched (resting) isolated ventricular myocytes (Kazanski et al. 2010b, 2011), which goes in hand with report by Dyachenko et al. (2008). During cellular stretch PTIO also leads to inhibition of MG-currents, including background ones. Blockers of NO-syntases *L*-NAME (20 mkmol/L, 100 mkmol/L) and *L*-NMMA (200 mkmol/L) completely prevent appearance of MG-current in response to cellular stretching. Therefore endogeneous NO is required for activation of MGC cardiomyocytes.

Investigation involving knockout mice (Fig. 8.11) with different NO-syntases missing showed that for presence of response of cardiac myocytes to mechanical

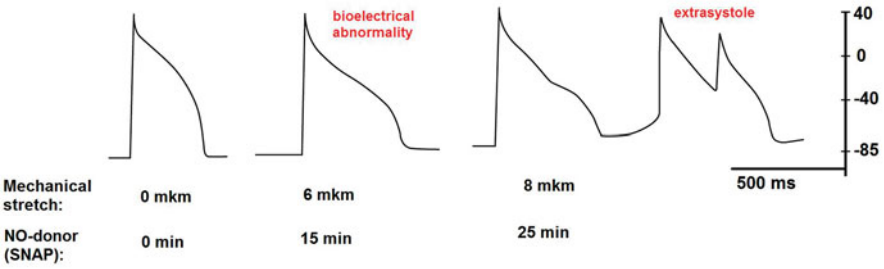

Fig. 8.12 Effects of nitric oxide on ventricular myocytes. The comparison of dynamics of effects of discrete stretching and NO-donor SNAP. Curves are modified from original recordings. (Kamkin et al. 2000; Abramochkin et al. 2012)

stimulus NOS3 is most important (Kazanski et al. 2010b, 2011). So in cardiomyocytes from wild type mice as well as in cardiomyocytes from NOS1 and NOS2 knock out mice MG-currents, appearing in response to cellular stretch, are identical and typical for according levels of stretch. In cardiomyocytes from NOS3-knockout mice on the contrary deformation does not trigger MG-currents.

Investigation of preparations of the right rat atria performed by means of microelectrode technique showed that NO-donor SNAP (3×10^{-4} mol/L) on the background of physiological level of tissue stretch triggers alterations of the repolarization phase of the cardiomyocyte action potential typical to "hump-like" depolarization, which leads to development of arrhythmias. Gadolinium (40 μmol/L) blocks this effect, which proves involvement of mechanosensitive ion channels in development of NO-induced abnormalities. Increase in SNAP concentration (to 6×10^{-4} mol/L), as well as tissue stretch eliminates NO-triggered "hump-like" depolarization (Abramochkin et al. 2012). Therefore NO at low concentrations activates mechanosensitive channels of cardiomyocytes, leading to mechanoinduced arrhythmias, while at high concentrations it inactivates them.

8.7 Conclusion and Perspectives

Possible mechanisms of NO effects were described in earlier publications (Kazansky et al. 2011). Major pathways of NO-mediated effects on ion channel activity in cardiac myocytes are activation of cGMP-dependent pathways (Han et al. 1996; Musialek et al. 1997; Wang et al. 2000; Vulcu et al. 2000; Ahmmed et al. 2001; Gallo et al. 2001; Núñez et al. 2006) and *S*-nitrosylation of reactive aminogroups of channels (Bai et al. 2004; Gómez et al. 2009). The key role in determination of the direction of the NO effect belongs to its concentration, which is convincingly proven by abovementioned data regarding NO effect on calcium and mechanosensitive channels of cardiac myocytes.

It is important to note that according to our experimental data NO effects are similar to effects of discrete cardiac tissue stretching (Fig. 8.12: Kamkin et al. 2000; Abramochkin et al. 2012).

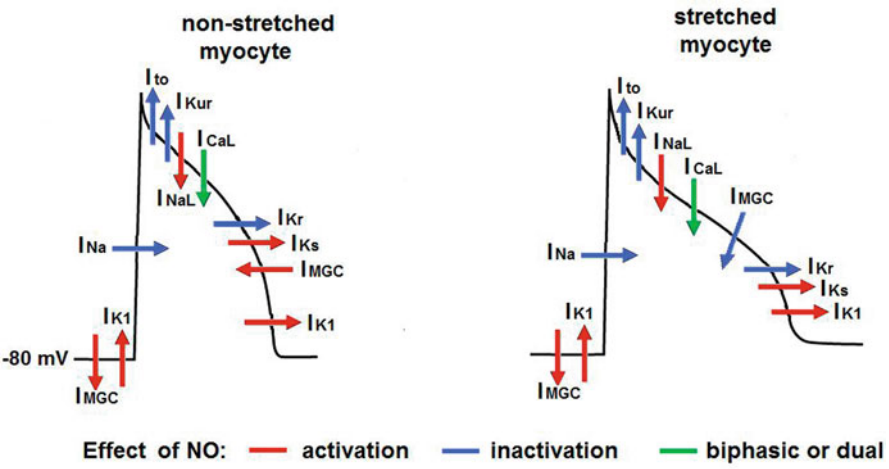

Fig. 8.13 Effects of nitric oxide on stretched and non-stretched ventricular myocyte currents

Figure 8.13 demonstrates summarized data regarding NO effects on ionic channels of cardiac myocytes.

Taking into consideration all abovementioned it is possible to confidently conclude that NO is one of the key physiological regulators of activity of cardiac cells, which mediates its effects via affecting cardiomyocyte transport systems, in particular altering activity of membrane ion channels.

Acknowledgments This work was supported by the Russian Foundation for Basic Research (grant no. 09-04-01277-a). Department of Fundamental and Applied Physiology (Professor and Chairman—Andre Kamkin) was supported by Ministry of Education and Science of the Russian Federation. The Order of Ministry of Education and Science of the Russian Federation No. 743 from 01 July 2010, Supplement, Event 4.4, the Period of Financing 2010–2019.

References

Abi-Gerges N, Fischmeister R, Méry P (2001) G protein mediated inhibitory effect of a nitric oxide donor on the Ltype Ca^{2+} current in rat ventricular myocytes. J Physiol 531(1):117–130

Abramochkin DV, Makarenko EYu, Mitrokhin VM, Tian Bo, Kalugin LYu, Sutiagin PV, Kamkin A (2012) Effect of nitric oxide on mechanoelectrical feedback. Bull Exp Biol Med 1:39–42 (Russian, English)

Ahern GP, Hsu S, Klyachko VA, Jackson MB (2000) Induction of persistent sodium current by exogenous and endogenous nitric oxide. J Biol Chem 275(37):28810–28815

Ahmmed GU, Xu Y, Dong PH, Zhang Z, Eiserich J, Chiamvimonvat N (2001) Nitric oxide modulates cardiac Na^{+} channel via protein kinase A and protein kinase G Circ Res 89:1005–1013

Bai C, Takahashi K, Masumiya H, Sawanobori T, Furukawa T (2004) Nitric oxide-dependent modulation of the delayed rectifier K^{+} current and the L-type Ca^{2+} current by ginsenoside Re, an ingredient of Panax ginseng, in guinea-pig cardiomyocytes. Br J Pharm 142:567–575

Bai C, Namekata I, Kurokawa J, Tanaka H, Shigenobu K, Furukawa T (2005) Role of nitric oxide in Ca^{2+} sensitivity of the slowly activating delayed rectifier K^+ current in cardiac myocytes. Circ Res 96:64–72

Bang L, Boesgaard S, Nielsen-Kudsk JE, Vejlstrup NG, Aldershvile J (1999) Nitroglycerin-mediated vasorelaxation is modulated by endothelial calcium-activated potassium channels. Cardiovasc Res 43:772–778

Campbell DL, Stamler JS, Strauss HC (1996) Redox modulation of L-type calcium channels in ferret ventricular myocytes. J Gen Physiol 108:277–293

Chiang C, Luk H, Wang T (2004) Swelling-activated chloride current is activated in guinea pig cardiomyocytes from endotoxic shock. Cardiovasc Res 62:96–104

Cuong DV, Kim N, Youm JB, Joo H, Warda M, Lee J, Park WS, Kim T, Kang S, Kim H, Han J (2006) Nitric oxide-cGMP-protein kinase G signaling pathway induces anoxic preconditioning through activation of ATP-sensitive K^+ channels in rat hearts. Am J Physiol Heart Circ Physiol 290:H1808–H1817

Dittrich M, Jureviacius J, Georget M, Rochais F, Fleischmann BK, Hescheler J, Fischmeister R (2001) Local response of *L*-type Ca^{2+} current to nitric oxide in frog ventricular myocytes. J Physiol 534(1):109–121

Donoso P, Sanchez G, Bull R, Hidalgo C (2011) Modulation of cardiac ryanodine receptor activity by ROS and RNS. Front Biosci 16:553–567

Dyachenko V, Christ A, Gubanov R, Isenberg G (2008) Bending of z-lines by mechanical stimuli: an input signal for integrin dependent modulation of ion channels? Prog Biophys Mol Biol 97(2-3):196–216

Dyachenko V, Rueckschloss U, Isenberg G (2009) Modulation of cardiac mechanosensitive ion channels involves superoxide, nitric oxide and peroxynitrite. Cell Calcium 45(1):55–64

Gallo MP, Ghigo D, Bosia A, Alloatti G, Costamagna C, Penna C, Levi RC (1998) Modulation of guinea-pig cardiac L-type calcium current bynitric oxide synthase inhibitors. J Physiol 506(3):639–651

Gallo MP, Malan D, Bedendi I, Biasin C, Alloatti G, Levi RC (2001) Regulation of cardiac calcium current by NO and cGMP-modulating agents. Pflügers Arch—Eur J Physiol 441:621–628

Gómez R, Núñez L, Vaquero M, Amorós I, Barana A, de Prada T, Macaya C, Maroto L, Rodrıguez E, Caballero R, López-Farré A, Tamargo J, Delpón E (2008) Nitric oxide inhibits Kv4.3 and human cardiac transient outward potassium current (I_{to1}). Cardiovasc Res 80:375–384

Gómez R, Caballero R, Barana A, Amorós I, Calvo E, López J, Klein H, Vaquero M, Osuna L, Atienza F, Almendral J, Pinto A, Tamargo J, Delpón E (2009) Nitric oxide increases cardiac I_{K1} by nitrosylation of cysteine 76 of $K_{ir}2.1$ channels. Circ Res 105:383–392

Han X, Shimoni Y, Giles WR (1994) An obligatory role for nitric oxide in autonomic control of mammalian heart rate. J Physiol 476(2):309–314

Han X, Shimoni Y, Giles WR (1995) A cellular mechanism for nitric oxide-mediated cholinergic control of mammalian heart rate. J Gen Physiol 106:45–65

Han X, Kobzik L, Balligand J-L, Kelly RA, Smith TW (1996) Nitric oxide synthase (NOS3)–mediated cholinergic modulation of Ca^{2+} current in adult rabbit atrioventricular nodal cells. Circ Res 78:998–1008

Han J, Kim K, Joo H, Kim E, Earm YE (2002) ATP-sensitive K^+ channel activation by nitric oxide and protein kinase G in rabbit ventricular myocytes. Am J Physiol Heart Circ Physiol 283:H1545–H1554

Hu H, Chiamvimonvat N, Yamagishi T, Marban E (1997) Direct inhibition of expressed cardiac *L*-type Ca^{2+} channels by *S*-nitrosothiol nitric oxide donors. Circ Res 81:742–752

Kamkin A, Kiseleva I, Isenberg G (2000) Stretch-activated currents in ventricular myocytes: amplitude and arrhythmogenic effects increase with hypertrophy. Cardivasc Res 48(3):409–420

Kamkin A, Kiseleva I, Isenberg G (2003) Ion selectivity of stretch-activated cation currents in mouse ventricular myocytes. Pflugers Arch—Europ J Physiol 446(2):220–231

Kazanski VE, Kamkin AG, Makarenko EY, Lysenko NN, Sutiagin PV, Bo T, Kiseleva IS (2010a) Role of nitric oxide in activity control of mechanically gated ionic channels in cardiomyocytes: NO-donor study. Bull Exp Biol Med 150(1):1–5

Kazanski VE, Kamkin AG, Makarenko EY, Lysenko NN, Sutiagin PV, Kiseleva IS (2010b) Role of nitric oxide in the regulation of mechanosesnsitive ionic channels in cardiomyocytes: contribution of NO-synthases. Bull Exp Biol Med 150(2):263–267

Kazanski V, Kamkin A, Makarenko E, Lysenko N, Lapina N, Kiseleva I (2011) The role of nitric oxide in the regulation of mechanically gated channels in the heart. In: Kamkin A, Kiseleva I (eds) Mechanosensitivity in Cells and Tissues 4. Mechanosensitivity and mechanotransduction. Springer, Berlin, pp 109–140

Kelly RA, Balligand JL, Smith TW (1996) Nitric oxide and cardiac function. Circ Res 79(3):363–380

Kirstein M, Rivet-Bastide M, Hatem S, Benardeau A, Mercadier J, Fischmeister R (1995) Nitric oxide regulates the calcium current in isolated human atrial myocytes. J Clin Invest 95:794–802

Kumar R, Namiki T, Joyner RW (1997) Effects of cGMP on L-type calcium current of adult and newborn rabbit ventricular cells. Cardiovasc Res 33:573–582

Levi RC, Alloatti G, Penna C, Gallo MP (1994) Guanylate-cyclase-mediated inhibition of cardiac I_{Ca} by carbachol and sodium nitroprusside. Pflugers Arch 426(5):419–426

Lim G, Venetucci L, Eisner DA, Casadei B (2008) Does nitric oxide modulate cardiac ryanodine receptor function? Implications for excitation–contraction coupling. Cardiovasc Res 77:256–264

Ljubkovic M, Shi Y, Cheng Q, Bosnjak Z, Jiang MT (2007) Cardiac mitochondrial ATP-sensitive potassium channel is activated by nitric oxide in vitro. FEBS Lett 581:4255–4259

Lu Z, Gao J, Zuckerman J, Mathias RT, Gaudette G, Krukenkamp I, Cohen IS (2007) Two-pore K^+ channels, NO and metabolic inhibition. Biochem Biophys Res Commun 363(1):194–196

Méry P, Pavoine C, Belhassen L, Pecker F, Fischmeister R (1993) Nitric oxide regulates cardiac Ca^{2+} current. J Biol Chem 268(35):26286–26295

Musialek P, Lei M, Brown HF, Paterson DJ, Casadei B (1997) Nitric oxide can increase heart rate by stimulating the hyperpolarization-activated inward current, I_f. Circ Res 81:60–68

Nakayama H, Bodi I, Correll RN, Chen X, Lorenz J, Houser SR, Robbins J, Schwartz A, Molkentin JD (2009) α1G-dependent *T*-type Ca^{2+} current antagonizes cardiac hypertrophy through a NOS3-dependent mechanism in mice. J Clin Invest 119:3787–3796

Nishimura N, Reien Y, Matsumoto A, Ogura T, Miyata Y, Suzuki K, Nakazato Y, Daida H, Nakaya H (2010) Effects of nicorandil on the cAMP-dependent Cl^- current in guinea-pig ventricular cells. J Pharmacol Sci 112:415–423

Núñez L, Vaquero M, Gómez R, Caballero R, Mateos-Cáceres P, Macaya C, Iriepa I, Gálvez E, López-Farré A, Tamargo J, Delpón E (2006) Nitric oxide blocks hKv1.5 channels by S-nitrosylation and by a cyclic GMP-dependent mechanism. Cardiovasc Res 72:80–89

Nuss HB, Houser SR (1993) T-type Ca^{2+} current is expressed in hypertrophied adult feline left ventricular myocytes. Circ Res 73(4):777–782

Petroff MG, Kim SH, Pepe S, Dessy C, Marbán E, Balligand JL, Sollott SJ (2001) Endogenous nitric oxide mechanisms mediate the stretch dependence of Ca^{2+} release in cardiomyocytes. Nat Cell Biol 3(10):867–873

Pinsky DJ, Patton S, Mesaros S, Brovkovych V, Kubaszewski E, Grunfeld S, Malinski T (1997) Mechanical transduction of nitric oxide synthesis in the beating heart. Circ Res 81(3):372–379

Sasaki N, Sato T, Ohler A, O'Rourke B, Marbán E (2000) Activation of mitochondrial ATP-dependent potassium channels by nitric oxide. Circulation 101:439–445

Schröder F, Klein G, Fiedler B, Bastein M, Schnasse N, Hillmer A, Ames S, Gambaryan S, Drexler H, Walter U, Lohmann SM, Wollert KC (2003) Single *L*-type Ca^{2+} channel regulation by cGMP-dependent protein kinase type I in adult cardiomyocytes from PKG I transgenic mice. Cardiovasc Res 60:268–277

Stoyanovsky D, Murphy T, Anno PR, Kim Y, Salama G (1997) Nitric oxide activates skeletal and cardiac ryanodine receptors. Cell Calcium 21(1):19–29

Taglialatela M, Pannaccione A, Iossa S, Castaldo P, Annunziato L (1999) Modulation of the K^+ channels encoded by the human ethera-gogo-related gene-1 (hERG1) by nitric oxide. Mol Pharm 56:1298–1308

Tamargo J, Caballero R, Gomez R, Valenzuela C, Delpon E (2004) Pharmacology of cardiac potassium channels. Cardiovasc Res 62:9–33

Tamargo J, Caballero R, Gomez R, Delpon E (2010) Cardiac electrophysiological effects of nitric oxide. Cardiovasc Res 87:593–600

Vandecasteele G, Eschenhagen T, Fischmeister R (1998) Role of the NO—cGMP pathway in the muscarinic regulation of the *L*-type Ca^{2+} current in human atrial myocytes. J Physiol 506(3):653–663

Vulcu SD, Wegener JW, Nawrath H (2000) Differences in the nitric oxidersoluble guanylyl cyclase signaling pathway in the myocardium of neonatal and adult rats. Eur J Pharm 406:247–255

Wahler GM, Dollinger SJ (1995) Nitric oxide donor SIN-l inhibits mammalian cardiac calcium current through cGMP-dependent protein kinase. Am J Physiol 268(37):45–54

Wang Y, Wagner MB, Joyner RW, Kumar R (2000) cGMP-dependent protein kinase mediates stimulation of L-type calcium current by cGMP in rabbit atrial cells. Cardiovasc Res 48:310–322

Wang X, Yin C, Xi L, Kukreja RC (2004) Opening of Ca^{2+}-activated K^{+} channels triggers early and delayed preconditioning against I/R injury independent of NOS in mice. Am J Physiol Heart Circ Physiol 287:H2070–H2077

Wang G, Strang C, Pfaffinger PJ, Covarrubias M (2007) Zn^{2+}-dependent Redox Switch in the Intracellular T1-T1 Interface of a Kv Channel. J Biol Chem 282(18):13637–13647

Wang H, Viatchenko-Karpinski S, Sun J, Györke I, Benkusky NA, Kohr MJ, Valdivia HH, Murphy E, Györke S, Ziolo MT (2010) Regulation of myocyte contraction via neuronal nitric oxide synthase: role of ryanodine receptor *S*-nitrosylation. J Physiol 588(15):2905–2917

Yoo S, Lee SH, Choi BH, Yeom JB, Ho WK, Earm YE (1998) Dual effect of nitric oxide on the hyperpolarization-activated inward current (If) in sino-atrial node cells of the rabbit. J Mol Cell Cardiol 30:2729–2738

Chapter 9
The Role of Ion Channels in Cellular Mechanotransduction of Hydrostatic Pressure

Kevin D. Champaigne and Jiro Nagatomi

9.1 Introduction

The sensation of pressure, followed by a resulting alteration of cellular function, may be critical to a number of organs and systems, including the vasculature (Folgering et al. 2008), intervertebral disks (Ishihara et al. 1996), the eye (Kwon et al. 2009), the renal system (Arnold et al. 2009), and the urinary system (Ferguson et al. 1997). Like temperature, hydrostatic pressure (HP), which is a pressure acting uniformly in all directions, is a thermodynamic state variable, and therefore can be considered a ubiquitous factor in all biological processes. However, there remains considerable debate as to whether physiologic levels of HP can cause a direct, detectable effect on cells which are generally considered incompressible, or whether HP is sensed indirectly via local tissue deformation or other mechanism.

Although the cell may not undergo significant mechanical deformation due to HP changes alone, numerous studies have shown effects of HP on cells and tissues, including changes in intracellular ion concentrations, gene expression, membrane trafficking, cell proliferation, and apoptosis (Ishihara et al. 1996; Haberstroh et al. 1999; Nagatomi et al. 2001, 2002, 2003; Ohashi et al. 2007; Stover and Nagatomi 2007; Nagatomi et al. 2009; Drumm et al. 2010; Huang et al. 2010). However, studies investigating the fundamental mechanism responsible for physiological HP mechanosensitivity are rare. Ion channels are known to be responsible for certain observed events under high pressures (up to 100 MPa) in deep sea animals and diving mammals including humans, where thermodynamic effects have been shown to directly alter channel open probabilities (Macdonald 2002). Such direct modulation of gating probabilities may also be involved with some observed effects on chondrocytes, which have been tested up to 50 MPa (Hall 1999). Normal physiological pressures of less than 20 kPa, though, have also been shown to cause effects in cells from the eye, the vestibular system, and the bladder, where alternative mechanisms are likely needed to provide pressure sensitivity (Macdonald and Fraser 1999).

J. Nagatomi (✉) · K. D Champaigne
Department of Bioengineering, Clemson University, 315 Rhodes Hall, Clemson, SC 29634-0905, USA
e-mail: jnagato@clemson.edu

A. Kamkin, I. Lozinsky (eds.), *Mechanically Gated Channels and their Regulation,* Mechanosensitivity in Cells and Tissues 6,
DOI 10.1007/978-94-007-5073-9_9,

It is not a simple task to effectively eliminate all potential extraneous sources of stimulation, such as fluid shear stress, while subjecting cells or tissues to controlled HP stimuli. Thus, experimental setups and techniques are critically important for generating valid pressure sensitivity results. Examples of approaches include, but are not limited to, the use of water column height adjustment, pressurization of the gas phase above liquid media, and direct mechanical pressurization of the liquid phase. Consideration of gas partial pressures, temperature, nutrients, fluid flow, pressure stability, and cell substrate stiffness, among other parameters, must be undertaken while continuing to provide functional experimental conditions. Although patch clamp techniques have most often been employed for investigating ion channel effects of high hydrostatic pressures, imaging with calcium-sensitive fluorescent dyes have thus far been most often used for physiological range HP ion channel research.

This review will first present evidence for the involvement of particular ion channels or transporters in cellular HP sensitivity for a number of organ systems and cell types across a range of physiologic pressures. Testing techniques which are able to isolate the effects of HP on cells will then be reviewed to not only provide the reader with potential methods for further experimentation, but also to better illustrate the application the hydrostatic pressure stimulus under physiological conditions. Finally, potential physical mechanisms by which an extracellular HP stimulus could elicit a cellular response, including example estimates of changes to physical parameters that would be experienced within physiological and pathological conditions, will be presented.

9.2 Ion Channel-mediated Pressure Mechanotransduction in Various Cell Types

9.2.1 Bladder

Mechanical parameters such as bladder wall tension or intravesical pressure due to bladder filling are sensed at the cellular level and contribute to both conscious sensation and reflex responses. The urothelium, the epithelial lining of the bladder luman, has been shown to contribute to bladder sensation through the release of neurotransmitters such as ATP, as well as to actively respond to bladder filling by increasing the surface area of the umbrella cells that line the bladder (Birder 2005; Apodaca et al. 2007). Malfunctions in these sensing abilities are likely to contribute to lower urinary tract dysfunction (de Groat 2004), but the mechanisms by which sensory transduction is accomplished at the cellular level within the lower urinary tract are not well understood.

The generally agreed understanding of bladder mechanosensory event sequence is that when urine volume reaches a certain threshold, an afferent nerve signal activates the pontine micturition center to induce bladder contraction and urethra relaxation,

which results in voluntary voiding (Yoshimura et al. 2008). However, there has been a long debate whether the bladder afferent is activated by the threshold volume, intravescical pressure, or wall tissue tension caused by the pressure (Downie and Armour 1992; Moss et al. 1997). An early work by Iggo, which was later supported by the work of others, demonstrated that increasing intravescical pressure due to passive filling or isotonic contraction both led to the afferent nerve responses, indicating that pressure and/or the associated wall tissue tension, play a major role in bladder mechanosensing (Iggo 1955). Indeed, spontaneous contraction of the bladder detrusor muscle, which would increase pressure in the bladder but not cause stretch of the bladder, wall increases the urge to urinate. In contrast, others have suggested that there exist "volume sensitive" afferents innervating the bladder which detect the stretch (change in the length of wall tissue) irrespective of the intravescical pressure (Moss et al. 1997; Morrison 1999; Shea et al. 2000; Zagorodnyuk et al. 2006). These concepts are supported by the existence of so-called stretch-sensitive ion channels on various cells within bladder wall (Araki et al. 2008) and evidence that bladder strips subjected to stretching evoke afferent responses (Moss et al. 1997). It is also still not clear whether tension or stretch is the direct stimuli on the nerve terminal or whether other cells such as smooth muscle or urothelial cells release neurotransmitters to activate chemical receptors on afferent nerves. These functional units are not necessarily exclusive and it is possible that more than one mechanism exists to complement or compensate each other.

Ferguson et al. first demonstrated that ATP is released from the urothelial cell layer following the application hydrostatic pressure to the mucosal (or apical) surface of the bladder wall in rabbits, and were the first to suggest that this release of ATP may be part of a mechanosensory pathway to detect bladder filling (Ferguson et al. 1997). Experiments by Wang et al. later showed that ATP was released by both the mucosal and serosal surfaces of isolated rabbit bladder tissue when stretched by the application of hydrostatic pressure to the apical surface of the umbrella cells (Wang et al. 2005), and that ATP signaling pathways regulate both exocytosis and endocytosis rates, thereby controlling apical membrane dynamics. Yu et al. further observed that modification of the apical membrane surface area requires activation of both a non-selective cation channel and a member of the epithelial sodium channel (ENaC) family, as well as an intact cytoskeleton (Yu et al. 2009).

Multiple members of the Transient Receptor Potential (TRP) family of cation-selective ion channels have been identified in the bladder (Everaerts et al. 2010), which are activated by widely varying stimuli and contribute to sensory perception in hearing, vision, taste, smell, and touch, as well as cellular regulation processes such as due to osmotic challenges (Venkatachalam and Montell 2007). The TRP family of proteins has been divided into 7 subfamilies (TRPV, TRPC, TRPM, TRPA, TRPN, TRPP, and TRPML), although the functional characteristics and sensing modalities often do not correspond to subfamily classification. Members of the ENaC/degenerin family of ion channels play critical roles in maintaining Na^+ homeostasis in a variety of tissues, including ENaCs and the homologous acid-sensing ion channel (ASIC). Both channels are highly Na^+ selective, amiloride sensitive, and have been found to be responsive to mechanical stimuli (Kashlan and Kleyman 2011).

Work by Olsen et al. (2011) investigated the response of rat urothelial cells to physiological levels of hydrostatic pressure as would be experienced during bladder filling. Unlike the experiments described above, where the urothelial tissues were stretched by the applied pressure difference, these experiments were performed on cells cultured on a rigid substrate, resulting in negligible stretch. Urothelial cells were prepared in separate dishes for each parameter group and subjected to hydrostatic pressure at 5, 10, 15, and 20 cm H_2O (0.5, 1, 1.5, 2 kPa), each for 5, 15, and 30 min. Supernatant media were collected before and after exposure of urothelial cells to pressure. The ATP release from the cultured cells into the supernatant media was significantly increased in response to the application of pure hydrostatic pressure stimulus of 10 cm H_2O when applied for 5 or 15 min. This ATP release was blocked by the broad TRP channel blocker ruthenium red, the ENaC channel blocker amiloride, the stretch activated channel blocker gadolinium (Gd^{3+}), or by the chelation of extracellular calcium with BAPTA. This implies that pressure sensation is dependent upon a serial pathway including ENaC channels and stretch-activated channels such as TRP channels, as well as Ca^{2+} influx from the extracellular space. However, whether these ion channels are activated by HP or via a separate secondary mechanism is yet to be demonstrated.

9.2.2 Optic Nerve Cells

Glaucoma is a chronic, degenerative optic neuropathy caused by the loss of retinal ganglion cell (RGC) axons, along with supporting glia and vasculature (Kwon et al. 2009). Elevated intraocular pressure (IOP) is an important risk factor for the development of glaucoma (Kumar et al. 2005), although glaucoma can occur without elevated IOP. Intraocular pressure is currently the only factor that can be modified by treatment, which has been shown to slow the onset and progression of glaucoma (Kwon et al. 2009). As such, numerous studies have been performed to attempt to identify the causative mechanism for the effect of HP on various cell types. Identified studies that have shown a potential connection between the mechanosensation of HP via ion channels and glaucoma are reviewed in this section.

A study by Sappington et al. investigated the contribution of the transient receptor potential vanilloid subunit 1 (TRPV1) channel to the release of interleukin-6 (IL-6) and the nuclear translocation of nuclear factor kappa B (NFκB) in microglial cells from rat retinas (Sappington and Calkins 2008). Calcium imaging revealed that $[Ca^{2+}]_i$ increases via calcium influx are observed following the application a hydrostatic pressure of $+70$ mmHg (9.3 kPa), which potentiates NFκB translocation to the nucleus and release of IL-6. Removal of extracellular calcium or blocking of all TRP channels via ruthenium red substantially reduced the effects of pressure, while targeted desensitization of the TRPV1 channels via iodo-resiniferatoxin (I-RTX) only reduced the response by approximately 25 %. The TRPV1 agonist capsaicin alone did not activate NFκB or cause IL-6 release. TPRV1 was shown by

immunohistochemistry to be diffusely distributed throughout the cell and on the plasma membrane, which was attributed to the presence of the channel on the endoplasmic reticulum as well as the cell membrane. Although the mechanism by which hydrostatic pressure caused the calcium influx was not identified, the fact that capsaicin was not able to induce the same effects as hydrostatic pressure implied that other pressure sensitive mechanisms are necessarily present.

Sappington et al. further probed the mechanisms by which increased HP causes increased retinal ganglion cell death through potential involvement of TRPV1 channels (Sappington et al. 2009). Expression of TRPV1 channels was verified in rat and mouse RGCs, and activation of TRPV1 channels by capsaicin was shown to increase RGC apoptosis rates in a dose-dependent manner. When exposed to an elevated HP of + 70 mmHg (9.3 kPa) for 48 h, RGC apoptosis rates increased from ambient levels by 36 %. This increase in apoptosis rate was significantly reduced in the presence of I-RTX, a TRPV1 antagonist, as well as through chelation of extracellular Ca^{2+} with EGTA, suggesting that an influx of Ca^{2+} via TRPV1 channels is at least partially responsible for HP-induced death of RGCs. The Ca^{2+} indicator dye fluo-4 was used to show a fourfold increase in $[Ca^{2+}]_i$ in RGC cell bodies and processes due to elevated HP. Use of antagonist I-RTX reduced the increase in $[Ca^{2+}]_i$ by 40 %, demonstrating that TRPV1 channel activation is a prominent factor in the increase in intracellular calcium in RGCs exposed to elevated HP.

A study by Mandal et al. (2009) found that elevated hydrostatic pressure activates the sodium/hydrogen exchanger-1 (NHE1) in rat optic nerve head astrocytes. Pressures of either 15 or 30 mmHg (2 or 4 kPa) applied for 2 h were found to cause phosphorylation of ERK1/2, ribosomal S6 protein kinase (p90RSK), and NHE1. The activation of NHE1 in HP exposed cells did not lead to baseline acidification of the cell cytoplasm, but did significantly increase the rate of intracellular pH recovery from induced acidification. This effect was abolished in the presence of either U0126, an MEK/ERK inhibitor, or dimethylamiloride, an NHE inhibitor, suggesting that HP induced NHE1 phosphorylation through the ERK pathway rather than directly inducing activation of NHE1.

A follow-up study by Mandal et al. (2010) was undertaken to investigate if intracellular calcium was involved in the upstream events that caused ERK1/2 and p90RSK phosphorylation. Cytoplasmic calcium levels of cells subjected to 15 mmHg (2 kPa) were measured using the ratiometric calcium indicator fura-2 AM. Control cells not exposed to increased HP were found to maintain a steady $[Ca^{2+}]_i$ of approximately 100 nM. In cells subjected to HP, this baseline level increased in a steady manner by approximately 27 nM in 15 min. This increase was unchanged when calcium-free medium was employed or in the presence of 4 mM nickel chloride, suggesting a release from an internal calcium store rather than an influx through the cell membrane. The increase was abolished by cyclopiazonic acid (CPA), a specific inhibitor of the sarcoendoplasmic reticulum Ca^{2+} pump, but not by xestospongin C, an IP3 receptor antagonist. Ruthenium Red and dantrolene, inhibitors of ryanodine receptor-mediated calcium release, abolished the calcium increase, suggesting a contribution of ryanodine-sensitive calcium stores. Treatment with dantrolene was further found

to abolish the increase in ERK1/2 phosphorylation due to HP, verifying that increased $[Ca^{2+}]_i$ precedes ERK activation in the response of astrocytes to HP stimuli.

9.2.3 Chondrocytes

Articular cartilage is typically subjected to loads up to 18 MPa in vivo during normal activities (Hodge et al. 1986). Upon compressive loading of the joint, HP of the fluid in the cartilage increases, which is maintained due to the low permeability of the tissue. Sustained pressure causes fluid to be slowly exuded from the tissue until a new equilibrium condition is reached, as balanced by the osmotic pressure due to the highly negatively-charged proteoglycan content of cartilage. Chondrocytes within the cartilage would experience the increase in HP pressure as a uniform normal stress (Elder and Athanasiou 2009). Numerous studies have subjected chondrocytes to HP stimuli of various levels and frequencies, and demonstrated a direct effect on extracellular matrix (ECM) composition, protein expression, chondroprotection, and cell differentiation (Elder and Athanasiou 2009; Grad et al. 2011). A subset of these studies are reviewed here that specifically investigated the role of membrane-bound transporters and ion channels in the mechanotranduction of HP by chondrocytes.

Hall (1999) studied the effects of HP on isolated bovine articular chondrocytes and found that increased HP inhibited both the Na/K pump (ouabain sensitive) and the Na/K/2Cl cotransporter (bumetanide sensitive), as well as the residual K^+ permeability. Specifically, static pressures of 0.1–50 MPa were applied for either 20 s or 10 min, and the resulting relative inhibition of the channels was observed. A 28 % reduction in K^+ flux through Na/K transporters was observed in response to a 2.5 MPa pressure applied for 10 min, with modestly increasing inhibition for higher pressures. A 24 % inhibition in the Na/K pump occurred for a 10 MPa stimulus applied for 20 s, again with increasing inhibition at higher pressures. This inhibition of the Na/K pump was not observed when the $[Na^+]_i$ was reduced below physiologic levels, and was reduced for elevated $[Na^+]_i$. The Na/K/2Cl cotransporter was shown to be inhibited up to 68 % by pressures of 15 MPa applied for 10 min, and by 52 % by pressures of 15 MPa applied for 20 s. The residual K^+ flux, occurring in the presence of ouabain and bumetanide, was additionally found to be inhibited by a pressure of greater than 7.5 MPa applied for 10 min. Based on these findings, the authors suggest that inhibition of these K^+ transport mechanisms could lead to decreased in $[K^+]_i$, which may alter matrix metabolism as occurs in cartilage under load.

Browning et al. (1999) investigated the effects of HP up to 30 MPa on the Na/H exchanger in isolated bovine articular chondrocytes when applied for 300 s. HP application in this regime was not found to affect the resting internal pH of chondrocytes. However, the recovery from induced acidification was found to be stimulated by HP, suggesting that the Na/H exchanger was activated by HP. This effect was dependent upon the presence of extracellular Na^+ and could be inhibited by the Na/H exchanger inhibitor ethylisopropylamiloride (EIPA, 10 mM). The stimulation

was also abolished by the non-specific kinase inhibitor staurosporine, which implies pressure sensitive phosphorylation is responsible for the effect. A further study by the same group (Browning et al. 2004) investigated the short-term effects of increased HP on isolated juvenile bovine articular chondrocytes. Specifically, pressures of 30 MPa applied for 30 s resulted in a 3-fold increase in intracellular calcium, largely caused by calcium release from intracellular stores. Increases in $[Ca^{2+}]_i$ due to pressures applied for 240 s were abolished by the removal of Ca^{2+} from the medium, implying an extracellular calcium source. These increases were also blocked by the inhibitors neomycin and thapsigargin, showing that an IP_3-mediated calcium release from internal calcium stores was occurring.

Mizuno (2005) attempted to characterize the calcium response of chondrocytes to the application of 0.5 MPa hydrostatic pressure for 5 min. Interestingly, no response was observed for cells cultured for just 2 days, presumably due to the lack of accumulated ECM. For cells cultured for 5 days, however, up to a twofold increase in $[Ca^{2+}]_i$ was observed, with the peak concentrations occurring 20–140 s after HP application. This transient increase in $[Ca^{2+}]_i$ returned to near-baseline levels within 300 s. The effect was reduced to 55 % of the unaltered pressure response by gadolinium, a blocker of stretch-activated channels, and to 36 % by dantrolene, an intracellular Ca^{2+} storage blocker. The effect was also blocked by using Ca^{2+} free medium with EGTA, but was not affected by verapamil, an L-type calcium channel blocker. Evidence provided by these studies provides a potential explanation of the mechanism by which the composition and structure of cartilage is modified by the applied loading regimen, with each effect potentially modifying the function of the associated chondrocytes.

9.2.4 Vestibular Cells

In the endolymphatic system, very low levels of hydrostatic pressure (changes as low as 0.5 cm H_2O or 50 Pa) has been postulated to cause endolymphatic hydrops or Meniere's Disease (Bohmer and Dillier 1990), which is characterized by vertigo, hearing loss, and tinnitus. In order to determine if ion channel currents in vestibular cells are modulated by HP, Düwel et al. (2003) quantified potassium currents in vestibular type II hair cells from guinea pig utricles using patch clamp techniques. HP was controlled within the range of 0.2 cm H_2O (20 Pa)–1 cm H_2O (100 Pa) by manipulating the height of the fluid bath during patch clamp experimentation. Significant increases in baseline K^+ current densities of 22 ± 14 % at $+40$ mV were observed after the application of just 0.5 cm H_2O. This pressure-sensitive K^+ current ($I_{K,p}$) occurred immediately upon the application of HP, remained elevated during the entire period of increased HP (2–4 min), and then receded after the HP stimuli was removed. No similar pressure-sensitive Ca^{2+} current was identified. $I_{K,p}$ was most effectively blocked with charybdotoxin, a blocker of Ca^{2+}-sensitive K^+ currents, which was able to consistently and reversibly block the current while not affecting other K^+ currents. A subsequent study (Düwel et al. 2005) demonstrated that cinnarizine and

nifedipine, blockers of voltage-gated Ca^{2+} currents which are sometimes prescribed to treat Meniere's disease, reduce $I_{K,p}$ by reducing Ca^{2+} influx. This $I_{K,p}$ current was shown to alter the membrane voltage response and subsequently the transmitter release by hair cells by acting as an increased depolarizing current (Dinh 2008), which could be modulated with cinnarizine (Haasler et al. 2009). Together, these findings potentially explain the diminished afferent activity in Meniere's disease patients.

9.2.5 Bone Cells

Mechanical loading on the skeleton affects bone homeostasis, with increases in loading activities leading to increased bone mineral density (Leblanc et al. 1990; Zerwekh et al. 1998) and decreases in loading activities leading to decreased bone mass (Krolner et al. 1983; Courteix et al. 1998). Mechanical stimulation, such as HP, strain, or fluid shear stress, has been postulated to be sensed by osteocytes, osteoblasts, or osteoclasts, thereby modulating the bone remodeling process (Chen et al. 2010). Multiple in vitro studies have shown that the application of HP to bone cells can affect differentiation, gene expression, cytoskeletal organization, and apoptosis (Nagatomi et al. 2001; Liu et al. 2010). Thus far, however, the role of ion channels or transporters in the response of bone cells to HP has not been specifically investigated. A recent study by Liu et al. (2010) has, however, demonstrated an increase in $[Ca^{2+}]_i$ due to cyclic HP on an osteocyte-like cell line. MLO-Y4 cells were subjected to cyclic HP with a 0.5 Hz triangular waveform and a peak pressure of 68 kPa for 1 or 2 h. Since TRP channels can be activated by hypo-osmotic stimulation and induce calcium ion influx in osteoblasts (Gomis et al. 2008), the authors suggested that a similar mechanism may be involved with cyclic HP mechanosensation.

9.3 Experimental Techniques for Ion Channel Pressure Mechanotransduction Research

Experiments involving low pressures must be carefully designed and executed to provide the proper pressure stimuli while maintaining all other conditions sufficiently constant to avoid false results. Various test configurations used to date and potential issues to be aware of when developing experiment setups and protocols are reviewed in this section.

9.3.1 Water Column

Perhaps the most straightforward approach to apply highly stable small hydrostatic pressures is simply to create a water column above the cells of sufficient height. This

technique was employed for the patch clamp experiments performed by Düwel et al. (2003), where the height of the fluid bath was controlled by adding and removing fluid while the cell remained patched. The cells were monitored under the microscope to make sure that the hair cells did not move upon fluid addition or removal. Extreme care must be taken to avoid fluid shear stress which would not be present in the control case, or perhaps to replicate the shear stress as close as possible by exchanging an equivalent volume of fluid at similar rates with the control cells.

Water column height adjustment was also used for portions of the work by Mandal et al. (2009, 2010) to expose cells to 15 mmHg pressure for 2 h. Control cells were placed in a horizontal tray containing the same volume of media in the same cell culture conditions. Both configurations were bubbled with 95 % air-5 % CO_2 to maintain constant gas tensions, and care was taken to place the gas outlet a similar distance from the cells and to use identical gas flow rates. Modifications of dissolved gas concentrations, pH, or nutrients must be avoided, particularly for longer term experiments. It has been shown (Lei et al. 2011) that increasing the height of the water column without proper controls can cause changes in gas tensions that can be the actual cause of effects attributed to HP. Within a standard column, gases must diffuse over an increased diffusion distance versus standard culture dishes with a thin layer of media, causing hypoxic conditions near the cells due to metabolism. This was avoided by Lei through the use of a horizontally oriented tube of media to provide similar diffusion conditions.

9.3.2 Gas Phase Pressurization

For cells cultured in media with gas, the HP experienced by cells is the sum of the gas pressure and the fluid pressure due to the height of the media above the cells. This configuration is well suited to experiments at high HPs, due to the relative ease of providing gases at high pressure. Figure 9.1 shows a typical system diagram for gas phase pressurization which employs a compressed gas source, electronic valves, a pressure transducer, and a computer (Stover and Nagatomi 2007).

A small container of water was included within the pressure chamber for this setup as well as a similar setup employed by Sappington et al. (Sappington and Calkins 2008; Sappington et al. 2009) to maintain humidity levels. Significant artifacts due to changes in pH, dissolved oxygen content, and dissolved carbon dioxide content must be ruled out by the experimenters as was done by these studies, since pH, pO_2, and pCO_2 will all be affected to some degree by increased gas pressure.

9.3.3 Liquid Phase Pressurization

Direct pressurization of the liquid phase can be achieved through the use of peristaltic (Mandal et al. 2010), isocratic (Mizuno 2005), or syringe pumps (Liu et al. 2010), among others. This technique is well suited to either low or high pressure application,

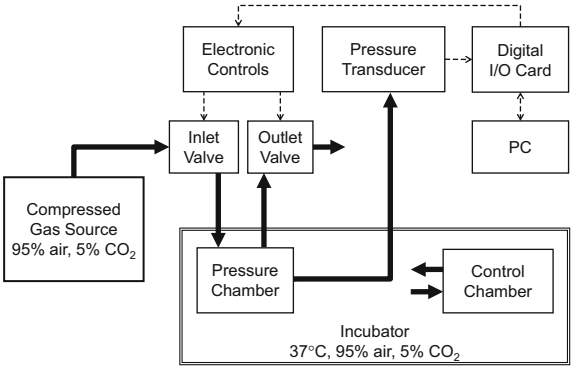

Fig. 9.1 Schematic of the computer-operated cyclic pressure system. Pressure levels within the sealed chamber were monitored by the transducer and controlled by the operation of inlet and outlet valves using custom written Labview software. Thin and thick lines indicate electrical and gas connections, respectively. The directions of electrical signals and gasflows are represented by dotted and solid arrows, respectively. (Reprinted with permission from Stover and Nagatomi 2007)

and it allows the simultaneous application of HP and fluid flow, thereby enabling the administration of drugs, channel blockers, or altered solution salt concentrations during experiments. System components of an innovative test configuration from Mandal et al., are shown in Fig. 9.2 (Mandal et al. 2010), where changing the outlet height directly controls the HP stimulus experienced by the cells in the imaging chamber. Pressure dampening is often required for such a system, as the peak to peak amplitude of the dynamic pressure swings from the peristaltic pump coupled with inflexible tubing can potentially exceed the static pressures desired. A similar design was implemented by Browning et al. (1999) however a computer operated back pressure controller was utilized rather than the manual height adjustment. Such a system could potentially be used for pressures greater than those for which height adjustment would be practical.

9.3.4 Considerations for Optical Microscopy under Pressurized Conditions

Optical imaging is often used in pressure experiments to perform ion concentration measurements or other indicators of ion channel or transporter activity. In such experiments, care must be taken to avoid introducing focus shift artifacts due to coverslip deformation under pressure. For relatively low pressures, increased thickness coverslips (#1.5 or greater) is often sufficient (Mandal et al. 2010), depending upon optical parameters. For high pressures, it may be necessary to decouple the cell layer from the pressure-retaining optical window to enable the use of stronger windows and to guarantee that cell responses to bending are not falsely attributed to HP.

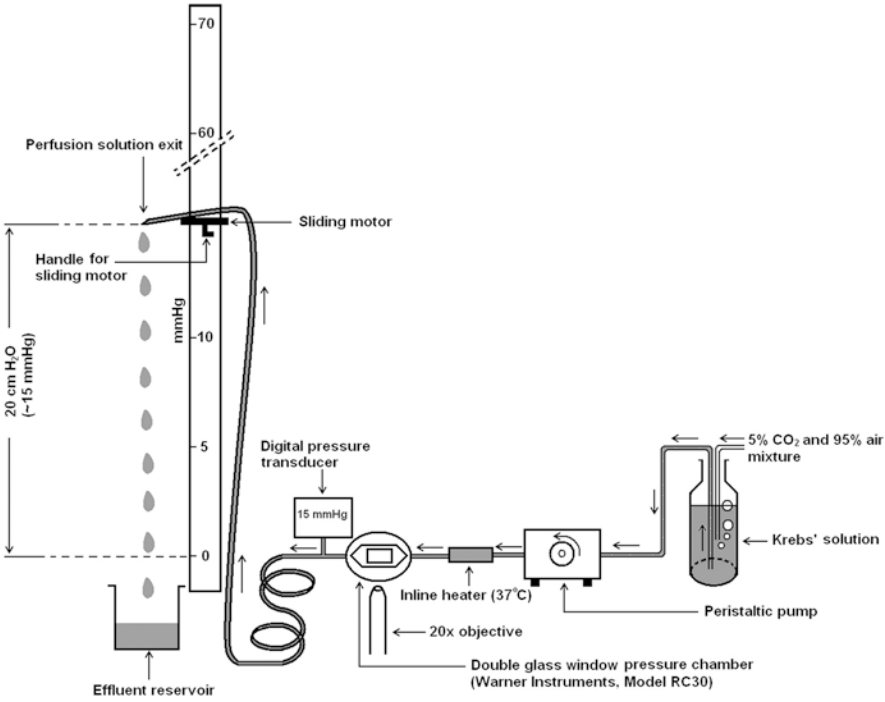

Fig. 9.2 Schematic diagram of HP application system. (Reprinted from Mandal et al. (2010) with permission)

The test configuration shown in Fig. 9.3, implemented by Mizuno (2005) demonstrates such a configuration, which uses a long working distance lens to image the cells while inverted above the pressure-containing optical window.

9.4 Potential Physical Mechanisms for Ion Channel Modulation by Hydrostatic Pressure

Provided that cells can be subjected to isolated hydrostatic pressure that elicits cellular/molecular responses as observed in numerous studies so far, in order to describe a cell as pressure sensitive, underlying physical mechanisms must be explained. As ion channels and transporters have been implicated in HP sensation in numerous cell types (Sect. 9.2), this section will outline a series of potential mechanisms by which relatively small pressures could yield electrophysiological responses, which would likely occur due to direct physical deformation, modified chemical reaction kinetics, or changes to lipid bilayer membrane properties.

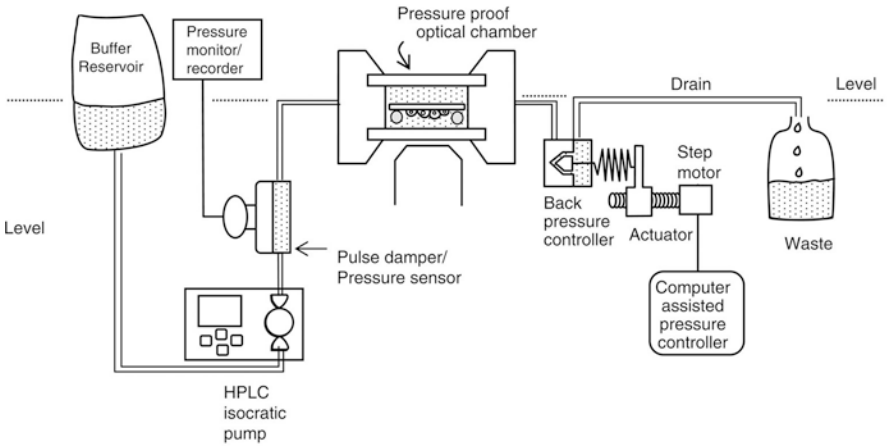

Fig. 9.3 Image acquisition system. Balanced salt solution (BSS) is injected into a pressure-proof chamber with an HPLC socratic pump. The hydrostatic pressure (HP) in the chamber is regulated with a needle valve attached to a spring and a computer-driven actuator. The chamber has sapphire glass windows (2 mm thick and 30 mm in diameter, 20-mm-diameter available optical field) and holds up to 10 MPa pressure. The coverslip was inverted and placed onto stainless steel suspension rails (0.5 mm thick) over the sapphire glass window in the chamber so that the cells opposed the sapphire glass window and faced the lens. Thus the cells were isolated from deformation of the sapphire glass during application of HP. (Reprinted from Mizuno (2005) with permission)

9.4.1 Physical Deformation

Perhaps the simplest potential mechanism for the sensation of hydrostatic pressure would involve direct cell membrane stretching, such as occurs with vascular endothelial cells due to blood pressure. Although endothelial cells would experience a small hydrostatic pressure increase as blood pressure increases due to the viscoelastic nature of blood vessels, this pressure would be quickly equalized with surrounding tissues through stretching of the vessel wall. Membrane stretch in vascular smooth muscle cells activates stretch-sensitive ion channels such as the transient receptor potential (TRP) channels, the amiloride-sensitive ENaC/ASIC channels and the potassium channels K_{2P} and K_{ir}, thereby contributing to the integrated myogenic response to changes in pressure (Folgering et al. 2008). Such a response is likely not associated with HP directly, which can cause confusion. Similar confusion is experienced when pressure is applied to the intracellular space by pressurization of the fluid within a patch clamp electrode, also causing the activation of stretch-activated ion channels (e.g. Kohler et al. 1998). This review only considers the sensation of hydrostatic pressure stimuli that do not cause observable membrane stretching.

Assuming a compressibility for erythrocytes of 4×10^{-10} Pa^{-1} (Shung et al. 1982), a 1 kPa load would produce a percent volume change of just 4×10^{-5} (Myers et al. 2007). Cells are therefore considered nearly incompressible, and it is unlikely that the direct bulk compression of the cell could be sensed. Alternatively, a related

theory states that differential compression of neighboring heterogeneous structures could cause detectible micro-strains which could activate ion channels (Macdonald and Fraser 1999). This could occur either between cells and substrates of differing stiffness or between intracellular components of differing compression moduli.

Direct conformational changes in membrane proteins such as ion channels due to hydrostatic pressure have been demonstrated for high pressures up to 100 MPa (Macdonald 2002), which directly modulate the gating of ion channels. However, such an effect has not been demonstrated for ion channels at small hydrostatic pressures of less than 20 kPa such as reviewed in this chapter (except for the chondrocyte experiments, which used pressures up to 50 MPa). Although such a conformation change is inherently a binary process that could be tuned to occur at a particular pressure level, local temperature variations and other uncontrolled effects would seem to make this an implausible sensing mechanism (Macdonald and Fraser 1999).

9.4.2 Modified Chemical Reaction Kinetics

Pressure is a variable in all chemical reactions that take place within the cell. A review by Myers et al. (2007) put forth a mechanism by which hydrostatic pressure may modulate the polymerization and depolymerization rates of cytoskeletal components, such as actin filaments and microtubules, thereby enabling a cellular mechanosensitive response. Indeed, studies have shown that high HP (4 or 70 MPa) can cause cytoskeletal disorganization and changes in cell shape (Haskin and Cameron 1993; Wilson et al. 2001). Changes in reaction rates for kinases, enzymes, etc. could have effects on cellular metabolism, protein expression, motility, apoptosis, or many other cellular processes. However, it is likely that with the small pressure levels considered here, some sort of a threshold effect or other amplification mechanism would be necessary to generate a discernible change due to reaction kinetics, which has not been demonstrated thus far.

9.4.3 Lipid Bilayer Membrane Properties

A lipid bilayer surrounds every cell and many intracellular compartments, providing chemical and electrical isolation, controlled passage of solutes, and anchoring locations for membrane bound proteins, among other functions. Membrane tension has been shown to mechanically gate certain stretch-sensitive ion channels (Hamill and Martinac 2001), and has been hypothesized to control endocytosis and exocytosis rates (Apodaca 2002). Membrane molecular order has been shown to increase when the membrane is exposed to increased hydrostatic pressure (or lower temperature) (Williams et al. 2001). Such increases in membrane order cause the lipid molecules of the membrane to become more closely packed, and thereby increase membrane tension (Winter et al. 2007), potentially activating stretch-activated ion channels.

Particularly interesting is the concept that pressure would reduce membrane fluidity in this way, raising the temperature of membrane phase transition from the gel state to the liquid crystalline state (Bravim et al. 2010). Such a phase transition could potentially provide increased sensitivity to very small pressure changes if properly tuned to the pressures of interest.

Rauch et al. (2010) recently presented a theoretical model of the control of the kinetics of fluid phase endocytosis (FPE) within cells and validated the model using published data for multiple, unique cellular phenomena. Using both thermodynamic and hydrodynamic modeling, the kinetics of FPE are shown to not be dependent upon membrane tension, but instead be modulated by membrane lipid number asymmetry and cytosolic hydrostatic pressure. Increasing the environmental HP or osmotic pressure was shown to favor exocytosis, which could potentially provide a sensing mechanism through autocrine signaling, ion channel trafficking, or membrane composition modification.

9.5 Conclusion and Perspectives

The lack of success thus far in identifying a single hydrostatic pressure-sensitive protein structure or complex, such as an ion channel, implies that the mechanosensation process of HP is likely a multifaceted process that exploits an unconventional sensing mechanism. Numerous studies have demonstrated downstream effects including altered gene expression, proliferation, and apoptosis rates. However, relatively few experiments have been performed to investigate the underlying mechanism responsible for the sensation of HP by cells. Thus far, most of these experiments have implicated ion channels or transporters, particularly members of the TRP and ENaC channel families. Interruption of particular stages of the pressure signaling cascade has been achieved, and indeed therapeutic drugs that affect ion channel function are clinically administered, but the fundamental mechanical transduction process involved in HP sensation remains to be discovered.

References

Apodaca G (2002) Modulation of membrane traffic by mechanical stimuli. Am J Physiol-Renal Physiol 282:F179-F190

Apodaca G, Balestreire E, Birder LA (2007) The Uroepithelial-associated sensory web. Kidney Int 72:1057–1064

Araki I, Du S, Kobayashi H, Sawada N, Mochizuki T, Zakoji H, Takeda M (2008) Roles of mechanosensitive ion channels in bladder sensory transduction and overactive bladder. Int J Urol 15:681–687

Arnold S, Vargas SL, Toma I, Hanner F, Willecke K, Janos PP (2009) Connexin 30 deficiency impairs renal tubular ATP release and pressure natriuresis. J Am Soc Nephrol 20:1724–1732

Birder LA (2005) More than just a barrier: urothelium as a drug target for urinary bladder pain. Am J Physiol-Renal Physiol 289:F489-F495

Bohmer A, Dillier N (1990) Experimental endolymphatic hydrops: are cochlear and vestibular symptoms caused by increased endolymphatic pressure? Ann Otol Rhinol Laryngol 99:470–476

Bravim F, de Freitas JM, Fernandes AAR, Fernandes PMB (2010) High hydrostatic pressure and the cell membrane Stress response of Saccharomyces cerevisiae. AnnNY AcadSci 1189:127–132

Browning JA, Walker RE, Hall AC, Wilkins RJ (1999) Modulation of Na^+ x H^+ exchange by hydrostatic pressure in isolated bovine articular chondrocytes. Acta Physiol Scand 166:39–45

Browning JA, Saunders K, Urban JPG, Wilkins RJ (2004) The influence and interactions of hydrostatic and osmotic pressures on the intracellular milieu of chondrocytes. Biorheology 41:299–308

Chen JH, Liu C, You LD, Simmons CA (2010) Boning up on Wolff's Law: Mechanical regulation of the cells that make and maintain bone. J Biomech 43:108–118

Courteix D, Lespessailles E, Peres SL, Obert P, Germain P, Benhamou CL (1998) Effect of physical training on bone mineral density in prepubertal girls: A comparative study between impact-loading and non-impact-loading sports. Osteoporosis Int 8:152–158

de Groat WC (2004) The urothelium in overactive bladder: Passive bystander or active participant? Urology 64:7–11

Downie JW, Armour JA (1992) Mechanoreceptor afferent activity compared with receptor field dimensions and pressure changes in feline urinary bladder. Can J Physiol Pharmacol 70:1457–1467

Drumm MR, York B, D, Nagatomi J (2010) Effect of Sustained Hydrostatic Pressure on Rat Bladder Smooth Muscle Cell Function. Urology 75:879–885

Düwel P, Jungling E, Westhofen M, Luckhoff A (2003) Potassium currents in vestibular type II hair cells activated by hydrostatic pressure. Neuroscience 116:963–972

Düwel P, Haasler T, Jungling E, Duong TA, Westhofen M, Luckhoff A (2005) Effects of cinnarizine on calcium and pressure-dependent potassium currents in guinea pig vestibular hair cells. Naunyn-Schmiedebergs Arch Pharmacol 371:441–448

Elder BD and Athanasiou KA (2009) Hydrostatic Pressure in Articular Cartilage Tissue Engineering: From Chondrocytes to Tissue Regeneration. Tissue Eng Part B-Rev 15:43–53

Everaerts W, Vriens J, Owsianik G, Appendino G, Voets T, De Ridder D, Nilius B (2010) Functional characterization of transient receptor potential channels in mouse urothelial cells. AJP—Renal Physiology 298:F692–F701

Ferguson DR, Kennedy I, Burton TJ (1997) ATP is released from rabbit urinary bladder epithelial cells by hydrostatic pressure changes—a possible sensory mechanism? J Physiol-London 505:503–511

Folgering JHA, Sharif-Naeini R, Dedman A, Patel A, Delmas P, Honore E (2008) Molecular basis of the mammalian pressure-sensitive ion channels: Focus on vascular mechanotransduction. Progress in Biophysics and Molecular Biology 97:180–195

Gomis A, Soriano S, Belmonte C, Viana F (2008) Hypoosmotic- and pressure-induced membrane stretch activate TRPC5 channels. J Physiol-London 586:5633–5649

Grad S, Eglin D, Alini M, Stoddart MJ (2011) Physical stimulation of chondrogenic cells In Vitro: A Review. Clin Orthop Rel Res 469:2764–2772

Haasler T, Homann G, Dinh TAD, Jungling E, Westhofen M, Luckhoff A (2009) Pharmacological modulation of transmitter release by inhibition of pressure-dependent potassium currents in vestibular hair cells. Naunyn-Schmiedebergs Arch Pharmacol 380:531–538

Haberstroh KM, Kaefer M, Retik AB, Freeman MR, Bizios R (1999) The effects of sustained hydrostatic-pressure on select bladder smooth muscle cell functions. J Urol 162:2114–2118

Hall AC (1999) Differential effects of hydrostatic pressure on cation transport pathways of isolated articular chondrocytes. J Cell Physiol 178:197–204

Hamill OP, Martinac B (2001) Molecular basis of mechanotransduction in living cells. Physiol Rev 81:685–740

Haskin C, Cameron I (1993) Physiological levels of hydrostatic pressure alter morphology and organization of cytoskeletal and adhesion proteins in MG-63 osteosarcoma cells. Biochem Cell Biol 71:27–35

Hodge WA, Fijan RS, Carlson KL, Burgess RG, Harris WH, Mann RW (1986) Contact pressures in the human hip joint measured in vivo. Proc Natl Acad Sci U S A 83:2879–2883
Huang Y, Haas C, Ghadiali SN (2010) Influence of Transmural Pressure and Cytoskeletal Structure on NF-kappa B Activation in Respiratory Epithelial Cells. Cell Mol Bioeng 3:415–427
Iggo A (1955) Tension receptors in the stomach and the urinary bladder. The Journal of Physiology 128:593–607
Ishihara H, McNally DS, Urban JPG, Hall AC (1996) Effects of hydrostatic pressure on matrix synthesis in different regions of the intervertebral disk. J Appl Physiol 80:839–846
Kashlan OB, Kleyman TR (2011) ENaC structure and function in the wake of a resolved structure of a family member. Am J Physiol-Renal Physiol 301:F684-F696
Kohler R, Distler A, Hoyer J (1998) Pressure-activated cation channel in intact rat endocardial endothelium. Cardiovasc Res 38:433–440
Krolner B, Toft B, Nielsen SP, Tondevold E (1983) Physical exercise as prophylaxis against involutional vertebral bone loss: a controlled trial. Clin Sci 64:541–546
Kumar V, Abbas AK, Fausto N (2005) Robbins and cotran pathologic basis of disease. Seventh edition. Elsevier Saunders
Kwon YH, Fingert JH, Kuehn MH, Alward WLM (2009) Mechanisms of Disease: Primary Open-Angle Glaucoma. N Engl J Med 360:1113–1124
Leblanc AD, Schneider VS, Evans HJ, Engelbretson DA, Krebs JM (1990) Bone mineral loss and recovery after 17 weeks of bed rest. J Bone Miner Res 5:843–850
Lei Y, Rajabi S, Pedrigi RM, Overby DR, Read AT, Ethier CR (2011) In Vitro Models for Glaucoma Research: Effects of Hydrostatic Pressure. Invest Ophthalmol Vis Sci 52:6329–6339
Liu C, Zhao Y, Cheung WY, Gandhi R, Wang LY, You LD (2010) Effects of cyclic hydraulic pressure on osteocytes. Bone 46:1449–1456
Macdonald AG (2002) Ion channels under high pressure. Comp Biochem Physiol A-Mol Integr Physiol 131:587–593
Macdonald AG, Fraser PJ (1999) The transduction of very small hydrostatic pressures. Comp Biochem Physiol A-Mol Integr Physiol 122:13–36
Mandal A, Shahidullah M, Delamere NA, Teran MA (2009) Elevated hydrostatic pressure activates sodium/hydrogen exchanger-1 in rat optic nerve head astrocytes. Am J Physiol-Cell Physiol 297:C111–C120
Mandal A, Shahidullah M, Delamere NA (2010) Hydrostatic Pressure-Induced Release of Stored Calcium in Cultured Rat Optic Nerve Head Astrocytes. Invest Ophthalmol Vis Sci 51:3129–3138
Mizuno S (2005) A novel method for assessing effects of hydrostatic fluid pressure on intracellular calcium: a study with bovine articular chondrocytes. Am J Physiol-Cell Physiol 288:C329–C337
Morrison J (1999) The activation of bladder wall afferent nerves. Exp Physiol 84:131–136
Moss NG, Harrington WW, Tucker MS (1997) Pressure, volume, and chemosensitivity in afferent innervation of urinary bladder in rats. Am J Physiol-Regul Integr Comp Physiol 272:R695-R703
Myers KA, Rattner JB, Shrive NG, Hart DA (2007) Hydrostatic pressure sensation in cells: integration into the tensegrity model. Biochem Cell Biol 85:543–551
Nagatomi J, Arulanandam BP, Metzger DW, Meunier A, Bizios R (2001) Frequency- and duration-dependent effects of cyclic pressure on select bone cell functions. Tissue Eng 7:717–728
Nagatomi J, Arulanandam BP, Metzger DW, Meunier A, Bizios R (2002) Effects of cyclic pressure on bone marrow cell cultures. J Biomech Eng-Trans ASME 124:308–314
Nagatomi J, Arulanandam BR, Metzger DW, Meunier A, Bizios R (2003) Cyclic pressure affects osteoblast functions pertinent to osteogenesis. Ann Biomed Eng 31:917–923
Nagatomi J, Wu YN, Gray M (2009) Proteomic analysis of bladder smooth muscle cell response to cyclic hydrostatic pressure. Cell Mol Bioeng 2:166–173
Ohashi T, Sugaya Y, Sakamoto N, Sato M (2007) Hydrostatic pressure influences morphology and expression of VE-cadherin of vascular endothelial cells. J Biomech 40:2399–2405
Olsen SM, Stover JD, Nagatomi J (2011) Examining the role of mechanosensitive ion channels in pressure mechanotransduction in rat bladder urothelial cells. Ann Biomed Eng 39:688–697

Rauch C, Pluen A, Foster N, Loughna P, Mobasheri A, Lagadic-Gossmann D, Counillon L (2010) On some aspects of the thermodynamic of membrane recycling mediated by fluid phase endocytosis: Evaluation of published data and perspectives. Cell Biochem Biophys 56:73–90

Sappington RM, Calkins DJ (2008) Contribution of TRPV1 to microglia-derived IL-6 and NF kappa B translocation with elevated hydrostatic pressure. Invest Ophthalmol Vis Sci 49:3004–3017

Sappington RM, Sidorova T, Long DJ, Calkins DJ (2009) TRPV1: Contribution to Retinal Ganglion Cell Apoptosis and Increased Intracellular Ca_2^+ with Exposure to Hydrostatic Pressure. Invest Ophthalmol Vis Sci 50:717–728

Shea VK, Cai R, Crepps B, Mason JL, Perl ER (2000) Sensory fibers of the pelvic nerve innervating the rat's urinary bladder. J Neurophysiol 84:1924–1933

Shung KK, Krisko BA, Ballard JO (1982) Acoustic measurement of erythrocyte compressibility. J Acoust Soc Am 72:1364–1367

Stover J, Nagatomi J (2007) Cyclic pressure stimulates DNA synthesis through the PI3 K/Akt signaling pathway in rat bladder smooth muscle cells. Ann Biomed Eng 35:1585–1594

Venkatachalam K, Montell C (2007) TRP channels. Annu Rev Biochem 76:387–417

Wang ECY, Lee JM, Ruiz WG, Balestreire EM, von Bodungen M, Barrick S, Cockayne DA, Birder LA, Apodaca G (2005) ATP and purinergic receptor-dependent membrane traffic in bladder umbrella cells. J Clin Invest 115:2412–2422

Williams EE, Stewart BS, Beuchat CA, Somero GN, Hazel JR (2001) Hydrostatic-pressure and temperature effects on the molecular order of erythrocyte membranes from deep-, shallow-, and non-diving mammals. Can J Zool-Rev Can Zool 79:888–894

Wilson RG, Trogadis JE, Zimmerman S, Zimmerman AM (2001) Hydrostatic pressure induced changes in the cytoarchitecture of pheochromocytoma (PC-12) cells. Cell Biol Int 25:649–666

Winter R, Lopes D, Grudzielanek S, Vogtt K (2007) Towards an understanding of the temperature/pressure configurational and free-energy landscape of biomolecules. J Non-Equilib Thermodyn 32:41–97

Yoshimura N, Kaiho Y, Miyazato M, Yunoki T, Tai CF, Chancellor MB, Tyagi P (2008) Therapeutic receptor targets for lower urinary tract dysfunction. Springer 437–448

Yu WQ, Khandelwal P, Apodaca G (2009) Distinct apical and basolateral membrane requirements for stretch-induced membrane traffic at the apical surface of bladder umbrella cells. Mol Biol Cell 20:282–295

Zagorodnyuk VP, Costa M, Brookes SJH (2006) Major classes of sensory neurons to the urinary bladder. Auton Neurosci-Basic Clin 126:390–397

Zerwekh JE, Ruml LA, Gottschalk F, Pak CYC (1998) The effects of twelve weeks of bed rest on bone histology, biochemical markers of bone turnover, and calcium homeostasis in eleven normal subjects. J Bone Miner Res 13:1594–1601

Chapter 10
Lipid-Mediated Mechanisms Involved in the Mechanical Activation of TRPC6 and TRPV4 Channels in the Vascular Tone Regulation

Ryuji Inoue, Yaopeng Hu, Yubin Duan and Kyohei Itsuki

10.1 Introduction

The circulatory system composed of the heart and blood vessels is constantly exposed to various forms of mechanical stresses such as blood pressure/flow, osmotic change, and direct deformation synchronized with the periodic cardiac contraction-relaxation cycle. There is now mounting evidence that these mechanical stimuli may be of essential significance to activate or modify the contractility, excitability, Ca^{2+} handling and metabolism of cells comprising the circulatory system (i.e. vascular smooth muscle and endothelial cells: dubbed as VSMCs and VECs respectively; cardiomyocytes and cardiac fibroblasts: dubbed as CMs and CFs, respectively) and actively participate in short- and long-term regulations of cardiovascular (CV) functions. There are many such well-characterized examples including the Frank-Starling mechanism, Bayliss effect (myogenic response), baroreceptor reflex and other circulatory reflexes, and the release of neurohormonal factors (e.g. renin, atrial natriuretic peptide, nitric oxide). These not only exert immediate hemodynamic effects on the CV system (CVS), but also alter the performance of CVS via changes in blood volume and osmolarity, as well as via long-term adaptive changes by the remodeling of CV tissues. It has been speculated that disruption of these regulations may lead to pathological conditions such as hypertension, arteriosclerosis, vasospasm, and cardiac hypertrophy (Johnson et al. 2008; Davis and Hill 1999; Heineke and Molkentin 2006; Davis 2009). Recent investigations have suggested that many of such mechanical responses in CVS may involve Ca^{2+} mobilization tightly associated with the transient receptor potential (TRP) proteins, a large cation channel family which belongs to the six membrane-spanning, voltage-dependent cation channel superfamily (Inoue et al. 2009b; Yin and Kuebler 2010).

TRP channels form a large non-voltage-gated nonselective cation channel (NSCC) family which shows diverse activation/regulation profiles. Their human

R. Inoue (✉) · Y. Hu · Y. Duan · K. Itsuki
Department of Physiology, Graduate School of Medical Sciences, Fukuoka University, Fukuoka 814-0180, Japan
e-mail: inouery@fukuoka-u.ac.jp

A. Kamkin, I. Lozinsky (eds.), *Mechanically Gated Channels and their Regulation,* Mechanosensitivity in Cells and Tissues 6,
DOI 10.1007/978-94-007-5073-9_10, © Springer Science+Business Media Dordrecht 2012

isoforms are classified into six subfamilies, i.e. TRPC1–7 (canonical or classical), TRPV1–6 (vanilloid), TRPM1–8 (melastatin), TRPP1–4 (polycystin), TRPML1–3 (mucolipin), and TRPA1 (ankyrin) (Ramsey et al. 2006; Flockerzi 2007). In general, TRPCs act as Ca^{2+}-permeable cation channels activated by diacylglycerol (DAG) and/or store-depletion upon stimulation of phospholipase C (PLC)-coupled receptors. In contrast, TRPV1–4, TRPM2–3, TRPM7–8, and TRPA1 act as physically- or chemically-activated NSCCs which are responsive to pungent, cooling and gustatory agents, membrane lipids, acidity, heat/cold, membrane stretch/shear stress, hyperosmolarity/hypoosmolarity, and ischemia/oxidative stress. The other TRPVs and TRPMs are constitutively activated (TRPV5, V6, M6, M7) or activated directly by an elevated $[Ca^{2+}]_i$ (TRPM4, M5), but also modulated by PLC-coupled receptor stimulation. Many of TRP channels show the polymodality of activation/modulation being responsive to several distinct stimuli (Ramsey 2006; Flockerzi 2007). In CVS, more than ten TRP members have been identified and implicated in a variety of CV functions and dysfunctions (Inoue et al. 2006; Watanabe et al. 2008; Yin and Kuebler 2010).

Although there is no direct proof yet, the majority of native mechanosensive (MS) channels involved in Ca^{2+} mobilization in the CVS share similarities with TRP channels expressed therein (Inoue et al. 2009b). Further, the activation/modulation of TRP channels seems intimately associated with membrane lipid mechanics and metabolism (Meves 2008; Suh and Hille 2008; Raghu and Hardie 2009; Lundbaek et al. 2010a). In the following, we therefore focus on the mechanical regulation of TRP channels in CVS particularly in terms of membrane lipid mediators, after introducing some general concepts about the mechanism for mechanical signal transduction and lipid-mediated regulation.

10.2 Diversity of Mechanical Signal Transduction

The strategies by which a cell can sense, transmit and transduce mechanical stimuli appear to have emerged in a very early stage of evolution. We can find such primitive cases in bacteria and archaea as MS channels which operate as a safety valve to release the osmolites in response to a sudden drop in environmental osmolarity (Martinac and Kloda 2003). In higher organisms which possess the cytoskeleton, more elaborated micro-architectures consisting of many mechanosensing/transducing molecules are organized so as to respond to more generalized forms of mechanical stimuli, e.g. compression, retraction, bending, torsion, and shear whereby to exert more complex biological functions.

In general, the mechanisms for mechanical signal transduction can be classified into several different categories depending on the timescale, mode and complexity of its operation (Inoue et al. 2009a, b);

- bilayer-dependent mechanism
- tethered mechanism
- mechanobiochemical conversion

- facilitated membrane trafficking
- enhanced gene transcription

The first one is the simplest and fastest form of mechanotransduction and is purely dependent on the cell membrane lipid bilayer. A typical exemplar is found for MS channels in *E. coli* and archaea, which are gated directly, even when reconstituted in artificial liposome, by changes in the bilayer deformation energy (**bilayer-dependent mechanism**; Sukharev et al. 1993; Corry and Martinac 2008). Because of the absence of intervening processes, the activation kinetics of MS channels by altered bilayer mechanics is as fast as micro- to milli-seconds. The mechanism for this type of fast mechanosensation/transduction has been most intensively investigated in prokaryotic MscL and MscS channels. By means of EPR spectroscopy with site-directed spin labeling, molecular dynamic simulation and statistical calculations, it is postulated that hydrophobic mismatch at the boundary of lipid bilayer and channel protein produced by membrane deformation (thinning, bending, altered elastic properties, etc.) causes conformational movements of channel gating apparatus, leading to the opening of the channels. In case of MscL, this occurs as a radial, iris-like broadening of a narrow constriction gate via increased tilt of pore-forming TM domains (Perozo et al. 2002; Corry and Martinac 2008). In vertebrates, many MS cation channels (MSCCs) with as-yet unidentified molecular entities have been recorded from acutely isolated CMs, VSMCs, and VECs and found to be activated on a millisecond scale (for review, Inoue et al. 2009b; Nilius et al. 2001). Although controversial (Dietrich et al. 2005; Gottlieb et al. 2008), some of expressed canonical transient receptor potential (TRP) channels (TRPC1 and TRPC6) may be (Maroto et al. 2005; Spassova et al. 2006), and more convincingly, two-pore domain K^+ channels (TREK-1, TAAK; Dedman et al. 2009), DEC/ENAC/ASICs family members (Drummond et al. 2008), and Piezo 1/2 (Coste et al. 2010), can be assigned to this category of MSCCs. Interestingly, many of these vertebrate MSCCs have been reported to be inhibited by an amphipathic *tarantula* venom peptide GsMTx-4, which has been suggested to directly act on the bilayer thereby changing its tension profile and elastic properties (Suchyna et al. 2000; Maroto et al. 2005; Spassova et al. 2006; Buxton et al. 2010; Bae et al. 2011). In contrast, GsMTx-4 has been reported to activate cold-sensing TRPA1 channel probably in a bilayer-mediated manner (Hill and Schaefer 2007).

In vertebrate audio-vestibular hair cells, there is a specialized tethered structure called 'tip-links'. This structure is believed to transduce the acoustic vibrations or head movements into electrical signals via the strength-dependent deflection (or resultant tension) of elastic stereocilia which then activates NSCCs (**tethered mechanism**). A similar tethered mechanism also appears to operate in *Drosophila*'s bristle and nematode's touch sensations (Tavernarakis and Driscoll 1997; Hamill and Martinac 2001; Christensen and Corey 2007). In the latter, it has been shown that several distinct *mec* genes encoding the extracellular matrix, transduction channel, intracellular scaffold and their linkers are indispensable for normal mechanotransduction, in which the deflective force is transmitted through intervening intracellular linkers (e.g. filamentous actin) to NSCCs (Tavernarakis and Driscoll 1997; Hamill and Martinac 2001). The molecular correlates of these MSCCs were originally

proposed to be TRPN1 and TRPA1 respectively. These TRP channels possess extraordinarily many ankyrin-like repeats on their N-termini that may enable the coupling of transduction channel to cytoskeleton. However, studies using loss-of function mutations or genetic deletion of these MSCC candidates do not support the obligatory involvement of these molecules (Christensen and Corey 2007). Other examples of the tethered MSCC model includes the renal epithelial TRPP2 channel, which physically interacts with TRPP1 and cytoskeletal components such as Hax-1, CD2AP, troponin I, tropomyosin-1, KIF3, mDia1, and α-actinin to form a mechanotransduction complex transmitting the displacing movement of primary cilia by fluid flow (Witzgall 2007; Chen et al. 2008); and the glomerular slit diaphragm TRPC6 channel which is physically associated with a putative mechanosensor podocin (Huber et al. 2006; Moller et al. 2009) and clustered with many slit diaphragm proteins such as nephrin, NEPH-1 CD2AP, ZO-1 and actin-associated cytoskeletal proteins (Lowik et al. 2009). Although there is still no compelling evidence to directly link them to mechanotransduction, the genetic mutations or impaired functions of these proteins are known to disrupt the glomerular 'filtration barrier' function and cause progressive proteinuric glomerulosclerosic diseases (Dietrich et al. 2010).

In higher organisms than bacteria, a dynamic and complex submembranous network of protein filaments (actin, microtubules, intermediate filaments) called the cytoskeleton exists, which provides mechanical support for the cell and also enables cell shape changes during division and migration. The intracellular network of cytoskeleton is a specialized framework which communicates with extracellular matrix via transmembrane proteins called integrins at focal contacts. It has been proposed that such cellular framework may serve as a pre-tensed architecture ('tensegrity' model; Ingber 2008) and is linked to intracellular signaling thereby converting the external mechanical forces into biochemical information (**mechanobiochemical conversion**). There are numerous reports that various forms of mechanical stimuli can activate cell surface receptors, G-proteins, or intracellular enzymes including adenylyl cyclase, protein kinase A (PKA), mitogen-activated protein kinases (MAPKs), non-receptor tyrosine kinase, thereby modulating ion channel activities (e.g. Martinez-Lemus et al. 2003; Hughes-Fulford 2004). For instance, the mechanical activation of $\alpha_4\beta_1$ and $\alpha_5\beta_1$ integrin-mediated pathways in VSMCs potentiate voltage-dependent Ca^{2+} channels via activation of Src and PKA producing vasoconstriction (Martinez-Lemus et al. 2003). In other cases, mechanical stimuli can more directly activate cell membrane-associated enzymes such as PLC and phospholipase A_2 (PLA_2) to generate functionally active lipid mediators, e.g. diacylglycerol (DAG) and arachidonic acid (AA). These lipid mediators then act directly or are further metabolized to modify a variety of cellular functions. The *Drosophila* TRP channels and many of mammalian TRP channels (e.g. TRPC subfamily, TRPV1/V4, TRPM2/M7/M8) likely undergo this type of regulation (see below). In addition to these, there is substantial evidence that mechanical stimuli facilitate the membrane insertion (**facilitated membrane trafficking**) or transcriptionally upregulate the expression (**enhanced gene transcription**) of many membrane proteins including TRP channels (Kanzaki et al. 1999; Guinamard et al. 2006; Oancea et al. 2006; Dalrymple et al. 2007; Fleming et al. 2007).

Table 10.1 Activation mechanisms for mechanosensitive TRPs in CVS. (Information derived from Inoue et al. (2009a). *nd*; not determined. *GPCR*: PLC- and $G_{q/11}$-protein-coupled receptor. For other abbreviations, see the text.)

	Distribution	Mode of mechanotransduction				
		Bilayer	Tethered	Mechanobiochemical	Trafficking	Transcription
TRPC1	CM, VEC, VSMC	Yes?	nd	nd	nd	Yes?
TRPC6	VEC, CM, CF, VSMC	Yes?	Yes (podocin?)	GPCR/PLC/DAG PLA_2/ω -hydroxylase/20-HETE	Yes	nd
TRPV1	Sensory n., VEC	nd	nd	Mediated by LOX-12 metabolites?, 20-HETE?	nd	nd
TRPV2	CM, VSMC	nd	nd	?	Yes	nd
TRPV4	CM, VEC, VSMC	nd	Yes (MAP7?)	PLA_2/epoxygenase/ 5′,6′-EET	nd	Yes?
TRPM7	CM,VEC, CF, VSMC	Yes?	nd	nd	Yes	nd
TRPP2	CM, VEC, VSMC	nd	Yes (TRPP1)	nd	nd	nd

Table 10.1 categorizes mechanically stimulated Ca^{2+} influx associated with several TRP isoforms in CVS in light of the above-mentioned mechanisms. It is noteworthy that the same TRP channel is often regulated at multiple levels of mechanotransduction, i.e. lipid bilayer, cytoskeletal dynamics, lipid mediators, membrane trafficking and gene transcription. This diversity of regulation is the characteristic features of mechanically-induced Ca^{2+} mobilization in CVS, and seemingly matches up with the promiscuous features of TRP channel activation intricately associated with membrane lipid mechanics and metabolism. In the next section, we will therefore see briefly what is generally known about lipid-mediated regulation of ion channels to gain more precise insight therein.

10.3 Mechanisms for the Lipid-Mediated Regulation of Ion Channels

Tight regulation of ion channels by membrane lipids is an emerging theme to understand their activation and inactivation kinetics and sensitivity to gating modification (Hilgemann et al. 2001; Meves 2008; Falkenburger et al. 2010). Particularly, phosphoinositide phosphates (PIPs) such as phosphatidylinositol 4,5-bisphosphate (PIP_2) and its metabolites by PLC, as well as PLA_2-related membrane phospholipid metabolites (i.e. AA and its metabolites), seem to play central roles in the regulation of TRP channel gating and functions. Several mammalian TRPC subfamily members (TRPC2, TRPC3/C6/C7) and the archetypal *Drosophila* TRP channels can be

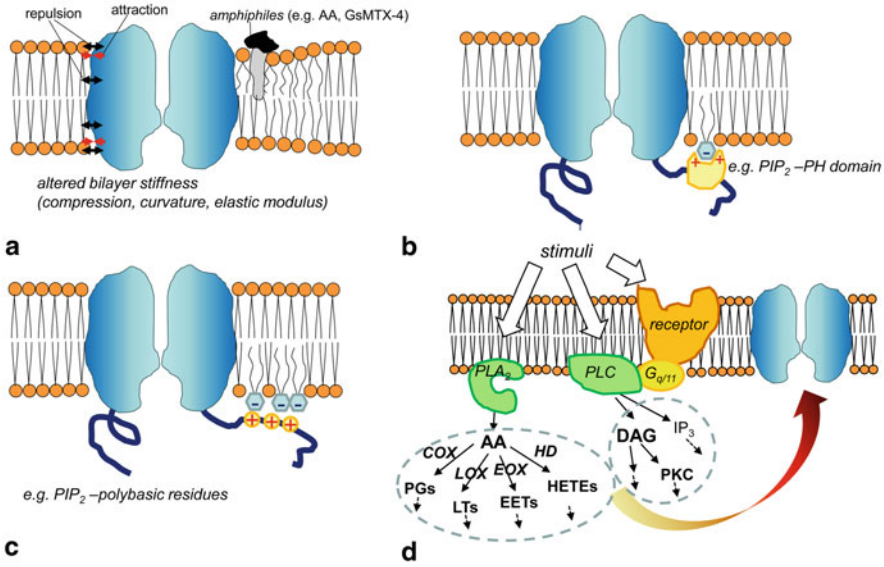

Fig. 10.1 Four representative mechanisms for lipid-mediated ion channel regulations. **a** 'bilayer-mediated'. **b** 'ligand-receotor' interaction. **c** 'electrostatic' interaction. **d** 'metabolization' or 'signaling'-mediated. Abbreviations not appearing in the text; *COX*: cyclooxygenase; *PGs*: prostaglandins; *LOX*: lipooxygenase; *LTs*: leucotriens; *EOX*: epoxygenase; *EETs*: epoxye-icosatrienoic acids; *HD*: ω-hydroxylase: *HETEs*: hydroxyeicosatetraenoic acids. For explanation, refer to the text

activated by DAG or its potential metabolites including AA and other poly- and mono-unsaturated fatty acids (linolenic, linoleic and oleic acids) (Putney 2007; Raghu and Hardie 2009). These effects do not need the activation of protein kinase C or further metabolization, thus probably being direct on channel gating. There is also increasing evidence that PIP_2 itself may have direct regulatory effects on many types of ion channels including TRP channels (Hilgemann 2001; Hille et al. 2008; Falkenburger et al. 2010). Similarly, AA and its metabolites generated through the lipooxygenase, cyclooxygenase, and cytochrome P450 pathways have been reported to exert effects on TRP channel gating (Meves 2008).

The mechanisms underlying such lipid actions can be summarized into at least four categories (Fig. 10.1); bilayer-mediated, ligand-receptor interaction, electrostatic interaction and metabolization- or signaling-mediated mechanisms.

10.3.1 Bilayer-Mediated Mechanism

Figure 10.1a demonstrates bilayer-mediated mechanism. By investigating the dis-joining kinetics of gramicidin channel monomers as a measure for the changes in the lipid bilayer elastic energy, many amphipathic membrane lipids such as AA, lysophosphatidylcholine, docosahexaenoic acid, oleic acid, eicosapentaenoic acid

have been shown to be reversibly absorbed in the bilayer membrane thereby being capable of changing the bilayer stiffness (Lundbaek et al. 2010a, b). Strikingly, many of them (e.g., AA, oleic acid, docosahexaenoic acid) are found to affect, at their concentrations to alter the bilayer stiffness; the activation/inactivation of voltage-dependent Na^+ and Ca^{2+} (N-type) and K^+ channels and large conductance Ca^{2+}-dependent K^+ channel; the desensitization of nicotinic ACh receptor channel and the ligand binding of $GABA_A$ receptor channel (Lundbaek et al. 2010a). These actions appear clearly different from the classical 'key and lock' or 'ligand and receptor' interaction, and thus may represent nonspecific but rather commonly occurring actions of membrane lipids on channel gating. There is no rigorous proof yet, but the effects of membrane lipids and an amphipathic neurotoxin GsMTx-4 on several TRP channels likely occur through this mechanism (see above). Of note, cholesterol which has been thought to increase the membrane rigidity, has indeed proved to increase the bilayer stiffness by using the gramicidin-based bilayer elastic energy measurement (Lundbaek et al. 2010a). Interestingly, the 'ionotropic' activation of TRPM3 channel by neurosteroids has been reported to be greatly enhanced by the depletion of cholesterol, which is counteracted by the exogenous application of cholesterol (Naylor et al. 2010). This might also involve the bilayer-mediated mechanism.

Although it is still uncertain, recent investigations have proposed that certain membrane-derived lipids such as linoleic acid may alleviate the intrinsic voltage-dependent inhibition (note: the authors describe this phenomenon as the relief of 'open channel block'), thereby increasing the activity of several TRP channels (*Drosophila* TRP and TRPL, TRPV3) presumably via bilayer-mediated mechanism (Parnas et al. 2009a, b).

10.3.2 Ligand-Receptor and Electrostatic Interactions

Figure 10.1b, c demonstrates ligand-receptor and electrostatic interactions. In stark contrast with the bilayer absorbing effects of lipids on ion channels, the interaction with PIPs appears more direct in that it requires specific or nonspecific binding to target proteins. The typical example of the former is the pleckstrin homology (PH) domain, which is found in many cyoplasmic signaling proteins including PLC. The PH domain consists of positively charged amino acid residues in a binding pocket that are positioned so as to optimize the interaction with the phosphorylated head groups of PIPs. This type of structure is a kind of 'ligand-receptor' interaction and may provide the specificity over different PIPs molecules. On the other hand, proteins bearing a long stretch of clustered polybasic residues can nonspecifically binds the acidic head groups of multiple PIPs molecules. The MARCKS (myristoylated alanine-rich C kinase substrate) protein is representative for this type of binding, which sequestrates PIP_2 in the inner bilayer leaflet when not phosphorylated by PKC or interacting with calmodulin (Suh and Hille 2008). Both specific binding via structured domains and nonspecific binding via clustered polybasic residues seem important for channels showing PIPs-sensitivity such as inward rectifying K^+

and TRP channels. A recent crystallographic study of Kir2.2 inward-rectifying K^+ channel revealed that binding of PIP_2 through both specific and nonspecific interactions with the transmembrane and cytoplasmic domains of the channel is essential for its opening (Hansen and MacKinnon 2011). Although controversial, PIP_2-mediated potentiation of TRPV1 is shown to be associated with its proximal C-terminal region containing polybasic amino acid residues (Ufret-Vincenty et al. 2011), whereas a study on TRPM8 has proposed that the very proximal C-terminal 'TRP-domain' may serve as a general PIP_2-binding pocket in TRP channels (Rohacs et al. 2005).

As for other membrane lipids, there is considerable paucity of information. However, a recent bioinformatic approach with the GDDA-BLAST tool has proposed a specific DAG-binding region (TRP_2) on the proximal N-terminus of TRPC3 channel, which is crucial for the functional expression of the channel protein (van Rossum et al. 2008). It has been proposed that positive regulation of TRPM2 channel by AA may be mediated by its specific binding domain on N-terminus (AA-responsive sequence: ARS) which is also requisite for the response to H_2O_2 (Hara et al. 2002).

10.3.3 Metabolization or Signaling-Mediated Mechanism

Figure 10.1d demonstrates metabolization or signaling-mediated mechanism. Many lipid-mediated regulations involve the multi-step activation of metabolizing and/or signaling molecules such as enzymes and adaptor/signaling proteins. A well-known example is the AA cascade, in which three biologically important lipid metabolites, i.e. prostaglandins/thromboxanes, leucotrienes, eicosatrienoic acids/hyroxyeicosatetraenoic acids, are further generated by cyclooxygenase, lipooxygenase, and cytochrome P450 enzymes. The classical pathway of PLC-mediated PIP_2 metabolization is to generate IP_3 and DAG, but there is a bypass to generate AA from DAG via DAG kinase and lipase. The consequences of the generation of these membrane lipid-derived second messengers are diverse, ranging from the direct activation/modulation of downstream effector proteins (e.g. IP_3 receptor, PKC, ion channels) to the sequential activation of enzymes (e.g. PI3 K/Akt/eNOS, MAPK cascade) which in most cases leads to the induction of transcriptional, translational and trafficking activities.

The considerations so far strongly suggest that the mechanisms of mechanotransduction intimately involve membrane lipid dynamics and metabolism, which have great influences on the regulation of TRP channel gating. This means that lipid-mediated regulation may be a general paradigm accounting for mechanical activation and resultant functions of many TRP channels.

In the following, to gain more precise insight, we will take two TRP channels, i.e. TRPC6 and TRPV4, as the representative lipid-regulated channels showing contrasting nature in CVS. These channels are the most ubiquitous and reportedly the first mechanosensitive TRP isoforms with well-investigated details in CVS (Inoue et al. 2009b). And their functional antagonism in VSMC and VEC seems to play a pivotal role in vascular tone regulation, via mutually interwined activation/regulation mechanisms through lipid dynamics and metabolism.

10.4 Lipid-Mediated Mechanisms Involved in Mechanical Activation of TRPs in Vascular Tone Regulation

10.4.1 Two Lipid Mediators DAG and 20-HETE Synergistically Regulate TRPC6 Channel in VSMC

The vascular tone is regulated by both neurohormonal and myogenic mechanisms. While the former indicates vasoconstrictor response to receptor agonists such as noradrenaline, vasopressin, and angiotensin II, the latter is defined as an intrinsic mechanosensitive mechanism independent of neural, metabolic and hormonal influences, which has been traditionally called 'myogenic response' (Davis and Hill 1999). In general, agonist-induced vasoconstrictor response occurs as the result of PLC-dependent Ca^{2+} mobilization and is responsible for raising the systemic vascular resistance and thereby blood pressure, for which the essential roles of TRPC6 and its homologues have been speculated (for review, see e.g. Inoue et al. 2006). In contrast, the role of myogenic response has been ascribed to local blood flow control through not yet firmly determined mechanosensitive mechanisms which are generally believed different from those of receptor-mediated mechanism. However, as will be seen below, such simple dichotomy may not be relevant, particularly in that membrane lipids associated with receptor-mediated metabolization would contribute to both vascular responses.

The 'myogenic response' or 'Bayliss effect' is a long-standing concept that has been used to explain the auto-regulatory response of small arteries. This mechanism is thought to be of critical importance to maintain the blood flow constant in response to blood pressure fluctuations in specialized circulations, i.e. cerebral, renal and coronary circulations (Davis and Hill 1999). The important characteristics of myogenic response include not only its dependence on extracellular Ca^{2+} and inhibition by VDCC or MSCC blockers (e.g. Gd^{3+} and GsMTx-4), but also its sensitivity to PLC inhibitors (Osol et al. 1993; Matsumoto et al. 1995; Davis and Hill 1999; Lee et al. 2007). This indicates that myogenic response would also be tightly linked to Ca^{2+} influx dependent on PLC-mediated phospholipid metabolization. There are indeed several reports showing that increased intravascular pressure promoted the hydrolysis of PIP_2 in a PLC-dependent manner (e.g. Narayanan et al. 1994), and that Ca^{2+} -permeable DAG-sensitive cationic conductances could be induced by membrane stretch (e.g. Park et al. 2003; Lee et al. 2007).

A recent study applying the antisense approach to organ-cultured cerebral artery unequivocally united the above independent observations to show that pressure-induced activation of a DAG-sensitive NSCC TRPC6 channel contributes to the development of myogenic tone (Welsh et al. 2002). More recently, Spassova et al. (2005) demonstrated that expressed TRPC6 channels can be directly gated by membrane stretch at both macroscopic current and single channel levels, which are inhibited by an amphipathic neurotoxin GsMTx-4. These observations led the authors to propose the 'bilayer-dependent' mechanism for TRPC6 channel activation (Fig. 10.2); both membrane deformation by stretch and DAG generated through

PLC-coupled receptor activation would directly activate TRPC6 channel in a 'bilayer-mediated' fashion. However, deletion of *trpc6* gene in mice could not confirm these observations. The myogenic response of cerebral artery from these mice was not compromised at all. This questioned the obligatory involvement of mechanical activation of TRPC6 channel in the myogenic response (Dietrich 2005). Instead, the same study found that compensatory overexpression of TRPC3 protein in TRPC6$^{-/-}$ mice rather produced vascular over-reactivity to both receptor and mechanical stimulations. These disparate results seemed difficult to reconcile each other, but subsequent studies proposed alternative views.

The fact that PIP_2 hydrolysis can be stimulated by mechanical stimuli does not necessarily mean that PLC should directly be activated by mechanical stimuli. Mederos et al. (2008) reported that, when $G_{q/11}$/PLC-coupled receptors [GPCRs; angiotensin (AT_1), endothelin (ET_A), muscarinic (M_5) and histamine (H_1) receptors] were overexpressed, various forms of mechanical stimuli, i.e. hypotonicity, cell inflation, cell stretch and negative pressure applied into patch pipette could activate coexpressed TRPC6 channels. This mechanical activation of TRPC6 channel was prevented by the PLC inhibitor U73122 or an inactive GTP analogue GDPβS, and even by the antagonist of overexpressed AT_1 receptor losartan. Importantly, pretreatment with losartan also attenuated the BRET signals reflecting the interaction between AT_1 receptor and its downstream signaling molecule β-arrestin, and suppressed (but not abolished) myogenic response of cerebral artery in the absence of AT_1 receptor agonist. These results together suggest that mechanical stimuli may directly activate empty GPCRs thereby activating the downstream PLC-dependent pathway thereby activating TRPC6 channel (Fig. 10.2). Thus, it is not surprising that vascular reactivity was not impaired in TRPC6$^{-/-}$ mice where compensatory upregulation of another DAG-sensitive NSCC TRPC3 may fully substitute the role of TRPC6 channel.

In strong support of this view, a recent independent study using the substituted cysteine accessibility mapping technique has shown that mechanical stimulation can actually cause the conformational change of unoccupied AT_1 receptor with an anticlockwise rotation and a shift of the 7th transmembrane^{TM} segment into a ligand binding pocket. Moreover, this effect was inhibited by the AT_1 receptor antagonist candesartan which probably stabilizes the AT_1 receptor in an inactive state (Yasuda et al. 2008). The mechanism by which mechanical stimuli causes the conformational change of AT_1 receptor remains still unclear. However, the most plausible explanation is that mechanical stimulation might increase the hydrophobic mismatch at the lipid – AT_1 receptor protein boundary, and the compensatory movement of the 7th TM segment to diminish this membrane 'frustration' energy might bring the receptor into the activated state. Nevertheless, even though the activation of PLC-coupled receptor is the primary mechanism, it does not preclude that TRPC6 channel could be activated by mechanically produced DAG through the bilayer-dependent mechanism described above.

Despite the importance of PLC-dependent mechanism, the myogenic response of cerebral artery was only partially inhibited by the AT_1 receptor antagonist losartan (Dietrich et al. 2005). In other types of arteries than cerebral artery such as resistance arteries (e.g. mesenteric arteries, skeletal muscle arterioles), it has been

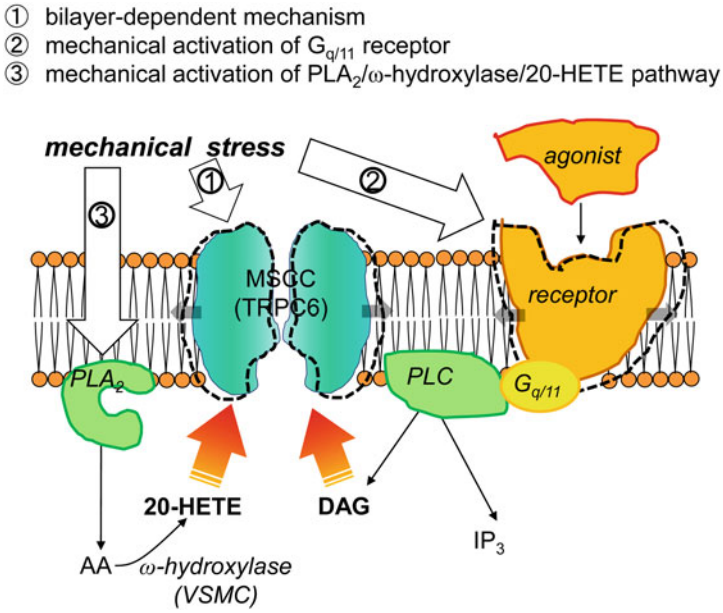

Fig. 10.2 Three hypothetical mechanisms for mechanical activation of TRPC6 channels. Mechanical stimuli applied to VSMC membrane may activate TRPC6 channel directly or indirectly through three distinct pathways, i.e. TRPC6 channel itself, PLC-coupled receptor, and PLA_2-dependent pathway. Note that all mechanisms could involve deformation energy due to altered membrane tension or bending in the initial step

known that noticeable myogenic response is induced only after vasoconstrictive receptor in VSMC is activated by its agonist, e.g. noradrenaline. Or conversely, agonist-induced vasoconstriction is enhanced by increased intravascular pressure or preexisting vascular wall tension (VanBavel et al. 1994; Meininger et al. 1991; Davis and Hill 1999). These observations suggest that there is a synergy between receptor-mediated and mechanically-induced signaling in VSMCs, which may involve an additional signaling pathway independent of PLC. The PLA_2-dependent pathway is one of plausible candidates to fit this idea. PLA_2 is activated by mechanical stimuli to generate AA, from which many vasoactive metabolites can be derived. Amongst them, 20-hydroxyeicosatetraenoic acid (20-HETE) has drawn particular attention, because it acts as a potent vasoconstrictor and is actively formed via cytochrome P450A family enzymes (ω-hydroxylase) in VSMCs (Harder et al. 1997; Marji et al. 2002; Roman 2002).

The formation of 20-HETE is dependent on perfusion pressure in cerebral artery (Gebremedhin et al. 2000), and overexpression of cytochrome P450A1 enzyme enhances the constrictor response to phenylephrine with increased production of 20-HETE in renal interlobar artery (Kaide et al. 2003). Furthermore, pharmacological inhibition of endogenous production of 20-HETE impaires the autoregulation of renal and cerebral blood flow in response to increased intravascular pressure (Zou

et al. 1994; Gebremedhin et al. 2000). These results have established the integral role of 20-HETE in the development of myogenic tone (Harder et al. 2011). The mechanism underlying the vasoconstrictor actions of 20-HETE in cerebral artery has been ascribed to the inhibition of Ca^{2+}-dependent K^+ channel (Zou et al. 1996) and potentiation of VDCC; both result in the enhancement of voltage-dependent Ca^{2+} influx by membrane depolarization, and activation of PKC which increases the Ca^{2+} sensitivity of contractile machinery (Harder et al. 1997, 2011).

To explore whether a similar mechanism operates in enhanced myogenic response by receptor stimulation, Inoue et al. (2009a) re-investigated the mechanical activation of TRPC6 in the light of synergy between receptor and mechanical stimulations. Both in expression system and A7r5 vascular myocytes, mechanical stimulation (hypotonicity, shear stress, intrapipette negative pressure, application of an amphipathic compound trinitrophenol) enhanced the activity of TRPC6 channel only after it was activated by GPCR agonists. Oppositely, when the mechanical stimuli were applied first, the subsequent activation of TRPC6 channel by agonists was greatly enhanced with more than 100-fold leftward shift of concentration-response relationship. The mechanical potentiation of receptor-activated TRPC6 channel was completely abrogated by siRNA knockdown of cytosolic PLA_2 and pharmacological inhibition of PLA_2 or 20-HETE production via ω/ω^--hydroxylase. Conversely, exogenous administration of 20-HETE, which could itself elicit a very small magnitude of cationic currents with atypical properties (Basora et al. 2003), resulted in remarkable potentiation of TRPC6 channel activities induced by a DAG analogue OAG. At the tissue level, pressure-induced contraction (myogenic response) of rat mesenteric artery was marginal in the absence of agonist, but was markedly enhanced by preceding weak α1-adrenoceptor stimulation. This enhancement was almost completely inhibited by the ω/ω-hydroxylase-specific blocker HET0016 (Fig. 10.3) or TRPC6 channel blockers Gd^{3+} and SK&F96365. In aggregate, these results suggest that, upon simultaneous receptor and mechanical stimulations, two lipid mediators derived from PLC- and PLA_2-dependent pathways, DAG and 20-HETE, may synergistically activate TRPC6 channels (Fig. 10.3). The specific receptors responsible for the actions of 20-HETE and DAG on TRPC6 channels have not yet been identified, but again, the possibility that both lipids may rather affect the channel activity via altered bilayer elastic energy (see above) cannot be ruled out.

In physiological settings, a certain amount of noradrenaline is continuously released from the sympathetic nerve ending because of its autonomic tone, and many vasoactive factors (e.g., vasopressin, angiotensin II, endothelin) are released from endocrine organs and VEC and circulating in the blood. VSMCs are constantly exposed to this vasoconstrictive neurohormonal drive. Under these conditions, the mechanical reactivity of peripheral arteries is expected to be enhanced or 'sensitized' by the above-mentioned mechanism. As described above, the enhanced myogenic response has been observed in resistance arteries which mainly contribute to systemic vascular resistance. This further implies that simultaneous operation of mechanical and receptor stimulations may greatly enhance the mechanical responsiveness of resistance arteries. Under normal conditions, this would help to more efficiently elevate decreased blood pressure, whereas in pathological conditions, it could exacerbate

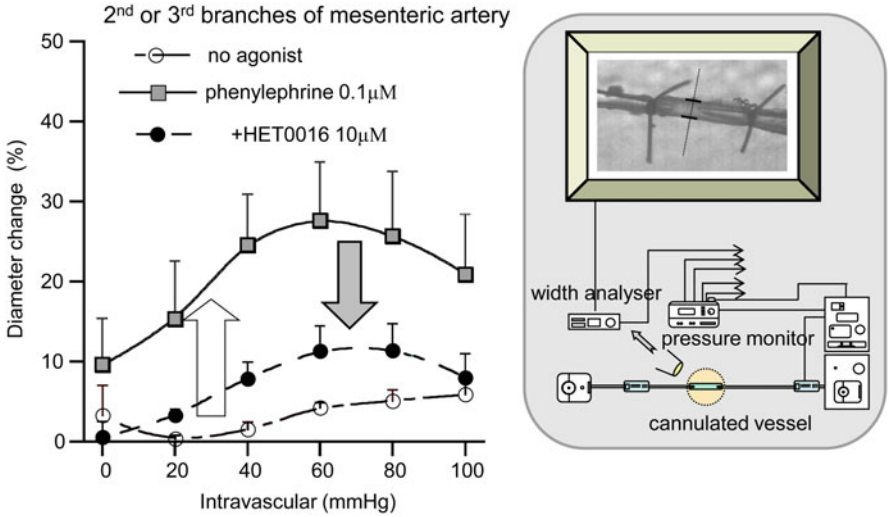

Fig. 10.3 Involvement of 20-HETE production in enhanced myogenic response in small mesenteric arteries. *Left*: myogenic response expressed as a % decrease of initial diameter before and after application of an α1-adrenergic agonist phenylephrine, in the presence or absence of the specific ω-hydroxylase blocker HET0016. *Right*: schematic representation of a set-up used for videomicroscopic diameter measurement of cannulated artery preparation. (Modified from Inoue et al. (2009b))

hypertensive propensity. A similar situation may also hold for the heart, since it is continuously subjected to mechanical loads and under tight neurohormonal regulation. Thus, the synergy between mechanical (PLA_2-meidated) and PLC-coupled receptor stimulations may be of general physiological and pathophysiological significance for the regulation of CVS functions.

In addition, contribution of 20-HETE to myogenic response has also been assigned to the activation of vasosensory TRPV1 (see below) in small branches of mesenteric artery (Scotland et al. 2004). The proposed hypothesis is that mechanically produced 20-HETE in VSMCs may activate TRPV1 channels in adjacent vasosensory terminals; which in turn triggers the release of substance P thereby evoking vasoconstriction via stimulation of neurokinin 1 receptor on the VSMC membrane. Although TRPV1 is known to be activated by several 12-LOX products (Hwang et al. 2000), it is not clear whether 20-HETE could exert the same action. Thus, physiological relevance of vasosensory TRPV1-mediated mechanism for local blood pressure/flow regulation remains to be determined.

10.4.2 EET Mediates the Activation of TRPV4 Channel in VECs

Blood stream continuously generates shear stress thereby facilitating the release of vasodilative agents from VECs such as nitric oxide (NO) (Busse and Fleming 2003).

The mechanism by which shear stress facilitates the NO production is diverse, but Ca^{2+} influx through mechanically activated TRPV4 channel in VEC is one of crucial steps contributing to NO production and resultant vasodilation or increased blood flow (Kohler et al. 2006; Hartmannsgrube et al. 2007; Loot et al. 2008). TRPV4 is abundantly expressed in VECs and activated by hypoosmolarity, shear stress, warm temperature and synthetic 4α-phorbols. The activity of TRPV4 channel is positively modulated by voltage and $[Ca^{2+}]_i$ and PKC-mediated phosphorylation (Nilius et al. 2004).

Mechanical activation of TRPV4 by hypoosmolarity is suppressed by the inhibitors for PLA_2 and cytochrome P450 epoxygenase which are responsible for the production of AA and its metabolites epoxyeicosatrienoic acid (EETs) respectively. Exogenous administration of anandamide, AA or 5′,6′-EET (but not other EETs except for 8′,9′-EET which shows only a weak activating effect) induced TRPV4-mediated Ca^{2+} responses but only 5′,6′-EET could elicit single channel activities in inside-out patch membrane (Watanabe et al. 2003). These results suggest that 5′,6′-EET is generated via mechanical activation of PLA_2/expoygenase pathway to act as a membrane-delimited lipid mediator responsible for mechanical activation of TRPV4 channel. A subsequent investigation with specific point mutagenesis revealed that activation of TRPV4 by hypoosmolarity or 5′,6′-EET critically depended on Tyr-591 and Arg-594 residues in the C-terminal part of the 4th TM segment (TM4). These amino acid residues were also necessary for heat- or 4αPDD-induced activation, which however additionally required hydrophobic residues (Leu584, Trp586) in the central part of TM4 as well as Tyr-556 in the third TM segment (Vriens et al. 2007). Through the comparison of chemical structures and efficacies to activate TRPV4 channel of 4α-phorbol esters and analogy to TRPV1 channel, it has been hypothesized that the C-terminal part of TM4 (Tyr-591 and Arg-594) may not contribute to the specific binding of TRPV4 agonists but rather be involved in the gating of TRPV4 channel per se (Vriens et al. 2007). These results raise the possibility that 5′,6′-EET might activate TRPV4 channel through a nonspecific 'bilayer-mediated' mechanism. It is an intriguing subject of further investigation to evaluate such potential bilayer-dependent action of 5′,6′-EET in the light of its effects on the gramicidin channel kinetics as described above (Lundbaek et al. 2010a).

The synergy of mechanical stimulation and PLC-coupled receptor has also been documented for TRPV4 channel. Besides the potentiating effect of PKC activation on TRPV4 channel (Nilius et al. 2004), it has been reported that receptor-activated IP_3R enhances hypotonicity-induced (i.e EET-mediated) activation of TRPV4 channel, via binding to the TRPV4C-terminal region harboring a CaM-binding motif (Fernandes et al. 2008; Garcia-Elias et al. 2008). Although the available information is still sparse, the above observations raise an intriguing idea that the synergistic operation of PLC and PLA_2 may serve as a common paradigm to amplify an otherwise marginal Ca^{2+} mobilization caused by either neurohormonal or mechanical stimulus alone.

In addition, mechanical activation of TRPV4 channel has been suggested to involve Src-mediated phosphorylation of N-terminal Tyr-110 residue. The point mutation of this residue resulted in impairment of shear stress- and hypoosmolarity-induced TRPV4 channel activation leaving the activating effect of 4αPDD unchanged

(Wegierski et al. 2009). It is uncertain however how Src-mediated Tyr-110 phosphorylation on the N-terminus could maintain the sensitivity of TRPV4 channel to mechanical stimuli. Whether some conformational changes induced directly or indirectly via auxiliary proteins by Tyr-110 phosphorylation may mediate the enhancement of mechanical activation of TRPV4 is a matter of future investigation.

10.4.3 Functional Antagonism between TRPC6 (and TRPC3) and TRPV4 Channels in Vascular Tone Regulation via Lipid-Mediate Regulation and their Therapeutic Significance in Future

In the vasculature, two AA metabolites derived form PLA_2-dependent pathway, EETs and 20-HETE are known to play reciprocal roles (Roman 2002; Busse and Fleming 2003). The former is actively produced in VECs, and thought to contribute to vasodilative response. In contrast, 20-HETE is derived mainly from VSMCs, and under pressurized conditions, considerable amount of 20-HETE is released into peripheral circulations from VSMCs. There is compelling evidence that altered production of EETs and 20-HETE is closely related to the onset and progression of hypertensive disorders (Fleming 2001; Roman 2002). Furthermore, recent studies have suggested that in both spontaneously hypertensive rats and patients with essential hypertension, expression of TRPC3 is upregulated relative to that of TRPC6 and Ca^{2+} mobilization associated with PLC-coupled receptor activation (i.e. through these TRPC channels) is exaggerated (Liu et al. 2005, 2006, 2009). In the early stage of essential hypertension, excessive activities of sympathetic nerves and renin-angiotensin system are commonly observed features (Johnson et al. 2008). This means that excessive activation of PLC-dependent pathway may play a key role in the onset/progression of the hypertension. Taking all these facts together, it is possible that disruption of the lipid-mediated regulation of DAG-sensitive TRPC subfamily members (i.e. TRPC3, TRPC6), particularly via their synergistic activation by PLC- and PLA_2-dependent pathways (i.e. via DAG, 20-HETE), may lead to abnormally elevated blood pressure, due to increased vascular reactivity and resistance and the exacerbating process of hypertension resulting from defective renal protection due to impaired myogenic response of renal arteries.

It has been reported that the production of 20-HETE in VSMCs is inhibited by NO, which binds and inactivates the heme moiety of cytochrome P450A enzymes via formation of nitrosyl-iron complexes (Harder et al. 1997, 2011). The production of NO is facilitated by shear stress-induced activation of TRPV4 channel in VECs via mechanically produced 5,6,-EET. Although $TRPV4^{-/-}$ is found to be normotensive (Willette et al. 2008), the vasodepressor effect of NO is strongly dependent on the activation of TRPV4 channels (Kohler et al. 2006; Hartmannsgrube et al. 2007; Loot et al. 2008; Willette et al. 2008). Moreover, NO released from VECs

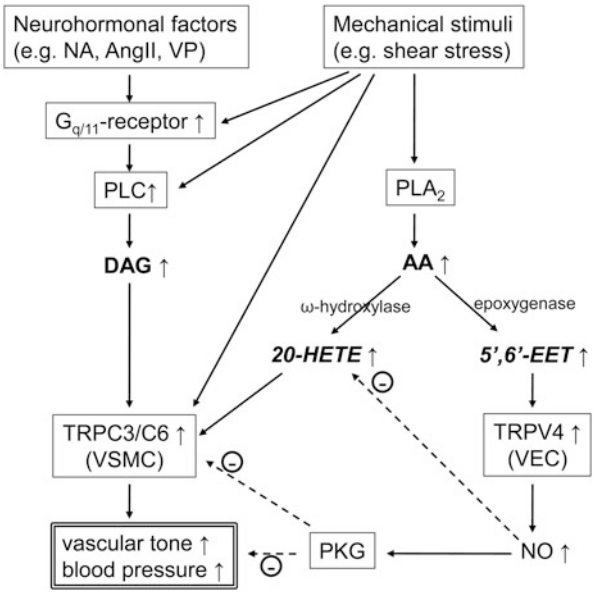

Fig. 10.4 Functional antagonism between TRPC3/C6 and TRPV4 channels in vascular tone regulation. The two membrane lipid-metabolizing pathways, PLC/DAG and PLA_2/cytochrome P450 enzymes are likely involved in mechanical activation of these channels, in which two lipid mediators, EET and 20-HETE may play antagonistic roles. Solid and dashed arrows indicate stimulatory and inhibitory effects on targets at the arrowheads, respectively

continously diffuses into VSMCs to activate protein kinase G (PKG). The activation of PKG has been reported to phosphorylate TRPC3 and TRPC6 channels and suppress Ca^{2+} influx into VSMCs (Kwan et al. 2004, 2006; Takahashi et al. 2008; Koitabashi 2010; Inoue et al. 2010) with enhanced Ca^{2+} uptake into the sarcoplasmic reticulum and decreased Ca^{2+} sensitivity of contractile machinery in VSMCs (Lincoln et al. 2001). All these can contribute to produce vasorelaxation and decrease blood pressure.

The above-mentioned mechanisms provide us a new conceptual framework of functional antagonism between TRPC6/C3 channels in VSMCs and TRPV4 channels in VECs via PLC/ω-hydroxylase/20-HETE and PLA_2/epoxygenase/EET, NO/PKG-mediated regulation of vascular tone and blood pressure (Fig. 10.4). This framework may become an important basis for developing a new therapeutic strategy toward more effective treatments of hypertensive disorders in future. A similar strategy can also be applied to the treatment of cardiac hypertrophy wherein both neurohormonal and mechanical activation of TRPC1/C3/C6 channels may play a pivotal role in concert with the calcineurin/NFAT-mediated signaling (Heineke and Molkentin 2006; Inoue et al. 2006, 2010).

Acknowledgments Part of this work is supported by Grants-in-aid for Scientific Research on Innovative Areas (No. 22136008) and Scientific Research (C) (No. 21590246), and a grant from Seizon Kagaku Institute to R.I. Support was also obtained as a member from an oversea funding granted to Dr. Juan Shi at the Department of Anatomy and K.K. Leung Brian Research Center, the Fourth Military Medical University Xi'an (National Natural Science Foundation of China: No. 30871004).

References

Bae C, Sachs F, Gottlieb PA (2011) The mechanosensitive ion channel Piezo1 is inhibited by the peptide GsMTx4. Biochemistry 50(29):6295–6300

Basora N, Boulay G, Bilodeau L, Rousseau E, Payet MD (2003) 20-hydroxyeicosatetraenoic acid (20-HETE) activates mouse TRPC6 channels expressed in HEK293 cells. J Biol Chem 278(34):31709–31716

Busse R, Fleming I (2003) Regulation of endothelium-derived vasoactive autacoid production by hemodynamic forces. Trends Pharmacol Sci 24(1):24–29

Buxton IL, Singer CA, Tichenor JN (2010) Expression of stretch-activated two-pore potassium channels in human myometrium in pregnancy and labor. PLoS One 5(8):e12372

Chen XZ, Li Q, Wu Y, Liang G, Lara CJ, Cantiello HF (2008) Submembraneous microtubule cytoskeleton: interaction of TRPP2 with the cell cytoskeleton. Febs J 275(19):4675–4683

Christensen AP, Corey DP (2007) TRP channels in mechanosensation: direct or indirect activation? Nat Rev Neurosci 8(7):510–521

Corry B, Martinac B (2008) Bacterial mechanosensitive channels: experiment and theory. Biochim Biophys Acta 1778(9):1859–1870

Coste B, Mathur J, Schmidt M, Earley TJ, Ranade S, Petrus MJ et al (2010) Piezo1 and Piezo2 are essential components of distinct mechanically activated cation channels. Science 330(6000): 55–60

Dalrymple A, Mahn K, Poston L, Songu-Mize E, Tribe RM (2007) Mechanical stretch regulates TRPC expression and calcium entry in human myometrial smooth muscle cells. Mol Hum Reprod 13(3):171–179

Davis PF (2009) Hemodynamic shear stress and the endothelium in cardiovascular pathophysiology. Nat Clin Pract 6(1):16–26

Davis MJ, Hill MA (1999) Signaling mechanisms underlying the vascular myogenic response. Physiol Rev 79(2):387–423

Dedman A, Sharif-Naeini R, Folgering JH, Duprat F, Patel A, Honore E (2009) The mechano-gated K(2P) channel TREK-1. Eur Biophys J 38(3):293–303

Dietrich A, Mederos YSM, Gollasch M, Gross V, Storch U, Dubrovska G et al (2005) Increased vascular smooth muscle contractility in TRPC6$^{-/-}$ mice. Mol Cell Biol 25(16):6980–6989

Dietrich A, Chubanov V, Gudermann T (2010) Renal TRPathies. J Am Soc Nephrol 21(5):736–744

Drummond HA, Grifoni SC, Jernigan NL (2008) A new trick for an old dogma: ENaC proteins as mechanotransducers in vascular smooth muscle. Physiology (Bethesda) 23:23–31

Falkenburger BH, Jensen JB, Dickson EJ, Suh BC, Hille B (2010) Phosphoinositides: lipid regulators of membrane proteins. J Physiol 588(Pt 17):3179–3185

Fernandes J, Lorenzo IM, Andrade YN, Garcia-Elias A, Serra SA, Fernandez-Fernandez JM et al (2008) IP_3 sensitizes TRPV4 channel to the mechano- and osmotransducing messenger 5′-6′-epoxyeicosatrienoic acid. J Cell Biol 181(1):143–155

Fleming I (2001) Cytochrome p450 and vascular homeostasis. Circ Res 89(9):753–762

Fleming I, Rueben A, Popp R, Fisslthaler B, Schrodt S, Sander A et al (2007) Epoxyeicosatrienoic acids regulate Trp channel dependent Ca^{2+} signaling and hyperpolarization in endothelial cells. Arterioscler Thromb Vasc Biol 27(12):2612–2618

Flockerzi V (2007) An introduction on TRP channels. Handb Exp Pharmacol 179:1–19

Garcia-Elias A, Lorenzo IM, Vicente R, Valverde MA (2008) IP_3 receptor binds to and sensitizes TRPV4 channel to osmotic stimuli via a calmodulin-binding site. J Biol Chem 283(46):31284–31288

Gebremedhin D, Lange AR, Lowry TF, Taheri MR, Birks EK, Hudetz AG et al (2000) Production of 20-HETE and its role in autoregulation of cerebral blood flow. Circ Res 87(1):60–65

Gottlieb P, Folgering J, Maroto R, Raso A, Wood TG, Kurosky A et al (2008) Revisiting TRPC1 and TRPC6 mechanosensitivity. Pflugers Arch 455(6):1097–1103

Guinamard R, Demion M, Magaud C, Potreau D, Bois P (2006) Functional expression of the TRPM4 cationic current in ventricular cardiomyocytes from spontaneously hypertensive rats. Hypertension 48(4):587–594

Hamill OP, Martinac B (2001) Molecular basis of mechanotransduction in living cells. Physiol Rev 81(2):685–740

Hansen SB, Tao X, MacKinnon R (2011) Structural basis of PIP_2 activation of the classical inward rectifier K^+ channel Kir2.2. Nature 477(7365):495–498

Hara Y, Wakamori M, Ishii M, Maeno E, Nishida M, Yoshida T et al (2002) LTRPC2 Ca^{2+}-permeable channel activated by changes in redox status confers susceptibility to cell death. Mol Cell 9(1):163–173

Harder DR, Lange AR, Gebremedhin D, Birks EK, Roman RJ (1997) Cytochrome P450 metabolites of arachidonic acid as intracellular signaling molecules in vascular tissue. J Vasc Res 34(3):237–243

Harder DR, Narayanan J, Gebremedhin D (2011) Pressure-induced myogenic tone and role of 20-HETE in mediating autoregulation of cerebral blood flow. Am J Physiol Heart Circ Physiol 300(5):H1557–1565

Hartmannsgruber V, Heyken WT, Kacik M, Kaistha A, Grgic I, Harteneck C et al (2007) Arterial response to shear stress critically depends on endothelial TRPV4 expression. PLoS ONE 2(9):e827

Heineke J, Molkentin JD (2006) Regulation of cardiac hypertrophy by intracellular signalling pathways. Nat Rev Mol Cell Biol 7(8):589–600

Hilgemann DW, Feng S, Nasuhoglu C (2001) The complex and intriguing lives of PIP2 with ion channels and transporters. Sci STKE 2001(111):re19

Hill K, Schaefer M (2007) TRPA1 is differentially modulated by the amphipathic molecules trinitrophenol and chlorpromazine. J Biol Chem 282(10):7145–7153

Huber TB, Schermer B, Muller RU, Hohne M, Bartram M, Calixto A et al (2006) Podocin and MEC-2 bind cholesterol to regulate the activity of associated ion channels. Proc Natl Acad Sci USA 103(46):17079–17086

Hughes-Fulford M (2004) Lessons learned about spaceflight and cell biology experiments. J Gravit Physiol 11(1):105–109

Hwang SW, Cho H, Kwak J, Lee SY, Kang CJ, Jung J et al (2000) Direct activation of capsaicin receptors by products of lipoxygenases: endogenous capsaicin-like substances. Proc Natl Acad Sci USA 97(11):6155–6160

Ingber DE (2008) Tensegrity-based mechanosensing from macro to micro. Prog Biophys Mol Biol 97(2–3):163–179

Inoue R, Jensen LJ, Shi J, Morita H, Nishida M, Honda A et al (2006) Transient receptor potential channels in cardiovascular function and disease. Circ Res 99(2):119–131

Inoue R, Jensen LJ, Jian Z, Shi J, Hai L, Lurie AI et al (2009a) Synergistic activation of vascular TRPC6 channel by receptor and mechanical stimulation via phospholipase C/diacylglycerol and phospholipase A2/omega-hydroxylase/20-HETE pathways. Circ Res 104(12):1399–1409

Inoue R, Jian Z, Kawarabayashi Y (2009b) Mechanosensitive TRP channels in cardiovascular pathophysiology. Pharmacol Ther 123(3):371–385

Inoue R, Shi J, Jian Z, Imai Y (2010) Regulation of cardiovascular TRP channel functions along the NO-cGMP-PKG axis. Exp Rev Clin Pharmacol 3(3):347–360

Johnson RJ, Feig DI, Nakagawa T, Sanchez-Lozada LG, Rodriguez-Iturbe B (2008) Pathogenesis of essential hypertension: historical paradigms and modern insights. J Hypertens 26(3):381–391

Kaide J, Wang MH, Wang JS, Zhang F, Gopal VR, Falck JR et al (2003) Transfection of CYP4A1 cDNA increases vascular reactivity in renal interlobar arteries. Am J Physiol Renal Physiol 284(1):F51–56

Kanzaki M, Zhang YQ, Mashima H, Li L, Shibata H, Kojima I (1999) Translocation of a calcium-permeable cation channel induced by insulin-like growth factor-I. Nat Cell Biol 1(3):165–170

Kohler R, Heyken WT, Heinau P, Schubert R, Si H, Kacik M et al (2006) Evidence for a functional role of endothelial transient receptor potential V4 in shear stress-induced vasodilatation. Arterioscler Thromb Vasc Biol 26(7):1495–1502

Koitabashi N, Aiba T, Hesketh GG, Rowell J, Zhang M, Takimoto E et al (2010) Cyclic GMP/PKG-dependent inhibition of TRPC6 channel activity and expression negatively regulates cardiomyocyte NFAT activation Novel mechanism of cardiac stress modulation by PDE5 inhibition. J Mol Cell Cardiol 48(4):713–724

Kwan HY, Huang Y, Yao X (2004) Regulation of canonical transient receptor potential isoform 3 (TRPC3) channel by protein kinase G. Proc Natl Acad Sci USA 101(8):2625–2630

Kwan HY, Huang Y, Yao X (2006) Protein kinase C can inhibit TRPC3 channels indirectly via stimulating protein kinase G. J Cell Physiol 207(2):315–321

Lee HA, Baek EB, Park KS, Jung HJ, Kim JI, Kim SJ et al (2007) Mechanosensitive nonselective cation channel facilitation by endothelin-1 is regulated by protein kinase C in arterial myocytes. Cardiovasc Res 76(2):224–235

Lincoln TM, Dey N, Sellak H (2001) Invited review: cGMP-dependent protein kinase signaling mechanisms in smooth muscle: from the regulation of tone to gene expression. J Appl Physiol 91(3):1421–1430

Liu D, Scholze A, Zhu Z, Kreutz R, Wehland-von-Trebra M, Zidek W et al (2005) Increased transient receptor potential channel TRPC3 expression in spontaneously hypertensive rats. Am J Hypertens 18(11):1503–1507

Liu D, Scholze A, Zhu Z, Krueger K, Thilo F, Burkert A et al (2006) Transient receptor potential channels in essential hypertension. J Hypertens 24(6):1105–1114

Liu D, Yang D, He H, Chen X, Cao T, Feng X et al (2009) Increased transient receptor potential canonical type 3 channels in vasculature from hypertensive rats. Hypertension 53(1):70–76

Loot AE, Popp R, Fisslthaler B, Vriens J, Nilius B, Fleming I (2008) Role of cytochrome P450-dependent transient receptor potential V4 activation in flow-induced vasodilatation. Cardiovasc Res 80(3):445–452

Lowik MM, Groenen PJ, Levtchenko EN, Monnens LA, Van Den Heuvel LP (2009) Molecular genetic analysis of podocyte genes in focal segmental glomerulosclerosis–a review. Eur J Pediatr 168(11):1291–1304

Lundbaek JA, Collingwood SA, Ingolfsson HI, Kapoor R, Andersen OS (2010a) Lipid bilayer regulation of membrane protein function: gramicidin channels as molecular force probes. J R Soc Interface 7(44):373–395

Lundbaek JA, Koeppe RE, Andersen OS (2010b) Amphiphile regulation of ion channel function by changes in the bilayer spring constant. Proc Natl Acad Sci USA 107(35):15427–15430

Marji JS, Wang MH, Laniado-Schwartzman M (2002) Cytochrome P-450 4 A isoform expression and 20-HETE synthesis in renal preglomerular arteries. Am J Physiol Renal Physiol 283(1):F60–67

Maroto R, Raso A, Wood TG, Kurosky A, Martinac B, Hamill OP (2005) TRPC1 forms the stretch-activated cation channel in vertebrate cells. Nat Cell Biol 7(2):179–185

Martinac B, Kloda A (2003) Evolutionary origins of mechanosensitive ion channels. Prog Biophys Mol Biol 82(1–3):11–24

Martinez-Lemus LA, Wu X, Wilson E, Hill MA, Davis GE, Davis MJ et al (2003) Integrins as unique receptors for vascular control. J Vasc Res 40(3):211–233

Matsumoto H, Baron CB, Coburn RF (1995) Smooth muscle stretch-activated phospholipase C activity. Am J Physiol 268(2 Pt 1):C458–465

Mederos y Schnitzler M, Storch U, Meibers S, Nurwakagari P, Breit A, Essin K et al (2008) Gq-coupled receptors as mechanosensors mediating myogenic vasoconstriction. Embo J 27(23):3092–3103

Meininger GA, Faber JE (1991) Adrenergic facilitation of myogenic response in skeletal muscle arterioles. Am J Physiol 260(5 Pt 2):H1424–1432

Meves H (2008) Arachidonic acid and ion channels: an update. Br J Pharmacol 155(1):4–16

Moller CC, Flesche J, Reiser J (2009) Sensitizing the Slit Diaphragm with TRPC6 ion channels. J Am Soc Nephrol 20(5):950–953

Narayanan J, Imig M, Roman RJ, Harder DR (1994) Pressurization of isolated renal arteries increases inositol trisphosphate and diacylglycerol. Am J Physiol 266(5 Pt 2):H1840–1845

Naylor J, Li J, Milligan CJ, Zeng F, Sukumar P, Hou B et al (2010) Pregnenolone sulphate- and cholesterol-regulated TRPM3 channels coupled to vascular smooth muscle secretion and contraction. Circ Res 106(9):1507–1515

Nilius B, Droogmans G (2001) Ion channels and their functional role in vascular endothelium. Physiol Rev 81(4):1415–1459

Nilius B, Vriens J, Prenen J, Droogmans G, Voets T (2004) TRPV4 calcium entry channel: a paradigm for gating diversity. Am J Physiol Cell Physiol 286(2):C195–205

Oancea E, Wolfe JT, Clapham DE (2006) Functional TRPM7 channels accumulate at the plasma membrane in response to fluid flow. Circ Res 98(2):245–253

Osol G, Laher I, Kelley M (1993) Myogenic tone is coupled to phospholipase C and G protein activation in small cerebral arteries. Am J Physiol 265(1 Pt 2):H415–420

Park KS, Kim Y, Lee YH, Earm YE, Ho WK (2003) Mechanosensitive cation channels in arterial smooth muscle cells are activated by diacylglycerol and inhibited by phospholipase C inhibitor. Circ Res 93(6):557–564

Parnas M, Katz B, Lew S, Tzarfaty V, Dadon D, Gordon-Shaag A et al (2009a) Membrane lipid modulations remove divalent open channel block from TRP-like and NMDA channels. J Neurosci 29(8):2371–2383

Parnas M, Peters M, Minke B (2009b) Linoleic acid inhibits TRP channels with intrinsic voltage sensitivity: implications on the mechanism of linoleic acid action. Channels (Austin) 3(3):164–6

Perozo E, Kloda A, Cortes DM, Martinac B (2002) Physical principles underlying the transduction of bilayer deformation forces during mechanosensitive channel gating. Nat Struct Biol 9(9):696–703

Putney JW Jr (2007) Inositol lipids and TRPC channel activation. Biochem Soc Symp(74):37–45

Raghu P, Hardie RC (2009) Regulation of Drosophila TRPC channels by lipid messengers. Cell Calcium 45(6):566–573

Ramsey IS, Delling M, Clapham DE (2006) An introduction to TRP channels. Annu Rev Physiol 68:619–647

Rohacs T, Lopes CM, Michailidis I, Logothetis DE (2005) $PI(4,5)P_2$ regulates the activation and desensitization of TRPM8 channels through the TRP domain. Nat Neurosci 8(5):626–634

Roman RJ (2002) P-450 metabolites of arachidonic acid in the control of cardiovascular function. Physiol Rev 82(1):131–185

Scotland RS, Chauhan S, Davis C, De Felipe C, Hunt S, Kabir J et al (2004) Vanilloid receptor TRPV1, sensory C-fibers, and vascular autoregulation: a novel mechanism involved in myogenic constriction. Circ Res 95(10):1027–1034

Spassova MA, Hewavitharana T, Xu W, Soboloff J, Gill DL (2006) A common mechanism underlies stretch activation and receptor activation of TRPC6 channels. Proc Natl Acad Sci USA 103(44):16586–16591

Suchyna TM, Johnson JH, Hamer K, Leykam JF, Gage DA, Clemo HF et al (2000) Identification of a peptide toxin from Grammostola spatulata spider venom that blocks cation-selective stretch-activated channels. J Gen Physiol 115(5):583–598

Suh BC, Hille B (2008) PIP_2 is a necessary cofactor for ion channel function: how and why? Annu Rev Biophys 37:175–195

Sukharev SI, Martinac B, Arshavsky VY, Kung C (1993) Two types of mechanosensitive channels in the Escherichia coli cell envelope: solubilization and functional reconstitution. Biophys J 65(1):177–183

Takahashi S, Lin H, Geshi N, Mori Y, Kawarabayashi Y, Takami N et al (2008) Nitric oxide-cGMP-protein kinase G pathway negatively regulates vascular transient receptor potential channel TRPC6. J Physiol 586(Pt 17):4209–4223

Tavernarakis N, Driscoll M (1997) Molecular modeling of mechanotransduction in the nematode Caenorhabditis elegans. Annu Rev Physiol 59:659–689

Ufret-Vincenty CA, Klein RM, Hua L, Angueyra J, Gordon SE (2011) Localization of the PIP_2 sensor of TRPV1 ion channels. J Biol Chem 286(11):9688–9698

van Rossum DB, Oberdick D, Rbaibi Y, Bhardwaj G, Barrow RK, Nikolaidis N et al (2008) TRP_2, a lipid/trafficking domain that mediates diacylglycerol-induced vesicle fusion. J Biol Chem 283(49):34384–34392

VanBavel E, Mulvany MJ (1994) Role of wall tension in the vasoconstrictor response of cannulated rat mesenteric small arteries. J Physiol 477(Pt 1):103–115

Vriens J, Owsianik G, Janssens A, Voets T, Nilius B (2007) Determinants of 4 alpha-phorbol sensitivity in transmembrane domains 3 and 4 of the cation channel TRPV4. J Biol Chem 282(17):12796–12803

Watanabe H, Vriens J, Prenen J, Droogmans G, Voets T, Nilius B (2003) Anandamide and arachidonic acid use epoxyeicosatrienoic acids to activate TRPV4 channels. Nature 424(6947):434–438

Watanabe H, Murakami M, Ohba T, Takahashi Y, Ito H (2008) TRP channel and cardiovascular disease. Pharmacol Ther 118(3):337–351

Wegierski T, Lewandrowski U, Muller B, Sickmann A, Walz G (2009) Tyrosine Phosphorylation Modulates the Activity of TRPV4 in Response to Defined Stimuli. J Biol Chem 284(5):2923–2933

Welsh DG, Morielli AD, Nelson MT, Brayden JE (2002) Transient receptor potential channels regulate myogenic tone of resistance arteries. Circ Res 90(3):248–250

Willette RN, Bao W, Nerurkar S, Yue TL, Doe CP, Stankus G et al (2008) Systemic activation of the transient receptor potential vanilloid subtype 4 channel causes endothelial failure and circulatory collapse: Part 2. J Pharmacol Exp Ther 326(2):443–452

Witzgall R (2007) TRPP2 channel regulation. Handb Exp Pharmacol 179:363–375

Yasuda N, Miura S, Akazawa H, Tanaka T, Qin Y, Kiya Y et al (2008) Conformational switch of angiotensin II type 1 receptor underlying mechanical stress-induced activation. EMBO Rep 9(2):179–186

Yin J, Kuebler WM (2010) Mechanotransduction by TRP channels: general concepts and specific role in the vasculature. Cell Biochem Biophys 56(1):1–18

Zou AP, Imig JD, Kaldunski M, Ortiz de Montellano PR, Sui Z, Roman RJ (1994) Inhibition of renal vascular 20-HETE production impairs autoregulation of renal blood flow. Am J Physiol 266(2 Pt 2):F275–F282

Zou AP, Fleming JT, Falck JR, Jacobs ER, Gebremedhin D, Harder DR et al (1996) 20-HETE is an endogenous inhibitor of the large-conductance Ca^{2+}-activated K^+ channel in renal arterioles. Am J Physiol 270(1 Pt 2):R228–R237

Chapter 11
Stretch Effects on Atrial Conduction: A Potential Contributor to Arrhythmogenesis

Michela Masè and Flavia Ravelli

11.1 Introduction

The existence of a close relationship between stretch and atrial arrhythmias is supported by large clinical and experimental evidence (see Ravelli 2003; Eckstein et al. 2008 for review). Clinical studies have reported an increased prevalence of arrhythmias for hearts that have been mechanically compromised by congestive heart failure (Packer 1985; Francis 1986), or exposed to pressure overload through hypertension (Sideris 1993) and aortic valve disease (Dreifus 1993). In addition, atrial dilatation is known to be an important independent risk factor for atrial fibrillation (AF) (Vaziri et al. 1994; Psaty et al. 1997), with left atrial size being a predictor of successful cardioversion and maintenance of sinus rhythm (Hoglund and Rosenhamer 1985; Brodsky et al. 1989). Consistently with clinical evidence, experimental studies in animal models have shown that both acute and chronic atrial stretch increase the vulnerability to atrial fibrillation (Boyden and Hoffman 1981; Solti et al. 1989; Sideris et al. 1994; Ravelli and Allessie 1997; Chorro et al. 1998; Neuberger et al. 2005, 2006). In particular, the arrhythmogenic role of stretch was demonstrated in the small rabbit heart, which, unable to sustain any atrial arrhythmia in normal conditions, could instead produce a fibrillatory response to electrical stimulation, if preconditioned by stretch (Ravelli and Allessie 1997). On the other hand, atrial dilatation can be a consequence of atrial fibrillation (Probst et al. 1973; Keren et al. 1987; Petersen et al. 1987; Sanfilippo et al. 1990; Suarez et al. 1991). The electrical remodeling induced by the arrhythmia is indeed accompanied by a progressive loss of atrial contractility and increase in atrial compliance, which determine an enlarged atrial volume (Wijffels et al. 1995; Schotten and Allessie 2001; Schotten et al. 2011). In this way, atrial dilatation contributes to the vicious circle which perpetuates AF (Allessie et al. 2002).

F. Ravelli (✉) · M. Masè
Laboratory of Biophysics and Biosignals and BIOTech, Department of Physics,
Faculty of Science, University of Trento, Via Sommarive 14, 38123, Povo-Trento, Italy
e-mail: ravelli@science.unitn.it

M. Masè
e-mail: mase@science.unitn.it

A. Kamkin, I. Lozinsky (eds.), *Mechanically Gated Channels and their Regulation,*
Mechanosensitivity in Cells and Tissues 6,
DOI 10.1007/978-94-007-5073-9_11,

Atrial stretch may contribute to the development and maintenance of atrial arrhythmias through the modulation of several electrophysiological parameters, promoting focal arrhythmias that trigger self-perpetuating AF or maintaining irregular activation through substrate modification. In experimental preparations stretch has been shown to induce both early and delayed afterdepolarizations able to trigger premature beats and atrial tachyarrhythmias (Nazir and Lab 1996; Kamkin et al. 2000), as well as to accelerate the firing rate (Kalifa et al. 2003) or increase the arrhythmogenic activity of the pulmonary veins (Chang et al. 2007). As concerns substrate modification, previous works in both isolated rabbit hearts (Ravelli and Allessie 1997) and humans (Tse et al. 2001) have shown a close relationship between the vulnerability of the atria to AF and the stretch-induced shortening of atrial refractoriness. A proarrhythmic factor has been also identified in the nonuniform modulation of local atrial refractory periods induced by stretch, which has been attributed to an heterogeneous distribution of wall stress in the intact human atrium (Satoh and Zipes 1996; Chen et al. 1999; Tse et al. 2001).

In addition to these factors, stretch may contribute to the formation of an arrhythmic substrate through the modulation of atrial conduction properties. Experimental and clinical studies on this issue remain, nevertheless, rather sparse, since stretch and speed represent a "complicated couple" to investigate (Allessie 2011). Macroscopic conduction properties are determined by a variety of microscopic factors, all of which can be potentially modulated by stretch, which results in variegate strain-velocity responses in different stretch ranges and tissue preparations (McNary et al. 2008). In addition, the reliable measurement of conduction velocity and stretch-induced changes poses important technical issues, as concerns the mapping system resolution, as well as the definition and estimation of conduction properties from experimental data (Allessie 2011; Ravelli et al. 2011).

In this chapter, we will review the experimental and clinical evidence which supports the role of stretch-induced conduction disturbances in the creation of an arrhythmic substrate. After an introduction concerning the methodological challenges and technical advancements involved in the investigation, the effects of acute stretch on macroscopic conduction properties will be described, as well as the potential microscopic determinants of the observed changes. The mechanisms through which stretch-induced conduction changes may contribute to the generation, maintenance and stabilization of arrhythmic conditions will be pointed out, complementing the conduction changes produced by acute stretch with the even more deleterious effects chronic dilatation.

11.2 Determination of Stretch Effects on Conduction: Methodological Aspects

The actual determination of stretch effects on atrial conduction in whole-heart preparations involves two principal methodological issues: the definition of dilatation protocols able to elicit significant electrophysiological responses, and the

development of methods for a reliable estimation of conduction properties from the available mapping data. The study of stretch-induced conduction changes in humans by minimally invasive techniques introduces further constraints, which make the task particularly challenging.

11.2.1 Atrial Dilatation Protocols

Acute changes in atrial volume/pressure have been obtained in intact heart animal models by a variety of dilatation protocols. The mainly used techniques include acute volume loading by normal saline solutions (Sideris et al. 1994; Satoh and Zipes 1996) or plasma expander (Wijffels et al. 1997) and inflation of a balloon catheter (Solti et al. 1989; Chorro et al. 1998). Changes in right and left atrial pressures over a wide range of values have been obtained in the Langendorff-perfused rabbit heart (Ravelli and Allessie 1997; Eijsbouts et al. 2003) using the experimental model of biatrial dilatation designed by Ravelli and Allessie (1997). Specifically, the experimental setup provides that the caval and pulmonary veins are ligated and the perfusion fluid entering the right atrium from the coronary sinus is allowed to leave the heart exclusively through a cannula in the pulmonary artery, while the inter-atrial septum is perforated to guarantee an equal pressure in both atria. In this way, the atrial pressure and degree of biatrial dilatation can be controlled simply adjusting the height of the pulmonary outflow cannula (Ravelli and Allessie 1997).

The possibility to extend the study of stretch effects to humans has originated from the observation that atrial pressure and size can be actually controlled by sequential atrioventricular (AV) pacing. Indeed, by monitoring atrial pressure and size in open chest anesthetized dogs during sequential AV pacing, Kaseda and Zipes (1988) showed that these parameters changed at varying AV intervals, with maximal increase in peak and mean atrial pressure and atrial size for AV intervals approaching zero. Based on this principle, stretch effects have been studied in humans by performing simultaneous AV pacing (see Fig. 11.1; Klein et al. 1990; Calkins et al. 1992; Chen et al. 1999; Tse et al. 2001; Ravelli et al. 2011), or during arrhythmic conditions, such as AV node reciprocating tachycardia (Klein et al. 1990), where near simultaneous activation of the atrium and ventricle spontaneously occurs at tachycardia rate. These protocols have been shown to elicit consistent electrophysiological changes in human atria, both in terms of refractory (Klein et al. 1990; Calkins et al. 1992; Chen et al. 1999; Tse et al. 2001) and conduction (Ravelli et al. 2011) properties.

11.2.2 Conduction Velocity Measurements

Different approaches and techniques have been used for the quantification of the conductive properties of the cardiac tissue. The choice of the technique strictly depends on the available mapping system (i.e., the number and displacement of the recording

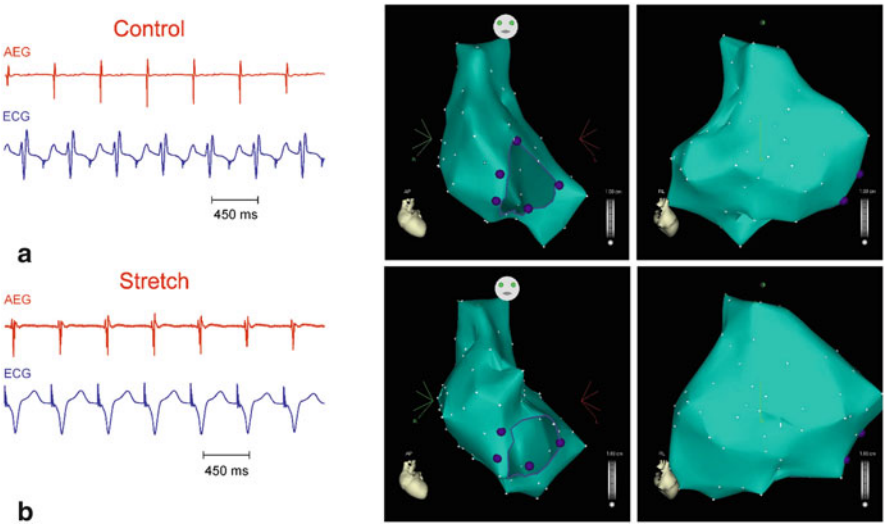

Fig. 11.1 Right atrial dilatation in humans during simultaneous AV pacing. Atrial electrograms (*AEG*) and surface electrocardiograms (*ECG, left* panels), showing the relative timing of atrial and ventricular activations during control (**a**) and simultaneous AV pacing (**b**), are displayed with the anterior and right lateral views of the CARTO-reconstructed right atrium (*central* and *right* panels, respectively). Note the dilatation of the atrial chamber during simultaneous AV pacing. (Modified from Ravelli et al. (2011), with permission)

sites), and determines different levels of estimation accuracy. With a limited number of recording sites available, rough estimates of atrial conduction properties have been obtained in terms of inter/intra-atrial conduction times, by calculating the delay between activation at two different atrial locations (Solti et al. 1989; Sideris et al. 1994). The accuracy of these measures is nevertheless undermined by the impossibility of defining the direction of wavefront propagation. Differently, accurate estimation of conduction properties have been obtained in animal models by mapping the cardiac surface by high-density regularly-spaced electrode grids (Lammers et al. 1990; Bayly et al. 1998; Eijsbouts et al. 2003) or optical mapping techniques (Sung et al. 2003; Mills et al. 2008). Indeed, the construction of phase-maps (Lammers et al. 1990), velocity maps (Eijsbouts et al. 2003) or model-fitted velocity vector fields (Bayly et al. 1998; Sung et al. 2003; Mills et al. 2008) from multisite data has allowed the detection and spatial tracing of activation wavefronts, as well as the local quantification and spatial mapping of conduction properties, leading to the identification of conduction inhomogeneities. Techniques developed for regular grid data are not straightforwardly applicable to clinically-obtained electroanatomic mapping data, since these usually present lower resolution, spatial scattering and irregular spacing. In order to comply with clinical data features, specific methods have been proposed, such as triangulation approaches acting on point triads (Kanagaratnam et al. 2002), linear (Fitzgerald et al. 2003) or cosine (Weber et al. 2010) model fitting of small datasets of points, and scattered-data interpolation techniques

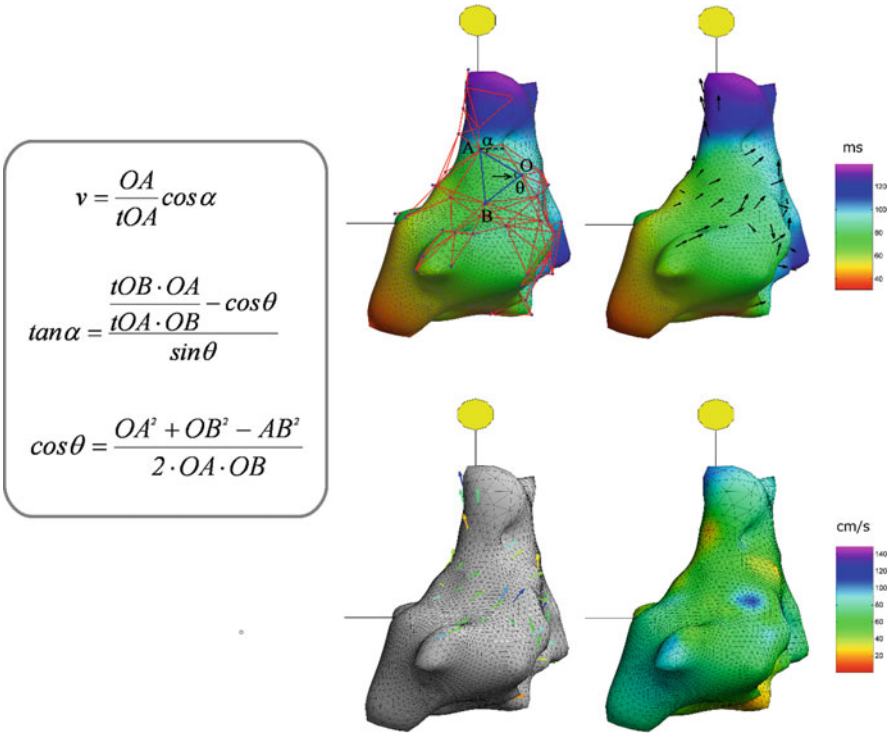

Fig. 11.2 Principles of triangulation method and velocity map construction from clinical mapping data. On the *left*, trigonometric equations used to calculate the velocity vector magnitude (v) and direction (α) from the activation time differences (tOA, tOB) and spatial distances (OA, OB, AB) between triangle vertices. On the right, automated construction of velocity maps by triangulation. In the upper panels, the distributions of eligible point triads (*left*) and averaged velocity vectors (*right*) are displayed over the colored right atrial activation map (*posterior* view). In the lower panels, conduction velocity vectors are color-coded according to their magnitude (*left*) and the corresponding conduction velocity map is obtained by velocity value interpolation (*right*). (Modified from Ravelli et al. (2011), with permission)

(Masè and Ravelli 2010). In particular, several studies (Kanagaratnam et al. 2002; Kojodjojo et al. 2006a, b, 2007; Ravelli et al. 2011) have shown the ability of the triangulation method to accurately measure wave propagation velocity in the direction of wavefront propagation with the access afforded by endocardial mapping in the conscious patient. The triangulation method is simply based on the principle that the magnitude and direction of conduction velocity vectors can be measured using the difference in local activation times and the spatial distance between triads of mapping points (see equations in Fig. 11.2), provided that a single planar wavefront propagates in the plane of measurements and uniform conduction properties are present in the triangle area. The accuracy of triangulation methods is, thus, conditioned by a careful choice of point triads, which have to satisfy spatial and temporal constraints (Kojodjojo et al. 2006a, b, 2007; Ravelli et al. 2011), in order to comply

with triangulation assumptions and limit the effects of inaccuracy factors, such as chamber curvature, local conduction heterogeneity, inaccuracies in activation time estimation, which may be present in real data. Methods for the automatic identification of eligible triads and the spatial averaging of velocity vectors (Ravelli et al. 2011) have been used to improve the basic triangulation method, in order to yield reliable estimates of local conduction velocity, as well as statistically consistent and homogeneous spatial mapping of velocity vectors (Fig. 11.2, right panels).

The measurement of conduction velocity in conditions of atrial stretch involves additional methodological issues. Stretch effects on cardiac conduction may indeed be estimated by two different velocity measures, based on either constant or changing electrode distance (Penefsky and Hoffman 1963; Rosen et al. 1981). "Penefsky and Hoffman (1963) suggested that the conduction velocity measured over a fixed distance was an "apparent" conduction velocity, whereas that measured between two moving sites on a lengthening tissue surface was a "true" conduction velocity" with "Penefsky and Hoffman (1963) suggested that the conduction velocity measured over a fixed distance, in basal and stretch conditions, was an "apparent" conduction velocity, whereas the "true" conduction velocity had to be measured between two moving sites on a lengthening tissue surface". Indeed, in unidimensional fiber preparations, velocity measurements performed at changing distance between marked points guaranteed conduction to occur on the same electrical pathway, i.e., between the same number of cells in both control and stretch conditions. Estimations of "true" conduction velocity have been proposed also in isolated rabbit heart mapping studies with bidimensional electrode arrays (Eijsbouts et al. 2003). Specifically, approximate "true" conduction velocity values were obtained by normalization of "apparent" velocity values for stretch level, assuming that the number of cells varied linearly with distance, as well as conduction properties and stretch levels were homogeneous over the tissue surface. Differently, in experimental settings where these conditions are not satisfactorily met, such as in whole chamber mapping studies (Sung et al. 2003; Mills et al. 2008; Ravelli et al. 2011), the effects of stretch have been quantified just in terms of "apparent" conduction velocity changes. On the other hand, the reconstruction of velocity vector fields from optical (Sung et al. 2003; Mills et al. 2008) or movable catheter (Ravelli et al. 2011) mapping data in these studies provided a global quantification of conduction properties during control and stretch conditions.

11.3 Effects of Acute Stretch on Cardiac Conduction

The relationship between acute mechanical strain and cardiac conduction has been studied since the sixties in a variety of experimental models, but just recently complemented with results from clinical human studies (Ravelli et al. 2011). In their seminal work of 1963, Penefsky and Hoffman (1963) first investigated the conduction changes induced at different strain levels in one-dimensional fiber strips from different animal species and cardiac tissue types. The study revealed a complex biphasic response of conduction velocity to stretch conditions, with an increase of conduction in the low strain range and a decrease in the high strain range. Since then

further studies have observed different types of strain-velocity relationships (McNary et al. 2008), which include biphasic (Penefsky and Hoffman 1963; Rosen et al. 1981; McNary et al. 2008), constant (Spear and More 1972; Reiter et al. 1997; Zhu et al. 1997), increasing (Deck 1964; Dominguez and Fozzard 1979; Tavi et al. 1996) and decreasing (Spear and More 1972; Solti et al. 1989; Sideris et al. 1994; Zabel et al. 1996; Chorro et al. 1998; Eijsbouts et al. 2003; Sung et al. 2003; Mills et al. 2008) behaviors. The heterogeneity of experimental findings may be partially due to the multiplicity of experimental protocols applied, which involved differences in dilatation protocol and stretch range, in animal model and cardiac tissue type, as well as in the definition and quantification of conduction properties. More homogeneous results have been reported in studies based on intact heart animal models and in human studies, where a depression of atrial (Solti et al. 1989; Sideris et al. 1994; Chorro et al. 1998; Eijsbouts et al. 2003; Ravelli et al. 2011) or ventricular (Sung et al. 2003; Mills et al. 2008) conduction was observed at increasing stretch levels. Details concerning the stretch-induced conduction disturbances observed in the atrial tissue will be provided in the following paragraphs for animal models and patient data, respectively.

11.3.1 Stretch-Induced Conduction Disturbances in Animal Model Atria

First evidence of the negative dromotropic effects of stretch on atrial conduction was provided in a dog model (Solti et al. 1989; Sideris et al. 1994), where interatrial conduction times measured in normal conditions were compared with values observed in presence of atrial stretch. Stretch was indeed shown to depress atrial conduction, with a lengthening of the interatrial conduction time when atrial pressure was acutely increased by transfusion (Sideris et al. 1994) or by balloon catheter inflation (Solti et al. 1989). A more accurate description of the phenomenon was provided by high-density mapping studies in the isolated rabbit heart (Chorro et al. 1998; Eijsbouts et al. 2003). Indeed, Chorro et al. (1998) observed a progressive and reversible global reduction of conduction velocity in the right atrium distended by balloon inflation, with conduction velocity decreasing from a control value of 73.3 ± 4.4 cm/s to 66.8 ± 5.1 cm/s to 55.2 ± 3.1 cm/s for average longitudinal dilatations of 24 and 41 %, respectively. Similarly, Eijsbouts et al. (2003) observed a progressive decrease of the normalized right atrial conduction velocity by 35 and 49 % in the rabbit heart, when the atrial pressure was augmented to 9 cm H_2O and 14 cm H_2O by raising the level of an outflow cannula in the pulmonary artery, after occlusion of the caval and pulmonary veins. More interestingly, the authors showed that atrial dilatation not only depressed conduction, but also promoted spatial inhomogeneities in conduction properties, suggesting that the underlying architecture of the atrial myocardium played a significant role in stretch-induced conduction disturbances. In particular, by pacing the atrium from four different atrial sites and computing corresponding high-density activation and velocity maps (Fig. 11.3), the authors revealed a significant increase in the incidence of slow conduction areas

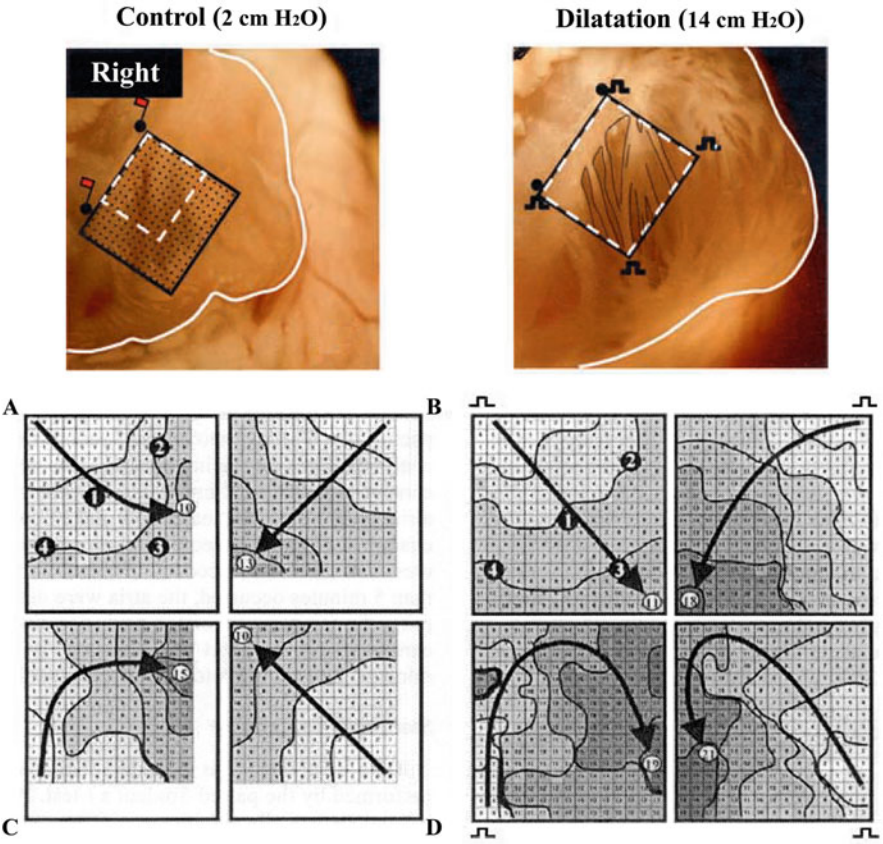

Fig. 11.3 Effects of acute stretch on right atrial conduction in the isolated rabbit heart. Upper panels. Photographs of the free wall of the right atrium at pressures of 2 cm H_2O (control, *left*) and 14 cm H_2O (dilatation, *right*). The mapping array is indicated by the black box and pacing sites are positioned at the box corners. The white dashed lines indicate the same tissue part at increasing degree of dilatation. Lower panels. High-density isochrones maps of the right atrial free wall during high-frequency stimulation from the four pacing sites (a, b, c and d). Note the less uniform conduction and crowding of isochrones during acute dilatation. (Modified from Eijsbouts et al. (2003), with permission)

and conduction block sites during atrial dilatation (right panels) in comparison with basal conditions (left panels), where conduction was instead mostly uniform. The lines of block prevalently occurred along the border of the crista terminalis and larger atrial trabeculae, which could be explained as the consequence of an heterogeneous distribution of wall stress over the atrial surface. The complex architecture of the atrial wall indeed exhibits large variations in orientation and size of muscle bundles, as well as large differences in wall thickness. Since an increase in atrial pressure should stretch the thinner part of the atrium more than the thicker regions (Satoh

and Zipes 1996), the thin epicardial layer, overlaying the trabecular network, may be more sensitive to acute stretch and potentially reach the critical value of conduction block earlier than the thicker bundles. The heterogeneous stretch response of the atrial wall, leading to the formation of lines of blocks and forcing the propagating wavefronts to follow the complex atrial architecture, may have significant consequences on the propagation of activation wavefronts and thus on arrhythmia stabilization.

11.3.2 Stretch-Induced Conduction Disturbances in Human Atria

The effects of acute atrial stretch on conduction properties have been recently analyzed in humans by Ravelli et al. (2011). The investigation was performed in the clinical setting during electrophysiological studies preceding ablation of paroxysmal supraventricular tachycardia. In order to make stretch induction and conduction mapping consistent with clinical practice and minimally invasive techniques, the authors combined simultaneous AV pacing to distend the atria, with electroanatomic mapping and triangulation techniques to quantify and spatially map conduction velocity. Specifically, right atrial mapping was performed by CARTO electroanatomic mapping system during proximal coronary sinus pacing (basal condition) and repeated during simultaneous AV pacing (stretch condition) at a fixed cycle length of 450–500 ms. In order to have an adequate spatial resolution, a mean of 80 mapping points were sampled during each step of the procedure, acquiring three-dimensional coordinates and corresponding activation times in each location. Automatic triangulation of data points was applied to compute conduction velocity vectors and to construct velocity maps and distributions in each patient (Fig. 11.4).

Simultaneous AV pacing produced an overall significant increase of right atrial volume from 72.0 ± 29.0 to 86.3 ± 31.3 ml, which, in turn, induced a depression of atrial conduction. Spatial mapping of conduction velocity in basal and stretch conditions (Fig. 11.4) revealed a significant stretch-induced increase in the extension of slow conduction regions and in the number of sites with velocity smaller than 30 cm/s (red spots in panel A), which resulted in a shift of the conduction velocity distribution towards lower velocity values (panel B). Similarly to the experimental findings in the isolated rabbit heart (Eijsbouts et al. 2003), slow conduction sites were mostly located on the trabecular lateral atrial wall. In the overall population of patients (Fig. 11.5) the authors observed that the 23 ± 14 % increase in atrial volume (left) was accompanied by a significant decrease of median conduction velocity (centre) from 65.8 ± 5.9 cm/s to 55.2 ± 7.2 cm/s and an increase of the incidence of slow conduction areas (right) from 10.3 ± 4.2 % to 15.9 ± 7.7 %.

These results extend to humans the findings obtained in experimental animal models, thus confirming the deleterious action of dilatation on atrial conduction properties, which involves slowed and heterogeneous propagation.

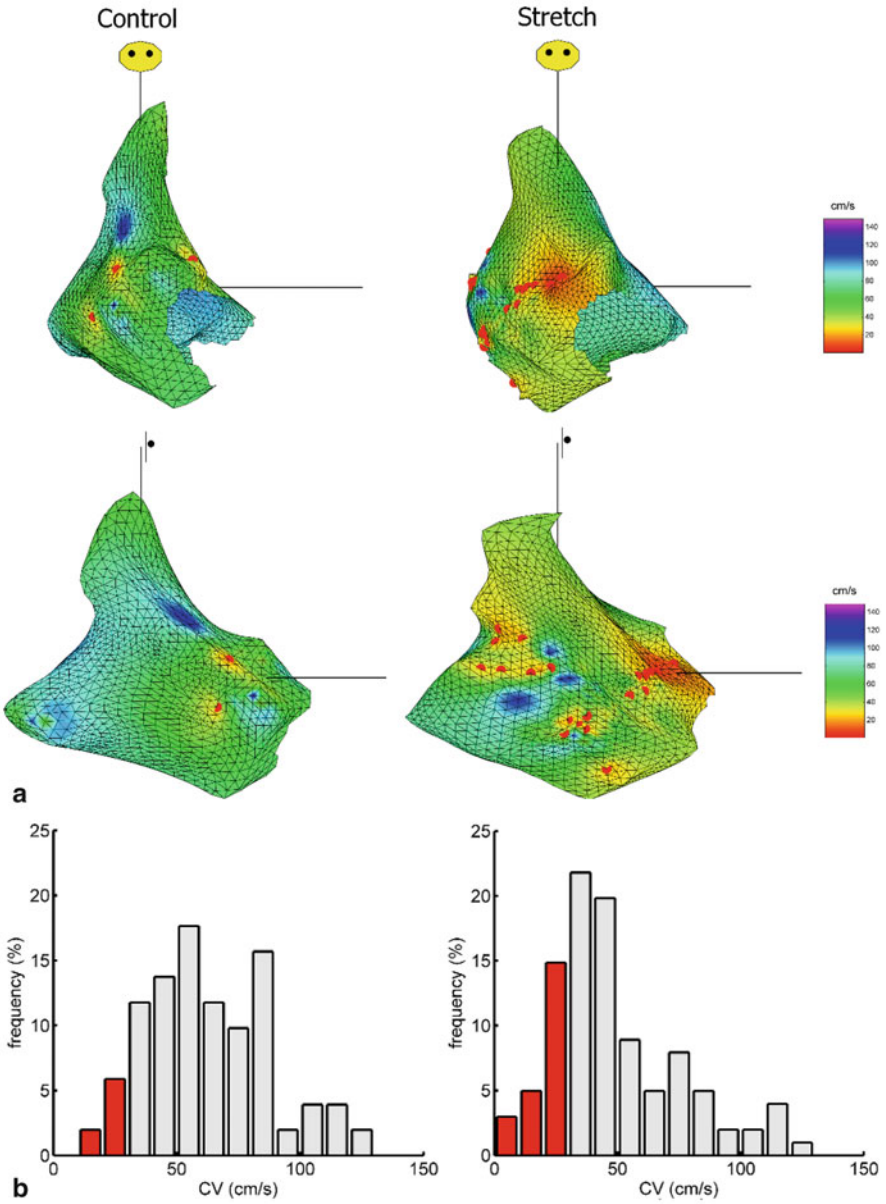

Fig. 11.4 Effects of acute atrial dilatation on conduction velocity (*CV*) distribution in the human right atrium. Anterior and right lateral views of the reconstructed interpolated CV maps (**a**) and corresponding CV histograms (**b**) are shown during control (*left*) and stretch conditions (*right*). *Red* spots in the map mark the slow conduction and local conduction block sites (CV < 30 cm/s). The incidence of slow conduction and block clearly increases during dilatation. (From Ravelli et al. (2011), with permission)

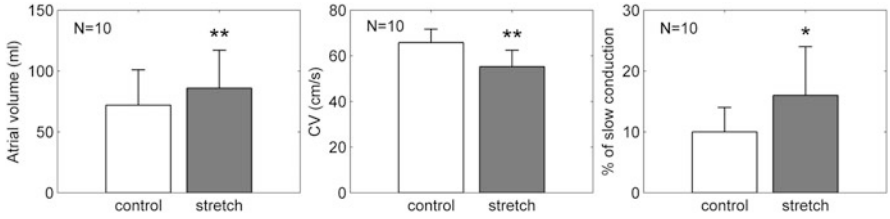

Fig. 11.5 Effects of atrial stretch on right atrial volume (*left*), median conduction velocity (CV, *centre*) and incidence of slow conduction (*right*) in the overall patient population (N = 10). * $p < 0.01$ and ** $p < 0.001$, respectively. (Modified from Ravelli et al. (2011), with permission)

11.4 Microscopic Determinants of Stretch-Induced Conduction Slowing

Propagation in cardiac tissue is a complex process that depends on the active electrical properties of myocyte membranes (membrane excitability and resting membrane potential), the passive (resistive and capacitive) properties of the cellular network (McNary et al. 2008), and the coupling with other non-myocyte cell populations (i.e., fibroblasts; Camelliti et al. 2005; Kamkin et al. 2005; Kohl et al. 2005). Stretch can affect all these properties and the relative contribution of these factors can result in different macroscopic outcomes for different stretch ranges and preparations.

Concerning active electrical properties, myocardial stretch has been associated with a slight depolarization of resting membrane potential, which is mainly attributed to an increased open state probability of stretch-activated ion channels (SAC; Hu and Sachs 1997; Zhang et al. 2000; Kamkin et al. 2003). At moderate levels of strain, membrane depolarization favors conduction by a reduction of the time to activation, while at larger strain the increased depolarization of the membrane leads to inactivation of the sodium channels, reducing upstroke velocity and slowing conduction (McNary et al. 2008). Stretch activated channels may also indirectly affect conduction properties by modulating action potential duration and refractory periods, as demonstrated in computational studies by the dependence of strain-velocity relationship on stimulation rate (Trayanova et al. 2004; Kuijpers et al. 2007; Sachse et al. 2007).

With regards to passive tissue properties, experimental and computer models have shown stretch to affect both resistive and capacitive properties of the cellular network. In computer models including the effects of stretch on tissue conductivity (Sachse et al. 2000, 2002; Kuijpers et al. 2007; McNary et al. 2008), moderate to large levels of stretch were generally assumed to increase the myocardial resistance associated to the cell interior by increasing cell length and decreasing cell cross-sectional area, while the intercellular resistance associated to gap junction was considered strain-independent (McNary et al. 2008). In experimental models, stretch has been shown to increase effective membrane capacitance (Mills et al. 2008), which could be the

result of an increased effective cell membrane surface area-to-volume ratio by uncovering of "surplus" sarcolemma and expansion of sarcolemmal vesicles (Kohl et al. 2003). Interestingly, Mills et al. (2008) have shown that these capacitive effects prevailed over resistive effects in the determination of conduction velocity. Although experimental evidence of the relation between stretch and gap-junction uncoupling is still lacking, it has been suggested that extreme levels of stretch could lead to closure of gap-junction channels, preventing intercellular current flow and conduction, and, possibly, contributing to the formation of conduction blocks (McNary et al. 2008).

In addition to the active and passive properties of myocytes, conduction may be modulated by the interactions between myocytes and other cell populations. In particular, fibroblasts have been recently proposed to play a role as electrical bridges or current sinks. (Camelliti et al. 2005; Kohl et al. 2005), Computer models of cardiac propagation including fibroblasts have indeed confirmed myocyte-fibroblast coupling to significantly affect conduction (Jacquemet and Henriquez 2008; Sachse FB et al. 2009). Since cardiac fibroblasts possess an inherent mechanosensitivity, with fibroblast membrane resistance and potential changing considerably with mechanical stimulation (Camelliti et al. 2005; Kamkin et al. 2005; Kohl et al. 2005), fibroblast-myocyte coupling may affect conduction differently, depending on the acute mechanical loading condition. Further investigation and experimental evidence are, nevertheless, required to better clarify the effective contribution of myocyte-fibroblast interaction in the conduction alterations produced by stretch.

The decrease in conduction velocity observed during acute dilatation in intact heart experimental models and clinical data may be ascribed to a prevalent effect of factors hindering conduction versus factors with facilitating effects, at the stretch level considered. Specifically, conduction disturbances might be the result of a SAC-induced reduction of excitability, an increased membrane capacitance and, potentially, of gap-junctional uncoupling. The possible role of stretch activated channels in stretch-induced disturbances has been indeed evidenced in a simulation study by Kuijpers et al. (2007). In a model of atrial tissue the authors showed that a depolarized resting membrane potential produced by SAC currents could slow conduction by inactivation of Na^+ channels and lowering of maximum upstroke velocity. As concerns the role of capacitive changes, the combination of experimental data and computer modeling in the isolated rabbit heart suggested that the stretch-induced slowing of ventricular conduction was consistent with a prevalent increase of membrane capacitance over reduced intercellular resistance, rather than be mediated by stretch-activated channels (Sung et al. 2003; Mills et al. 2008). The effects on conduction of electrical uncoupling have been investigated by multisite optical mapping in linear strands of cultured neonatal rat ventricular myocytes by Rohr et al. (1998). The authors found that gap junctional uncoupling could have even stronger effects on conduction velocity than a reduction of excitability. In addition, while the latter caused an uniform slowing of conduction, electrical uncoupling made cellular activation patterns change from uniform to highly discontinuous, due to the pronounced spatial differences in the degree of electrical coupling among cells (Rohr et al. 1998). The effects of stretch on gap-junctional coupling and the extent to which electrical coupling has

to decrease to affect wavefront propagation are, however, still a matter of debate and require further investigation.

In addition to the actual depression of conduction, characterized by the slowing of the excitation wavefront along the direction of propagation, the macroscopic decrease of conduction velocity measured in experimental and clinical settings may be due also to an increase in the tortuosity of the trajectories of impulse propagation at the microscopic level, due to the presence of non-excitable blocks (Allessie 2011). This would be consistent with the significant increase in the number of slow conduction sites and lines of conduction block observed during dilatation in both animal (Eijsbouts et al. 2003) and human atria (Ravelli et al. 2011). The presence of these barriers may indeed force the activation wavefront to deviate from a straight course, lengthening the conduction time between recording sites. For instance, zigzag conduction with tortuous routes around unexcitable barriers has been revealed to underline the macroscopic slow conduction areas present in the papillary muscles of patients with myocardial infarction (de Bakker et al. 1993).

Further high-density mapping studies should be performed to elucidate the actual microscopic determinants of stretch-induced conduction disturbances, assessing the relative contribution of depressed conduction and tortuosity of propagation patterns, in order to identify potential targets of therapeutic approaches.

11.5 Contribution of Stretch-Induced Conduction Disturbances to the Arrhythmic Substrate

The previously described conduction impairment induced by conditions of acute atrial dilatation may constitute an important factor for the development of a substrate for atrial arrhythmias. The impairment of conduction may even worsen in presence of prolonged atrial stretch conditions, such as during chronic atrial dilatation, and play a crucial role in the long-term stabilization of atrial fibrillation.

11.5.1 Acute Stretch Contribution

Both animal (Solti et al. 1989; Sideris et al. 1994; Chorro et al. 1998) and human (Ravelli et al. 2011) studies have reported stretch-induced conduction changes to be paralleled by an increased vulnerability of the atria to the development of arrhythmias, suggesting the potential role of conduction disturbances in the creation of an arrhythmic substrate. Experimental data from the distended dog atria showed that the stretch-induced lengthening of interatrial conduction times was accompanied by an augmented propensity to atrial arrhythmias (Solti et al. 1989; Sideris et al. 1994). Indeed, in conditions of left atrial dilatation by balloon inflation, atrial arrhythmias could be regularly induced by an early extrastimulus or burst pacing. As well,

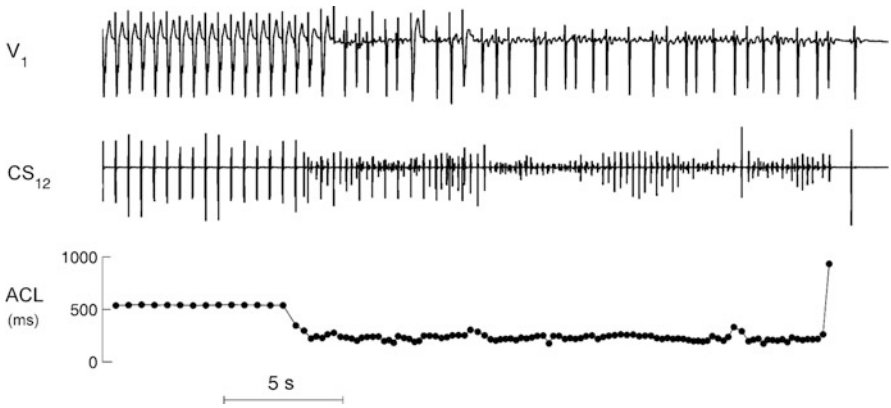

Fig. 11.6 Spontaneous occurrence of atrial fibrillation (*AF*) during acute atrial dilatation by simultaneous AV pacing. ECG (V1), coronary sinus (*CS*) electrogram and atrial cycle length (*ACL*) series recorded during simultaneous AV pacing in a representative patient developing AF. (Modified from Ravelli et al. (2011), with permission)

spontaneous episodes of atrial tachycardia occurred in 38 % of the dilated dog atria (Solti et al. 1989). Similarly, Sideris et al. (1994) observed a higher (57.9 vs 12.5 %) induction of AF by rapid atrial pacing at high (> 14 mmHg) vs low (< 10 mmHg) atrial pressures during transfusion-bleeding. In the isolated rabbit heart, Chorro et al. (1998) showed that the decrease of conduction velocity due to atrial dilatation was accompanied by an increasing number of pacing-induced arrhythmia episodes with respect to basal conditions (22 episode at 24 % longitudinal dilatation vs 5 episodes at control). Finally, in humans, Ravelli et al. (2011) observed a higher occurrence of spontaneous arrhythmic episodes during atrial dilatation (Fig. 11.6), in parallel with conduction impairment. Indeed, while during control condition atrial fibrillation never occurred, during acute atrial dilatation by simultaneous AV pacing six over ten patients developed 15 episodes of AF, four of which had durations longer than ten seconds.

Stretch-induced conduction slowing and increased conduction heterogeneity could both act as predisposing factors for the genesis, modulation and persistence of arrhythmias based on abnormal impulse propagation and reentrant mechanisms. Indeed, the decrease of conduction velocity may contribute to the shortening of the wavelength of excitation (i.e., the product between refractory period and conduction velocity), promoting the formation of reentries of small dimension and allowing an increase of the maximal number of wavelets coexisting on the atrial surface. On the other hand, an increased heterogeneity of electrophysiological properties may favor the formation of unidirectional conduction blocks, as well as provide a central obstacle for reentrant activity (Allessie et al. 1988). The favoring role of heterogeneous conduction on reentry formation has been stressed by Spach and Dolber (1986), who showed that, in nonuniform anisotropic tissue, reentry can occur in very small circuits, within small areas of few mm^2.

Stretch-induced conduction changes may not only favor the onset and maintenance of atrial arrhythmias, but may also modulate the rate of reentrant arrhythmias, such as atrial flutter. The small beat-to-beat variability of atrial flutter cycle length has been indeed correlated to periodic variations of atrial volume/pressure due to hemodynamic changes associated with ventricular contraction and respiration (Lammers et al. 1991; Ravelli et al. 1994, 2008; Masè et al. 2008; Masè et al. 2009). According to the recently formulated mechano-electrical feedback paradigm (Ravelli et al. 2008), changes in atrial volume should modulate atrial flutter rate via direct alteration of circuit size and mechano-electrical modulation of conduction velocity. Specifically, cyclical conditions of acute atrial stretch due to ventricular systole and inspiration would lengthen the reentrant circuit pathway as well as slow the reentrant wavefront, leading to a periodic prolongation of the revolution time around the flutter circuit.

11.5.2 Chronic Stretch Contribution

Large experimental and clinical evidence has demonstrated that chronic atrial dilatation causes an increased stability of AF (Eckstein et al. 2008; Schotten et al. 2011). Interestingly, this occurs in absence of shortening of atrial refractoriness, and is instead related to an increased heterogeneity in conduction. Animal models of chronic atrial dilatation have, indeed, shown that chronic stretch conditions induce severe structural alterations, which concur to a progressive loss of integrity of the lateral connection between neighboring muscle bundles, and yield to macroscopic conduction disturbances and substrate formation. Proarrhythmic structural alterations have been mainly identified in fibrosis (Boyden and Hoffman 1981; Verheule et al. 2003, 2004), myocyte hypertrophy (Ausma et al. 1997; Neuberger et al. 2005, 2006), altered expression and/or distribution of connexin proteins (Haugan et al. 2006; Takeuchi et al. 2006).

Specifically, in a canine model of chronic left atrial dilatation (4–5 weeks) due to mitral regurgitation (MR, see Fig. 11.7a; Verheule et al. 2003, 2004) combined histological analysis (upper panels) and high-resolution optical mapping (lower panels) revealed the presence of areas with inflammatory infiltrates and increased fibrosis, which affected propagation, leading to strong curvature of activation wavefronts, pronounced regional conduction slowing and a marked dependence on propagation direction during high-frequency pacing and premature stimuli introduction. An increased duration of AF episodes was observed concurrently with these alterations, suggesting that the higher stability of AF could be associated with chronic stretch-induced structural changes leading to increased conduction heterogeneity. Similarly, in a goat model exposed to four weeks of complete AV block (Fig. 11.7b; Neuberger et al. 2005, 2006) atrial dilatation was paralleled by a gradual prolongation of AF duration, although no changes in the values or dispersion of the atrial effective refractory period were observed. Atrial mapping during high-rate pacing instead revealed a

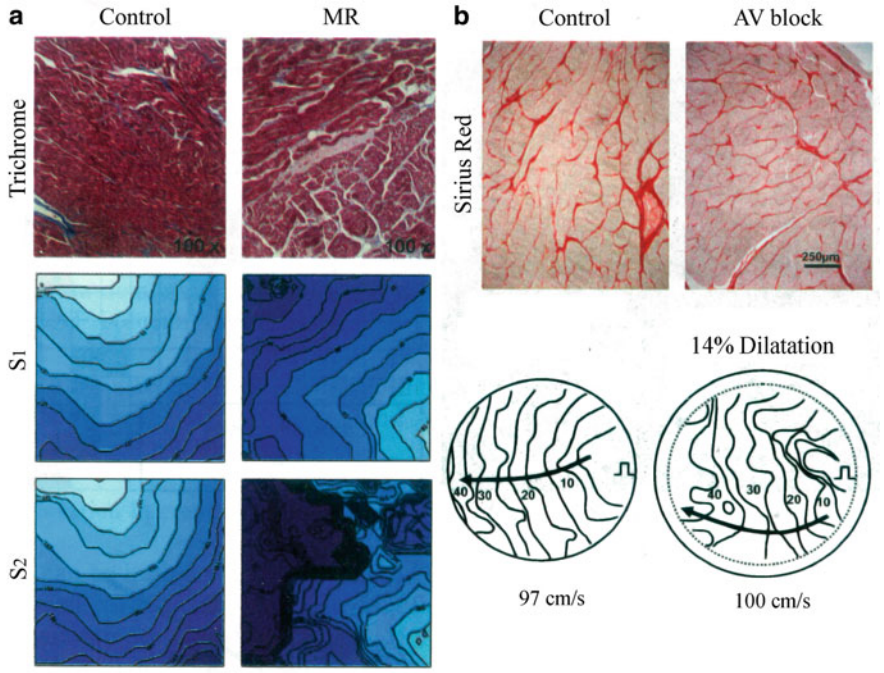

Fig. 11.7 Atrial structure (*upper* panels) and conduction pattern (*lower* panels) in a canine model of chronic left atrial dilatation due to mitral regurgitation (*MR*) (**a**) and in a goat model of biatrial dilatation due to chronic complete AV block (**b**). The dog model presented areas of fibrosis (in *blue*, trichrome staining) and inflammatory infiltrates, which determined slow conduction with strong wavefront curvature at closely coupled premature stimulation (S2). In the goat model, chronic AV block did not increase fibrosis (in *red*, Sirius *red* staining), but areas of slow heterogeneous conduction were revealed by high-frequency pacing. (Modified from Eckstein et al. (2008), with permission)

higher incidence of areas with slow conduction in the chronically-dilated atria (lower panels), which was correlated with an increased myocyte hypertrophy, without signs of fibrosis or alterations in connexin distribution (upper panels). Differently, a significant reduction in the expression levels of both Cx40 and Cx43 protein was observed in a rabbit model with arterio-venous shunt leading to chronic overload (Haugan et al. 2006). In these dogs atrial conduction velocity was significantly decreased, and the atria were more vulnerable to the induction of atrial tachyarrhythmias by burst pacing with respect to control dogs (Hirose et al. 2005). Alterations in the distribution of Cx43, with no changes in expression level, were revealed by confocal microscopy in patient with AF and atrial dilatation (Takeuchi et al. 2006). Nevertheless observations in different clinical studies are not consistent and the actual role of altered connexin distribution patterns in the formation of a substrate for AF remains to be elucidated (Duffy and Wit 2008).

It is worth to notice that the different micro-structural alterations, produced by different chronic dilatation models, had an increased heterogeneity of conduction in common. The connection between structural alterations and conduction properties has been investigated in a series of simulation studies by Spach et al. (Spach and Boineau 1997; Spach et al. 2000, 2004), using a detailed mathematical cell model with well-defined microstructure. Computer simulations showed that in presence of fibrosis and increased transverse fiber separation, transverse propagation might become discontinuous and discrete time delay in activation might appear between adjoining myocytes or myocycte bundles (Spach and Boineau 1997). Similarly, non-uniform distribution of gap-junction and increased cell size had strong effects on conduction anisotropy, leading to pronounced propagation delays between myocyte during transverse propagation (Spach et al. 2000, 2004). Simulation results evidence that with the loss of side-to-side fiber coupling, the myocardial architecture may fail to reestablish a smoothed wavefront at the macroscopic level. As well, spatial nonuniformities of electrical loading may give rise to conduction block and favor reentry (Spach and Boineau 1997).

The progressive loss of integrity between neighboring muscle bundles produced by fibrosis and/or cell hypertrophy, and the consequent electrical dissociation may play a crucial role in the development of a substrate of persistent AF, as shown in both humans and animal models (Spach and Dolber 1986; Allessie et al. 2010; Verheule et al. 2010). In particular, increased longitudinal dissociation, characterized by lines of block running parallel to the atrial musculature, has been recently revealed by epicardial mapping in patients with longstanding AF and structural heart disease involving chronic atrial stretch (Allessie et al. 2010). Similarly, pronounced dissociation of fibrillation waves with large activation time differences has been observed in goats with long-term AF (6 months) with respect to short-term AF (3 weeks), in parallel with an increased myocyte hypertrophy and increased endomysial fibrosis (Verheule et al. 2010). In addition to longitudinal dissociation, electrical dissociation might occur also between different layers of the atrial wall, i.e., between the epicardial layer and the endocardial bundle network (de Groot et al. 2010; Everett et al. 2010; Eckstein et al. 2011). In a recent study in the goat model of persistent AF, Eckstein et al. (2011) have shown that epi-endocardial dissociation can occur as a consequence of AF-induced structural remodeling, and be the result of a progressive electrical uncoupling between the epicardial layer and the endocardial bundle network, instead of a transmural dispersion of refractoriness. Electrical uncoupling resulted both in dyssynchronous activation of the epicardial and endocardial bundle network and in differences in the direction of propagation, which transformed fibrillatory conduction in a three-dimensional process. This transition from a two to a three-dimensional arrhythmic substrate may be of crucial importance in the stabilization of the fibrillatory process. Dissociation of the endocardial and epicardial layers may indeed lead to a consistent increase of the functional area available for wavefront propagation and provide transmural bifurcation and pivot points, prerequisite of epicardial breakthrough events, which more frequently occur in complex substrates of AF (de Groot et al. 2010).

All these findings provide evidence for the crucial role of stretch-induced conduction disturbances in the progressive stabilization of AF, and suggest the potential mechanisms of contribution of conduction changes to the formation of an increasingly complex and multi-dimensional fibrillatory substrate.

11.6 Conclusions and Perspectives

In this chapter we have explored the experimental and clinical evidence which supports the strong interrelation between stretch, conduction impairment and atrial arrhythmias. Starting from seminal experiments on unidimensional fiber preparation and passing through intact heart animal models, the investigation has finally ventured into the measurement of stretch-induced conduction changes in humans in the clinical setting, taking advantage of the progressive advancement of mapping system and signal processing techniques. Evidence gathered in both animal and human atrial models indicates stretch to induce a slowing and increased heterogeneity of conduction, factors which can consistently contribute to the creation of an arrhythmic substrate. Data from high-resolution mapping are now required in order to correlate the macroscopic impairment of conduction with its microscopic determinants, distinguishing an actual depression of the propagated action potential from an increased tortuosity of propagation pathways. A second crucial issue, which needs to be deepened, relies on the effects of prolonged dilatation on atrial conduction and arrhythmia vulnerability, and, in particular, on the time course, irreversibility, and signaling pathways, which may determine structural changes in the chronically dilated myocardium. Acquisition and integration of multiscale data and computer modeling may help to bridge the gap between micro and macroscopic perspectives, in order to identify potential targets for the prevention and treatment of stretch-induced conduction disturbances and arrhythmias, and, thus, to interrupt the deleterious circle formed by the stretch, conduction and atrial fibrillation.

Acknowledgement Michela Masè is recipient of a fellowship supported by Fondazione Cassa di Risparmio di Trento e Rovereto.

References

Allessie MA (2011) Stretch and speed: a complicated couple. J Cardiovasc Electrophysiol 22(4):402–404

Allessie MA, Lammers WJEP, Rensma PL, Schalij MJ, Kirchhof CJHJ (1988) Determinants of reentry in cardiac muscle. Progr Cardiol 1(2):3–15

Allessie MA, de Groot NM, Houben RP, Schotten U, Boersma E, Smeets JL, Crijns HJ (2010) Electropathological substrate of long-standing persistent atrial fibrillation in patients with structural heart disease: longitudinal dissociation. Circ Arrhythm Electrophysiol 3(6):606–615

Allessie M, Ausma J, Schotten U (2002) Electrical, contractile and structural remodeling during atrial fibrillation. Cardiovasc Res 54(2):230–246

Ausma J, Wijffels M, Thone F, Wouters L, Allessie M, Borgers M (1997) Structural changes of atrial myocardium due to sustained atrial fibrillation in the goat. Circulation 96(9):3157–3163

Bayly PV, KenKnight BH, Rogers JM, Hillsley RE, Ideker RE, Smith WM (1998) Estimation of conduction velocity vector fields from epicardial mapping data. IEEE Trans Biomed Eng 45(5):563–571

Boyden PA, Hoffman BF (1981) The effects on atrial electrophysiology and structure of surgically induced right atrial enlargement in dogs. Circ Res 49(6):1319–1331

Brodsky MA, Allen BJ, Capparelli EV, Luckett CR, Morton R, Henry WL (1989) Factors determining maintenance of sinus rhythm after chronic atrial fibrillation with left atrial dilatation. Am J Cardiol 63(15):1065–1068

Calkins H, el Atassi R, Kalbfleisch S, Langberg J, Morady F (1992) Effects of an acute increase in atrial pressure on atrial refractoriness in humans. PACE 15(11 Pt 1):1674–1680

Camelliti P, Borg TK, Kohl P (2005) Structural and functional characterization of cardiac fibroblast. Cardiovasc Res 65:40–51

Chang SL, Chen YC, Chen YJ, Wangcharoen W, Lee SH, Lin CI, Chen SA (2007) Mechanoelectrical feedback regulates the arrhythmogenic activity of pulmonary veins. Heart 93(1):82–88

Chen YJ, Tai CT, Chiou CW, Wen ZC, Chan P, Lee SH, Chen SA (1999) Inducibility of atrial fibrillation during atrioventricular pacing with varying intervals: role of atrial electrophysiology and the autonomic nervous system. J Cardiovasc Electrophysiol 10(12):1578–1585

Chorro FJ, Egea S, Mainar L, Canoves J, Sanchis J, Llavador E, Lopez-Merino V, Such L (1998) Acute changes in wavelength of the process of auricular activation induced by stretching. Experimental study. Rev Esp Cardiol 51(11):874–883

de Bakker JM, van Capelle FJ, Janse MJ, Tasseron S, Vermeulen JT, de Jonge N, Lahpor JR (1993) Slow conduction in the infarcted human heart. 'Zigzag' course of activation. Circulation 88(3):915–926

de Groot NM, Houben RP, Smeets JL, Boersma E, Schotten U, Schalij MJ, Crijns H, Allessie MA (2010) Electropathological substrate of longstanding persistent atrial fibrillation in patients with structural heart disease: epicardial breakthrough. Circulation 122(17):1674–1682

Deck KA (1964) Changes in the resting potential and the cable properties of Purkinje fibers during stretch. Pflugers Arch Gesamte Physiol Menschen Tiere 280:131–140

Dominguez G, Fozzard HA (1979) Effect of stretch on conduction velocity and cable properties of cardiac Purkinje fibers. Am J Physiol 237(3):C119–C124

Dreifus LS (1993) Arrhythmias in valvular heart disease. Cardiovasc Clin 23:65–74

Duffy HS, Wit AL (2008) Is there a role for remodeled connexins in AF? No simple answers. J Mol Cell Cardiol 44(1):4–13

Eckstein J, Verheule S, de Groot NM, Allessie M, Schotten U (2008) Mechanisms of perpetuation of atrial fibrillation in chronically dilated atria. Prog Biophys Mol Biol 97(2–3):435–451

Eckstein J, Maesen B, Linz D, Zeemering S, van Hunnik A, Verheule S, Allessie M, Schotten U (2011) Time course and mechanisms of endo-epicardial electrical dissociation during atrial fibrillation in the goat. Cardiovasc Res 89(4):816–824

Eijsbouts S, Van Zandvoort M, Schotten U, Allessie M (2003) Effects of acute atrial dilation on heterogeneity in conduction in the isolated rabbit heart. J Cardiovasc Electrophysiol 14(3):269–278

Everett TH, Wilson EE, Hulley GS, Olgin JE (2010) Transmural characteristics of atrial fibrillation in canine models of structural and electrical atrial remodeling assessed by simultaneous epicardial and endocardial mapping. Heart Rhythm 7(4):506–517

Fitzgerald TN, Rhee EK, Brooks DH, Triedman JK (2003) Estimation of cardiac conduction velocities using small data sets. Ann Biomed Eng 31(3):250–261

Francis GS (1986) Development of arrhythmias in the patient with congestive heart failure: pathophysiology, prevalence and prognosis. Am J Cardiol 57(3):3B–7B

Haugan K, Miyamoto T, Takeishi Y, Kubota I, Nakayama J, Shimojo H, Hirose M (2006) Rotigaptide (ZP123) improves atrial conduction slowing in chronic volume overload-induced dilated atria. Basic Clin Pharmacol Toxicol 99(1):71–79

Hirose M, Takeishi Y, Miyamoto T, Kubota I, Laurita KR, Chiba S (2005) Mechanism for atrial tachyarrhythmia in chronic volume overload-induced dilated atria. J Cardiovasc Electrophysiol 16(7):760–769

Hoglund C, Rosenhamer G (1985) Echocardiographic left atrial dimension as a predictor of maintaining sinus rhythm after conversion of atrial fibrillation. Acta Med Scand 217(4):411–415

Hu H, Sachs F (1997) Stretch-activated ion channels in the heart. J Mol Cell Cardiol 29(6):1511–1523

Jacquemet V, Henriquez CS (2008) Loading effect of fibroblast-myocyte coupling on resting potential, impulse propagation, and repolarization: insights from a microstructure model. Am J Physiol Heart Circ Physiol 294(5):H2040–H2052

Kalifa J, Jalife J, Zaitsev AV, Bagwe S, Warren M, Moreno J, Berenfeld O, Nattel S (2003) Intra-atrial pressure increases rate and organization of waves emanating from the superior pulmonary veins during atrial fibrillation. Circulation 108(6):668–671

Kamkin A, Kiseleva I, Wagner KD, Leiterer KP, Theres H, Scholz H, Gunther J, Lab MJ (2000) Mechano-electric feedback in right atrium after left ventricular infarction in rats. J Mol Cell Cardiol 32(3):465–477

Kamkin A, Kiseleva I, Wagner KD, Bohm J, Theres H, Gunther J, Scholz H (2003) Characterization of stretch-activated ion currents in isolated atrial myocytes from human hearts. Pflugers Arch 446(3):339–346

Kamkin A, Kiseleva I, Lozinsky I, Scholz H (2005) Electrical interaction of mechanosensitive fibroblasts and myocytes in the heart. Basic Res Cardiol 100(4):337–345

Kanagaratnam P, Rothery S, Patel P, Severs NJ, Peters NS (2002) Relative expression of immunolocalized connexins 40 and 43 correlates with human atrial conduction properties. J Am Coll Cardiol 39(1):116–123

Kaseda S, Zipes DP (1988) Contraction-excitation feedback in the atria: a cause of changes in refractoriness. J Am Coll Cardiol 11(6):1327–1336

Keren G, Etzion T, Sherez J, Zelcer AA, Megidish R, Miller HI, Laniado S (1987) Atrial fibrillation and atrial enlargement in patients with mitral stenosis. Am Heart J 114(5):1146–1155

Klein LS, Miles WM, Zipes DP (1990) Effect of atrioventricular interval during pacing or reciprocating tachycardia on atrial size, pressure, and refractory period. Contraction-excitation feedback in human atrium. Circulation 82(1):60–68

Kohl P, Cooper PJ, Holloway H (2003) Effects of acute ventricular volume manipulation on in situ cardiomyocyte cell membrane configuration. Prog Biophys Mol Biol 82(1–3):221–227

Kohl P, Camelliti P, Burton FL, Smith GL (2005) Electrical coupling of fibroblasts and myocytes: relevance for cardiac propagation. J Electrocardiol 38(4 Suppl):45–50

Kojodjojo P, Kanagaratnam P, Markides V, Davies DW, Peters N (2006a) Age-related changes in human left and right atrial conduction. J Cardiovasc Electrophysiol 17(2):120–127

Kojodjojo P, Kanagaratnam P, Segal OR, Hussain W, Peters NS (2006b) The effects of carbenoxolone on human myocardial conduction: a tool to investigate the role of gap junctional uncoupling in human arrhythmogenesis. J Am Coll Cardiol 48(6):1242–1249

Kojodjojo P, Peters NS, Davies DW, Kanagaratnam P (2007) Characterization of the electroanatomical substrate in human atrial fibrillation: the relationship between changes in atrial volume, refractoriness, wavefront propagation velocities, and AF burden. J Cardiovasc Electrophysiol 18(3):269–275

Kuijpers NH, ten Eikelder HM, Bovendeerd PH, Verheule S, Arts T, Hilbers PA (2007) Mechanoelectric feedback leads to conduction slowing and block in acutely dilated atria: a modeling study of cardiac electromechanics. Am J Physiol Heart Circ Physiol 292(6):H2832–H2853

Lammers WJ, Schalij MJ, Kirchhof CJ, Allessie MA (1990) Quantification of spatial inhomogeneity in conduction and initiation of reentrant atrial arrhythmias. Am J Physiol 259(4 Pt 2):H1254–H1263

Lammers WJ, Ravelli F, Disertori M, Antolini R, Furlanello F, Allessie MA (1991) Variations in human atrial flutter cycle length induced by ventricular beats: evidence of a reentrant circuit with a partially excitable gap. J Cardiovasc Electrophysiol 2(5):375–387

Masè M, Ravelli F (2010) Automatic reconstruction of activation and velocity maps from electro-anatomic data by radial basis functions. Conf Proc IEEE Eng Med Biol Soc 12608–2611

Masè M, Glass L, Ravelli F (2008) A model for mechano-electrical feedback effects on atrial flutter interval variability. Bull Math Biol 70(5):1326–1347

Masè M, Disertori M, Ravelli F (2009) Cardiorespiratory interactions in patients with atrial flutter. J Appl Physiol 106(1):29–39

McNary TG, Sohn K, Taccardi B, Sachse FB (2008) Experimental and computational studies of strain-conduction velocity relationships in cardiac tissue. Prog Biophys Mol Biol 97(2–3):383–400

Mills RW, Narayan SM, McCulloch AD (2008) Mechanisms of conduction slowing during myocardial stretch by ventricular volume loading in the rabbit. Am J Physiol Heart Circ Physiol 295(3):H1270–H1278

Nazir SA, Lab MJ (1996) Mechanoelectric feedback and atrial arrhythmias. Cardiovasc Res 32(1):52–61

Neuberger HR, Schotten U, Verheule S, Eijsbouts S, Blaauw Y, van Hunnik A, Allessie M (2005) Development of a substrate of atrial fibrillation during chronic atrioventricular block in the goat. Circulation 111(1):30–37

Neuberger HR, Schotten U, Blaauw Y, Vollmann D, Eijsbouts S, van Hunnik A, Allessie M (2006) Chronic atrial dilation, electrical remodeling, and atrial fibrillation in the goat. J Am Coll Cardiol 47(3):644–653

Packer M (1985) Sudden unexpected death in patients with congestive heart failure: a second frontier. Circulation 72(4):681–685

Penefsky Z, Hoffman B (1963) Effect of stretch on mechanical and electrical properties of the cardiac muscle. Am J Physiol 204:433–438

Petersen P, Kastrup J, Brinch K, Godtfredsen J, Boysen G (1987) Relation between left atrial dimension and duration of atrial fibrillation. Am J Cardiol 60(4):382–384

Probst P, Goldschlager N, Selzer A (1973) Left atrial size and atrial fibrillation in mitral stenosis. Factors influencing their relationship. Circulation 48(6):1282–1287

Psaty BM, Manolio TA, Kuller LH, Kronmal RA, Cushman M, Fried LP, White R, Furberg CD, Rautaharju PM (1997) Incidence of and risk factors for atrial fibrillation in older adults. Circulation 96(7):2455–2461

Ravelli F, Masè M, Disertori M (2008) Mechanical modulation of atrial flutter cycle length. Prog Biophys Mol Biol 97(2–3):417–434

Ravelli F, Masè M, Del Greco M, Marini M, Disertori M (2011) Acute atrial dilatation slows conduction and increases AF vulnerability in the human atrium. J Cardiovasc Electrophysiol 22(4):394–401

Ravelli F (2003) Mechano-electric feedback and atrial fibrillation. Progr Biophys Mol Biol 82(1–3):137–149

Ravelli F, Allessie M (1997) Effects of atrial dilatation on refractory period and vulnerability to atrial fibrillation in the isolated Langendorff-perfused rabbit heart. Circulation 96(5):1686–1695

Ravelli F, Disertori M, Cozzi F, Antolini R, Allessie MA (1994) Ventricular beats induce variations in cycle length of rapid (type II) atrial flutter in humans. Evidence of leading circle reentry. Circulation 89(5):2107–2116

Reiter MJ, Landers M, Zetelaki Z, Kirchhof CJ, Allessie MA (1997) Electrophysiological effects of acute dilatation in the isolated rabbit heart: cycle length-dependent effects on ventricular refractoriness and conduction velocity. Circulation 96(11):4050–4056

Rohr S, Kucera JP, Kleber AG (1998) Slow conduction in cardiac tissue, I: effects of a reduction of excitability versus a reduction of electrical coupling on microconduction. Circ Res 83(8):781–794

Rosen MR, Legato MJ, Weiss RM (1981) Developmental changes in impulse conduction in the canine heart. Am J Physiol 240(4):H546–H554

Sachse FB, Seemann G, Riedel C, Werner CD, Dössel O (2000) Modeling of the cardiac mechano-electrical feedback. Int J Bioelectromagn 2(2)

Sachse FB, Seemann G, Riedel C (2002) Modeling of cardiac excitation propagation taking deformation into account. Proc BIOMAG 2002:839–841

Sachse FB, Hunter GA, Weiss DL, Seemann G (2007) A framework for modeling of mechano-electrical feedback mechanisms of cardiac myocytes and tissues. Conf Proc IEEE Eng Med Biol Soc 2007:160–163

Sachse FB, Moreno AP, Seemann G, Abildskov JA (2009) A model of electrical conduction in cardiac tissue including fibroblasts. Ann Biomed Eng 37(5):874–889

Sanfilippo AJ, Abascal VM, Sheehan M, Oertel LB, Harrigan P, Hughes RA, Weyman AE (1990) Atrial enlargement as a consequence of atrial fibrillation. A prospective echocardiographic study. Circulation 82(3):792–797

Satoh T, Zipes DP (1996) Unequal atrial stretch in dogs increases dispersion of refractoriness conducive to developing atrial fibrillation. J Cardiovasc Electrophysiol 7(9):833–842

Schotten U, Allessie M (2001) Electrical and mechanical remodeling of the atria: What are the underlying mechanisms, the time course and the clinical relevance? In: Raviele A (ed) Cardiac Arrhythmias 2001. Springer, Milan, pp 345–352

Schotten U, Verheule S, Kirchhof P, Goette A (2011) Pathophysiological mechanisms of atrial fibrillation: a translational appraisal. Physiol Rev 91(1):265–325

Sideris DA (1993) High blood pressure and ventricular arrhythmias. Eur Heart J 14(11):1548–1553

Sideris DA, Toumanidis ST, Thodorakis M, Kostopoulos K, Tselepatiotis E, Langoura C, Stringli T, Moulopoulos SD (1994) Some observations on the mechanism of pressure related atrial fibrillation. Eur Heart J 15(11):1585–1589

Solti F, Vecsey T, Kekesi V, Juhasz-Nagy A (1989) The effect of atrial dilatation on the genesis of atrial arrhythmias. Cardiovasc Res 23(10):882–886

Spach MS, Boineau JP (1997) Microfibrosis produces electrical load variations due to loss of side-to-side cell connections: a major mechanism of structural heart disease arrhythmias. PACE 20(2 Pt 2):397–413

Spach MS, Dolber PC (1986) Relating extracellular potentials and their derivatives to anisotropic propagation at a microscopic level in human cardiac muscle. Evidence for electrical uncoupling of side-to-side fiber connections with increasing age. Circ Res 58(3):356–371

Spach MS, Heidlage JF, Dolber PC, Barr RC (2000) Electrophysiological effects of remodeling cardiac gap junctions and cell size: experimental and model studies of normal cardiac growth. Circ Res 86(3):302–311

Spach MS, Heidlage JF, Barr RC, Dolber PC (2004) Cell size and communication: role in structural and electrical development and remodeling of the heart. Heart Rhythm 1(4):500–515

Spear JF, More EN (1972) Stretch-induced excitation and conduction disturbances in the isolated rat myocardium. J Electrocardiol 5(1):15–24

Suarez GS, Lampert S, Ravid S, Lown B (1991) Changes in left atrial size in patients with lone atrial fibrillation. Clin Cardiol 14(8):652–656

Sung D, Mills RW, Schettler J, Narayan SM, Omens JH, McCulloch AD (2003) Ventricular filling slows epicardial conduction and increases action potential duration in an optical mapping study of the isolated rabbit heart. J Cardiovasc Electrophysiol 14(7):739–749

Takeuchi S, Akita T, Takagishi Y, Watanabe E, Sasano C, Honjo H, Kodama I (2006) Disorganization of gap junction distribution in dilated atria of patients with chronic atrial fibrillation. Circ J 70(5):575–582

Tavi P, Laine M, Weckstrom M (1996) Effect of gadolinium on stretch-induced changes in contraction and intracellularly recorded action- and afterpotentials of rat isolated atrium. Br J Pharmacol 118(2):407–413

Trayanova N, Li W, Eason J, Kohl P (2004) Effect of stretch-activated channels on defibrillation efficacy. Heart Rhythm 1(1):67–77

Tse HF, Pelosi F, Oral H, Knight BP, Strickberger SA, Morady F (2001) Effects of simultaneous atrioventricular pacing on atrial refractoriness and atrial fibrillation inducibility: role of atrial mechanoelectrical feedback. J Cardiovasc Electrophysiol 12(1):43–50

Vaziri SM, Larson MG, Benjamin EJ, Levy D (1994) Echocardiographic predictors of nonrheumatic atrial fibrillation. The Framingham Heart Study. Circulation 89(2):724–730

Verheule S, Wilson E, Everett T, Shanbhag S, Golden C, Olgin J (2003) Alterations in atrial electrophysiology and tissue structure in a canine model of chronic atrial dilatation due to mitral regurgitation. Circulation 107(20):2615–2622

Verheule S, Wilson E, Banthia S, Everett TH, Shanbhag S, Sih HJ, Olgin J (2004) Direction-dependent conduction abnormalities in a canine model of atrial fibrillation due to chronic atrial dilatation. Am J Physiol Heart Circ Physiol 287(2):H634–H644

Verheule S, Tuyls E, van Hunnik A, Kuiper M, Schotten U, Allessie M (2010) Fibrillatory conduction in the atrial free walls of goats in persistent and permanent atrial fibrillation. Circ Arrhythm Electrophysiol 3(6):590–599

Weber FM, Schilling C, Seemann G, Luik A, Schmitt C, Lorenz C, Dossel O (2010) Wave-direction and conduction-velocity analysis from intracardiac electrograms-a single-shot technique. IEEE Trans Biomed Eng 57(10):2394–2401

Wijffels MC, Kirchhof CJ, Dorland R, Allessie MA (1995) Atrial fibrillation begets atrial fibrillation. A study in awake chronically instrumented goats. Circulation 92(7):1954–1968

Wijffels MC, Kirchhof CJ, Dorland R, Power J, Allessie MA (1997) Electrical remodeling due to atrial fibrillation in chronically instrumented conscious goats: roles of neurohumoral changes, ischemia, atrial stretch, and high rate of electrical activation. Circulation 96(10):3710–3720

Zabel M, Portnoy S, Franz MR (1996) Effect of sustained load on dispersion of ventricular repolarization and conduction time in the isolated intact rabbit heart. J Cardiovasc Electrophysiol 7(1):9–16

Zhang YH, Youm JB, Sung HK, Lee SH, Ryu SY, Ho WK, Earm YE (2000) Stretch-activated and background non-selective cation channels in rat atrial myocytes. J Physiol 523:607–619

Zhu WX, Johnson SB, Brandt R, Burnett J, Packer DL (1997) Impact of volume loading and load reduction on ventricular refractoriness and conduction properties in canine congestive heart failure. J Am Coll Cardiol 30(3):825–833

Chapter 12
Early Activation of Intracellular Signals after Myocardial Stretch: Anrep Effect, Myocardial Hypertrophy and Heart Failure

Horacio E. Cingolani, María C. Villa-Abrille, Claudia I. Caldiz, Irene L. Ennis, Oscar H. Cingolani, Patricio E. Morgan, Ernesto A. Aiello and Néstor Gustavo Pérez

12.1 Introduction

The link between the Anrep effect and myocardial hypertrophy and failure, although obvious–since this effect is the result of myocardial strain- was not appreciated until we proposed it in the 2005 edition of the book "Mechanosensitivity in Cells and Tissues". Previous experiments by Izumo and Sadoshima (Sadoshima et al. 1993), Ito et al. (1993) and Yamazaki et al. (1996) performed in neonatal cardiomyocytes showed that mechanical stretch induces the release of preformed angiotensin II (A2) to the surrounding media, yet these findings were never linked to the Anrep effect, a phenomenon originally described in the open chest dog model (von Anrep 1912). Furthermore, Ito et al. (1993) showed that in stretched-conditioned medium where A2 was released, the hypertrophic signals were abolished by interfering with the endothelin (ET) action, finding that is in agreement with our own results demonstrating that stretching adult myocardium releases A2 (or activates the AT1 receptor by deformation) triggering the release and/or formation of ET (for review see Cingolani et al. 2011a).

12.2 The Anrep Effect

Although the contractile performance of the heart is under continuous neurohormonal and electrophysiological influence, the heart possesses intrinsic mechanisms, adapting to different hemodynamic conditions by changing its cardiac output. An

H. E. Cingolani (✉) · M. C. Villa-Abrille · C. I. Caldiz · I. L. Ennis · P. E. Morgan · E. A. Aiello · N. G. Pérez
Centro de Investigaciones Cardiovasculares, Facultad de Ciencias Médicas, Universidad Nacional de La Plata, Calle 60 y 120, 1900 La Plata, Argentina
e-mail: cicmes@infovia.com.ar

O. H. Cingolani
Division of Cardiology, Johns Hopkins University Hospital, 720 Rutland Avenue, Ross 835, Baltimore, MD 21205, USA

A. Kamkin, I. Lozinsky (eds.), *Mechanically Gated Channels and their Regulation,* Mechanosensitivity in Cells and Tissues 6,
DOI 10.1007/978-94-007-5073-9_12,

increase in ventricular end diastolic volume, induced by increasing aortic resistance to ejection or venous return, leads to a more powerful contraction. This occurs immediately and is the well-known Frank-Starling mechanism that allows the heart to increase its output after an increase in venous return or to eject the same stroke volume against a greater afterload. However, over the next 10 or 15 min after the sudden stretch, there is a further increase in myocardial performance and the end diastolic volume returns towards its original value. The time constant of this phenomenon will depend on several factors such as species differences, temperature, coronary blood flow, etc. In 1912, von Anrep showed that after clamping the ascending aorta in a dog (acutely decreasing outflow and increasing intraventricular pressures), its heart initially dilated. This was followed by a progressive decline in heart volumes towards initial values over the next minutes (von Anrep 1912). Von Anrep interpreted these findings as secondary to a positive inotropic effect mediated by the release of cathecolamines by the adrenal glands, which were receiving low blood flow. In 1959 Rosenblueth et al. (1959) called attention to the fact that both, an increase in heart rate (Bowditch effect) and in afterload augmented the contractility in the isolated canine right ventricle, "the two staircase phenomenon". Sarnoff, in 1960, coined the term "homeometric autoregulation" to define the decrease in left ventricular end diastolic volume after the initial increase in diastolic volume that occurs after an increase in afterload (Sarnoff et al. 1960). Since both reports (Rosenblueth et al. 1959; Sarnoff et al. 1960) were based on experiments performed in isolated hearts, the possibility of a positive inotropic effect due to the release of cathecolamines by the adrenal glands was ruled out.

In 1973, Parmley and Chuck reproduced this phenomenon in isolated strips of ventricular myocardium (Parmley and Chuck 1973). They showed that if the length of the muscle was increased, there were corresponding rapid and slow increases in developed force. The rapid change in force is thought to be the basis of the Frank-Starling mechanism and occurs secondary to an increase in myofilament Ca^{2+} sensitivity (Hofmann and Fuchs 1988). The slow force response (SFR) after a change in length is due to a progressive increase in the Ca^{2+} transient, as demonstrated by Allen and Kurihara in 1982 (Allen and Kurihara 1982) and later on confirmed by other authors, including us (Kentish and Wrzosek 1998; Alvarez et al. 1999). Parmley and Chuck also ruled out the possible role played by cathecolamines at the nerve endings in the development of the SFR, since the response was also present in isolated muscles from reserpinized animals (Parmley and Chuck 1973).

Although the cellular and molecular bases of the Frank-Starling mechanism (or "heterometric autoregulation") are well-known and involve mainly an increase in the response of cardiac myofilaments to calcium (Hofmann and Fuchs 1988), the mechanism of the Anrep effect (homeometric autoregulation) is less understood. It is accepted that the increase in cardiac contractility that develops during the 10–15 min following muscle stretch can be quantitatively explained by a progressive increase in calcium transients (Allen and Kurihara 1982; Kentish and Wrzosek 1998; Alvarez et al. 1999). However, the source for this increase in calcium was less understood. It could not be explained by a hyperactive sarcoplasmic reticulum (SR) (Kentish and Wrzosek 1998) nor by an increased transarcolemmal calcium current (Hongo et al.

1996). The mechanism leading to the increase in the calcium transient was clarified by experiments performed in our laboratory that demonstrated a link between calcium influx and an autocrine/paracrine response to muscle stretch (Cingolani et al. 1998, 2003a; Alvarez et al. 1999; Perez et al. 2001, 2011; Caldiz et al. 2007; Villa-Abrille et al. 2010).

12.3 The Autocrine/Paracrine Loop Triggered by Myocardial Stretch

As stated before, the stretch of cardiac muscle increases developed force in two phases. The first phase, which occurs rapidly, is generally attributed to enhanced myofilament responsiveness to calcium and is probably not affected by the autocrine/paracrine mechanism. The second phase (SFR) occurs gradually and is due to an increase in the calcium transient amplitude as a result of the autocrine/paracrine mechanism. The SFR was proposed to be the in vitro equivalent of the Anrep phenomenon and its genesis was unknown until we proposed that Na^+/H^+ exchanger (NHE-1) activation was the main step in the autocrine/paracrine mechanism leading to the increase in contractility by increasing intracellular sodium and calcium (Alvarez et al. 1999).

Most intracellular pathways leading to cardiac hypertrophy and failure are triggered by increases in intracellular calcium levels. Actually, the rise in cardiac muscle calcium causing the SFR or Anrep effect occurs as fast as 10–15 min after stretch. It is surprising that most investigators working in the field of excitation-contraction coupling and cardiac mechanics have not established a link between the Anrep effect and cardiac hypertrophy and failure. Interestingly, while several years ago we proposed the crucial role of the NHE-1 in the SFR development, more recently, elegant experiments by Wakabayashi's group demonstrated that NHE-1 activation is sufficient to generate calcium signals causing cardiac hypertrophy and failure (Nakamura et al. 2008).

An attractive idea, albeit speculative, will be that the fate of the myocardium may be determined during the first few minutes after stretch (i.e. it is possible that a pharmacological intervention that prevents the development of the Anrep effect might blunt the subsequent hypertrophy and failure). Approximately 23 million people are affected with heart failure, and 2 million new cases of heart failure are diagnosed each year worldwide. All the basic studies mentioned in this chapter need to be considered when designing new therapeutic strategies in the treatment of cardiac hypertrophy and failure. A clear understanding of the early triggering mechanisms that stretch imposes to the myocardium will allow us to design novel weapons to win the battle against this major disease.

In the next sections, we will present the experimental evidence that led us to propose the autocrine/paracrine mechanism underlying the SFR, as well as its resemblance to signals that have been described for cardiac hypertrophy development and heart failure.

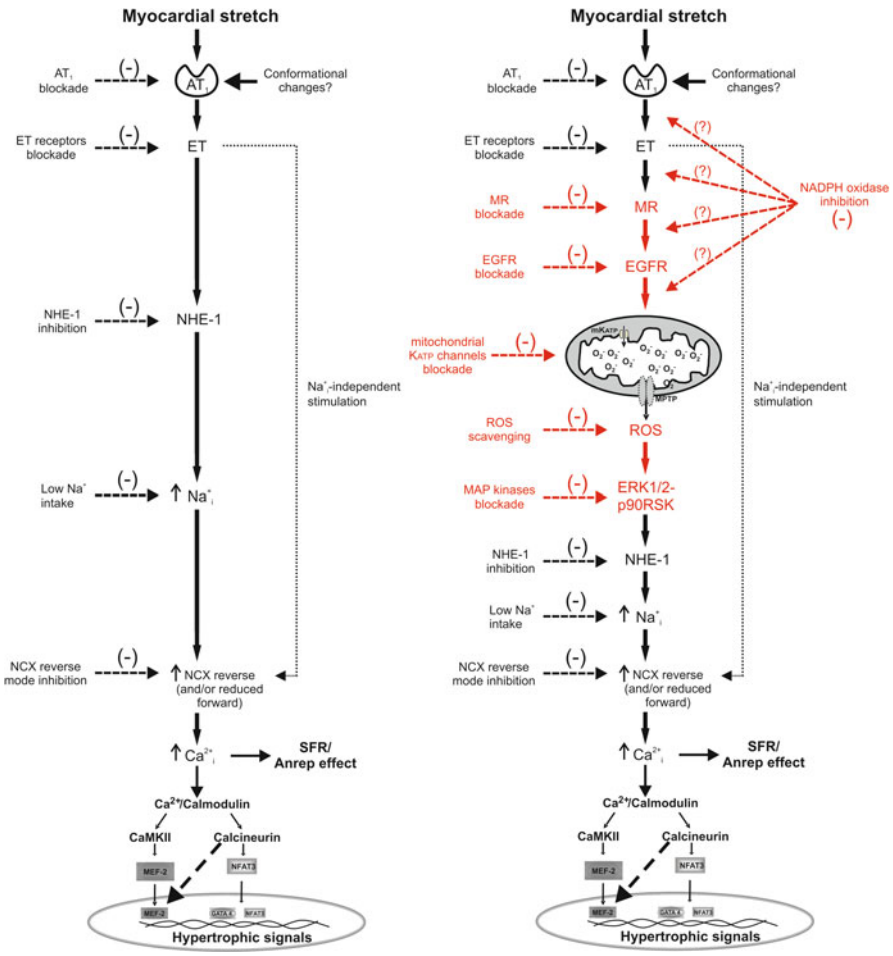

Fig. 12.1 State of knowledge of the chain of events triggered by myocardial stretch at 2005 (*left* panel) and the updated sequence at 2011 (*right* panel)

12.4 Recent Advances in the Anrep Effect and Myocardial Hypertrophy and Failure

Figure 12.1 (left panel) depicts the state of knowledge on this subject when we wrote the chapter in the 2005 edition of the present book. In summary, the chain of events hypothesized at that time comprised the following: (1) AT1 receptor activation, (2) release/formation of ET, (3) NHE-1 hyperactivity, (4) increase in intracellular Na^+ concentration, and (5) increase in Ca^{2+} transient amplitude through the Na^+/Ca^{2+} exchanger (NCX).

On the right panel of Fig. 12.1 we present the recent advances in this particular field, stressing the idea that myocardial hypertrophy and failure begins with cardiac

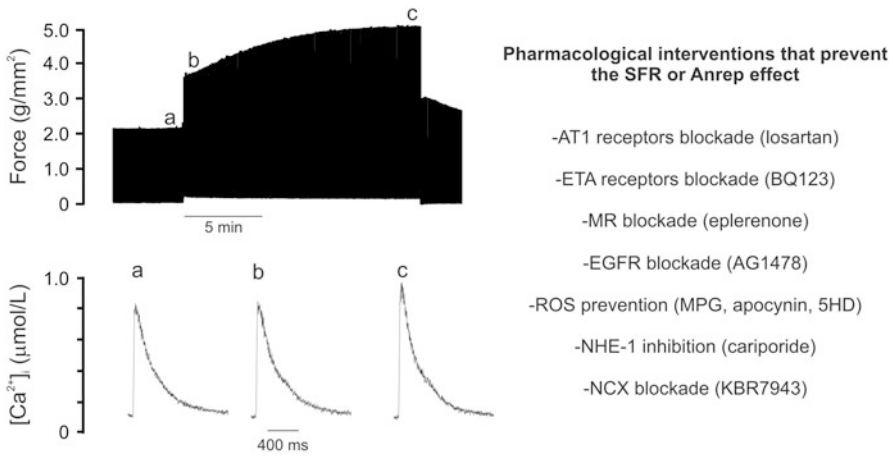

Fig. 12.2 Left: Contractile response to stretch of an isolated papillary muscle. The first increase in force (from "a" to "b", *top*) occurs without changes in the Ca^{2+} transient ("a" to "b", *bottom*) while the SFR (from "b" to "c", *top*) is due to an increase in the Ca^{2+} transient ("b" to "c", *bottom*). Right: Pharmacological interventions proved to inhibit the SFR. (Modified with permission from Cingolani et al. (2001))

strain-triggered intracellular pathways that are in part common to hypertrophy and failure development and the mechanical counterpart, the so called SFR. Our updated proposal is that the chain of events triggered by myocardial stretch is as follows: (1) release of A2, (2) release/formation of ET, (3) MR activation, (4) transactivation of the EGFR, (5) NADPH oxidase activation, (6) mitochondrial reactive oxygen species (ROS) production, (7) activation of redox-sensitive kinases, (8) NHE-1 hyperactivity, (9) increase in intracellular Na^+ concentration, and (10) increase in Ca^{2+} transient amplitude through the NCX.

The left panel of Fig. 12.2 shows the typical behavior of a control papillary muscle before and after stretch. The first increase in force occurs immediately after stretch without changes in the Ca^{2+} transient and is attributed to the Frank-Starling mechanism. The SFR is the mechanical result of a chain of intracellular signals triggered by the stretch that ends with an increase in the Ca^{2+} transient. The pharmacological interventions that abolished the SFR or Anrep effect are summarized in the right panel of Fig. 12.2. Note the relationships between these interventions and the therapeutic treatments used to regress myocardial hypertrophy or to treat heart failure.

During the 5–6 years after the 2005 chapter was written, the followings steps were added to the sequence of the SFR generation:

12.4.1 The Critical Role of Mitochondrial ROS in the Activation of Redox Sensitive Kinases Leading to the Anrep Effect

The participation of ROS as intracellular signalling markers of A2/ET-1 in the myocardium is a well accepted fact (Sugden and Clerk 2006). In fact, we have

demonstrated that a low dose of A2 (1 nmol/L) increases sarcomere shortening of isolated cat cardiomyocytes through an autocrine crosstalk with endogenous ET-1 (Cingolani et al. 2006), being this effect dependent on ROS production. Both peptides, A2 and ET-1, are well known activators of the NADPH oxidase (Giordano 2005; Kimura et al. 2005b) and through this action it has been reported a phenomenon called "ROS-induced ROS-release", by which a small amount of ROS triggers a greater ROS production from the mitochondria (Zorov et al. 2000; Brandes 2005; Kimura et al. 2005a). The fact that ROS were implicated in myocardial strain-triggered hypertrophy (Pimentel et al. 2006), lead us to explore the possibility that the ROS-induced ROS-release mechanism would underlie the SFR. Figure 12.3a shows that stretch -in addition to its mechanical effect- induces an increase in intracellular ROS formation of approximately 30 % above baseline levels. Furthermore, scavenging ROS with N-(2-mercaptopropionyl)-glycine (MPG) or EUK8 inhibited both stretch-induced increase in ROS (Fig. 12.3a) and the SFR (Fig. 12.3b). We also found that ROS scavenging inhibited the increase in $[Na^+]_i$ that occurs in response to stretch (Fig. 12.3c).

These results allow us to hypothesize that activation of NAPDH oxidase after stretch would produce a small amount of O_2^-, which may open the ATP-sensitive mitochondrial potassium (mKATP) channels and produce a larger amount of O_2^- enough to generate the SFR. Experimental evidence supports these assumptions since the SFR was abolished after NADPH oxidase inhibition (apocynin or diphenyleneiodonium chloride, DPI) or after blockade of mKATP channels (5-hydroxydecanoate, 5HD, or glibenclamide) (Fig. 12.4a). Furthermore, the NHE-1-induced increase in $[Na^+]_i$ underlying the SFR was also abolished by these interventions (Fig. 12.4b).

In this context, it appears reasonable to speculate that stretch-mediated mitochondrial ROS production leads to phosphorylation and activation of the NHE-1. Actually, ROS-mediated activation of NHE-1 has been reported to be due to redox sensitive kinase-mediated phosphorylation of the exchanger cytosolic tail, being MEK, ERK1/2 and p90rsk kinases the favourite candidates (Rothstein et al. 2002). In this regard: (1) RAS-dependent activation of these kinases has been reported after stretch in neonatal cardiomyocytes (Pimentel et al. 2006); (2) we have detected significant increases in ERK1/2 and p90rsk phosphorylation after stretch (Fig. 12.5) that were abolished with 1 μmol/L losartan (Fig. 12.5); and (3) inhibition of MEK (a kinase upstream ERK1/2) also blunted the SFR (Fig. 12.5).

12.4.2 The Role of Epidermal Growth Factor Receptor (EGFR) in the SFR Development

It has been recently established that transactivation of the EGFR is the primary mechanism underlying G-protein coupled receptor (GPCR) agonist activation of ERK1/2 and its downstream intracellular pathways (Lemarie et al. 2008). Furthermore, myocardial stretch (Anderson et al. 2004; Duquesnes et al. 2009), myocardial hypertrophy (Kagiyama et al. 2002), and ET-1 signaling (Asakura et al. 2002) have

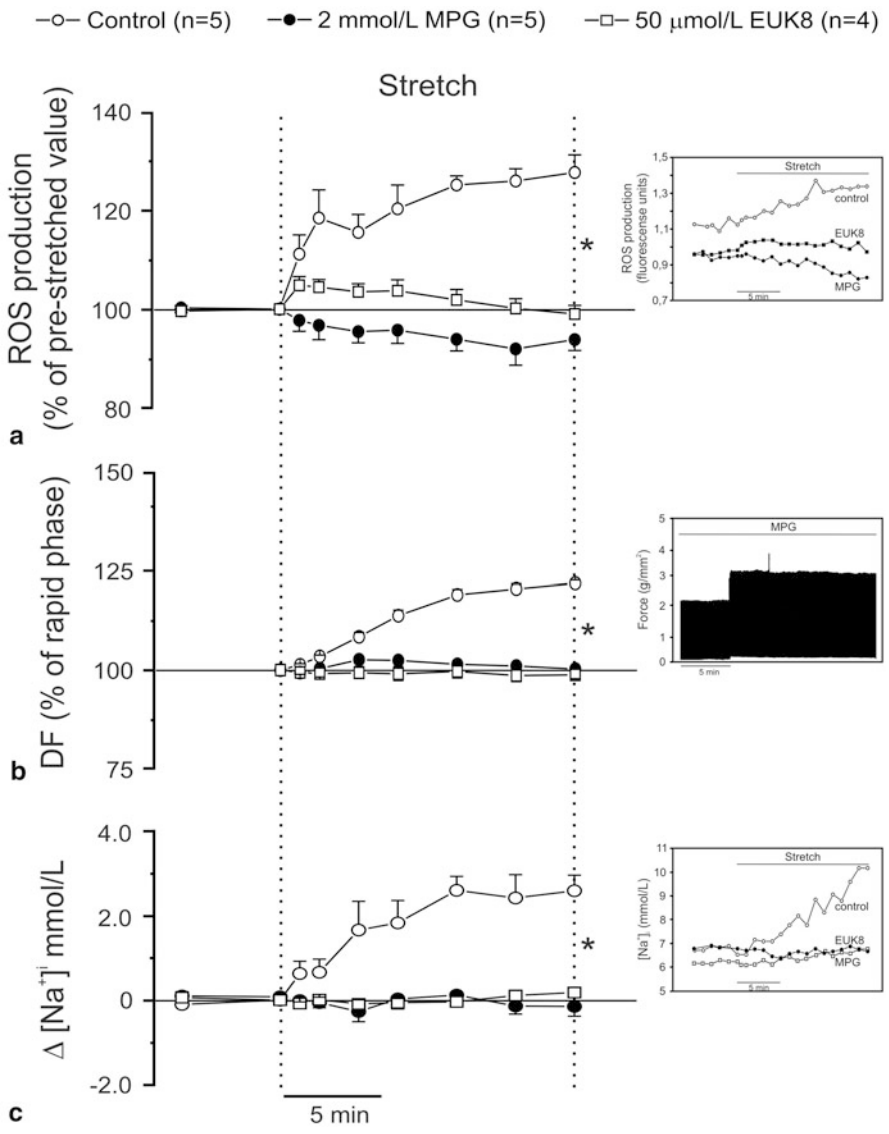

Fig. 12.3 Myocardial stretch induced an intracellular ROS increase of ~30 % above the baseline levels that was cancelled by the ROS scavengers MPG and EUK8 (Panel **a**). MPG and EUK8 also cancelled the slow force response (expressed as percent of initial rapid phase) (Panel **b**). Furthermore, ROS scavenging also blunted stretch-induced increase in $(Na^+)_i$ (Panel **c**). Insets show original raw data. * indicates $P < 0.05$ control vs. MPG and EUK8. *DF* = developed force. (Modified with permission from Caldiz et al. (2007))

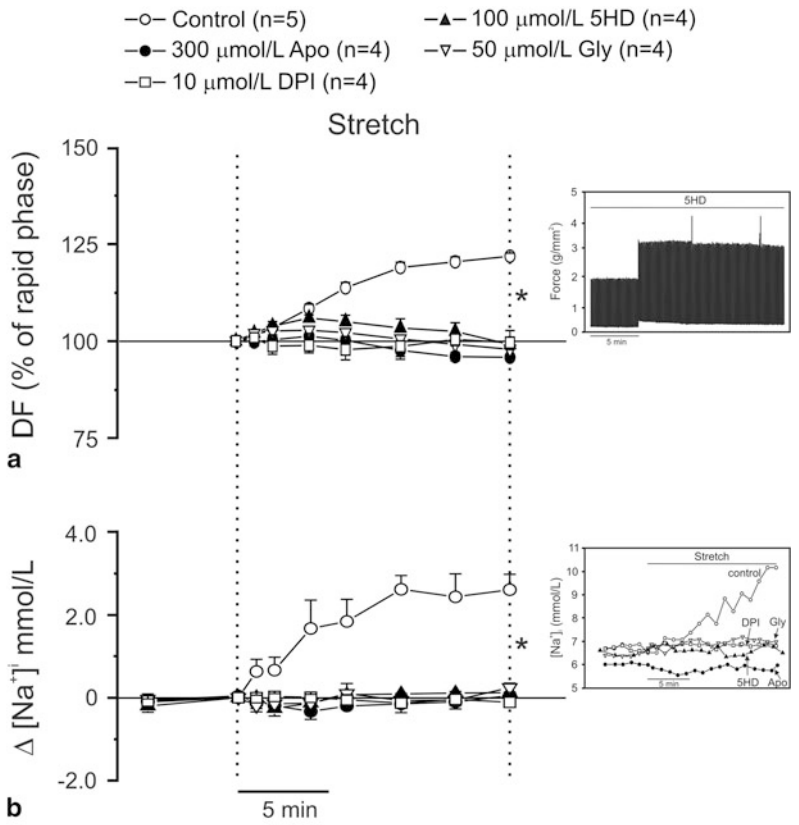

Fig. 12.4 NADPH oxidase inhibition by apocynin (*Apo*) or diphenyleneiodonium chloride (*DPI*) as well as mK_{ATP} channels blockade with 5-hydroxydecanoate (*5HD*) or glybenclamide (*Gly*) abolished slow force response (expressed as percent of initial rapid phase) (Panel **a**). All these interventions also cancelled NHE-1-mediated increase in $[Na^+]_i$ that accompanied the slow force response (Panel **b**). Insets show original raw data. * indicates $P < 0.05$ control vs. all other groups. *DF* = developed force. (Modified with permission from Caldiz et al. (2007))

been shown to involve EGFR transactivation. The possibility that this receptor was playing a role in the chain of events following myocardial stretch was examined. To this aim we explored whether inhibiting EGFR transactivation would impact on the SFR. Several mediators are known to be involved in the transactivation process, but the precise communication between GPCR and EGFR remains not entirely understood (Wetzker and Bohmer 2003). One proposed mediator is Src tyrosine kinase (Wetzker and Bohmer 2003); thus, as a first step in probing our hypothesis, we inhibited Src kinase with the specific tyrosine kinase inhibitor PP1. Figure 12.6b shows that PP1 (1 μmol/l) completely abolished the SFR. Another proposed mediator (Krieg et al. 2004; Szokodi et al. 2008) of EGFR transactivation is heparin-binding EGF (HB-EGF). HB-EGF is generated through extracellular proteolytic cleavage of proHB-EGF by the action of a matrix metalloproteinase (MMP). To test the

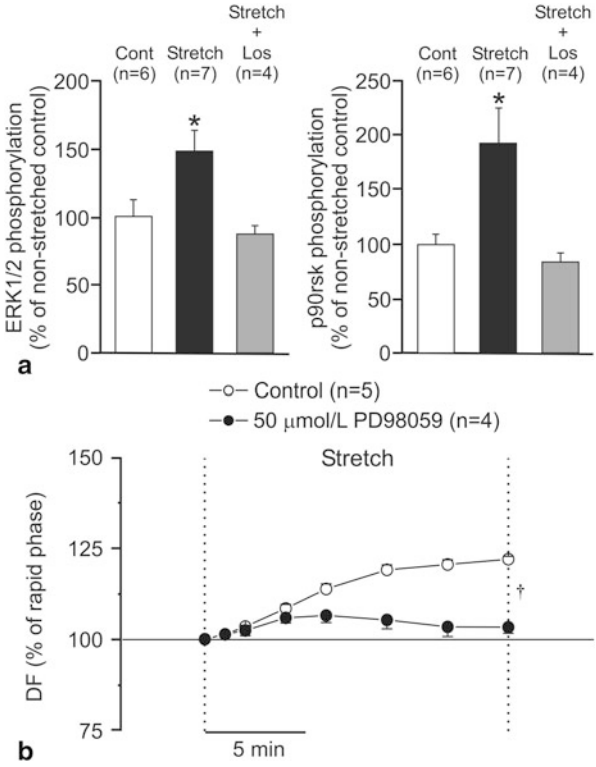

Fig. 12.5 **a** Myocardial stretch significantly increased ERK1/2 and p90rsk phosphorylation, effect that was cancelled by losartan (Los). **b** Inhibition of MEK (a kinase upstream ERK1/2 and downstream RAS) by PD98059 cancelled the SFR (expressed as percent of the initial rapid phase). *DF* = developed force. * indicates $P < 0.05$ vs. non-stretched control (cont); † indicates $P < 0.05$ control vs. PD98059. (Modified with permission from Caldiz et al. (2007))

contribution of this signaling pathway to the SFR, we inhibited MMP with MMP inhibitor III (MMPI), which specifically targeted MMPs 1, 2, 3, 7 and 13. MMPI (3 μmol/l) did not completely eliminate the SFR, but significantly reduced its magnitude by <60 % (Fig. 12.6c) providing further support to the notion that EGFR transactivation was required for a fully developed SFR. Finally, we specifically inhibited the EGFR with AG1478 (1 μmol/l), which is known to prevent receptor phosphorylation, and consequently its activation. Under these conditions, the SFR was completely abolished (Fig. 12.6d). Thus, these three interventions that interfered with the mechanism of EGFR transactivation significantly decreased the SFR confirming that EGFR transactivation plays an essential role in the development of the SFR in cat myocardium.

12.4.3 Activation of Redox Sensitive Kinases and NHE Phosphorylation after Myocardial Stretch. Role of the EGFR Transactivation

We (Cingolani et al. 2005; Caldiz et al. 2007) and others (Zhang et al. 2009) previously showed that the SFR depends on the activation of NHE-1, which is a target

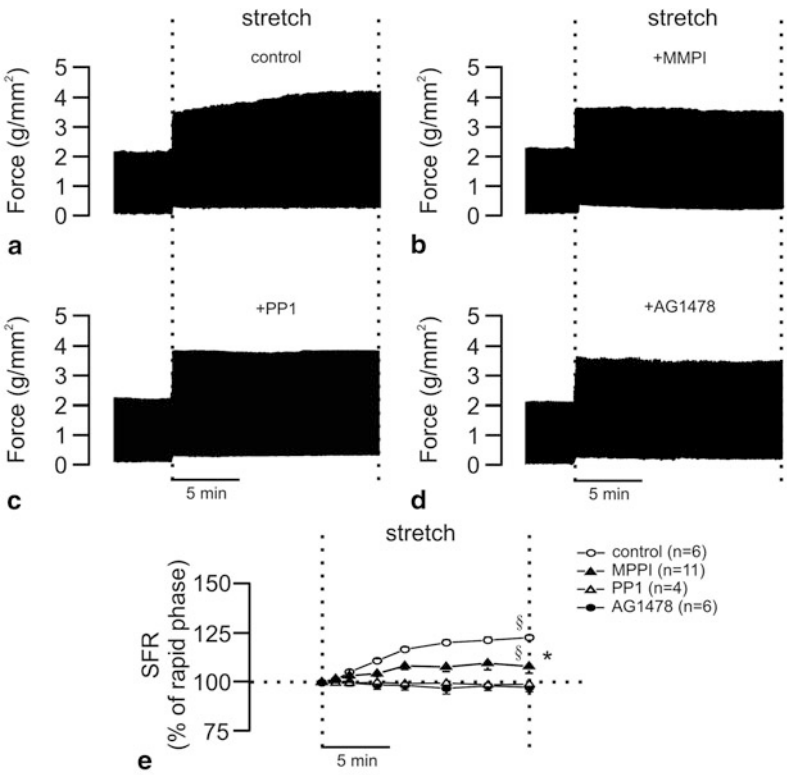

Fig. 12.6 SFR and EGFR transactivation. (**a**) a typical force record from a cat papillary muscle subjected to an increase in length from 92 to 98 % of Lmax; the biphasic response to stretch can be seen (vertical dotted lines indicate stretching interval). (**b**–**d**), same as **a** but from muscles pretreated with matrix metalloproteinase inhibitor (MMPI, **b**), the Src kinase inhibitor PP1 (**c**) or the EGFR blocker AG1478 (**d**), interventions that cancel EGFR transactivation. As can be seen, all these pharmacological interventions prevented the development of the SFR to stretch. (**e**), the averaged results obtained under the different experimental conditions expressed as a percentage of the initial rapid phase. *$P < 0.05$ control curve vs. others (2-way ANOVA). §$P < 0.05$ vs. initial rapid phase (for the sake of clarity, significance is indicated only for 15 min of stretch. (Modified with permission from Villa-Abrille et al. (2010))

of the redox sensitive kinases, ERK1/2. Others showed that ROS stimulated NHE-1 through MAPK (Rothstein et al. 2002; Haworth et al. 2003; Fliegel and Karmazyn 2004; Akram et al. 2006), and we recently proposed that stretch induced the mitochondrial production of ROS (Caldiz et al. 2007). We detected a significant increase in ERK1/2 phosphorylation after myocardial stretch. This effect was cancelled by pre-treatment with either AG1478 or PP1 (Fig. 12.7), two inhibitors of EGFR transactivation that also blocked the mechanical response. These findings showed that the prevention of EGFR activation is able to cancel both the increase in ERK1/2 phosphorylation and the mechanical response to stretch.

Additionally, we estimated the levels of NHE-1 phosphorylation at Ser703 with a phospho-Ser 14-3-3 binding motif antibody. Figure 12.8 shows that phosphory-

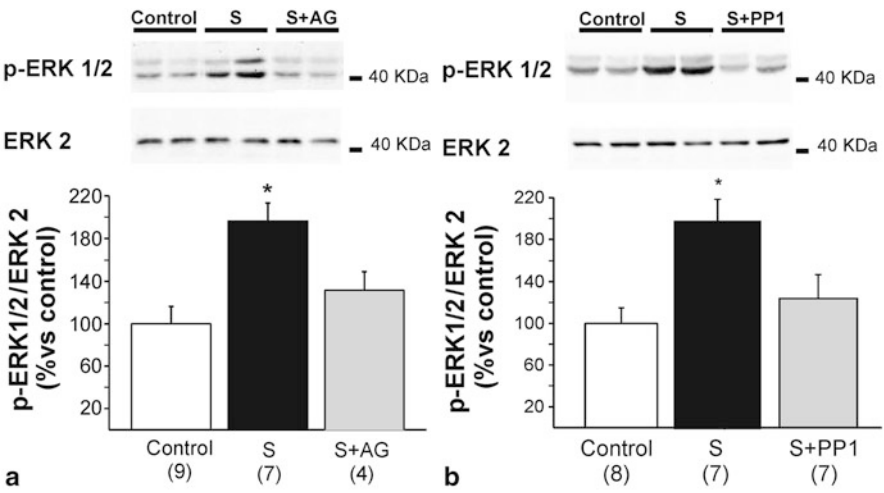

Fig. 12.7 ERK1/2 phosphorylation after stretch. Myocardial stretch (S) significantly increased ERK1/2 phosphorylation. This effect was blunted either by EGFR blockade with AG1478 (AG) (**a**) or by Src kinase inhibition with PP1 (**b**), demonstrating that EGFR transactivation after stretch is necessary for ERK1/2 phosphorylation. AG1478 and PP1 alone did not modify basal ERK1/2 phosphorylation (92 ± 4 %, $n = 4$, and 107 ± 8 %, $n = 4$, of control respectively). $^{*}P < 0.05$ vs. non-stretched control (control). (Modified with permission from Villa-Abrille et al. (2010))

lation at the 14-3-3 binding motif was increased after myocardial stretch, and this increase was prevented with AG1478. Our results support the concept that GPCR induced-EGFR transactivation plays a role in the chain of events that lead to NHE-1 phosphorylation and SFR development.

Recently, it has been demonstrated that the Anrep effect was absent in a transgenic mouse lacking thrombospondin-4 (Cingolani et al. 2011b), a matricellular protein that is normally expressed at modest levels in the heart under normal conditions, but has been shown to be elevated in animals as well as humans with heart failure. Interestingly, the thrombospondin-4 molecule carries an EGF-like repeat, and as mentioned before, mice not expressing this protein not only had the Anrep effect blunted, but also failed to phosphorylate ERK1/2, as controls did. Surprisingly, these mice showed a phenotype of dilated cardiomyopathy after their aortas were banded, suggesting that a complex- not yet completely understood- cross-talk between the extracellular matrix and myocytes takes place after stretch. Further studies will continue to address the mechanistic role these matricellular proteins have in the development of heart failure.

12.4.4 Activation of the MR as a Consequence of Muscle Stretch

The link between A2 or its AT1 receptor and the mineralocorticoid receptor (MR) is an accepted fact (Lemarie et al. 2008, 2009; Grossmann and Gekle 2009). Although

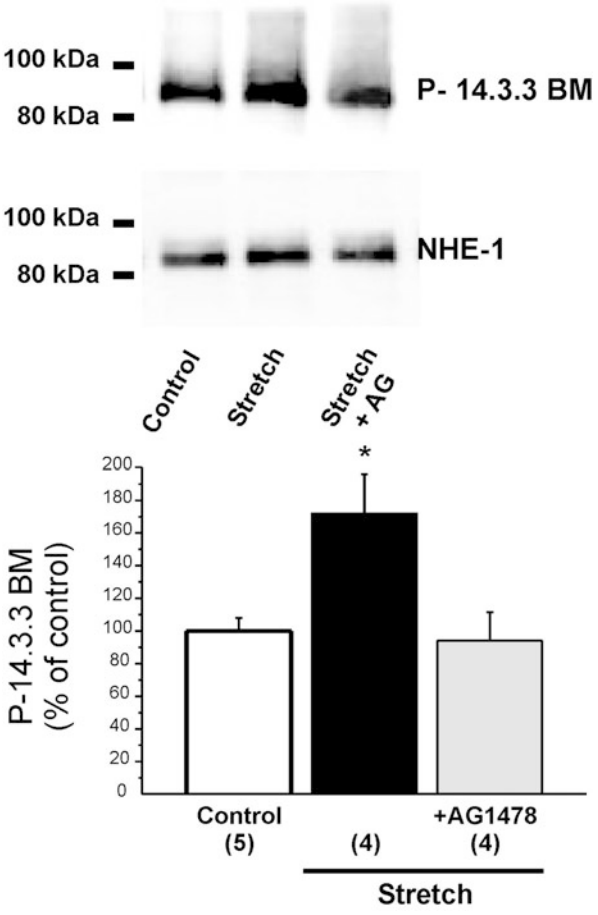

Fig. 12.8 Stretch-induced NHE-1 phosphorylation. Myocardial stretch significantly increased NHE-1 phosphorylation at Ser703 estimated by a phospho-Ser 14-3-3 binding motif antibody. This effect was cancelled when the EGFR was blocked by AG1478 (AG). These results support a role of the EGFR transactivation in the chain of events leading to NHE-1 phosphorylation and SFR development. AG1478 alone did not modify basal NHE-1 phosphorylation (93 ± 4 % of control, $n = 4$). $^{*}P < 0.05$ vs. control. (Modified with permission from Villa-Abrille et al. (2010))

still somewhat controversial, aldosterone (ALD), which is known to be regulated by A2, appears to be synthesized and/or released by cardiac muscle (Gomez-Sanchez et al. 2004; Chai and Danser 2006); (Silvestre et al. 1998, 1999; Takeda et al. 2000). We have recently hypothesized that if a crosstalk between A2 and the MR occurs during ROS production, and at the same time A2 and ROS are crucial for SFR development, therefore MR inhibition would blunt the SFR. In this section we will present evidence that MR activation is involved in the signalling pathway leading to the Anrep effect.

Figure 12.9 shows that MR activation is necessary to promote ROS formation by a physiological concentration of A2 (1 nmol/L), since the increase in superoxide anion formation of ~50 % was suppressed after blocking MR with spironolactone or eplerenone. This effect was also suppressed by blocking AT1, ET1 (type A) receptor or EGFRs, by inhibiting NADPH oxidase, or by targeting mitochondria; and it was unaffected by glucocorticoid receptor inhibition.

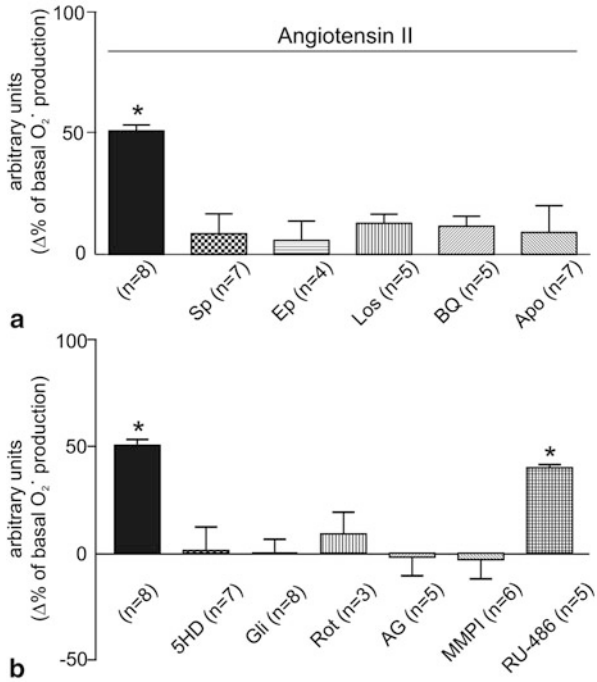

Fig. 12.9 Superoxide anion production induced by angiotensin II. **a** MR blockade with spirolactone (*Sp*, 10 μmol/L) or eplerenone (*Ep*, 10 μmol/L) abrogated the effect of 1 nmol/L A2 on the basal rate of O_2^- production. This effect was also blunted by the AT1 and ET_A receptor antagonists losartan (*Los*, 1 μmol/L) and BQ123 (*BQ*, 10 μmol/L), respectively, and by NADPH oxidase inhibition with apocynin (*Apo*, 300 μmol/L). **b** A2-induced O_2^- formation was also blunted by targeting mitochondria with 5HD (100 μmol/L), glibenclamide (*Gli*, 50 μmol/L), or rotenone (*Rot*, 10 μmol/L), and by preventing EGFR activation either by EGFR blockade with AG1478 (*AG*, 1 μmol/L) or by inhibiting the metalloproteinase involved in EGFR transactivation with MMPI (3 μmol/L). Glucocorticoid receptor inhibition with Ru-486 (10 μmol/L) did not influence the effect of A2. $^*P < 0.05$ vs. basal O_2^- production. (Modified with permission from Caldiz et al. (2011))

All interventions except AT1 receptor blockade blunted the increase in superoxide anion promoted by an equipotent dose of ET-1 (1 nmol/L), confirming that ET receptor activation is downstream of AT1 receptor (not shown, (Caldiz et al. 2011)). Similarly, an increase in superoxide anion promoted by an equipotent dose of ALD (10 nmol/L) was blocked by spironolactone or eplerenone, by preventing EGFR transactivation, but not after inhibiting glucocorticoid receptors or protein synthesis, suggesting a non-genomic MR effect (Fig. 12.10a). Combination of ALD and ET-1 did not further increase superoxide anion formation (Fig. 12.10b). ALD increased phosphorylation of the redox-sensitive kinases ERK1/2, p90RSK, and the NHE-1, effects that were eliminated by eplerenone or by preventing EGFR transactivation (not shown, see ref. Caldiz et al. 2011).

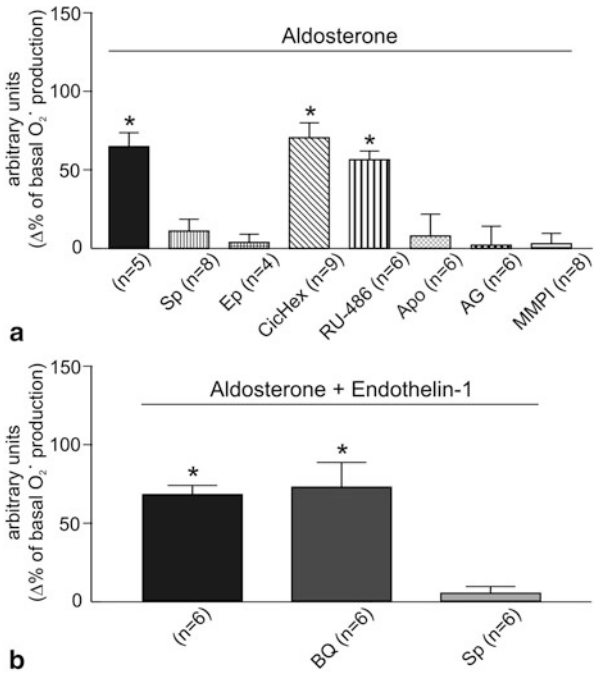

Fig. 12.10 Superoxide anion production induced by aldosterone. **a** The effect of ALD at a concentration (10 nmol/L) that mimicked the effect of A2 and ET on the basal rate of $O_2^{\cdot}$ production was suppressed by spirolactone (*Sp*) and eplerenone (*Ep*), but not by the glucocorticoid receptor inhibitor Ru-486 or by preventing protein synthesis with cycloheximide (*CicHex*, 7 mmol/L). This demonstrates that MR activation has nongenomic consequences and excludes the possibility of glucocorticoid receptor activation. On the other hand, as shown for A2 and ET, the ALD-mediated increase in ROS formation was prevented by NADPH oxidase inhibition (*Apo*) and by preventing EGFR activation (AG and MMPI). This suggests that transactivation occurs in the direction of activated MR to EGFR, and that metalloproteinase activation downstream of MR is crucial for EGFR transactivation. **b** The combination of ALD and ET did not promote any further increase in $O_2^{\cdot}$ production. Under this condition, mitochondrial $O_2^{\cdot}$ production was abrogated by spironolactone (*Sp*), but unaffected by ET_A receptor blockade with BQ123 (*BQ*), indicating that the only possible sequence of events is from ET_A to MR. *P $<$ 0.05 vs. basal $O_2^{\cdot}$ production. (Modified with permission from Caldiz et al. (2011))

Finally, the SFR was suppressed by MR blockade, by preventing EGFR transactivation or by scavenging ROS, but it was unaffected by glucocorticoid receptor blockade or protein synthesis inhibition as shown in Fig. 12.11. These results clearly suggest that MR activation is a necessary step in stretch-triggered mitochondrial ROS that mediates the activation of redox-sensitive kinases upstream NHE-1, leading to de Anrep effect.

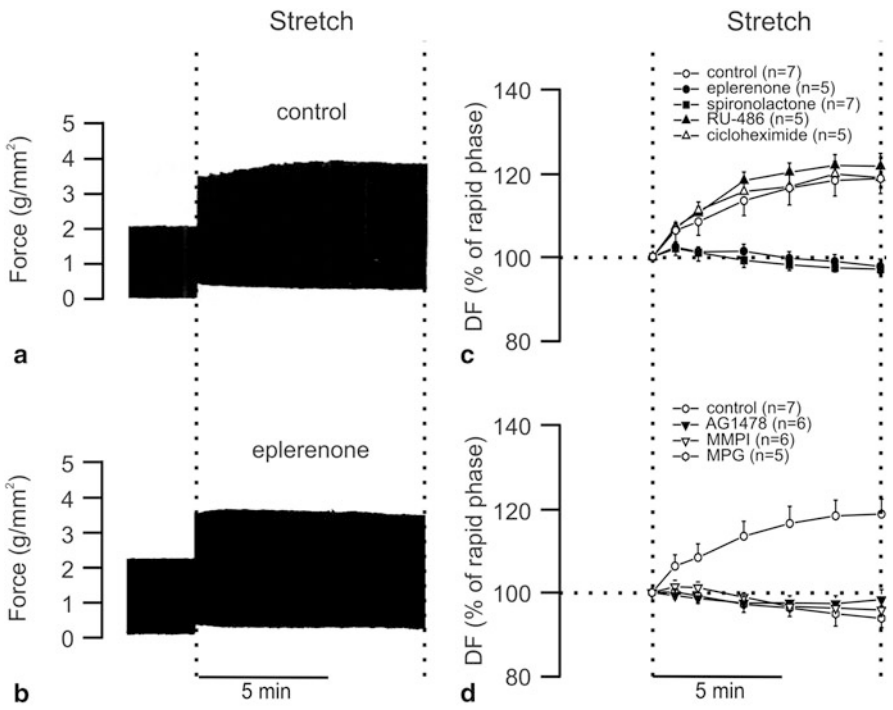

Fig. 12.11 SFR and MR activation. **a** Typical force record from rat papillary muscle subjected to an increase in length from 92 to 98 % of Lmax. The biphasic force response to stretch can be observed. **b** Same as (**a**) but from a muscle pre-treated with the MR blocker eplerenone, demonstrating that prevention of MR activation after stretch eliminated the SFR. **c** Averaged results of the SFR expressed as percentages of the initial rapid phase. MR blockade, not only by eplerenone but also by spironolactone, completely suppressed the SFR. However, the SFR was unaffected by the glucocorticoid receptor inhibitor Ru-486 or the protein synthesis inhibitor cycloheximide. **d** As reported previously in cat myocardium (Villa-Abrille et al. 2010) the SFR required EGFR transactivation, since it was blunted either by direct EGFR inhibition (AG1478) or by blocking transactivation with MMPI. Furthermore, the SFR was suppressed by the ROS scavenger MPG, supporting the notion that ROS formation is a key factor in the chain of events leading to the Anrep effect. (Modified with permission from Caldiz et al. (2011))

12.5 Direct Measurements of NHE-1 Stimulation by Aldosterone: Transactivation of the EGFR

Fujisawa et al. (2003) demonstrated that mineralocorticoid/salt-induced rat cardiac fibrosis and hypertrophy was prevented by the selective NHE-1 blocker cariporide. It has also been reported that ALD upregulates the expression and function of NHE-1 (Ebata et al. 1999; Karmazyn et al. 2003; Barbato et al. 2004; Matsui et al. 2007) and that selective blockade of this transporter prevents and/or reverts left ventricular hypertrophy in various animal models (Cingolani and Ennis 2007). According to

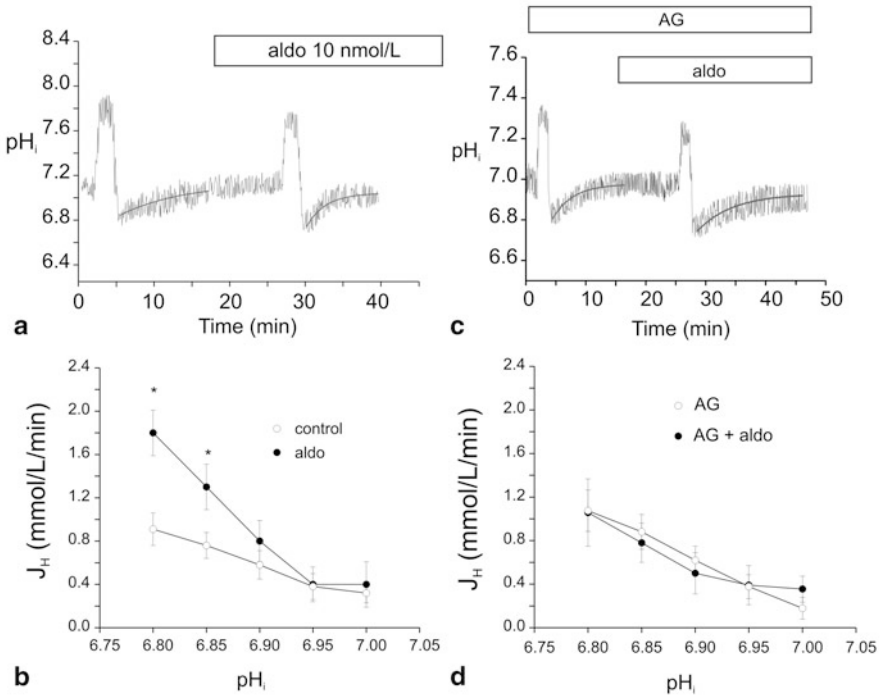

Fig. 12.12 Aldosterone induced activation of the NHE-1 and its blockade by inhibiting the EGFR. Panel **a**: representative traces of pH_i during the application of two consecutive ammonium pulses (20 mmol/L NH_4Cl), in the absence (*first* pulse) and presence of 10 nmol/L ALD (aldo, *second* pulse). ALD was applied 10 min before the second pulse. Panel **b**: average proton efflux J_H, carried by the NHE-1, before (*first* pulses, closed *circles*, n = 5) and after application of 10 nmol/L ALD (*second* pulses, open circles, n = 5). J_H is significantly enhanced by ALD. *P < 0.05 vs. control. Panel **c**: representative traces of pH_i during the application of two consecutive ammonium pulses (20 mmol/L NH_4Cl), in the absence (*first* pulse) and presence of 10 nmol/L ALD (*second* pulse). The EGFR blocker AG1478 (*AG*, 1 μmol/L) was applied 10 min before the first pulse and maintained throughout the experiment. ALD was applied 10 min before the second pulse. Panel **d**: average proton efflux J_H, carried by the NHE-1, before (*first* pulses, open *circles*, n = 4) and after application of 10 nmol/L ALD (*second* pulses, closed *circles*, n = 4) in the continuous presence of 1 μmol/L AG1478. The transactivation of the EGFR by ALD leads to the activation of the NHE-1. (Modified with permission from De Giusti et al. (2011))

these data and in agreement with our previous results on the SFR described above, we have recently shown that ALD increases NHE-1 activity in rat ventricular myocytes through a non-genomic pathway (Fig. 12.12a, b) (De Giusti et al. 2011).

As commented above, EGFR activation represents one of the signaling pathways involving ALD (Grossmann and Gekle 2007; Grossmann et al. 2007). It has been shown that the MR blocker spironolactone reduces the EGFR mRNA synthesis after cerebral ischemia (Dorrance et al. 2001). Accordingly, Grossmann et al. (2007) reported that MR activation by ALD enhanced EGFR expression via an interaction

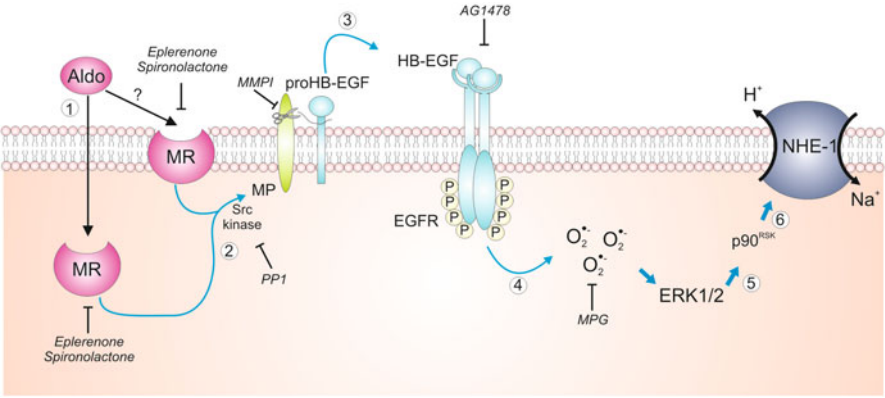

Fig. 12.13 Signaling cascade involved in the aldosterone-induced NHE-1 stimulation in rat cardiomyocytes. The activation of the MR by ALD (*Aldo*) (1) leads to EGFR transactivation. This mechanism is mediated by the activation of the src-kinase (2) and the metalloproteinases. HB-EGF is released from the cell surface following shedding of the extracellular domain (ectodomain shedding) by this zinc-dependent metalloproteinases (3). HB-EGF binds to the EGFR and increases the production of superoxide anion (O_2-) (4). These reactive oxygen species (*ROS*) stimulates the redox-sensitive kinase ERK1/2 (5), which phosphorylates the kinase $p90^{RSK}$. This kinase phosphorylates the NHE-1 (6), stimulating its activity. Eplerenone (*eple*) and spironolactone (*spiro*) (MR blockers), PP1 (src-kinase inhibitor), MMPI (metalloproteinases blocker) and MPG (*ROS* scavenger) were employed to investigate pathways 1–4 (Ref. (De Giusti et al. 2011)). The inhibitor of the EGFR kinase AG1478 (AG) was used to evaluate the transactivation of this receptor by aldosterone. (Modified with permission from De Giusti et al. (2011))

with the EGFR promoter of vascular smooth muscle. In addition to these genomic effects, non-genomic actions of ALD involving EGFR transactivation have also been reported (Grossmann and Gekle 2008, 2009). Consistent with this evidence, we have recently shown that ALD enhances NHE-1 activity via transactivation of EGFR (Fig. 12.12c, d) (De Giusti et al. 2011). The stimulatory effect of this hormone on NHE-1 was blocked by the inhibitor of the Src-kinase PP1 and the blocker of metalloproteinases MMPI (De Giusti et al. 2011).

As commented above, these proteases release HB-EGF from its precursor, proHB-EGF. Figure 12.13 depicts that activation of EGFR by HB-EGF increases the production of intracellular ROS and triggers the ERK1/2 pathway, which phosphorylates p90RSK (De Giusti et al. 2011).

This kinase, in turn, phosphorylates Serine703 of the NHE-1, leading to the activation of the transporter. As noted in Fig. 12.13, at least a fraction of the total amount of MR appears to be linked to the sarcolemma, likely co-localized to the EGFR (Grossmann et al. 2010) and/or associated to caveolin-1 (Krug et al. 2011). This data would explain the binding of ALD to the sarcolemmal fraction reported by Le Moellic et al. (2004). In addition, non genomic effects of ALD altering stimulation of a GPCR (GPR30) has been recently reported in vascular smooth muscle and endothelial cells (Gros et al. 2011).

12.6 Molecular Approach Targeting the Anrep Effect: Silencing NHE-1 Expression by Interference RNA

Gene silencing by RNA interference is a natural process occurring in cells by which a specific mRNA is degraded and therefore the expression of the encoded protein prevented. This mechanism is mediated by a double-stranded RNA (dsRNA) of approximately 18–23 nucleotides of length present inside the cell, known as siRNA (small interfering RNA) (Mello and Conte 2004; Kim and Rossi 2007). Briefly, through a multiple step pathway, one of the RNA strands of the siRNA is matched to a complementary mRNA which in turn is cleaved and ultimately degraded. In the research arena, in vivo or in vitro delivery of siRNA molecules to cells provides a powerful tool to specifically silence a single type of protein (Akhtar and Benter 2007; Kim and Rossi 2007). This technology has several advantages: (1) It is highly specific and can differentiate between members of the same family and even between isoforms of the same protein; (2) It has a lasting effect whose extension varies according to the strategy used to deliver the siRNA or modifications of the siRNA molecule; (3) It can be reversed; (4) It is relatively easy to obtain a siRNA. Moreover, siRNA technology has the potential to be used in the therapeutic field, to validate a protein as a suitable target whose inhibition would mediate the cure or alleviation of a disease. After finding the target protein, a synthetic drug could be designed to treat the disease. However, the RNA interference methodology also allows consideration of the siRNA molecule itself as a possible therapeutic tool (Kim and Rossi 2007). Delivery of siRNA molecules into the cell portends several challenges, starting with penetration of the plasma membrane, stability of siRNA inside and outside the cell, toxicity, and triggering of immune responses (Akhtar and Benter 2007; Kim and Rossi 2007; Manjunath et al. 2009).

Classic pharmacological techniques to inhibit a desired protein in vivo have several disadvantages compared to interference RNA: (1) The drug distributes broad-wide in the organism, condition that may affect undesired targets or generate side effects; (2) It is very difficult to make a drug that can differentiate between members of the family or isoforms; (3) Drug concentration change along time therefore requiring frequent administration.

Pharmacological inhibition of NHE-1 was beneficial in different experimental models of cardiac pathologies (Ennis et al. 1998, 2003; Karmazyn 1999; Avkiran and Marber 2002; Camilion de Hurtado et al. 2002; Engelhardt et al. 2002; Cingolani et al. 2003b). However, clinical trials with NHE-1 inhibitors like GUARDIAN (Theroux et al. 2000), ESCAMI (Zeymer et al. 2001) and EXPEDITION (Mentzer et al. 2008) failed to provide such benefits, and one of these studies was suspended due to undesired cerebrovascular side effects (Mentzer et al. 2008). Although the mechanism for this negative effect is still not clear, it could be related to blockade of NHE-1 activity in the brain where NHE-1 function seems to be essential, since animals lacking NHE-1 showed aberrant phenotype that included ataxia and epileptic-like seizures (Cox et al. 1997; Bell et al. 1999). It is possible then, that pharmacological inhibition of NHE-1 affects the exchanger in tissues other than the myocardium where its role is crucial or, even inhibits an unrelated protein required for normal function (Villafuerte et al. 2007). Activation of the RNA interference

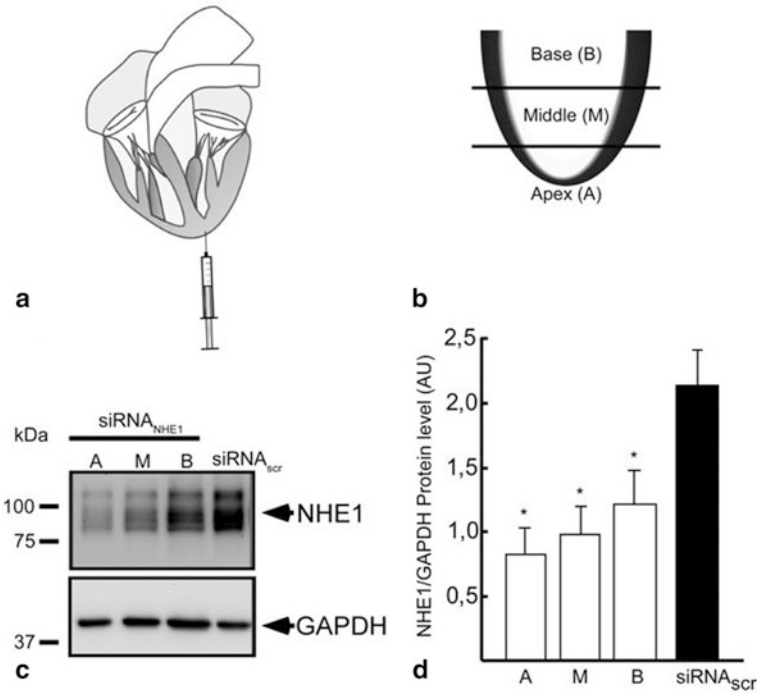

Fig. 12.14 NHE-1 expression reduction distally from the injection site. **a** Mice were injected once in the apex of the left ventricle with naked siRNA$_{NHE-1}$ or siRNA$_{scramble}$ (siRNA$_{SCR}$) as shown in the heart scheme, and sacrificed after 72 h. **b** Left ventricle was divided into three parts (apex, *middle*, and base) to evaluate NHE-1 expression. **c** Representative immunoblots of lysates of the different fractions of the left ventricle. **d** Average expression of protein, quantified by densitometry and normalized to the amount of GAPDH ($n = 7$, $^*P < 0.05$ vs. siRNA$_{SCR}$). (Modified with permission from Morgan et al. (2011))

pathway appeared to be a suitable method to specifically block the NHE-1 because it spares the other nine members of the protein family. In our laboratory, we designed two different approaches to target the NHE-1 protein exclusively in the heart: (a) the delivery of naked siRNA, and (b) the delivery of siRNA using the lentivirus backbone. The use of viral vectors for delivering siRNA inside the cells facilitates its entry and provides a long lasting inhibition of a protein. Disadvantages of this strategy are potential changes of the gene expression after integration of viral DNA in the host genome and generation of immune responses. The use of naked siRNA has the advantage of preventing a massive immune response, but carries the difficult task of crossing the plasma membranes, allowing optimal propagation, mainly due to its size and electrostatic charge. Furthermore, it is more susceptible to be degraded by nucleases producing a less lasting silencing effect.

We have demonstrated that after a week of a single injection of naked siRNA$_{NHE-1}$ to the left ventricle, an extensive reduction of the NHE-1 expression and function took place (Morgan et al. 2011) (Fig. 12.14).

These results, suggests the ability of siRNA molecules to spread through the myocardium and reduce NHE-1 expression and activity faraway from the injection

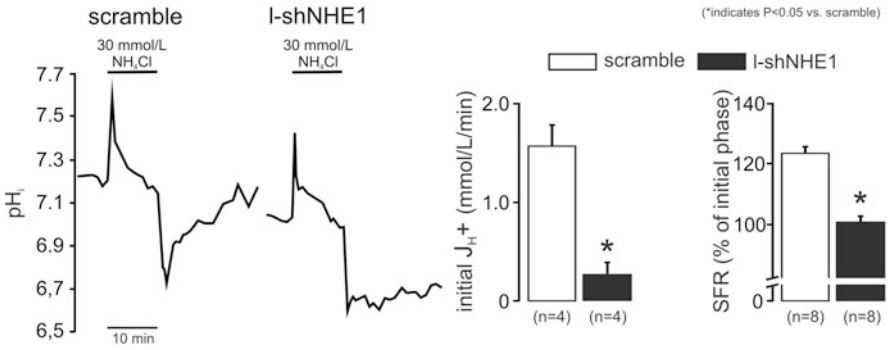

Fig. 12.15 Functional activity of the NHE-1 was evaluated by the recovery of pH_i after an acidic load (NH_4^+ prepulse) in isolated papillary muscles where the SFR was also tested. The original pH_i recordings (*left*) as well as the averaged initial H^+ fluxes (J_H^+, *middle*) clearly demonstrate the significant depression of NHE-1 activity in l-shNHE1 injected muscles compared to scramble. Furthermore, silencing the NHE-1 blunted the SFR (*right*). *$P < 0.05$ vs. scramble

site. In agreement with our findings, Kizana et al. (2009) demonstrated that siRNA molecules can move through cultured neighbour neonatal rat ventricle myocytes when coupled by gap junctions. Accordingly, it was found in different cultured cells that siRNA molecules can travel from one cell to another through gap junctions (Valiunas et al. 2005; Wolvetang et al. 2007) if connexin 43 (the predominant connexin isoform in adult hearts (Dhein 1998) is expressed (Valiunas et al. 2005). This local injection of siRNA in the left ventricle did not produce any effect on other organs, which allowed concluding that the procedure was successful in limiting the effects of siRNA to the heart (Morgan et al. 2011).

We have also recently incorporated the siRNA sequence able to mediate specific NHE-1 knockdown into a lentiviral vector (l-shNHE1) and injected into the left ventricular wall of Wistar rats (Pérez et al. 2011). A separated group of rats injected with a vector expressing a non-silencing sequence (scramble) served as control. Confocal microscopy analysis of heart tissue revealed spreading of l-shNHE1 (DsRed tagged) from the sites of injection throughout the myocardium. Hearts with l-shNHE1 showed reduced NHE-1 protein expression (44 ± 8 % of controls, $n = 4$, $P < 0.05$) that correlated with depressed pH_i recovery after acidosis and abolishment of the SFR (Fig. 12.15), despite preserved ERK1/2 activation (in % of control: stretch 241 ± 10 $n = 5$; stretch l-shNHE1 285 ± 36 $n = 6$). These data provide unequivocal support to our proposal that NHE-1 activation is crucial to the Anrep effect.

12.7 Potential Link Between NHE-1 Activation and Cardiac Hypertrophy and Failure

Cardiac hypertrophy is known to be one of the main cardiovascular risk factors and a poor prognostic sign associated with nearly all forms of heart failure (Koren et al. 1991; Lloyd-Jones et al. 2002). Most intracellular pathways leading to pathological

cardiac hypertrophy and failure converge at the increase in intracellular calcium levels and downstream activation of the calcineurin-dependent transcriptional pathway. The rise in calcium may occur through different mechanisms. One of them is an increase in intracellular Na^+ resulting from enhanced function of the NHE-1, which drives the NCX to increase cytosolic calcium. As stated before, after cardiac muscle is stretched, an autocrine/paracrine chain of steps occur in which AT1 receptor activation is an early event (Sadoshima et al. 1993). This pathway also involves NADPH oxidase-dependent mitochondrial reactive oxygen species release, which itself activates the NHE-1 redox-sensitive kinase$p90^{RSK}$, among others.

Enhanced NHE-1 activity as a possible mechanism involved in cardiac hypertrophy and failure was previously reported in the hypertrophic myocardium of adult spontaneously hypertensive rats (SHR) (Perez et al. 1995), in human ventricular myocytes from hearts with chronic end-stage heart failure (Yokoyama et al. 2000), in a pressure-volume overload model of cardiac hypertrophy and failure in rabbits (Baartscheer et al. 2008), in the hypertrophied heart of a type 2 diabetic rat model (Darmellah et al. 2007) and in neonatal rats (Dulce et al. 2006).

Interestingly, Nakamura et al. (2008) have recently demonstrated in vitro that NHE-1 hyperactivity is sufficient to generate calcium signals required for cardiac hypertrophy to take place. Although in vivo physiological data supporting the involvement of this mechanism in the transition to chronic cardiac hypertrophy and its consequences is scant, Baartscheer et al. (2005) have shown in elegant experiments that long-term NHE-1 inhibition with cariporide in rabbits with combined pressure and volume overload cardiac hypertrophy and failure attenuated hypertrophy and decreased the previously augmented diastolic calcium without significant alteration of systolic calcium (Fig. 12.16).

An increased activity of calcineurin in the myocardium of the SHR, and its suppression by the antihypertrophic treatment has been reported previously (Zou et al. 2002; Ennis et al. 2007). Similarly, in the hypertrophied myocardium of rats with salt-sensitive hypertension, an increase in the activity of calcineurin and its prevention by treatment with an AT1 blocker has been reported (Nagata et al. 2002). We were the first to report that the regression of cardiac hypertrophy caused by NHE-1 inhibition was accompanied by normalization of the activity of the calcineurin pathway and preservation or even improvement of cardiac function. (Ennis et al. 2007). NHE-1 inhibition by decreasing $[Na^+]_i$ diminishes calcium either by decreasing calcium entry (reverse mode) or by increasing calcium efflux (forward mode) through the NCX. At first glance, it may appear difficult to understand how a decrease in cytosolic calcium induced by NHE-1 inhibition can improve myocardial contractility in the long term. However, the preservation of cardiac function after regression of cardiac hypertrophy seems not to be unique to the regression of cardiac hypertrophy induced by NHE-1 inhibition (Esposito et al. 2002). In the myocardium, intracellular calcium is compartmentalized in such way that the contractile pool is different from the pool that regulates reactive signaling. In agreement with this, it has been suggested that calcineurin, as well as CaMKII are preferentially activated by specific sub-cellular calcium pools (Frey et al. 2004; Wu et al. 2010). Therefore we can speculate that the decrease in diastolic calcium might be sensed by the calcium calmodulin-calcineurin

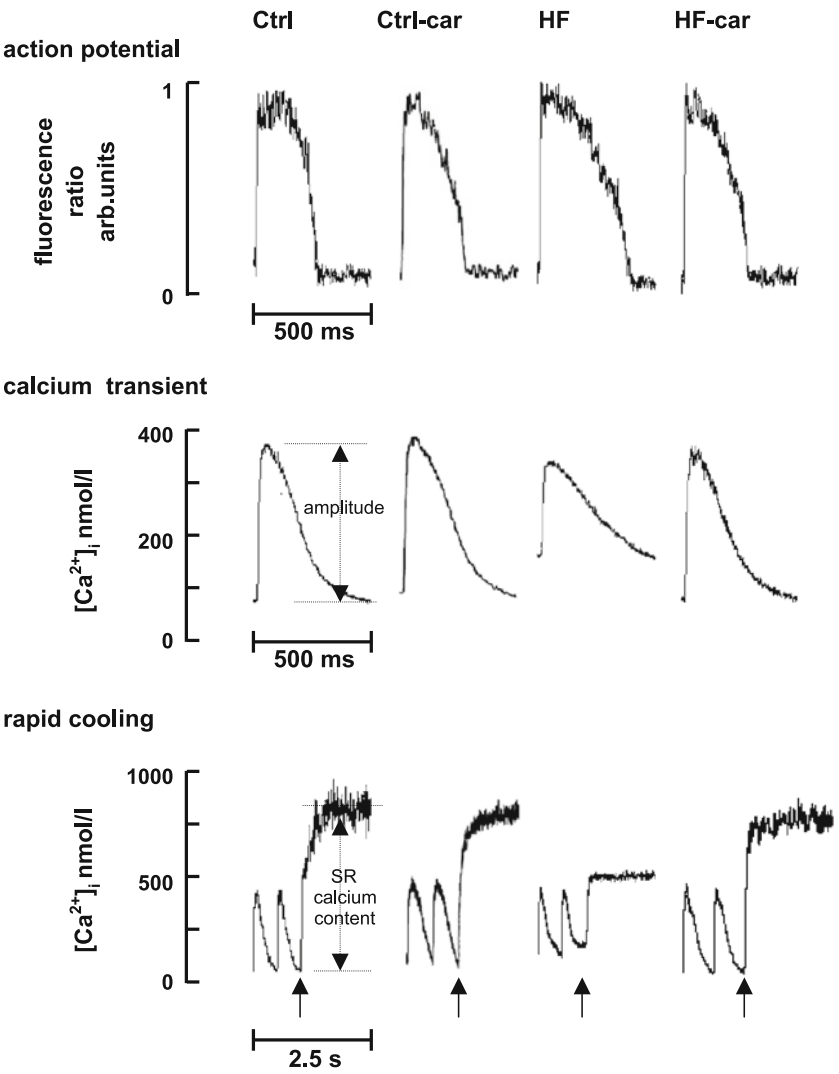

Fig. 12.16 Prevention of cardiac hypertrophy and normalization of the previously augmented diastolic Ca^{2+} observed in rabbits with cardiac hypertrophy and failure (caused by combined pressure and volume overload) treated during 3 months with the NHE-1 inhibitor cariporide. Action potentials (*top*) and Ca^{2+} transients (*bottom*) in isolated myocytes from control (*Ctrl*), control plus cariporide (*Ctrl*-car), heart failure (*HF*), and heart failure plus cariporide (*HF*-car) groups. (Modified with permission from Baartscheer et al. (2005))

pathway, but not by the contractile machinery. Moreover, a negative inotropic effect of calcineurin through different mechanisms has been described (Sah et al. 2002; Li et al. 2003), and a positive inotropic effect could therefore be expected with the phosphatase deactivation.

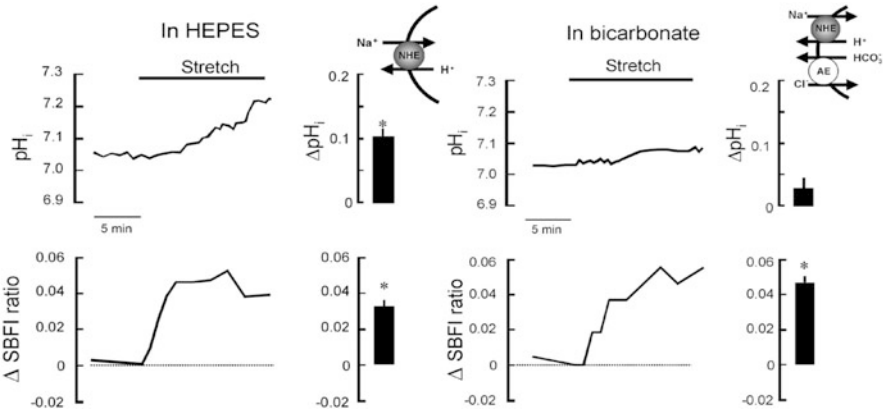

Fig. 12.17 Representative experiments showing that in the presence of bicarbonate, NHE-1 activation by stretch causes elevation of $[Na^+]_i$ (assessed by SBFI 340/380 fluorescence ratio) but not of pH_i, due to the simultaneous activation of the AE. (Modified with permission from Cingolani et al. (2003))

In our scheme, stretch-triggered NHE-1 activation is the main step leading to cardiac hypertrophy and failure. The experiments that originally induced us to consider the activation of NHE-1 after myocardial stretch were performed in the absence of bicarbonate in the medium, where the only active pH_i regulating mechanism was this exchanger (Cingolani et al. 1998). Therefore, the increase in pH_i served as a "marker" for NHE-1 activation by A2-ET. This activation was protein kinase C-dependent since chelerythrine prevented it (Cingolani et al. 1998). It is interesting to emphasize that the NHE-1 exchanges one intracellular H^+ for one extracellular Na^+, therefore, its activation would be followed by an increase in both $[Na^+]_i$ and pH_i. However, during our experiments it became evident that the increase in pH_i occurred only in the absence of bicarbonate in the medium. In contrast, when bicarbonate was present in the media, the simultaneous activation by the stretch of the NHE-1 and the Na^+ independent Cl^-/HCO_3^- exchanger (AE) precluded significant changes in pH_i but not in $[Na^+]_i$ (Fig. 12.17). Regarding the intracellular signals leading to activation of NHE-1 by ET, they are not fully understood. If we consider that part of the positive inotropic effect of ET-1 is the result of endogenously generated ROS (Sand et al. 2003) and that ROS, through MAPK pathways, phosphorylate the cytosolic tail of the NHE-1 increasing its activity (Rothstein et al. 2002), we could suggest that ROS may be involved in the activation of the NHE-1 after stretch.

As pointed out before, the increase in $[Na^+]_i$ induced by NHE-1 activation is the most important step in the chain of events leading to its mechanical counterpart, the SFR, and perhaps portending implications in the mechanism(s) that lead to myocardial hypertrophy and failure (Gray et al. 2001). In connection with this, we have demonstrated that exogenous applied A2 stimulates AE activity through endogenous ET (Camilión de Hurtado et al. 2000). Therefore, under physiological conditions, stretch will be followed by a sequential release of A2 and ET leading

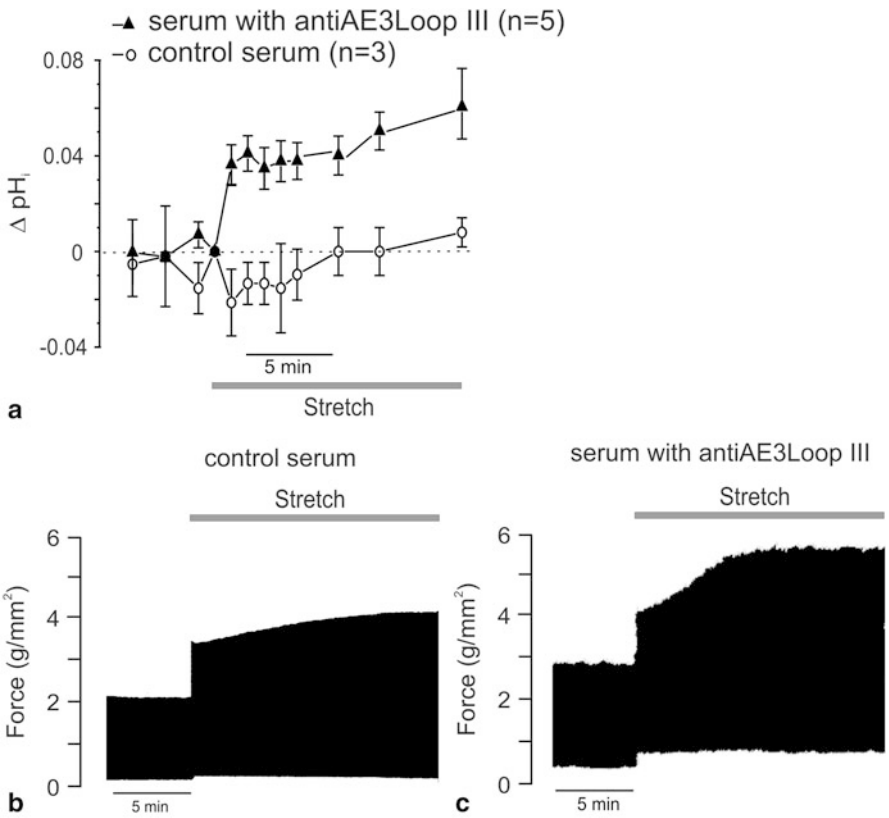

Fig. 12.18 When the AE activation is prevented by a functional antibody (antiAE3Loop III) an increase in pH_i takes place (panel **a**), Thus, the SFR in this condition results from the increase in the calcium transient plus an increase in myofilament calcium responsiveness due to cytosolic alkalization and, therefore, the SFR to stretch is greater (compare panels **b** and **c**). (Modified with permission from Cingolani et al. (2003a))

to the simultaneous activation of NHE and AE. The rise in pH_i induced by NHE-1 activation might be prevented by AE, but this is not the case for the increase in $[Na^+]_i$, due to its Na^+ independency. This increase in $[Na^+]_i$ will trigger an increase in calcium influx (and consequently the calcium transient) by reducing the NCX forward mode and/or favoring its reverse mode of operation. Instead, when the activation of the AE is prevented by a functional antibody, an increase in $[Na^+]_i$ takes place (Fig. 12.18a) together with an increase in pH_i. The mechanical counterpart may therefore result from the increase in calcium transient and also from the increase in myofilament calcium responsiveness due to cytosolic alkalization (Fabiato and Fabiato 1978; Mattiazzi et al. 1979; Orchard and Kentish 1990). In agreement with the latter, Fig. 12.18b, c shows that in the presence of the AE antibody, the stretch of a cat papillary muscle produces a greater SFR.

It may be argued that the Na^+/K^+ATPase should prevent the increase in $[Na^+]_i$ elicited by NHE-1 hyperactivity, however, Bers et al. (2003) have shown that the changes in $[Na^+]_i$ necessary to alter the Na^+ pump activity should be greater than those detected by us after the stretch. Furthermore, we should consider that an enhanced activity of the pump would be probably detected due to the increase in $[Na^+]_i$ after stretch, but not enough to normalize the $[Na^+]_i$. In other words, the rise in $[Na^+]_i$ detected during the SFR should be higher if the pump was inhibited. We may also speculate that, similarly to the Na^+ pump lag hypothesis for the force-frequency relationship, the greater Na^+ entry is balanced by an increased Na^+ pump activity, but only at the cost of elevated $[Na^+]_i$ and hence increased calcium entry. In contrast, the changes in $[Na^+]_i$ detected after stretch may suffice to alter the activity of the NCX, specially if the NHE and the NCX are co-localized (Petrecca et al. 1999; Brette et al. 2002). Accordingly, we recently showed that the positive inotropic effect of exogenous A2 or ET-1 is accompanied by a cariporide-sensitive increase in $[Na^+]_i$ (Fig. 12.19) (Perez et al. 2003). Additionally, the fact that ET receptors blockade with TAK044 canceled the A2-induced rise in $[Na^+]_i$ reinforces the role of ET as mediator of A2 effects (Perez et al. 2003).

Although the role of NHE-1 activation early after stretch leading to the SFR development (and possibly to cardiac hypertrophy and failure) has been detected in different species including cat (Perez et al. 2001; Caldiz et al. 2007), human (von Lewinski et al. 2004), rabbit (Luers et al. 2005), and rat (Alvarez et al. 1999; Calaghan and White 2004) myocardium, involvement of stretch-operated channels in this response was recently proposed in mouse ventricular muscle by Ward et al. (2008), who showed that canonical transient receptor-operated channels (TRPC) are sensitive to stretch in mice myocardium. Furthermore, Takahashi et al. (2007) showed TRPC sensitivity to A2 in human coronary artery smooth muscle cells. Interestingly, it was proposed that TRPC channels were necessary mediators of pathological cardiac hypertrophy in mice, in part through calcineurin-NFAT signaling (Wu et al. 2010), a pathway that we showed to be sensitive to NHE-1 inhibition in rats (Ennis et al. 2007). This discrepancy may be explained by two alternative hypotheses: (1) the TRPC channels were involved in one or some of the steps in the chain of events described previously; i.e., to induce A2 release after stretch or (2) by species differences.

Regarding whether some early intracellular signals triggered by the autocrine/paracrine mechanism, (i.e; NHE-1 activation) persists over time, we recently explore this in a mouse model of cardiac hypertrophy and failure by transverse aortic constriction (TAC). After 7 weeks of TAC, cardiac hypertrophy and decreased myocardial performance was detected, along with enhanced oxidative stress, as well as increased activity of redox-sensitive $p90^{RSK}$ kinase and NHE-1 phosphorylation. Selective AT1 receptors blockade with losartan prevented $p90^{RSK}$ and NHE-1 activation and decreased hypertrophy development, preserving contractility in spite of a higher workload (Cingolani et al. 2010, 2011c). It is important to highlight that losartan treatment did not restore wall thickness to control values (it remained ~24 % higher than controls), but certainly reduced it to levels "necessary" to counteract for the increase in pressure induced by the aortic constriction. In other words, an excessive

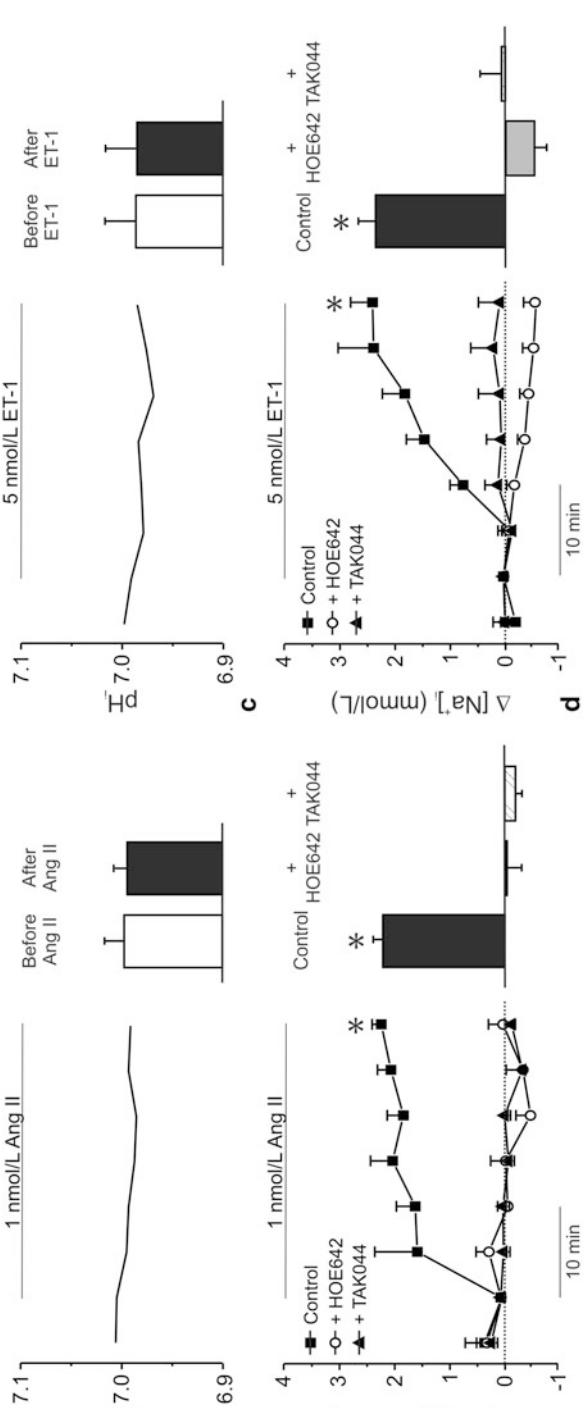

Fig. 12.19 The positive inotropic effect of exogenous Ang II or ET-1 is accompanied by a cariporide-sensitive rise in $[Na^+]_i$. Panel **a**: Typical experiment and averaged results of the effect of a low dose of A2 on pH_i. Panel **b**: Time course of $[Na^+]_i$ changes induced by A2 and averaged values after 30 min, in control and after NHE-1 inhibition with cariporide (HOE642) or ET receptors blockade (TAK044). Panels **c** and **d**: Same as A and B respectively, but after addition of an equipotent dose of exogenous ET-1. Note that despite the lack of pH_i change, there is an A2-induced NHE-1 stimulation detected by the increase in $[Na^+]_i$ that requires available ET receptors and that this effect can be mimicked by an equipotent dose of exogenous ET-1. *$P < 0.05$ vs pre-peptide control value. (Modified with permission from Perez et al. (2003))

cardiac hypertrophy was eliminated. Interestingly, in spite of the increase in wall stress seen with losartan in the present study, the reduction in cardiac hypertrophy was accompanied by an increased cardiac performance. These findings suggest that the degree of cardiac hypertrophy prevented by losartan was maladaptive or "inappropriate", a concept previously coined by others (Mureddu et al. 2009). In this regard, it seems that pressure overload may trigger multiple intracellular signaling pathways in addition to enhanced AT1 receptor stimulation. Whereas some of these may be deleterious, others may benefit the heart allowing it to adapt to different stressors. The hypothetical proposal to explain these striking findings is schematized in Fig. 12.20.

12.7.1 Hypertrophic Signals Triggered by NHE-1

The possible link between the SFR and myocardial hypertrophy and failure is supported by the fact that an enhanced activity of NHE-1 is detected in several models of cardiac hypertrophy (Kusumoto et al. 2001; Engelhardt et al. 2002). In the hypertrophied myocardium of SHR (Wang et al. 2003), an increased activity of NHE-1 has been detected (Perez et al. 1995; Schussheim and Radda 1995) due to a kinase-dependent posttranslational phosphorylation of its cytosolic tail (Siczkowski et al. 1995; Ennis et al. 1998). The regression of myocardial hypertrophy produced by several pharmacological interventions was accompanied by normalization of the NHE-1 activity (Ennis et al. 1998; Alvarez et al. 2002). Moreover, chronic treatment of SHR rats with NHE-1 inhibitors caused load-independent regression of cardiomyocyte hypertrophy and fibrosis (Camilion de Hurtado et al. 2002; Cingolani et al. 2003b), although the latter effect took longer than the regression of myocyte size (Cingolani et al. 2003b), possibly as a reflection of the slower turnover rate of collagen metabolism (Weber and Brilla 1991).

Based on our previous results in adult multicellular cardiac preparations, hypertensive cardiac hypertrophy and failure are caused by an autocrine/paracrine chain of events triggered by myocardial stretch that begins with the activation of the AT1 receptors followed by the release/formation of endothelin-1 (ET-1), MR activation, EGFR transactivation and stimulation of the NHE-1 (Cingolani et al. 2005; Villa-Abrille et al. 2010; Caldiz et al. 2011). The increased production of ROS that results from A2/ET-1 stimulation of the NADPH oxidase may be responsible for ERK1/2-p90^{RSK} activation and NHE-1 stimulation (Caldiz et al. 2007; Garciarena et al. 2008). NHE-1 hyperactivity leads to an increase in intracellular Na^+ concentration that promotes cytoplasmic calcium overload through the NCX (Cingolani et al. 2005). Calcium is widely recognized as one of the main pro-hypertrophic intracellular signal. It activates several intracellular pathways like calcineurin, nuclear factor of activated T cells (NFAT), calcium/calmodulin-dependent kinase II, protein kinase C and possibly other intracellular signaling pathways. Calcineurin is a pro-hypertrophic serine-threonine protein phosphatase that is activated in response to sustained elevations of intracellular levels of calcium. Once activated, calcineurin

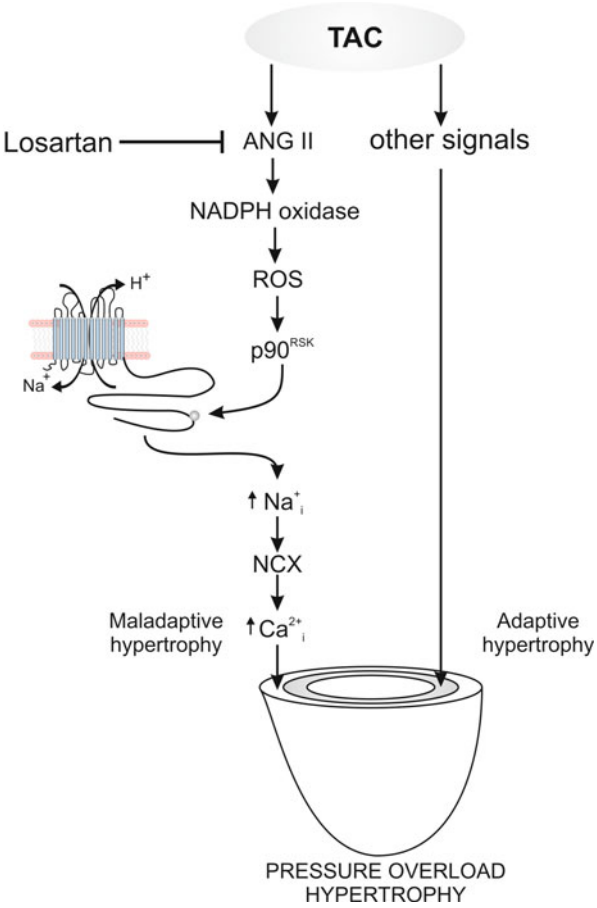

Fig. 12.20 Schematic representation of the proposed signaling pathway involved in the prevention of cardiac hypertrophy by AT1 receptors blockade. In our scheme, the AT1 receptors-sensitive part of the TAC-induced CH is maladaptive and related to redox-sensitive $p90^{RSK}$ activation, NHE-1 phosphorylation/activation, increase in intracellular Na^+ and the consequent increase in intracellular calcium through the NCX. The increased calcium concentration would then activate the calcineurin-NFAT signaling pathway responsible for triggering an abnormal cardiac growth. On the other hand, the same mechanical stimulus (*stretch* of cardiac muscle) may trigger other prohypertrophic signals intended to compensate for the increased wall stress ("adaptive hypertrophy") (Catalucci et al. 2008). The reason for an improvement in cardiac performance accompanying the regression in cardiac hypertrophy due to AT1 receptors blockade is not apparent to us at present. However, we could speculate about cancellation of the negative inotropic effect assigned to calcineurin phosphatase activation (Sah et al. 2002; Li et al. 2003). (Modified with permission from Cingolani et al. (2011c))

directly dephosphorylates NFATs within the cytoplasm and promotes their translocation into the nucleus to induce the transcription of several genes. In SHR, Ennis et al. (2007) described that NHE-1 blockade regressed cardiac hypertrophy, decreased myocardial BNP, calcineurin Aβ and nuclear NFAT expression. Additionally, they demonstrated by echocardiography, a reduction in left ventricular wall thickness

without changes in cavity dimensions or a significant decrease in blood pressure (Ennis et al. 2007).

Emerging evidence indicates that NHE-1 can be activated by ROS (Sabri et al. 1998; Snabaitis et al. 2002). Less well explored is the possibility that the increased ROS production, in addition to its role played upstream to NHE-1, may be induced by a rise in $[Na^+]_i$ secondary to NHE-1 hyperactivity. Javadov et al. (2005, 2006) showed in rats with myocardial infarction that NHE-1 inhibition was able to prevent cardiac hypertrophy and decreased the vulnerability of mitochondria to calcium. In addition, they attributed the anti-hypertrophic effect of NHE-1 inhibition to the decreased generation of mitochondrial-derived ROS. In relation to this, we recently reported that the cardiac superoxide production induced by A2 was reduced under NHE-1 inhibition (Javadov et al. 2006; Garciarena et al. 2008). Moreover, the decrease in infarct size and level of tissue lipoperoxidation, induced by ROS scavengers administered during the reperfusion, can be mimicked by specific blockade of NHE-1 (Fantinelli et al. 2006). Therefore, NHE-1 inhibition may exert its beneficial effects by decreasing $[Na^+]_i$ and/or ROS production. Both $[Na^+]_i$ and ROS target the NCX to modify its activity, and therefore target calcium either at the bulk of the cytosol, or to more restricted spaces.

12.8 Conclusion and Perspectives. Possible Applications in the Clinical Arena

The RALES trial in 1999, the EPHESUS in 2003 and the EMPHASIS-HF in 2010, called attention to the beneficial effects of ALD antagonism in the treatment of heart failure. Cardiovascular disease and specially heart failure is one of the most important health problems in the world. Cardiac hypertrophy is known to be the main entrance door to the failing heart. As described above, cardiac hypertrophy and failure are triggered by intracellular signals that occur following myocardial stretch. Surprisingly, investigators working in the area of cardiac mechanics did not often extrapolate their early findings seen after stretch to the development of cardiac hypertrophy and/or failure. The reason for this could be that time frames in which these two phenomena occur are quite different. However, the long journey toward myocardial hypertrophy and failure begins with one step, and this first step may well be the autocrine/paracrine intracellular signaling pathway triggered by myocardial stretch as was proposed by Izumo and Sadoshima in neonatal cardiac myocytes (Sadoshima et al. 1993) and by us (Cingolani et al. 1998; Alvarez et al. 1999; Perez et al. 2001; Caldiz et al. 2007; Villa-Abrille et al. 2010) in adult multicellular preparations.

Current treatment against cardiac failure is mainly based on inhibition of hormones (A2, ALD, catecholamines). Despite the term “ALD inhibition” has been widespread used, this is often misleading and should be replaced by MR antagonism, mainly because ALD is not the only agonist binding to and activating MR (Mihailidou et al. 2009). Although several studies have demonstrated the important benefits of MR

antagonists in heart failure, their clinical use remains lower than expected and the exact mechanism of the beneficial effect is still unknown.

In 1990 Swedberg et al. (1990) established a relationship between plasma levels of ALD and mortality in patients with heart failure. This finding called attention to the possibility of predicting indexes of morbidity and mortality in patients suffering from this disease with excessive plasma levels of ALD. On the other hand, Karl Weber's laboratory carried out several investigations demonstrating that ALD itself is able to increase myocardial fibrosis independently of blood pressure level (for review see (Gandhi et al. 2011)). Furthermore, it was also shown that spironolactone, an MR blocker with diuretic properties developed by Searle laboratories, abolished these effects.

Contemporarily, several research labs reported that MR are not only expressed in classical ALD target tissues, but also in many others, including smooth and cardiac muscle.

The most potent stimulator of ALD synthesis is A2. Consequently, interfering with A2 actions should decrease systemic ALD levels. However, despite complete vascular angiotensin converting enzyme inhibition plasma ALD levels were elevated in patients with heart failure (Jorde et al. 2002). Even the combination of angiotensin converting enzyme inhibition and A2 antagonism only transiently reduces ALD plasma levels in patients with heart failure (McKelvie et al. 1999) suggesting A2 independent ALD production. This phenomenon known as ALD escape and whose underlying mechanism has not been completely clarified yet constitutes a strong proof to directly inhibit MR activation on top of angiotensin converting enzyme inhibition or AT1 blockers in the treatment of heart failure.

Among MR inhibitors, spironolactone was the first marketed compound in the early 1960s, and although proved to be clinically useful, it also showed tolerability problems due to painful gynecomastia or menstrual disturbances due to its androgenic and progesteronergic effects. Nevertheless, it was the only compound approved to be used in the RALES in 1663 patients with severe heart failure (Class III-IV NYHA). The trial was discontinued after a mean follow-up period of 24 months, because interim analysis determined that spironolactone reduced the risk of death by 30 %. Later on, more specific compounds that inhibit MR were developed, and after several years of delay Searle patented eplerenone in 1984. Eplerenone was tested in a clinical study called EPHESUS performed on 6642 patients with acute myocardial infarction complicated with left ventricular systolic dysfunction (ejection fraction less than 40 %). Treatment started 3–14 days after myocardial infarction and was maintained during 16 months. The results were positive, favoring the active treatment arm, and the main difference with RALES was that most of the patients in EPHESUS were receiving beta blockers (75 % vs. 11 % in RALES). All cause mortality decreased by ~15 % and sudden cardiac death by ~21 %. Interestingly, a post hoc analysis of the EPHESUS (Pitt et al. 2005) showed a reduction of all cause mortality by ~31 % as early as 30 days after eplerenone treatment. One important fact to emphasize, specially after the widely spread concept that high levels of ALD characterizes heart failure, is that plasma levels of ALD and Na^+ were in the normal range in both RALES and EPHESUS trials at randomization, and the beneficial effects were seen

early, probably before the "ALD escape" took place. These findings may suggest that: (1) MRs are activated by ligands other than ALD, or (2) cytosolic MRs are activated by increased intracellular levels of ALD independently of its plasma levels (Silvestre et al. 1998).

In contrast with the two mentioned clinical trials, the recently published EMPHASIS (Zannad et al. 2010, 2011) was carried out on patients with less severe heart failure. This study enrolled 2737 patients with heart failure class II and III of the NYHA and left ventricular ejection fraction of no more than 35 %. The trial was stopped prematurely according to their rules, after a median follow-up of 21 months, due to the excess of benefit in reducing the risk of cardiovascular death or hospitalization for heart failure, obtained by anti-aldosteronic therapy with eplerenone, which was then extended to both arms of the trail. Another clinical trial which is currently running is the TOPCAT. This study will test the effects of MR inhibition in patients suffering from heart failure with left ventricular ejection fraction of at least 45 %. TOPCAT will probably end in 2013.

Finally, ALBATROS is a clinical trial designed to asses the potential superiority of MR inhibition early after myocardial infarction. The study will evaluate the intravenous bolus of potassium camreonate followed by a daily dose of 25 mg of spironolactone for 6 months on top of standard therapy in 1600 patients with myocardial infarction.

Although clinical evidence undoubtedly showed beneficial effects of treating heart failure patients with MR blockers, the mechanisms by which MR antagonism provide cardiovascular protection are not completely understood. In this regard, our own results assigning a crucial role for MR activation as an early hypertrophic signal triggered by myocardial stretch (presented before in this chapter) encouraged us to suggest that prevention of oxidative stress and NHE-1 activation should be considered as a potential key factor for the salutary effects of ALD antagonism in humans.

References

Akhtar S, Benter IF (2007) Nonviral delivery of synthetic siRNAs in vivo. J Clin Invest 117: 3623–3632

Akram S, Teong HF, Fliegel L, Pervaiz S, Clement MV (2006) Reactive oxygen species-mediated regulation of the Na^+-H^+ exchanger 1 gene expression connects intracellular redox status with cells' sensitivity to death triggers. Cell Death Differ 13:628–641

Alvarez BV, Perez NG, Ennis IL, Camilion de Hurtado MC, Cingolani HE (1999) Mechanisms underlying the increase in force and Ca^{2+} transient that follow stretch of cardiac muscle: a possible explanation of the Anrep effect. Circ Res 85:716–722

Alvarez BV, Ennis IL, De Hurtado MC, Cingolani HE (2002) Effects of antihypertensive therapy on cardiac sodium/hydrogen ion exchanger activity and hypertrophy in spontaneously hypertensive rats. Can J Cardiol 18:667–672

Allen DG, Kurihara S (1982) The effects of muscle length on intracellular calcium transients in mammalian cardiac muscle. J Physiol 327:79–94

Anderson HD, Wang F, Gardner DG (2004) Role of the epidermal growth factor receptor in signaling strain-dependent activation of the brain natriuretic peptide gene. J Biol Chem 279:9287–9297

Asakura M, Kitakaze M, Takashima S, Liao Y, Ishikura F, Yoshinaka T, Ohmoto H, Node K, Yoshino K, Ishiguro H, Asanuma H, Sanada S, Matsumura Y, Takeda H, Beppu S, Tada M, Hori M, Higashiyama S (2002) Cardiac hypertrophy is inhibited by antagonism of ADAM12 processing of HB-EGF: metalloproteinase inhibitors as a new therapy. Nat med 8:35–40

Avkiran M, Marber MS (2002) Na^+/H^+ exchange inhibitors for cardioprotective therapy: progress, problems and prospects. J Am Col Cardiol 39:747–753

Baartscheer A, Schumacher CA, van Borren MM, Belterman CN, Coronel R, Opthof T, Fiolet JW (2005) Chronic inhibition of Na^+/H^+-exchanger attenuates cardiac hypertrophy and prevents cellular remodeling in heart failure. Cardiovasc Res 65:83–92

Baartscheer A, Hardziyenka M, Schumacher CA, Belterman CN, van Borren MM, Verkerk AO, Coronel R, Fiolet JW (2008) Chronic inhibition of the Na^+/H^+ – exchanger causes regression of hypertrophy, heart failure, and ionic and electrophysiological remodelling. Br J Pharmacol 154:1266–1275

Barbato JC, Rashid S, Mulrow PJ, Shapiro JI, Franco-Saenz R (2004) Mechanisms for aldosterone and spironolactone-induced positive inotropic actions in the rat heart. Hypertension 44:751–757

Bell SM, Schreiner CM, Schultheis PJ, Miller ML, Evans RL, Vorhees CV, Shull GE, Scott WJ (1999) Targeted disruption of the murine Nhe1 locus induces ataxia, growth retardation, and seizures. Am J Physiol 276:C788–C795

Bers DM, Barry WH, Despa S (2003) Intracellular Na^+ regulation in cardiac myocytes. Cardiovasc Res 57:897–912

Brandes RP (2005) Triggering mitochondrial radical release: a new function for NADPH oxidases. Hypertension 45:847–848

Brette F, Komukai K, Orchard CH (2002) Validation of formamide as a detubulation agent in isolated rat cardiac cells. Am J Physiol 283:H1720–H1728

Calaghan S, White E (2004) Activation of Na^+-H^+ exchange and stretch-activated channels underlies the slow inotropic response to stretch in myocytes and muscle from the rat heart. J Physiol 559:205–214

Caldiz CI, Garciarena CD, Dulce RA, Novaretto LP, Yeves AM, Ennis IL, Cingolani HE, Chiappe de Cingolani G, Perez NG (2007) Mitochondrial reactive oxygen species activate the slow force response to stretch in feline myocardium. J Physiol 584:895–905

Caldiz CI, Diaz RG, Nolly MB, Chiappe de Cingolani GE, Ennis IL, Cingolani HE, Perez NG (2011) Mineralocorticoid receptor activation is crucial in the signalling pathway leading to the Anrep effect. J Physiol 589:6051–6061

Camilión de Hurtado MC, Alvarez BV, Ennis IL, Cingolani HE (2000) Stimulation of myocardial Na^+-independent Cl^--HCO^{3-} exchanger by angiotensin II is mediated by endogenous endothelin. Circ Res 86:622–627

Camilión de Hurtado MC, Portiansky EL, Perez NG, Rebolledo OR, Cingolani HE (2002) Regression of cardiomyocyte hypertrophy in SHR following chronic inhibition of the Na^+/H^+ exchanger. Cardiovasc Res 53:862–868

Catalucci D, Latronico MV, Ellingsen O, Condorelli G (2008) Physiological myocardial hypertrophy: how and why? Front Biosci 13:312–324

Cingolani et al. (2003) In: The Sodium-Hydrogen Exchanger. From molecule to its role in disease, pp. 255–262 Kluwer Academic Publishers

Cingolani HE, Ennis IL (2007) Sodium-hydrogen exchanger, cardiac overload, and myocardial hypertrophy. Circulation 115:1090–1100

Cingolani HE, Alvarez BV, Ennis IL, Camilion de Hurtado MC (1998) Stretch-induced alkalinization of feline papillary muscle: an autocrine-paracrine system. Circ Res 83:775–780

Cingolani HE, Pérez NG, Camilión de Hurtado MC (2001) An autocrine/paracrine mechanism triggered by myocardial stretch induces changes in contractility. NIPS 16:88–91

Cingolani HE, Chiappe GE, Ennis IL, Morgan PG, Alvarez BV, Casey JR, Dulce RA, Perez NG, Camilion de Hurtado MC (2003a) Influence of Na^+-independent Cl^--HCO^{3-} exchange on the slow force response to myocardial stretch. Circ Res 93:1082–1088

Cingolani HE, Rebolledo OR, Portiansky EL, Perez NG, Camilion de Hurtado MC (2003b) Regression of hypertensive myocardial fibrosis by $Na^{(+)}/H^{(+)}$ exchange inhibition. Hypertension 41:373–377

Cingolani HE, Perez NG, Aiello EA, de Hurtado MC (2005) Intracellular signaling following myocardial stretch: an autocrine/paracrine loop. Regul Pept 128:211–220

Cingolani HE, Villa-Abrille MC, Cornelli M, Nolly A, Ennis IL, Garciarena C, Suburo AM, Torbidoni V, Correa MV, Camilionde Hurtado MC, Aiello EA (2006) The positive inotropic effect of angiotensin II: role of endothelin-1 and reactive oxygen species. Hypertension 47:727–734

Cingolani OH, Perez NG, Mosca SM, Schinella GR, Console GM, Ennis IL, Escudero EM, Cingolani HE (2010) AT1 receptor blockade with losartan prevents Maladaptive hypertrophy in pressure overload by inhibiting ROS release. Hypertension 56:e119 (Abstract)

Cingolani HE, Ennis IL, Aiello EA, Perez NG (2011a) Role of autocrine/paracrine mechanisms in response to myocardial strain. Pflugers Arch 426(1):29–38

Cingolani OH, Kirk JA, Seo K, Koitabashi N, Lee DI, Ramirez-Correa G, Bedja D, Barth AS, Moens AL, Kass DA (2011b) Thrombospondin-4 is required for stretch-mediated contractility augmentation in cardiac muscle. Circ Res 109:1410–1414

Cingolani OH, Perez NG, Ennis IL, Alvarez MC, Mosca SM, Schinella GR, Escudero EM, Console G, Cingolani HE (2011c) In vivo key role of reactive oxygen species and NHE-1 activation in determining excessive cardiac hypertrophy. Pflugers Arch 462:733–743

Cox GA, Lutz CM, Yang CL, Biemesderfer D, Bronson RT, Fu A, Aronson PS, Noebels JL, Frankel WN (1997) Sodium/hydrogen exchanger gene defect in slow-wave epilepsy mutant mice. Cell 91:139–148

Chai W, Danser AH (2006) Why are mineralocorticoid receptor antagonists cardioprotective? N-S Arch Pharmacol 374:153–162

Darmellah A, Baetz D, Prunier F, Tamareille S, Rucker-Martin C, Feuvray D (2007) Enhanced activity of the myocardial Na^+/H^+ exchanger contributes to left ventricular hypertrophy in the Goto-Kakizaki rat model of type 2 diabetes: critical role of Akt. Diabetologia 50:1335–1344

De Giusti VC, Nolly MB, Yeves AM, Caldiz CI, Villa-Abrille MC, Chiappe de Cingolani G, Ennis IL, Cingolani HE, Aiello EA (2011) Aldosterone stimulates the cardiac Na^+/H^+ exchanger via transactivation of the epidermal growth factor receptor. Hypertension 58:912–919

Dhein S (1998) Gap junction channels in the cardiovascular system: pharmacological and physiological modulation. Trends Pharmacol Sci 19:229–241

Dorrance AM, Osborn HL, Grekin R, Webb RC (2001) Spironolactone reduces cerebral infarct size and EGF-receptor mRNA in stroke-prone rats. Am J Physiol Regul Integr Comp Physiol 281:R944–R950

Dulce RA, Hurtado C, Ennis IL, Garciarena CD, Alvarez MC, Caldiz C, Pierce GN, Portiansky EL, Chiappe de Cingolani GE, Camilion de Hurtado MC (2006) Endothelin-1 induced hypertrophic effect in neonatal rat cardiomyocytes: involvement of Na^+/H^+ and Na^+/Ca^{2+} exchangers. J Mol Cell Cardiol 41:807–815

Duquesnes N, Vincent F, Morel E, Lezoualc'h F, Crozatier B (2009) The EGF receptor activates ERK but not JNK Ras-dependently in basal conditions but ERK and JNK activation pathways are predominantly Ras-independent during cardiomyocyte stretch. Int J Biochem Cell Biol 41:1173–1181

Ebata S, Muto S, Okada K, Nemoto J, Amemiya M, Saito T, Asano Y (1999) Aldosterone activates Na^+/H^+ exchange in vascular smooth muscle cells by nongenomic and genomic mechanisms. Kidney Int 56:1400–1412

Engelhardt S, Hein L, Keller U, Klambt K, Lohse MJ (2002) Inhibition of Na^+-H^+ exchange prevents hypertrophy, fibrosis, and heart failure in beta(1)-adrenergic receptor transgenic mice. Circ Res 90:814–819

Ennis IL, Alvarez BV, Camilion de Hurtado MC, Cingolani HE (1998) Enalapril induces regression of cardiac hypertrophy and normalization of pHi regulatory mechanisms. Hypertension 31:961–967

Ennis IL, Escudero EM, Console GM, Camihort G, Dumm CG, Seidler RW, Camilion de Hurtado MC, Cingolani HE (2003) Regression of isoproterenol-induced cardiac hypertrophy by Na^+/H^+ exchanger inhibition. Hypertension 41:1324–1329

Ennis IL, Garciarena CD, Escudero EM, Perez NG, Dulce RA, Camilion de Hurtado MC, Cingolani HE (2007) Normalization of the calcineurin pathway underlies the regression of hypertensive

hypertrophy induced by Na^+/H^+exchanger-1 (NHE-1) inhibition. Can J Physiol Pharm 85:301–310

Esposito G, Rapacciuolo A, Naga Prasad SV, Takaoka H, Thomas SA, Koch WJ, Rockman HA (2002) Genetic alterations that inhibit in vivo pressure-overload hypertrophy prevent cardiac dysfunction despite increased wall stress. Circulation 105(1):85–92

Fabiato A, Fabiato F (1978) Effects of pH on the myofilaments and the sarcoplasmic reticulum of skinned cells from cardiace and skeletal muscles. J Physiol 276:233–255

Fantinelli JC, Cingolani HE, Mosca SM (2006) Na^+/H^+ exchanger inhibition at the onset of reperfusion decreases myocardial infarct size: role of reactive oxygen species. Cardiovasc Pathol 15:179–184

Fliegel L, Karmazyn M (2004) The cardiac Na-H exchanger: a key downstream mediator for the cellular hypertrophic effects of paracrine, autocrine and hormonal factors. Biochem Cell Biol 82:626–635

Frey N, Barrientos T, Shelton JM, Frank D, Rütten H, Gehring D, Kuhn C, Lutz M, Rothermel B, Bassel-Duby R, Richardson JA, Katus HA, Hill JA, Olson EN (2004) Mice lacking calsarcin-1 are sensitized to calcineurin signaling and show accelerated cardiomyopathy in response to pathological biomechanical stress. Nat Med 10(12):1336–1343

Fujisawa G, Okada K, Muto S, Fujita N, Itabashi N, Kusano E, Ishibashi S (2003) Na/H exchange isoform 1 is involved in mineralocorticoid/salt-induced cardiac injury. Hypertension 41:493–498

Gandhi MS, Kamalov G, Shahbaz AU, Bhattacharya SK, Ahokas RA, Sun Y, Gerling IC, Weber KT (2011) Cellular and molecular pathways to myocardial necrosis and replacement fibrosis. Heart Failure Rev 16:23–34

Garciarena CD, Caldiz CI, Correa MV, Schinella GR, Mosca SM, Chiappe de Cingolani GE, Cingolani HE, Ennis IL (2008) Na^+/H^+ exchanger-1 inhibitors decrease myocardial superoxide production via direct mitochondrial action. J Appl Physiol 105:1706–1713

Giordano FJ (2005) Oxygen, oxidative stress, hypoxia, and heart failure. J Clin Invest 115:500–508

Gomez-Sanchez EP, Ahmad N, Romero DG, Gomez-Sanchez CE (2004) Origin of aldosterone in the rat heart. Endocrinology 145:4796–4802

Gray RP, McIntyre H, Sheridan DS, Fry CH (2001) Intracellular sodium and contractile function in hypertrophied human and guinea-pig myocardium. Pflugers Arch 442:117–123

Gros R, Ding Q, Sklar LA, Prossnitz EE, Arterburn JB, Chorazyczewski J, Feldman RD (2011) GPR30 expression is required for the mineralocorticoid receptor-independent rapid vascular effects of aldosterone. Hypertension 57:442–451

Grossmann C, Gekle M (2007) Non-classical actions of the mineralocorticoid receptor: misuse of EGF receptors? Mol Cell Endocrinol 277:6–12

Grossmann C, Gekle M (2008) Nongenotropic aldosterone effects and the EGFR: interaction and biological relevance. Steroids 73:973–978

Grossmann C, Gekle M (2009) New aspects of rapid aldosterone signaling. Mol Cell Endocrinol 308:53–62

Grossmann C, Krug AW, Freudinger R, Mildenberger S, Voelker K, Gekle M (2007) Aldosterone-induced EGFR expression: interaction between the human mineralocorticoid receptor and the human EGFR promoter. Am J Physiol Endocrinol Metab 292:E1790–E1800

Grossmann C, Husse B, Mildenberger S, Schreier B, Schuman K, Gekle M (2010) Colocalization of mineralocorticoid and EGF receptor at the plasma membrane. Biochim Biophys Acta 1803:584–590

Haworth RS, McCann C, Snabaitis AK, Roberts NA, Avkiran M (2003) Stimulation of the plasma membrane Na^+/H^+ exchanger NHE1 by sustained intracellular acidosis. Evidence for a novel mechanism mediated by the ERK pathway. J Biol Chem 278:31676–31684

Hofmann PA, Fuchs F (1988) Bound calcium and force development in skinned cardiac muscle bundles: effect of sarcomere length. J Mol Cell Cardiol 20:667–677

Hongo K, White E, Le Guennec JY, Orchard CH (1996) Changes in $[Ca^{2+}]i$, $[Na^+]i$ and Ca^{2+} current in isolated rat ventricular myocytes following an increase in cell length. J Physiol 491(Pt 3): 609–619

Ito H, Hirata Y, Adachi S, Tanaka M, Tsujino M, Koike A, Nogami A, Murumo F, Hiroe M (1993) Endothelin-1 is an autocrine/paracrine factor in the mechanism of angiotensin II-induced hypertrophy in cultured rat cardiomyocytes. J Clin Invest 92:398–403

Javadov S, Huang C, Kirshenbaum L, Karmazyn M (2005) NHE-1 inhibition improves impaired mitochondrial permeability transition and respiratory function during postinfarction remodelling in the rat. J Mol Cell Cardiol 38:135–143

Javadov S, Baetz D, Rajapurohitam V, Zeidan A, Kirshenbaum LA, Karmazyn M (2006) Antihypertrophic effect of Na^+/H^+ exchanger isoform 1 inhibition is mediated by reduced mitogen-activated protein kinase activation secondary to improved mitochondrial integrity and decreased generation of mitochondrial-derived reactive oxygen species. J Pharmacol Exp Ther 317:1036–1043

Jorde UP, Vittorio T, Katz SD, Colombo PC, Latif F, Le Jemtel TH (2002) Elevated plasma aldosterone levels despite complete inhibition of the vascular angiotensin-converting enzyme in chronic heart failure. Circulation 106:1055–1057

Kagiyama S, Eguchi S, Frank GD, Inagami T, Zhang YC, Phillips MI (2002) Angiotensin II-induced cardiac hypertrophy and hypertension are attenuated by epidermal growth factor receptor antisense. Circulation 106:909–912

Karmazyn M (1999) The role of the myocardial sodium-hydrogen exchanger in mediating ischemic and reperfusion injury. From amiloride to cariporide. Ann N Y Acad Sci 874:326–334

Karmazyn M, Liu Q, Gan XT, Brix BJ, Fliegel L (2003) Aldosterone increases NHE-1 expression and induces NHE-1-dependent hypertrophy in neonatal rat ventricular myocytes. Hypertension 42:1171–1176

Kentish JC, Wrzosek A (1998) Changes in force and cytosolic Ca^{2+} concentration after length changes in isolated rat ventricular trabeculae. J Physiol 506(Pt 2):431–444

Kim DH, Rossi JJ (2007) Strategies for silencing human disease using RNA interference. Nat Rev 8:173–184

Kimura S, Zhang GX, Nishiyama A, Shokoji T, Yao L, Fan YY, Rahman M, Abe Y (2005a) Mitochondria-derived reactive oxygen species and vascular MAP kinases: comparison of angiotensin II and diazoxide. Hypertension 45:438–444

Kimura S, Zhang GX, Nishiyama A, Shokoji T, Yao L, Fan YY, Rahman M, Suzuki T, Maeta H, Abe Y (2005b) Role of NAD(P)H oxidase- and mitochondria-derived reactive oxygen species in cardioprotection of ischemic reperfusion injury by angiotensin II. Hypertension 45:860–866

Kizana E, Cingolani E, Marban E (2009) Non-cell-autonomous effects of vector-expressed regulatory RNAs in mammalian heart cells. Gene Ther 16:1163–1168

Koren MJ, Devereux RB, Casale PN, Savage DD, Laragh JH (1991) Relation of left ventricular mass and geometry to morbidity and mortality in uncomplicated essential hypertension. Ann Intern Med 114:345–352

Krieg T, Cui L, Qin Q, Cohen MV, Downey JM (2004) Mitochondrial ROS generation following acetylcholine-induced EGF receptor transactivation requires metalloproteinase cleavage of proHB-EGF. J Mol Cell Cardiol 36:435–443

Krug AW, Pojoga LH, Williams GH, Adler GK (2011) Cell membrane-associated mineralocorticoid receptors? New evidence. Hypertension 57:1019–1025

Kusumoto K, Haist JV, Karmazyn M (2001) Na^+/H^+ exchange inhibition reduces hypertrophy and heart failure after myocardial infarction in rats. Am J Physiol 280:H738–H745

Le Moellic C, Ouvrard-Pascaud A, Capurro C, Cluzeaud F, Fay M, Jaisser F, Farman N, Blot-Chabaud M (2004) Early nongenomic events in aldosterone action in renal collecting duct cells: PKCalpha activation, mineralocorticoid receptor phosphorylation, and cross-talk with the genomic response. J Am Soc Nephrol 15:1145–1160

Lemarie CA, Paradis P, Schiffrin EL (2008) New insights on signaling cascades induced by cross-talk between angiotensin II and aldosterone. J Mol Med 86:673–678

Lemarie CA, Simeone SM, Nikonova A, Ebrahimian T, Deschenes ME, Coffman TM, Paradis P, Schiffrin EL (2009) Aldosterone-induced activation of signaling pathways requires activity of angiotensin type 1a receptors. Circ Res 105:852–859

Li J, Yatani A, Kim SJ, Takagi G, Irie K, Zhang Q, Karoor V, Hong C, Yang G, Sadoshima J, Depre C, Vatner DE, West MJ, Vatner SF (2003) Neurally-mediated increase in calcineurin activity regulates cardiac contractile function in absence of hypertrophy. Cardiovasc Res 59:649–657

Luers C, Fialka F, Elgner A, Zhu D, Kockskamper J, von Lewinski D, Pieske B (2005) Stretch-dependent modulation of $[Na^+]i$, $[Ca^{2+}]i$, and pHi in rabbit myocardium – a mechanism for the slow force response. Cardiovasc Res 68:454–463

Lloyd-Jones DM, Larson MG, Leip EP, Beiser A, D'Agostino RB, Kannel WB, Murabito JM, Vasan RS, Benjamin EJ, Levy D (2002) Lifetime risk for developing congestive heart failure: the Framingham Heart Study. Circulation 106:3068–3072

Manjunath N, Wu H, Subramanya S, Shankar P (2009) Lentiviral delivery of short hairpin RNAs. Adv Drug Deliver Rev 61:732–745

Matsui S, Satoh H, Kawashima H, Nagasaka S, Niu CF, Urushida T, Katoh H, Watanabe Y, Hayashi H (2007) Non-genomic effects of aldosterone on intracellular ion regulation and cell volume in rat ventricular myocytes. Can J Physiol Pharm 85:264–273

Mattiazzi AR, Cingolani HE, de Castuma ES (1979) Relationship between calcium and hydrogen ions in heart muscle. Am J Physiol 237:H497–H503

McKelvie RS, Yusuf S, Pericak D, Avezum A, Burns RJ, Probstfield J, Tsuyuki RT, White M, Rouleau J, Latini R, Maggioni A, Young J, Pogue J (1999) Comparison of candesartan, enalapril, and their combination in congestive heart failure: randomized evaluation of strategies for left ventricular dysfunction (RESOLVD) pilot study. The RESOLVD Pilot Study Investigators. Circulation 100:1056–1064

Mello CC, Conte D Jr (2004) Revealing the world of RNA interference. Nature 431:338–342

Mentzer RM Jr, Bartels C, Bolli R, Boyce S, Buckberg GD, Chaitman B, Haverich A, Knight J, Menasche P, Myers ML, Nicolau J, Simoons M, Thulin L, Weisel RD (2008) Sodium-hydrogen exchange inhibition by cariporide to reduce the risk of ischemic cardiac events in patients undergoing coronary artery bypass grafting: results of the EXPEDITION study. Ann Thorac Surg 85:1261–1270

Mihailidou AS, Loan Le TY, Mardini M, Funder JW (2009) Glucocorticoids activate cardiac mineralocorticoid receptors during experimental myocardial infarction. Hypertension 54:1306–1312

Morgan PE, Correa MV, Ennis IL, Diez AA, Perez NG, Cingolani HE (2011) Silencing of sodium/hydrogen exchanger in the heart by direct injection of naked siRNA. J Appl Physiol 111(2):566–572

Mureddu GF, Cioffi G, Stefenelli C, Boccanelli A, de Simone G (2009) Compensatory or inappropriate left ventricular mass in different models of left ventricular pressure overload: comparison between patients with aortic stenosis and arterial hypertension. J Hypertens 27:642–649

Nagata K, Somura F, Obata K, Odashima M, Izawa H, Ichihara S, Nagasaka T, Iwase M, Yamada Y, Nakashima N, Yokota M (2002) AT1 receptor blockade reduces cardiac calcineurin activity in hypertensive rats. Hypertension 40(2):168–174

Nakamura TY, Iwata Y, Arai Y, Komamura K, Wakabayashi S (2008) Activation of Na^+/H^+ exchanger 1 is sufficient to generate Ca^{2+} signals that induce cardiac hypertrophy and heart failure. Circ Res 103:891–899

Orchard CH, Kentish JC (1990) Effects of changes of pH on the contractile function of cardiac muscle. Am J Physiol 258:C967–C981

Parmley WW, Chuck L (1973) Length-dependent changes in myocardial contractile state. Am J Physiol 224:1195–1199

Perez NG, Alvarez BV, Camilion de Hurtado MC, Cingolani HE (1995) pHi regulation in myocardium of the spontaneously hypertensive rat. Compensated enhanced activity of the Na^+-H^+ exchanger. Circ Res 77:1192–1200

Perez NG, de Hurtado MC, Cingolani HE (2001) Reverse mode of the Na^+–Ca^{2+} exchange after myocardial stretch: underlying mechanism of the slow force response. Circ Res 88:376–382

Perez NG, Villa-Abrille MC, Aiello EA, Dulce RA, Cingolani HE, Camilion de Hurtado MC (2003) A low dose of angiotensin II increases inotropism through activation of reverse $Na^{(+)}/Ca^{(2+)}$ exchange by endothelin release. Cardiovasc Res 60:589–597

Perez NG, Nolly MB, Roldan MC, Villa-Abrille MC, Cingolani E, Portiansky EL, Alvarez BV, Ennis IL, Cingolani HE (2011) Silencing of NHE-1 blunts the slow force response to myocardial stretch. J Appl Physiol 111:874–880

Petrecca K, Atanasiu R, Grinstein S, Orlowski J, Shrier A (1999) Subcellular localization of the Na^+/H^+ exchanger NHE1 in rat myocardium. Am J Physiol 276:H709–H717

Pimentel DR, Adachi T, Ido Y, Heibeck T, Jiang B, Lee Y, Melendez JA, Cohen RA, Colucci WS (2006) Strain-stimulated hypertrophy in cardiac myocytes is mediated by reactive oxygen species-dependent Ras S-glutathiolation. J Mol Cell Cardiol 41:613–622

Pitt B, White H, Nicolau J, Martinez F, Gheorghiade M, Aschermann M, van Veldhuisen DJ, Zannad F, Krum H, Mukherjee R, Vincent J (2005) Eplerenone reduces mortality 30 days after randomization following acute myocardial infarction in patients with left ventricular systolic dysfunction and heart failure. J Am Coll Cardiol 46:425–431

Rosenblueth A, Alanis J, Lopez E, Rubio R (1959) The adaptation of ventricular muscle to different circulatory conditions. Arch Int Physiol Biochim 67:358–373

Rothstein EC, Byron KL, Reed RE, Fliegel L, Lucchesi PA (2002) H(2)O(2)-induced Ca^{2+} overload in NRVM involves ERK1/2 MAP kinases: role for an NHE-1-dependent pathway. Am J Physiol 283:H598–H605

Sabri A, Byron KL, Samarel AM, Bell J, Lucchesi PA (1998) Hydrogen peroxide activates mitogen-activated protein kinases and Na^+-H^+ exchange in neonatal rat cardiac myocytes. Circ Res 82:1053–1062

Sadoshima J, Xu Y, Slayter HS, Izumo S (1993) Autocrine release of angiotensin II mediates stretch-induced hypertrophy of cardiac myocytes in vitro. Cell 75:977–984

Sah R, Oudit GY, Nguyen TT, Lim HW, Wickenden AD, Wilson GJ, Molkentin JD, Backx PH (2002) Inhibition of calcineurin and sarcolemmal Ca^{2+} influx protects cardiac morphology and ventricular function in K(v)4.2 N transgenic mice. Circulation 105:1850–1856

Sand C, Peters SL, Pfaffendorf M, van Zwieten PA (2003) The influence of endogenously generated reactive oxygen species on the inotropic and chronotropic effects of adrenoceptor and ET-receptor stimulation. N-S Arch Pharmacol 367:635–639

Sarnoff SJ, Mitchell JH, Gilmore JP, Remensnyder JP (1960) Homeometric autoregulation in the heart. Circ Res 8:1077–1091

Schussheim AE, Radda GK (1995) Altered Na^+-H^+—exchange activity in the spontaneously hypertensive perfused rat heart. J Mol Cell Cardiol 27:1475–1481

Siczkowski M, Davies JE, Ng LL (1995) Na^+-H^+ exchanger isoform 1 phosphorylation in normal Wistar-Kyoto and spontaneously hypertensive rats. Circ Res 76:825–831

Silvestre JS, Robert V, Heymes C, Aupetit-Faisant B, Mouas C, Moalic JM, Swynghedauw B, Delcayre C (1998) Myocardial production of aldosterone and corticosterone in the rat. Physiological regulation. J Biol Chem 273:4883–4891

Silvestre JS, Heymes C, Oubenaissa A, Robert V, Aupetit-Faisant B, Carayon A, Swynghedauw B, Delcayre C (1999) Activation of cardiac aldosterone production in rat myocardial infarction: effect of angiotensin II receptor blockade and role in cardiac fibrosis. Circulation 99:2694–2701

Snabaitis AK, Hearse DJ, Avkiran M (2002) Regulation of sarcolemmal Na^+/H^+exchange by hydrogen peroxide in adult rat ventricular myocytes. Cardiovasc Res 53:470–480

Sugden PH, Clerk A (2006) Oxidative stress and growth-regulating intracellular signaling pathways in cardiac myocytes. Antioxidants and redox signaling 8:2111–2124

Swedberg K, Eneroth P, Kjekshus J, Wilhelmsen L (1990) Hormones regulating cardiovascular function in patients with severe congestive heart failure and their relation to mortality. CONSENSUS Trial Study Group. Circulation 82:1730–1736

Szokodi I, Kerkela R, Kubin AM, Sarman B, Pikkarainen S, Konyi A, Horvath IG, Papp L, Toth M, Skoumal R, Ruskoaho H (2008) Functionally opposing roles of extracellular signal-regulated

kinase 1/2 and p38 mitogen-activated protein kinase in the regulation of cardiac contractility. Circulation 118:1651–1658

Takahashi Y, Watanabe H, Murakami M, Ohba T, Radovanovic M, Ono K, Iijima T, Ito H (2007) Involvement of transient receptor potential canonical 1 (TRPC1) in angiotensin II-induced vascular smooth muscle cell hypertrophy. Atherosclerosis 195:287–296

Takeda Y, Yoneda T, Demura M, Miyamori I and Mabuchi H (2000) Cardiac aldosterone production in genetically hypertensive rats. Hypertension 36:495–500

Theroux P, Chaitman BR, Danchin N, Erhardt L, Meinertz T, Schroeder JS, Tognoni G, White HD, Willerson JT, Jessel A (2000) Inhibition of the sodium-hydrogen exchanger with cariporide to prevent myocardial infarction in high-risk ischemic situations. Main results of the GUARDIAN trial. Guard during ischemia against necrosis (GUARDIAN) Investigators. Circulation 102:3032–3038

Valiunas V, Polosina YY, Miller H, Potapova IA, Valiuniene L, Doronin S, Mathias RT, Robinson RB, Rosen MR, Cohen IS, Brink PR (2005) Connexin-specific cell-to-cell transfer of short interfering RNA by gap junctions. J Physiol 568:459–468

Villa-Abrille MC, Caldiz CI, Ennis IL, Nolly MB, Casarini MJ, Chiappe de Cingolani GE, Cingolani HE, Perez NG (2010) The Anrep effect requires transactivation of the epidermal growth factor receptor. J Physiol 588:1579–1590

Villafuerte FC, Swietach P, Vaughan-Jones RD (2007) Common inhibitors of membrane H^+-transport also inhibit carbonic anhydrase The FASEB Journal 21. (Abstract)

von Anrep G (1912) On the part played by the suprarenals in the normal vascular reactions of the body. J Physiol 45:307–317

von Lewinski D, Stumme B, Fialka F, Luers C, Pieske B (2004) Functional relevance of the stretch-dependent slow force response in failing human myocardium. Circ Res 94:1392–1398

Wang Y, Meyer JW, Ashraf M, Shull GE (2003) Mice with a null mutation in the NHE1 Na^+-H^+ exchanger are resistant to cardiac ischemia-reperfusion injury. Circ Res 93:776–782

Ward ML, Williams IA, Chu Y, Cooper PJ, Ju YK, Allen DG (2008) Stretch-activated channels in the heart: contributions to length-dependence and to cardiomyopathy. Prog Biophys Mol Biol 97:232–249

Weber KT, Brilla CG (1991) Pathological hypertrophy and cardiac interstitium. Fibrosis and renin-angiotensin-aldosterone system. Circulation 83:1849–1865

Wetzker R, Bohmer FD (2003) Transactivation joins multiple tracks to the ERK/MAPK cascade. Nat Rev Mol Cell Biol 4:651–657

Wolvetang EJ, Pera MF, Zuckerman KS (2007) Gap junction mediated transport of shRNA between human embryonic stem cells. Biochem Biophys Res Commun 363:610–615

Wu X, Eder P, Chang B, Molkentin JD (2010) TRPC channels are necessary mediators of pathologic cardiac hypertrophy. Proc Natl Acad Sci USA 107:7000–7005

Yamazaki T, Komuro I, Kudoh S, Zou Y, Shiojima I, Hiroi Y, Mizuno T, Maemura K, Kurihara H, Aikawa R, Takano H, Yazaki Y (1996) Endothelin-1 is involved in mechanical stress-induced cardiomyocyte hypertrophy. J Biol Chem 271:3221–3228

Yokoyama H, Gunasegaram S, Harding SE, Avkiran M (2000) Sarcolemmal Na^+/H^+ exchanger activity and expression in human ventricular myocardium. J Am Coll Cardiol 36:534–540

Zannad F, McMurray JJ, Drexler H, Krum H, van Veldhuisen DJ, Swedberg K, Shi H, Vincent J, Pitt B (2010) Rationale and design of the Eplerenone in Mild Patients Hospitalization And SurvIval Study in Heart Failure (EMPHASIS-HF). Eur J Heart Fail 12:617–622

Zannad F, McMurray JJ, Krum H, van Veldhuisen DJ, Swedberg K, Shi H, Vincent J, Pocock SJ, Pitt B (2011) Eplerenone in patients with systolic heart failure and mild symptoms. New Engl J Med 364:11–21

Zeymer U, Suryapranata H, Monassier JP, Opolski G, Davies J, Rasmanis G, Linssen G, Tebbe U, Schroder R, Tiemann R, Machnig T, Neuhaus KL (2001) The Na^+/H^+ exchange inhibitor eniporide as an adjunct to early reperfusion therapy for acute myocardial infarction. Results of the evaluation of the safety and cardioprotective effects of eniporide in acute myocardial infarction (ESCAMI) trial. J Am Coll Cardiol 38:1644–1650

Zhang YH, Dingle L, Hall R, Casadei B (2009) The role of nitric oxide and reactive oxygen species in the positive inotropic response to mechanical stretch in the mammalian myocardium. Biochim Biophys Acta 1787:811–817

Zorov DB, Filburn CR, Klotz LO, Zweier JL, Sollott SJ (2000) Reactive oxygen species (ROS)-induced ROS release: a new phenomenon accompanying induction of the mitochondrial permeability transition in cardiac myocytes. J Exp Med 192:1001–1014

Zou Y, Yamazaki T, Nakagawa K, Yamada H, Iriguchi N, Toko H, Takano H, Akazawa H, Nagai R, Komuro I (2002) Continuous blockade of L-type Ca^{2+} channels suppresses activation of calcineurin and development of cardiac hypertrophy in spontaneously hypertensive rats. Hypertens Res 25:117–124

Chapter 13
Recent Aspects of Angiotensin II Action in the Heart. Implications for Myocardial Ischemia and Heart Failure

Walmor C. De Mello

13.1 Introduction

Recent advances in cardiovascular research indicate that different factors like the release of inflammatory cytokines, endothelin, aldosterone, oxidative stress and angiotensin II are involved in cardiac remodeling at cellular and molecular levels. The activation of the renin angiotensin system plays an important role through the formation of angiotensin II and the activation of AT1 receptors which are involved in generation of fibrosis and ventricular hypertrophy.

13.2 Renin Angiotensin Aldosterone System and Cardiac Remodeling

The renin angiotensin system (RAS) is classically conceptualized as an enzymatic cascade in which renin derived from the juxtaglomerular cells of the kidney, acts on angiotensinogen originated from the liver generating angiotensin I which is converted to angiotensin II by the angiotensin converting enzyme (ACE). Angiotensin II activates AT1 receptors causing vasoconstriction and the release of aldosterone which retains water and sodium in the organism. Two enzymes are involved in the convertion of angiotensin I into angiotensin II: ACE and chymase (Urata et al. 1994). Although chymase has been reported to be the main enzyme in human heart responsible for Ang I to Ang II conversion, its *physiological* role in vivo is still unclear. It is possible that chymase utilizes circulating/tissue PA12 (Urata et al. 1994) because elevated chymase activity and Ang II generation in various cardiovascular disease states suggests a possible pathophysiological role(s) for chymase-dependent PA12 processing (Droggel and Wanstall 2004; Miyazaki et al. 2006).

W. C. De Mello (✉)
Department of Pharmacology, School of Medicine, Medical Sciences Campus, UPR, San Juan, PR 00936-5067, USA
e-mail: walmor.de-mello@upr.edu

A. Kamkin, I. Lozinsky (eds.), *Mechanically Gated Channels and their Regulation,* Mechanosensitivity in Cells and Tissues 6,
DOI 10.1007/978-94-007-5073-9_13, © Springer Science+Business Media Dordrecht 2012

The CONSENSUS trial emphasized the importance of inhibition of the renin angiotensin system to prolong survival in patients with heart failure (CONSENSUS Trial 1987)- a conclusion confirmed by the SOLVD program (SOLVD Investigators 1991). Studies performed in animal models of heart failure indicated that angiotensin II antagonism not only prevents interstitial fibrosis (De Mello and Specht 2006) and ventricular hypertrophy (Cohn and Tognoni 2001; Pfeffer et al. 2003) but also reduces the downregulation of Ca^{2+} ATPase (SERCA2a) and improves intracellular Ca^{2+} handling (Bruckschegel et al. 1995; Zierhut et al. 1996) which occurs during heart failure (Kuo et al. 1992; Cory et al. 1993). Interestingly, valsartan preserved the density of beta-receptors and concurrently restored SR function increasing the Ca^{2+}-uptake and preventing the Ca^{2+}-leak) in an animal model of heart failure (Tokuhisa et al. 2006). Valsartan also acts on the presynaptic angiotensin-II receptor, and inhibits norepinephrine release and stimulate norepinephrine uptake back into the synaptic pool, which results in a reduction of the adrenergic signals (Tokuhisa et al. 2006).

Although clinical trials have shown that the blockade of the renin angiotensin system reduces the end-organ damage in patients with hypertension and heart failure (De Mello and Frohlich 2011; Cohn and Tognoni 2001; Pfeffer et al. 2003; Gavras and Gavras 2002; Varagic et al. 2008) AT1 receptor blockers (ARBs) or angiotensin converting enzyme (ACE) inhibitors are unable to achieves complete blockade of the renin angiotensin system. On the other hand, the duration of the receptor blockade changes with the compound used (Gavras and Gavras 2002). It is accepted however, that ARBs significantly reduced end point of morbidity and mortality and significantly improves symptoms and signs in patients with heart failure (De Mello and Frohlich 2011; Gavras and Gavras 2002; Varagic et al. 2008; Pitt and Segal 2000).

Part of the influence of Ang II on cardiac remodeling is caused by a decrease of oxidative stress. Indeed, significant improvements were seen with both AT1 receptor blockers and tempol on NOX activity and insulin-mediated activation/phosphorylation of Akt (Browe and Baumgarten 2004) Decrease of the downstream signaling of angiotensin II-induced AT1 receptor activation caused by AT1 receptor blockers, results in less oxidative stress leading to de novo synthesis of several proteins like the nitric oxide synthase and the tumor necrosis factor-alpha in heart cells. Furthermore, there is evidence that AT1 receptors can activate the epidermal growth factor (EGF) at the surface of plasma cell membrane increasing cell growth (Tang et al. 2000). All these findings substantiate the notion that Ang II plays an important role on cardiac remodeling.

13.3 On the Role of a Local RAS

Accumulating evidence supports the notion that different components of the renin angiotensin system are taken up by different tissues (Kurdi et al. 2005) thereby influencing the synthesis of Ang II locally (De Mello and Frohlich 2011; De Mello and Danser 2000; Re 2003; De Mello and Re 2009; De Mello 2004a). Moreover,

the synthesis of several of these components has been detected in the heart (Kurdi et al. 2005). Studies in humans showed that the gradients of Ang II across the heart were increased in patients with congestive heart failure- a finding correlated with wall stress (Serneri et al. 2001). In the failing heart, the local angiotensin II concentration is increased and the extent of cardiac angiotensin II release is related to the pathological signs of heart failure (Serneri et al. 2001).

The precise role of the different components of the RAS on heart pathology is not completely understood (De Mello and Frohlich 2011). Transgenic mouse models have been developed to examine the role of the RAS on cardiac remodeling and the results were quite contradictory because in some models ventricular hypertrophy or fibrosis, are seen whereas in others not (Reudelhuber et al. 2007). The conclusion in some of these studies is that cardiac hypertrophy is much more dependent on hemodynamic changes than on local angiotensin II levels (Reudelhuber et al. 2007). In hypertensive transgenic mouse lacking the synthesis of angiotensinogen, for instance, the local synthesis of angiotensinogen is involved but not essential in the development of cardiac hypertrophy and fibrosis (Bader 2002). Generation of Ang II in the heart elicited by a αMHC promoter to target the cardiac expression of a fusion protein that directly releases Ang II caused a 20 fold elevation of the cardiac levels of the peptide without increment of circulating levels of the Ang II. In this model no hypertrophy was produced (van Katz et al. 2001).

Other studies, however, indicate that upregulation of Ang II generation in the ventricles of transgenic animals lead to ventricular hypertrophy (Mazzolai et al. 1998) supporting the view that local production of Ang II is responsible for cardiac remodeling (Mazzolai et al. 1998).

Is important to emphasize that in the majority of these studies hypertrophy was used as the main parameter to measured the pathological effect of enhanced cardiac Ang II and the influence of the peptide on other cellular functions like cell metabolism, cell communication and generation of cardiac arrhythmias-so important in heart failure, are not considered. As whole evidence is available that the local renin angiotensin system is involved in cardiac pathology, especially during heart failure, diabetes and hypertension (De Mello and Frohlich 2011).

13.4 On the Intracrine Renin Angiotensin Aldosterone System (RAAS)

Concerning the presence of renin in the cardiac cells evidence is available that under normal conditions cardiac renin is dependent on its uptake from plasma (Danser et al. 1994). However; renin expression is increased after myocardial infarction (Passier et al. 1996) as well as after stretch of cardiomyocytes (Malhotra et al. 1999). A renin transcript that does not encode a secretory signal and remains inside the cell, is overexpressed during myocardial infarction (Clausmeyer et al. 1999) indicating that intracellular renin has functional properties. Indeed, when renin or angiotensin II are dialyzed into cardiac myocytes from the failing heart, cell communication is reduced

and the inward calcium current is increased (De Mello 1994, 1998). As expected, the decrease of gap junction conductance leads to generation electrical uncoupling and mechanical desynchronization (De Mello 1994, 2004a). Recent observations performed on the intact ventricle of the failing heart indicated that the intracellular injection of Ang II increased the action potential duration- an effect related to the inhibition of the potassium conductance through PKC activation (De Mello 2011). This means that intracellular Ang II changes cardiac excitability from within.

These findings lead to the concept that the intracrine renin angiotensin system can be then considered an important functional component of the local renin angiotensin aldosterone system and might be involved in the generation cellular hypertrophy (Kumar et al. 2008) and cardiac arrhythmias (De Mello and Frohlich 2011). Although the factors involved in the activation of the intracrine RAAS are not well known, it is possible that mechanical stretch or genetic remodeling of the failing heart be involved (De Mello 2006).

Furthermore, a soluble form of ACE is secreted in the interstitium of heart muscle by proteolytic cleavage of the membrane anchor (Costerrousse et al. 1997) might be involved in the local formation of Ang II. An intracellular renin receptor [RER] has been recently described (Schefe et al. 2006) which when activated by renin, promotes the translocation of a transcription factor (PLZF) to the nucleus with consequent expression of several genes. The intracellular localization was confirmed using different constructs and studies of mutagenesis and colocalization. Indeed, mutagenesis of the atypical C-terminal ER-retention signal strongly reduced the perinuclear localization of the renin receptor (Schefe et al. 2006). Furthermore, a transcription factor promyelocytic zinc finger protein (PLZF) was identified as a direct protein interaction partner of the C-terminal domain of the renin receptor and following the activation of RER by renin, PLZF is translocated from the cytoplasm to the nucleus providing positive or negative regulation of target genes (Schefe et al. 2006). Renin stimulation also increased PI3-K-85α messenger RNA whereas small interfering RNA against PLZF abolished this effect (Schefe et al. 2006). Moreover, experiments performed on PLZF knockout mice supported the view that PLZF is an upstream regulator of RER (Schefe et al. 2006).

Other receptors like mannose-6 phosphate receptors, could internalize renin and prorenin (Saris et al. 2001) and the intracellular Ang II formation elicited by renin internalization, might explain the severe cardiac damage seen in transgenic rats expressing the mouse ren-2nd renin gene (Kantachuverisi et al. 2001). Although the precise role of the intracellular renin receptor (Nguyen et al. 2002) on heart muscle is not known, the possibility that its activation by internalized renin or by a renin transcript (Clausmeyer et al. 1999) lead to changes in cell communication and inward calcium current cannot be discarded.

13.5 Ang II, Cell Swelling and Activation of Ionic Channels

Cell volume activates stretch-sensitive ion channels and is an important contributor to metabolism, protein synthesis and gene expression (Baumgarten 2006; Baumgarten and Clemo 2003; Lang et al. 1998). Mechanical stress or cell swelling for instance,

stimulates protein kinase C (Richter et al. 1987) and increases tyrosine phosphorylation of several proteins (Ruwhof and Laarse 2000; Dagnino et al. 1992), a finding particularly relevant because it is known that Ang II changes the inward calcium current in the heart through the activation of PKC and tyrosine kinases (De Mello 1998). Evidence is available that mechanical stretch activates JAK/STAT pathway in rat cardiomyocytes a finding of possible significance to myocardial ischemia because the hypotonic stress induced by myocardial ischemia, leads to accumulation of metabolites intracellularly with consequent cell swelling due to water entering the cells (Lang et al. 1998; Sackin 1995).

Cell swelling which activates several ionic channels, changes the action potential duration and alters cardiac excitability. The K(v) 4.2/4.3 channels, which are the primary subunits of I (to, fast), are regulated by cell volume through phosphorylation/dephosphorylation of serine/threonine phosphatases (Wang et al. 2005) and their activation by cell swelling, facilitates the generation of cardiac arrhythmias. On the other hand, the activation of swelling-activate chloride current ($\mathbf{I}_{Cl,swell}$) by mechanical stress has different electrophysiologic effects including membrane depolarization and reduction of action potential duration (Baumgarten and Clemo 2003; Lang et al. 1998). It is known, for instance, that Angiotensin II causes cell swelling and increases $I_{Cl,swell}$ in the failing and in the normal heart (De Mello 2009; De Mello 2008).

Recently it has been shown that that the renin angiotensin aldosterone system is involved in the regulation of cell volume in normal as well as in the failing heart (De Mello 2008). Indeed, in myocytes isolated from the failing ventricle and exposed to renin plus angiotensinogen or to Ang II an increase of cell volume was seen concurrently with the inhibition of the sodium pump (De Mello 2008). The activation of the Na-K-2Cl cotransporter is involved in the effect of Ang II because bumetanide abolished the swelling induced by the peptide (De Mello 2008). It is important to recognize, however, that the regulation of cell volume involves other components like ion channels and their voltage dependence and that the cell swelling induced by Ang II causes the activation of ionic channels like the swelling-activate chloride current ($\mathbf{I}_{Cl,\ swell}$) which have electrophysiologic effects including membrane depolarization and reduction of action potential duration (De Mello 2009; Baumgarten and Clemo 2003). The peptide causes cell swelling and increases ($\mathbf{I}_{Cl,\ swell}$) in the failing and in the normal heart (De Mello 2009; Baumgarten 2006). This finding is of particular interest because the activation of this current seems involved in generation of early afterdepolarizations in the failing ventricle (De Mello 2009). Ang (1–7), which has been found to counteract many effects of Ang II (Ferrario et al. 1997), reduces the heart cell volume and decreases the swelling-activate chloride current ($\mathbf{I}_{Cl,\ swell}$) (De Mello 2009)—an effect that might be involved in the decrease of incidence of cardiac arrhythmias during ischemia/reperfusion (De Mello 2004b; Ferreira et al. 2001). Since cell swelling induced by myocardial ischemia or heart failure, represents an important arrhythmogenic mechanism which are potentiated by the activation of the plasma RAS, the formation of Ang (1–7) might be of benefit to the ischemic heart. Therefore, the activation of the ACE2/ Ang (1–7)/Mas receptor axis might be involved in the regulation of heart cell volume by counteracting the effect of Ang II (De Mello 2010). Failure of the heart cell to regulate its volume through a lack of

activation of the regulatory volume decrease (RVD) has serious consequences for cardiac function because inhibition of the RVD is commonly associated with cell shrinkage (Lang et al. 1998).

Interestingly, the intracellular administration of Ang II or renin reversed the cell swelling caused by hypotonic solution –an effect associated with the activation of the sodium pump (De Mello 1998). The physiological meaning of this finding is not known and further studies will be needed to clarify the relevance of this finding.

In conclusion, these novel findings lead to the concept that the renin angiotensin system is not only involved in regulation of blood volume but also contributes to the regulation of cell volume with extracellular renin and Ang II increasing the cell volume and the intracrine RAS reducing it.

13.6 AT1 Receptors as Mechanosensors Independent of Angiotensin II

Evidence is now available that AT1 receptors are sensitive to mechanical stress showing a specific change in its conformation without the involvement of Ang II (Yasuda et al. 2008; Zou et al. 2004). The membrane-stretch-induced conformational changes were suggested for the AT_1R (Yasuda et al. 2008) based on a model of the bovine rhodopsin crystal structure (Okada et al. 2004; Palczewski et al. 2000). The conformation of such a mechanically activated receptor is different from the active receptor conformation induced by agonists (Gether 2000). The lack of action of Ang II on these experiments was supported by the finding that no increase in Ang II concentration in the medium was seen with stretch and the concentration of the peptide in the extracellular medium was not enough to activate the extracellular signal-regulated protein kinase (ERK) in cardiomyocytes (Zou et al. 2004) The agonist-independent activation of the AT_1 receptor can be inhibited by inverse agonists, but not by neutral antagonists, through the specific drug-receptor interactions (Gether 2000). This lead to the conclusion that AT1 is a mechanical force-transducing molecule that mediates mechanical stress-induced cellular responses (Yasuda et al. 2008; Zou et al. 2004) (see Fig. 13.1). Indeed, information gained over the last decade changed our concept on receptors which are now considered as highly dynamic structures that exist in equilibriums between active and inactive conformations changing out view of a yes/no process (Gether 2000). Therefore, an agonist is recognized as a molecule that can stabilize an active conformation while an inverse agonist (*i.e.,* an antagonist with negative intrinsic activity) is a molecule that can stabilize an inactive conformation (see Gether 2000). Antagonists, on the other hand, inhibit responses in competition with agonists, but they are not able to reduce the constitutive activity of the receptor or the agonist-independent receptor activity (Miura 2005). Some AT1 receptor blockers have an inverse agonist activity including olmesartan, valsartan and candesartan (Miura 2005).

These observations indicate that the pressure overload imposed on the heart of angiotensinogen-deficient mice, generated cardiac hypertrophy supporting the view

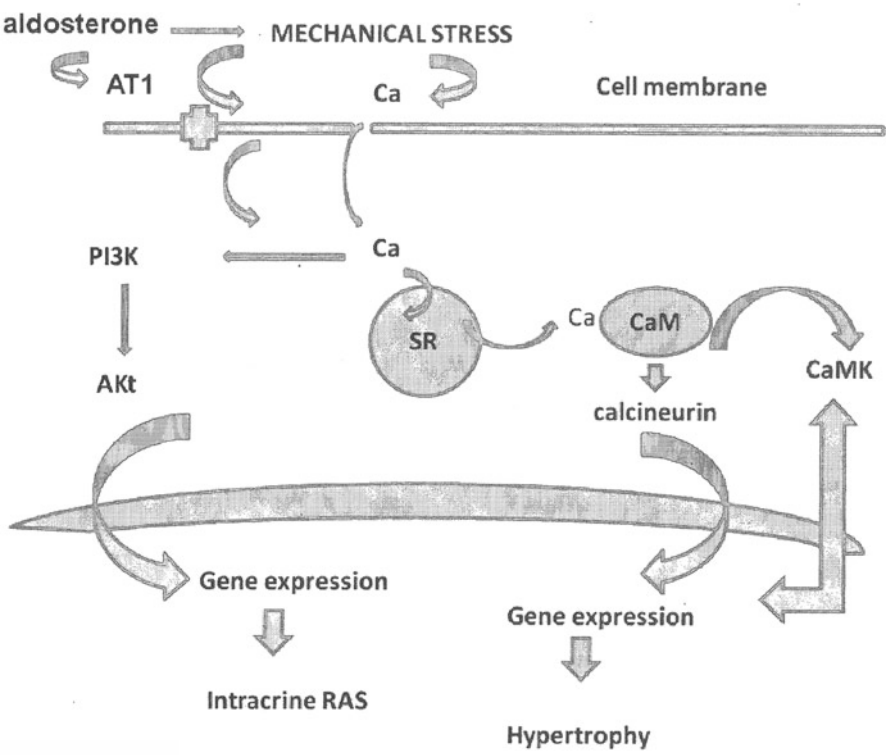

Fig. 13.1 Diagram showing the influence of mechanical stretch, AT1 receptors and aldosterone on gene expression with consequent generation of ventricular hypertrophy and possible activation of the intracrine renin angiotensin system

that mechanical stress can induce hypertrophy in absence of Ang II (De Mello 2008). However, many issues remain to be solved including how mechanical stress activates the AT1 receptor and how candesartan exerts an inverse agonism is not known (De Mello 2008). The possibility exists that changes in membrane tension elicits a conformational alteration in the AT1 receptor or that the activation of mechanosensors such as LIM protein within the disc (Knoll et al. 2002) or that the activation of integrin-linked kinase (Bendig et al. 2006) are able to the activate the AT1 receptor.

Mechanical forces in cardiac muscle involves different components including the extracellular matrix, adherent junctions at intercalated discs and costameric proteins at focal adhesions (Knoll et al. 2002; Cox et al. 2008). Despite the fact that the mechanism by which cells sense mechanical stimulation is poorly understood. Our present concept indicates that stretch signals are sensed and transduced by multiple protein complexes responsible for sensing (Cox et al. 2008) and that the information has to be transmitted to the nucleus with consequent change in gene expression including increased expression of fetal genes (Han et al. 2004; Ruwhof and Laarse 2000) (see Fig. 13.1). It was found that mechanical stretch-induced cSrc protein tyrosine kinase activation is mediated through the actin-filament associated protein

(Han et al. 2004). According to these authors the mechanical forces can be transmitted along the cytoskeleton and associated proteins and enzyme-related to signal transduction converting physical forces into biochemical reactions (Cox et al. 2008; Han et al. 2004). Mechanical stress may also be coupled to intracellular signals that are responsible for the hypertrophic response via integrins (Linke 2008; Knoll et al. 2002; Kamkin et al. 2000; Lang et al. 1998) and the cytoskeleton or via sarcolemmal proteins, such as phospholipases, ion channels and ion exchangers. The signal transduction pathways might involve the mitogen-activated protein kinases (MAPK), the janus kinase/signal transducers and activators of transcription (JAK/STAT) pathway) (Lang et al. 1998). On the other hand, the stress signal may be directly transmitted to the nucleus. Furthermore, through an increase in intracellular Ca^{2+} concentration, the stress signal may stimulate the calcium/calmodulin-dependent phosphatase calcineurin (Komuro et al. 1990). How the activation of AT1 receptor by mechanical stretch induces cardiac remodeling is not completely known.

The concept that the AT1 receptor is a mechanosensor might indicate that during myocardial ischemia, when there is upregulation of AT1 expression, gene expression is increased (Kudoh et al. 2003). Prolonged stretch of neonatal rat cardiomyocytes in culture, for instance, induces fetal gene expression (Dagnino et al. 1992; Richter et al. 1987; Komuro et al. 1990; Kudoh et al. 2003; Wang et al. 2005). Ca^{2+} is involved in stretch-induced gene expression because voltage-dependent Ca^{2+} channel blockers like nifedipine suppress BNP gene expression by mechanical stress (Richter et al. 1987; Dagnino et al. 1992; Kudoh et al. 2003; Komuro et al. 1990).

Evidence is available that integrins are involved in the response to mechanical stress (Linke 2008; Knoll et al. 2002) and that Ang II increases the expression of integrins (Kawano et al. 2000). It is then conceivable that a decline in Ang II levels in the plasma and in the heart influences the effect of pressure overload on cardiac remodeling by reducing the expression of integrins. Although the possibility that AT1 is a mechanoreceptor in humans is not completely clear, it is possible that the activation of the renin angiotensin system and its consequent increment of arterial blood pressure represent an important factor in the activation of signaling pathways related to mechanosensor receptors.

13.7 Shear Stress, Mechanical Deformation and Activation of Kinases

Shear stress is known to enhance the activities of several kinases involved in phosphorylation of signaling proteins in endothelial cells (Kuo et al. 1992), what raises the possibility that the endocardium might be also involved in the regulation of heart cell function. Indeed, the endocardium-endothelial (EE) dysfunction play a role in cardiac pathology and mechanical stress, as well as various hormones and cytokines can initiate EE dysfunction (Kuo et al. 1992). Chronic deformation of surface cell membrane like that seen in heart failure, essential hypertension and myocardial ischemia causes mechanical stress. Although mechanosensitive channels (MSCs) are

involved in different cellular responses during physiological and pathological conditions, our present knowledge of their pharmacology is meager. Pharmacologic agents able to modulate the activity of these channels like lanthanide gadolinium, streptomycin and a peptide toxin (GsMTx-4), prevent the generation of cardiac arrhythmias by altering the tension-sensing lipid bilayer or the cytoskeleton but not by interacting directly with these channels (Subramanyan et al. 2010). Further studies, however, are needed to rule out the direct participation of the channels.

13.8 Conclusion and Perspectives

These novel findings show the importance of mechanical stress and cell swelling on heart pathology particularly during myocardial ischemia, hypertension and heart failure, which are sources of mechanical stress. Changes in gene expression and activation of stretch-sensitive ionic channels lead to the generation of cardiac arrhythmias. The role of mechanical stress generated by pressure overload, by itself, can induce cardiac remodeling which is certainly potentiated by the activation of the renin angiotensin aldosterone system.

The evidence that mechanical stress induces biochemical changes including alterations of gene expression provides an important avenue for future studies on the role of mechanosensors on cardiac remodeling during hypertension, heart failure or myocardial ischemia.

Acknowledgement Supported in part by grants HL 34148 and GM 61838 from NIH.

References

Bader M (2002) Role of the local renin-angiotensin system in cardiac damage: a minireview focussing on transgenic animal models. J Mol Cell Cardiol 34:1455–1462

Baumgarten CM (2006) Cell volume regulation of cardiac myocytes: a leaky boat gets a new bilge pump. J Gen Physiol 128:487–489

Baumgarten CM, Clemo HF (2003) Swelling-activated chloride channels in cardiac physiology and pathophysiology. Prog Biophys Mol Biol 122:689–670

Bendig G, Grimmler M, Huttner IG, Wessels G et al (2006) Integrin-linked kinase, a novel component of the cardiac mechanical stretch sensor, controls contractility in the zebrafish heart. Genes Dev 20:2361–2372

Browe DM, Baumgarten CM (2004) Angiotensin II (AT1) receptors and NADPH oxidase regulate Cl- current elicited by b1 integrin stretch bin rabbit ventricular myocytes. J Gen Physiol 124:273–287

Bruckschlegel G, Holmer SR, Jandeleit K, Grimm D, Muders F, Kromer EP et al (1995) Blockade of the renin-angiotensin system in cardiac pressure-overload hypertrophy in rats. Hypertension 25:250–259

Cohn JN, Tognoni G (2001) A randomized trial of the angiotensin receptor blocker valsartanin chronic heart failure. N Engl J Med 345:1667–1675

Clausmeyer S, Sturebecher R, Peters J (1999) An alternative transcript of the rat renin gene can result in a truncated prorenin that is transported into adrenal mitochondria. Cir Res 84:337–344

CONSENSUS Trial Study Group (1987) Effects of enalapril on mortality in severe congestive heart failure. Results of the Cooperative North Scandinavian Enalapril Survival Study (CONSENSUS). N Engl J Med 316:1429–1435

Cory CR, McCutcheon LJ, O'Grady M, Pang AW et al (1993) Compensatory downregulation of myocardial Ca^{2+} channel in SR from dogs with heart failure. Am J Physiol 264:H926–H9237

Costerousse O, Danilov S, Alhenc-Gelas F (1997) Genetics of angiotensin I-converting enzyme. Clin Exp Hypertens 19:659–669

Cox L, Umans L, Cornelis F, Huylebroeck D, Zwijsen A (2008) A broken heart: a stretch too far: an overview of mouse models with mutations in stretch-sensor components. Int J Cardiol 131:33–44

Dagnino L, Lavigne JP, Nomer M (1992) Increased transcripts for b-type natriuretic peptide in spontaneous hypertensive rats. Quantitative polymerase chain reaction for atrial and brain natriuretic peptide transcripts. Hypertension 20:690–700

Danser AHJ, van K JP, Admiraal PJJ et al (1994) Cardiac renin and angiotensins; uptake from plasma versus in situ synthesis. Hypertension 24:37–48

De Mello WC (1994) Is an intracellular renin angiotensin system involved in the control of cell communication in heart? J Cardiovasc Pharmacol 23:640–646

De Mello WC (1998) Intracellular angiotensin II regulates the inward calcium current in cardiac myocytes. Hypertension 32:076–082

De Mello WC (2004a) Heart failure: how important is cellular sequestration? The role of the renin angiotensin aldosterone system. J Mol Cell Cardiol 37:431–438

De Mello WC (2004b) Angiotensin (1–7) re-establishes impulse conduction in cardiac muscle during ischemia/reperfusion. The role of the sodium pump. J Renin Angiotensin Aldosterone Syst 5:203–208

De Mello WC (2006) Cardiac intracrine renin angiotensin system. Part of genetic reprogramming? Regul Pept 133:10–12

De Mello WC (2008) Intracellular and extracellular renins have opposite effects on the regulation of heart cell volume. Implications to myocardial ischemia. J Renin Angiotensin Aldosterone Syst 9:112–118

De Mello WC (2009) Cell swelling, impulse conduction and cardiac arrhythmias in the failing heart. Opposite effects of angiotensin II and angiotensin (1–7) on cell volume regulation. Mol Cell Biochem 330:211–217

De Mello WC (2010) Angiotensin (1–7) reduces the cell volume of swollen cardiac cells and decreases the swelling-dependent chloride current. Implications for cardiac arrhythmias and myocardial ischemia. Peptides 31:2322–2324

De Mello WC (2011) Intracrine action of angiotensin II in the intact ventricle of the failing heart: angiotensin II changes cardiac excitability from within. Mol Cell Biochem 358:309–315

De Mello WC, Danser AHJ (2000) Angiotensin II and the heart. On the intracrine renin angiotensin system. Hypertension 35:1183–1188

De Mello WC, Frohlich ED (2011) On the local cardiac renin angiotensin system. Basic and clinical implications. Peptides 32(8):1774–1779

De Mello WC, Re RN (2009) Systemic versus local renin angiotensin systems. An overview. In: De Mello WC, Frohlich ED (eds) Renin Angiotensin System and cardiovascular Disease Humana Press, Springer, New York, pp 1–5

De Mello WC, Specht P (2006) Chronic blockade of angiotensin II AT1receptors increased cell communication, reduced fibrosis and improved impulse propagation in the failing heart. J Renin Angiotensin Aldosterone Syst 7:201–205

Droggel SA, Wanstall JC (2004) Vascular chymase: pathophysiological role and therapeutic potential of inhibition. *Cardiovasc* Res 61:653–662

Ferrario C, Chapell M, Tallant EK et al (1997) Counterregulatory actions of angiotensin (1–7). Hypertension 30:535–541

Ferreira AJ, Santos RA, Almeida AP (2001) Angiotensin (1–7); cardioprotective effect in myocardial ischememia/reperfusion. Hypertension 38:665–668

Gavras I, Gavras H (2002) Angiotensin II as a cardiovascular risk factor. J Hum Hypertens 16(Suppl 2):S2–S6

Gether U (2000) Uncovering molecular mechanisms involved in activation of G protein-coupled receptors. Endocr Rev 21:90–113
Han B, Bai XH, Lodyga M, Xu J, Burton B et al (2004) Conversion of mechanical forces into biochemical signaling. J Biol Chem 279:54793–54801
Kamkin A, Kiseleva I, Isenberg G (2000) Stretch-activated currents in ventricular myocytes: amplitude and arrhythmogenic effects increase hypertrophy. Cardiovasc Res 48:409–420
Kantachuverisi S, Fleming S, Peters J, Peters B, Brooker G, Lammie AG, McGrath I et al (2001) Controlled hypertension, a transgenic toggle switch reveals differential mechanisms underlying vascular disease. J Biol Chem 276:36727–36733
Kawano H, Cody RJ, Graf K, Goetze S, Kawano Y et al (2000) Angiotensin II enhances integrin and alpha-actinin expression in adult rat cardiac fibroblasts. Hypertension 35:273–279
Komuro I, Kaida T, Shibazaki Y et al (1990) Stretching cardiac myocytes stimulates protooncogene expression. J Biol Chem 265:3595–3598
Knoll R, Hoshijima M, Hoffman HM, Person V et al (2002) The cardiac mechanical stretch sensor machinery involves a Z disc complex that is defective in a subset of human dilated cardiomyopathy. Cell 111:943–955
Kumar R, Singh VP, Baker KM (2008) The intracellular renin angiotensin system: implications in cardiovascular remodeling. Curr Opin Nephrol Hypertens 17:168–173
Kudoh S, Akazawa H, Takano H et al (2003) Stretch- modulation of second messengers: effects on cardiomyocytes ion transport. Prog Biophys Mol Biol 82:57–66
Kuo TH, Tsang W, Wang KK, Carlock L (1992) Simultaneous reduction of the sarcolemmal and SR calcium ATPase activities and gene expression in cardiomyopathic hamster. Biochim Biophys Acta 1138:343–349
Kurdi M, De Mello WC, Booz GW (2005) Working outside the system: an uptodate on unconventional behavior of the renin angiotensin system components. Intern J Biochem Cell Biol 37:1357–1367
Lang F, Busch GL, Ritter M, Volkl H et al (1998) Functional significance of cell volume regulatory mechanisms. Physiol Rev 78:247–306
Linke WA (2008) Sense and stretch ability: The role of titin and titin-associated proteins in myocardial stress-sensing and mechanical dysfunction. Cardiovasc Res 77:637–648
Malhotra R, Sadoshima J, Broscius FC, Izumo S (1999) Mechanical stretch and angiotensin II differentially upregulated the renin angiotensin system in cardiac myocytes in vitro. Circ Res 85:137–146
Mazzolai L, Nussberger J, Aubert JF et al (1998) Blood pressure-independent cardiac hypertrophy induced by locally activated renin angiotensin system. Hypertension 31:1324–1330
Miura S (2005) Angiotensin II receptor blocker as an inverse agonist: a current perspective. Curr Hypertens Rev 1:115–121
Miyazaki M, Takai S, Jin D, Muramatsu M (2006) Pathological roles of angiotensin II produced by mast cell chymase and the effects of chymase inhibition in animal models. Pharmacol Ther 112:668–676
Nguyen G, Delarue F, Burckle C, Bouzir L et al (2002) Pivotal role of the renin/ prorenin receptor in angiotensin II production and cellular response to renin. J Clin Invest 109:1417–1427
Okada T, Sugihara M, Bondar AN, Elstner M, Entel P, Buss V (2004) The retinal conformation and its environment in rhodopsin in light of a new 2.2 Å crystal structure. J Mol Biol 342:571–583
Palczewski K, Kumasaka T, Hori T, Behnke CA, Motoshima H, et al (2000) Crystal structure of rhodopsin: a G protein-coupled receptor. Science 289:739–745
Passier RCJJ, Smits JFM, Verluyten MJA, Daemen MJAP (1996) Expression and localization of renin and angiotensinogen in rat heart after myocardial infarction. Am J Physiol 271:H1040–H1048
Pitt B, PA, Segal R et al (2000) Effect of losartan compared with captopril on mortality in patients with symptomatic heart failure: ramdomised trial –the Losartan Heart Failure Survival Study ELITE. Lancet 355:1582–1587

Pfeffer MA, Swedberg K, Granger CB, Held P, McMurray JJ et al (2003) Effects of candesartan on mortality and morbidity in patients with chronic heart failure: the CHARM-Overall programme. Lancet 362:759–766

Re RN (2003) The implication of intracrine hormone action for physiology and medicine. Am J Physiol heart Circ Physiol 284:H751–H757

Re RN, Cook JL (2008) The basis of an intracrine physiology. J Clin Pharmacol 48:344–350

Reudelhuber TL, Bernstein KE, Delafontaine P (2007) Is angiotensin II a direct mediator of left ventricular hypertrophy? Hypertension 49:1196–1201

Richter, EA, Cleland PJ, Rattigan S, Clark MG (1987) Contraction-associated translocation of protein kinase C in rat skeletal muscle. FEBS Lett 217:232–236

Ruwhof C, van der Laarse (2000) A mechanical stress-induced cardiac hypertrophy: mechanisms and signal transduction pathways. Cardiov Res 47:23–37

Sackin H (1995) Stretch activated ion channels. Kidney Int 48:1134–1147

Saris JJ, Derks FH, Lamers JM, Saxena PR et al (2001) Cardomyocytes bind and activate native human prorenin: role of soluble mannose-6 phosphate receptors. Hypertension 37:710–715

Serneri GG, Boddi M, Cecione I et al (2001) Cardiac angiotensin II formation in the clinical course of heart failure and its relationship with left ventricular function. Circ Res 88:961–968

Schefe JH, Menk M, Reinemund J et al (2006) A novel signal transduction cascade involving direct physical interaction of the renin/prorenin receptor with the transcription factor promyelocytic zinc finger protein. Circ Res 99:1355–1366

The SOLVD Investigators (1991) Effect of enalapril on survival in patients with reduced left ventricular ejection fractions and congestive heart failure. N Engl J Med 325:293–302

Subramanyan M, Takahashi N, Hagesawa Y et al (2010) Inhibition of protein kinase AKt1 by apoptosis signal regulating kinase^{-1} (ASK1) is involved in apoptotic inhibition of regulatory volume decrease. J Biol Chem 285:6109–6117

Tang H, Nishishita T, Fitzgerard T, Landon EJ, Inagami T (2000) Inhibition of AT1 receptor internalization by concavalin A blocks angiotensin II—induce ERK activation but not AT1 receptor internalization. J Biol Chem 275:13420–13426

Tokuhisa T, Yano M, Obayashi M, Noma TN et al (2006) Receptor function, rendering isoproterenol-induced failing heart less susceptible to Ca^{2+}-Leak induced by oxidative stress. Circulation J 70:777–786

Urata H, Hoffmann S, Ganten D (1994) Tissue Angiotensin II System in the Human Heart. Eur Heart J 15(Suppl D):68–78

van Katz JP, Methot D, Paradis P, Silversides DW, Reudelhuber TL (2001) Use of a biological pump to study chronic peptide hormone action in transgenic mice. Direct and indirect effects of angiotensin II on the heart. J Biol Chem 276:44012–44017

Varagic J, Frohlich ED, Sucic D, Ahn J et al (2008) AT1 receptor antagonism attenuates target organ effects of salt excess in SHR's without affecting pressure. Am J Physiol Heart Circ 294:H853–H858

Wang GL, Wang GX, Yamamoto S, Ye L et al (2005) Molecular mechanisms of regulation of fast-inactivating voltage-dependent transient outward K^+ current in mouse heart by cell volume changes. J Physiol 568:423–443

Yasuda N, Akazawa H, Qin Y, Zou Y, Komuro I (2008) A novel mechanism of mechanical stress-induced angiotensin II type 1–receptor activation without the involvement of angiotensin II. N-S Arch Pharm 377:393–399

Yasuda N, Miura S, Akazawa H, Tanaka T, Qin Y et al (2008) Conformational switch of angiotensin II type 1 receptor underlying mechanical stress-induced activation. EMBO Rep 9:179–186

Zierhut W, Studer R, Laurent D, Kastner S, Allegrini P, Whitebread S et al (1996) Left ventricular wall stress and sarcoplasmic reticulum Ca^{2+}-ATPase gene expression in renal hypertensive rats: Dose dependent effects of ACE inhibition and AT1 receptor blockade. Cardiovasc Res 31:758–768

Zou Y, Akazawa H, Qin Y, Sano M, Takano H et al (2004) Mechanical stress activates angiotensin II type 1 receptor without the involvement of angiotensin II. Nat Cell Biol 6:499–506

Chapter 14
Mechanosensitivity of Pancreatic β-cells, Adipocytes, and Skeletal Muscle Cells: The Therapeutic Targets of Metabolic Syndrome

Koichi Nakayama, Yoshiyuki Tanabe, Kazuo Obara and Tomohisa Ishikawa

14.1 Introduction

Mechanotransduction describes the molecular and cellular processes that transduce mechanical/physical forces, such as hemodynamic factors, exercise, and osmotic change, into biochemical signals, followed by diverse intracellular signaling and cell responses, thus enabling organisms from bacteria to human beings to adapt to their physical surroundings (Jaalouk and Lammerding 2009). As mechanosensing and its feedback system are fundamental for physiological homeostasis, failures in mechanotransduction would cause various pathological conditions.

The cardiovascular system is known to be particularly sensitive to mechanical stimuli such as cardiac contraction, blood pressure, and blood flow. We have recently reviewed specific mechanotransduction signaling involved in myogenic responses of cerebral arteries (Nakayama et al. 2010): Spatial and temporal interactions of mechanosensitive kinases including Rho/Rho-kinase, protein kinase C, and tyrosine kinase were discussed. These kinases are also activated in experimental canine cerebral vasospasm after subarachnoid hemorrhage, and play an important role in the development of the vasospasm. Thus, the mechanism underlying stretch-induced contraction and cerebral vasospastic episode may overlap.

The metabolic syndrome is characterized by a group of metabolic risk factors, including diabetic diseases, abdominal obesity, atherogenic dyslipidemia, elevated blood pressure, and prothrombotic and proinflammatory states in one person (Scott et al. 2004). Progression of the metabolic syndrome leads to increased risk of coronary heart disease and other vascular occlusive diseases related to plaque buildup in arterial walls. It is a well-documented fact that non-sensory cells and tissues

K. Nakayama (✉) · Y. Tanabe
Department of Molecular and Cellular Pharmacology, Faculty of Pharmaceutical Sciences, Iwate Medical University, Yahaba, Iwate 028-3694, Japan
e-mail: nakyamk@iwate-med.ac.jp

K. Obara · T. Ishikawa
Department of Pharmacology, School of Pharmaceutical Sciences, University of Shizuoka, 52-1 Yada, Suruga-ku, Shizuoka City, Shizuoka 422-8526, Japan

A. Kamkin, I. Lozinsky (eds.), *Mechanically Gated Channels and their Regulation,* Mechanosensitivity in Cells and Tissues 6,
DOI 10.1007/978-94-007-5073-9_14,

derived from mesenchyme, including stromal cells like cardiac, smooth, and skeletal muscles, endothelial cells, fibroblasts, and osteoblasts are mechanosensitive. Adipocytes are also derived from mesenchyme, while pancreatic β-cells are derived from endodermal epithelium. Interestingly, these latter two types of cells are also mechanosensitive. Thus it is worth extending the research field of mechanotransduction into pancreatic β-cells, adipocytes, and skeletal muscle cells, all of which are related to the core concerns in metabolic syndrome.

Pancreatic β-cells are inflated by a high glucose level, which leads to insulin secretion independently of the well-documented K_{ATP} channel-dependent mechanism. Adipocytes subjected to mechanical stretching show a variety of phenotype and functional changes. Moreover, passive stretching in skeletal muscle cells promotes surface expression of glucose transporter 4 (GLUT4) and facilitates glucose uptake. Thus it seems possible that the level of blood glucose may be controlled via mechanosensitive mechanisms, which may open the way to a new therapeutic strategy of diabetic diseases.

The present article focuses on the unitary discussion of three peripheral organs from the view point of mechanosensitivity/mechanotransduction. We provide herein some new insights into the mechanotransduction of pancreatic β-cells, adipocytes, and skeletal muscle cells, based on our series of published papers and those of others in related fields, i.e., how the cell/tissue is sensing mechanical force, and transducing it into intracellular signaling and other events related to energy metabolism.

14.2 Pancreatic β-Cell

14.2.1 Introduction

Glucose-stimulated insulin secretion (GSIS) from pancreatic β-cells is attributed to a sequence of events; acceleration of metabolism, closure of ATP-sensitive K^+ (K_{ATP}) channels, membrane depolarization, activation of voltage-dependent Ca^{2+} channels (VDCC), and a rise in cytosolic free Ca^{2+} concentration ($[Ca^{2+}]_c$) through Ca^{2+} influx (Ashcroft and Rorsman 1990; Newsholme et al. 2010). A major aspect of GSIS is, therefore, the induction of electrical activity. The membrane potential of β-cells at sub-stimulatory glucose concentrations is normally between −60 and −70 mV and the cells are electrically silent. The elevation of glucose concentration results in a gradually developing depolarization, and action potentials are generated when the membrane potential reaches the threshold potential. This K_{ATP} channel-dependent triggering signal is essential for GSIS. The K_{ATP} channels of β-cells are a heteromultimer composed of the pore-forming Kir6.2 and the sulfonylurea receptor SUR1 (Drews et al. 2010). However, GSIS is unlikely to be exclusively dependent only on the K_{ATP} channel-dependent mechanism. GSIS consists of two phases; a transient and marked first phase, followed by a sustained flat or gradually increasing second phase. The possible mechanisms underlying the two phases of GSIS have been previously reviewed (Straub and Sharp 2002; Henquin 2009). The first phase

is currently ascribed to a rapid, K_{ATP} channel–dependent increase in $[Ca^{2+}]_c$ that triggers exocytosis of a readily releasable pool of insulin granules. The second phase requires both the triggering $[Ca^{2+}]_c$ elevation and the augmentation of exocytosis via a K_{ATP} channel–independent mechanism. The latter pathway has been estimated under the conditions where the involvement of K_{ATP} channels is eliminated by either K_{ATP} channel openers or blockers (Komatsu et al. 2001). Although the second phase has been suggested to be caused by various possible mechanisms, the molecular mechanism still remains to be established.

Functional K_{ATP} channels are well known to be essential for β-cell activity. However, the ionic mechanism triggering insulin secretion, especially in the second phase, is still a matter of debate. Evidence has been accumulating that inhibition of K_{ATP} channels is not the sole ionic mechanism underlying the depolarization in response to glucose elevation in β-cells. For example, low concentrations of glucose decreased $^{42}K^+$ or $^{86}Rb^+$ efflux from pancreatic islets, probably reflecting K_{ATP} channel inhibition; however, the K^+ conductance was little affected or rather transiently increased when the concentration of glucose exceeded approximately 8.3 mM (Henquin 1978; Carpinelli and Malaisse 1981). Moreover, K_{ATP} channels were shown to be inhibited by glucose within the range 0–5 mM with no further effect of higher concentrations (Ashcroft et al. 1988; Best 2002a). Consistent with these findings, the membrane conductance of β-cells was the minimum at threshold concentrations of glucose but rather increased at stimulatory glucose concentrations (Best 2000). Moreover, glucose depolarized the membrane potential even in the β-cells where K_{ATP} channels were completely inhibited by sulfonylurea K_{ATP} channel blockers (Best 2002a) and in the β-cells from Kir6.2 knock-out mice (Ravier et al. 2009). In the β-cells from SUR1 knock-out mice, although they displayed action potentials even at low glucose concentrations, changes in action potential frequency, percentage of time with action potentials, and interburst length were still observed when glucose concentration was raised (Düfer et al. 2004). It is thus highly possible that ionic mechanisms other than K_{ATP} channel inhibition are involved in the membrane depolarization induced by higher concentrations of glucose in β-cells. In particular, the alternative ionic mechanisms may be of importance in pathophysiological conditions, as in type 2 diabetes mellitus, where insulin secretion during hyperglycemia cannot be satisfactorily explained by the closure of K_{ATP} channels. The responses to β-cell swelling have been postulated as one of the candidate mechanisms.

14.2.2 β-Cell Swelling Induced by High-Concentration Glucose

Of particular interest is the fact that glucose causes the swelling of β-cells (Semino et al. 1990; Miley et al. 1997; Takii et al. 2006). Glucose-induced β-cell swelling is dependent on glucose metabolism, because it is not evoked by 3-*O*-methylglucose, a non-metabolizable glucose analogue (Miley et al. 1997; Davies et al. 2007). The mechanisms can be explained as follows: The elevation of glucose concentration accelerates glycolysis, leading to an accumulation of lactate, a product of non-oxidative

phosphorylation. The expression of the plasma membrane monocarboxylate transporter MCT1, which transports lactate as well as pyruvate, is unusually low in β-cells (Best et al. 1992; Zhao et al. 2001). This modification would serve a role to prevent the loss of glucose-derived pyruvate from β-cells; on the other hand, it would lead to intracellular lactate accumulation when the cells are exposed to high concentrations of glucose. Indeed, there is evidence that an accumulation of lactate formed from methylglyoxal leads to β-cell swelling (Best et al. 1999). The intracellular accumulation of lactate would result in intracellular hyperosmolarity, producing cell swelling (Best et al. 1992; Sekine et al. 1994). A controversial point, however, exists regarding the capacity of β-cells to generate lactate during glucose stimulation. As well as MCT1, lactate dehydrogenase (LDH), which converts pyruvate to lactate, displays very low expression levels in β-cells (Sekine et al. 1994), suggesting that LDH activity in β-cells may not be sufficient to convert pyruvate generated from glucose to lactate. As an alternative mechanism for glucose-induced β-cell swelling, an involvement of Na^+/H^+ and Cl^-/HCO_3^- exchangers is proposed. These exchangers are of importance in the extrusion of H^+ and HCO_3^- generated by glucose metabolism (Grapengiesser et al. 1989; Shepherd and Henquin 1995). Their activation increases the intracellular concentrations of Na^+ and Cl^-, leading to intracellular hyperosmolarity (Best et al. 1997). Since osmotic β-cell swelling induces insulin secretion (Blackard et al. 1975; Best et al. 1996a; Drews et al. 1998), the swelling due to high-concentration glucose is expected to be one of the mechanisms underlying GSIS.

14.2.3 Volume-Regulated Anion Channels

Volume-regulated anion channels (VRAC) are ubiquitously expressed in mammalian cells and are known to play a pivotal role in the cell volume regulation system, regulatory volume decrease (RVD), which occurs after hypotonicity-induced cell swelling (Eggermont et al. 2001; Sardini et al. 2003). In pancreatic β-cells, several lines of evidence, most of which have been reported by Best and co-workers (see review by Best et al. 2010), suggest that VRAC activated during RVD could also be an important mechanism for GSIS: (i) osmotic cell swelling activates VRAC in β-cells (Kinard and Satin 1995; Best et al. 1996b; Drews et al. 1998); (ii) glucose activates Cl^- currents with features resembling VRAC currents (Best 1999; Best 2002b; Jakab et al. 2002); and (iii) both the glucose-activated Cl^- currents and the swelling-induced insulin release are inhibited by a selective VRAC inhibitor DCPIB (Best et al. 2004). Since equilibrium potential of Cl^- has been shown to be around −30 mV (Kinard and Satin 1995; Drews et al. 1998), the activation of VRAC would induce inward current, leading to membrane depolarization. However, the physiological role of VRAC besides RVD in β-cells is not fully understood. Recently, the non-metabolizable analogue 3-*O*-methylglucose as well as glucose has been shown to induce VRAC currents (Dossena et al. 2011), implying that the activation of VRAC by glucose may be independent of glucose metabolism.

14.2.4 Stretch-Activated Cation Channels

Osmotic cell swelling mechanically stretches the plasma membrane. It is thus expected that stretch-activated cation channels (SAC) participate in the responses to hypotonic stimulation in β-cells. However, little information exists about SAC in β-cells. In isolated rat pancreatic β-cells, we have demonstrated that hypotonic stimulation induces membrane depolarization, produces outwardly rectifying cation currents, and increases insulin secretion, and that all these responses are sensitive to relatively low concentration of Gd^{3+} (Takii et al. 2006). The hypotonicity-induced insulin secretion was also inhibited by other cation channel blockers, such as amiloride, 2-APB, and ruthenium red (Takii et al. 2006). We have also obtained similar results in mouse pancreatic β-cells (Ishikawa, unpublished data). Thus, SAC is also suggested to be involved in the insulin secretion induced by β-cell swelling.

In other cell types, some transient receptor potential (TRP) channels are proposed as candidates of SAC. The TRP superfamily is one of the largest families of cation channels and subdivided into major branches; TRPC, TRPA, TRPM, TRPP, TRPV, TRPML, and TRPN (Nilius et al. 2007). There is increasing evidence that numerous TRP channels are expressed in β-cells, i.e., TRPC1-6, TRPM2-5, and TRPV1, 2, 4 (Islam 2011; Jacobson and Philipson 2007). These channels allow for β-cells to respond to a variety of stimulations including glucose, leading to membrane depolarization, $[Ca^{2+}]_c$ elevation, insulin secretion, cell survival, and apoptosis. At least ten mammalian TRPs have been suggested to exhibit mechanosensitivity, i.e., TRPC1, 5, and 6; TRPV1, 2, and 4; TRPM3 and 7; TRPA1; and TRPP2 (Inoue et al. 2009). Since the $[Ca^{2+}]_c$ elevation induced by hypotonic stimulation was sensitive to relatively low concentrations of ruthenium red in β-cells isolated from rats (Takii et al. 2006) and mice (Ishikawa, unpublished data), ruthenium red-sensitive channels, i.e., TRPV family or TRPA1, may be involved in the hypotonicity-induced responses. Among them, TRPV4 is a good candidate of SAC in β-cells. A recent study in the mouse β-cell line MIN6 has shown that human islet amyloid polypeptide (hIAPP) triggers $[Ca^{2+}]_c$ elevation, which corresponded with the appearance of hIAPP aggregates, alterations in the surface membrane morphology of MIN6 cells, and a reduction of cell viability. Small interference RNA against TRPV4 prevented hIAPP-induced $[Ca^{2+}]_c$ rises and reduced hIAPP-triggered cell death. It is thus suggested that TRPV4 may sense physical changes in the plasma membrane induced by hIAPP aggregation (Casas et al. 2008). Another candidate may be TRPV2. In MIN6 cells, TRPV2 has been shown to be translocated from the cytosol to the plasma membrane by insulin and participate in GSIS (Hisanaga et al. 2009). However, there is no indication how gating of TRPV2 is modulated in β-cells. Further studies are necessary to determine the molecular identity of SAC activated by cell swelling in β-cells.

14.2.5 Perspectives

There is increasing evidence that insulin secretion is not exclusively dependent on the K_{ATP} channel-dependent mechanism. β-Cell swelling induced by high-concentration

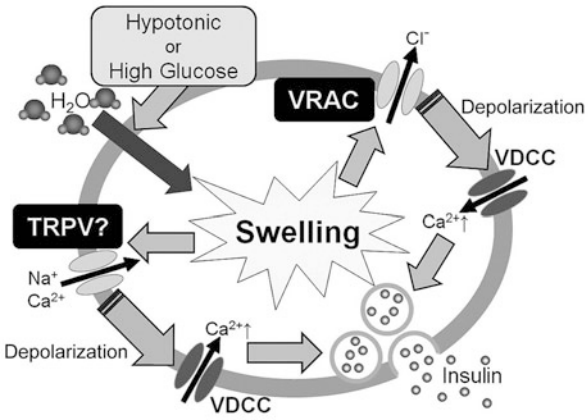

Fig. 14.1 Mechanisms for β-cell swelling-induced insulin secretion. β-Cell swelling activates volume-regulated anion channels (*VRAC*) and/or stretch-activated cation channels, possibly TRPV, thereby causing membrane depolarization and subsequent activation of voltage-dependent Ca^{2+} channels (VDCC), thus elevating insulin secretion

glucose may be one aspect of the K_{ATP} channel-independent mechanism. The regulation of cell volume is important in β-cells, in which high rates of glucose metabolism increase intracellular osmolality. The involvement of VRAC in the membrane depolarization and insulin secretion induced by β-cell swelling has been extensively studied; however, several reports have argued against this proposition by showing that hypotonicity-induced insulin secretion persists even in the presence of Cl^- channel blockers such as niflumic acid and DIDS (Kinard et al. 2001; Straub and Sharp 2002; Takii et al. 2006). Thus, the possibility still remains that mechanisms independent of VRAC are involved in the osmotic insulin secretion. Another potential candidate is mechanosensitive TRP channels; however, information available on them is limited (Fig. 14.1).

One major reason for this is the lack of specific inhibitors for TRP channel isoforms. Their study would be facilitated through RNA interference in cell culture and global mouse knockouts. Future studies with these techniques will elucidate the role of mechanosensitive TRP channels in K_{ATP} channel-independent GSIS as well as β-cell swelling-induced insulin secretion.

14.3 Adipocyte

14.3.1 Introduction

Recent advances in adipocyte research have established that adipose tissue not only serves as a means of energy storage in the form of triglycerides but also exerts secretory/endocrine functions. Adipocytes are the major cellular component of parenchymal adipose tissue, and are mesoderm or neuroectoderm in origin. The differentiation and hypertrophy (maturation) of adipocytes are fundamental processes involved in obesity. Mechanical stimuli such as stretching and rubbing of fat and skeletal muscle during gymnastic exercise or massage are believed to decrease

obesity as well. It is now considered that adipocytes are well equipped with possible candidates for mechanosensor molecules. These include chloride channels (Inoue et al. 2010) and TRP channels (Zhang et al. 2007), caveolae (Parton and Simons 2007; Pilch et al. 2007), kinases, including Rho-kinase (Hara et al. 2011), and focal adhesion proteins as well as stress fibers (Hara et al. 2011). In this regard, there have been quite a few papers as to the mechanosensitivity of adipocytes, i.e., how adipocytes respond to mechanical stimuli. Furthermore, adipocytes play a pivotal role in the secretion of hormones and cytokines/adipokines. Obese and matured adipose tissues produce a variety of proinflammatory adipokines, causing chronic inflammation. It has become clear that this obesity-induced chronic inflammation plays a key role in the development and progression of metabolic syndrome, including type-2 diabetes, hypertension, and pernicious obesity. Here, we present an overview of how adipocytes respond to mechanical stimuli with particular reference to the cell differentiation and the functions of secretory/endocrine gland, as well as adipose tissue inflammation, and their pharmacological interventions.

14.3.2 How does Mechanical Stress Act on Differentiation of Adipocytes?

14.3.2.1 Cyclic Stretching

Maturation of adipocytes can occur all throughout life irrespective of age from the pre-existing cluster of adipoprogenitor cells (preadipocytes). Thus both the proliferation and differentiation of preadipocytes into mature adipocytes are issues of particular importance from a pathophysiological point of view.

Tanabe et al. (2004) first reported the effect of cyclic stretching on adipocyte differentiation. The optimum cyclic stretching with a frequency of 1 Hz was applied to 3T3-L1 cells in the induction medium for 45 h (induction period) while undergoing adipocyte differentiation. After 45 h of induction, the cells subjected to cyclic stretching were oriented perpendicular to the axis of stretching. Thus, uniaxial stretching induces a phenotypic change in cytoskeletal structures of adipocytes, similar to that often observed in vascular endothelial cells subjected to hemodynamic forces such as blood pressure and blood flow. Furthermore, Oil-Red-O staining revealed that the accumulation of lipid droplets was significantly inhibited in the 3T3-L1 cells subjected to cyclic stretching.

As to the molecular mechanism of adipocyte differentiation, at least three members of CCAAT-enhancer-binding proteins (C/EBP) family (C/EBPα, β, and δ) and the γ-isoform of the peroxisome proliferator-activated receptor (PPAR) family (PPARγ1 and γ2) play pivotal roles in the regulation of adipipocyte differentiation, in particular, from preadipocyte to mature adipocyte (Rangwala and Lazar 2000; Rosen and Spiegelman 2000). Only the application of cyclic stretching during the late phase of induction could inhibit the adipocyte differentiation of 3T3-L1 cells, which was accompanied by the downregulation of PPARγ1 and γ2 without any change in the expression of mRNA transcript for C/EBP (Tanabe et al. 2004).

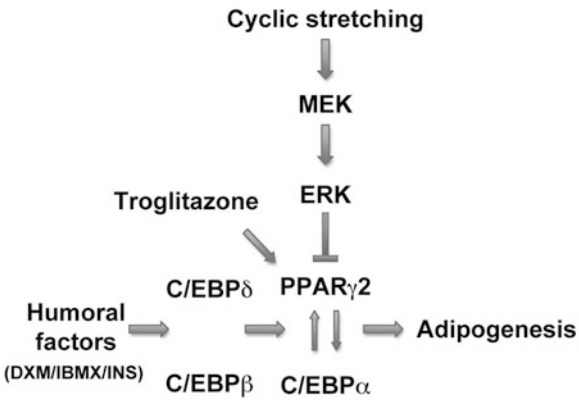

Fig. 14.2 Schematic diagram indicating inhibitory effect of cyclic/dynamic stretching on the process of differentiation involved in adipogenesis. Note that adipocyte differentiation is inhibited by mechanical stretching through ERK-mediated downregulation of a transcription factor PPARγ2. Troglitazone, a thiazolidinedione, accelerates the differentiation process, while cyclic stretching counteracts the process. (See in detail Tanabe et al. (2004))

14.3.2.2 MEK/ERK Pathway and Rho/Rho-Kinase Activity

Several lines of evidence have suggested that mechanical stimuli evoke the mitogen-activated protein kinase kinase/extracellular signal-regulated kinase (MEK/ERK) pathway in various types of cells (Tibbles and Woodgett 1999; Yamboliev et al. 2000). The stretch-induced blockade of adipocyte differentiation was reversed by PD98,059, an inhibitor of MEK, with concomitant restoration of the expression of PPARγ2 at the mRNA and protein levels. In contrast, the expression of PPARγ1 mRNA, which was reduced in response to the stretching condition, was not restored by PD98,059. PD98,059 also restored lipid droplet accumulation. Furthermore, the differentiation inhibited by stretching was also restored by a synthetic PPARγ ligand such as troglitazone. Therefore, inhibition of adipocyte differentiation in response to cyclic stretching is mainly attributable to the reduced expression of PPARγ2, which is negatively controlled by activation of the MEK/ERK system (Fig. 14.2).

Mechanical stress also activates Rho/Rho-kinase and the subsequent signaling. Hara et al. (2011) investigated whether activation of Rho/Rho-kinase in adipose tissue participates in the development of obesity. 3T3-L1 cells were subjected to direct application of static mechanical stretching for a 72-hour duration. Rho-kinase activity and stress fiber formation were increased as lipid accumulated and cells swelled after the differentiation into adipocytes. Rho-kinase activation induces the expression of cytokines and chemokines that are adipocytic in origin such as tumor necrosis factor α (TNFα) and monocyte chemotactic activating factor 1 (MCP-1). Consistently, mature adipocytes were abundant in the mRNA transcripts encoding TNFα and MCP-1.

14.3.2.3 Dynamic and Static Stretching

Shoham et al. (2012) have reported that static mechanical stretching at the static tensile strains of 12 % to the substrata accelerates lipid production in 3T3-L1 adipocytes

by activating the MEK pathway. Thus, the input pathway of static mechanical stretching seems to be similar to that of cyclic stretching. However, a PPARγ inhibitor, GW 9662, had no apparent effect on the adipocyte differentiation, indicating an alternative signaling pathway not yet revealed may be involved in the adipocyte differentiation.

It is considered that dynamic/cyclic stretching more effectively activates electrical and subsequent events than static stretching (Johansson and Mellander 1975). For instance, in vascular smooth muscle, the dynamic stretching mobilizes both extra- and intracellular-activator Ca^{2+}, while the static one promotes mainly influx of Ca^{2+} through L-type Ca^{2+} and other ion channels (Obara et al. 2001; Nakayama et al. 2010). Thus it appears possible that static and dynamic stretching evokes different cell signaling in adipocytes. However, as to mechanical stress in adipose cells and tissues, one needs to be careful when interpreting the results obtained. Although confluent cultures of 3T3-L1 cells undergo differentiation into adipocytes with or without stretching, this "without stretching" means that static tensile strain somehow always exists on the cell surface even when adipocytes are cultured on the surface of substrate. 3T3-L1 cells accumulate lipid droplets without any intentional procedure for stretching in the mature phase. Accordingly, Hara et al. (2011) have proposed a scheme depicting the vicious cycle of adipose tissues in obesity. The lipid deposition evokes adipocyte hypertrophy leading to further stretched cell membrane. Mechanical stretching and possibly some additional factors promote Rho-kinase activity, which contributes to both adipokine expression and recruitment of inflammatory cells, including macrophages, to adipose tissues. In turn, the chronic low-grade inflammatory process is accelerated (chronic inflammation), and lipid is further accumulated in a vicious cycle manner. It presumes that this vicious cycle of adipose tissue can take place only when adipocytes and surrounding tissues are properly adhered to each other for expanding (Fig. 14.3). The appropriate interaction between the cellular and extracellular matrix along with proper angiogenesis are particularly important for the development of adipose tissue *in vivo* (Han et al. 2011). As the developed network of blood vessels also nourishes the inflated-adipose tissues filled with lipid, it may be said that the state of chronic inflammation *in vivo* is caused by adipose tissues in concert with vascular tissues (adipogenesis-angiogenesis interaction) (Manabe 2011). Thus, hypertrophied adipose tissues together with an invading network of blood vessels and immune cells *in vivo* induce much more dysregulated production of proinflammatory mediators relative to the production of anti-inflammatory adipokines (e.g., adiponectin), which leads to adverse metabolic and cardiovascular consequences.

14.3.3 Mechanical Stress and Endocrine Function of Adipose Tissues

It is a well-documented fact that adipocytes/adipose tissue function as the largest secretory organs in the whole body. *In vivo*, the clusters of small size adipocytes under non-inflammatory conditions primarily secrete adiponectin, pref-1, and other anti-inflammatory and anti-obese factors such as leptin. However, mature and

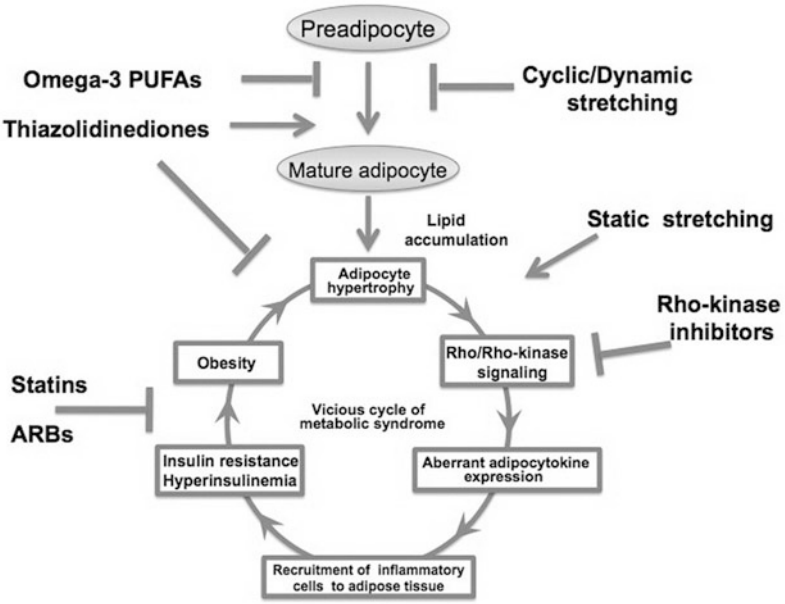

Fig. 14.3 Possible inhibitory actions of several cardiovascular drugs on vicious cycle of adipose tissues in obesity. Once adipocyte has matured, it begins to accumulate lipid in the cell, leading to hypertrophied adipocyte, and stretching of surface membrane. Mechanical stretching together with other factors activates Rho/Rho-kinase signaling and subsequent proinflammatory processes including expression of adipocytokines, recruitment of macrophages, and vascular invasion, which further accelerate systemic insulin resistance, hyperinsulinemia, and obesity. This vicious cycle contributes to the progress of metabolic syndrome and further complicates obesity. Cyclic stretching in combination with several drugs such as Rho-kinase inhibitors, statins, and angiotensin AT_1 receptor blockers (*ARBs*), may interrupt this vicious cycle

fat-accumulated adipocytes (large adipocytes) induce the expression of cytokines and chemokines that are adipocytic in origin such as tumor necrosis factor (TNFα) and MCP-1. The secreted chemokine recruits immune cells such as M1 macrophages, T cells and neutrophiles. Moreover, vascular networks invaded by the cluster of mature adipocytes further propagate inflammatory cascades, leading to a state of chronic inflammation responsible for systematic insulin resistance and other metabolic abnormalities (Nishimura et al. 2008; Manabe 2011). Thus, in order to clarify the effect of mechanical stress on the adipocytic endocrine function, i.e., how mechanical stress acts directly and locally on adipose tissues *in vivo*, it is inevitably necessary to carry out long-term experiments in conscious animals *in vivo*.

14.3.3.1 Rho/Rho-Kinase-Dependent Endocrine Function in Diet-Induced Obesity

Hara et al. (2011) reported that mice fed a high-fat diet showed increased adipocyte size, Rho-kinase activity, and stress-fiber formation in adipose tissue, as well as body

weight gain compared to mice fed a low-fat diet. Abundance of the mRNA transcripts encoding the adipocytokines TNFα and MCP-1 increased in adipose tissue of mice fed a high-fat diet. Conversely, abundance of the mRNA encoding adiponectin was decreased in mice fed a high-fat diet. Rho-kinase activity was increased after stretching in mature adipocytes. Furthermore, the expression of the mRNA transcripts encoding TNFα and MCP-1 was increased, whereas that encoding adiponectin was decreased. Fasudil and Y-27362, Rho-kinase inhibitors, reduced lipid accumulation and Rho-kinase activity in the mature cells. These are consistent with the *in vivo* data obtained in the diet-induced obese mice and dominant negative-RhoA transgenic mice. It is thus likely that lipid accumulation in adipocytes activates Rho/Rho-kinase signaling at least in part through mechanical stretching and implicates Rho/Rho-kinase signaling in adipose tissue in obesity.

14.3.3.2 Local Vibration and Metabolic and Endocrine Functions of Adipocytes

We have investigated *in vivo* effects of mechanical vibration on adipose tissues in conscious mice. Male ddY mice fed a high-fat diet and weighing about 50 g received mechanical vibration (100 Hz for 30 min) on the lower abdomen twice a day for up to 16 days. The daily abdominal vibrations significantly lowered triglyceride content in adipose tissues and plasma concentration of free fatty acids without any changes in body weight, daily food intake, or plasma concentration of corticosterone, a stress maker. Moreover, the vibrations decreased expression of adipogenic transcription factors such as PPARγ2 and sterol-regulatory element-binding protein-1c (SREBP-1c), while the expression of anti-adipogenic preadipocyte factor Pref-1 was increased. The increased Pref-1 is expected to induce a lowering of triglyceride content and the downregulation of adipokines such as leptin, resistin, and adiponectin in the epidermal adipose tissues, leading to a decrease in nonesterified fatty acids (NEFAs) in blood plasma. Thus, the daily abdominal vibrations can affect gene expression, endocrine, and metabolic function of adipose tissues, which would lead to a beneficial effect on obese-related diseases. However, the local vibration also induced the expression of pro-inflammatory genes; arginase-1, interleukin-10 (IL-10), and colony-stimulating factor Mgl-1, which are characteristic to M2 macrophages (alternatively-activated macrophages), and IL-6, IL-1β, MCP-1, and COX2, which are characteristic to M1 macrophages (classically-activated macrophages). Thus, mechanical stress such as vibration in combination with anti-inflammatory pharmacological interventions as mentioned below could improve the balance between proinflammatory factors and anti-inflammatory ones.

14.3.4 Mechanical Stress and Pharmacological Interventions

Metabolic syndrome is considered to be a kind of chronic inflammatory state. Of the many cardiovascular drugs, several drug groups can also be used against proinflam-

matory processes often encountered in metabolic syndrome including hypertension and obesity. They include inhibitors of Rho/Rho-kinase, fasudil and Y-2736, eicosapentaenoic acid (EPA) and docosahexanoic acid (DHA), ω-3 poly-unsaturated fatty acids, thiazolidinediones (TZDs), insulin-sensitizers, angiotensin AT_1 receptor blockers (ARBs), and HMG-CoA reductase inhibitor statins.

14.3.4.1 Rho/Rho-Kinase Inhibitors

Rho/Rho-kinase and subsequent signaling might be activated by stretching cell membrane when mature adipocytes become hypertrophic in obesity (Hara et al. 2011). Direct application of static stretching to mature adipocytes increased the expression of the mRNA transcripts encoding TNFα and MCP-1 and stress fiber formation, whereas the expression of the mRNA encoding adiponectin was decreased. These changes in mRNA abundance were inhibited by the Rho-kinase inhibitor Y-27632 or fasudil. Thus, lipid accumulation in adipocytes is likely to activate Rho/Rho-kinase signaling, at least in part, through mechanical stretching. The activated signaling further accelerates inflammatory changes in adipose tissue in obesity in a vicious cycle manner. This vicious cycle could be interrupted by the Rho-kinase inhibitors, which may provide a novel therapeutic strategy for obesity and related diseases, including insulin resistance and atherosclerosis (Hara et al. 2011) (See Fig. 14.3).

14.3.4.2 ω-3 Polyunsaturated Fatty Acids, EPA and DHA

A variety of endogenous and exogenous lipids and fatty acids play an important role in adipocyte differentiation. EPA and DHA are fish-oil-derived ω-3 polyunsaturated fatty acid (PUFA) possessing a variety of pharmacological actions, including antithrombic, anti-inflammatory, anti-atherogenic, and antiarrhythmic activities (Kris-Etherton et al. 2002; Holub and Holub 2004). Furthermore, ω-3 PUFA modulates gene expression involved in lipid homeostasis in adipocytes. When EPA was concomitantly applied with cyclic stretching, adipocyte differentiation was significantly reduced, although EPA alone had no effect on the differentiation (Tanabe et al. 2008). EPA could be a substrate of COX2, the expression of which was strongly augmented by stretching. A selective COX2 inhibitor NS-398 attenuated the combined effect of stretching and EPA. Thus, stretching and EPA are suggested to exhibit a synergistic effect on the inhibition of adipocyte differentiation through stretch-induced COX2 production. In contrast, DHA is not a direct substrate for either COX1 or COX2 (Hirafuji et al. 2003), indicating no apparent synergistic effects with stretching.

14.3.4.3 PPARγ Agonist Thiazolidinediones

Thiazolidinediones (TZD) are agonistic ligands for peroxisome proliferator-activating receptor γ (PPARγ), a group of nuclear hormone receptors. The activated

receptor migrates to the DNA, which is involved in the regulation of genes related to glucose and lipid metabolism. PPARγ agonists have been reported to possess anti-inflammatory activity, suggesting their possible use for treatment of inflammatory and autoimmune diseases (Straus and Glass 2007). One of the adverse actions of TZD is obesity due to a decrease in leptin levels and an acceleration of adipocyte differentiation. Cyclic stretching inhibited the accelerating action of TZD on the adipocyte differentiation assessed in 3T3-L1 cells (Tanabe et al. 2004). TZD also shows anti-inflammatory action by increasing adiponectin and by decreasing certain interleukins, e.g., IL-6, and vascular endothelial growth factor (VEGF)-induced angiogenesis. Thus, mechanical stretching may ameliorate the adverse action of TZD in obesity and enhance the pleiotropic action of TZD in the therapy of type2 diabetes (Tanabe et al. 2004).

14.3.4.4 AT_1 Receptor Blockers and Statins

Angiotensin II (AngII) type 1 receptor (AT_1R), a GTP binding protein-coupled receptor (GPCR), plays a crucial role in the regulation of cardiovascular homeostasis. In addition to circulating and local AngII, evidence has accumulated that mechanical stress including high blood pressure can activate AT_1R and induces cardiac hypertrophy (Zou et al. 2004; Yasuda et al. 2008) and vascular myogenic contraction (Voets and Nilius 2009). The mechanical strain is transmitted via Gq proteins coupled to AT_1R (Akazawa and Komuro 2010) or other adaptor proteins such as β-arrestins (Rakesh et al. 2010). The agonist-independent activation of AT_1R can be inhibited by inverse AT_1R agonists such as candesartan and olmesartan (Miura et al. 2006). AT_1R blockers (ARBs) substantially lower the risk for type 2 diabetes, and improves insulin sensitivity in animal models of insulin resistance. A specific subset of ARBs such as telmisartan and irbesartan has been shown to stimulate PPARγ activity independently of their AT_1R blocking actions (Schupp et al. 2004). The pleiotropic effects of ARBs including blocking the action of mechanical stress emerge as an important pharmacological characteristic for AT_1R and other GPCRs, which determine the efficacy to protect tissue and cells against cardiovascular and metabolic diseases.

The HMG-CoA reductase inhibitor statins have been clinically used to slow down the progression of atherosclerosis by inhibiting the rate-limiting step of biosynthesis of cholesterol. However, statins are now also shown to possess non-lipid lowering benefits, i.e., pleiotropic actions (Lefer 2002). The pleiotropic effects of statins have been often argued to occur in cardiovascular tissues. Pravastatin and rivastatin act inhibitory on the adipose tissue inflammation and toll-like receptor-4 (TLR4)-mediated signaling in macrophages (Abe et al. 2008). However, some statins including atorvastatin inhibited adipocyte maturation and expression of glucose transporter 4 (GLUT4).

There is so far no information available as to the effect of mechanical stretching in combination with statins on glycemic control in adipocytes. It would be important to recognize obesity, which is a crucial cause of metabolic syndrome, as a chronic inflammatory disease and to fully clarify how pharmacological interventions toward

cardiovascular and metabolic diseases in combination with mechanical stress act on adipose tissues *in vivo*.

14.3.5 Perspectives

It has become clear that the intercommunication between the central nervous system and peripheral organs, including pancreatic β-cells, adipocytes, and skeletal muscle cells is important for the maintenance of homeostasis in energy-glucose metabolism (Devaskar 2001; Sandoval et al. 2009). This intercommunication has often been discussed from the view point of the neurohumoral axis. However, the intercommunication among these peripheral organs is also important. The balance of anti- and pro-inflammatory cytokines, for instance, adiponectin and plasminogen-activator inhibitor-1 (PAI-1), respectively, released from adipocyte by mechanical and other stimuli also strongly affects not only insulin secretion but also the sensitivity of adipocyte and skeletal muscle cells to insulin (Corgosinho et al. 2011; Lumeng and Saltiel, 2011). Moreover, the adipogenesis coupled with vascular angiogenesis (Nishimura et al. 2008; Manabe 2011), an alternative kind of intercommunication, plays a pivotal role in the process of chronic inflammation and metabolic syndrome.

14.4 Skeletal Muscle

14.4.1 Introduction

The skeletal muscle is the main tissue involved in glucose disposal *in vivo*, and its function is exquisitely regulated by several stimuli including muscle contractions and insulin (Holloszy 2003). The major cellular mechanism for disposal of an exogenous glucose load is glucose transport into skeletal muscle. The principal glucose transporter protein in skeletal muscle is GLUT4, which is one isoform of glucose transporter proteins containing 12-transmembrane domains. Muscle contraction and insulin increase the glucose transport which can be rapidly induced by translocation of GLUT4 from intracellular vesicles to the plasma membrane and/or transverse tubules (T-tubules) (Dombrowski et al. 1996; Holloszy 2003) and possibly by increased intrinsic activity of GLUT4 (reviewed in Furtado et al. 2003). The GLUT4 translocation induced by muscle contraction and insulin is mediated by distinct signaling pathways, and their maximal effects on muscle glucose uptake are additive (Holloszy 2003). GLUT4 is thus a major mediator of glucose removal from the circulation and a key regulator of whole-body glucose homeostasis.

Muscle contraction is accompanied by mechanical stimuli such as passive stretching or deformation of cells and tissues. Stretching of skeletal muscle results in changes in cellular metabolism, including glucose transport (Ihlemann et al. 1999; Ito et al. 2006). Indeed, mechanical stretching per se has been reported to increase the glucose transport in skeletal muscle without force-producing contraction (Ihlemann

et al. 1999; Ito et al. 2006), as well as in cultured L6 (Mitsumoto et al. 1992) and C2C12 myotubes (Iwata et al. 2007). We have further shown that passive stretching induces the translocation of GLUT4 only to the plasma membrane, but not to T-tubules, in rat skeletal muscle, whereas active contraction and insulin stimulate the translocation of GLUT4 to both the plasma membrane and T-tubules (Ito et al. 2006). Thus, passive stretching is likely to play a major role in skeletal muscle glucose transport. However, there is still controversy as to which intracellular signaling pathways that mediate the effects of mechanical stretching on glucose transport.

14.4.2 Mechanosensors in Skeletal Muscle

Many molecules have been proposed as a mechanosensor in skeletal muscle, including SAC (Spangenburg and McBride 2006) and integrins (Zanchi and Lancha 2008); however, none of them are definitive. Skeletal muscle may have multiple mechanosensors, which all integrate the mechanical information into anabolic or catabolic responses.

14.4.2.1 Stretch-Activated Channels (SAC)

SAC was first discovered by patch clamping in skeletal muscle (Guharay and Sachs 1984), but the molecular identity of the channel is still unknown. SAC in skeletal muscle is permeable to Ca^{2+} as well as Na^{+} (Franco and Lansman 1990) and activated by stretching of the membrane. TRP channels are a good candidate to account for SAC. Several members of the TRPC, TRPV and TRPM subfamilies are expressed in skeletal muscle. The most prominent TRP channels are TRPC1, C3, C4 and C6, TRPV2 and V4 as well as TRPM4 and M7. TRPC1 is well characterized TRP in skeletal muscle, and can be activated by membrane stretching (Maroto et al. 2005). Even though many studies point to TRPC1 as being a stretch-activated channel (Ducret et al. 2006), this topic remains controversial, with tissue-specific investigations of TRPC1 function often providing negative results (Dietrich et al. 2007).

14.4.2.2 Integrin

There is increasing evidence indicating that integrin plays an important role in mechanotransduction (Sasamoto et al. 2005). Integrin is a heterodimeric complex composed of α and β subunits. There are 19α and 8β mammalian subunit isoforms (Humphries 2000). In skeletal muscle, integrin is limited to seven subunit subtypes, i.e., α1, α3, α4, α5, α6, α7, and αv subunits, all associated with β1 subunit (Schwander et al. 2003). Recently, we found that stretch-induced glucose uptake is inhibited by JB1 A, an integrin β1 blocking antibody (Ni et al. 1998), in cultured L6 myotubes

(Obara et al., unpublished observation), suggesting the involvement of integrin in stretch-induced glucose uptake into skeletal muscle.

14.4.3 Possible Mediators of Mechanotransduction

Iwata et al. (2007) have shown that mechanical stretch-stimulated glucose uptake is insensitive to wortmannin, an inhibitor of phosphoinositide 3-kinase (PI3K), whereas the effect of insulin is completely abolished by the PI3K inhibitor. These results suggest that the stretch signaling pathway mediates skeletal muscle glucose uptake through a pathway independent of insulin. Passive stretching of skeletal muscle is suggested to mimic the effects of muscle contractions on cellular metabolism, including glucose uptake (Ihlemann et al. 1999). It is thus hypothesized that the stimulation of glucose uptake by mechanical stretching may be mediated by pathways similar to those stimulated by contractions/exercise.

14.4.3.1 AMP-Activated Protein Kinase

AMP-activated protein kinase (AMPK) is a serine/threonine protein kinase activated by various stresses leading to the depletion of cellular ATP (Hardie et al. 1998). AMPK consists of one catalytic subunit (α) and two noncatalytic subunits (β, γ). AMPK is proposed to be a key mediator of glucose uptake into skeletal muscle during contractions and exercise. The α2-containing complex of AMPK is the primary catalytic isoform and activated during exercise (Musi et al. 2001; Wojtaszewski et al. 2000). The pharmacological activator of AMPK, adenosine analogue 5-aminoimidazole 4-carboxamide ribonucleoside (AICAR), can increase glucose uptake (Hayashi et al. 1998). However, there is apparent disassociation between AMPK activation and glucose uptake during exercise (Derave et al. 2000). Moreover, AMPK α2 knockout abolishes AICAR-induced glucose uptake, but has no inhibitory effect on contraction-induced glucose uptake (Jørgensen et al. 2004). Thus, it is likely that AMPK has the ability to increase glucose uptake, but is not essential for contraction-stimulated glucose uptake. AMPK is also unlikely to be involved in the stimulation of glucose uptake by mechanical stretching. In cultured C2C12 myotubes, compound C, an inhibitor of AMPK, completely inhibited the glucose transport induced by AICAR but not that induced by stretching (Iwata et al. 2007). This notion is also supported by our observation that mechanical stretching has no apparent effect on AMPK activity in mouse skeletal muscle *in vitro* (Ito et al. 2006).

14.4.3.2 Ca^{2+} and Ca^{2+}/Calmodulin-Dependent Protein Kinase

The experiments with caffeine, which induces release of Ca^{2+} from sarcoplasmic reticulum (SR) of isolated skeletal muscle without membrane depolarization, have

shown that raising $[Ca^{2+}]_c$ increases glucose uptake (Holloszy and Narahara 1967). Studies from several groups have shown that increases in $[Ca^{2+}]_c$ during skeletal muscle contraction provide the signal leading to contraction-induced increases in glucose transport (Holloszy and Narahara 1967; Clausen et al. 1975; Wijesekara et al. 2006). This possibility is supported by the observation that a Ca^{2+} ionophore ionomycin or ryanodine, which elicits the release of Ca^{2+} from SR, induces glucose uptake into C2C12 myotubes accompanied by an elevation of $[Ca^{2+}]_c$ below the contraction threshold (Iwata et al. 2007).

Cyclic stretch-dependent Ca^{2+} influx is suggested to be essential in several stretch-dependent signal transductions (Inou et al. 2002; Wang et al. 2001). In contrast, intracellular Ca^{2+} stores seem also to serve as a mechanotransducer in the stretch-induced signaling pathway in multiple cell types (Taskinen and Ruskoaho 1996). The stretching of C2C12 myotubes has been shown to induce a rapid increase in $[Ca^{2+}]_c$ (Iwata et al. 2007). The depletion of extracellular Ca^{2+} did not affect the glucose uptake induced by cyclic stretching and the inhibition of Ca^{2+} release from intracellular Ca^{2+} storage sites completely prevented stretch-stimulated glucose uptake in C2C12 myotubes (Iwata et al. 2007) and in mouse soleus muscle (Obara unpublished observation).

Ca^{2+}/calmodulin-dependent protein kinases (CaMK) are activated by Ca^{2+} (Soderling 1999), and CaMK is involved in the stimulation of muscle glucose uptake (Chin 2005). The inhibition of CaMK by KN93, a specific inhibitor of CaMK (Sumi et al. 1991; Corcoran and Means 2001), leads to a decrease in the glucose transport stimulated by cyclic stretching in C2C12 myotubes (Iwata et al. 2007) and by contraction in rodent skeletal muscles (Wright et al. 2004). These findings suggest that stretch-stimulated glucose transport appears to be dependent on the Ca^{2+}/CaMK signaling pathway. Three CaMKs, i.e., CaMKI, CaMKII, and CaMKIV, are activated by Ca^{2+}, and all of the CaMKs are inhibited by KN93 (Corcoran and Means 2001). CaMKII, but not CaMKI or CaMKIV, is expressed in human skeletal muscle (Rose et al. 2006). The activation of CaMKII by Ca^{2+} mediates the contraction-induced increases in glucose transport in rat epitrochlearis muscle (Wright et al. 2004). It is thus likely that stretch-stimulated glucose transport is mediated by the Ca^{2+}/CaMKII-dependent signaling pathway.

14.4.3.3 Nitric Oxide

Nitric oxide (NO) is a gas synthesized by the enzyme nitric oxide synthase (NOS). Three NO synthase (NOS) isoforms, i.e., NOS1 (neuronal NOS; nNOS), NOS2 (inducible NOS; iNOS), and NOS3 (endothelial NOS; eNOS), have been described: NOS1 and NOS3 are constitutively expressed and Ca^{2+}/calmodulin-dependently activated, while the expression of NOS2 is induced by cytokines (Moncada et al. 1991). Several isoforms have been identified that result from alternative splicing of the nNOS gene. Of these nNOS isoforms, nNOSμ is the most prevalent isoform expressed in skeletal muscle fibers (Silvagno et al. 1996). The involvement of NO in glucose uptake into skeletal muscle is suggested by several lines of evidence: The

NO donor sodium nitroprusside (SNP) increases glucose uptake in skeletal muscle independently of insulin (Balon and Nadler 1997) and NOS inhibitors attenuate or abolish increases in glucose uptake during contractions in rodent skeletal muscle (Balon and Nadler 1997; Ross et al. 2007). Moreover, skeletal muscle contraction has been shown to increase cGMP formation (Lau et al. 2000), suggesting that NO increases contraction-induced glucose uptake via the NO/cGMP pathway. NO seems also to mediate glucose uptake induced by mechanical stretching as well as contractions. Cyclic stretching has been shown to increase nNOS expression and NO production (Tidball et al. 1998; Zhang et al. 2004), and to stimulate glucose uptake in C2C12 myotubes (Iwata et al. 2007). We have confirmed that N^{G}-nitro-L-arginine methylester (L-NAME), an inhibitor of NOS, inhibits glucose uptake induced by cyclic stretching in mouse soleus muscle (Obara, unpublished observation). NO is thus likely to mediate increased glucose uptake during cyclic stretching as well as during contraction. In this regard, identifying the pathways through which NO acts during mechanical stretching is still needed.

14.4.3.4 p38 Mitogen-Activated Protein Kinase

A potential role of p38 mitogen-activated protein kinase (p38 MAPK) in the contraction- and insulin-stimulation of glucose transport in skeletal muscle is suggested (Somwar et al. 2000; 2002). Somwar et al. (2002) showed that p38 MAPK mediates an increase in glucose transport by activating GLUT4 although it is not involved in GLUT4 translocation to the cell surface. In adult rat skeletal muscle, exercise and contraction increase the phosphorylation and activity of multiple isoforms (α, β, and γ) (Goodyear et al. 1996). Of these isoforms, γ-isoform (p38 γMAPK) is highly regulated by muscle contraction (Boppart et al. 2000). Recently, it has been reported that p38 γMAPK decreases contraction-stimulated glucose uptake by affecting intrinsic GLUT4 activity in skeletal muscle of mice (Ho et al. 2004). Although we observed that total phosphorylation of p38 MAPK isoforms was increased by mechanical stretching in mouse skeletal muscle, it is possible that an isoform such as p38 γMAPK may negatively regulate glucose uptake induced by passive stretching, resulting in a small glucose uptake despite large translocation of GLUT4 to the plasma membrane (Ito et al. 2006).

14.4.4 Perspectives

Mechanical stretching increases skeletal muscle GLUT4 translocation from intracellular vesicles to the surface membrane and increases glucose uptake, but it is clear that insulin- and contraction-independent pathways are involved. The mechanisms by which mechanical stretching increases glucose uptake into skeletal muscle are not fully elucidated, but may involve Ca^{2+}/CaMKII, p38 MAPK, and NO signaling (Fig. 14.4). In addition, β1 subunit-containing integrins seem to locate upstream of the mechanotransduction cascade. It is likely that more than one pathway is involved

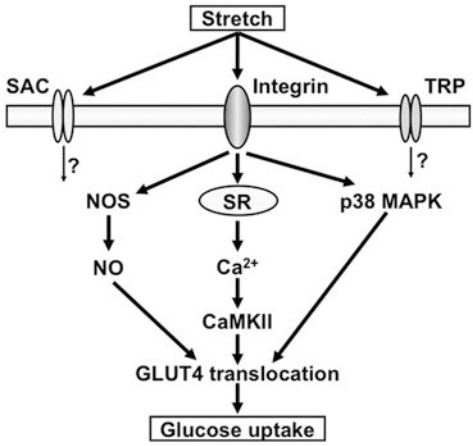

Fig. 14.4 Possible mechanisms involved in stretch-induced glucose uptake. *SAC*, stretch-activated channel; *TRP*, transient receptor potential channel; *NOS*, nitric oxide synthase; *NO*, nitric oxide; *SR*, sarcoplasmic reticulum; p 38 MAPK, p 38 mitogen-activated protein kinase; CaMKII, Ca^{2+}/calmodulin dependent protein kinase type II; GLUT4, glucose transporter 4

in signaling of GLUT4 translocation and glucose uptake stimulated by mechanical stretching and that overlapping of pathways and redundancy may occur; if one pathway is inadequate or blocked, another pathway may be upregulated.

14.5 Conclusion and Perspectives

In this review, we have provided a brief review of currently available knowledge on the cellular and molecular mechanisms as to the mechanosensitivity of pancreatic β-cells, adipocytes and skeletal muscle cells. All of these cells and tissues play a critical role in the energy metabolism, and are related to a core concern in the metabolic syndrome. As has been well documented, skeletal muscle cells are always subjected to mechanical stress during muscle contraction such as exercise, and other various motions. However, as shown in this review, both β-cells and adipocytes are also quite mechanosensitive. In this regard, there are quite a few papers as to the mechanosensitive mechanisms of these cells and tissues. It has become clear that these cells and tissues react differentially in their functions when subjected to mechanical stress. It is now considered that the obesity-induced chronic inflammation is critical in the development and progression of metabolic syndrome. While research concerning pharmacological intervention and mechanosensitivity seems to be still in its infancy, we believe that further study of mechanosensitivity/mechanotransduction in cells and tissues, particularly that involved in the metabolic syndrome and cardiovascular complications, will aid in further recognizing the importance of biomechanical factors in physiological and pathophysiological conditions, and will open up a new era of novel therapeutic remedies.

Acknowledgments The present study was supported in part by grants-in-aid for scientific research from the Ministry of Education, Culture, Sports, Science, and Technology of Japan, and by grants from the Shizuoka Research and Development Foundation. We also appreciate Iwate Medical

University and University of Shizuoka for their continuous support. We also express our special thanks to Dr. Paul Langman for his excellent revision of our English.

References

Abe M, Matsuda M, Kobayashi H, Miyata Y, Nakayama Y, Komuro R, Fukuhara A, Shimomura I (2008) Effects of statins on adipose tissue inflammation: their inhibitory effect on MyD88-independent IRF3/IFN-β pathway in macrophages. Arterioscler Thromb Vasc Biol 28:871–877

Akazawa H, Komuro I (2010) Mechanical stress induces cardiomyocyte hypertrophy through agonist-independent activation of angiotensin II type receptor. In: Kamkin A, Kiseleva I (eds) Mechanosensitivity in cells and tissues. Mechanosensitivity of the heart. Springer, pp 83–95

Ashcroft FM, Rorsman P (1990) ATP-sensitive K^+ channels: a link between B-cell metabolism and insulin secretion. Biochem Soc Trans 18:109–111

Ashcroft FM, Ashcroft SJ, Harrison DE (1988) Properties of single potassium channels modulated by glucose in rat pancreatic β-cells. J Physiol 400:501–527

Balon TW, Nadler JL (1997) Evidence that nitric oxide increases glucose transport in skeletal muscle. J Appl Physiol 82:359–363

Best L (1999) Cell-attached recordings of the volume-sensitive anion channel in rat pancreatic B-cells. Biochim Biophys Acta 1419:248–256

Best L (2000) Glucose-sensitive conductances in rat pancreatic β-cells: contribution to electrical activity. Biochim Biophys Acta 1468:311–319

Best L (2002a) Evidence that glucose-induced electrical activity in rat pancreatic β cells does not require K_{ATP} channel inhibition. J Membr Biol 185:193–200

Best L (2002b) Study of a glucose-activated anion-selective channel in rat pancreatic β-cells. Pflügers Arch 445:97–104

Best L, Trebilcock R, Tomlinson S (1992) Lactate transport in insulin-secreting β-cells: contrast between rat islets and HIT-T15 insulinoma cells. Mol Cell Endocrinol 86:49–56

Best L, Miley HE, Yates AP (1996a) Activation of an anion conductance and beta-cell depolarization during hypotonicity-induced insulin release. Exp Physiol 81:927–933

Best L, Sheader EA, Brown PD (1996b) A volume-activated anion conductance in insulin-secreting cells. Pflügers Arch 431:363–370

Best L, Brown PD, Tomlinson S (1997) Anion fluxes, volume regulation and electrical activity in the mammalian pancreatic β-cell. Exp Physiol 82:957–966

Best L, Miley HE, Brown PD, Cook LJ (1999) Methylglyoxal causes swelling and activation of a volume-sensitive anion conductance in rat pancreatic β-cells. J Membr Biol 167:65–71

Best L, Yates AP, Decher N, Steinmeyer K, Nilius B (2004) Inhibition of glucose-induced electrical activity in rat pancreatic β cells by DCPIB, a selective inhibitor of volume-sensitive anion currents. Eur J Pharmacol 489:13–19

Best L, Brown PD, Sener A, Malaisse WJ (2010) Electrical activity in pancreatic islet cells: The VRAC hypothesis. Islets 2:59–64

Blackard WG, Kikuchi M, Rabinovitch A, Renold AE (1975) An effect of hyposmolarity on insulin release in vitro. Am J Physiol 228:706–713

Boppart MD, Asp S, Wojtaszewski JF, Fielding RA, Mohr T, Goodyear LJ (2000) Marathon running transiently increases c-Jun NH2-terminal kinase and p38 activities in human skeletal muscle. J Physiol 526:663–669

Carpinelli AR, Malaisse WJ (1981) Regulation of ^{86}Rb outflow from pancreatic islets: the dual effect of nutrient secretagogues. J Physiol 315:143–156

Casas S, Novials A, Reimann F, Gomis R, Gribble FM (2008) Calcium elevation in mouse pancreatic beta cells evoked by extracellular human islet amyloid polypeptide involves activation of the mechanosensitive ion channel TRPV4. Diabetologia 51:2252–2262

Chin ER (2005) Role of Ca^{2+}/calmodulin-dependent kinases in skeletal muscle plasticity. J Appl Physiol 99:414–423

Clausen T, Elbrink J, Dahl-Hansen AB (1975) The relationship between the transport of glucose and cations across cell membranes in isolated tissues. IX. The role of cellular calcium in the activation of the glucose transport system in rat soleus muscle. Biochim Biophys Acta 375:292–308

Corcoran EE, Means AR (2001) Defining Ca^{2+}/calmodulin-dependent protein kinase cascades in transcriptional regulation. J Biol Chem 276:2975–2978

Corgosinho FC, de Piano A, Sanches PL, Campos RM, Silva PL, Carnier J, Oyama LM, Tock L, Tufik S, de Mello MT, Damaso AR (2011) The role of PAI-1 and adiponectin on the inflammatory state and energy balance in obese adolescents with metabolic syndrome

Davies SL, Brown PD, Best L (2007) Glucose-induced swelling in rat pancreatic α-cells. Mol Cell Endocrinol 264:61–67

Derave W, Ai H, Ihlemann J, Witters LA, Kristiansen S, Richter EA, Ploug T (2000) Dissociation of AMP-activated protein kinase activation and glucose transport in contracting slow-twitch muscle. Diabetes 49:1281–1287

Devaskar SU (2001) Neurohumoral regulation of body weight gain. Pediatric Diabetes 2:131–144

Dietrich A, Kalwa H, Storch U, Mederos Y, Schnitzler M, Salanova B, Pinkenburg O, Dubrovska G, Essin K, Gollasch M, Birnbaumer L, Gudermann T (2007) Pressure-induced and store-operated cation influx in vascular smooth muscle cells is independent of TRPC1. Pflügers Arch 455:465–477

Dombrowski L, Roy D, Marcotte B, Marette A (1996) A new procedure for the isolation of plasma membranes, T tubules, and internal membranes from skeletal muscle. Am J Physiol Endocrinol Metab 270:E667–E676

Dossena S, Gandini R, Tamma G, Vezzoli V, Nofziger C, Tamplenizza M, Salvioni E, Bernardinelli E, Meyer G, Valenti G, Wolf-Watz M, Fürst J, Paulmichl M (2011) The molecular and functional interaction between ICln and HSPC038 proteins modulates the regulation of cell volume. J Biol Chem 286:40659–40670

Drews G, Zempel G, Krippeit-Drews P, Britsch S, Busch GL, Kaba NK, Lang F (1998) Ion channels involved in insulin release are activated by osmotic swelling of pancreatic B-cells. Biochim Biophys Acta 1370:8–16

Drews G, Krippeit-Drews P, Düfer M (2010) Electrophysiology of islet cells. Adv Exp Med Biol 654:115–163

Ducret T, Vandebrouck C, Cao ML, Lebacq J, Gailly P (2006) Functional role of store-operated and stretch-activated channels in murine adult skeletal muscle fibres. J Physiol 575:913–924

Düfer M, Haspel D, Krippeit-Drews P, Aguilar-Bryan L, Bryan J, Drews G (2004) Oscillations of membrane potential and cytosolic Ca^{2+} concentration in $SUR1^{-/-}$ beta cells. Diabetologia 47:488–498

Eggermont J, Trouet D, Carton I, Nilius B (2001) Cellular control of volume-regulated anion channels. Cell Biochem Biophys 35:263–274

Franco A Jr, Lansman JB (1990) Stretch-sensitive channels in developing muscle cells from a mouse cell line. J Physiol 427:361–380

Furtado LM, Poon V, Klip A (2003) GLUT4 activation: thoughts on possible mechanisms. Acta Physiol Scand 178:287–296

Goodyear LJ, Chung PY, Sherwood D, Dufresne SD, Moller DE (1996) Effects of exercise and insulin on mitogen-activated protein kinase signaling pathway in rat skeletal muscle. Am J Physiol Endocrinol Metab 271:E403–E408

Grapengiesser E, Gylfe E, Hellman B (1989) Regulation of pH in individual pancreatic β-cells as evaluated by fluorescence ratio microscopy. Biochim Biophys Acta 1014:219–224

Guharay F, Sachs F (1984) Stretch-activated single ion channel currents in tissue-cultured embryonic chick skeletal muscle. J Physiol 352:685–701

Han J, Lee JE, Jin J, Lim JS, Oh N, Kim K, Chang SI, Shibuya M, Kim H, Koh GY (2011) The spatiotemporal development of adipose tissue. Development 138:5027–5037

Hara Y, Wakino S, Tanabe Y, Saito M, Tokuyama H, Washida N, Tatematsu S, Yoshioka K, Homma K, Hasegawa K, Minakuchi H, Fujimura K, Hosoya K, Hayashi K, Nakayama K, Itoh H (2011) Rho and Rho-kinase activity in adipocytes contributes to a vicious cycle in obesity that may involve mechanical stretch. Sci Signal 4:ra3

Hardie DG, Carling D, Carlson M (1998) The AMP-activated/SNF1 protein kinase subfamily: metabolic sensors of the eukaryotic cell? Annu Rev Biochem 67:821–825

Hayashi T, Hirshman MF, Kurth EJ, Winder WW, Goodyear LJ (1998) Evidence for 5' AMP-activated protein kinase mediation of the effect of muscle contraction on glucose transport. Diabetes 47:1369–1373

Henquin JC (1978) D-glucose inhibits potassium efflux from pancreatic islet cells. Nature 271:271–273

Henquin JC (2009) Regulation of insulin secretion: a matter of phase control and amplitude modulation. Diabetologia 52:739–751

Hirafuji M, Machida T, Hamaue N, Minami M (2003). Cardiovascular protective effects of n-3 polyunsaturated fatty acids with special emphasis on docosahexaenoic acid. J Pharmacol Sci 92:308–316

Hisanaga E, Nagasawa M, Ueki K, Kulkarni RN, Mori M, Kojima I (2009) Regulation of calcium-permeable TRPV2 channel by insulin in pancreatic β-cells. Diabetes 58:174–184

Ho RC, Alcazar O, Fujii N, Hirshman MF, Goodyear LJ (2004) p38 g MAPK regulation of glucose transporter expression and glucose uptake in L6 myotubes and mouse skeletal muscle. Am J Physiol Renal Physiol 286:R342–R349

Holloszy JO (2003) A forty-year memoir of research on the regulation of glucose transport into muscle. Am J Physiol Endocrinol Metab 284:E453–E467

Holloszy JO, Narahara HT (1967) Enhanced permeability to sugar associated with muscle contraction: studies of the role of Ca^{+}. J Gen Physiol 50:551–562

Holub DJ, Holub BJ (2004) Omega-3 fatty acids from fish oils and cardiovascular disease. Mol Cell Biochem 263:217–225

Humphries MJ (2000) Integrin structure. Biochem Soc Trans 28:311–339

Ihlemann J, Ploug T, Galbo H (2001) Effect of force development on contraction induced glucose transport in fast twitch rat muscle. Acta Physiol Scan. 171:439–444

Ihlemann J, Ploug T, Hellsten Y, Galbo H (1999) Effect of tension on contraction-induced glucose transport in rat skeletal muscle. Am J Physiol Endocrinol Metab 277:E208–E214

Inou H, Ishiguro N, Sawazaki S, Amma H, Miyazu M, Iwata H, Sokabe M, Naruse K (2002) Uni-axial cyclic stretch induces the activation of transcription factor nuclear factor kappaB in human fibroblast cells. FASEB J 16:405–407

Inoue R, Jian Z, Kawarabayashi Y (2009) Mechanosensitive TRP channels in cardiovascular pathophysiology. Pharmacol Ther 123:371–385

Inoue H, Takahashi N, Okada Y, Konishi M (2010) Volume-sensitive outwardly rectifying chloride channel in white adipocytes from normal and diabetic mice. Am J Physiol Cell Physiol 298:C900–C909

Islam MS (2011) TRP channels of islets. Adv Exp Med Biol 704:811–830

Ito Y, Obara K, Ikeda R, Ishii M, Tanabe Y, Ishikawa T, Nakayama K (2006) Passive stretching produces Akt- and MAPK-dependent augmentations of GLUT4 translocation and glucose uptake in skeletal muscle of mice. Pflügers Arch 451:803–813

Iwata M, Hayakawa K, Murakami T, Naruse K, Kawakami K, Inoue-Miyazu M, Yuge L, Suzuki S (2007) Uniaxial cyclic stretch-stimulated glucose transport is mediated by a Ca^{2+}-dependent mechanism in cultured skeletal muscle cells. Pathobiology 74:159–168

Jaalouk DE, Lammerding J (2009) Mechanotransduction gone awry. Nature Reviews, Molecular Cell Biology 10:63–73 (Focus on mechanotransduction)

Jacobson DA, Philipson LH (2007) TRP channels of the pancreatic beta cell. Handb Exp Pharmacol 179:409–424

Jakab M, Furst J, Gschwentner M, Botta G, Garavaglia ML, Bazzini C, Rodighiero S, Meyer G, Eichmueller S, Woll E, Chwatal S, Ritter M, Paulmichl M (2002) Mechanisms sensing and modulating signals arising from cell swelling. Cell Physiol Biochem 12:235–258

Johansson B, Mellander S (1975) Static and dynamic components in the vascular myogenic response to passive changes in length as revealed by electrical and mechanical recordings from the rat portal vein. Circ Res 36:76–83

Jørgensen SB, Viollet B, Andreelli F, Frøsig C, Birk JB, Schjerling P, Vaulont S, Richter EA, Wojtaszewski JF (2004) Knockout of the α2 but not α1 5'-AMP-activated protein kinase isoform abolishes 5-aminoimidazole-4-carboxamide-1-β-4-ribofuranosidebut not contraction-induced glucose uptake in skeletal muscle. J Biol Chem 279:1070–1079

Kinard TA, Satin LS (1995) An ATP-sensitive Cl^- channel current that is activated by cell swelling, cAMP, and glyburide in insulin-secreting cells. Diabetes 44:1461–1466

Kinard TA, Goforth PB, Tao Q, Abood ME, Teague J, Satin LS (2001) Chloride channels regulate HIT cell volume but cannot fully account for swelling-induced insulin secretion. Diabetes 50:992–1003

Komatsu M, Sato Y, Aizawa T, Hashizume K (2001) K_{ATP} channel-independent glucose action: an elusive pathway in stimulus-secretion coupling of pancreatic β-cell. Endocr J 48:275–288

Kris-Etherton PM, Harris WS, Appel LJ (2002) Fish consumption, fish oil. omega-3 fatty acids, and cardiovascular disease. Circulation 106:2747–2757

Lau KS, Grange RW, Isotani E, Sarelius IH, Kamm KE, Huang PL, Stull JT (2000) nNOS and eNOS modulate cGMP formation and vascular response in contracting fast-twitch skeletal muscle. Physiol. Genomics 2:21–27

Lefer DJ (2002) Statins as potent anti-inflammatory drugs. Circulation 106:2041–2042

Lumeng CN, Saltiel AR (2011) Inflammatory links between obesity and metabolic disease. J Clin Invest 121:2111–2117

Manabe I (2011) Chronic inflammation links cardiovascular, metabolic and renal diseases. Circ J 75:2739–2748

Maroto R, Raso A, Wood TG, Kurosky A, Martinac B, Hamill OP (2005) TRPC1 forms the stretch-activated cation channel in vertebrate cells. Nat Cell Biol 7:179–85

Miley HE, Sheader EA, Brown PD, Best L (1997) Glucose-induced swelling in rat pancreatic β-cells. J Physiol 504:191–198

Mitsumoto Y, Downey GP, Klip A (1992) Stimulation of glucose transport in L6 muscle cells by long-term intermittent stretch-relaxation. FEBS Lett 301:94–98

Miura S, Fujino M, Hanzawa H, Kiya Y, Imaizumi S, Matsuo Y, Tomita S, Uehara Y, Karnik S, Yanagisawa H, Koike H, Komuro I, Saku K (2006) Molecular mechanism underlying inverse agonist of angiotensin II type 1 receptor. J Biol Chem 281:19288–19295

Moncada S, Palmer RM, Higgs EA (1991) Nitric oxide: physiology, pathophysiology, and pharmacology. Pharmacol Rev 43:109–142

Musi N, Hayashi T, Fujii N, Hirshman MF, Witters LA, Goodyear LJ (2001) AMP-activated protein kinase activity and glucose uptake in rat skeletal muscle. Am J Physiol Endcrino Metab 280:E677–E684

Nakayama K, Obara K, Ishikawa T, Nishizawa S (2010) Specific mechanotransduction signaling involved in myogenic responses of the cerebral arteries. In: Kamkin A, Kiseleva I (eds) Mechanosensitivity in cells and tissues. Mechanosensitivity of the heart. Springer, pp 453–481

Newsholme P, Gaudel C, McClenaghan NH (2010) Nutrient regulation of insulin secretion and beta-cell functional integrity. Adv Exp Med Biol 654:91–114

Ni H, Li A, Simonsen N, Wilkins JA (1998) Integrin activation by dithiothreitol or Mn^{2+} induces a ligand-occupied conformation and exposure of a novel NH_2-terminal regulatory site on the beta1 integrin chain. J Biol Chem 273:7981–7987

Nilius B, Owsianik G, Voets T, Peters JA (2007) Transient receptor potential cation channels in disease. Physiol Rev 87:165–217

Nishimura S, Manabe I, Nagasaki M, Hosoya Y, Yamashita H, Fujita H, Ohsugi M, Tobe K, Kadowaki T, Nagai R, Sugiura S (2008) In vivo imaging in mice reveals local cell dynamics and inflammation in obese adipose tissue. J Clin Invest 118:710–721

Obara K, Saito M, Yamanaka A, Uchino M, Nakayama K (2001) Involvement of different activator Ca^{2+} in the rate-dependent stretch-induced contractions of canine basilar artery. Jpn J Physiol 51:327–335

Parton RG, Simons K (2007) The multiple faces of caveolae. Nat Rev Mol Cell Biol 8:185–194

Pilch PF, Souto RP, Liu L, Jedrychowski MP, Berg EA, Costello CE, Gygi SP (2007) Cellular spelunking: exploring adipocyte caveolae. J Lipid Res 48:2103–2111

Rakesh K, Yoo BS, Kim IM, Salazar N, Kim KS, Rockman HA (2010) β-Arrestin-biased aginism of the angiotensin receptor induced by mechanical stress. Sci Signal 3:p. ra46

Rangwala SM, Lazar MA (2000) Transcriptional control of adipogenesis. Annu Rev Nutr 20:535–559

Ravier MA, Nenquin M, Miki T, Seino S, Henquin JC (2009) Glucose controls cytosolic Ca^{2+} and insulin secretion in mouse islets lacking adenosine triphosphate-sensitive K^+ channels owing to a knockout of the pore-forming subunit Kir6.2. Endocrinology 150:33–45

Rose AJ, Kiens B, Richter EA (2006) Ca^{2+}-calmodulin dependent protein kinase expression and signaling in skeletal muscle during exercise. J Physiol 574:889–903

Rosen ED, Spiegelman BM (2000) Molecular regulation of adipogenesis. Annu Rev Cell Dev Biol 16:145–171

Ross RM, Wadley GD, Clark MG, Rattigan S, McConell GK (2007) Local nitric oxide synthase inhibition reduces skeletal muscle glucose uptake but not capillary blood flow during in situ muscle contraction in rats. Diabetes 56:2885–2892

Sandoval DA, Obici S, Seeley RJ (2009) Targting the CNS to treat type 2 diabetes. Nature Rev Drug Discov 8:386–398

Sardini A, Amey JS, Weylandt K-H, Nobles M, Valverde MA, Higgins CF (2003) Cell volume regulation and swelling-activated chloride channels. Biochim Biophys Acta 1618:153–162

Sasamoto A, Nagino M, Kobayashi S, Naruse K, Nimura Y, Sokabe M (2005) Mechanotransduction by integrin is essential for IL-6 secretion from endothelial cell in response to uniaxial continuous stretch. Am J Physiol Cell Physiol 288:C1012–1022

Schupp M, Janke J, Clasen R, Unger T, Kintscher U (2004) Angiotensin type 1 receptor blockers induce peroxisome proliferator–activated receptor-g activity. Circulation 109:2054–2057

Schwander M, Leu M, Stumm M, Dorchies OM, Ruegg UT, Schittny J, Muller U (2003) Beta1 integrins regulate myoblast fusion and sarcomere assembly. Dev Cell 4:673–685

Scott M, Grundy H, Brewer B Jr, Cleeman JI, Smith SC Jr, Lenfant C (2004) Definition of metabolic syndrome: Report of the national heart, lung, and blood institute/American heart association conference on scientific issues related to definition. Circulation 109:433–438

Sekine N, Cirulli V, Regazzi R, Brown LJ, Gine E, Tamarit-Rodriguez J, Girotti M, Marie S, MacDonald MJ, Wollheim CB (1994) Low lactate dehydrogenase and high mitochondrial glycerol phosphate dehydrogenase in pancreatic β-cells. Potential role in nutrient sensing. J Biol Chem 269:4895–4902

Semino MC, Gagliardino AM, Bianchi C, Rebolledo OR, Gagliardino JJ (1990) Early changes in the rat pancreatic B cell size induced by glucose. Acta Anat (Basel) 138:293–296

Shepherd RM, Henquin JC (1995) The role of metabolism, cytoplasmic Ca^{2+}, and pH-regulating exchangers in glucose-induced rise of cytoplasmic pH in normal mouse pancreatic islets. J Biol Chem 270:7915–7921

Shoham N, Gottlieb R, Sharabani-Yosef O, Zaretsky U, Benayahu D, Gefen A (2012) Static mechanical stretching accelerates lipid production in 3T3-L1 adipocytes by activating the MEK signaling pathway. Am J Physiol Cell Physiol 302:C429–C441

Silvagno F, Xia H, Bredt DS (1996) Neuronal nitric-oxide synthase-mu, an alternatively spliced isoform expressed in differentiated skeletal muscle. J Biol Chem 271:11204–11208

Soderling TR (1999) The Ca-calmodulin-dependent protein kinase cascade. Trend Biochem. Sci 24:232–236

Somwar R, Perreault M, Kapur S, Taha C, Sweeney G, Ramlal T, Kim DY, Keen J, Côte CH, Klip A, Marette A (2000) Activation of p38 mitogen-activated protein kinase alpha and beta by insulin and contraction in rat skeletal muscle: potential role in the stimulation of glucose transport. Diabetes 49:1794–1088

Somwar R, Koterski S, Sweeney G, Sciotti R, Djuric S, Berg C, Trevillyan J, Scherer PE, Rondinone CM, Klip A (2002) A dominant-negative p38 MAPK mutant and novel selective inhibitors of p38 MAPK reduce insulin-stimulated glucose uptake in 3T3-L1 adipocytes without affecting GLUT4 translocation. J Biol Chem 277:50386–50395

Spangenburg EE, McBride TA (2006) Inhibition of stretch-activated channels during eccentric muscle contraction attenuates p70S6 K activation. J Appl Physiol 100:129–135

Straub SG, Sharp GW (2002) Glucose-stimulated signaling pathways in biphasic insulin secretion. Diabetes Metab Res Rev 18:451–463

Straus DS, Glass CK (2007) Anti-inflammatory actions of PPAR ligands: new insights on cellular and molecular mechanisms. Trends Immunol 28:551–558

Sumi M, Kiuchi K, Ishikawa T, Ishii A, Hagiwara M, Nagatsu T, Hidaka H (1991) The newly synthesized selective Ca^{2+}/calmodulin dependent protein kinase II inhibitor KN-93 reduces dopamine contents in PC12h cells. Biochem Biophys Res Commun 181:963–975

Takii M, Ishikawa T, Tsuda H, Kanatani K, Sunouchi T, Kaneko Y, Nakayama K (2006) Involvement of stretch-activated cation channels in hypotonically induced insulin secretion in rat pancreatic β-cells. Am J Physiol Cell Physiol 291:C1405–C1411

Tanabe Y, Koga M, Saito M, Matsunaga Y, Nakayama K (2004) Inhibition of adipocyte differentiation by mechanical stretching through ERK-mediated downregulation of PPARγ2. J Cell Sci 117:3605–3614

Tanabe Y, Matsunaga Y, Saito M, Nakayama K (2008) Involvement of cyclooxygenase-2 in synergistic effect of cyclic stretching and eicosapentaenoic acid on adipocyte differentiation. J Pharmacol Sci 106:478–484

Taskinen P, Ruskoaho H (1996) Stretch-induced increase in atrial natriuretic peptide secretion is blocked by thapsigargin. Eur J Pharmacol 308:295–300

Tibbles LA, Woodgett JR (1999) Review The stress-activated protein kinase pathways. Cell Mol Life Sci 55:1230–1254

Tidball JG, Lavergne E, Lau KS, Spencer MJ, Stull JT, Wehling M (1998) Mechanical loading regulates NOS expression and activity in developing and adult skeletal muscle. Am J Physiol 275:C260–C266

Voets, T, Nilius B (2009) TRPCs, GPCRs and the Bayliss effect. EMBO J 28:4–5

Wang JG, Miyazu M, Matsushita E, Sokabe M, Naruse K (2001) Uniaxial cyclic stretch induces focal adhesion kinase (FAK) tyrosine phosphorylation followed by mitogen-activated protein kinase (MAPK) activation. Biochem Biophys Res Commun 288:356–361

Wijesekara N, Tung A, Thong F, Klip A (2006) Muscle cell depolarization induces a gain in surface GLUT4 via reduced endocytosis independently of AMPK. Am J Physiol Endocrinol Metab 290:E1276–E1286

Wojtaszewski JFP, Nielsen P, Hansen BF, Richter EA, Kiens B (2000) Isoform-specific and exercise intensity-dependent activation of 5'-AMP-activated protein kinase in human skeletal muscle. J Physiol 528:221–226

Wright DC, Hucker KH, Holloszy JO, Han DH (2004) Ca^{2+} and AMPK both mediate stimulation of glucose transport by muscle contractions. Diabetes 53:330–335

Yamboliev IA, Hedges JC, Jack LM, Mutnick JLM, Adam LP, Gerthoffer WT (2000) Evidence for modulation of smooth muscle forceby the p38 MAP kinase/HSP27 pathway. Am J Physiol Heart Circ Physiol 278:H1899–H1907

Yasuda N, Miura S, Akazawa H, Tanaka T, Qin Y, Kiya Y, Imaizumi S, Fujino M, Ito K, Zou Y, Fukuhara S, Kunimoto S, Fukuzai K, Sato T, Ge J, Mochizuki N, Nakaya H, Saku K, Komuro I (2008) Conformational switch of angiotensin II type 1 receptor underlying mechanical stress-induced activation. EMBO Rep 9:179–186

Zanchi NE, Lancha AH Jr (2008) Mechanical stimuli of skeletal muscle: implications on mTOR/p70s6k and protein synthesis. Eur J Appl Physiol 102:253–263

Zhang JS, Kraus WE, Truskey GA (2004) Stretch-induced nitric oxide modulates mechanical properties of skeletal muscle cells. Am J Physiol Cell Physiol 287:C292–C299

Zhang LL, Liu D Y, Ma LQ, Luo ZD, Cao TB, Zhong J, Yan ZC, Wang LJ, Zhao ZG, Zhu SJ, Schrader M, Thilo F, Zhu MZ, Tepel M (2007) Activation of transient receptor potential vanilloid type-1 channel prevents adipogenesis and obesity. Circ Res 100:1063–1070

Zhao C, Wilson MC, Schuit F, Halestrap AP, Rutter GA (2001) Expression and distribution of lactate/monocarboxylate transporter isoforms in pancreatic islets and the exocrine pancreas. Diabetes 50:361–366

Zou Y, Akazawa H, Qin Y, Sano M, Takano H, Minamino T, Makita N, Iwanaga K, Zhu W, Kudoh S, Toko H, Tamura K, Kihara M, Nagai T, Fukamizu A, Umemura S, Iiri T, Fujita T, Komuro I (2004) Mechanical stress activates angiotensin II type 1 receptor without the involvement of angiotensin II. Nat Cell Biol 6:499–506

Chapter 15
The Role of the Primary Cilium in Chondrocyte Response to Mechanical Loading

Angus K. T. Wann, Clare Thompson and Martin M. Knight

15.1 Introduction

All cells experience external mechanical forces whether it is compression, tension, fluid shear, hydrostatic pressure or a combination of these. Mechanical signals are converted to biochemical and structural changes within the cell through a process of mechanotransduction which ultimately regulates cell function. Indeed this process of mechanotransduction and response to mechanical environment is fundamental to many aspects of cell behaviour including stem cell differentiation, cell polarity and developmental tissue patterning, tissue homeostasis and response to injury. However the fundamental mechanotransduction pathways and how they are specialised for different cell types and associated biomechanical environments, is as yet unclear. Emerging into this context is the primary cilium, a hitherto under-rated and ignored cellular structure whose function and importance are only just being recognised. In the 70s and 80s, pioneering studies by Jensen, Poole and others, described the structure of the primary cilium in a variety of tissues (Albrecht-Buehler and Bushnell 1980; Jensen et al. 1979; Poole et al. 1985, 1997). However it took another 30 years before the primary cilium began to be recognised as an organelle of fundamental importance for cell and tissue function and pathology. It is now acknowledged that the primary cilium plays a central role in processes that include cell fate and development, cell cycle regulation, chemosensation and cell migration (Gerdes et al. 2009). Of particular relevance to this book is the finding that primary cilia function as mechanoreceptors in an increasing range of cell types. In this chapter we explore the role of the chondrocyte primary cilium in responding to the complex and demanding mechanical environment which is so critical to articular cartilage homeostasis and function.

M. M. Knight (✉) · A. K. T. Wann · C. Thompson
Institute of Bioengineering, School of Engineering and Materials Science,
Queen Mary University of London, Mile End Rd, E1 4NS, London, UK
e-mail: m.m.knight@qmul.ac.uk

A. Kamkin, I. Lozinsky (eds.), *Mechanically Gated Channels and their Regulation,*
Mechanosensitivity in Cells and Tissues 6,
DOI 10.1007/978-94-007-5073-9_15,

15.2 The Structure of the Primary Cilium

The primary cilium is a specialized membranous projection or compartment with a unique framework of microtubules made of acetylated α-tubulin. Unlike motile cilia such as those found on the airway epithelium, there is only one primary cilium per cell. The primary cilium consists of an axoneme that extends out from the basal body which is a modified form of the more mature of the two centrioles. The axoneme exhibits what is described as a "9 + 0" microtubule structure possessing nine outer doublet microtubules arranged around a central core as shown in Fig. 15.1. This structure differs from that of motile cilia which exhibit a "9 + 2" structure comprising the same 9 doublet microtubules as the primary cilium but with an additional central pair which helps to confer motility on these cilia. The ciliary axoneme is ensheathed in a lipid bilayer, the ciliary membrane, which is contiguous with the plasma membrane but has a distinct composition of membrane proteins (Ostrowski et al. 2002; Teilmann et al. 2005; Teilmann and Christensen 2005). A region at the base of the cilium called the ciliary necklace separates these two membrane compartments (Gilula and Satir 1972).

Ciliogenesis, the formation of a cilium, is intrinsically linked with the cell cycle. In proliferating cells cilia assembly typically occurs during G_1 whilst cilia resorption and disassembly occurs upon entry into the cell cycle prior to mitosis (Christensen et al. 2008; Kim et al. 2011; Li et al. 2011; Pan and Snell 2007; Robert et al. 2007). Upon exiting mitosis the mother-centriole dissociates from the core of the mitotic spindle to become the basal body. The basal body moves to the cell surface, associating with golgi-derived vesicles en-route, and docks at an actin-rich assembly site where it nucleates outgrowth of ciliary microtubules (Dawe et al. 2007). Electron microscopy has identified several cilia structures that support the basal body in its role not only as an anchor for the cilium, but also as a gatekeeper of protein import and export. These include the striated rootlet (Hagiwara et al. 1997), distal and sub-distal appendages (Ringo 1967) and transition zone fibres (Anderson 1972). The latter, in particular, forms a region at the base of the cilium called the transition zone which contains several protein complexes that regulate selective import and transport of ciliary proteins (Garcia-Gonzalo et al. 2011; Williams et al. 2011). This occurs in a cell type-specific manner, thus controlling the protein composition of the cilium and potentially enabling cilia structure and function to be specialised in different cell types. Thus in virtually every tissue, a set of specific receptors becomes Localised or localized to the ciliary membrane which are adapted to detect particular environmental signals.

The process of intraflagellar transport (IFT) is responsible for building and maintaining the structure of the primary cilium, as shown schematically in Fig. 15.2 (Berbari et al. 2009; Haycraft et al. 2007; Huangfu and Anderson 2005; Pazour and Witman 2003). IFT is the bidirectional transport of raft-like transport modules, IFT particles, along the length of the cilium (Davenport and Yoder 2005; Haycraft and Serra 2008). Assembly of IFT particles occurs at the base of the cilium such that proteins, including the structural protein tubulin, are transported in the antereograde

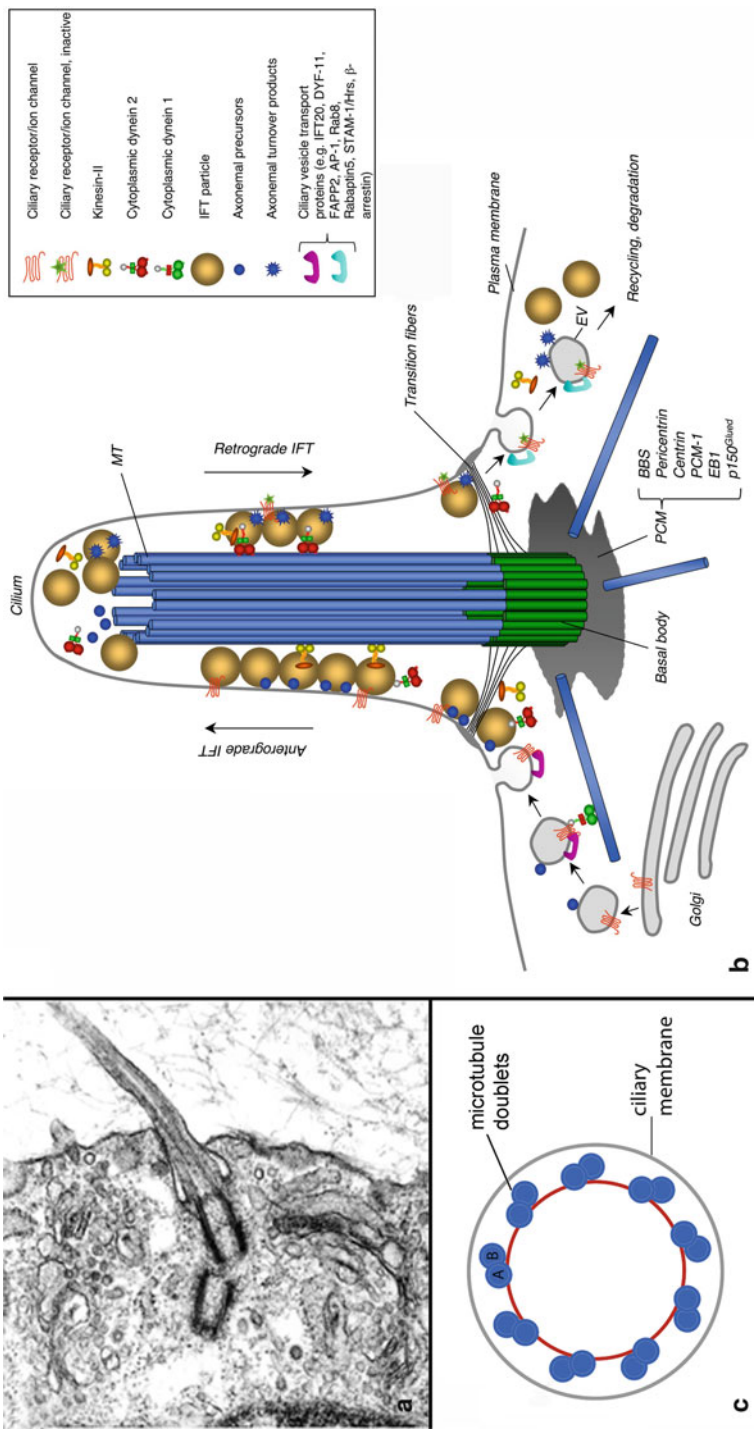

Fig. 15.1 The primary cilium. **a** TEM image showing the primary cilium for a chondrocyte within articular cartilage (Reproduced with permission from CA Poole). **b** Schematic diagram showing the structure of the primary cilium and the mechanism of assembly and disassembly via intraflagellar transport. (Based on figure from Pedersen and Rosenbaum, and reproduced with permission (Pedersen and Rosenbaum, 2008)). **c** Schematic cross section of the primary cilium showing the characteristic '9 + 0' formation of microtubule doublets

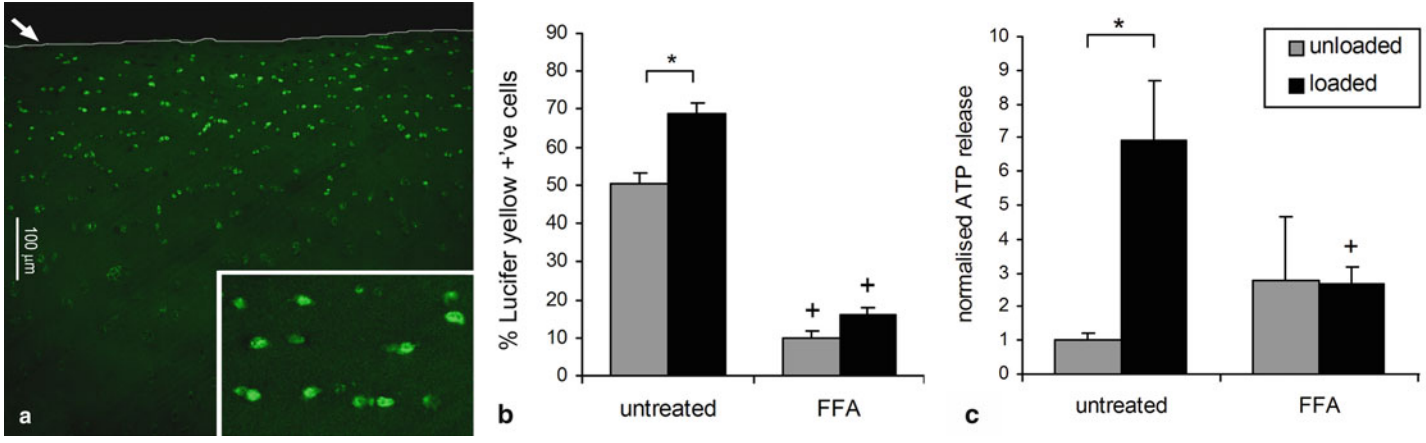

Fig. 15.2 Chondrocytes express hemichannels which open to release ATP upon mechanical stimulation. **a** Confocal immunofluorescence showing the expression of the hemichannel protein, connexin 43, in human articular cartilage. Inset shows higher magnification. Adapted from (Knight et al. 2009). **b** Hemichannel opening in response to mechanical loading as shown by the percentage of Lucifer yellow cells in unloaded and loaded chondrocyte-agarose constructs. Lucifer yellow uptake was blocked by the hemichannel inhibitor, flufenamic acid (*FFA*) confirming the specificity of the Lucifer yellow assay. **c** Mechanical loading activates ATP release measured in the culture media following a 1hour period of cyclic loading. The release of ATP was blocked by the hemichannel inhibitor, flufenamic acid (*FFA*). (Adapted from (Garcia and Knight 2010))

direction to the tip of the cilium, where they become fully assembled and correctly localized (Qin et al. 2004). Antereograde transport is driven by the Kinesin II motor complex which is composed of three subunits; KIF3A, KIF3B and KAP (Davenport and Yoder 2005). Once at the tip Kinesin II is inactivated, this facilitates both cargo release and return of the raft to the base of the cilium- a process driven by cytoplasmic dyenin 1b (Krock et al. 2009; Perrone et al. 2003; Schafer et al. 2003).

Ciliary tubulin undergoes several highly conserved post-translational modifications which include; detyrosination, glutamylation, glycylation and acetylation (Verhey and Gaertig 2007; Westermann and Weber 2003). Such modifications function to stabilize the axonemal microtubules and can be used to visualize the cilium with immunocytochemistry as they are more abundant than elsewhere in the cell (Jensen et al. 2004). Despite these modifications the cilium remains a highly dynamic structure. Assembly continually occurs at the axonemal tip, but once a set length is reached, the cilium does not extend further as microtubule assembly is balanced by simultaneous disassembly. Microtubule disassembly is an active process and several mechanisms for how this occurs have been identified (Cao et al. 2009; Pugacheva et al. 2007; Prodromou et al. 2012).

15.3 The Primary Cilium as a Mechanosensor

Mechanotransduction is the process by which mechanical force or associated deformation or strain is translated into a cellular response (for review see Farge 2011; Kolahi and Mofrad 2010; Schwartz 2010; Schwartz and DeSimone 2008; Shivashankar 2011). The mechanisms and signalling pathways involved appear to depend on the cell type and the precise nature of the mechanical environment. Even within a single cell type different loading modalities, durations, magnitudes and rates elicit a variety of cellular responses. Consequently a plethora of mechanotransduction and mechanosensitive processes have been identified with associated interplay and redundancy within these pathways. However, the primary cilium has emerged as a putative mechanotransducer involved in mechanotransduction in a variety of cell types. In particular the primary cilium has been identified as a flow sensor in osteocytes, vasculature endothelium and kidney tubular epithelia (Lu et al. 2008; Malone et al. 2007; Nauli et al. 2011; Praetorius and Spring 2003). Studies suggest that flow rate-dependent deflection of the cilium initiates a signalling cascade involving the polycystin ion channel complex on the axoneme and related intracellular calcium signalling (Lu et al. 2008; Nauli et al. 2003; Praetorius and Spring 2001). In bone, it is suggested that loading initiates fluid flow through the canaliculae which is detected by deflection of the primary cilia present on the osteocytes (Malone et al. 2007). This mechanotransduction process regulates bone resorption and formation which underpins bone mechanoregulation as defined by Wolff's Law and the Mechanostat principal (Frost 1987).

15.4 Cartilage Mechanotransduction

Articular cartilage is the specialised soft tissue that covers the articulating surfaces within synovial joints where it functions to reduce stress to the underlying bone and to provide a low friction, low wear weight-bearing surface. As such, articular cartilage is subjected to a demanding and complex mechanical environment, consisting of compressive and shear strain, hydrostatic pressure and fluid flow. This mechanical loading environment is critical to the health and homeostasis of the tissue maintaining the balance between synthesis and catabolism of the extracellular matrix which provides the tissue with its mechanical functionality. It is well established that mechanical loading regulates matrix synthesis and composition based on *in vivo* studies and those using cartilage explants or isolated cells *in vitro*. Furthermore removal of this physiological loading or exposure to excessive loading is linked to cartilage degradation and association pathologies such as osteoarthritis. In addition, cartilage development and patterning is also dependent on transduction of appropriate mechanical forces.

The chondrocyte is the only cell type within articular cartilage and is responsible for detecting the mechanical environment and regulating the composition, structure and function of the extracellular matrix. In particular this is achieved by mechanoregulation of the synthesis of extracellular matrix proteins, such as collagen II and the proteoglycan aggrecan, as well as proteases, such as ADAMTS5 and MMP13, which breakdown the matrix. Although chondrocyte mechanotransduction is clearly of immense importance in cartilage physiology, the mechanisms involved are unclear.

Extensive studies suggest that chondrocytes respond to a wide range of physiological mechanical stimuli including cell deformation, fluid shear, hydrostatic pressure, and associated physicochemical changes such as electrical streaming potentials, pH and osmolarity (for review see Urban, 1994). However the mechanotransduction pathways involved are less well defined. Studies indicate that mechanical loading may initiate downstream changes in cell function through the activation of intracellular calcium signalling pathways (D'Andrea et al. 2000; Edlich et al. 2004; Edlich et al. 2001; Erickson et al. 2001; Guilak et al. 1999; Kono et al. 2006; Mizuno, 2005; Ohashi et al. 2006; Pingguan-Murphy et al. 2005; Roberts et al. 2001; Wilkins et al. 2003). More recently, our group, and others, have reported that chondrocytes subjected to mechanical loading release ATP (Garcia and Knight 2010; Millward-Sadler and Salter 2004) which activates P2 purine receptors leading to global calcium transients (Pingguan-Murphy et al. 2006, 2005). Until recently the mechanosensitive mechanism of ATP release in chondrocytes was unknown. In all cell types there is still debate about the physiological transport mechanisms that facilitate ATP release with three putative mechanisms namely; anion channels, connexin hemichannels and exocytosis of ATP-filled vesicles. Studies from our group have now established that chondrocytes express connexin 43 hemichannels (Fig. 15.2a) and that cyclic compression opens these hemichannels as shown by the uptake of Lucifer Yellow which is blocked by the inhibitor flufenamic acid (Fig. 15.2b). Furthermore the mechanically induced opening of the hemichannels facilitates the release of ATP as

confirmed by inhibition with flufenamic acid (Fig. 15.2c). Chondrocytes express the apparatus for the reception of the extracellular ATP in the form of a selection of P2X and P2Y receptors (Knight et al. 2009) such that blocking of these receptors prevents mechanically activated calcium signalling (Pingguan-Murphy et al. 2006). Furthermore we have also shown that this purinergic mechanotransduction ATP-calcium pathway is responsible for the characteristic compression induced up-regulation of proteoglycan synthesis in articular chondrocytes (Chowdhury and Knight 2006).

15.5 The Role of the Chondrocyte Primary Cilium in Mechanotransduction

The chondrocyte primary cilium has been postulated to play a role in cartilage tissue homeostasis and development (Kaushik et al. 2009; McGlashan et al. 2007). However it is only very recently that studies have shown for the first time that the primary cilium is involved in chondrocyte mechanotransduction (Wann et al. 2012). These studies from Knight's group at Queen Mary University of London in collaboration with Poole and McGlashan in New Zealand used immortalized chondrocytes from Wild-type (WT) and *Tg737* Oak Ridge Polycystic Kidney (ORPK) mice provided by collaboration with Haycraft at Medical University of South Carolina. Hypomorphic allele mutation of the *Tg737* gene (IFT88) disrupts polaris expression, interrupting ciliogenesis and resulting in severely stunted or absent primary cilia (Fig. 15.3a). ORPK chondrocytes did not exhibit the classic compression-induced calcium transients induced in WT cells subjected to compressive loading (Fig. 15.3c, d, e). However, interestingly ORPK cells did respond to load with increased release of ATP (Fig. 15.3e). Thus the absence of mechanically induced calcium signalling in ORPK cells without a primary cilium is not caused by the loss of mechanically activated ATP release. Instead the primary cilium appears to regulate mechanotransduction downstream of the initial connexin mediated release of ATP.

Studies also examined whether the disruption of the mechanotransduction pathway in ORPK cells influenced extracellular matrix synthesis (Wann et al. 2012). Indeed, whilst chondrocytes derived from wild type mice showed a characteristic mechanically-induced up-regulation of proteoglycan synthesis, no such mechanosensitive regulation of matrix synthesis at gene or protein level was seen in ORPK cells (Fig. 15.4). Thus these studies reveal that the primary cilium is essential for chondrocyte mechanotransduction via ATP induced calcium signalling (Wann et al. 2012). However, in contrast to separate cilia-mediated mechanotransduction pathways in other cell types (Malone et al. 2007; Masyuk et al. 2006; Praetorius and Spring 2001), it is the connexin hemichannels, independent of the chondrocyte primary cilium, that function as the initial mechanoreceptors. Interestingly, the fact that the primary cilium is essential for both purinergic signalling and transduction of extracellular ATP into intracellular calcium transients, suggests that the cilium may be involved in cell physiology beyond mechanotransduction.

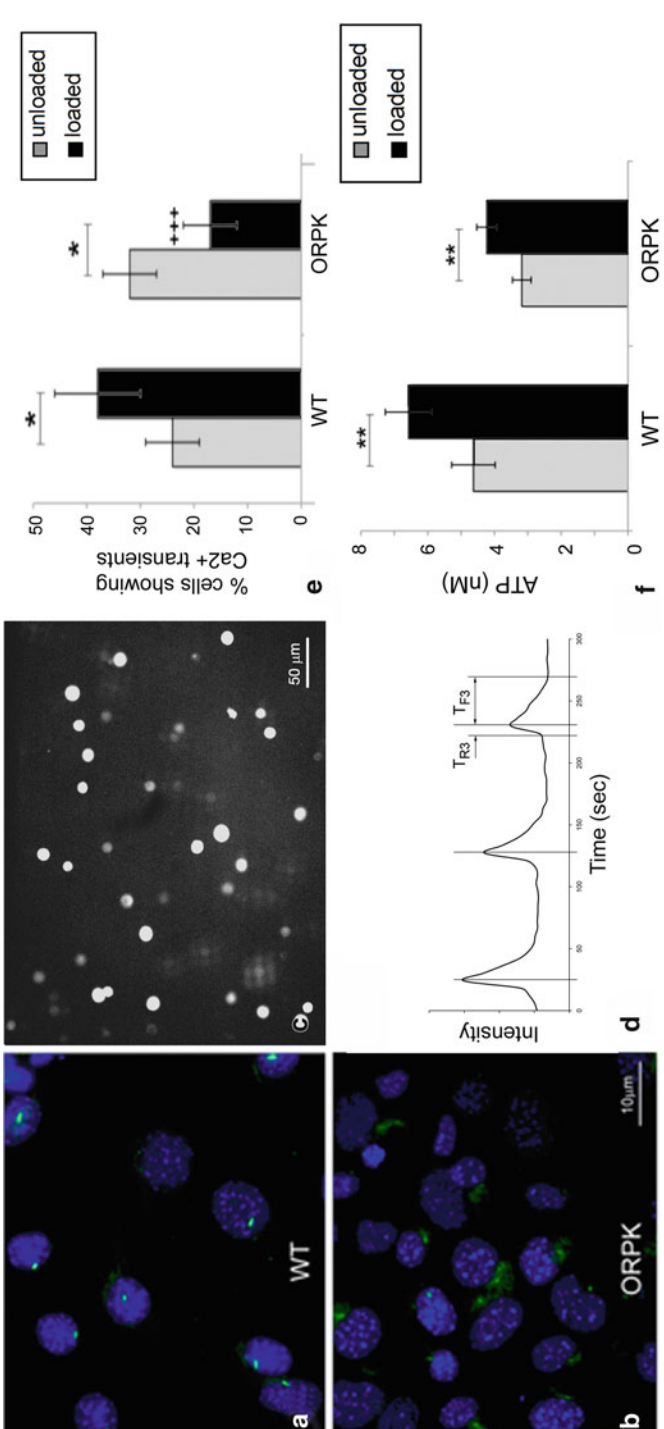

Fig. 15.3 Loss of primary cilia disrupts mechanically induced calcium signalling but does not influence mechanically induced ATP release. **a** Confocal immunofluorescence showing the presence of primary cilia labelled with acetylated α-tubulin (*green*) in wild type (*WT*) chondrocytes cultured in monolayer. Nuclei labelled with DAPI (*blue*). **b** Primary cilia are absent from ORPK chondrocytes which lack IFT88. **c** A single image from a confocal time series showing isolated chondrocytes in agarose labelled with the intracellular calcium indicator Fluo4-AM. **d** Typical intracellular calcium transients within a single chondrocyte quantified by measuring temporal changes in Fluo4 intensity. **e** Cyclic compressive loading of chondrocytes in agarose constructs significantly increases the percentage of cells showing calcium transients in WT chondrocytes ($p < 0.05$). By contrast, in ORPK cells loading produces a significant reduction in the percentage of cells showing calcium transients ($p < 0.05$). **f** Compressive loading also up-regulates the release of ATP in both WT and ORPK chondrocytes ($p < 0.01$). Cumulative ATP release was measured in the culture media surrounding an individual construct after a 1 h loading period or equivalent unloaded control. (Adapted from (Wann et al. 2012))

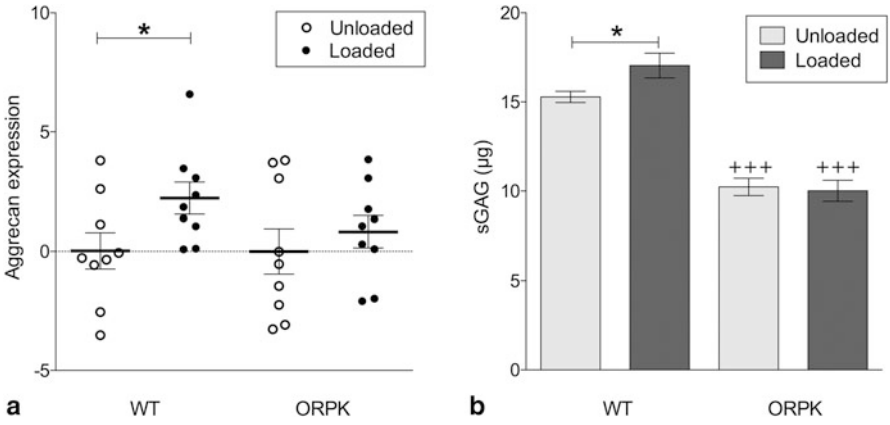

Fig. 15.4 Primary cilia are required for mechanosensitive up-regulation of extracellular matrix synthesis in chondrocytes. **a** Compressive loading of chondrocytes in agarose significantly up-regulates aggrecan gene expression for WT chondrocytes ($p < 0.05$) but not ORPK chondrocytes which lack a primary cilium. Gene expression was measured by qPCR following 1 h cyclic compression. **b** Compressive loading of WT chondrocytes in agarose stimulates synthesis of sulphated glycosaminoglycan (*sGAG*) measured after a 24 period of cyclic compression ($p < 0.05$). By contrast ORPK cells in agarose exhibit significantly reduced levels of sGAG synthesis compared to WT cells ($p < 0.001$) and a complete absence of any mechanosensitive changes in sGAG synthesis. (Adapted from (Wann et al. 2012))

15.6 Hedgehog Signalling and Other Cilia-Mediated Pathways

In addition to mechanotransduction, primary cilia are also involved in a variety of other signalling pathways. Loss of cilia, or cilia dysfunction has been linked to a series of related genetic disorders such as Bardet Biedel Syndrome and Polycystic Kidney Disease, which are collectively termed ciliopathies (for review see (Waters and Beales 2011)). In addition to defects in cell cycle regulation and mechanotransduction, these ciliopathies have helped to identify a number of other fundamental signalling pathways which are dependent upon a fully functioning primary cilium. Interestingly, emerging evidence suggests that many of these pathways are themselves mechanosensitive.

Common characteristics of ciliopathies include skeletal patterning defects such as polydactyly, and abnormalities of the central nervous system, both of which are indicative of defects in Hedgehog (Hh) signalling. Hh signalling is crucial for embryonic development and regulates the morphogenesis of a variety of tissues and organs (Athar et al. 2006; Ehlen et al. 2006; King et al. 2008; Nagase et al. 2008). The Hh receptor, Patched localizes to the primary cilium and maintains the pathway in an 'OFF state' through the inhibition of a second transmembrane protein, Smoothened (Rohatgi et al. 2007). In vertebrates, Patched not only inhibits Smoothened activation, but also its localization in the cilium (Rohatgi et al. 2007). Smoothened regulates the processing of a family of bi-functional transcription factors called Gli proteins. In the absence of Hh ligands full-length Gli activators are processed to their truncated repressor forms, this is suggested to take place within the cilium and is dependent

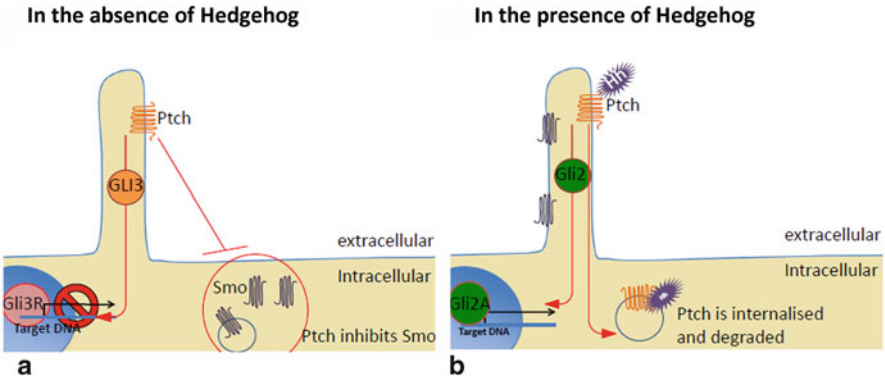

Fig. 15.5 Schematic diagram showing a simplified overview of the Hedgehog signalling pathway. **a** In the absence of Hedgehog (*Hh*) ligands the hedgehog receptor Patched (*Ptch*) localises to the primary cilium where it inhibits the function of Smoothened (*Smo*). Smo is held in an inactive conformation and prevented from entering the cilium, the mechanism by which this is achieved is unclear. Smo regulates the processing of a family of bifunctional transcription factors called Gli proteins. As a consequence of Smo inhibition, Gli transcription factors are either degraded or processed to their repressor forms (Gli3R) within the cilium resulting in the repression of Hh target genes. **b** When Hedgehog (*Hh*) ligands bind to Ptch, the receptor is internalised and targeted for proteasomal degradation releasing the inhibition on Smo. Smo undergoes an activating conformational change and enters the cilium where it inhibits the degradation and processing of Gli transcription factors, and promotes formation of Gli activators (Gli2A) and thus gene transcription. Several additional components are required for this signalling pathway such as Supressor of fused (*SuFu*), KIF7 and Rab23 (not shown) for review see. (Cohen 2010)

upon components of the IFT machinery (Haycraft et al. 2005; May et al. 2005). When Hh ligands bind to Patched, Smoothened inhibition is released. Smoothened then translocates to the primary cilium where it inhibits Gli processing, allowing full length Gli activators to move to the nucleus where they activate the expression of Hh-regulated genes (Day and Yang 2008; Huangfu and Anderson 2005; Huangfu et al. 2003; Milenkovic et al. 2009; Rohatgi et al. 2007; Varjosalo and Taipale 2008; Veland et al. 2009). The Hh signalling pathway described above is shown schematically in Fig. 15.5 and reviewed by Wong et al (Wong and Reiter 2008).

The cilium also houses other signalling pathway components important to both development and homeostasis. These include receptor tyrosine kinases (Christensen et al. 2012) and the PDGF receptor (PDGFR), which is trafficked into the cilium in growth arrested cells (Schneider et al. 2005). Ligand-dependent activation of PDGFR is followed by Akt activation and activation of the Mek1/2-Erk1/2 pathways, with Mek1/2 being phosphorylated within the cilium and at the basal body (Schneider et al. 2005) which ultimately regulates cell cycle progression and cellular migration via NHE-1 (Christensen et al. 2008; Jones et al. 2012; Kim et al. 2011; Schneider et al. 2010).

Non-canonical wnt signalling also takes places on the cilium resulting in the breakdown of β-catenin and the inhibition of wnt target genes (Corbit et al. 2008). For review of the interaction between the primary cilium and the wnt signalling pathway

see Gerdes et al (Gerdes and Katsanis 2008). The signalling of polycystin 1 and 2 is another cilia-dependent pathway thought to converge on many downstream effectors including STAT1, P100, beta catenin and intracellular calcium stores (Dalagiorgou et al. 2010; Kim et al. 1999; Lal et al. 2008; Low et al. 2006; Nauli et al. 2003; Pazour et al. 2002; Praetorius and Spring 2001). Furthermore, in some cell types certain signalling proteins are specifically localised to the ciliary axoneme suggesting that the primary cilium is critical in these signalling pathways. Examples of these ciliary signalling proteins include somatostatin receptors in neurons (Handel et al. 1999) and adenylate cylclase isoforms in neurons, osteocytes and synovial fibroblasts (Bishop et al. 2007; Malone et al. 2007; Ou et al. 2009).

15.7 Mechanoregulation of Hedgehog Signalling in Chondrocytes

In cartilage, Indian hedgehog (Ihh) is the major hedgehog protein regulating chondrocyte proliferation and differentiation during skeletal development. Ihh is essential for endochondral ossification which is the predominant mechanism of bone formation (for review see (Ehlen et al. 2006)).

In 2001, Wu et al demonstrated a novel function for Ihh in cartilage, as a mechanotransduction mediator (Wu et al. 2001). Using cyclic compression of isolated embryonic sternal chondrocytes in 3D-culture, they determined Ihh gene expression was induced by mechanical stress. Ihh induction was sensitive to the stretch-activated ion channel blocker gadolinium and stimulated chondrocyte proliferation via the induction of BMP2/4 (Wu et al. 2001). The mechanoregulation of Ihh expression appears to be under the control of specific mechanosensitive microRNAs (Guan et al. 2011) and is influenced by the presence of the oligomeric extracellular matrix proteins, matrillins (Kanbe et al. 2007; Le et al. 2001). Consequent elimination of functional matrillins in the chondrocyte pericellular matrix abrogates mechanical activation of Hh signalling (Kanbe et al. 2007). The classification of Ihh as a 'mechanosensitive' gene has been further strengthened by studies in the avian embryonic limb (Nowlan et al. 2008). Nowlan et al. compared the in vivo gene expression pattern of Ihh with patterns of biophysical stimuli induced by embryonic muscle contraction (Nowlan et al. 2008a, b). These studies revealed the expression pattern of Ihh colocalises with regions of high strain and fluid velocity and that this colocalisation is disrupted in limbs immobilised with the neuromuscular blocking agent decamethonium bromide (Nowlan et al. 2008). The rat tempromandibular joint (*TMJ*) has been used to investigate the function of mechanosensitive of Ihh expression in vivo during post-natal development (hjTang et al. 2004; Rabie and Al-Kalaly 2008). Mechanical stress to the TMJ induces Ihh gene expression within the proliferative layer of the condylar cartilage growth plate (hjTang et al. 2004), expression increases with greater loading (Ng et al. 2006; Rabie and Al-Kalaly 2008). Ihh expression is associated with increased proliferation of chondroprogenitor cells resulting in increased cartilage growth (hjTang et al. 2004; Ng et al. 2006).

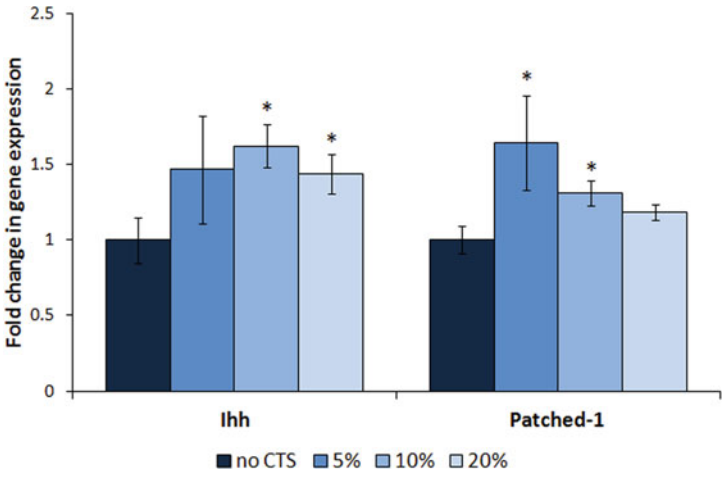

Fig. 15.6 Cyclic tensile strain upregulates Ihh gene expression and activates hedgehog signalling in adult articular chondrocytes. The expression of Ihh is significantly increased in chondrocytes subjected to cyclic tensile strain (*CTS*) at 5, 10 and 20 % strain compared to no CTS controls ($p < 0.05$). Gene expression was measured by qPCR following 1 h CTS. Changes in Patched1 gene expression were monitored as a measure of hedgehog pathway activation. Patched1 gene expression was significantly increased by 5 and 10 % CTS compared to no CTS controls ($p < 0.05$), however no significant changes were observed at 20 % strain indicating the pathway is not activated by this regime

The function of Ihh in adult cartilage is poorly understood. Current studies from the authors based at Queen Mary, London, have shown Ihh expression is also mechanosensitive in bovine articular chondrocytes isolated from adult tissue and subjected to cyclic tensile strain, which leads to strain-dependent Hh pathway activation (Fig. 15.6). The magnitude of Ihh gene expression is much lower than previously reported (Shao et al. 2011; Wu et al. 2001). This difference potentially arises due to the use of adult articular chondrocytes rather than chondrocytes isolated from embryonic chick sterna (Wu et al. 2001) or rat cartilage growth plates (Shao et al. 2011), as used in previous studies. It is also unlikely that chondrocytes in these different animals and different locations will be exposed to the same mechanical environment and may have adapted their responses accordingly.

Recent studies explore the role of the primary cilium in loading-induced Ihh signalling. Chondrocyte-specific ablation of *kif3a*, a component of the kinesin II IFT motor complex, using Col2a-Cre-mediated recombination, results in a loss of primary cilia in the post-natal murine TMJ (Kinumatsu et al. 2011). Loss of primary cilia in condylar cartilage results in abnormal hedgehog signalling producing defects in chondrocyte maturation, intramembranous bone formation, and chondrogenic condylar growth (Kinumatsu et al. 2011). Similarly, *in vitro* studies using rat growth plate chondrocytes demonstrate hedgehog signal transduction in response to hydrostatic pressure requires a fully functioning primary cilium (Shao et al. 2011). A role for the primary cilium in the maintenance of articular cartilage has also recently been demonstrated using the *Tg737*^{orpk} mouse (Ift88-deficient, see above) (Chang

et al. 2012). Mutant articular cartilage was thicker with a reduced overall stiffness and was consequently more prone to the development of osteoarthritis. Hh signalling was increased in the cartilage of ORPK mice, a phenomenon previously reported in osteoarthritis (Lin et al. 2009). This increase in Hh signalling was proposed to occur due to reduced cilia-mediated repression of the Hh signal (Chang et al. 2012).

Cartilage is not the only tissue in which the expression of Hh proteins is mechanically regulated. In vascular smooth muscle, strain produced a reduction in the expression of sonic hedgehog (Shh), another member of the Hedgehog protein family (Varjosalo and Taipale 2008). This resulted in decreased expression of several components of the hedgehog signalling pathway leading to increased apoptosis and reductions in cell number which could be rescued by addition of recombinant Shh (Morrow et al. 2007). This study implies there may be tissue-specific mechanisms regulating Hh signalling in response to mechanical cues.

15.8 Mechanoregulation of Primary Cilia Structure

As cilia-mediated signalling pathways, such as Hh signalling and mechanotransduction, are starting to be characterised, other studies have focused on primary cilia structure with a view to understanding the complex structure-function relationship. Indeed, an increasing number of studies are showing that length and associated anterograde and retrograde IFT, are correlated to functionality (Besschetnova et al. 2010; Tran et al. 2008) and in some case to disease as in certain ciliopathies (Mokrzan et al. 2007). In the case of motile, cilia-like flagella this is considerably easier, the molecular characterization of the mechanisms that regulate cilia length is much further ahead (Berman et al. 2003; Nguyen et al. 2005; Rosenbaum 2003; Tam et al. 2003, 2007; Wang et al. 2004). However, regulation of primary cilia length appears to involve a wide range of possible mechanisms including the cAMP-PKA system, the PKC- Mitogen-activated (MAP) Protein Kinases, a large range of actin and tubulin related proteins, many cell-cycle related proteins, Gelectins, FGF signaling, and Hypoxia-inducible factors (HIFs) (Abdul-Majeed et al. 2011; Besschetnova et al. 2010; Cruz et al. 2010; Kim et al. 2010; Kinzel et al. 2010; Li et al. 2011; Lopes et al. 2010; Massinen et al. 2011; May-Simera et al. 2010; Miyoshi et al. 2009; Neugebauer et al. 2009; Ou et al. 2009; Palmer et al. 2011; Pugacheva et al. 2007; Rondanino et al. 2011; Sharma et al. 2011; Thiel et al. 2011; Verghese et al. 2009, 2011). The primary cilia disassembly pathways are perhaps better defined and include prominent roles for tubulin de-acetylases and cell cycle related kinases such as Aurora A (Hubbert et al. 2002; Pugacheva et al. 2007; Prodromou et al. 2012).

At its most extreme cilia length regulation, in the form of rapid disassembly, often takes place in polarized cell types where the cilium is facing into a lumen. Here fluid-flow induced shear forces exert influence over structure producing a feedback loop which regulates epithelial cilia-mediated mechanotransduction (Besschetnova et al. 2010; Iomini et al. 2004). Thus fluid shear-mediated deflection of the primary cilium activates calcium signalling thereby reducing intracellular cAMP concentrations leading to cilium shortening and decreased mechanotransductive signalling

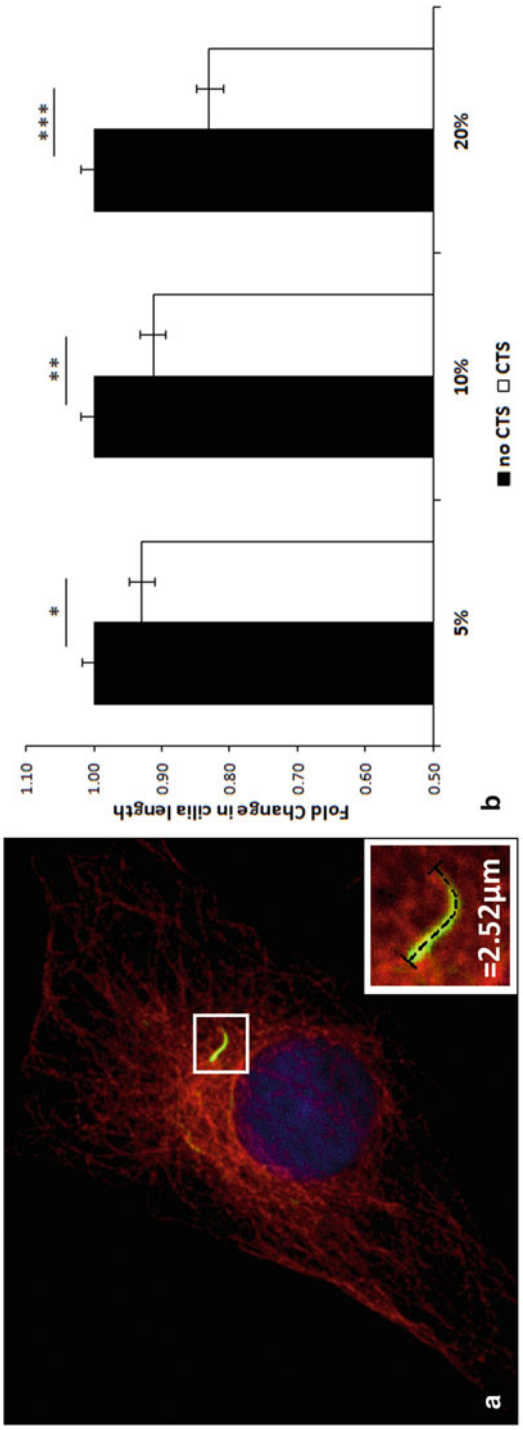

Fig. 15.7 Cyclic tensile strain induces primary cilia disassembly and reduces cilia length in a strain-dependent manner. **a** Immunofluorescent labelling of the chondrocyte primary cilium. Primary cilia in bovine articular chondrocytes were labelled with acetylated α-tubulin (*green*) and β-tubulin (*red*), the cilia appears yellow as these two labels colocalise. Nuclei labelled with DAPI (*blue*). The length of the primary cilium was determined by measuring the distance from base to tip (*dashed line*) using Leica Lite confocal software. **b** Chondrocytes were subjected to cyclic tensile strain (*CTS*) at 5, 10 and 20 % strain for 1 h, 0.33 Hz. Mean primary cilia length was significantly reduced by CTS ($p < 0.05$) in a strain dependent manner compared to no CTS controls

(Besschetnova et al. 2010). Similarly for articular chondrocytes, mechanical loading influences primary cilia structure and length with studies showing strain-dependent reductions in cilia length following cyclic compression (McGlashan et al. 2010) or cyclic tension (Fig. 15.6). These data suggests the reported variation in primary cilia length observed between different zones of the articular cartilage (Farnum and Wilsman 2011; McGlashan et al. 2008) may be the result of established differences in the mechanical environment within each zone (Guilak et al. 1995). This is supported by the fact that zonal differences in cilia length and prevalence are more pronounced in load bearing regions of the joint and that cilia are shorter and more oriented in regions experiencing high levels of strain compared with low (Farnum and Wilsman 2011). Interesting recent studies by the authors suggest that the reduction in primary cilia length observed at high strain magnitudes (20 % cyclic tensile strain), prevents the mechanosensitive up-regulation of Hh signalling (Fig. 15.6 and 15.7). It remains to be seen whether this is part of a physiological feedback mechanism as in epithelial cells subjected to fluid flow or whether this is a pathological injury response.

15.9 Conclusion and Perspectives

The first pioneering studies by Poole and Jensen and others, characterising the presence of primary cilia in cartilage and other musculoskeletal tissues were largely over looked for many years. It is only recently that the importance of the chondrocyte primary cilium in cartilage physiology has begun to be recognised. In particular chondrocyte primary cilia are now know to be essential for cartilage development. More specifically cilia are required for chondrocyte mechanotransduction and the maintenance of a functional extracellular matrix in response to a dynamic mechanical environment. The primary cilium also functions as a centre for hedgehog signalling which is required for development and which has recently been found to be involved in the pathogenesis of osteoarthritis. Interestingly, hedgehog signalling is stimulated by mechanical loading which also regulates primary cilia structure. Furthermore, recent studies demonstrate the inflammatory cytokines, present in the osteoarthritis, regulate primary cilia structure as part of the mechanism controlling downstream catabolic response (Wann and Knight 2012). All these studies support an emerging link between mechanical forces, primary cilia structure and cilia function. This is likely to be of fundamental importance for articular cartilage in health and disease. Furthermore the understanding of these mechanosensitive relationships may lead to the development of novel therapeutic strategies.

References

Abdul-Majeed S, Moloney BC, Nauli SM (2011) Mechanisms regulating cilia growth and cilia function in endothelial cells. Cell Mol Life Sci 69:165–173

Albrecht-Buehler G, Bushnell A (1980) The ultrastructure of primary cilia in quiescent 3T3 cells. Exp Cell Res 126:427–437

Anderson RG (1972) The three-dimensional structure of the basal body from the rhesus monkey oviduct. J Cell Biol 54:246–265

Athar M, Tang X, Lee JL, Kopelovich L, Kim AL (2006) Hedgehog signalling in skin development and cancer. Exp Dermatol 15:667–677

Berbari NF, O'Connor AK, Haycraft CJ, Yoder BK (2009) The primary cilium as a complex signaling center. Curr Biol 19:R526–R535

Berman SA, Wilson NF, Haas NA, Lefebvre PA (2003) A novel MAP kinase regulates flagellar length in Chlamydomonas. Curr Biol 13:1145–1149

Besschetnova TY, Kolpakova-Hart E, Guan Y, Zhou J, Olsen BR, Shah JV (2010) Identification of signaling pathways regulating primary cilium length and flow-mediated adaptation. Curr Biol 20:182–187

Bishop GA, Berbari NF, Lewis J, Mykytyn K (2007) Type III adenylyl cyclase localizes to primary cilia throughout the adult mouse brain. J Comp Neurol 505:562–571

Cao M, Li G, Pan J (2009) Regulation of cilia assembly, disassembly, and length by protein phosphorylation. Methods Cell Biol 94:333–346

Chang CF, Ramaswamy G, Serra R (2012) Depletion of primary cilia in articular chondrocytes results in reduced Gli3 repressor to activator ratio, increased Hedgehog signaling, and symptoms of early osteoarthritis. Osteoarthritis Cartilage 20:152–161

Chowdhury TT, Knight MM (2006) Purinergic pathway suppresses the release of.NO and stimulates proteoglycan synthesis in chondrocyte/agarose constructs subjected to dynamic compression. J Cell Physiol 209:845–853

Christensen ST, Pedersen SF, Satir P, Veland IR, Schneider L (2008) The primary cilium coordinates signaling pathways in cell cycle control and migration during development and tissue repair. Curr Top Dev Biol 85:261–301

Christensen ST, Clement CA, Satir P, Pedersen LB (2012) Primary cilia and coordination of receptor tyrosine kinase (RTK) signalling. J Pathol 226:172–184

Cohen MM Jr (2010) Hedgehog signaling update. Am J Med Genet A 152A:1875–1914

Corbit KC, Shyer AE, Dowdle WE, Gaulden J, Singla V, Chen MH, Chuang PT, Reiter JF (2008) Kif3a constrains beta-catenin-dependent Wnt signalling through dual ciliary and non-ciliary mechanisms. Nat Cell Biol 10:70–76

Cruz C, Ribes V, Kutejova E, Cayuso J, Lawson V, Norris D, Stevens J, Davey M, Blight K, Bangs F, Mynett A, Hirst E, Chung R, Balaskas N, Brody SL, Marti E, Briscoe J (2010) Foxj1 regulates floor plate cilia architecture and modifies the response of cells to sonic hedgehog signalling. Development 137:4271–4282

D'Andrea P, Calabrese A, Capozzi I, Grandolfo M, Tonon R, Vittur F (2000) Intercellular Ca^{2+} waves in mechanically stimulated articular chondrocytes. Biorheology 37:75–83

Dalagiorgou G, Basdra EK, Papavassiliou AG (2010) Polycystin-1: function as a mechanosensor. Int J Biochem Cell Biol 42:1610–1613

Davenport JR, Yoder BK (2005) An incredible decade for the primary cilium: a look at a once-forgotten organelle. Am J Physiol Renal Physiol 289:1159–1169

Dawe HR, Farr H, Gull K (2007) Centriole/basal body morphogenesis and migration during ciliogenesis in animal cells. J Cell Sci 120:7–15

Day TF, Yang Y (2008) Wnt and hedgehog signaling pathways in bone development. J Bone Joint Surg Am 90(Suppl 1):19–24

Erickson GR, Alexopoulos LG, Guilak F (2001) Hyper-osmotic stress induces volume change and calcium transients in chondrocytes by transmembrane, phospholipid, and G-protein pathways. J Biomech 34:1527–1535

Ehlen HW, Buelens LA, Vortkamp A (2006) Hedgehog signaling in skeletal development. Birth Defects Res C Embryo Today 78:267–279

Edlich M, Yellowley CE, Jacobs CR, Donahue HJ (2004) Cycle number and waveform of fluid flow affect bovine articular chondrocytes Biorheology 41:315–322

Edlich M, Yellowley CE, Jacobs CR, Donahue HJ (2001) Oscillating fluid flow regulates cytosolic calcium concentration in bovine articular chondrocytes. J Biomech 34:59–65

Farge E (2011) Mechanotransduction in development. Curr Top Dev Biol 95:243–265
Farnum CE, Wilsman NJ (2011) Orientation of Primary Cilia of Articular Chondrocytes in Three-Dimensional Space. Anat Rec (Hoboken) 294(3):533–549
Frost HM (1987) The mechanostat: a proposed pathogenic mechanism of osteoporoses and the bone mass effects of mechanical and nonmechanical agents. Bone Miner 2:73–85
Garcia M, Knight MM (2010) Cyclic loading opens hemichannels to release ATP as part of a chondrocyte mechanotransduction pathway. J Orthop Res 28:510–515
Garcia-Gonzalo FR, Corbit KC, Sirerol-Piquer MS, Ramaswami G, Otto EA, Noriega TR, Seol AD, Robinson JF, Bennett CL, Josifova DJ, Garcia-Verdugo JM, Katsanis N, Hildebrandt F, Reiter JF (2011) A transition zone complex regulates mammalian ciliogenesis and ciliary membrane composition. Nat Genet 43:776–784
Gerdes JM, Katsanis N (2008) Ciliary function and Wnt signal modulation. Curr Top Dev Biol 85:175–195
Gerdes JM, Davis EE, Katsanis N (2009) The vertebrate primary cilium in development, homeostasis, and disease. Cell 137:32–45
Gilula NB, Satir P (1972) The ciliary necklace. A ciliary membrane specialization. J Cell Biol 53:494–509
Guan YJ, Yang X, Wei L, Chen Q (2011) MiR-365: a mechanosensitive microRNA stimulates chondrocyte differentiation through targeting histone deacetylase 4. FASEB J
Guilak F, Ratcliffe A, Mow VC (1995) Chondrocyte deformation and local tissue strain in articular cartilage: a confocal microscopy study. J Orthop Res 13:410–421 Guilak F, Zell RA, Erickson GR, Grande DA, Rubin CT, McLeod KJ, Donahue HJ (1999) Mechanically induced calcium waves in articular chondrocytes are inhibited by gadolinium and amiloride. J Orthop Res 17:421–429
Guilak F, Zell RA, Erickson GR, Grande DA, Rubin CT, McLeod KJ, Donahue HJ (1999) Mechanically induced calcium waves in articular chondrocytes are inhibited by gadolinium and amiloride. J Orthop Res 17:421–429
Hagiwara H, Aoki T, Ohwada N, Fujimoto T (1997) Development of striated rootlets during ciliogenesis in the human oviduct epithelium. Cell Tissue Res 290:39–42
Handel M, Schulz S, Stanarius A, Schreff M, Erdtmann-Vourliotis M, Schmidt H, Wolf G, Hollt V (1999) Selective targeting of somatostatin receptor 3 to neuronal cilia. Neuroscience 89:909–926
Haycraft CJ, Serra R (2008) Cilia involvement in patterning and maintenance of the skeleton. Curr Top Dev Biol 85:303–332
Haycraft CJ, Banizs B, Aydin-Son Y, Zhang Q, Michaud EJ, Yoder BK (2005) Gli2 and Gli3 localize to cilia and require the intraflagellar transport protein polaris for processing and function. PLoS Genet 1:e53
Haycraft CJ, Zhang Q, Song B, Jackson WS, Detloff PJ, Serra R, Yoder BK (2007) Intraflagellar transport is essential for endochondral bone formation. Development 134:307–316
hjTang GH, Rabie AB, Hagg U (2004) Indian hedgehog: a mechanotransduction mediator in condylar cartilage. J Dent Res 83:434–438
Huangfu D, Anderson KV (2005) Cilia and Hedgehog responsiveness in the mouse. Proc Natl Acad Sci USA 102:11325–11330
Huangfu D, Liu A, Rakeman AS, Murcia NS, Niswander L, Anderson KV (2003) Hedgehog signalling in the mouse requires intraflagellar transport proteins. Nature 426:83–87
Hubbert C, Guardiola A, Shao R, Kawaguchi Y, Ito A, Nixon A, Yoshida M, Wang XF, Yao TP (2002) HDAC6 is a microtubule-associated deacetylase. Nature 417:455–458
Iomini C, Tejada K, Mo W, Vaananen H, Piperno G (2004) Primary cilia of human endothelial cells disassemble under laminar shear stress. J Cell Biol 164:811–817
Jensen CG, Jensen LC, Rieder CL (1979) The occurrence and structure of primary cilia in a subline of Potorous tridactylus. Exp Cell Res 123:444–449
Jensen CG, Poole CA, McGlashan SR, Marko M, Issa ZI, Vujcich KV, Bowser SS (2004) Ultrastructural, tomographic and confocal imaging of the chondrocyte primary cilium in situ. Cell Biol Int 28:101–110

Jones TJ, Adapala RK, Geldenhuys WJ, Bursley C, AbouAlaiwi WA, Nauli SM, Thodeti CK (2012) Primary cilia regulates the directional migration and barrier integrity of endothelial cells through the modulation of hsp27 dependent actin cytoskeletal organization. J Cell Physiol 227:70–76

Kanbe K, Yang X, Wei L, Sun C, Chen Q (2007) Pericellular matrilins regulate activation of chondrocytes by cyclic load-induced matrix deformation. J Bone Miner Res 22:318–328

Kaushik AP, Martin JA, Zhang Q, Sheffield VC, Morcuende JA (2009) Cartilage abnormalities associated with defects of chondrocytic primary cilia in Bardet-Biedl syndrome mutant mice. J Orthop Res 27:1093–1099

Kim E, Arnould T, Sellin LK, Benzing T, Fan MJ, Gruning W, Sokol SY, Drummond I, Walz G (1999) The polycystic kidney disease 1 gene product modulates Wnt signaling. J Biol Chem 274:4947–4953

Kim J, Lee JE, Heynen-Genel S, Suyama E, Ono K, Lee K, Ideker T, Aza-Blanc P, Gleeson JG (2010) Functional genomic screen for modulators of ciliogenesis and cilium length. Nature 464:1048–1051

Kim S, Zaghloul NA, Bubenshchikova E, Oh EC, Rankin S, Katsanis N, Obara T, Tsiokas L (2011) Nde1-mediated inhibition of ciliogenesis affects cell cycle re-entry. Nat Cell Biol 13:351–360

King PJ, Guasti L, Laufer E (2008) Hedgehog signalling in endocrine development and disease. J Endocrinol 198:439–450

Kinumatsu T, Shibukawa Y, Yasuda T, Nagayama M, Yamada S, Serra R, Pacifici M, Koyama E (2011) TMJ development and growth require primary cilia function. J Dent Res 90:988–994

Kinzel D, Boldt K, Davis EE, Burtscher I, Trumbach D, Diplas B, Attie-Bitach T, Wurst W, Katsanis N, Ueffing M, Lickert H (2010) Pitchfork regulates primary cilia disassembly and left-right asymmetry. Dev Cell 19:66–77

Knight MM, McGlashan SR, Garcia M, Jensen CG, Poole CA (2009) Articular chondrocytes express connexin 43 hemichannels and P2 receptors — a putative mechanoreceptor complex involving the primary cilium? J Anat 214:275–283

Kolahi KS, Mofrad MR (2010) Mechanotransduction: a major regulator of homeostasis and development. Wiley Interdiscip Rev Syst Biol Med 2:625–639

Kono T, Nishikori T, Kataoka H, Uchio Y, Ochi M, Enomoto K (2006) Spontaneous oscillation and mechanically induced calcium waves in chondrocytes. Cell Biochem Funct 24:103–111

Krock BL, Mills-Henry I, Perkins BD (2009) Retrograde intraflagellar transport by cytoplasmic dynein-2 is required for outer segment extension in vertebrate photoreceptors but not arrestin translocation. Invest Ophthalmol Vis Sci 50:5463–5471

Lal M, Song X, Pluznick JL, Di Giovanni V, Merrick DM, Rosenblum ND, Chauvet V, Gottardi CJ, Pei Y, Caplan MJ (2008) Polycystin-1 C-terminal tail associates with beta-catenin and inhibits canonical Wnt signaling. Hum Mol Genet 17:3105–3117

Le AX, Miclau T, Hu D, Helms JA (2001) Molecular aspects of healing in stabilized and non-stabilized fractures. J Orthop Res 19:78–84

Li A, Saito M, Chuang JZ, Tseng YY, Dedesma C, Tomizawa K, Kaitsuka T, Sung CH (2011) Ciliary transition zone activation of phosphorylated Tctex-1 controls ciliary resorption, S-phase entry and fate of neural progenitors. Nat Cell Biol 13:402–411

Lin AC, Seeto BL, Bartoszko JM, Khoury MA, Whetstone H, Ho L, Hsu C, Ali AS, Alman BA (2009) Modulating hedgehog signaling can attenuate the severity of osteoarthritis. Nat Med 15:1421–1425

Lopes SS, Lourenco R, Pacheco L, Moreno N, Kreiling J, Saude L (2010) Notch signalling regulates left-right asymmetry through ciliary length control. Development 137:3625–3632

Low SH, Vasanth S, Larson CH, Mukherjee S, Sharma N, Kinter MT, Kane ME, Obara T, Weimbs T (2006) Polycystin-1, STAT6, and P100 function in a pathway that transduces ciliary mechanosensation and is activated in polycystic kidney disease. Dev Cell 10:57–69

Lu CJ, Du H, Wu J, Jansen DA, Jordan KL, Xu N, Sieck GC, Qian Q (2008) Non-random distribution and sensory functions of primary cilia in vascular smooth muscle cells. Kidney Blood Press Res 31:171–184

Malone AM, Anderson CT, Tummala P, Kwon RY, Johnston TR, Stearns T, Jacobs CR (2007) Primary cilia mediate mechanosensing in bone cells by a calcium-independent mechanism. Proc Natl Acad Sci USA 104:13325–13330

Massinen S, Hokkanen ME, Matsson H, Tammimies K, Tapia-Paez I, Dahlstrom-Heuser V, Kuja-Panula J, Burghoorn J, Jeppsson KE, Swoboda P, Peyrard-Janvid M, Toftgard R, Castren E, Kere J (2011) Increased expression of the dyslexia candidate gene DCDC2 affects length and signaling of primary cilia in neurons. PLoS One 6:e20580

Masyuk AI, Masyuk TV, Splinter PL, Huang BQ, Stroope AJ, LaRusso NF (2006) Cholangiocyte cilia detect changes in luminal fluid flow and transmit them into intracellular Ca^{2+} and cAMP signaling. Gastroenterology 131:911–920

May-Simera HL, Kai M, Hernandez V, Osborn DP, Tada M, Beales PL (2010) Bbs8, together with the planar cell polarity protein Vangl2, is required to establish left-right asymmetry in zebrafish. Dev Biol 345:215–225

May SR, Ashique AM, Karlen M, Wang B, Shen Y, Zarbalis K, Reiter J, Ericson J, Peterson AS (2005) Loss of the retrograde motor for IFT disrupts localization of Smo to cilia and prevents the expression of both activator and repressor functions of Gli. Dev Biol 287:378–389

McGlashan SR, Haycraft CJ, Jensen CG, Yoder BK, Poole CA (2007) Articular cartilage and growth plate defects are associated with chondrocyte cytoskeletal abnormalities in Tg737orpk mice lacking the primary cilia protein polaris. Matrix Biol 26:234–246

McGlashan SR, Cluett EC, Jensen CG, Poole CA (2008) Primary cilia in osteoarthritic chondrocytes: from chondrons to clusters. Dev Dyn 237:2013–2020

McGlashan SR, Knight MM, Chowdhury TT, Joshi P, Jensen CG, Kennedy S, Poole CA (2010) Mechanical loading modulates chondrocyte primary cilia incidence and length. Cell Biol Int 34:441–446

Milenkovic L, Scott MP, Rohatgi R (2009) Lateral transport of Smoothened from the plasma membrane to the membrane of the cilium. J Cell Biol 187:365–374

Millward-Sadler SJ, Salter DM (2004) Integrin-dependent signal cascades in chondrocyte mechanotransduction. Ann Biomed Eng 32:435–446

Miyoshi K, Kasahara K, Miyazaki I, Asanuma M (2009) Lithium treatment elongates primary cilia in the mouse brain and in cultured cells. Biochem Biophys Res Commun 388:757–762

Mizuno S (2005) A novel method for assessing effects of hydrostatic fluid pressure on intracellular calcium: a study with bovine articular chondrocytes. Am J Physiol Cell Physiol 288:C329–337

Mokrzan EM, Lewis JS, Mykytyn K (2007) Differences in renal tubule primary cilia length in a mouse model of Bardet-Biedl syndrome. Nephron Exp Nephrol 106:e88–e96

Morrow D, Sweeney C, Birney YA, Guha S, Collins N, Cummins PM, Murphy R, Walls D, Redmond EM, Cahill PA (2007) Biomechanical regulation of hedgehog signaling in vascular smooth muscle cells in vitro and in vivo. Am J Physiol Cell Physiol 292:C488–C496

Nagase T, Nagase M, Machida M, Fujita T (2008) Hedgehog signalling in vascular development. Angiogenesis 11:71–77

Nauli SM, Jin X, Hierck BP (2011) The mechanosensory role of primary cilia in vascular hypertension. Int J Vasc Med 2011:376281

Nauli SM, Alenghat FJ, Luo Y, Williams E, Vassilev P, Li X, Elia AE, Lu W, Brown EM, Quinn SJ, Ingber DE, Zhou J (2003) Polycystins 1 and 2 mediate mechanosensation in the primary cilium of kidney cells. Nat Genet 33:129–137

Neugebauer JM, Amack JD, Peterson AG, Bisgrove BW, Yost HJ (2009) FGF signalling during embryo development regulates cilia length in diverse epithelia. Nature 458:651–654

Ng TC, Chiu KW, Rabie AB, Hagg U (2006) Repeated mechanical loading enhances the expression of Indian hedgehog in condylar cartilage. Front Biosci 11:943–948

Nguyen RL, Tam LW, Lefebvre PA (2005) The LF1 gene of Chlamydomonas reinhardtii encodes a novel protein required for flagellar length control. Genetics 169:1415–1424

Nowlan NC, Murphy P, Prendergast PJ (2008a) A dynamic pattern of mechanical stimulation promotes ossification in avian embryonic long bones. J Biomech 41:249–258

Nowlan NC, Prendergast PJ, Murphy P (2008b) Identification of mechanosensitive genes during embryonic bone formation. PLoS Comput Biol 4:e1000250

Ohashi T, Hagiwara M, Bader DL, Knight MM (2006) Intracellular mechanics and mechanotransduction associated with chondrocyte deformation during pipette aspiration. Biorheology 43:201–214

Ostrowski LE, Blackburn K, Radde KM, Moyer MB, Schlatzer DM, Moseley A, Boucher RC (2002) A proteomic analysis of human cilia: identification of novel components. Mol Cell Proteomics 1:451–465

Ou Y, Ruan Y, Cheng M, Moser JJ, Rattner JB, Van Der Hoorn FA (2009) Adenylate cyclase regulates elongation of mammalian primary cilia. Exp Cell Res 315:2802–2817

Palmer KJ, MacCarthy-Morrogh L, Smyllie N, Stephens DJ (2011) A role for Tctex-1 (DYNLT1) in controlling primary cilium length. Eur J Cell Biol 90:865–871

Pan J, Snell W (2007) The primary cilium: keeper of the key to cell division. Cell 129:1255–1257

Pazour GJ, Witman GB (2003) The vertebrate primary cilium is a sensory organelle. Curr Opin Cell Biol 15:105–110

Pazour GJ, San Agustin JT, Follit JA, Rosenbaum JL, Witman GB (2002) Polycystin-2 localizes to kidney cilia and the ciliary level is elevated in orpk mice with polycystic kidney disease. Curr Biol 12:R378–R380

Pedersen LB, Rosenbaum JL (2008) Intraflagellar transport (IFT) role in ciliary assembly, resorption and signalling. Curr Top Dev Biol 85:23–61

Perrone CA, Tritschler D, Taulman P, Bower R, Yoder BK, Porter ME (2003) A novel dynein light intermediate chain colocalizes with the retrograde motor for intraflagellar transport at sites of axoneme assembly in chlamydomonas and Mammalian cells. Mol Biol Cell 14:2041–2056

Pingguan-Murphy B, Lee DA, Bader DL, Knight MM (2005) Activation of chondrocytes calcium signalling by dynamic compression is independent of number of cycles. Arch Biochem Biophys 444:45–51

Pingguan-Murphy B, El-Azzeh M, Bader DL, Knight MM (2006) Cyclic compression of chondrocytes modulates a purinergic calcium signalling pathway in a strain rate- and frequency-dependent manner. J Cell Physiol 209:389–397

Poole CA, Flint MH, Beaumont BW (1985) Analysis of the morphology and function of primary cilia in connective tissues: a cellular cybernetic probe? Cell Motil 5:175–193

Poole CA, Jensen CG, Snyder JA, Gray CG, Hermanutz VL, Wheatley DN (1997) Confocal analysis of primary cilia structure and colocalization with the Golgi apparatus in chondrocytes and aortic smooth muscle cells. Cell Biol Int 21:483–494

Praetorius HA, Spring KR (2001) Bending the MDCK cell primary cilium increases intracellular calcium. J Membr Biol 184:71–79

Praetorius HA, Spring KR (2003) The renal cell primary cilium functions as a flow sensor. Curr Opin Nephrol Hypertens 12:517–520

Prodromou NV, Thompson C, Osborn DP, Kogger KF, Asworth R, Beales PL, Knight MM, Chapple JP (2012) Heat shock induces rapid resorption of primary cilia. J Cell Sci (Epub)

Pugacheva EN, Jablonski SA, Hartman TR, Henske EP, Golemis EA (2007) HEF1-dependent Aurora A activation induces disassembly of the primary cilium. Cell 129:1351–1363

Qin H, Diener DR, Geimer S, Cole DG, Rosenbaum JL (2004) Intraflagellar transport (IFT) cargo: IFT transports flagellar precursors to the tip and turnover products to the cell body. J Cell Biol 164:255–266

Rabie AB, Al-Kalaly A (2008) Does the degree of advancement during functional appliance therapy matter? Eur J Orthod 30:274–282

Ringo DL (1967) Flagellar motion and fine structure of the flagellar apparatus in Chlamydomonas. J Cell Biol 33:543–571

Robert A, Margall-Ducos G, Guidotti JE, Bregerie O, Celati C, Brechot C, Desdouets C (2007) The intraflagellar transport component IFT88/polaris is a centrosomal protein regulating G1-S transition in non-ciliated cells. J Cell Sci 120:628–637

Roberts SR, Knight MM, Lee DA, Bader DL (2001) Mechanical compression influences intracellular Ca^{2+} signaling in chondrocytes seeded in agarose constructs. J Appl Physiol 90:1385–1391

Rohatgi R, Milenkovic L, Scott MP (2007) Patched1 regulates hedgehog signaling at the primary cilium. Science 317:372–376

Rondanino C, Poland PA, Kinlough CL, Li H, Rbaibi Y, Myerburg MM, Al-bataineh MM, Kashlan OB, Pastor-Soler NM, Hallows KR, Weisz OA, Apodaca G, Hughey RP (2011) Galectin-7 modulates the length of the primary cilia and wound repair in polarized kidney epithelial cells. Am J Physiol Renal Physiol 301:F622–F633

Rosenbaum J (2003) Organelle size regulation: length matters. Curr Biol 13:R506–R507

Schafer JC, Haycraft CJ, Thomas JH, Yoder BK, Swoboda P (2003) XBX-1 encodes a dynein light intermediate chain required for retrograde intraflagellar transport and cilia assembly in Caenorhabditis elegans. Mol Biol Cell 14:2057–2070

Schneider L, Clement CA, Teilmann SC, Pazour GJ, Hoffmann EK, Satir P, Christensen ST (2005) PDGFRalphaalpha signaling is regulated through the primary cilium in fibroblasts. Curr Biol 15:1861–1866

Schneider L, Cammer M, Lehman J, Nielsen SK, Guerra CF, Veland IR, Stock C, Hoffmann EK, Yoder BK, Schwab A, Satir P, Christensen ST (2010) Directional cell migration and chemotaxis in wound healing response to PDGF-AA are coordinated by the primary cilium in fibroblasts. Cell Physiol Biochem 25:279–292

Schwartz MA (2010) Integrins and extracellular matrix in mechanotransduction. Cold Spring Harb Perspect Biol 2:a005066

Schwartz MA, DeSimone DW (2008) Cell adhesion receptors in mechanotransduction. Curr Opin Cell Biol 20:551–556

Shao YY, Wang L, Welter JF, Ballock RT (2011) Primary cilia modulate Ihh signal transduction in response to hydrostatic loading of growth plate chondrocytes. Bone 50(1):79–84

Sharma N, Kosan ZA, Stallworth JE, Berbari NF, Yoder BK (2011) Soluble levels of cytosolic tubulin regulate ciliary length control. Mol Biol Cell 22:806–816

Shivashankar GV (2011) Mechanosignaling to the cell nucleus and gene regulation. Annu Rev Biophys 40:361–378

Tam LW, Dentler WL, Lefebvre PA (2003) Defective flagellar assembly and length regulation in LF3 null mutants in Chlamydomonas. J Cell Biol 163:597–607

Tam LW, Wilson NF, Lefebvre PA (2007) A CDK-related kinase regulates the length and assembly of flagella in Chlamydomonas. J Cell Biol 176:819–829

Teilmann SC, Christensen ST (2005) Localization of the angiopoietin receptors Tie-1 and Tie-2 on the primary cilia in the female reproductive organs. Cell Biol Int 29:340–346

Teilmann SC, Byskov AG, Pedersen PA, Wheatley DN, Pazour GJ, Christensen ST (2005) Localization of transient receptor potential ion channels in primary and motile cilia of the female murine reproductive organs. Mol Reprod Dev 71:444–452

Thiel C, Kessler K, Giessl A, Dimmler A, Shalev SA, von der Haar S, Zenker M, Zahnleiter D, Stoss H, Beinder E, Abou Jamra R, Ekici AB, Schroder-Kress N, Aigner T, Kirchner T, Reis A, Brandstatter JH, Rauch A (2011) NEK1 mutations cause short-rib polydactyly syndrome type majewski. Am J Hum Genet 88:106–114

Tran PV, Haycraft CJ, Besschetnova TY, Turbe-Doan A, Stottmann RW, Herron BJ, Chesebro AL, Qiu H, Scherz PJ, Shah JV, Yoder BK, Beier DR (2008) THM1 negatively modulates mouse sonic hedgehog signal transduction and affects retrograde intraflagellar transport in cilia. Nat Genet 40:403–410

Urban JP (1994) The chondrocyte: a cell under pressure. Br J Rheumatol 33:901–908

Varjosalo M, Taipale J (2008) Hedgehog: functions and mechanisms. Genes Dev 22:2454–2472

Veland IR, Awan A, Pedersen LB, Yoder BK, Christensen ST (2009) Primary cilia and signaling pathways in mammalian development, health and disease. Nephron Physiol 111:39–53

Verghese E, Ricardo SD, Weidenfeld R, Zhuang J, Hill PA, Langham RG, Deane JA (2009) Renal primary cilia lengthen after acute tubular necrosis. J Am Soc Nephrol 20:2147–2153

Verghese E, Zhuang J, Saiti D, Ricardo SD, Deane JA (2011) In vitro investigation of renal epithelial injury suggests that primary cilium length is regulated by hypoxia-inducible mechanisms. Cell Biol Int 35:909–913

Verhey KJ, Gaertig J (2007) The tubulin code. Cell Cycle 6:2152–2160

Wang S, Luo Y, Wilson PD, Witman GB, Zhou J (2004) The autosomal recessive polycystic kidney disease protein is localized to primary cilia, with concentration in the basal body area. J Am Soc Nephrol 15:592–602

Wann AK, Zuo N, Haycraft CJ, Jensen CG, Poole CA, McGlashan SR, Knight MM (2012) Primary cilia mediate mechanotransduction through control of ATP-induced Ca^{2+} signaling in compressed chondrocytes. FASEB J 26:1663–1671

Wann AK and Knight MM (2012) Primary cilia elongation in response to interleukin-1 mediates the inflammatory response. Cell Mol Life Sci 69:2967–2977

Waters AM, Beales PL (2011) Ciliopathies: an expanding disease spectrum. Pediatr Nephrol 26:1039–1056

Westermann S, Weber K (2003) Post-translational modifications regulate microtubule function. Nat Rev Mol Cell Biol 4:938–947

Wilkins RJ, Fairfax TP, Davies ME, Muzyamba MC, Gibson JS (2003) Homeostasis of intracellular Ca^{2+} in equine chondrocytes: response to hypotonic shock. Equine Vet J. 35:439–443

Williams CL, Li C, Kida K, Inglis PN, Mohan S, Semenec L, Bialas NJ, Stupay RM, Chen N, Blacque OE, Yoder BK, Leroux MR (2011) MKS and NPHP modules cooperate to establish basal body/transition zone membrane associations and ciliary gate function during ciliogenesis. J Cell Biol 192:1023–1041

Wong SY, Reiter JF (2008) The primary cilium at the crossroads of mammalian hedgehog signaling. Curr Top Dev Biol 85:225–260

Wu Q, Zhang Y, Chen Q (2001) Indian hedgehog is an essential component of mechanotransduction complex to stimulate chondrocyte proliferation. J Biol Chem 276:35290–35296

Index

A. Kamkin, I. Lozinsky (eds.), *Mechanically Gated Channels and their Regulation,* Mechanosensitivity in Cells and Tissues 6,
DOI 10.1007/978-94-007-5073-9, © Springer Science+Business Media Dordrecht 2012